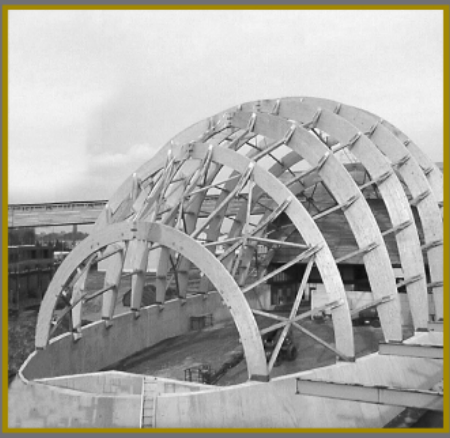
WOODHEAD PUBLISHING IN MATERIALS



# Advances in structural adhesive bonding

Edited by David A. Dillard

CRC

WP

# Advances in structural adhesive bonding

© Woodhead Publishing Limited, 2010

## Related titles:

*Adhesive bonding: science, technology and applications*
(ISBN 978-1-85573-741-9)
This important collection reviews key research on adhesive behaviour and applications in sectors as diverse as construction and automotive engineering. The book is divided into three main parts: fundamentals, mechanical properties and applications. Part I focuses on the basic properties of adhesives, surface assessment and treatment. Part II concentrates on understanding how adhesives perform under stress and the factors affecting fatigue and failure. The final part of the book reviews industry specific applications in areas such as building and construction, transport and electrical engineering.

*Bonding elastomers: a review of adhesives and processes*
(ISBN 978-1-85957-495-9)
This review has been written as a practical approach to bonding various kinds of elastomers to substrates such as steel and plastics, as used in the manufacture of diverse products such as rubber covered rolls, urethane fork lift wheels, rubber lining for chemical storage or solid rocket motors, engine bushes and mounts, seals for transmissions, electrical power connectors and military tank track pads.

*Engineering and structural adhesives*
(ISBN 978-1-85957-436-2)
The report discusses the types of adhesives in use, properties, advantages and disadvantages, and applications. It is very clearly written, well referenced and provides an excellent overview of a rapidly developing field. The author is an expert with many years of experience in adhesive research and development. The review is accompanied by around 400 abstracts from papers and books in the Rapra Polymer Library database, to facilitate further reading on this subject. A subject index and a company index are included.

Details of these and other Woodhead Publishing materials books can be obtained by:

- visiting our web site at www.woodheadpublishing.com
- contacting Customer Services (e-mail: sales@woodheadpublishing.com; fax: +44 (0) 1223 893694; tel.: +44 (0) 1223 891358 ext. 130; address: Woodhead Publishing Limited, Abington Hall, Granta Park, Great Abington, Cambridge CB21 6AH, UK)

If you would like to receive information on forthcoming titles, please send your address details to: Francis Dodds (address, tel. and fax as above; e-mail: francis.dodds@woodheadpublishing.com). Please confirm which subject areas you are interested in.

© Woodhead Publishing Limited, 2010

# Advances in structural adhesive bonding

Edited by

David A. Dillard




**CRC Press**
**Boca Raton Boston New York Washington, DC**

WOODHEAD PUBLISHING LIMITED
Oxford Cambridge New Delhi

© Woodhead Publishing Limited, 2010

Published by Woodhead Publishing Limited, Abington Hall, Granta Park, Great Abington, Cambridge CB21 6AH, UK
www.woodheadpublishing.com

Woodhead Publishing India Private Limited, G-2, Vardaan House, 7/28 Ansari Road, Daryaganj, New Delhi – 110002, India
www.woodheadpublishingindia.com

Published in North America by CRC Press LLC, 6000 Broken Sound Parkway, NW, Suite 300, Boca Raton, FL 33487, USA

First published 2010, Woodhead Publishing Limited and CRC Press LLC
© Woodhead Publishing Limited, 2010
The authors have asserted their moral rights.

This book contains information obtained from authentic and highly regarded sources. Reprinted material is quoted with permission, and sources are indicated. Reasonable efforts have been made to publish reliable data and information, but the authors and the publishers cannot assume responsibility for the validity of all materials. Neither the authors nor the publishers, nor anyone else associated with this publication, shall be liable for any loss, damage or liability directly or indirectly caused or alleged to be caused by this book.

Neither this book nor any part may be reproduced or transmitted in any form or by any means, electronic or mechanical, including photocopying, microfilming and recording, or by any information storage or retrieval system, without permission in writing from Woodhead Publishing Limited.

The consent of Woodhead Publishing Limited does not extend to copying for general distribution, for promotion, for creating new works, or for resale. Specific permission must be obtained in writing from Woodhead Publishing Limited for such copying.

Trademark notice: Product or corporate names may be trademarks or registered trademarks, and are used only for identification and explanation, without intent to infringe.

British Library Cataloguing in Publication Data
A catalogue record for this book is available from the British Library.

Library of Congress Cataloging in Publication Data
A catalog record for this book is available from the Library of Congress.

Woodhead Publishing ISBN 978-1-84569-435-7 (book)
Woodhead Publishing ISBN 978-1-84569-805-8 (e-book)
CRC Press ISBN 978-1-4398-0217-5
CRC Press order number: N10053

The publishers' policy is to use permanent paper from mills that operate a sustainable forestry policy, and which has been manufactured from pulp which is processed using acid-free and elemental chlorine-free practices. Furthermore, the publishers ensure that the text paper and cover board used have met acceptable environmental accreditation standards.

Typeset by Replika Press Pvt Ltd, India
Printed by TJ International Limited, Padstow, Cornwall, UK

© Woodhead Publishing Limited, 2010

# Contents

*Contributor contact details* *xiii*

## Part I Adhesive selection

1 Key issues in selecting the right adhesive 3
*E. J. C. Kellar, TWI, UK*

1.1 Introduction 3
1.2 Adhesive chemistry 4
1.3 Adhesive form and structure 10
1.4 Adhesive cure mechanism 11
1.5 Substrate compatibility 12
1.6 Surface pretreatment 13
1.7 Joint function and operating environment 13
1.8 Joint design 14
1.9 Manufacturing demands 14
1.10 Quality control 14
1.11 Testing and evaluation 15
1.12 End of life requirements 16
1.13 Aesthetics 16
1.14 Adhesive selector software 16
1.15 Internet provision 17
1.16 Future trends 18

2 Advances in epoxy adhesives 20
*K. J. Abbey, Lord Corporation, USA*

2.1 Introduction 20
2.2 Main applications and limitations of epoxy adhesives 21
2.3 Recent developments in epoxy adhesives 22
2.4 Sources of further information and advice 30
2.5 References 31

© Woodhead Publishing Limited, 2010

3 Advances in polyurethane structural adhesives 35
*B. Burchardt, Sika Services AG, Switzerland*

3.1 Introduction 35
3.2 Characterisation of structural adhesives 38
3.3 Chemistry 48
3.4 Design principles 54
3.5 Surface treatment strategy 57
3.6 Applications for PUR adhesives 57
3.7 Conclusions 65
3.8 References 65

4 Advances in structural silicone adhesives 66
*C. White and K. Tan, National Institute of Standards and Technology, USA; A. Wolf, Dow Corning Corporation, Germany; and L. Carbary, Dow Corning Corporation, USA.*

4.1 Introduction 66
4.2 Properties of silicone structural adhesives 67
4.3 Product forms and cure chemistry 69
4.4 Silicone adhesive formulations 74
4.5 Applications of silicone structural adhesives 81
4.6 Conclusions 89
4.7 Future trends 90
4.8 Sources of further information and advice 90
4.9 References 91

5 Advances in anaerobic and cyanoacrylate adhesives 96
*P. Klemarczyk, Henkel Corporation, USA; and J. Guthrie, Henkel Loctite RD&E, Ireland*

5.1 Introduction to anaerobic adhesives 96
5.2 Chemistry of anaerobic adhesives 98
5.3 Recent developments in anaerobic adhesive technology 103
5.4 Introduction to cyanoacrylate adhesives 110
5.5 Cyanoacrylate adhesive formulations and adhesive types 114
5.6 Advances in cyanoacrylate technology 124
5.7 Summary 126
5.8 Future trends 127
5.9 Acknowledgement 127
5.10 References 127

6 Advances in acrylic structural adhesives 132
*P. C. Briggs, IPS Corporation, USA; and G. L. Jialanella, The Dow Chemical Company, USA*

6.1 Introduction 132

© Woodhead Publishing Limited, 2010

6.2 Classification of acrylic structural adhesives 137
6.3 Advantages and disadvantages and unique characteristics of acrylic structural adhesives 140
6.4 Applications of acrylic structural adhesives 145
6.5 Manufacturers 149
6.6 Future trends 149
6.7 References 150

7 Advances in nanoparticle reinforcement in structural adhesives 151
*A. C. Taylor, Imperial College London, UK*

7.1 Introduction: opportunities and limitations in nanoparticle reinforcement 151
7.2 Types of nanoparticles and their key attributes 153
7.3 Methods of nanoparticle incorporation 158
7.4 Typical property variations available through nanoparticle reinforcement 161
7.5 Future trends 172
7.6 Sources of further information and advice 174
7.7 Conclusions 175
7.8 References 176

Part II Adherends, surfaces and pre-treatments

8 Improvements in bonding metals (steel, aluminium) 185
*A. Kwakernaak, J. Hofstede, J. Poulis and R. Benedictus, Delft University of Technology, The Netherlands*

8.1 Introduction: key problems in metal bonding 185
8.2 Developments in the range of adhesives for metal 186
8.3 Developments in surface treatment techniques for metal 196
8.4 Developments in joint design 206
8.5 Developments in modelling and testing the effectiveness of adhesive bonded metal joints 220
8.6 Future trends 228
8.7 Sources of further information and advice 229
8.8 References 230

9 Advances in bonding plastics 237
*G. L. Jialanella, The Dow Chemical Company, USA*

9.1 Introduction 237
9.2 Adhesion mechanisms in bonding plastics 238
9.3 Surface characteristics affecting plastic bonding 246

© Woodhead Publishing Limited, 2010

9.4 Surface treatments used in bonding plastics 247
9.5 Uses of organoboron chemistry in plastic bonding 256
9.6 Limitations of plastic bonding 258
9.7 Future trends 261
9.8 References 262

10 Bonding of polymer matrix composites 265
*K. D. Fernholz, Ford Motor Company, USA*
10.1 Introduction 265
10.2 Preteatment and surface characterization in composite bonding 271
10.3 Composite joint design considerations 274
10.4 Modeling and testing composite joints 277
10.5 Future trends in aerospace and automotive composites 281
10.6 Sources of further information and advice 287
10.7 Acknowledgements 288
10.8 References 288

Part III Joint design

11 Selecting the right joint design and fabrication techniques 295
*K. Dilger, Technical University Braunschweig, Germany*
11.1 Introduction 295
11.2 Basics 296
11.3 Selecting the right joint design 299
11.4 Fabrication techniques 301
11.5 Joints for different materials 302
11.6 Graphic representation of adhesive joints in engineering drawings 310
11.7 Conclusions and outlook 311
11.8 References 313

12 Life prediction for bonded joints in composite material based on actual fatigue damage 316
*G. Meneghetti, M. Quaresimin and M. Ricotta, University of Padova, Italy*
12.1 Introduction 316
12.2 Recent results for fatigue behaviour of single lap bonded joints 318
12.3 Overview and analysis of fatigue damage mechanics (nucleation and propagation) 322

© Woodhead Publishing Limited, 2010

12.4 The life prediction model 332
12.5 Generalised stress intensity factor (SIF) approach and assessment of the life to crack initiation 333
12.6 The crack propagation phase 338
12.7 Life prediction procedure and application 343
12.8 Discussion and conclusions 347
12.9 References 348

13 Improving adhesive joint design using fracture mechanics 350
*D. A. Dillard, Virginia Polytechnic Institute and State University, USA*
13.1 Introduction 350
13.2 Fracture mechanics overview 354
13.3 Measuring adhesion fracture energies 357
13.4 Designing to resist fracture 360
13.5 Issues related to mixed mode fracture 367
13.6 Design insights from fracture mechanics 372
13.7 Design implications of other singularities 375
13.8 Numerical analysis 376
13.9 Future trends 379
13.10 Conclusions 380
13.11 References 381

14 Developments in testing adhesive joints 389
*B. Duncan, National Physical Laboratory, UK*
14.1 Introduction 389
14.2 Current and emerging types of testing 392
14.3 Specimen manufacture issues 410
14.4 Test variables 415
14.5 Detection of failure 421
14.6 Case study in the use of joint tests: cryogenic liquid containment system 424
14.7 Case study in the use of joint tests: using T joints to validate materials models 428
14.8 Future trends 431
14.9 Acknowledgements 432
14.10 Sources of further information and advice 432
14.11 References 434

15 Advances in testing adhesively bonded composites 437
*J.-Y. Cognard, ENSIETA, France; P. Davies, IFREMER, France; and L. Sohier, Université de Bretagne Occidentale (UBO), France*
15.1 Introduction 437

© Woodhead Publishing Limited, 2010

15.2 State of the art 438
15.3 Examples of results from traditional tests of adhesively bonded composites 439
15.4 Modified Arcan test 449
15.5 Characterization of composite assemblies with the modified Arcan test 456
15.6 Conclusion and future trends 463
15.7 References 464

Part IV Environmental effects and durability of adhesives

16 Designing adhesive joints for fatigue and creep load conditions 469
*I. Ashcroft, Loughborough University, UK; and P. Briskham, Coventry University, UK*

16.1 Introduction 469
16.2 Fatigue in adhesive joints 472
16.3 Creep in adhesive joints 484
16.4 Creep–fatigue interactions in adhesive joints 497
16.5 Applications of fatigue and creep analysis of adhesively bonded joints 499
16.6 Overall summary and future trends 510
16.7 References 511

17 Improving bonding at high and low temperatures 516
*L. F. M. da Silva, University of Porto, Portugal*

17.1 Introduction: key problems caused by high and low temperature conditions 516
17.2 Shrinkage of the adhesive 517
17.3 Effect of differential thermal expansion 518
17.4 Effect of temperature on adhesive properties 522
17.5 Modelling high and low temperature conditions 528
17.6 Experimental joint strength results in high and low temperature conditions 532
17.7 Techniques for optimising adhesive bonds in high and low temperature conditions 534
17.8 Summary and future trends 540
17.9 Sources of further information and advice 541
17.10 Acknowledgements 541
17.11 References 542

© Woodhead Publishing Limited, 2010

18 Assessing and improving bonding in wet conditions 547
*K. Tan, C. White and D. Hunston, National Institute of Standards and Technology, USA; B. Vogt, Arizona State University, USA; and A. Haag, Haag Chemistry LLC, USA*

18.1 Introduction 547
18.2 Testing and modeling adhesive bonds in wet conditions 548
18.3 Techniques for optimizing adhesive bonds in wet conditions 559
18.4 Future trends 567
18.5 References 568

19 Improving bonding in hostile chemical environments 574
*W. Broughton, National Physical Laboratory, UK*

19.1 Introduction 574
19.2 Chemical agents and degradation mechanisms 575
19.3 Chemical resistance testing 587
19.4 Modelling and predictive analysis 602
19.5 Optimizing chemical resistance of adhesive joints 606
19.6 Future trends 608
19.7 Sources of further information and advice 609
19.8 Acknowledgements 609
19.9 References 609
19.10 Appendix: Standards 611

*Index* *617*

© Woodhead Publishing Limited, 2010

# Contributor contact details

(* = main contact)

## Chapter 1

Dr Ewen J. C. Kellar
TWI
Granta Park
Great Abington
Cambridge
CB21 6AL
UK

E-mail: ewen.kellar@twi.co.uk

## Chapter 2

Dr K. J. Abbey
Lord Corporation
Thomas Lord Research Center
110 Lord Drive
Cary, NC 27511
USA

E-mail: kirk_abbey@lord.com

## Chapter 3

Dr Bernd Burchardt
Market Research Manager
Sika Services AG
Tüffenwies 16
CH-8048 Zürich
Switzerland

E-mail: burchardt.bernd@ch.sika.com

## Chapter 4

C. C. White* and K. Tan
National Institute of Standards and Technology
Building & Fire Research Laboratory
100 Bureau Dr., Mail Stop 8615
Gaithersburg, MD 20899-8615
USA

E-mail: christopher.white@nist.gov

A. T. Wolf
Dow Corning Corporation
Rheingaustrasse 34
D-65201 Wiesbaden
Germany

E-mail: andreas.wolf@dowcorning.com

L. D. Carbary
Dow Corning Corporation
Midland
MI 48686
USA

E-mail: l.carbary@dowcorning.com

© Woodhead Publishing Limited, 2010

## Chapter 5

Dr P. Klemarczyk*
Henkel Corporation
One Henkel Way
Rocky Hill, CT 0607
USA

E-mail: phil.klemarczyk@us.henkel.com

Dr J. Guthrie
Henkel Loctite RD&E
Tallaght Business Park, Whitestown
Dublin 24
Ireland

E-mail: john.guthrie@ie.henkel.com

## Chapter 6

Dr P. C. Briggs
IPS Corporation
600 Ellis Road
Durham, NC 27703
USA

Dr G. L. Jialanella*
The Dow Chemical Company
Dow Automotive
1250 Harmon Road
Auburn Hills, MI 48326
USA

E-mail: gljialanella@dow.com

## Chapter 7

Dr A. C. Taylor
Department of Mechanical Engineering
Imperial College London
South Kensington Campus
London SW7 2AZ
UK

E-mail: a.c.taylor@imperial.ac.uk

## Chapter 8

A. Kwakernaak*, J. C. J. Hofstede, J. A. Poulis and R. Benedictus
Adhesion Institute
Faculty of Aerospace Engineering
Delft University of Technology
Kluyverweg 1
2629 HS Delft
The Netherlands

E-mail: a.kwakernaak@tudelft.nl

## Chapter 9

Dr G. L. Jialanella
The Dow Chemical Company
Dow Automotive
1250 Harmon Road
Auburn Hills, MI 48326
USA

E-mail: gljialanella@dow.com

© Woodhead Publishing Limited, 2010

## Chapter 10

K. D. Fernholz
Materials and Processes Department
Research & Advanced Engineering
Ford Motor Company
MD 3182/RIC Building
PO Box 2053
Dearborn, MI 48121-2053
USA

E-mail: kfernhol@ford.com

## Chapter 11

Professor K. Dilger
Technical University Braunschweig
Institute of Joining and Welding
Langer Kamp 8
38106 Braunschweig
Germany

E-mail: k.dilger@tu-bs.de

## Chapter 12

Professor Marino Quaresimin*
Department of Management and Engineering
University of Padova
Stradella San Nicola 3
I-36100 Vicenza
Italy

E-mail: marino.quaresimin@unipd.it

Dr Giovanni Meneghetti and Dr Mauro Ricotta
Department of Mechanical Engineering
University of Padova
Via Venezia 1
I-35131 Padova
Italy

## Chapter 13

Professor David A. Dillard
Adhesive and Sealant Science Professor
Engineering Science and Mechanics Department
Virginia Polytechnic Institute and State University
Blacksburg
VA 24061-0219
USA

Email: dillard@vt.edu

## Chapter 14

B. C. Duncan
National Physical Laboratory
Teddington
TW11 0LW
UK

E-mail: bruce.duncan@npl.co.uk

## Chapter 15

Professor J.-Y. Cognard
Brest Laboratory of Mechanics and Systems
ENSIETA
29806 Brest Cedex 09
France

E-mail: jean-yves.cognard@ensieta.fr

Dr P. Davies*
Materials and Structures group
IFREMER
Brest Centre
29280 Plouzané
France

E-mail: peter.davies@ifremer.fr

© Woodhead Publishing Limited, 2010

Dr L. Sohier
Brest Laboratory of Mechanics and Systems
Université de Bretagne Occidentale (UBO)
29285 Brest Cedex
France

E-mail: Laurent.sohier@univ-brest.fr

## Chapter 16

Dr I. A. Ashcroft*
Wolfson School of Mechanical and Manufacturing Engineering
Loughborough University
Leicestershire
LE11 3TU
UK

E-mail: i.a.ashcroft@lboro.ac.uk

Dr P. Briskham
Faculty of Engineering & Computing
Coventry University
CV1 5FB
UK

E-mail: p.briskham@coventry.ac.uk

## Chapter 17

Dr L. F. M. da Silva
Department of Mechanical Engineering
Faculty of Engineering
University of Porto
Rua Dr Roberto Frias
4200-465 Porto
Portugal

E-mail: lucas@fe.up.pt

## Chapter 18

K. T. Tan, C. C. White* and D. L. Hunston
National Institute of Standards and Technology
Building & Fire Research Laboratory
100 Bureau Dr., Mail Stop 8615
Gaithersburg, MD 20899-8615
USA

E-mail: christopher.white@nist.gov

B. D. Vogt
Department of Chemical Engineering
Arizona State University
Tempe, AZ 85284
USA
E-mail: bryan.vogt@asu.edu

A. P. Haag
Haag Chemistry LLC
Bozeman, MT 59718
USA

E-mail: haagap@q.com

## Chapter 19

Dr W. R. Broughton
Bio, Polymeric and Composite Materials Group
Materials Division
National Physical Laboratory
Hampton Road
Teddington, TW11 0LW
UK

E-mail: bill.broughton@npl.co.uk

© Woodhead Publishing Limited, 2010

# 1

# Key issues in selecting the right adhesive

EWEN J. C. KELLAR, TWI, UK

**Abstract**: In a world where there are many hundreds of commercially available adhesives, spanning many chemical compositions, physical forms and curing requirements, it is very daunting for an engineer to make an appropriate selection based on an application he or she is working on. In addition to the nature of the adhesive, other important factors to consider include surface pretreatment, substrate compatibility, joint design, manufacturing demands, quality control and end of life requirements. This chapter seeks to introduce the reader to the key areas associated with adhesive selection and provide an overview of the selection approach. Additionally, this chapter provides some comment on what is available to assist engineers with selection in terms of software and web resources and concludes with some thoughts on future trends and drivers which are likely to affect the adhesives industry and end-users alike.

**Key words**: adhesive forms, adhesive selection, chemistry, end of life, internet resource, selection software, surface pretreatment.

## 1.1 Introduction

It is difficult to estimate the total number of commercial structural adhesives that are available to the modern engineer but it most likely equates to several hundreds worldwide. Add to this the fact that some formulations span several brands differing perhaps only in product name or in some small change in filler or additive and the task of effective adhesive selection has the potential to become overwhelming. Thankfully, if a systematic approach is adopted, considering a number of key parameters, selection can be simplified. However, it should be stressed that all selection must be followed up with an appropriate test programme to ensure fitness for purpose. The major key parameters include:

- adhesive chemistry
- adhesive form/structure
- mode or type of adhesive cure
- substrate compatibility
- surface pretreatment
- joint function and operating environment
- joint design
- manufacturing demands



© Woodhead Publishing Limited, 2010

- quality control/quality assurance (QA/QC)
- testing and evaluation
- end of life requirements
- aesthetics.

Depending upon the application, different selection parameters will adopt different levels of priority and it is not uncommon for an iterative approach to be taken. Initial application requirements will be put forward by the engineer or designer, which at first pass appear to be of the utmost priority but upon subsequent review there may be other factors that have a greater impact upon selection. For example, a key requirement that is often stated is that the adhesive should be as strong as possible. This might result in the selection of a rigid heat cure epoxy, but the epoxy may exhibit a very low strain to failure of say, <0.3%, which would be very strong but could result in catastrophic failure with little or no yield. A re-evaluation of the design might point to the fact that a better candidate may be a 'weaker' toughened epoxy or acrylic adhesive which fails at greater strain levels (e.g. 1–5%). The joint is more robust and a greater volume of adhesive carries the applied load. Another example might be for a glass bonding application where structural performance is superseded by aesthetic requirements and a water-clear 'colour' is preferred over other superior properties.

Although virtually all of the parameters listed are covered in greater detail in subsequent chapters of this book, it is useful to introduce them in a way that emphasises the complex interrelationships that they have with each other.

## 1.2 Adhesive chemistry

The majority of structural adhesives are based upon six main types of chemical composition:

- epoxy (or epoxide)
- polyurethane
- reactive acrylic
- toughened acrylic
- anaerobic acrylic
- cyanoacrylate
- silicone

Each chemical type offers a range of properties which often overlap each other but also possess some unique attributes. In recent years, innovative chemists have formulated many hybrid systems (e.g. epoxy/acrylic and epoxy/polyurethane) designed to bridge the remaining gaps and so provide the adhesives engineer with an almost continuous palette of joining materials

© Woodhead Publishing Limited, 2010

from which to choose. However, the base resin chemistry is only one part of the final adhesive product. Adhesives contain other components in quantities ranging from >10% to <0.01%, each selected for specific property-modifying attributes including adhesion promotion, thermal expansion control, toughening, rheology control, bond-line control, thermal/electrical conduction, colouring, cure control, mix ratio control, and so on. In most cases the full properties of the adhesive are regarded as proprietary information and are rarely, if ever, disclosed. That said, general adhesive properties are still defined by the base chemistry:

### 1.2.1 Epoxy (epoxide)

This is probably still the main workhorse of structural adhesive formulations. They bond well to a wide range of materials, especially metals, ceramics and most polymers, including many thermoplastics. They exhibit good chemical resistance, produce few volatiles during curing and have low shrinkage values. Therefore they have the capacity to form extremely strong and durable bonds with most materials in well-designed joints.

Owing to the nature of the chemistry and the curing reaction, great versatility in formulation can be achieved since there are many resins and many different hardeners. They are available in a wide variety of forms, from low-viscosity liquids to solid pastes or films. Development of toughened formulations has dramatically increased the demanding uses of these adhesives in many industries.

Throughout all the variations, the mechanism of curing (termed addition) is always the same. This mechanism requires precise quantities of resin and hardener, hence the need for accurate mix ratios, and the thorough mixing of resin and hardener in two-part systems. Without these, curing will be affected and inferior properties may result, typically lower strength and stiffness and reduced environmental resistance.

Two-part epoxy adhesives start to react under ambient conditions once the two components have been mixed together and as such are often termed room-temperature (RT) curing adhesives. The reaction is strongly influenced by temperature and as a rule of thumb the reaction rate approximately doubles for every 10°C rise in temperature, that is, an epoxy which takes 1 hour to cure at 20°C, will cure in ~15 minutes at 40°C. Conversely the cure time will double as the temperature drops by 10°C. Complete cure times at ambient temperatures for two-part systems range from a few minutes to several days. It should be noted that, with only a few exceptions, at temperatures below 10°C, the rate of cure decreases significantly and the level of cross-linking may be compromised, giving rise to limited levels of cure, that is, lower cohesive strength, reduced modulus and lower resistance to aggressive environments.

© Woodhead Publishing Limited, 2010

Single-part epoxy adhesives are available in liquid, paste or film form. These adhesives require heat to cure. The resin and hardener are premixed but curing does not occur because the catalyst is in an inactive form at room temperature. It only becomes reactive as the temperature is raised, usually in excess of 100°C. The higher the temperature, the faster the reaction becomes and, in some instances, times of less than 10 minutes can be obtained.

### 1.2.2 Polyurethane

These adhesives, often abbreviated to PU or PUR, will bond to most materials, including plastics, glass, stone and metals. PU adhesives are chemically reactive formulations that may be one-part or two-part systems. They provide strong impact-resistant joints and have better low-temperature (cryogenic) strength than most other adhesives. For two-part systems, cure can be controlled via small quantities of catalyst and can range from several hours to a few seconds. Single-part formulations are partially polymerised and chemically stable until cure is initiated through exposure to atmospheric moisture. The cure rate is diffusion controlled and as such is relatively slow. Full cure is normally hours to days.

Polyurethanes find major uses in the bonding of glass fibre reinforced plastics (GRP), direct glazing of automobiles and lamination of insulation panels and flexible packaging materials. They are also used extensively as adhesives and sealants in the construction and marine industries.

### 1.2.3 Reactive acrylic

These adhesives are supplied as two-part systems comprising a viscous resin and a low volume activator. The activator is often carried in a volatile solvent which flashes off upon application. The resin is applied to the other substrate and when the joint is made, the two surfaces are brought together and the cure then proceeds rapidly (normally a few minutes). This approach has the benefit of starting only when the joint is formed and allows components to be prepared minutes or even hours before final assembly.

Reactive acrylic adhesives have a preference toward bonding plastic systems such as acrylonitrile butadiene styrene (ABS), polycarbonate, poly (methyl methacrylate) (PMMA) and so on but care should be taken to avoid stress cracking which can happen in some instances.

### 1.2.4 Toughened acrylic

Toughened acrylic adhesives are relatively fast curing (minutes to hours) systems, offer high strength and toughness and have more flexibility than many common epoxies. A key property is that they tolerate minimal surface

© Woodhead Publishing Limited, 2010

preparation and bond well to a very wide range of materials, especially plastics. Available primarily as two-part adhesives, the two components are combined either in a similar manner to that seen for epoxies or at the point of dispensing (mixing may or may not be necessary). The cure mechanism (based upon free radical chemistry) is such that acrylics are tolerant of imperfect mixing ratios.

Although toughened acrylics match or even better epoxy systems in many properties, they still exhibit much higher levels of shrinkage during cure, meaning that gap filling is more limited unless very high levels of filler are added, which may compromise mechanical properties.

### 1.2.5 Anaerobic acrylic

Anaerobic adhesives are often known as 'locking compounds', being used to secure, seal and retain turned, threaded, or similarly close fitting parts. They are also used to bond coaxial assemblies and to seal flange faces. At least one component within the joint must be metallic. As a member of the acrylic family of adhesives, they are often in the form of low viscosity liquids, although they can be formulated into pastes or thixotropic systems. They are single-part adhesives which cure when air or, more specifically, oxygen is excluded, hence the name anaerobic.

Under the influence of anaerobic conditions alone, the cure rate is quite slow; in the presence of metal the cure rate is much faster and this, in practice, is how they are used, confined between closely fitting metal parts. The close fit excludes air and the metal surface speeds the rate of cure to a commercially useful degree.

These adhesives have the advantage that material outside the joint does not normally cure and can be wiped off after the assembly has reached handling strength. They are unique among adhesives in that they are formulated to possess different strength characteristics, ranging from relatively weak materials, which allow the easy dismantling of large parts, to very strong materials for permanent fixing. Within each strength band there will usually be several products with different viscosities, allowing different gaps to be filled at the same level of controlled strength. They can also be toughened (see toughened adhesives section) to provide greatly improved peel and impact values.

### 1.2.6 Cyanoacrylate

These adhesives primarily cure through reaction with the thin film of moisture adsorbed on the surfaces to be bonded. They need close fitting joints and usually solidify in seconds, which has resulted in them being given the universal generic name of 'superglues'. Preferred materials include most

© Woodhead Publishing Limited, 2010

non-porous materials especially plastics and rubber.

Curing requires that the moisture found on most surfaces is neutral or slightly alkaline. Any acidic substrate, such as many hardwoods (e.g. oaks), will tend to inhibit the cure and in extreme cases prevent curing altogether. As the adhesive actually consists of very low molecular weight monomer or oligomer components, the curing reaction should be more properly termed polymerisation. Cyanoacrylates are therefore thermoplastic systems and as such are susceptible to creep, especially at elevated temperatures. They are rarely, if ever used at temperatures above 110°C. Additionally, the lack of cross-linking can cause a sensitivity to some organic solvents and to moisture exposure.

Most grades of adhesive are low viscosity liquids and therefore need close fitting joints as they are unable to act as gap fillers. However, newer developments with gelled variants allow cure in wider gaps and application to vertical surfaces.

### 1.2.7 Silicone

Silicone adhesives are not known for their high strength, but are appreciated for their flexibility and their ability to function over a wide temperature range (from cryogenic conditions to over 250°C). They are available in single or two-part forms. The latter are mixed and dispensed in a similar way to other two-part systems, such as epoxies and toughened acrylics, whilst the former behave like single-part polyurethanes, i.e. cure through the diffusion of atmospheric moisture. However, unlike PUs the cure mechanism is condensation in type and either alcohol or acid (usually acetic) is evolved.

A main use for silicone adhesives is for glass bonding either as structural glazing on buildings or for tank fabrication. However, they can also be found in many electronic and medical products where the benefits of high temperature resistance and/or very high levels of flexibility are exploited.

### 1.2.8 Other systems

Although the adhesives covered above form the vast majority of commercially available systems, there are other more specialised systems that may need to be considered for some of the more challenging applications. The main ones to be aware of are:

- Cyanate esters, polyimides and polybismalaeimides: few adhesives are suitable for prolonged use at temperatures between 250°C and 375°C. For specialist aerospace and electronic applications, in cases where brittle ceramic adhesives are not appropriate, more exotic synthetic polymers must be considered. The imide and cyanate ester adhesives are the most

© Woodhead Publishing Limited, 2010

established types in this class. They are available as liquids or films, but are relatively expensive and difficult to handle. However, they are superior to most other adhesive types with regard to long-term strength retention at elevated temperatures.

- Phenol/resorcinol-based systems: phenolics were the first structural adhesives for metals and have a long history of successful use for joining metals and wood. Although the starting materials used to make the two adhesive types in this group are different, they are chemically similar and the curing mechanism is the same. Consequently they can be considered together. During the curing reaction, which must be done at elevated temperatures, water is a by-product. This means that either the substrates must be porous or a high pressure must be imposed to prevent the formation of voids. The brittle, basic resins can be modified with other more rubbery polymers (to give vinyl or nitrile phenolics). These types of adhesive are particularly durable at both elevated temperatures and in harsh environments and would see much greater use in engineering industries if they were easier to use and less susceptible to shock.
- Amino or urea: These are usually two-part systems consisting of resin and hardening agents and based on products from the reaction of urea and formaldehyde. Curing is normally achieved under pressure but without heat, although heating can be used to accelerate the cure. As the adhesive cures, water is liberated and this tends to limit their use to porous substrates. Due to their poor environmental resistance they are normally used in the manufacture of interior wooden structures

### 1.2.9 Solvent cements

These straddle the area between adhesive and welding. They consist of a solution of low molecular weight oligomer in a suitable solvent. They are used to bond specific corresponding thermoplastic polymer materials, the commonest being polyvinyl chloride (PVC) and acrylic systems. The solvent enables the polymer surfaces to be softened, allowing transport of the oligomeric components into the polymer. These two phenomena have the effect of plasticising the polymer, enabling effective diffusion to take place across the bond area. The oligomer also serves as a partial gap-filling component, although the high levels of solvent require that the bond gap is as tight as possible, otherwise voids will form as the solvent diffuses out of the joint. Additionally, the presence of solvent within the polymer and the bond area requires that the joint be left for a period of time to ensure diffusion of any volatiles away from the joint. If formed correctly the joint can be classified as a structural weld, examples include pipe joining, acrylic structures and so on.

© Woodhead Publishing Limited, 2010

### 1.2.10 Structural pressure sensitive adhesives

Although PSAs would not immediately come to mind as structural bonding materials, there is a class of predominantly acrylic-based adhesives which will bond a wide range of materials. They normally exist in a supported tape form where the carrier tape can either be made from a similar or related solid material, that is, foamed acrylic or from a film such as polyethylene terephthalate (PET). PSAs have the unusual property of requiring pressure to induce a strong bond and although the adhesive never really cures, once pressure and a duration of several hours have passed, the adhesive becomes firmly adhered to the substrate. Essentially pressure and time enable the adhesive (a semi-solid) to wet-out the substrate fully and facilitate bonding. So it is possible to remove/reposition the adhesive relatively easily if the tape is lifted within a few seconds/minutes after application but not if left for longer periods. The semi-solid nature of the adhesive means that creep under sustained loading and/or elevated temperatures is a real possibility. PSAs are available in a wide variety of forms and carrier media and will stick to almost all substrates to some extent.

## 1.3 Adhesive form and structure

Adhesives exist in a wide variety of physical forms, in part dictated by the chemistry but also by virtue of the applications that they are designed for. The main forms are:

- two-part liquids/pastes (e.g. epoxy, polyurethane, toughened acrylic, reactive acrylic, silicone)
- single-part liquids/pastes (e.g. epoxy, polyurethane, anaerobic acrylic, UV cure acrylic, cyanoacrylate, silicone, solvent cement)
- single/double sided tapes (e.g. PSA acrylic, PSA silicone)
- films with and without carrier (e.g. epoxy, polyimide, cyanate ester)
- single-part solid (blocks, chips, rods) (e.g. hot melt).

The key influence of chemistry over the form supplied is based upon the curing mechanism:

- Two-part adhesives comprising two liquids at room temperature will be most likely to react chemically when they are brought into contact, although the level of mixing required will be dictated by the chemical reaction mechanism. Reactive acrylics merely require surface-to-surface contact between the two components as the reaction is free radical-based whereas the epoxy reaction between resin and hardener is addition in type and requires the reactive groups to be intimately mixed for complete cure to occur.
- Single-part systems either have both components mixed together but in

© Woodhead Publishing Limited, 2010

a non-reactive state (i.e. solid and liquid as in the case of single-part epoxy systems) or are single component systems which use an external agent or energy source to initiate cure such as moisture cure polyurethane adhesives or UV cure acrylics.

- Pressure sensitive tapes are usually non-chemically curing adhesives and the tape carrier provides the most convenient means of dispensing such systems.
- Adhesive films are often solid or semi-solid versions of single-part liquid/paste adhesives, where a carrier in the form of a woven/non-woven substrate (nylon, polyester, cotton etc) is often used to support the film, provide additional levels of toughness and to act as a bond-line thickness control layer. It should be stressed that unsupported film systems are produced too.

Although chemistry is very important, the types of application that the adhesive has been formulated for dominate the final physical form. Adhesives are, in the majority of cases, complex mixtures of materials, including reactive agents which provide structure and adhesion, rheology modifiers, fillers to control shrinkage, thermal expansion and bondline control, adhesion promoters, toughening agents, colourings, cure initiators, and so on. Applications for which the adhesive is targeted may require the adhesive to be applied:

- in vertical or overhanging locations
- to have high levels of bond-line control
- to cure on demand.

It is for this reason that some adhesives, most notably the epoxies, can contain the same basic chemistry but exist in many different forms depending upon what is required with regard to the method of application, joint type, joint dimensions, cure type, end properties and so on.

## 1.4 Adhesive cure mechanism

The method by which an adhesive is cured will influence selection in a number of ways. Some applications require a very rapid cure which could be met by using a suitable adhesive, perhaps a two-part toughened acrylic system over an epoxy with similar mechanical performance. However, if the bond area is very large, a rapid cure system may require a rate of mixing and dispensing that may not be possible, in other words the adhesive starts to gel at the point of initial application before the joint can be made. In this instance, a slower curing formulation may be more appropriate or one in which the cure can be controlled in another way, by heat, radiation, pressure and so on. When smaller joints are produced in very high volumes, the adhesive used may require a very rapid cure to minimise the amount of

© Woodhead Publishing Limited, 2010

jigging required, for example through the use of a cyanoacrylate or a UV/blue light cure adhesive.

In other applications, there may be a need to apply a very specific amount of adhesive (in terms of bond-line thickness and coverage) over a large bond area, such as in composite bonding. A film adhesive would be the best candidate in this case owing to the fact that it can be cut precisely to shape and easily placed in position. The adhesive will not cure until the joint is assembled and the necessary pressure and temperature applied. Should there be a need to make an adjustment to the positioning of the adhesive, the joint can be disassembled and the changes made right up until the curing procedure is carried out.

It is important to recognise, however, that often the type of substrate(s) to be bonded can influence the range of curing mechanisms that could be applied. For example, where one or both of the substrates is transparent, a radiation type of cure (UV/blue light) adhesive would be a preferred choice, as the adhesive can be irradiated directly through the adherend. In the case of more thermally sensitive components, a high temperature heat cure may exceed the operating limits of the materials and cause distortion, melting or even degradation.

Finally, the economics of the manufacturing process can have a significant impact on the choice of curing and type of adhesive. A two-part or single-part room temperature curing system normally requires little more than investment in the appropriate mixing dispensing equipment, whereas additional equipment is required to cure other systems (UV/blue light source, ovens, autoclaves, etc.).

## 1.5 Substrate compatibility

The nature of the substrate may also have an influence on the type of adhesive that can be used. The influence may be positive or negative depending upon the type of sensitivity. In the case of some plastics that are susceptible to stress cracking (e.g. polycarbonates, polystyrene, ABS etc.), adhesives that contain low molecular weight components may act as solvents, causing whitening or blooming of the polymer in contact with the adhesive. Good examples of this include cyanoacrylates (the adhesive monomer becomes a solvent), toughened acrylics (methacrylic monomer can be present) and metal surfaces where copper ions are present that can stimulate the rate of cure. Sensitivity can also influence the curing mechanism, for example for cyanoacrylates, both the pH of the surface and the presence/absence of adsorbed water can have an effect. A low pH and/or water will promote cure, whereas a high pH and absence of water will inhibit cure. This is the reason why cyanoacrylate adhesives are so good at bonding skin. In contrast, adhesives based upon epoxy chemistry are much less substrate sensitive.

© Woodhead Publishing Limited, 2010

Anaerobic adhesives require contact with metals to facilitate cure. Although any metal will do, some will enhance the rate of cure such as copper, whereas others, such as zinc, may require a secondary catalyst or primer. Bonding to non-metals will require the application of an appropriate primer/catalyst if the bond is to be successful.

## 1.6 Surface pretreatment

The way in which the surface is pretreated prior to bonding can also influence the types of adhesive that may be considered for an application. Normally it is recommended that the adherend surface is adequately prepared, be it a simple solvent wipe or a more complex set of processes such as etching or anodising. However, there are some instances where the surface either cannot be prepared in advance or the manufacturing process is driven in such a way that other factors dictate that the surface is less than ideal. Two examples that highlight this are:

- Within the automotive industry there is a need to apply adhesive directly to 'as-received' pressed parts which can be contaminated by the thin layer of press-oil required to lubricate the forming process. Throughput and cost considerations mean that precleaning is not possible, but the adhesive, once cured, is still required to fulfil structural demands in a reliable and consistent manner. Adhesives developed to address this requirement are normally single-part heat curing epoxy systems which have the capacity to displace and absorb surface oil during the curing stage, enabling the surface to be fully wetted and a structural bond to develop. Most other adhesives would not tolerate such conditions.
- There is sometimes a need to carry out an adhesive bonding operation to a wet substrate or one that is under water. Adhesive systems exist which rely upon one of the components (the hardener in the case of epoxies) to displace fully the water and wet the surface.

## 1.7 Joint function and operating environment

Adhesive selection is also influenced by what the joint has to do in service, whether it has to:

- tolerate adverse environments (wet, acid, alkaline, solvent, etc.)
- experience extremes in temperatures
- survive high loading levels or impact conditions
- be dismantled at a later date
- conform aesthetically, i.e. colour match, transparency, fillet profile, etc.
- or some other function.

© Woodhead Publishing Limited, 2010

Some or all of these factors may control the form or type of adhesive that should be considered. A brittle, high strength adhesive would not be suitable for a structure that has to suffer impact loading, as in the motor-sports sector, whereas an opaque adhesive may not be considered for a glass bonding application.

## 1.8 Joint design

The design of the joint may also influence selection in that the joint area and/or bond-line thickness may be very small or it may be very large, in which case very different types or forms of adhesive may be required. Where very high levels of joint tolerance are present, as in composite to metal or composite to composite bonding, a film adhesive may be more suitable than a paste system. However, some joints may have a very complex geometry where access to all areas is difficult. An appropriate adhesive may have to be one that can be injected or run into the joint from a particular position, thereby eliminating solid or semi-solid adhesives or pastes. In contrast, joint surfaces may be in vertical or overhead positions, requiring an adhesive that can be applied directly but must not run. Such an application requires thixotropic adhesive formulations.

## 1.9 Manufacturing demands

Manufacturing demands may have a significant impact upon adhesive selection in terms of many often diverse factors such as volume of adhesive required, storage, dispensing needs, curing equipment, performance, price, training and so on. Additionally if the bonding operation can be carried out in a controlled environment (e.g. dry, ambient conditions with appropriate ventilation, etc.), many more adhesives can be considered compared to bonding outdoors at high or low air temperatures or at high levels of humidity/rain. For many two-part adhesives, curing will only occur very slowly or not at all at temperatures below 10°C but at elevated temperatures greater than 30°C or 35°C as would occur in many parts of the world, cure would happen in minutes or seconds, which could be too fast.

## 1.10 Quality control

In addition to risks to life and property, a poor quality bonded product will potentially destroy consumer and fabricator confidence. To address this, many adhesives have been developed to assist with more effective quality control (QC). Examples include adhesives with fillers of a particular diameter to control bondline thickness and to manage shrinkage during cure and film adhesives which are supplied within a tight thickness tolerance and which

© Woodhead Publishing Limited, 2010

also often contain a carrier which will control minimum thicknesses. Some epoxy adhesives will tolerate surfaces contaminated with oil and others have a preference towards a particular type of pretreatment, thereby ensuring consistent bond strength. Recently some adhesives have been formulated to change colour, indicating when full cure has been achieved in a similar fashion to the indications that have been developed for white emulsion paint. Other adhesives are tolerant of adverse storage conditions and others can be cured over a wide range of temperatures without adverse effects.

Another way in which adhesives can be selected/developed for QC purposes is via colouring agents that aid visual inspection. In some automotive applications, structural adhesives used in critical chassis assembly are coloured according to the mode of application. For example a robot may apply a blue version of the adhesive, whereas an operator may require to touch up the bond with a red coloured system thus ensuring that any aspects of human interaction can be identified during the life of the product. Obviously the colouring is selected to have no effect on the adhesive performance. Another very common aspect is to produce two-part adhesives where each component is a different colour, thereby enabling thorough mixing to be easily observed. It should be stressed however, that regardless of the adhesive selected, effort should always be made to control all variables (external and internal) within the bonding process.

## 1.11 Testing and evaluation

Practical testing and evaluation of adhesives forms the applied basis for adhesive selection. Individual expertise, desktop searching and discussions with suppliers may help to produce a short-list of candidates but nothing can substitute for a practical assessment of the adhesive, ideally within the actual application. Testing can take many forms and is highly dependent upon what is actually required of the bonded joint. In the majority of cases, testing will be mechanical, usually measuring the strength and/or other properties of the joint. The specifics of the test will most often be defined by the type of load or environmental condition to be investigated (i.e. peel, shear, impact, high/low temperature, humidity, etc.) which in turn will define the test specimen geometry. The most usual approach is to identify the appropriate standard (ISO, BSI, ASTM, etc.) and to use this as the basis from which to obtain the data. A thorough review of such tests and associated standards is given in a later chapter.

Testing may also be based on handling requirements such as ease of application and rheology or even appearance or colour. It should be remembered that adhesives should be tested for each unique application separately owing to the fact that many, often subtle, factors can influence joint performance.

© Woodhead Publishing Limited, 2010

## 1.12 End of life requirements

The need to consider end of life requirements is becoming ever more relevant to all aspects of product fabrication and engineering and adhesively bonded joints are no exception. For the majority of adhesives cured through chemical cross-linking, reversible bonding is not trivial and may even be considered impossible in most cases. However, some systems and approaches are becoming available that challenge this perception. Additives that act as susceptors (e.g. carbon nanotubes, ferromagnetic materials, etc.) can be used to generate heat under the action of an external electromagnetic field which in turn could be used as a trigger to disrupt the joint and allow for disassembly. Another technology that is being commercialised takes the form of tiny microspheres filled with hydrocarbon liquid which, when subjected to a certain input of heat, expand to many times their original size, literally blowing the joint apart.

Alternatively, advantage may be taken of corrosive or swelling agents such as solvents or acids which could attack, soften or dissolve the adhesive within the joint. This may lead to selection of an adhesive or adhesive group with known susceptibility to a particular agent, which is very unlikely to be seen in the normal operating environment.

## 1.13 Aesthetics

Although in the vast majority of applications the adhesive remains hidden within the joint, there are instances where some/all of the adhesive can be visible, such as in the fillet area and where bonding of transparent/translucent components is done. In these situations, the colour and the rheology of the adhesive can play a dominant role in selection. In the case of colour, other than transparent, adhesives can take a wide range of pigments and if the volume/value is sufficiently large, a bespoke version of the adhesive could be formulated. For glass bonding, transparent adhesives are most often selected. Rheology influences the way the adhesive flows upon application and crucially when the joint is closed when the fillet is being formed. Manually altering the fillet profile is time consuming and can be very difficult to control, especially for complex structural shapes.

## 1.14 Adhesive selector software

### 1.14.1 Stand-alone systems

Despite the fact that there is a software program available to help with almost everything, the area of adhesive selection appears to be remarkably sparse. Extensive searching has revealed only two stand-alone systems available to the end user. Of these, one is almost out of print and the other is available only in the German language.

© Woodhead Publishing Limited, 2010

EASel (Engineering Adhesive Selector) was originally developed from a product specific selection tool by the late Dr Bill Lees, technical director of Permabond (now Bondmaster) and entitled PAL (Permabond Adhesive Locator). Despite being written in a purely text-based format in the mid to late 1980s owing to the limitations of operating systems at the time (MSDOS), it was a relatively powerful tool which took the user through a series of probing questions about the particular application before arriving at a short-list of possible Permabond adhesive candidates to consider. The program was based upon a series of deselection rules which are outlined in Bill Lees' book (Chapter 5 in *Adhesives in Engineering Design*, by W.A. Lees, 1984, published by The Design Council, London) whereby the software progressively eliminated less likely candidates as the questions progressed. There was even an option to apply a less rigorous filter allowing a greater number of adhesives to be presented, together with reasons why they might not be so suitable.

In a desire to make the software more accessible to a wider audience, the program was rewritten, taking advantage of the then new graphical user interface that Windows® offered. The result (mid 1990s), in collaboration with TWI, was EASel, an elegant stand-alone program which lived on the desktop. It was operated through a number of toggle-based icons which updated possible adhesive candidate icons in real time. Within the program was also a highly comprehensive surface preparation guide, more detailed descriptions of the major adhesive families and useful suggestions where appropriate. The program was distributed in the form of two floppy disks available from TWI. Unfortunately for a number of reasons, including copyright issues, the software was never updated and is now not compatible with the most recent versions of Windows, leaving the software almost inaccessible.

Gluedo is a software program developed by a German research and technology organisation, IFF GmbH based in Ismaning (info@iff-gmbh.de). It is described as an adhesive selection and information system which it claims provides assistance both with the design and the fabrication of adhesive joints. Unfortunately the software seems to be available only in the German language which severely limits its end-user audience.

Such a severe shortage of selection software is perplexing, especially when the task of adhesive selection is so important. It would appear that currently the only way to obtain even a basic level of guidance is to consult a book such as this or to make direct contact with adhesive suppliers and/or the relatively limited number of experts in the field.

## 1.15 Internet provision

In this ever-increasingly connected world, there is a general trend to provide assistance in an on-line format, either via electronic forms, which will be

© Woodhead Publishing Limited, 2010

acted upon by an expert when received, or through smart websites with embedded software. The benefits of the latter are that the response has the potential to be similar to that of a stand-alone system, which it is accessible to a truly global audience and can be potentially updated regularly although in many cases this is not always done. In preparation for this book a detailed search was carried out and it was found that the level of interactive support was very low. Most of the major adhesives suppliers provide comprehensive information on their websites via datasheets and selection charts, but this normally assumes that the user has some knowledge about the subject and also that the information being provided is correct for the application in mind. Some websites have attempted to include 'smart' product search forms which proved (to the author) to be somewhat unwieldy and frustrating, whilst others have much simpler input pages which are essentially structured electronic email enquiries. No commercial site was identified that provided any assistance with adhesive selection via embedded software similar to EASel or Gluedo.

However, within the internet as a whole, several sites were identified that offered considerably more assistance/information. Notable examples include Specialchem – Adhesives and Sealants (www.specialchem4adhesives.com), the Adhesives Design Toolkit (www.adhesivestoolkit.com) and the Adhesive and Sealant Council (www.adhesives.org). The Specialchem and the Adhesive and Sealant Council sites are both primarily commercially driven, basing revenue through on-screen advertising and membership subscription fees. The latter site also possesses a step through question input section reminiscent of the old PAL selection software. However it is relatively easy to arrive at a no-product result and no explanation is provided about what are the key deselection factors. That said, both sites are extremely informative with many articles on adhesive properties, selection and related topics. The Adhesives Design Toolkit was developed through UK government funding between 2000 and 2005 and provides a range of information both in the form of text based documents and also via embedded software modules, assisting the user through interactive input. Key functions include adhesive selection, simple joint stress analysis and adhesive supplier location. The adhesive selection module is based upon the deselection logic of PAL and EASel and, although primarily text based, it does offer the user the ability to open or close the specificity of the search and will indicate which selection factors could be most significant.

## 1.16 Future trends

Adhesive selection has for many years been driven by a wide range of factors as outlined above and in many ways industry is quite resistant to change. Once an adhesive has been selected and qualified, the desire or ability to change

© Woodhead Publishing Limited, 2010

to a potentially superior system may be significantly reduced as the cost of requalifiying or the implementation of a new curing system or dispensing robot may be too high. However, in these changing times, industry pull or technology push may still be sufficient to enable change. The reduction in manufacturing time or energy consumption or a change in material may necessitate a change of adhesive or influence the type of adhesive that could be used. Alternatively technological developments may produce an adhesive or adhesive system with very desirable properties, for example high strength, cure on demand, little/no surface preparation, ability to bond difficult substrates and so on. It is highly likely that adhesive selection will be assisted through the development of better computer programs, linked to computer-aided design and finite element analysis capability, although to date successful modelling of adhesive bonds has met with limited success.

Other factors which may influence adhesive selection include environmental and health and safety legislation in terms of reduction of carbon footprint (energy consumption associated with production and/or cure), reduction/elimination of volatile organic components (VOCs), reduction of hazardous components (carcinogens, mutagenic agents, etc.). One example of note relates to the pretreatment needs of aluminium, especially for the aerospace sector. Currently the 'best' treatment requires exposure of the surface to Cr(VI) ions usually from chromic acid. Cr(VI) is a known carcinogen and its use is being phased out through legislation. At present there is no universally acknowledged replacement within the aerospace sector although much research is being carried out. It is inevitable, however, that either a pretreatment and/or adhesive system will be developed to replace the current system and this in turn may influence adhesive selection.

Finally, adhesive technology like all aspects of business today is affected by global developments. Companies will be bought and sold and although many brands will remain constant, adhesives may be subject to subtle changes which may or may not have an influence on their properties. In particular, raw products may be sourced from alternative suppliers or geographical locations. Whilst this may not affect generic properties such as lap shear strength, other less-well characterised properties may be altered. Examples could include cure shrinkage, thermal coefficient of expansion, susceptibility of fillers to leaching/degradation and thermal conduction. The end result of such changes will mean that the end user needs to be ever vigilant and monitor key properties specific to that application on a regular basis.

© Woodhead Publishing Limited, 2010

# 2
# Advances in epoxy adhesives

K. J. ABBEY, Lord Corporation, USA

**Abstract**: Epoxy adhesives have the widest range of application of the various classes of adhesives arising principally from their extremely broad set of performance properties. Two continuing trends appear in the literature relating to epoxy systems: control of cure rate and methods of improving toughness. There has also been a marked increase in the exploration of formulations containing raw materials derived from renewable resources.

**Key words**: epoxy adhesives, nano-fillers, toughness.

## 2.1 Introduction

Epoxy adhesives have the widest range of application of the various classes of adhesives arising principally from the extremely broad set of performance properties. This is a result of the diversity of curatives available. These curatives include catalysts for cationic, anionic, or coordination polymerization of the oxirane moiety itself to a plethora of compounds with nucleophilic sites used in a roughly equal stoichiometry for ring opening addition reactions. Two introductory statements by Drake (1997) are still true today: 'While little is generally new, there exists a host of specific advances which define the broad synergism extant in structural adhesives sciences and technology today' and 'There is no universally accepted definition for a structural (or engineering) adhesive'. A structural adhesive as used here will be one that can bear a substantial load, generally of high strength and modulus in the use environment.

Almost all commercial adhesives contain a number of additional components including fillers, extenders, pigments, toughening agents, wetting agents, rheology modifiers, adhesion promoters and plasticizers. The formulation of a particular adhesive is often fine tuned to a particular customer's end use and process of assembly. Formulations also continue to be extended to include mixtures demonstrating other cure chemistry, referred to as hybrid systems, to gain properties encompassing both types of chemistry.

Two overriding trends appear in the literature relating to epoxy systems: control of cure rate and methods of improving toughness. The term, 'snap cure' appeared in the early 1990s and has been applied solely to microelectronic applications. This term refers to a cure in a very short time period, but not necessarily at a low temperature. A broader terminology such as 'fast cure'



© Woodhead Publishing Limited, 2010

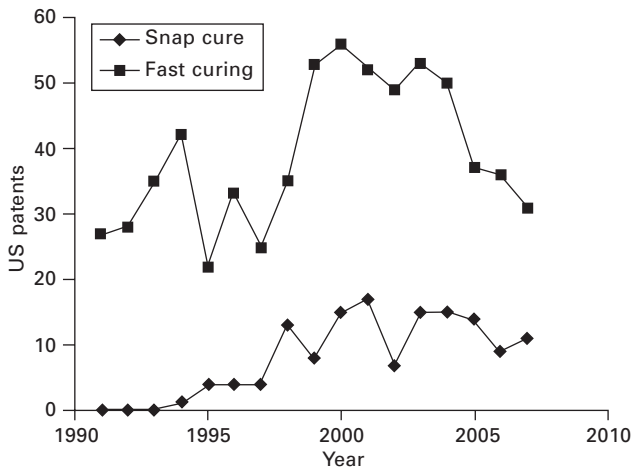
or 'rapid cure' appears in earlier literature and in greater abundance in the patent literature (Fig. 2.1).

With the recent rapid escalation of oil prices and the increased concern about global warming, there has also been a marked increase in the exploration of formulations containing raw materials derived from renewable resources and on 'greener' routes to epoxy resins. This chapter will not address the closely related topic of substrate surface cleaning and treatment which is important to durable bonding.

## 2.2 Main applications and limitations of epoxy adhesives

Structural epoxy adhesives have been used in numerous industries including construction, electrical and electronic, medical, and all branches of transportation. The distribution of use is not uniform, but heavily loaded towards the transportation segment. For most structural applications, cure at elevated temperatures is required to achieve ultimate strength. This is a consequence of most structural epoxy adhesives relying upon step-growth polymerization and the glass transition temperature of the intermediate oligomers leading to vitrification before complete reaction (Fava, 1968; French *et al.*, 1970; Acitelli *et al.*, 1971). The construction industry, in particular, most often must work with adhesives that cure entirely at ambient temperature.

Fields such as electronics and medicine or dentistry have other special restrictions. In electronics, ionic impurities, particularly halide and trace metal ions must be severely limited. Because most commercial epoxy resins are produced by reaction of epichlorohydrin with some base polyol, most




*2.1* Recent US patent activity related to fast cure epoxy compositions.

© Woodhead Publishing Limited, 2010

often a bisphenol, further purification of the product epoxy resin is required. Alternatively, a more expensive synthetic process must be used that avoids introducing chloride. Recent advancements have been made in catalytic processes using hydrogen peroxide or oxygen. Monnier and Muehlbauer (1990) were the first to invent a process using oxygen and a supported silver catalyst to prepare epoxide-functional molecules from olefins without allylic hydrogen atoms: butadiene, *t*-butylethylene, vinyl furan and methyl vinyl ketone.

Several subsequent patents have appeared claiming improvements in the catalyst and process. Monnier and Muehlbauer (1992) extended the compounds epoxidized to include norbornene and norbornadiene by using a thallium promoter. Mikawa and Uchida (2003) have further refined this type of air oxidation to form epoxy materials by using thallium and alkali metals on supports of particular particle size. Yonehara *et al*. (2008) disclosed a process using aqueous hydrogen peroxide for epoxidation with a tungsten catalyst. Khan *et al*. (2007) claim high selectivity and conversion and detailed background discussion of earlier less preferred processes is given.

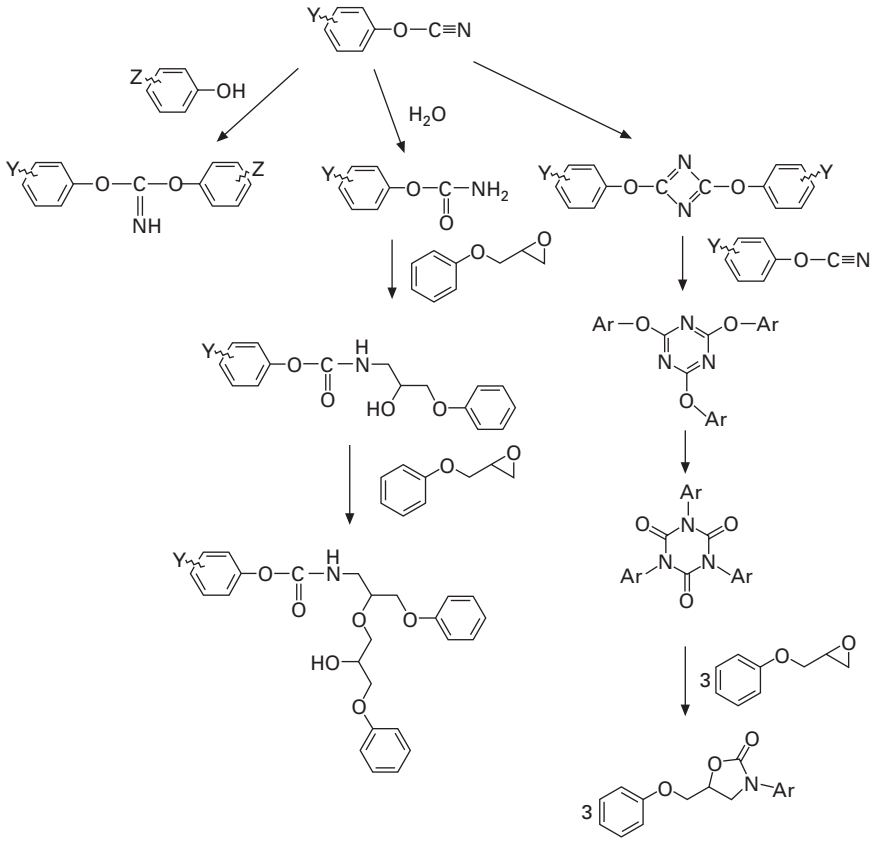
Many electronic packaging adhesives and encapsulants utilize frozen, catalyzed anhydride–epoxy cure chemistry. In recent years, the use of anhydrides in formulated epoxies has become a health concern because of the irritancy of the anhydrides.

The continued, rapid evolution of microelectronics has engendered much patent activity on adhesives and sealants, many of which are epoxy based. The structural load is not in the same domain as some other uses, but fatigue in thermal cycling, where mismatch in thermal expansion coefficient places considerable stress on the joints and susceptibility to disbonding when dropped are clearly important drivers. Medical, dental, and veterinarian applications require materials of low toxicity and compatible with living tissue. This has limited the utility of epoxies relative to other adhesive technologies that are more readily biodegradable. The use of high temperature, medical grade epoxy adhesives in catheters and endoscopes have been claimed to provide the ability to withstand autoclaving so that the tools may be reused (Uram, 2006).

## 2.3 Recent developments in epoxy adhesives

Various epoxy hybrid systems have been investigated. Systems comprising aryl cyanate esters were first described by Kubens *et al*. (1971). Reaction of the epoxy functionality with the triazine ring formed from the cyanate ester is known to result in oxazolidinone rings, but the reaction can be more complex, as shown by Grenier-Loustalot and Lartigau (1997) in Fig. 2.2. To preserve the high temperature properties of the cyanate ester resin, Ryang (1989) has proposed using an epoxy terminated siloxane resin, as a toughening

© Woodhead Publishing Limited, 2010



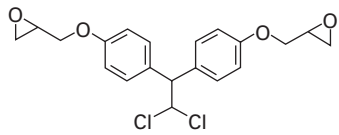
*2.2* Aryl cyanate ester–epoxy reactions (based on Grenier-Loustalot and Lartigau, 1997).

agent. Thermal gravimetric analysis showed essentially the same weight loss as the pure cyanate resin system. A DOT (2002) study describes improved fire resistance using a combination of cyanate ester and epoxy resin based on a chlorine-containing bisphenol, 1,1-dichloro-2,2-bis(4-hydroxyphenyl) ethane (bisphenol-C), (Fig. 2.3).

Blends of epoxy resins with polyamides have been known since the 1960s. These hybrids, which are noted for their peel strength and low temperature properties, are often prepared as film adhesives from an alcoholic solution. A series of papers by Gupta *et al*. (2003, 2004, 2005, 2008) approach this quite differently by anionically polymerizing caprolactam *in situ* in an epoxy resin concurrent with curing the epoxy.

A reactive epoxy modified structural acrylic adhesive has been claimed to result in improved heat resistance (Dawdy, 1984). Self-healing of polymers and composites has received considerable attention in recent years including

© Woodhead Publishing Limited, 2010




2.3 Structure of bisphenol-C diglycidyl ether.

thermosetting epoxy systems (Wu *et al.*, 2008, p 494). The healing agent can be an epoxy material or the result of other types of chemistry, such as olefin metathesis. The healing materials can be contained in hollow fibers or encapsulated in various polymeric agents including urea-formaldehyde.

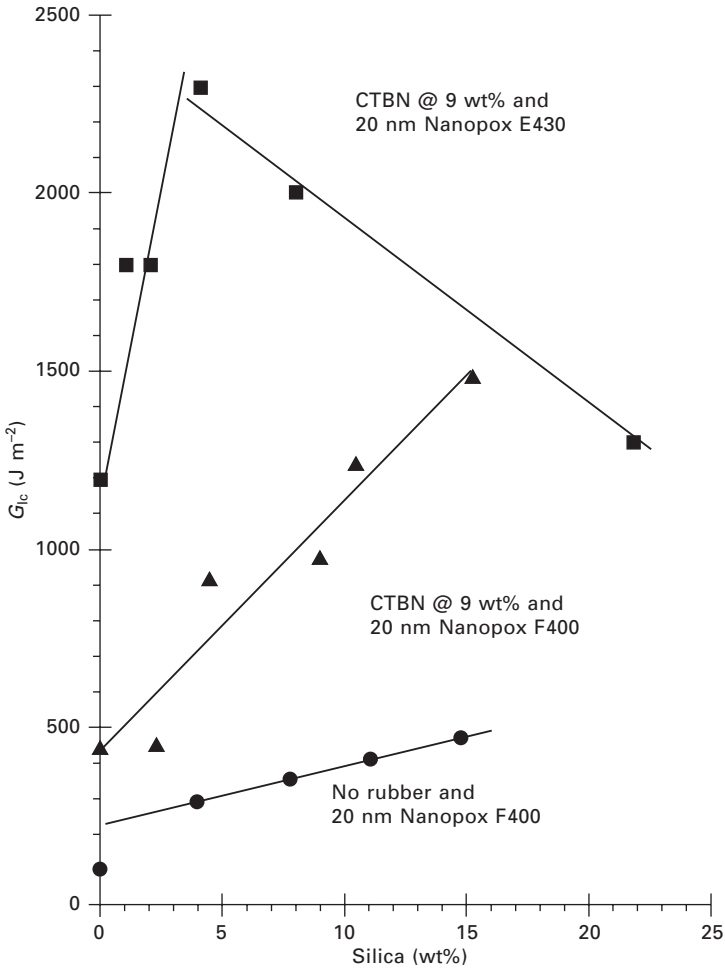
### 2.3.1 Toughening

Many cured, unmodified epoxy compositions are inherently brittle, especially those of interest for structural adhesive and high strength composite applications. Early on, efforts to improve their resistance to fracture and to understand how these materials fail were made (Sultan and McGarry, 1973). The use of reactive liquid rubber was an early success and is still the benchmark for gauging improvements (Riew, 1973, 1977; Riew *et al.*, 1976). Much research is still being expended attempting to provide further improvements. Rubber toughened compositions with improved heat resistance as experienced in 'overbake' conditions in automotive paint bake cycles are the subject of a patent by Eagle and Lutz (2008). The composition includes liquid rubber modified epoxy resins, phenol-blocked polyether urethane resin as a reactive toughener and other components.

The recent focus on nano-fillers includes many studies demonstrating improvements in impact and/or fracture energy. Ragosta *et al.* (2005) has shown improvements using nano-silica compared to micrometer-sized silica. This effect has been shown to be synergistic with rubber toughening (Kinloch *et al.*, 2003) in an ambient cured epoxy adhesive. Kinloch *et al.* (2005) and later Liang *et al.* (2007) have demonstrated the same effect in a heat cured adhesive, as shown in Fig. 2.4.

Oldak *et al.* (2007) have shown that piperidine-catalyzed cure of epoxy composition with varying amounts of triblock copolymer (Arkema, Inc. Nanostrength™ E20, a polystyene-block-polybutadiene-block-poly(methyl methacrylate)) leads to much better toughening when cured at 160°C than at 120°C. At the lower temperature, the rubber particles are clustered whereas at the higher temperature, they remain well dispersed inclusions that are mostly less than a tenth of a micrometer in size. There is also no plateau in the fracture toughness ($K_{Ic}$) up to 25% loading (~4.8 MPa-m$^{0.5}$) and the sample was transparent for the high temperature work, whereas at 120°C a maximum of 2.7 MPa-m$^{0.5}$ was found at 10% loading.

© Woodhead Publishing Limited, 2010




*2.4* Effect of nano-silica filler on epoxy fracture energy, $G_{Ic}$, for a two-part, rubber modified composition, ■ (Liang *et al.*, 2007) and a one-part, anhydride composition with, ▲, and without rubber modification, ● (Kinloch *et al.*, 2005).

The use of epoxy-terminated, hyperbranched resins also show advantages over linear, functional liquid rubber (Boogh *et al.*, 1999; Mezzenga *et al.*, 2000, 2001; Mezzenga and Månson, 2001). Because of their globular nature, the solution viscosity of the mixed composition is about an order-of-magnitude lower than for the linear elastomer system that yields similar toughness.

Studies on using high temperature thermoplastics as toughening agents for epoxy systems continue to be investigated. Poly(aryl-ether-sulfone) modified with varying levels of ether phosphine oxide as comonomer were studied by Wang *et al.* (1998) at 10 wt% and 20 wt% loading in 4,4′-

© Woodhead Publishing Limited, 2010

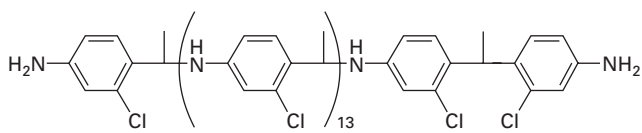
diaminodiphenylsulfone cured DGEBA (diglycidyl ether of bisphenol A). A peak in $K_{Ic}$ versus phosphine oxide content was found with both loadings at 10–20% phosphine oxide content in the copolymers. The largest increase in $K_{Ic}$, ~50%, was with the 20% polymer loading. As with other evaluations of thermoplastic additives, the improvement in toughness is not nearly as great as with rubber inclusions. However, the high temperature strength and modulus is not sacrificed in such systems.

Another approach to toughening has been taken by Maity *et al.* (2008). They prepared an oligomeric condensate from *m*-chloroaniline and acetaldehyde with an average degree of polymerization of about 16 (Fig. 2.5). This oligomer was incorporated into the epoxy adhesive by either a one or two step process. In the two-step process, the oligomer was prereacted with the epoxy resin at 80°C for an hour before being mixed with triethylene tetramine. An izod unnotched impact test showed a five to six-fold improvement at ten parts oligomer per hundred parts epoxy resin. The two-step process was better than the single-step process.

## 2.3.2 Renewable materials

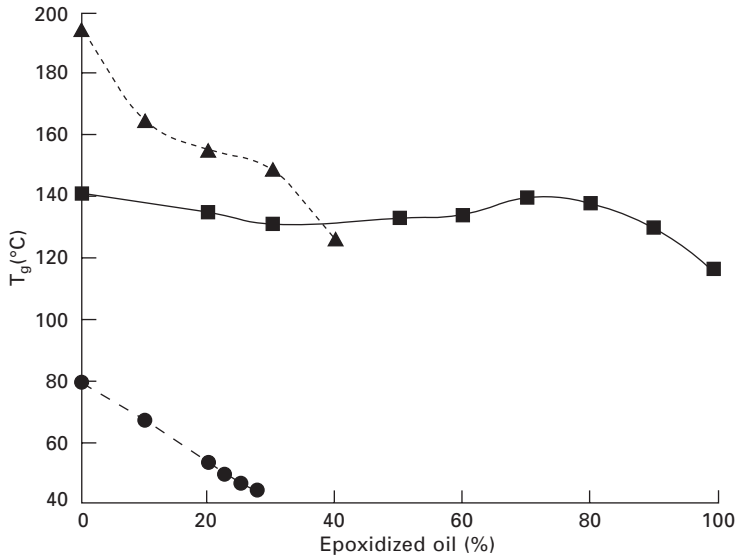
The emphasis on environmentally sound use of the earth's resources (DOE, 1999) has put pressure on structural adhesive manufacturers to devise formulations that have a lesser impact on our environment.

Generally, epoxy adhesives have been resistant to environmental degradation. Indeed, a key attribute has been that these adhesives survive intact in many harsh environments. Without sacrificing this aspect of their nature, a lesser environmental impact is possible by incorporating ingredients derived from renewable resources while reducing reliance on petroleum (DOE, 1999). The vegetable oil-based epoxy resins have received renewed attention (Miyagawa *et al.*, 2004a, 2004b; Park *et al.*, 2004; Chandrashekhara *et al.*, 2005). However, even when they are used as a partial replacement for more conventional bisphenol-based epoxies, the $T_g$ and modulus of derived materials are generally significantly depressed because they are flexible and do not phase separate on cure. Figure 2.6 shows the effects for amine cured, anhydride cured and cationically cured blends. Only the anhydride cured material maintains a fairly constant $T_g$ over a broad composition range (Miyagawa *et al.*, 2004a).




*2.5* Idealized structure for chloroaniline–acetaldehyde condensate (Maity *et al.,* 2008).

© Woodhead Publishing Limited, 2010




2.6 Effect of added vegetable oil based epoxy resins on modulus at various temperatures on cure chemistry. ■, Miyagawa *et al.* (2004a); ●, Miyagawa et al. (2004b); ▲, Park *et al.* (2004).

Recently Chevron-Philips has been investigating mercaptan curatives based on further derivatization of epoxidized soy oil (Brown *et al.*, 2006). Cross-linked compositions derived from epoxy resin cured with these polymercaptans are claimed in a subsequent filing (Byers *et al.*, 2007).

The use of bio-based fibers for epoxy reinforcement is also receiving much attention especially in less developed parts of the world. Cellulose fiber has been used as a reinforcing thixotrope by Grace and Sullivan (1995). Straw from various crops has been reacted with phenol and acid to generate an extract which was subsequently converted to an epoxy resin by reaction with epichlorohydrin for use as an adhesive (Zhang *et al.*, 2008).

### 2.3.3 Applications

*Construction*

The growing use of fiber-reinforced polymer (FRP) composites in construction, including pultruded shapes, bridge decks, internal and external reinforcements for concrete and even masonry, has often led to the use of epoxy adhesives in their joining as reviewed by Bakis *et al.* (2002). Adhesively bonded pultruded shapes used in bridge decks provide a weight reduction of the dead load, allowing for increased live load at the same time as improving structural stiffness and strength. Among several challenges identified, several relate to aspects of the composite and adhesive: design of joints and attachment

© Woodhead Publishing Limited, 2010

of stringers, fatigue behavior, environmental effects and ultimate strength. This work was being implemented as FRP prices began to fall in the late 1980s. This, combined with the rapidly failing infrastructure, opened up the opportunity to use FRP for repairs.

Various methods of repair are being used to extend the life of existing steel reinforced concrete pillars such as those found in bridge supports. One method gaining in popularity is a process called 'near-surface mounting technique' wherein grooves are cut into the concrete pillar in an axial orientation and carbon FRP, made for example by pultrusion with epoxy-bound carbon, is bonded in place. More recently, this near surface mounting was extended to reinforced concrete slabs (Bonaldo *et al.*, 2008; Barros and Fortes, 2005).

Research is continuing at numerous sites. Ecole Polytechnique Federale de Lausanne, Composite Construction Laboratory (EPFL, 2008) has active projects on adhesive systems. Sika (1998) provides a family of products specifically targeted for the construction market.

A widely publicized failure of an epoxy-bonded structure leading to a fatality was the collapse of the tunnel ceiling in Boston's 'Big Dig' in 2006. While the National Transporation Safety Board found blame in many places, the structural cause of the failure was the slow creep of the epoxy adhesive used to mount the anchor bolts (NTSB, 2007). This type of structural application, the overhead suspension of heavy concrete ceiling panels, had been designed with a maximum load of 11 565 N per anchor (8007 N dead load and 3559 N live load) but was specified at 17 792 N with a safety factor of four or 71 171 N load capacity. In tests after the failure, the epoxy adhesive used was shown to exhibit significant creep even at 4448 N load (NTSB, 2007, p 90).

### *Aerospace*

While bonding of aircraft predates powered flight, the use of epoxy adhesives was first used in 1960 on the Convair B-58 supersonic bomber (Minford, 1993, p 4). This was an epoxy-phenolic adhesive rated for higher temperature use with a sandwiched aluminum honeycomb. Broader application of epoxy adhesives soon followed. Combinations of mechanical fastening with adhesive bonding have included techniques such as rivbonding, weldbonding and clinchbonding.

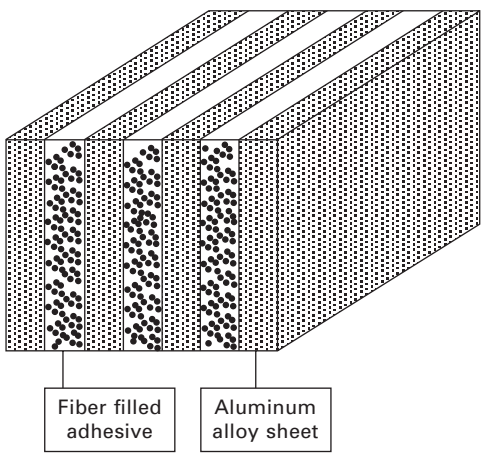
An extensive investigation of adhesives in military aviation was undertaken with Douglas Aircraft Company by the US Air Force entitled 'Primary Adhesively Bonded Structures Technology' (PABST) in 1975 (Shannon *et al.*, 1978; Potter, 1979). Four adhesive/primer systems from different manufacturers were considered: EA9628/EA9202 (Hysol), FM55/XA3950 (3M), M1133/6740 (Narmco) and FM73/BR127 (American Cyanamid). All adhesives had woven carriers except for the American Cyanamid adhesive

© Woodhead Publishing Limited, 2010

which was a Dacron mat. Phosphoric acid anodized aluminum substrate was used.

Rider (2002) has examined two surface treatments of titanium alloy (Ti–6Al–4V) with regard to military aircraft repaired by the royal Australian Air Force with rubber toughened epoxy adhesive (FM73 or FM300, Cytec-Fiberite). Grit-blast and epoxy silane treatment performed better than Pasa-Jell, but the durability was not as good as an aluminum bonded repair.

Fiber metal laminates (FML) began to be developed in the 1950s. The history of this technology is related in a story-book format by Vlot (2001) and with more technical detail by Vlot and Gunnink (2001). Figure 2.7 is a diagram illustrating the concept where the adhesive layers containing unidirectional fibers are sandwiched between ultra-thin metal sheets. The thickness of the total laminate is about 2 mm using aluminum foil of 0.2–0.5 mm and the adhesive/glass fiber layers 0.125–0.16 mm. The chief advantages of this structure are the improved damage tolerance relative to either the metal of the same overall thickness or of a fiber composite of this thickness with a reduced weight relative to the metal itself. The first commercial product was given the name Arall (aramid reinforced aluminum laminate) by Vogelesang (Vlot, 2001, p 43) and launched by ALCOA in 1982 (Vlot, 2001, p 64). Fatigue cracking in this material under the conditions of cabin pressurization limited Arall's success, but a switch to R-glass fiber from Saint Gobain, given the acronym Glare (glass reinforced laminate), resolved the fatigue issue (Roebroeks, 1991). Later, the use of the stronger S2-glass from Owens and Corning became available. The Airbus A380 was the first commercial craft to use Glare panels in fuselage segments. In 2006, Glare




2.7 Diagram of multi-layered aluminum–glass-fiber/epoxy laminate being used in the Airbus A380.

© Woodhead Publishing Limited, 2010

was available in six main commercial grades depending on the fiber direction in the various layers and the type of aluminum (Botelho *et al.*, 2006).

Similarly, two surface treatments of epoxy adhesives, either $TiO_2$ plasma spray on titanium grade 2 or chromic acid anodization on either titanium grade 2 or grade 5 (Amantini *et al.*, 2004) have been examined for FMLS made with titanium. The anodization surface treatment gave a superior performance.

One look to the future is provided by Renton *et al.* (2004, p 991) where the prognosis of structural bonding in military aircraft in combination with advanced composite design, including 3-D weaving, is strong.

## 2.4 Sources of further information and advice

Several major reviews of epoxy adhesives have appeared in the past 15 years. The most comprehensive is that of Petrie (2006) with some references from 2004. The specialized topic of toughening in epoxy resins was reviewed by Unnikrishnan and Thachil (2006) with references into 2003. Minford (1993) addressed aluminum bonding broadly including an extensive discussion on the selection of epoxy adhesives (Minford, 1993, p 147–170) with 150 references into 1991. Further, Minford (1993, 524–583) addresses uses of bonded aluminum in numerous markets including aerospace, auto and truck, construction, appliances and others. A published guide from the US Department of the Interior provides information on concrete repair including epoxy adhesive use (GCR, 1996).

*Table 2.1* Websites of interest for epoxy adhesives

| Publisher | Web address | Comments |
|---|---|---|
| Specialchem S A | www.specialchem4adhesives.com | Commercial: offers training, articles of interest, advertisements from raw material vendors |
| Adhesion Society, Inc. | www.adhesionsociety.org | Professional society: site includes links to other web sites of interest for adhesives and adhesion |
| Adhesive and Sealant Council, Inc. | www.adhesives.org | Non-profit trade organization: site to educate those relatively unfamiliar with adhesive technology |
| Adhesive and Sealant Council, Inc. | www.ascouncil.org | Non-profit trade organization |
| VertMarkets, Inc. | www.adhesivesandsealants.com | Commercial: supplier enabler connecting buyers with suppliers |

© Woodhead Publishing Limited, 2010

Other recent books with chapters concerning epoxy adhesives generally include Pizzi and Mittal (2003) and Adams (2005). Yacobi and Hubert (2003) focus on photonic applications.

Several websites provide information regarding adhesives in general, see Table 2.1.

## 2.5 References


Acitelli, M A, Prime, R B and Sacher, E (1971), 'Kinetics of epoxy cure: (1) The system bisphenol-A diglycidyl ether/m-phenylene diamine', *Polymer*, **12**, 335–43.

Adams, R D (2005), *Adhesive Bonding; Science, Technology and Applications*, CRC Press, Boca Raton.

Amantini, L, Bellachioma, M, Cavallo, G, Marchetti, M and Corradi, S, (2004), 'Study of advanced composite structures for high temperature applications', *Convegno IGF XVII Bologna 2004*, Session VI, Italian Group of Fracture (Groupo Italiano Frattura), Cassino, Italy.

Bakis, C E, Bank, L C, Brown, V L, Cosenza, E, Davalos, J F, Lesko, J J, Machida, A, Rizkalla, S H and Trianafillou, T C (2002), 'Fiber-reinforced polymer composites for construction–state-of-the-art review', *J Compos Construct*, **6**(2), 73–87.

Barros, J A O and Fortes, A S (2005), 'Flexural strengthening of concrete beams with CFRP laminates bonded into slits', *Cement Concrete Compos*, **27**, 471–80.

Bonaldo, E, Barros, J A O and Lourenco, P B (2008), 'Efficient stengthening technique to increase the flexural resistance of existing RC slabs', *J Compos Construct*, **12**(2), 149–59.

Boogh, L, Pettersson, B and Månson, J.-A E (1999) 'Dendritic hyperbranched polymers as toughenersfor epoxy resins', *Polymer*, **40**, 2249–61.

Botelho, E C, Silva, R A, Pardini, L C and Rezende, M C (2006), 'A review on the development and properties of continuous fiber/epoxy/aluminum hybrid composites for aircraft structures', *Materials Res*, **9**(3), 247–56.

Brown, C W, Refvik, M D and Herron, S J (2006), *Thiol Ester Compositions and Processes for Making and Using Same*, US Pat Appl 20 060 036 110.

Byers, J D, Refvik, M D, Brown, C E and Matson, M S (2007), *Mercaptan-hardened Epoxy Polymer Composition and Processes for Making and Using Same*, US Pat Appl 20 070 112 100.

Chandrashekhara, K, Sundararaman, S, Flanigan, V and Kapila, S (2005), 'Affordable composites using renewable materials', *Mater Sci Eng A*, **412**, 2–6.

Dawdy, T H (1984), *Epoxy Modified Structural Adhesives having Improved Heat Resistance*, US Patent 4 467 071.

DOE (1999), *Technology Roadmap for Plant/Crop-Based Renewable Resources 2020*, (US Department of Energy), Washington DC. http://www1.eere.energy.gov/biomass/pdfs/technology_roadmap.pdf

DOT (2002), 'Fire-resistant cyanate ester-epoxy blends', DOT/FAA/AR-02/53, (US Department of Transportation), Washington DC. http://www.tc.faa.gov/its/worldpac/techrpt/ar02-53.pdf

Drake, R (1997), 'Structural adhesives technology: two decades of enduring progress', in *Proceedings 20th Annual 'Anniversary' Meeting of the Adhesion Society,* Drzal, L T and Schreiber, H P (eds), The Adhesion Society, Blacksburg, VA, 187–9.


© Woodhead Publishing Limited, 2010

Eagle, G G and Lutz, A (2008), *Heat-resistant Structural Epoxy Resins*, US Pat Appl 20 080 251 202.

EPFL (Ecole Polytechnique Federale de Lausanne), (2008), Composite Construction Laboratory, http://www.cclab.ch/

Fava, R A (1968), 'Differential scanning calorimetry of epoxy resins', *Polym (London)* **9**, 137–51.

French, D M, Strecker, R A H and Tompa, A S (1970), 'The maximum extent of reaction in gelled systems', *J Appl Polym Sci,* **14**, 599–610.

Grace, M J and Sullivan, C (1995), 'Cellulose fiber as a reinforcing thixotrope in adhesives and sealants', *Adhesives Age*, July.

GCR, (1996), *Guide to Concrete Repair*, US Department of the Interior, Bureau of Reclamation, Technical Service Center, Denver.

Grenier-Loustalot, M-F and Lartigau, C J (1997), 'Influence of the stoichiometry of epoxy-cyanate systems (non-catalyzed and catalyzed) on molten state reactivity', *Polym Sci A: Polym Chem*, **35**, 3101–15.

Gupta, A, Singhal, R and Nagpal, A K (2003), 'Crosslinking reaction of epoxy resin (diglycidyl ether of bisphenol A) by anionically polymerized polycaprolactam I. Mechanism and optimization', *J Appl Polym Sci*, **89**, 3237–47.

Gupta, A, Singhal, R and Nagpal, A K (2004), 'Reactive blends of epoxy resin (DGEBA) crosslinked by anionically polymerized polycaprolactam: process of epoxy cure and kinetics of decomposition', *J Appl Polym Sci*, **92**, 687–97.

Gupta, A, Singhal, R and Nagpal, A K, (2005) 'Reactive blends of epoxy resin (DGEBA) crosslinked by anionically polymerized polycaprolactam. II. Mechanical and electrical properties', *J Appl Polym Sci*, **96**, 537–49.

Gupta, A, Singhal, S K, Katiyar, S, Singhal, R and Nagpal, A K (2008), 'Reactive blends of epoxy resin (DGEBA) cross-linked by anionically polymerized polycaprolactam: adhesive property and chemical resistance', *Polym-Plast Techn Eng*. **47**, 223–36.

Khan; N H, Razi Abdi, S H, Kureshy, R I, Singh, S, Ahmad, I, Jasra, R V and Ghosh, P K (2007), *Catalytic Process for the Preparation of Epoxides from Alkenes*, US Pat 7 235 676.

Kinloch, A J, Lee, J H, Taylor, A C, Sprenger, S, Eger, C and Egan, D (2003), 'Toughening structural adhesives via nano- and micro-phase inclusions', *J. Adhesion*, **79**, 867–73.

Kinloch, A J, Mohammed, R D, Taylor, A C, Eger, C, Sprenger, S and Egan, D (2005), 'The effect of silica nano particles and rubber particles on the toughness of multiphase thermosetting epoxy polymers', *J Mater Sci*, **40**, 5083–6.

Kubens, R, Schultheis, H, Wolf, R, Grigat, E, Schminke, H-D and Putter, R (1971), *Resins Based on Aromatic Cyanic Acid Esters and Polyepoxide Compounds*, US Patent 3 562 214.

Liang, Y L, Oldak, R K and Pearson, R A (2007), 'Particle size effect in rubber-glass sphere toughened epoxies', in *Proceedings 30th Annual Meeting of the Adhesion Society,* Jagota, A (ed), The Adhesion Society, Blacksburg, VA, 343–5.

Maity, T, Samanta, B C and Banthia, A K (2008), 'Amine functional chloroaniline acetaldehyde condensate-modified epoxy networks', *J Appl Polym Sci*, **110**, 3717–26.

Mezzenga, R and Månson, J A E (2001), 'Thermo-mechanical properties of hyperbranched polymer modified epoxies', *J Mater Sci*, **36**, 4883–91.

Mezzenga, R, Boogh, L and Petterson, B (2000), 'Chemically induced phase separated

© Woodhead Publishing Limited, 2010

morphologies in epoxy resin-hyperbranched polymer blends', *Macromol Symp*, **149**, 17–22.

Mezzenga, R, Plummer, C J G, Boogh, L and Månson, J A E (2001), 'Morphology build-up in dendritic hyperbranched polymer modified epoxy resins: modeling and characterization', *Polymer*, **42**, 305–17.

Mikawa, M and Uchida, S-I (2003), *Catalyst for Production of Epoxides and Methods for Production Thereof and Epoxides*, US Pat 6 600 056.

Minford, J D (1993), *Handbook of Aluminum Bonding Technology and Data,* Marcel Dekker, New York.

Miyagawa, H, Mohanty, A K, Misra, M and Drzal, L T (2004a), 'Thermo-physical and impact properties of epoxy containing epoxidized linseed oil, 1 anhydride-cured epoxy', *Macromol Mater Eng*, **289**, 629–35.

Miyagawa, H, Mohanty, A K, Misra, M and Drzal, L T (2004b), 'Thermo-physical and impact properties of epoxy containing epoxidized linseed oil, 2 amin-cured epoxy', *Macromol Mater Eng*, **289**, 636–41.

Monnier, J R and Muehlbauer, P J (1990), *Selective Monoepoxidation of Olefins*, US Pat 4 897 498.

Monnier, J R and Muehlbauer, P J (1992), *Selective Epoxidation of Diolefins and Aryl Olefins*, US Pat 5 138 077.

NTSB (2007), *Ceiling Collapse in the Interstate 90 Connector Tunnel, Boston, Massachusetts*, National Transportation Safety Board, Accident Report NTSB/HAR-07/02, PB2007-916203, Washington DC. http://www.ntsb.gov. July 10, 2006.

Oldak, R K, Hydro, R M and Pearson, R A (2007), 'On the use of triblock copolymers as toughening agents for epoxies', in *Proceedings 30th Annual Meeting of the Adhesion Society,* Jagota, A (ed), The Adhesion Society, Blacksburg, VA, 153–6.

Park, S-J, Jin, F-L and Lee, J-R (2004), 'Effect of biodegradable epoxidized castor oil on physicochemical and mechanical properties of epoxy resins', *Macromol Chem Phys*, **205**, 2048–54.

Petrie, E M (2006), *Epoxy Adhesive Formulations*, McGraw-Hill, New York.

Pizzi, A and Mittal, K L (2003), *Handbook of Adhesive Technology*, Marcel Dekker, New York.

Potter, D L (1979), *Primary Adhesively Bonded Structure Technology (PABST). Design Handbook for Adhesive Bonding*, Defense Technical Information Center, Accession Number: ADA082078.

Ragosta, G, Abbate, M, Musto, P, Scarinzi, G and Mascia, L (2005), 'Epoxy-silica particulate nanocomposites: Chemical interactions, reinforcement and fracture toughness', *Polymer*, **46**(23),10 506–16.

Renton, J, Olcott, D, Roeseler, B, Batzer, R, Baron, B and Velicki, A (2004), 'Future of flight vehicle structures (2002–2023)', *J Aircraft*, **41**(5), 986–98.

Rider, A N (2002), *The Durability of Epoxy Adhesive Bonds Formed with Titanium alloy*, http://www.dsto.defence.gov.au/corporate/reports/DSTO-TR-1333.pdf; DSTO Aeronautical and Maritime Research Laboratory, Melbourne, Vic.

Riew, C K (1973), *Phenol Terminated Carboxy Containing Diene Elastomers*, US Pat 3 770 698.

Riew, C K (1977), *Reaction Products of Non-cycloaliphatic Epoxy Resins and Amine-terminated Liquid Polymers and Process for Preparation Thereof*, US Pat 4 055 541.

Riew, C K, Siebert, A R and Rowe, E H (1976), *Compositions Containing Epoxy Resin, Chain Extender, Functionally Terminated Elastomer and Curing Agent*, US Pat 3 966 837.

© Woodhead Publishing Limited, 2010

Roebroeks, G (1991), '*Towards Glare – The Development of a Fatigue Insensitive and Damage Tolerant Aircraft Material*', Dissertation, Aerospace Engineering, Delft University of Technology, The Netherlands.

Ryang, H-S (1989), *Curable Resin Systems Containing Cyanate Ester Functional Oxazolinylpolysiloxanes*, US Pat 4 797 454.

Shannon, R W, Stifel, P, Beger, R, Hughes, E J and Rutherford, J L (1978), *Primary Adhesively Bonded Structure Technology (PABST). General Material Property Data*, Defense Technical Information Center, Accession Number: ADA077891.

Sika (1998), *Technology and Concepts for Sika® CarboDur® Structural Strengthening System*, S&W 3.99.98 SIK3.13/© Sika AG, Switzerland.

Sultan, J N and McGarry, F J (1973), 'Effect of rubber particle size on deformation mechanisms in glassy state', *Polym Eng Sci*, **13**(1), 29–34.

Unnikrishnan, K P and Thachil, E T (2006), 'Toughening of epoxy resins', *Designed Monomers Polym*, **9**(2), 129–52.

Uram, M (2006), *Autoclavable Endoscope*, US Pat 6 997 868.

Vlot A (2001), *Glare, History of the Development of a New Aircraft Material*, Kluwer Academic Publishers, Boston.

Vlot, A and Gunnink, J W (2001), *Fibre Metal Laminates,* Kluwer Academic Dordrecht.

Wang, J, Wang, S, Qing, J, Kwon, O, McGrath, J E and Ward, T C (1998), 'Toughness of epoxy resins with poly(ether phosphine oxide-co-ether sulfone)', in *Proceedings 21st Annual Meeting of the Adhesion Society,* 22–25 February, Savannah, Georgia. The Adhesion Society, Blacksburg VA, 434–6.

Wu, D Y, Meure, S and Solomon, D (2008), 'Self-healing polymeric materials: A review of recent developments', *Prog Polym Sci*, **33**, 479–522.

Yacobi, B G and Hubert, M (2003), *Adhesive Bonding in Photonics Assembly and Packaging*, American Scientific, Stevenson Ranch, CA.

Yonehara, K, Sumida, Y and Hirata, K (2008), Liquid Phase Oxygenation Reaction Using Tungsten Species, US Pat 7 425 519.

Zhang, Y, Sun, Y and Zhang, W (2008), 'Method for preparing epoxy resin adhesive by straw liquification', *Faming Zhuanil Shenquing Gongkai Shuomingshu*, CN 101 168 653 A.

© Woodhead Publishing Limited, 2010

# 3
# Advances in polyurethane structural adhesives

BERND BURCHARDT, Sika Services AG, Switzerland

**Abstract**: This chapter discusses a broad definition of structural adhesives and the main elements for their characterisation, with a specific focus on polyurethanes. Using some typical examples, test results from different polyurethane adhesives demonstrate the large variety of polyurethane formulations. A new application is the combination of epoxy and polyurethane to obtain crash-resistant adhesives with unmatched properties. Another innovation is the development of high modulus, single-component moisture curing adhesives with latent hardeners. More than any other adhesive technology, polyurethane chemistry allows adhesives to be tailor-made for a specific application. This makes polyurethane adhesives the most versatile bonding technology and the key to successful lightweight design.

**Key words**: structural bonding with polyurethane adhesives, mechanical characterisation of adhesives, crash resistant adhesives, 1C polyurethane adhesives with latent hardener.

## 3.1 Introduction

### 3.1.1 Education

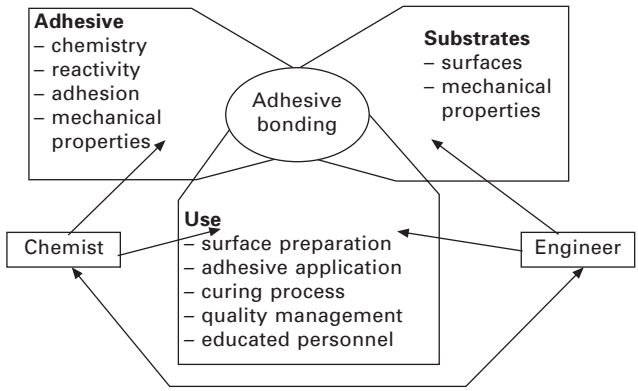
Structural adhesive bonding is a key technology in building lightweight structures. This chapter describes a wide variety of polyurethane (PUR) adhesives and how adhesive bonding technology can be used successfully by engineers. Knowledge of structural adhesive bonding among engineers and chemists is rather limited, but to take advantage of its benefits requires specific know how and the combined expertise of chemists and engineers (Fig. 3.1). Fraunhofer IFAM in Bremen, Germany (Klebtechnisches Zentrum) has offered a university level education in structural adhesive bonding since 1994. The adhesive bonding engineer degree course is certified by the German Welding Association (Deutscher Verband für Schweisstechnik DVS) and provides basic knowledge in structural bonding.

### 3.1.2 Definition of structural adhesive bonding

What is the goal of structural bonding? It is to build a complex structure from different parts that fulfils a required function for a desired lifetime. Bonding under the definition of 'structural' has nothing to do with the strength of an



© Woodhead Publishing Limited, 2010




*3.1* Skills necessary for structural bonding.

adhesive, but is concerned with engineering principles. The key to successful structural bonding is to design an adhesive for a particular function, or to select the best one for that function from existing adhesive systems.

An engineer must be able to calculate how much load can be transferred based on the adhesive, the design of the bonded area, the material properties of the substrates, the expected load and the required stiffness of the bonded structure. They must also assess how an adhesive can contribute to the structure and durability under the expected operating conditions. Ultimately, this can be calculated using finite element methods (FEM) and this chapter will highlight how PUR adhesives can be designed using these techniques to meet specific functions.

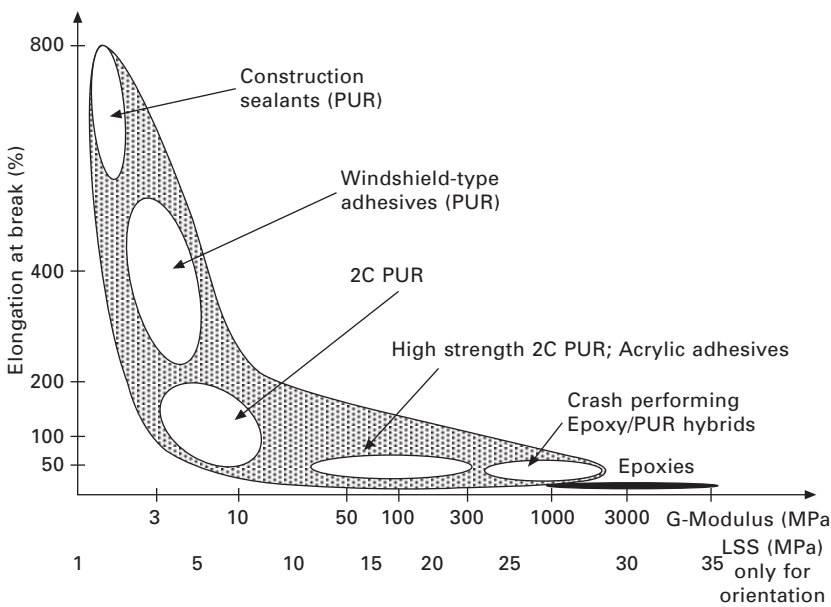
Structural adhesives with significant load-bearing capabilities, which are resistant to creep and durable at the required working temperature are usually reactive systems, where organic molecules such as monomers or prepolymers are cured to a polymer. The three-dimensional, covalently bonded polymer network created is a prerequisite for structural performance and the chemical cross-link reaction between the reactive components of the adhesives creates a polymer with the required mechanical properties. Adhesives must have a liquid stage during application, otherwise there will be no surface wetting, which is essential for building up adhesion. This implies that structural adhesives are usually two-component (2C) systems. There are, however, single-component (1C) systems, where there is no need to mix components on application. This is usually the case where the reactive component does not react at room temperature (in the case of heat curing systems), or where the second component comes from ambient moisture without mixing (moisture curing system).

© Woodhead Publishing Limited, 2010

### 3.1.3 Positioning of PUR adhesives

PUR adhesives compete with other compounds for structural functions, including epoxies (EP) and acrylics. There are also other structural adhesives, such as polyimides, silicones and polysulfides, but these will not be compared with PUR in this chapter. Non-cross-linked hotmelts have a very limited use as structural adhesives, despite the fact that they are easy to disassemble for recycling purposes. The high glass transition temperature $T_g$ requires specific processing, especially for metals, which need preheating or surface pretreatment to obtain the necessary wetting for good adhesion on metal substrates.

Figure 3.2 shows the three most commonly used structural adhesives in terms of their shear modulus, elongation and lap shear strength (LSS). There is an approximately reciprocal correlation between shear modulus ($G$) on the logarithmic scale and elongation and these two mechanical properties are the key to understanding the usability of the adhesive. The shear modulus determines the stiffness of a bonded structure in combination with the design of the substrates and the elongation shows whether substrates with different thermal elongation can be bonded together with a longer bond line. Lap shear strength increases only linearly compared to $G$ and is mentioned for comparison.




*3.2* Landscape of adhesives.

© Woodhead Publishing Limited, 2010

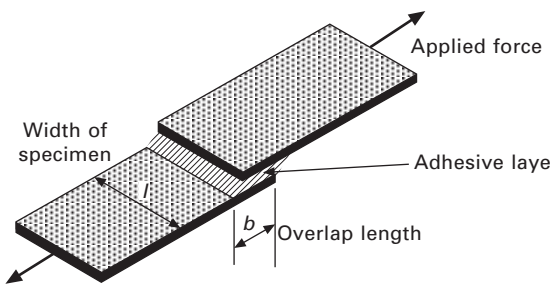
In Fig 3.2, PURs encompass the entire grey area and are therefore the most versatile adhesive technology, making them unique in this respect. They can be adjusted across the whole range of mechanical properties, from very soft and elastic, like a rubber, to very rigid. An adhesive formulator has to understand how variables like cross-link density, chain length, molecular building blocks and number of functional groups influence the mechanical properties of the PUR. The challenge for a good structural adhesive is to achieve a shear modulus as high as possible with sufficient elongation at break, shifting the position of the adhesive towards the upper right corner in Fig. 3.2. Basic information on how to formulate PUR adhesives can be read in, for example, Meier-Westhues (2007).

## 3.2 Characterisation of structural adhesives

Adhesives are complex systems, which implies that many parameters can be used for a detailed characterisation. In this chapter, the focus will be on lap shear strength (LSS), shear modulus ($G$), stress–strain curve, elongation at break, glass transition temperature ($T_g$) and temperature dependence of mechanical properties, durability and ageing behaviour under different climatic conditions.

### 3.2.1 Lap shear strength

In technical data sheets, structural adhesives are usually characterised by LSS, determined according to DIN 53283. The design of the test samples is shown in Fig. 3.3, where the width I is usually 25 mm and the overlap length $b$ is 12.5 mm. The LSS values give an indication of the strength of an adhesive, but can never be used to calculate the strength of a bonded structure, since this is strongly related to the geometry of the samples and the mechanical properties of the substrates. When measuring the LSS of high strength PUR or EP adhesives with thin metal sheets (e.g. 1.6 mm with Al and 1.0 mm with steel) the strength is usually determined by the yield strength of the




*3.3* Lap shear specimen.

© Woodhead Publishing Limited, 2010

substrate. As soon as the metal starts to yield, the stress at the end of the overlap becomes too high and the adhesive cracks. In special cases, such as crash-resistant EP/PUR hybrid adhesives, the metal breaks first (Fig. 3.4). Only the strength of the metal is measured in this case.

Assuming a yield strength of 280 MPa, thickness of 1.0 mm and width of 25 mm, the yield stress will be 7000 kN. With a bonded area of 300 $mm^2$, this results in a calculated LSS of 23.3 MPa. Testing the same adhesive according to DIN 54451 often gives an LSS of more than 40 MPa, but since LSS is easy to measure, it can be used for quick quality tests to check surface preparation and the control of adhesive batches.

### 3.2.2 Shear modulus *G*

The key figure for a structural adhesive is the shear modulus, *G*. With *G*, the mechanical properties of the bonded joint can be calculated using finite element methods (FEM) (Equation 3.1).

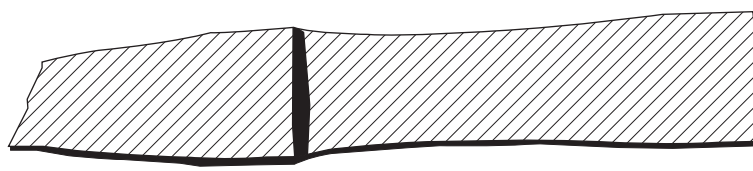
$$k = c \times \frac{A_k}{d} \text{ (N mm}^{-1}\text{)} \qquad [3.1]$$

where $k$ is the spring constant in the adhesive layer, $c$ is the stiffness, $A_k$ is the bonding area and $d$ is the adhesive layer thickness.

There is in principle no difference to other substrates such as metals but, in contrast to metals, adhesives are based on organic polymers and the respective dependence of their mechanical properties on temperature must be taken into account when designing a bonded structure.

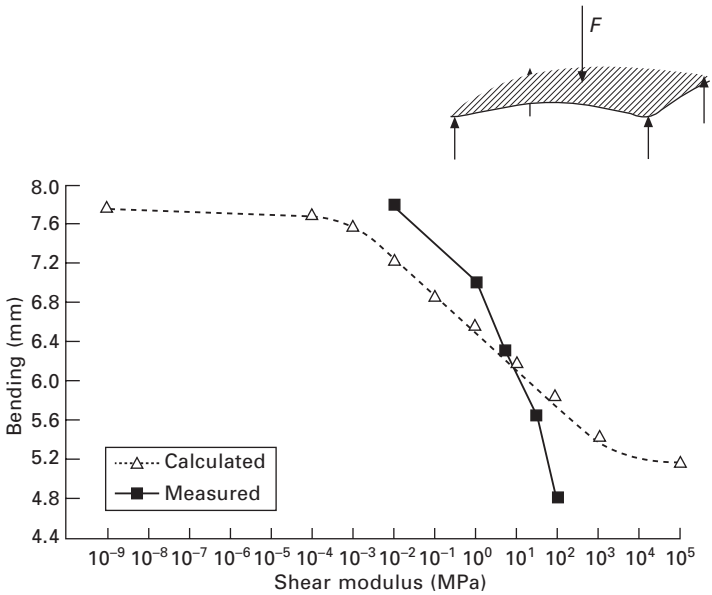
It is interesting to see the influence of shear modulus on a tightly bonded structure, as described by Deimel (1993) in a diploma thesis which compared calculated and measured bending stiffness of a car sun roof lid where the inner and outer metal sheets had been bonded together. Four adhesives with different *G* were used, and the calculated and measured stiffness in bending strength correlated well, even when the measured stiffness was slightly higher (Fig. 3.5).

In this example, almost 90% of the maximum achievable bending stiffness was reached with a *G* value of 100 MPa. Since this was an application where the bonding transferred the forces into the very thin (0.8 mm) outer steel and



*3.4* Bonded lap shear specimen broken in the steel (1mm gauge).

© Woodhead Publishing Limited, 2010




*3.5* Comparison of calculated and measured stiffness of a sun roof lid.

where no surface marking was allowed, 1000 MPa adhesive could not be used. The practical requirement was bending of less than 6 mm, otherwise the sun roof lid would be blown away by wind forces at speeds above 200 km $h^{-1}$.

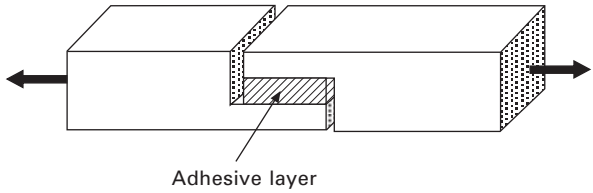
This case demonstrates there is no need for a particularly high value of $G$ to achieve the maximum increase in stiffness for a structure. This is important because it offers opportunities to reduce $G$, thus increasing elongation at break, which will increase the durability and impact resistance of bonded structures and enable bonding of materials with different thermal elongation.

$G$ is measured for the thick adherend lap shear specimen (Fig. 3.6). The overlap length is 12 mm, substrate thickness at the bonded area (depending on the substrate) between 6 and 10 mm, width 20 mm and overall length 88 mm. The thickness of the adhesive layer varies according to requirements (between 0.3 and 5 mm). Various articles by Schlimmer (2004–2006) discuss this topic.

### 3.2.3 Stress–strain diagram

The stress–strain curve is measured for the thick adherend test specimen according to DIN 54451. Typical curves are shown in the following diagrams

© Woodhead Publishing Limited, 2010




*3.6* Specimen for the thick adherent test.

comparing Epoxy, PUR standard and EP/PUR hybrid crash-resistant adhesives.

Figure 3.7 reflects the different behaviour of PUR adhesives depending on their strength. In all cases, there is a significant strain before the adhesives break, which makes them more robust in real applications since the danger of a sudden failure is reduced.

A stress–strain diagram gives important information about the mechanical properties of an adhesive (Fig. 3.8):

- *G*, which can be measured from the slope of the curve as the secant modulus within one-third of the maximum stress (interval 1). This value is then used in FEM calculations. *G* and Young's modulus, *E*, are linked by the Poisson ratio ν, which is around 0.35 to 0.40 in these adhesives.

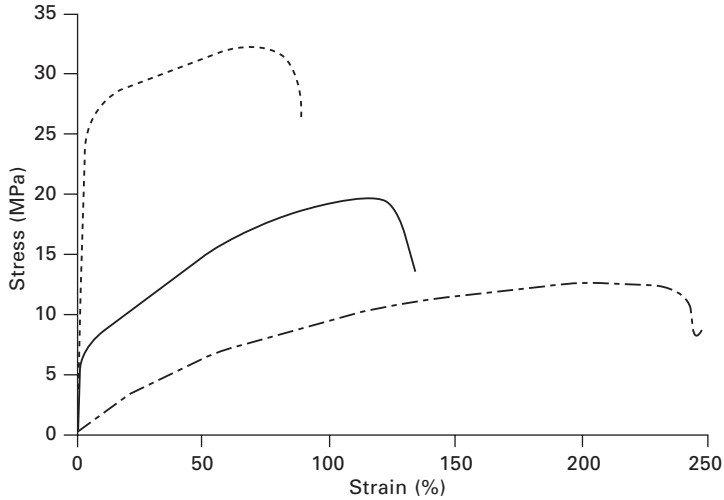
$$E = G \bullet 2 \bullet (1 + \nu) \quad [3.2]$$

  where *E* is the elastic modulus, *G* is the shear modulus and ν is the Poisson ratio.
- The maximum stress, which is often significantly higher than that measured with LSS in the case of high strength adhesives (interval 2).
- The elongation at break, which shows the behaviour of the adhesive in cases of overload and thus gives information about the fail-safe behaviour of the adhesive (interval 3). It is important to be aware that the shape of this curve also depends on the test speed and on temperature.

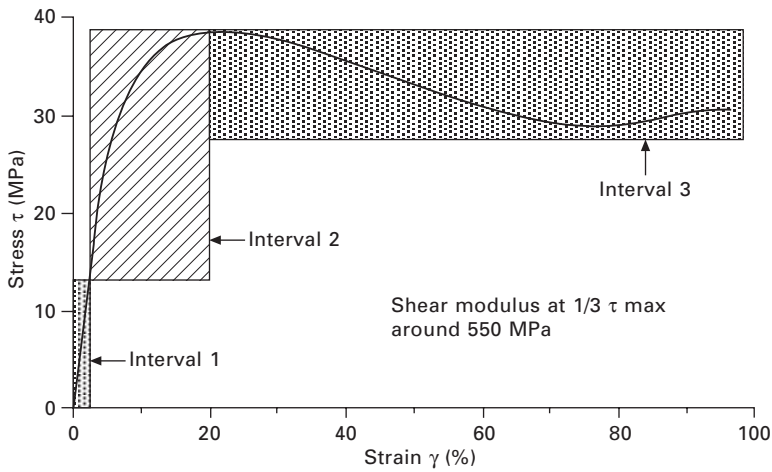
Whereas *G* from the stress–strain curve can be used for FEM calculations, the maximum shear strength has only limited practical importance in inferring joint behaviour. It is only an indication of what might be the maximum possible load in a one-time event (e.g. a crash), but owing to possible yield deformation of the substrates, real bonded structures will often fail in the substrates before they reach such high strength levels.

Figure 3.9 shows a modified stress–strain diagram, where real elongation in mm rather than percentage of deformation is plotted against adhesive thickness on the x-axis. Comparing 2C EP, PUR and acrylic structural adhesives in this way shows that the EP has almost no elongation, whereas the 2C PUR and the 2C acrylic behave similarly, with significant deformation. Based on

© Woodhead Publishing Limited, 2010




*3.7* Stress–strain diagram for different PUR adhesives. ------, EP/PUR crash resistant; _____, PUR (high strength); _ _ _, PUR (medium strength).

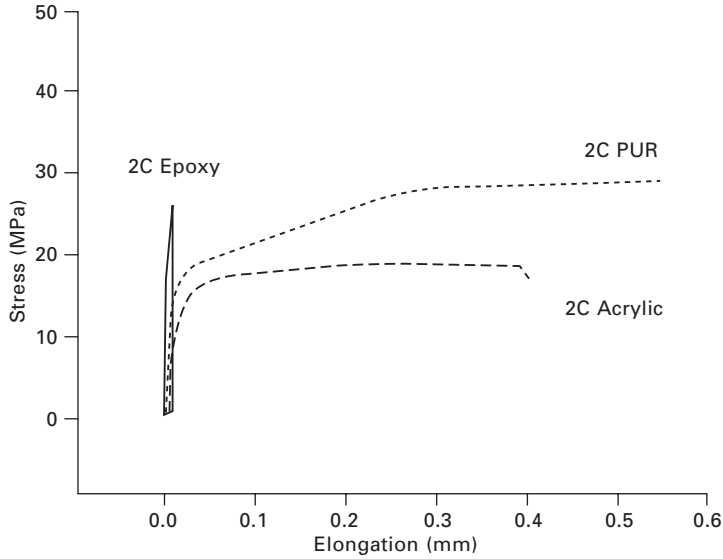



*3.8* Stress–strain diagram of a crash resistant adhesive.

this behaviour, PUR and acrylic adhesives often compete in the market for the same applications.

In many practical applications using PUR adhesives, the standard working load for a structural bond does not exceed 3–5% of the maximum load in terms of LSS (Burchardt *et al.*, 2006), because this includes all the necessary reduction factors, like temperature dependence and ageing. In such cases, structural adhesives work as ideal elastic and do not creep. This can be read from Wöhler diagrams, because the remaining load after $10^8$ cycles correlates with experiments with permanent static load over a long period

© Woodhead Publishing Limited, 2010




*3.9* Stress–elongation comparison of standard 2C structural adhesives.

of time (this was also found for 1C heat cured EP adhesive in automotive applications).

Elongation at break is usually measured with dog-bone samples of the bulk material. The values will differ, since with bonded lap shear specimen, the adhesive is loaded by shear forces and not by tension and size and adherent properties also influence the result. The thick adherend test will therefore give better information regarding what elongation (strain) can be used in bonded structures.

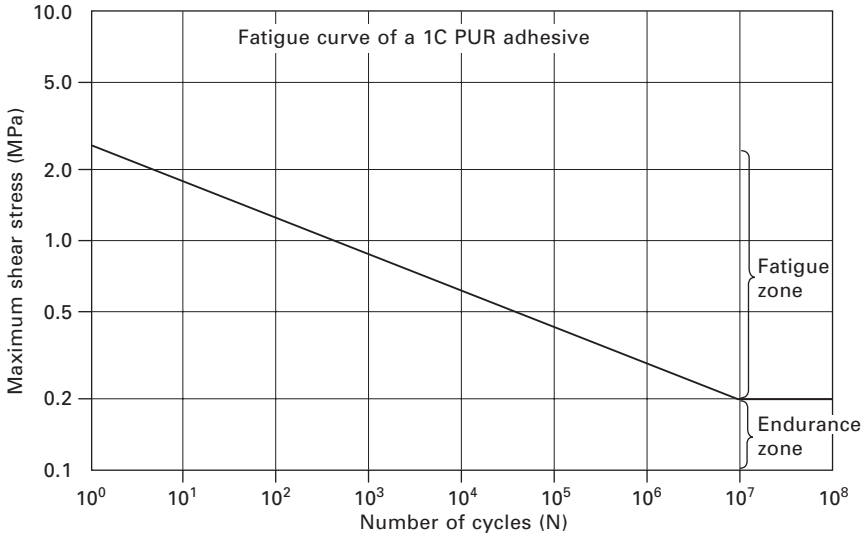
### 3.2.4 Durability

Engineers must design products with an expected lifetime and must be sure that, even under worst-case assumptions, the structure will not fail. To assess the predicted lifetime of a bonded structure, the process for steel structures can be used, applying different loads cyclically to create a Wöhler diagram.

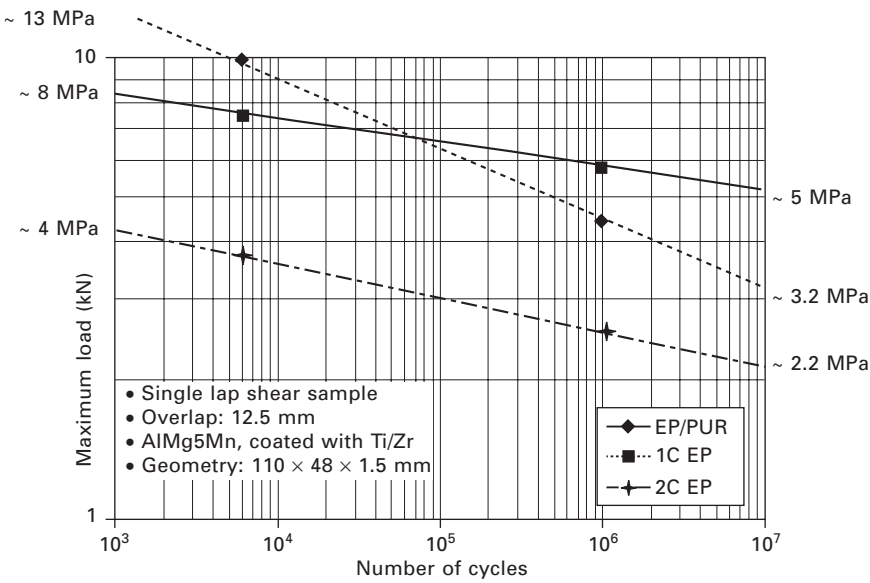
To create such a diagram, more than ten samples are stressed at different load levels and the number of cycles up to failure is plotted in a double logarithmic chart. When lap shear samples are used, there is always an initial load level to prevent compression of the specimen, which would create bending forces and lead to premature failure. From such a diagram, the long-term durability, after 10 or 20 million cycles, can be determined. In many cases for PUR adhesives this level also marks the limit of permanent static load of an adhesive bond.

© Woodhead Publishing Limited, 2010

Figures 3.10 to 3.12 show Wöhler curves for different types of adhesives. This is a curve typical of windshield-type 1C PUR adhesives. The endurance zone after 10 million cycles also correlates with static load tests over years, where loads of 0.20 to 0.25 MPa were sustained and the samples did not creep.

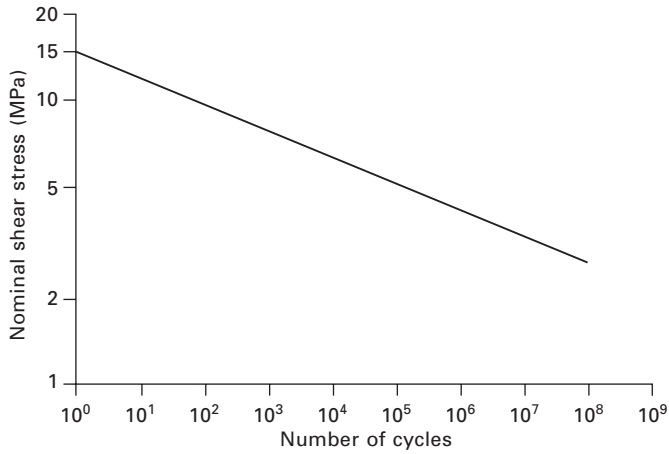



*3.10* Wöhler curve for a 1C PUR adhesive.




*3.11* Comparison of Wöhler curves for different types of adhesives.

© Woodhead Publishing Limited, 2010




*3.12* Wöhler curve for a high strength 2-C PUR adhesive.

Figure 3.11 shows a comparison of structural adhesives used for joining metal sheets in the automotive industry. The heat curing 1C EP starts with the highest load level of 13 MPa, which is not surprising since its initial lap shear value measured with the thick adherend test reaches 70 MPa. The PUR-modified EP adhesive has an initial shear strength of only 25 MPa and starts at 8 MPa, but after 10 million cycles the result reveals a substantially higher residual load level of 6 MPa compared with the 1C EP adhesive at 4.2 MPa. The 2C EP adhesive also starts with a higher lap shear strength of 35 MPa, but under cyclic loading it shows only half of the performance of the EP/PUR hybrid adhesive. The tendency for cracks is lower in case of the EP/PUR hybrid, owing to the toughening effect of the PUR, which results in higher load levels. EP/PUR hybrid adhesives are used in automobile car bodies to replace spot weld bonding of metal sheets.

The Wöhler curve for a high strength 2C PUR (Fig. 3.12) ends with a stress level at about 3 MPa, which is about 20% of the initial stress. Taking into account the additional decrease when working above the glass transition temperature $T_g$, the reduction to a level of 3–5% of initial load is the reasonable assumed permanent stress.

These three examples show that the whole range of mechanical strength for different grades of adhesives can be measured by this method. These tests do, however, take time, because the frequency for the tests must be in the range of 10 Hz to a maximum of 50 Hz, since the adhesives, especially those with lower $G$ and higher elongation, are heated up by the mechanical energy which is put into the system. Engineers do not really trust adhesive bonding technology because of bad experiences owing to failures of adhesively bonded parts. Most cases of failure are linked to problems with the design of the bonded structure, especially when using brittle high

© Woodhead Publishing Limited, 2010

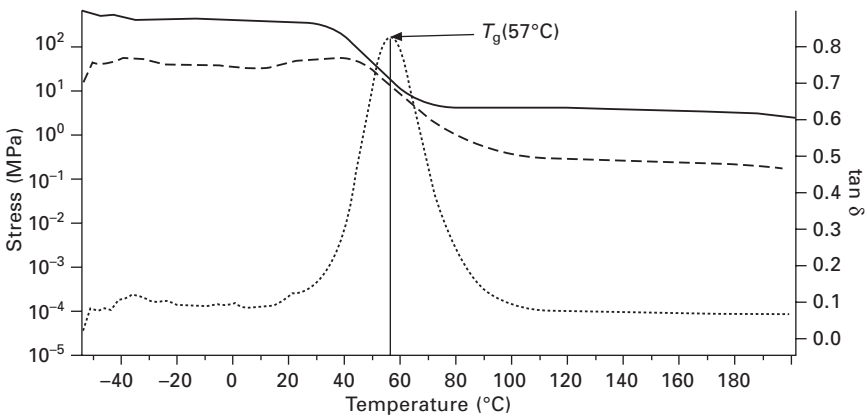
strength adhesives. Adhesives can fail under the designed load after a few cycles if the calculated LSS is used to obtain the dimensions of the bonded area without understanding that the loads at the ends of the overlap are too high owing to uneven stress distribution.

### 3.2.5 Glass transition temperature and temperature dependence of mechanical properties

The glass transition temperature ($T_g$) is usually measured by dynamic mechanical thermo analysis (DMTA) (Fig. 3.13). The curve for the storage modulus $G'$ shows the change in mechanical properties depending on the temperature. The quotient between loss modulus and storage modulus is tan δ, which is often used as an indication for $T_g$. But the reduction in the mechanical strength of an adhesive has already started at temperatures about 20°C lower than can be read from the curve $G'$.

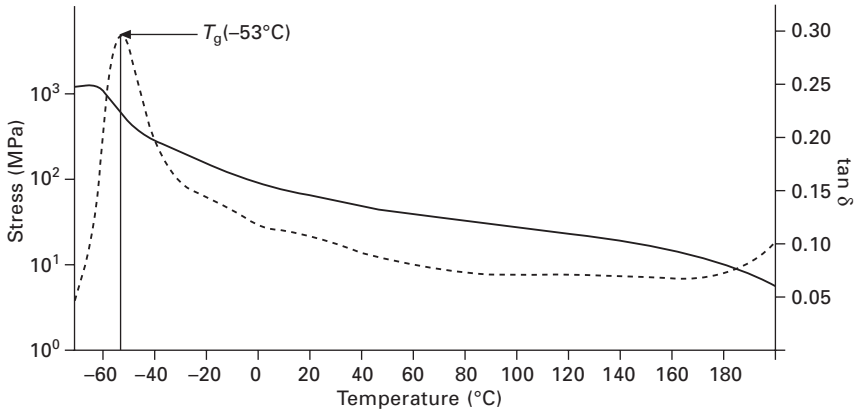
The importance of $T_g$ is often overestimated. Many PUR adhesives work very well above their $T_g$. Of course a large decrease in mechanical properties within the temperature range under service life conditions is often not acceptable, but the residual mechanical strength can be taken into account and can be calculated. For example, 1C PUR windshield adhesives have a $T_g$ of –50°C and therefore always work successfully above their $T_g$.

Figure 3.14 shows a 1C PUR offering a high modulus over a wide temperature range. In comparison with the DMTA of the high strength 2C PUR shown in Fig. 14, the $G'$ value of this 1C PUR above 60°C is higher and the decrease with temperature is very low. This represents a new generation of 1C PUR adhesives which maintain their mechanical properties over a wide temperature range. An LSS specimen bonded with an EP adhesive with a




*3.13* DMTA measurement of a high strength 2C PUR. —, $G'$ (storage modulus); – – $G''$ (loss modulus); ·····, tan δ curve.

© Woodhead Publishing Limited, 2010




*3.14* DMTA of high modulus 1C PUR adhesive. For key to traces, see Fig. 3.13.

$T_g$ above 80°C failed under a permanent static load of 2 MPa (about 5% of its maximum shear strength) within 18 months. Under identical conditions, a windshield adhesive with a $T_g$ below –50°C failed with a static load of 0.28 MPa (about 5% of its maximum shear strength). In conclusion, it is not the $T_g$ that is important but the load which the adhesive can sustain over its lifetime under service. The Wöhler diagram of the adhesive provides this information. And more than 30 years of windshield bonding in transportation confirms that adhesives have excellent durability even when working above their $T_g$.

### 3.2.6 Adhesion and ageing of adhesives

Durability is not only influenced by cyclic load but also by environmental factors such as temperature, UV radiation, chemicals, oxygen and solvents. In general, moisture has the biggest effect. It diffuses into the polymer matrix and acts like a plasticiser, or has a long-term influence on the adhesion on the substrates.

Polyurethanes with polyether as the backbone polymer usually have a high diffusion rate for moisture vapour. This may lead to adhesion problems on metals since the adhesion takes place on the metal oxide on the surface. This oxide layer is attacked by the intrusion of moisture, which will destroy the oxide layer over the long term if not properly protected by the appropriate surface treatment.

The bulk of the PUR adhesive itself is rather insensitive to moisture intrusion. In moisture-curing adhesives, saturation with moisture will not lead to a decrease in *G*. This is in contrast to EP systems, which, after tests under cataplasma conditions (+70°C, 100% humidity), show up to a 40%

© Woodhead Publishing Limited, 2010

drop in *G* measured at room temperature. Owing to the high initial lap shear values, this does not become obvious in lap shear tests because the results are determined by the substrate yield strength. There are a number of test cycles that combine temperature change, humidity and salt, especially designed for the automotive industry. All automotive manufacturers have their own test cycles, but all combine these elements and end up with similar results. However, the cycles are usually designed to achieve results in a very short period of time, which sometimes creates effects not observed in real life (especially when combining temperatures above 70°C with 100% humidity).

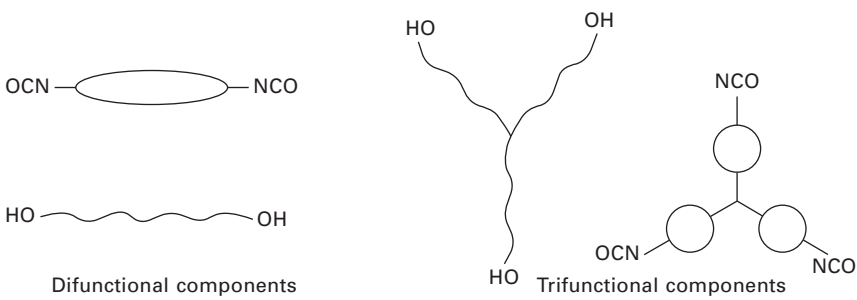
When bonding on plastic substrates, such as fibre-reinforced composites or thermoplastic parts, moisture diffusion is of less importance but the migration of smaller molecules, such as plasticisers, stabilisers or catalysts, becomes important and can influence the strength of the adhesive or the quality of adhesion. The large variety of adhesives and substrates makes it necessary to test compatibility and adhesion for a given material combination in each individual case. For all currently used substrates, specific surface treatments are available to create the desired adhesion over the required service life.

## 3.3 Chemistry

### 3.3.1 Building blocks

This chapter will not go into a detailed chemistry of polyurethanes, but it is important to understand how to combine the building blocks in order to achieve the required properties. Polyurethanes offer a wide range of possibilities for formulation. The chemistry of polyurethanes is described in the literature (Meier-Westhues, 2007), but the key determining factors which influence the properties of the cured polymer are outlined here schematically because the right polymer design is key to obtaining the desired properties (Fig. 3.15).

Polyurethanes are mainly built up via difunctional and trifunctional OH-terminated molecules which react with di- or tri-isocyanates. The chain length




*3.15* Schematic building blocks for polyurethanes.

© Woodhead Publishing Limited, 2010

and stiffness of the chain determine the mechanical properties of the final polymer. The chain may consist of polyethers, which makes them flexible and hydrophilic, polyesters, which provide more rigidity, polycarbonates, or other OH-or NH-terminated molecules (in the case of NH-terminated molecules, the cured product will be a polyurea). The concentration of trifunctional molecules, which can be either the OH- or the isocyanate component, determines the cross-link density and is an important influencing factor for stiffness. A structural adhesive must have trifunctional groups to guarantee a covalent three-dimensional network, otherwise the polymer would have thermoplastic properties.

Aromatic isocyanates like diphenymethan 4-4′-diisocyanate (MDI) and toluenediisocyanate (TDI), as well as aliphatics like isophoronediisocyanate (IPDI) and the aliphatic hydrogenated MDI (H12MDI), are used in adhesive formulations (Meier-Westhues, 2007). Polyether-based PUR exhibit a high water permeation, which is not always desired, especially when bonding metals, because moisture penetration can lead to degradation of the oxide layer of the metal. This can be reduced by suitable surface treatments. Using other, more hydrophobic OH-terminated building blocks reduces moisture diffusion and thus also corrosion on metals. But the properties of the different adhesives have to be balanced carefully, because reducing the hydrophilic properties of the adhesive results in diminished wetting and adhesion on polar surfaces.

PUR adhesives based on aromatic isocyanates do not resist UV radiation. If such formulations are exposed to UV, they must either be shielded from light or a good UV-stabilising system must be used. Bonding on glass is therefore critical, because the UV radiation destroys the adhesion zone. The principles of protecting such bonds are outlined in Burchardt *et al.* (2006).

For some applications, volume shrinkage caused by curing plays an important role. When a thick adhesive layer cannot move during curing because of distance holders or other design constraints, the shrinkage creates significant stress, which reduces the load-bearing capabilities of the bonded joint. PURs based on prepolymers have reduced shrinkage and lower heat development during curing, thus offering additional advantages.

The building blocks of adhesives also show different reactivity and catalysts are needed to adjust the reaction speed. But since catalysts also influence the back reaction, which may occur at temperatures above 150°C, it is recommended that as little catalyst as possible be used when formulating adhesives for high temperature resistance. Reactions that are too fast also create problems with wetting, because the liquid adhesive must first wet the surface completely to get adhesion before it cures and if the curing is faster than the wetting, the adhesion will be significantly reduced.

© Woodhead Publishing Limited, 2010

### 3.3.2 Crash-resistant adhesives

Crash-resistant adhesives are based on a combination of an EP system with PUR elements. The EP provides the matrix resin with good adhesion on oily metals and a high $T_g$. The PUR component generates *in situ* elastic nanophases during curing of the adhesive, creating high energy absorption in case of impact, as the nanophases act as crack stoppers. Such adhesives exhibit an unmatched performance in terms of mechanical strength in combination with toughness. Figure 3.16 demonstrates the principle, where nanoparticles have formed from a homogenous liquid phase after curing.

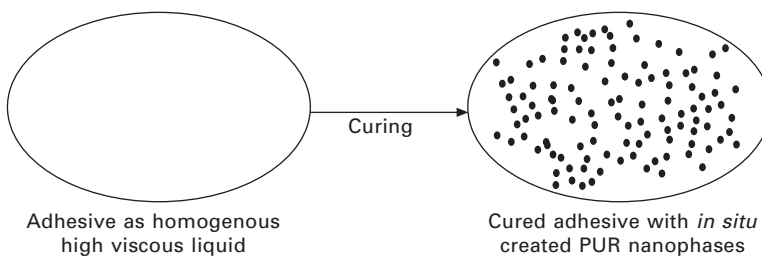
These adhesives are used in automotive applications to build up the steel body, replacing welding operations. It should be noted that the adhesive cannot absorb the energy of a crash itself because this is the task of the metal structure, but must hold the structure (e.g. a beam) together so that the metal can fold as predicted and calculated. In comparison with spot welded beams, the folding of bonded beams is more regular, resulting in a higher energy absorption compared with welding and thus increasing the safety of the passengers (Schulenburg and Kramer, 2004).

Figure 3.17 shows the impact peel tester measurements of the peel forces for a crash-resistant adhesive and a high quality structural adhesive already used in automotive applications. For the crash-resistant adhesive, the average peel forces are three times higher and the time to tear the impact peel wedge through the specimen 25% longer.

The new generation of 1C heat-curing adhesives allows a weight reduction of around 20% in conventional steel car bodies with even better durability and without additional cost, if the production process is designed around this technology (Burchardt *et al.*, 2009).

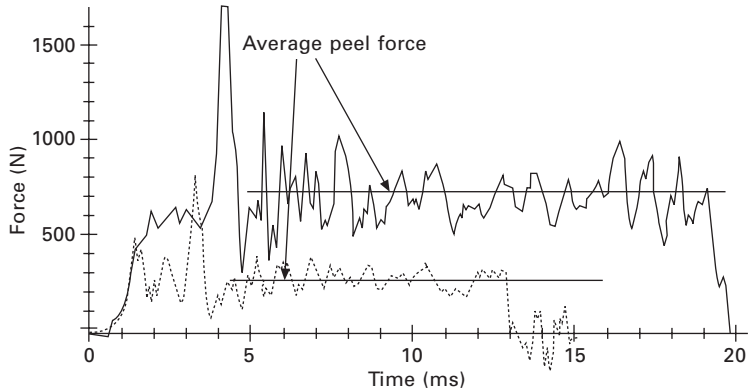
### 3.3.3 Reactivity of 2C PUR adhesives

In general there is a distinction between 1C and 2C PUR adhesives. From a practical point of view this is easily understandable, but it is not the complete story. All PUR adhesives have isocyanate groups which react with NH- or




*3.16* Formation of nanophases during curing.

© Woodhead Publishing Limited, 2010




*3.17* Peel force measurements. —, structural crash-resistant adhesive, ·····, structural adhesive. The time is recorded for rupture through the whole length of the sample.

OH functional groups and build a cross-link network, so there are always at least two reaction partners which form the final adhesive polymer. The simplest way to separate the two components is to put them into different cans and mix before use. The curing speed then depends on the reactivity of the reaction partners and the catalyst amount and this can be adjusted to the required production speed. The open time usually varies between 10 minutes and 2 hours and depends strongly on temperature. The curing time is then roughly ten times longer and also depends strongly on temperature. These are typical values for standard 2C PUR adhesives.

### 3.3.4 Reactivity of moisture curing adhesives

Based on the earlier definition of structural bonding, 1C PURs provide the largest number of adhesives for structural bonding applications. Formulating 1C PURs requires detailed chemistry. They are moisture curing, which means they react with water as the second component. 1C moisture curing PURs are easy to apply and can be used in so many applications that ongoing developments have further improved these adhesives mitigating their inherent disadvantages.

*Slow curing speed*

To accelerate the cross-link reaction of a moisture curing adhesive, water must be added. This is not easy because mixing even a very small amount of water into a water repellent, highly viscous material is not easy. But it can be achieved by adding a specially formulated water-containing paste (booster) via a short static mixer. In this case, homogenous mixing (which

© Woodhead Publishing Limited, 2010

is necessary for 2C PUR) is not required. The curing speed is faster than in a 2C system since the reactivity of water is greater than that of the OH-functional groups in standard 2C systems. Curing will also occur, although slowly, without booster paste through ambient moisture. Booster systems can be used when thick bondlines are required in materials with no or slow water vapour diffusion. A challenge in such applications is the tendency for bubble formation caused by fast curing with a large amount of water.

*Slow strength build-up*

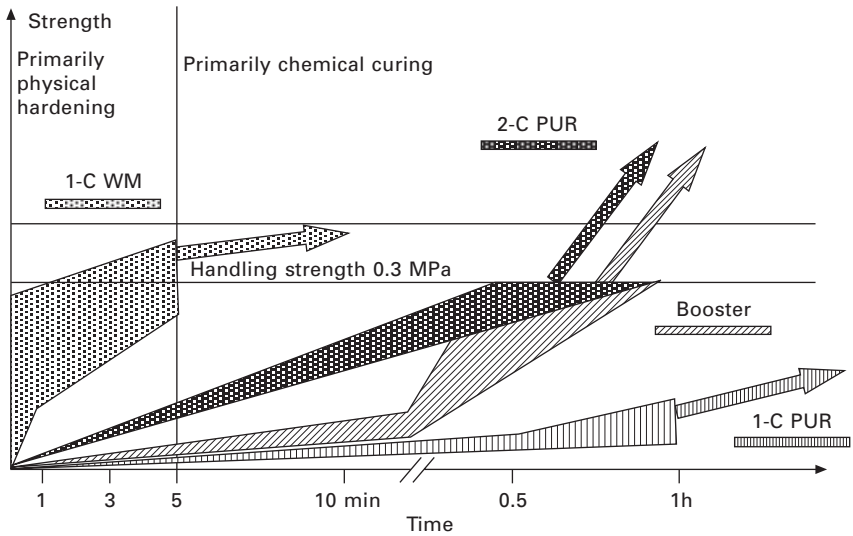
The amount of catalyst only influences the skinning time taken to obtain a tack free surface. Curing occurs through diffusion of moisture into the adhesive and this process is only controlled through the speed of water diffusion, which is also dependent on temperature and humidity and on the hydrophilic/hydrophobic properties of the polymer backbone. Environmental conditions like temperature and humidity significantly influence the curing speed.

*Low initial strength*

Slow curing requires longer fixation times to reach the necessary initial strength. One way to gain the handling strength required for installing automotive windshields more quickly is by warming the adhesives. They will then offer some initial strength immediately after cooling, thus reducing the time before the car can be used (safe drive away time) to 1 hour instead of 24 hours. It sounds simple, but in practice it is rather tricky since, if the adhesive cools too fast, there may be disbonding because the build-up of cohesion is much faster than that of adhesion and this may cause stress cracks. Careful balancing of the desired warm-melt properties is required. Headlight cover shields are bonded to the box with a non-crystalline, rubber-like warm-melt adhesive, which is leak-proof, immediately after assembly. After application, it has the consistency of a butyl rubber tape. Its final mechanical performance is acquired through reaction with water, like other moisture curing adhesives. 1C reactive hotmelt PURs have been developed to reduce the time for strength build-up to a few minutes. Such systems are used for lamination applications in automotive interior parts, furniture, sandwich panels and other applications where fast production speed must be combined with a temperature resistance of more than 100°C.

Various different strategies for reaching the desired handling strength are shown in Fig. 3.18, where the difference in the build-up of strength and curing speed is shown diagrammatically. The handling strength in this example is defined at 0.3 MPa, but this clearly depends on the application. This level, 0.3 MPa, will allow the bonding of windshields without the glass slipping after installation.

© Woodhead Publishing Limited, 2010




*3.18* Comparison of strength build up and curing speed of different PUR technologies.

In order to achieve handling strength very quickly, that is in less than 5 minutes, physical hardening of the adhesive is required, since rapid chemical curing cannot be handled under real production conditions owing to the necessary reaction speed. Curing of warm-melt systems (warm-melt means a change into a lower, viscous phase between 40 and 80°C) to the final strength is usually slower than other moisture curing systems.

The standard 2C PUR starts curing immediately after mixing and increases in viscosity, whereas the booster keeps its viscosity for a latent period and then cures even faster than the 2C PUR. Compared with these fast systems, the standard 1C PUR cures very slowly.

### *Bubbling*

A drawback of moisture curing systems is the release of $CO_2$ when curing. This limits the number of free isocyanate groups in the prepolymer, since if there are too many reactive groups, this will increase $CO_2$ release to levels too high to be absorbed by fillers or evaporated fast enough from the inside of the adhesive. This is not only a cosmetic issue, but also leads to a reduction in strength and sets the limits when formulating a higher modulus moisture curing adhesive.

To overcome this drawback, latent hardeners based on aldimines can be used. These latent hardeners are hydrolysed to the amine and the corresponding aldehyde, which evaporates and usually has a strong odour. Unfortunately, the odour is often unacceptable to customers. A newly developed aldimine

© Woodhead Publishing Limited, 2010

latent harder that releases a higher molecular weight, odour-free aldehyde, increases the strength of a 1C moisture curing adhesive to a *G* value of more than 20 MPa (Burckhardt, 2009). This invention also facilitates the use of booster systems because it reduces the tendency to bubble at a significantly higher strength level.

Latent hardener technology allows the use of 1C systems at strength levels previously reserved for 2C PUR. In addition, as can be seen in Fig. 3.14, these adhesives have a $T_g$ below –50°C but offer a very low temperature dependence for strength, providing a significantly higher *G* value at 100°C than a standard 2C PUR (compared with Fig. 3.13).

## 3.4 Design principles

### 3.4.1 Bonding area

The main design principles are described in a standard book on adhesive bonding by Habenicht (2006). It is clear that adhesive bonding only works if the bonding surface area is sufficient to transfer the expected load. Under many conditions, it is better to use an adhesive with higher elongation and lower strength combined with a larger surface area. This allows more even stress distribution, which results in bonding less sensitive to overload. The picture below illustrates the difference between elastic bonding and rigid bonding. The stress distribution shows that, with a short overlap length, a stronger adhesive can bear higher loads than an elastic adhesive (compare the areas under the curve marked rigid and elastic), whereas with a longer overlap length, the increase in load-bearing capabilities does not increase proportionally, as is more or less the case with the elastic adhesive (Fig. 3.19). In bonding fibre composite structures, an adhesive that is too strong can lead to a failure between the matrix and the fibres because local stress is too high. This type of failure can be avoided by using an adhesive with lower strength but higher elongation, although a larger bonding area is required to transfer the required load.

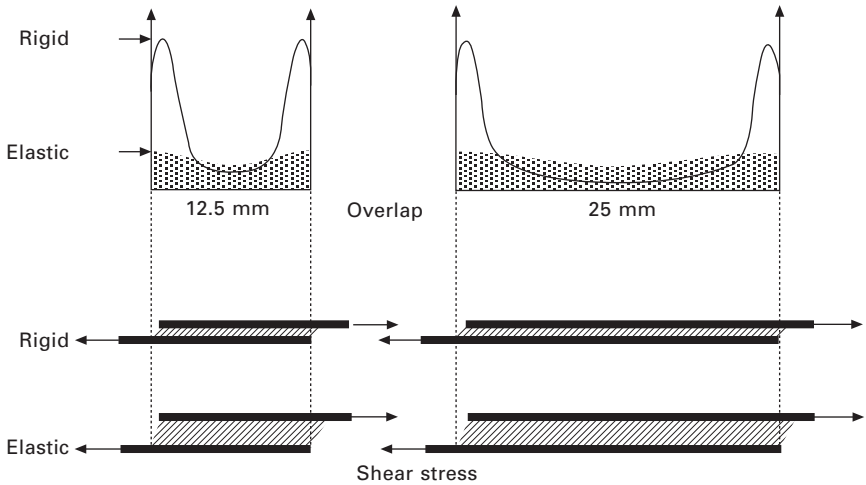
### 3.4.2 Bondline thickness

Bonding strength for adhesives with high elongation is less dependent on the thickness of the bondline, as can be seen in Fig. 3.20.

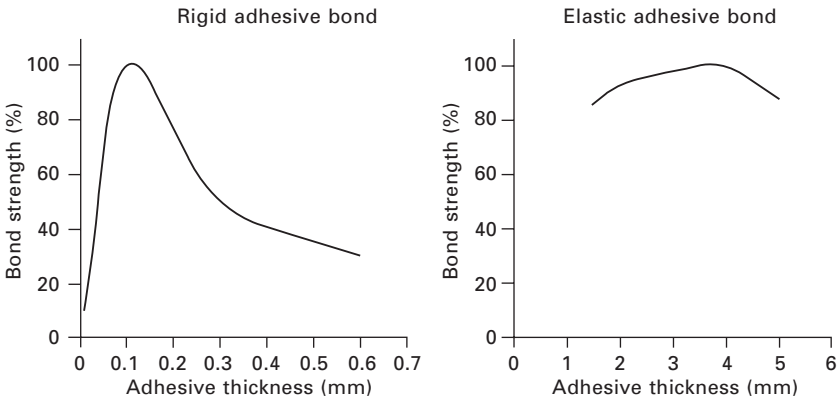
Whereas a standard EP adhesive shows a decrease of 80% when the thickness of the layer is increased to 3 mm, the elastic adhesive retains almost the same strength level over a wide range. This characteristic is necessary in practical applications with large parts and significant tolerances.

The big advantage of PUR adhesives is that they can be designed to offer the best compromise between stiffness and stress distribution for specific

© Woodhead Publishing Limited, 2010




*3.19* Schematic view of the stress distribution comparing rigid and elastic bonding.




*3.20* Strength dependence on bondline thickness.

substrates. The stiffness of the whole bonded part depends on *G*, but in reality its influence on a complete bonded structure is of less importance. This was described above (in Section 3.2.2 and Fig. 3.5). Even a lower *G* adhesive can increase the stiffness of a structure dramatically. This has been demonstrated by windshield bonding in automotive applications, where torsional stiffness increases by more than 70% when front and rear glass is bonded into the body. It also applies to other applications where rectangular frames are attached to a panel through bonding. The additional gain in stiffness is only incremental above a certain modulus. In the case of glass bonding, a too-high modulus leads to an increase in breakage rate because of higher stresses transferred into the glass. In this case, the shear modulus

© Woodhead Publishing Limited, 2010

should not surpass 5 MPa. Since there is a broad range of PUR adhesives, it may become difficult to choose the adhesive with the right mechanical properties. The relevant information on $G$ is not usually available in the standard technical datasheets, but calculating and predicting the achievable bond strength and expected stress or deformation caused by different thermal elongation of the substrates is not possible without $G$. Therefore an adhesive engineer always has to ask for this data.

### 3.4.3 Stress through thermal elongation

When bonding dissimilar materials, stress resulting from differences in thermal elongation must be considered carefully. This calculation is simplified in the example of a bonded bus roof (Fig. 3.21 and Equation 3.3). When using a lower $G$ adhesive (2 MPa), the calculation can be done on the basis of linear elastic behaviour, taking into account only the need to accommodate the difference in thermal elongation.

$$\Delta I = I_0 \times \Delta\alpha \times \Delta T \qquad [3.3]$$

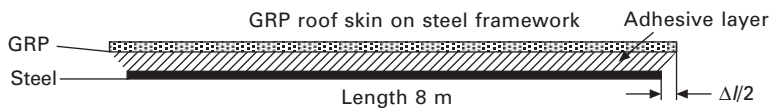
where $\Delta I = 8\ \text{m} \times 8 \times 10^{-6} \times \text{K}^{-1} \times 70\text{K}$

$\Delta I = 4.5$ mm is the difference in linear expansion, $I_0$ is the length of object, $\Delta\alpha = \alpha_{GRP} - \alpha_{steel}$ is the difference in the coefficients of linear expansion and $\alpha_{GRP} = 20 \times 10^{-6} \times \text{K}^{-1}$ and $\alpha_{steel} = 12 \times 10^{-6} \times \text{K}^{-1}$.

A glass fibre composite roof with a length of 8 m is bonded on a steel bus structure and, assuming a temperature difference of 70 K, there is a difference of 4.5 mm, which has to be held by the elastic adhesive. The roof assembly is free to move at both ends (no rivets, no bolts as additional fixation) and the change in length at either end is half of the total differential movement, 2.25 mm.

As a general rule for such elastic bonding applications, based on 30 years' experience with such applications, the thickness of the adhesive layer must be greater than the total change in length (Burchardt *et al.*, 2006). This ensures that the maximum strain for the adhesive at either end does not exceed 50%. In the example, the minimum thickness of the adhesive should be 4.5 mm.

The situation becomes more complex when bonding steel and aluminium parts. Temperature differences will then create either a deformation of the bonded parts or, if the structure is too stiff, a corresponding stress in the bondline, which may lead to failure and cracks.




*3.21* Difference in thermal elongation.

© Woodhead Publishing Limited, 2010

## 3.5 Surface treatment strategy

The most important element for successful structural bonding is adhesion on the surfaces of the substrates. Small changes on the surfaces may lead to a different adhesion profile, so a proper surface treatment is required in all structural bonding applications. This is a real challenge for adhesive applications since adhesion cannot be predicted or calculated for an individual surface. It also cannot be detected after bonding using non-destructive methods. Mistakes in surface treatment can lead to failure in the long term owing to the influence of environmental factors like moisture. Since adhesion properties for structural bonding applications must always be tested, efficient test methods are required in order to guarantee good adhesion for the whole service life.

Specific surface treatment strategies are available for the most commonly encountered surfaces on metals, composites or plastic substrates and adhesive formulators know how to achieve the desired adhesion. It is of no real value to list the numerous successful pretreatment methods in this chapter, it is more important to understand the principles of the right strategy.

The first goal of pretreatment is to remove all contaminants and loose oxide layers from the surface. For composite or plastic substrates, the plasticisers or release agents used to prevent moulding must be removed. In many cases abrading followed by coating with a primer or adhesion promoter is successful. Cleaning with solvents has the same function, but is less common owing to health and safety hazards and environmental restrictions on volatile organic compound (VOC) consumption. This also applies to primers, which usually contain VOCs. Water-based primers are available for 1C PUR windshield adhesives.

The second goal of pretreatment is to obtain good wetting. Modern physical methods that treat the surface with high energy processes are often very successful. Such methods include low pressure plasma or atmospheric plasma. They create polar functional groups even on very unpolar surfaces like polypropylene, thus enabling good adhesion for the more polar PUR adhesives. They are also able to burn organic contaminants, creating an active surface. After pretreatment, it is recommended either to bond the activated surfaces within a short period of time or to apply a primer, which will allow the transport of pretreated parts and later bonding without reactivation. In either case, adhesion on the surfaces of the substrates must be tested.

## 3.6 Applications for PUR adhesives

Here we describe some typical structural bonding applications where polyurethanes are used. Other adhesives may be used for similar applications, but no other adhesive system can match such a broad spectrum of uses.

© Woodhead Publishing Limited, 2010

### 3.6.1 Buses

The frame structure of modern buses obtains its stiffness by bonding the roof, the side panels, the front end and the floor onto the structure (Fig. 3.22). Owing to the size of the bus, the tolerances and the production speed, 1C PURs are commonly used. When higher production speeds are required, 2C PURs with mechanical properties similar to 1C PURs can be used.

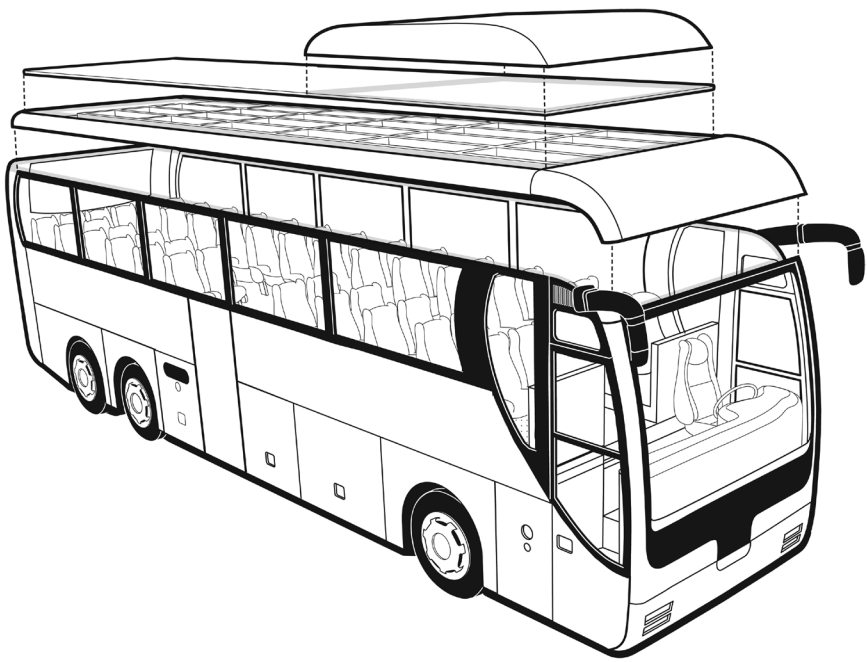
The bonded panels contribute significantly to the stiffness of the bus, enabling lightweight structures to be built. In the same way, bonded windows increase the overall stiffness of the structure (Fig. 3.23).

### 3.6.2 Rail

In rail applications, the bonding of windows is state-of-the-art. Figure 3.24 shows the complete front end of the train, made from glass fibre composite, which is also bonded onto the metal frame.

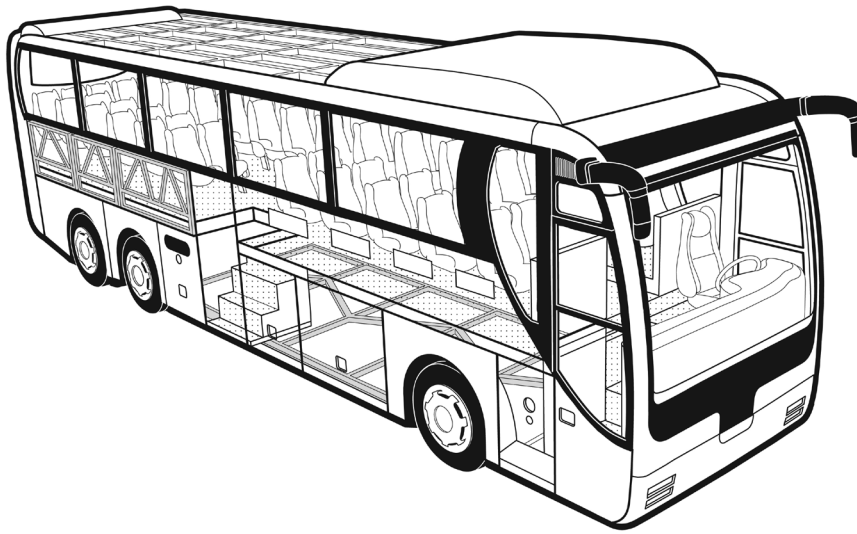
### 3.6.3 Automotive

Figure 3.25 shows some of the numerous applications of PUR adhesives in the automotive industry. In the body shop, a 2C structural adhesive is used to

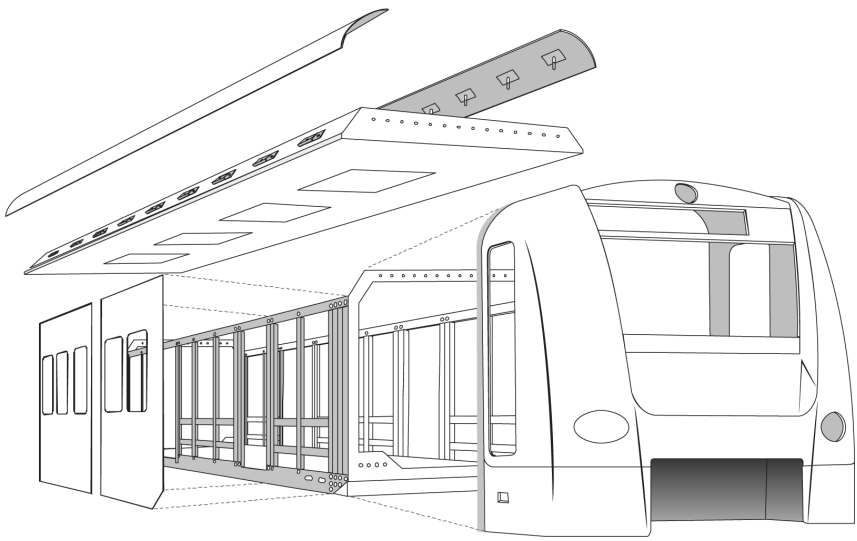


*3.22* Bonding of the roof and air conditioning systems in bus production.

© Woodhead Publishing Limited, 2010



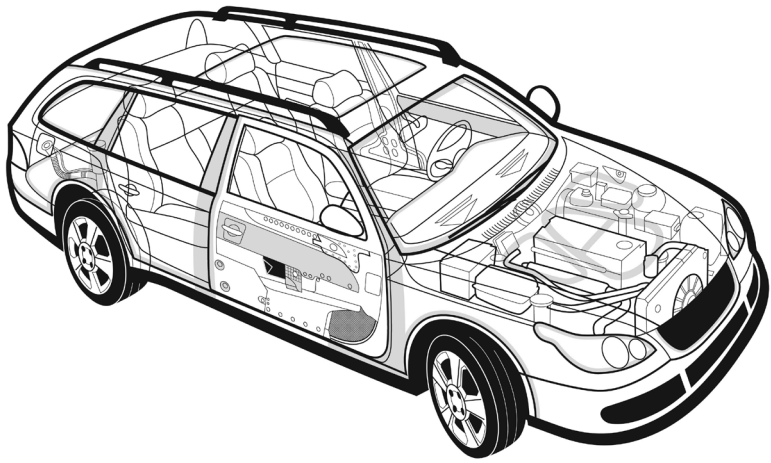
*3.23* Bonding of floor and side panels in buses.



*3.24* Bonding in rail applications.

bond the inner and outer metal sheets of aluminium hoods. This increases the stiffness of the hood without any surface marking. Modified crash-resistant PUR adhesives which are used in the hybrid joining of spot-welded flanges, provide additional stiffness to the complete body structure. The windshields are installed with warm applied 1C PUR, avoiding any additional fixation. The

© Woodhead Publishing Limited, 2010



*3.25* Several automotive applications.

headlights are bonded with a rubber-like warm melt 1C PUR and a carbon fibre composite roof is installed with a 2C PUR. For interior trim parts, 1C PUR reactive hotmelts are used for laminating fabrics onto door trims which have to withstand high stresses at temperatures at about 100°C. The bolts needed for fixing trim parts are also bonded with 1C reactive hotmelts.

### 3.6.4 Marine

Figure 3.26 shows the application of 1C PUR adhesives in leisure boat production. In this example, the hull is made of glass fibre composite. Since large tolerances in the bondline are expected, a thick adhesive layer is necessary. The adhesive is not applied as a bead but in large dots. This allows better access to moisture and so speeds up curing.

On luxury ships with teak decks, the teak is bonded with 1C PUR onto the deck, thus providing a smooth surface without any bolts and the joints are filled with a PUR sealant (deck caulking).

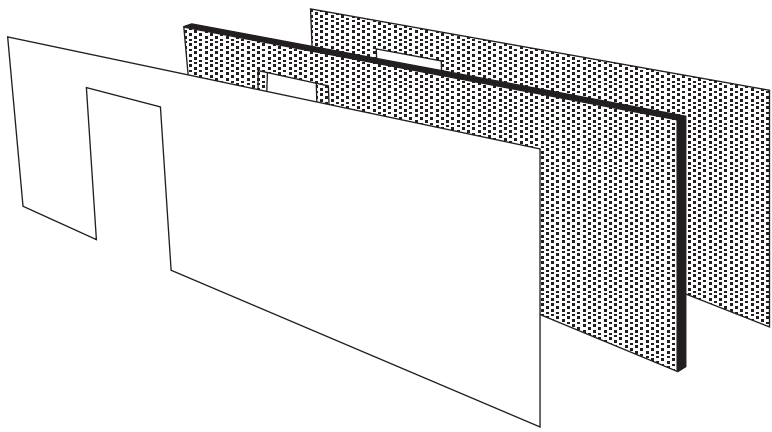
### 3.6.5 Sandwich panels

Sandwich panels are used as insulation walls in buildings and on trucks (Fig. 3.27). 2C PURs or 1C reactive PUR hotmelts are used in their production. The 2C PURs cost less but need more time to reach the required handling strength for panels stored in a stack. The handling strength for production of reactive PUR hotmelts is reached on the assembly line and the increase in productivity compensates for the higher cost of the adhesive. Owing to the large bonded area, the mechanical properties are of minor importance, but the system must cross-link, otherwise a static load would lead to the

© Woodhead Publishing Limited, 2010



*3.26* Adhesive applications in a leisure boat.



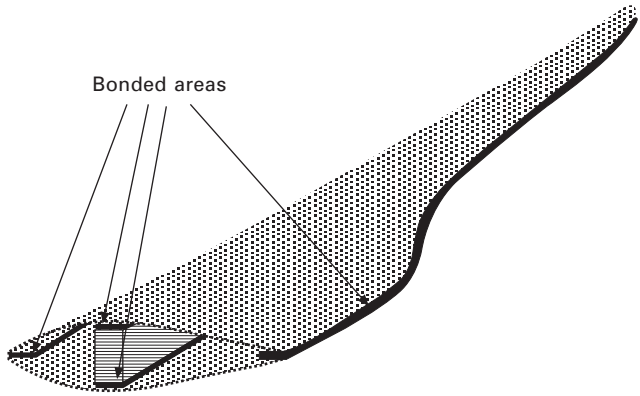
*3.27* Bonding of sandwich panels.

panels bending under load. Panels used for buildings or inside ships need a fire-rated PUR adhesive.

### 3.6.6 Rotor blades for wind turbines

Figure 3.28 shows the areas bonded with 2C PUR on rotor blades. The two half-shells around the perimeter and a reinforcement bar inside are bonded with a structural PUR adhesive. In this application, the adhesive has to withstand tens of millions of cyclic loads and also needs a high $E$ to minimise bending of the blade. Owing to the size of the parts, with lengths of up to 50 m, there are large tolerances and the adhesive must also work at thicknesses of more than 20 mm.

© Woodhead Publishing Limited, 2010




*3.28* Principle design of rotor blades for wind turbines.

### 3.6.7 Laminated beams

Structural bonding of wood has been practised for hundreds of years. To achieve high strength, moisture-stable wooden joints, 1C PUR prepolymers are the preferred adhesive today. Figure 3.29 shows a roof structure made with beams laminated using 1C PURs. With this technology, much larger spans can be achieved than those using beams made from single tree trunks.

Wooden panels bonded with finger joints are stacked in several layers (Fig. 3.30). The number of layers is not limited and therefore the beams can be made to order for the designed load (Fig. 3.31).

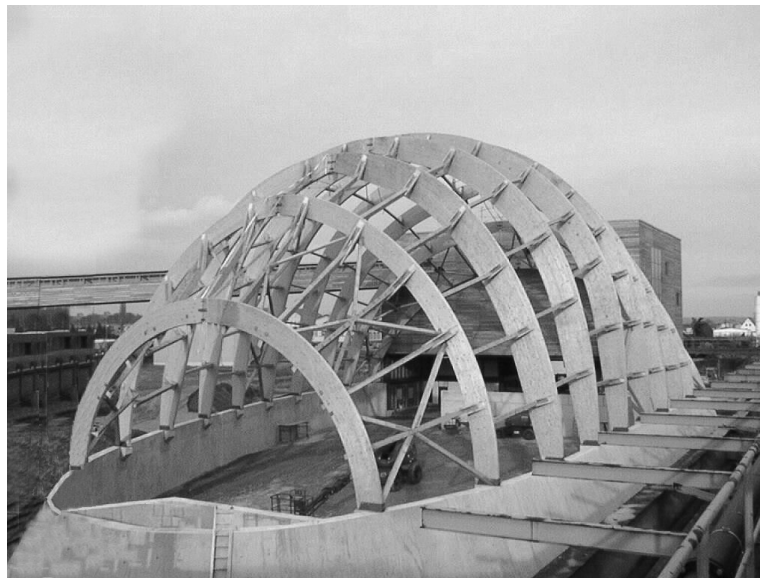
PUR adhesives have inherently good adhesion on wood and the mechanical strength usually surpasses that of the wood itself. This technology allows the use of wooden structures for larger buildings, thus contributing to ecological construction practices. With regard to emissions from the adhesive during its service life, PURs are unmatched since cured adhesives have zero emissions.

### 3.6.8 Windows

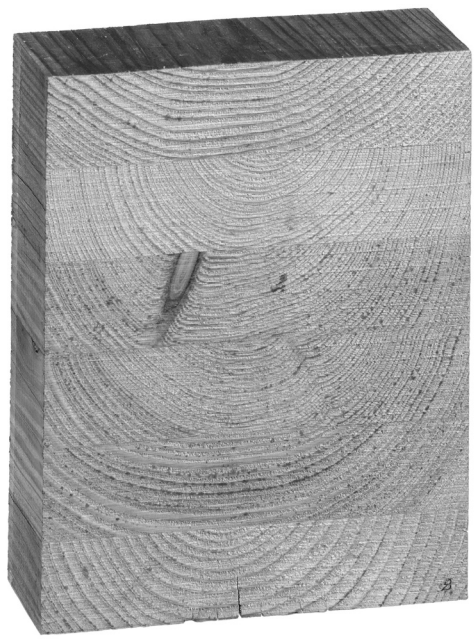
A new method of producing windows is based on the same principles as windshield bonding in automobiles. The adhesive uses the glass as an integral part of the window, increasing the stiffness of the window and thus reducing the weight of the frames, since steel reinforcement bars are no longer needed. A further benefit is that production can be simplified and automated.

The left-hand picture in Fig. 3.32 shows a rebate bonding directly on the edges of the insulating glass. In this application, the compatibility of the insulating glass sealant/adhesive has to be considered, since migration of small molecules such as plasticisers, stabilisers or catalysts can influence

© Woodhead Publishing Limited, 2010

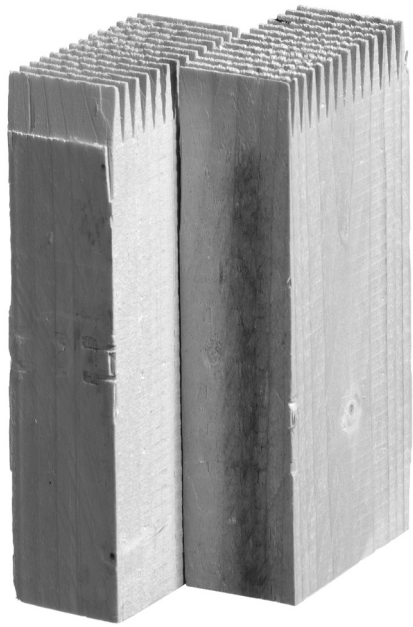


*3.29* Roof structure built with laminated beams (with kind permission of Purbond AG, Switzerland).

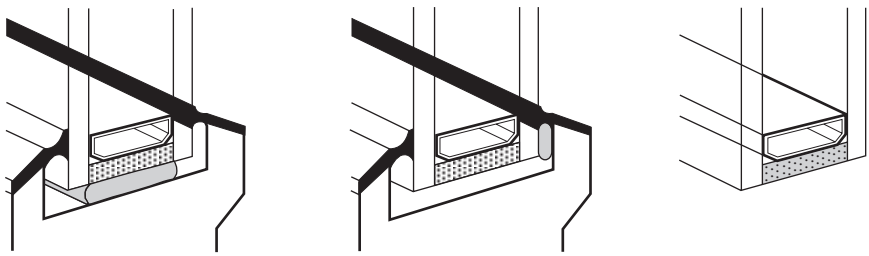


*3.30* Layers of bonded wooden panels for laminated beams (with kind permission of Purbond AG, Switzerland).

© Woodhead Publishing Limited, 2010



*3.31* Finger joint design for the bonding panels for laminated beams (with kind permission of Purbond AG, Switzerland).




*3.32* Different designs (a, b, c) for bonding insulating glass into a window frame.

durability. In the middle picture, the bonding is on the glass side. In this case it is important to have enough UV-protection when using a PUR adhesive. The right-hand picture shows the edge adhesive of the insulating glass, which is a 2C PUR and provides the correct mechanical properties for the rebate bonding, reduces diffusion of water vapour into and argon out of the insulating layer and offers the necessary compatibility for rebate bonding. Deformation of the window through differences in thermal elongation should be considered carefully, since even a small bending of the window would lead to leakage, reducing the energy efficiency of the window system.

© Woodhead Publishing Limited, 2010

## 3.7 Conclusions

Structural bonding systems must be designed by skilled engineers. The engineers have to understand how the chemistry of PUR adhesives allows the creation of tailor-made adhesives for a given application. Thus they do not start with an existing adhesive, but by defining the properties required and then designing the adhesive for this purpose. The mechanical and adhesion properties of the substrates and the adhesives have to be taken into account when designing the bonded structure. The properties of these structures can be calculated and the durability can be predicted using methods similar to those for plastic and metal structures. Adhesion tests are always necessary to qualify a structural bond. A few examples show the wide variety of possible applications.

Considering all these aspects, adhesive bonding is the joining technology of choice, in particular for durable, lightweight structures built up from different materials. Polyurethanes are the most versatile technology base for such adhesives.

## 3.8 References

Burchardt B, Diggelmann K, Koch S, Lanzendörfer B, Wappmann R and Wolf J (2006), *Elastic Bonding*, second revised edition, Verlag Moderne Industry, München.

Burchardt B, Schulenburg J O and Linnenbrink M (2009), 'The latest developments in hybrid joining: New building blocks for lightweight structures', *Adhesion Extra, Adhesives and Sealants*, **10**, 22–27.

Burckhardt U (2009), *Moisture-hardened Polyurethane Compositions Containing Compounds Comprising Aldimine,* USPTO Patent Application 20090159204.

Deimel A (1993), *Einfluss der Klebstoffsteifigkeit auf das Verformungsverhalten geklebter Fahrzeugkomponenten*, Diploma Thesis, Fachhochschule München.

Habenicht G (2006), *Kleben, Grundlagen, Technologien, Anwendungen*, 5. Auflage Springer-Verlag, Berlin, Heidelberg.

Klebtechnisches Zentrum http://www.ifam.fraunhofer.de/index.php?seite=/2804/technologietransfer/ktzentrum/ (Accessed July 27)

Meier-Westhues U (2007), *Polyurethane – Lacke, Kleb- und Dichtstoffe*, Vincentz Network, Hannover.

Schlimmer M (2004–2006), *Berechnung und Auslegung von Klebverbindungen*, Zeitschrift Adhäsion, Wiesbaden, Vieweg und Teubner GWV Fachverlage, Teil 1-5, 5-12 (2004) und 1-3 (2005), 5-6 (2006).

Schulenburg J O and Kramer A (2004), 'Structural adhesives: Improvements in vehicle crash performance', *SAE Transactions*, **113**(5), 111–114.

© Woodhead Publishing Limited, 2010

# 4

# Advances in structural silicone adhesives

C. WHITE and K. TAN,
National Institute of Standards and Technology, USA;
A. WOLF, Dow Corning Corporation, Germany; and
L. CARBARY, Dow Corning Corporation, USA

**Abstract**: This chapter presents the latest research on silicone structural adhesives. Beginning with an introduction to silicone adhesives, this chapter discusses chemical and physical properties of silicone adhesives which make them versatile and cost-effective solutions in a wide variety of applications. Developments in the chemistry and formulation of silicone adhesives are then reviewed. The final section of this chapter concentrates on advances in the use of silicone adhesives in construction, electronics, domestic applications, renewable energy, automotive and aerospace industries.

**Key words**: silicone, structural adhesives, silicone formulation, silicone chemistry.

## 4.1 Introduction

A structural adhesive is a substance that fastens together elements to produce high modulus, high strength, permanent bonds. It must be capable of transmitting structural stress without loss of structural integrity within design limits. Thus, it substantially contributes to the structural integrity of continuously stressed assemblies during their expected service lives under relatively severe service environments. There are many types of structural adhesive, including epoxy, silicone, urethane and acrylic. Silicone structural adhesives can be further classified as liquid-applied, curable, elastomeric materials. They behave as a liquid during their application, which is important in order to achieve good wetting of the substrate surfaces, and cure to form a high molecular weight, rigid, cross-linked, solid elastomer. By nature, silicones have lower cohesive strength than other structural adhesives such as epoxies; however, this property is an advantage in a number of applications. The lower strength and modulus mean that silicones are excellent for repair and rework applications and are ideally suited for applications that require a certain level of stress flexibility in the adhesive joint. The latter need typically arises when the adhesive joint must be capable of absorbing a certain amount of movement, for instance, resulting from differences in thermal expansion between the substrates, vibration of the components, exterior loads, and so on. Silicone structural adhesives provide excellent adhesion to a wide range of



© Woodhead Publishing Limited, 2010

substrates, are capable of operating over a wide range of service temperatures and have long service lives even in harsh environments. Furthermore, they can be formulated for either high or low electric and thermal conductivities. Because of these unique properties, they are used in a wide range of electric, electronic, automotive, domestic appliance and construction applications.

## 4.2 Properties of silicone structural adhesives

Silicone adhesives often are referred to as structural sealants or adhesive sealants, which may lead people to the conclusion that these materials will not perform as a structural adhesive. However, because of their flexibility, silicones can perform as either adhesive or sealant, thereby making them a versatile and cost-effective solution in a wide variety of applications. Silicones occupy the regime between inorganic silicates and organic polymers and exhibit some of the properties of their extremes owing to the combination of the partially ionic siloxane (Si–O–Si) bond and the organic substituent groups. Because of these unique features of their polymeric backbone, silicone adhesives and sealants possess:

- easy wet-out
- low toxicity
- ability to wet difficult (low surface energy) substrates, good adhesion to a wide variety of substrates
- excellent elastomeric properties (high movement capability, high elastic recovery (85–98%), low creep, good fatigue resistance)
- environmental resistance (including but not limited to ultraviolet- (UV), moisture-, oxygen- and ozone-resistance)
- high temperature resistance (up to 300°C)
- flexibility, including cold temperature flexibility (down to –90°C or –115°C for one- and two-part formulations, respectively)
- electrical properties ranging from high resistivity to high conductivity
- fire resistant properties
- high gas permeability
- chemical resistance
- effective sealing, even of larger gaps, against a variety of fluid types
- high optical clarity (adhesive can be formulated from opaque to optically clear).

These properties are discussed in greater details below. Owing to their low modulus of elasticity (typically below 10 MPa), silicone adhesives have gained popularity in structural and semi-structural applications requiring flexible bonding, resistance to environmental extremes and high durability of the adhesive bond.

© Woodhead Publishing Limited, 2010

Most silicone adhesives have a very low level of toxicity; this explains the use of certain silicone adhesive grades in biomedical applications, including class II and class III medical devices, as defined by the European Economic Community Medical Device Directive (The European Parliament and the Council of the European Union, 2007). Special formulations are also available for applications involving food contact.

When applied in their liquid state, silicone adhesives wet most substrates, even under difficult conditions, because of their low surface tension (ca. 21–22 mN $m^{-1}$). When formulated with suitable adhesion promoters, they exhibit very good adhesion to a wide variety of substrates. Silicone adhesives also display excellent self-adhesion. Silicones have a critical surface tension of wetting (24 mN $m^{-1}$), which is higher than their own surface tension. This enables liquid silicones to spread on cured silicones, a process that promotes film formation and surface coverage as a first step to good adhesion.

Cured silicone adhesives display good elastomeric properties, such as high movement capability, high elastic recovery (85–98%) and low creep. These properties are also much less temperature dependent than those of other common organic adhesives. Their good fatigue resistance allows them to withstand repetitive movement in the adhesive joint caused by flexible flanges, equipment or component vibration, as well as temperature cycling of joints with high differential thermal expansion of substrates.

Cured silicone adhesives display extraordinary environmental resistance (Wolf, 1999). The lack of chromophores (light-absorbing groups) along the polymeric backbone and the high Si–O bond energy provide inherent resistance to sunlight. With proper selection of the organo substituents in the siloxane polymer (e.g. fluoro-organo, phenyl, etc.), silicone adhesives can meet the most demanding chemical resistance requirements, even in high-temperature applications. Silicone adhesives display good resistance to oxidation by ozone and oxygen. The oxidation of the hydrocarbon side groups results in the formation of carbonyl groups (Israeli *et al.*, 1992a, 1992b, 1993, 1995). Because carbonyl groups do not interact strongly with other chemical groups in silicone polymers, the oxidation has little effect on the mechanical properties of the adhesive. Silicone adhesives display extreme low temperature flexibility, standard formulations remain flexible down to –60°C, special one-part (condensation cure) formulations down to –90°C and special two-part formulations down to –115°C. Cured silicone adhesives display excellent high temperature stability. Certain products can be used in applications involving continuous exposure to 260–300°C or intermittent exposure up to 340–350°C. The excellent environmental resistance of silicones is consistent with the fact that, even after prolonged service periods in extreme climates, silicone adhesives show comparatively minor changes in physical properties (Oldfield and Symes, 1996).

© Woodhead Publishing Limited, 2010

In general, silicone adhesives are good insulators and are characterized by high dielectric strength, high volume resistivity, low dielectric constant and a low dissipation factor. The low dissipation factor is a desirable property because it minimizes the waste of electrical energy as heat. However, by changing the type and amount of compounding ingredients, the formulator of the adhesive is able to influence its electrical properties over a wide range.

Cured silicones display favorable fire performance characteristics, for example a low heat release rate and an insensitivity of burn rate to fire severity, and the key combustion products exhibit minimal toxicity to humans. Indeed, pyrolysis of silicones results in the formation of carbon dioxide, water, amorphous silica and low yields of carbon monoxide, but no other polymer-specific toxic gases are generated. The combustion products demonstrate minimal potential for corrosive damage. A substantial portion of the amorphous silica generated during the combustion process is deposited on the fuel-generating, burning surface, resulting in the formation of a silica char. These surface silica deposits are believed to contribute to the unique burning characteristics of silicones, that is, the relatively low heat release rate and the minimal dependence of heat release rate on applied external heat flux (fire severity).

The large free volume and mobility of silicone polymer chains give rise to a high diffusion coefficient and high permeability of gases or vapors. For many applications, high gas permeability is a desirable property. For instance, the higher moisture transmission rate of silicone at ambient and lower temperatures allows the formulation of fast-curing one-part systems that cure at temperatures as low as –40°C. For applications in which high permeability is not desired, special silicones with reduced permeability have been developed or system solutions are available.

Silicone adhesives are effective in sealing even larger gaps against a variety of fluids such as oil, water, coolant liquid or air. Their large gap-filling capability often allows the relaxation of surface flatness requirements and provides for ease of alignment and assembly. Since the rheology of silicone adhesives can be varied over a wide range and tailored to the specific requirements of the application, their application process can be easily automated.

## 4.3 Product forms and cure chemistry

Products are available in a variety of forms, from paste-like non-slump materials to flowable self-leveling adhesives. Both single- and multi-component versions are available. Silicone adhesives can be formulated based on different chemistry of the cure; however, the vast majority of commercial products sold are based on condensation cure chemistry. Most of these products are applied and cured under ambient conditions and are,

© Woodhead Publishing Limited, 2010

therefore, termed room-temperature vulcanizing (RTV) products. Specialty condensation-curable hot-melt adhesives also exist. Other specialty silicone structural adhesives are based on either RTV or high-temperature vulcanizing (HTV) addition-cure or light-induced photo-cure chemistry. Combination of photo-cure chemistry with other (shadow) cure (RTV/low-temperature vulcanizing (LTV)) chemistry exists, ensuring that the adhesive cures fully in regions not directly reached by radiation.

### 4.3.1 Condensation cure chemistry (RTV)

One-part condensation cure silicone adhesives are based on siloxane polymers with hydrolyzable groups attached to the polymer chain ends combined with a hydrolyzable silane cross-linker, which also acts as a water scavenger to maintain the shelf-stability of the unopened container. Once the one-part package is opened, atmospheric moisture reacts with the hydrolyzable groups, resulting in the formation of silanol (Si–OH) groups. The terminal silanol groups formed initiate condensation reactions under acidic or mild basic conditions. Thus, one-part cure systems depend on atmospheric moisture to initiate cure and cure proceeds from the outside into the interior of the material. The cure by-products, which diffuse out of the RTV silicone and may cause a characteristic smell during cure, include alcohols (Brown and Hyde, 1964; Weyenberg, 1967; Smith and Hamilton, 1972), ketoximes (Sweet, 1965), carboxylic acids (Ceyzeriat, 1964; Bruner, 1962a, 1962b; Beers, 1968, 1981; Kulpa, 1967), amides (Goelitz *et al.*, 1968; Sattlegger *et al.*, 1968), hydroxylamines (Pande and Ridenour, 1969; Boissieras *et al.*, 1967; Murphy, 1967; Boissieras and Ceyzeriat, 1969), ketones (Takago *et al.*, 1974; Takago, 1979) and amines (Nitzsche and Wick, 1962; Hittmair *et al.*, 1968; Nitzsche *et al.*, 1972). Alkoxy-, oximo- and enoxysilane cross-linkers eliminate by-products displaying a pH-neutral chemical reaction, that is they are neither acidic nor basic and, therefore, are the key component of neutral, non-corrosive cure chemistry. Amidosilane-based cure chemistry is also considered to be neutral, although it may cause corrosion on sensitive substrates (for instance, stress corrosion has been observed on brass in contact with benzamide-cure silicone). The acetoxysilane-based cure system releases acetic acid; aminoxy- and aminosilane-based cures form alkaline hydroxylamine or amine by-products. Neither acidic nor alkaline cure products should be employed in contact with substrates that are susceptible to corrosion. It is important to keep the acid curing materials away from cementitious and alkaline substrates to minimize acid–base reactions resulting in poor bonding.

In many cases, the cure by-products are sufficiently acidic or basic to act as condensation catalysts; these are referred to as self-catalytic cure systems. While these systems provide good depth of cure, an additional condensation

© Woodhead Publishing Limited, 2010

catalyst generally is required to achieve a tack-free surface. This condensation catalyst may be a tin compound (White *et al*., 1983) such as stannous octoate and dibutyltin dilaurate, or an organotitanate (Smith and Hamilton, 1972). Titanates are employed primarily in neutral cure (alkoxy, amide or oxime) systems, while tin catalysts are added to acetoxy-, oxime- and amine-cure formulations. There is also the option of formulating alkoxy-cure systems with tin catalysts; however, in order to achieve good shelf-stability, the system must be kept free of water and silanol (White *et al*., 1983; Dziark, 1983; Lucas and Dziark, 1984; Chung, 1985).

In two-part condensation cure systems, the silane cross-linker and catalyst are packaged together as one reactive component, with the mixture of polymer and filler as the unreactive component. The two components must be mixed shortly before application. Once mixed, the cross-linking reaction proceeds without the need for external, atmospheric moisture. To achieve successful completion of cure and good heat stability of the cured material, it is important to ensure that the cure by-products completely leave the curing adhesive. The key benefit of two-part condensation cure systems is their ability to achieve deep-section cure and high 'green strength' within a few hours. For full development of physical properties, several days may be required to eliminate fully cure by-products from the bulk.

As in one-part systems, the condensation cure involves a functional silicone chain-end, typically silanol, and a polyfunctional silane. Suitable cross-linkers are tri-, tetra- or multi-functional materials, such as alkyl orthosilicate esters, and esters of ortho- (Brod and Schweitzer, 1958) or meta-silicic acid (polyalkylsilicates) (Polmanteer, 1960). *N*-propyl orthosilicate and tetraethyl orthosilicate are the most commonly used cross-linkers in two-part systems. Generally, the same condensation cure catalysts that apply to one-part systems are also employed in two-part systems.

Hot melt silicone adhesives are solventless thermoplastic compositions that are applied at elevated temperatures above the melting or softening point of the composition. This allows the heated hot melt to be transferred and applied in a flowable viscous liquid state. Upon cooling, the hot melt returns to a semi-solid state. The compositions of hot melt silicone adhesives are quite similar to those of pressure-sensitive adhesives. Silicone hot melts are based on high levels (commonly 60% and above) of a silicate resin and appropriate amounts of reactive and non-reactive silicone polymers to provide viscous, semi-solid systems at room temperature. A refinement of this technology is the incorporation of reactive end groups on the polymer chains that post-cure over time via regular RTV chemistry to a temperature-insensitive, cross-linked state that has enhanced performance characteristics (Cifuentes *et al*., 1994, 1996, 1999, 2003; Vincent *et al*., 1994; Strong *et al*., 1995; Be *et al*., 2004). Reactive hot melts combine the advantages of conventional liquid reactive adhesives, such as resistance to high temperature creep and

© Woodhead Publishing Limited, 2010

solvents, with typical hot melt attributes such as zero volatile content, easy dispensing, and high green strength.

### 4.3.2 Addition cure chemistry (RTV and LTV)

There are numerous applications in which condensation-cure silicone adhesives are not suitable. This is because they are relatively slow to cure, require moisture to cure (one-part) and evolve by-products that cause shrinkage. Adhesives used in automotive, electronics, microelectronics, microelectromechanical systems, avionic, and other 'hi-tech' applications usually are confined to very small volumes, which can make access to moisture difficult. Also, their proximity to very sensitive mechanical or electronic components requires a cure system that does not evolve reactive chemicals. Addition cure systems based on thermally induced reactions respond to the bonding needs that are not met by the condensation cure systems.

Cross-linking is accomplished in the RTV or LTV thermal addition cure system via a hydrosilation reaction whereby a Si–H group in a low molecular weight siloxane is added to a vinyl group in a siloxane polymer (Anonymous, 1967). The vinyl group may also be located on the siloxane oligomer and the silicon hydride group on the polymer. Generally, however, a Si–H polyfunctional siloxane oligomer plays the role of the cross-linker and the siloxane polymer is blocked at the vinyl end. This reaction occurs readily at room temperature in the presence of a platinum catalyst and can be accelerated by heat. The platinum catalyst can exist in a variety of forms; more commonly used are chloroplatinic acid, $H_2PtCl_6$, and its complexes with vinyl-functional cyclic siloxanes, such as tetramethyltetravinyl-cyclotetrasiloxane (Eckberg, 1982a) or linear siloxanes, such as divinyltetramethyldisiloxane (Eckberg, 1982b). The platinum–siloxane complexes have better compatibility with the siloxane medium and achieve similar cure rates at a lower addition level.

The addition cure has a number of advantages when compared with the condensation cure system. First, it does not produce any cure by-products and therefore does not give rise to any odor or shrinkage upon cure; second, it achieves almost instant homogenous deep-section cure at elevated temperature; third, it is not prone to aging in high service temperature. The main disadvantages are its easy inhibition by a number of electron-donating substances, such as amines and organosulfur compounds and the fact that it requires special proprietary adhesion promoters in order to achieve good adhesion (see Stein *et al.*, 1994, 2002; Stein, 1994, 1996; Stein and Davis, 1995a, 1995b; Stein and Rubinsztajn, 1995; Hara, 1999; Ahn and Lutz, 2002; and literature cited therein). Without incorporation of adhesion promoters, the cross-linked siloxane structure does not contain substantial amounts of any reactive groups after completion of an addition cure. Moreover, the Si–H and Si–$CH{=}CH_2$ groups are not particularly reactive towards many chemical

© Woodhead Publishing Limited, 2010

groups found on surfaces of common substrates. It is therefore expected that no coupling between the polymeric network and the substrate will take place during application and cure, unless special adhesion promoters are added to the formulation.

Because the hydrosilation reaction in the presence of a platinum catalyst occurs readily at room temperature, one-part addition-cure RTV systems are not feasible. Still, one-part products can be formulated that are shelf-stable at room temperature, but for which the cure is triggered by a slight increase in temperature, for example up to 60°C to 80°C. In this LTV cure system, the platinum is sequestered by chelation with an inhibitor, usually a conjugated polar species. Sequestered cure systems generally have a rather short shelf life, typically only a few days. Another interesting approach is based on the microencapsulation of the platinum catalyst (see Evans *et al*., 1993, and literature cited therein). Cure is then activated either by heating the composition above the melt temperature of the encapsulating shell or by addition of a suitable solvent.

For two-component compositions, the platinum catalyst, as well as the fillers and a part of the vinyl functional siloxane polymer represent one package (part A), while the silicon hydride material and the remaining part of the vinyl functional siloxane polymer represent the other package (part B). The two components are mixed together in the proper ratio at the point of application. Cure of these 'uninhibited' formulations initiates immediately upon mixing. Therefore, in order to extend the pot-life and simplify application, two-part addition cure formulations often contain a 'cure inhibitor' or 'cure retarder'. These are chemicals containing carbon–carbon triple bonds capable of complexing the platinum catalyst. Ethynylcyclohexanol (Ikeno and Fujiki, 1992), 3-methyl-3-hydroxy-1-butyne (Fujiki, 1996), $(HCCCH_2O)_3SiMe$ (Nishiwaki and Urabe, 1994), and dialkyl acetylenedicarboxylates (Eckberg, 1982b; Melancon, 1985; Brummer *et al*., 2003) are some of the cure retarders referred to in the patent literature. As in the above-described one-part systems, cure is triggered by a slight increase in temperature.

### 4.3.3 Electron-beam and photo-cure induced addition chemistry

Other addition cure systems that have emerged in recent years are the UV and electron beam (EB) radiation cure systems. UV curing is initiated by excitation of a photo-initiator through absorption of photons of UV radiation, while EB curing involves ionization of adhesives with high energy electrons. The development of these systems has been prompted by the ever-increasing need for fast cure rates and low cure temperatures. The UV cure system is more common than the EB-based system for general applications in silicone adhesives. Although both UV radiation and thermal curing offer rapid cure

© Woodhead Publishing Limited, 2010

rates, there are several advantages gained from using UV radiation instead of heat for curing silicone systems. The main benefit is that a low cure temperature allows deposition and cure of the adhesive on heat-sensitive substrates like polyolefins and other plastic materials. Also, UV curing requires minimal energy, thus eliminating major energy losses typically encountered in thermal cure systems. The UV cure system contains an epoxy or a vinyl ether functionalized polydimethylsiloxane (PDMS) polymer and a photo-catalyst (Stein and Eckberg, 1990). The latter, a diaryliodonium salt, is photolytically decomposed to form an active acid that polymerizes the epoxy or vinyl ether groups and cross-links the network. Theoretically, this system offers the advantages of the thermal cure systems that include fast cure and low temperature processing. However, these systems are sensitive to atmospheric humidity and the possible toxicity of the catalyst may be an issue.

## 4.4 Silicone adhesive formulations

Formulations of silicone adhesives are based on the following ingredients:

- reactive and/or non-reactive siloxane polymer
- reactive and/or non-reactive silicone resin
- plasticizer
- cross-linker
- catalyst
- adhesion promoter
- reinforcing, semi-reinforcing, and/or non-reinforcing (extending) fillers
- special additives.

The functionalities of the reactive components (polymer, cross-linker, adhesion promoter) and the nature of the catalyst depend on the cure chemistry of the formulation. For example, the reactive polymer may have functionalities of silanol, oximosiloxy, alkoxysiloxy, alkoxysilylethylene, vinyldimethylsiloxy, or other reactive groups, depending on the cure chemistry utilized. Tables 4.1 and 4.2 provide an overview of the different formulation ingredients and their functions in condensation and addition cure systems, respectively (De Buyl, 2001).

### 4.4.1 Polymers

*Silanol-terminated PDMS polymer*

RTV condensation cure adhesives are formulated from $\alpha,\omega$-silanol-endblocked siloxane polymers with a molecular weight of about 20,000–200,000 Daltons, corresponding to a viscosity of about 1 Pa s to 300 Pa s.

© Woodhead Publishing Limited, 2010

*Table 4.1* Formulation ingredients and their functions (condensation cure chemistry)

| Component | Typical chemical | Function |
|---|---|---|
| Polymer | Hydroxyl ~SiOH, | Backbone required to form the elastomeric network |
| Plasticizer | Trimethylsiloxy-endblocked-PDMS | Adjustment of mechanical properties such as hardness, viscoelasticity, rheology |
| Reinforcing fillers (active) | Fumed Silica ($SiO_2$); Precipitated calcium carbonate ($CaCO_3$); Carbon black | Thixotropic reinforcing agents (non-slump), adjustment of mechanical properties (cohesion); provide toughness for the elastomer as opposed to brittle materials |
| Non-reinforcing fillers (passive) | Ground calcium carbonate ($CaCO_3$) | Reduce formulation cost; adjust rheology and mechanical properties |
| Cross-linkers | Acetoxy ~$Si(OOCCH_3)_3$<br>Alkoxy ~$Si(OR)_3$<br>Oxime ~$Si(ON{=}CRR')_3$<br>Amine ~$Si(NHR)_3$ | Cross-linking of the polymeric component; provide network structure |
| Specific additives | Catalysts: organo-Sn, -Ti, -Pt, -Zn, -Rh<br>Adhesion promoter: X-$CH_2CH_2CH_2$-$Si(OR)_3$;<br>Water scavenger;<br>Pigments;<br>Rheology additive | Control of the rate of the curing process<br>Enhance the adhesive bonding properties against substrates<br>Prolonging shelf life<br>Offering wide range of colors<br>Adjust ease-of-use characteristics and features |

*Table 4.2* Formulation ingredients and their functions (addition cure chemistry)

| Component | Polymer/additive | Function |
|---|---|---|
| Polymer | Alkenyl functionalized PDMS | Backbone of silicone cured network |
| Cross-linker | Si–H functionalized polymer | Cross-link alkenyl PDMS |
| Catalyst | Platinum-based complex | Fast cure at room or high temperature |
| Inhibitor | Various organic or organosilicone types | Delays cure at room temperature and increases pot life |
| Inorganic or organic filler | Silica, carbon black | Reinforces mechanical strength |
| Pigment | Various metallic oxides | Color/thermal stability |
| Adhesion promoter | Various silanes and proprietary complex compounds | Enhance adhesion of silicone to specific substrates; prolonged durability |

### *Vinyldimethylsiloxy-terminated PDMS polymer*

RTV/LTV addition cure systems are formulated from vinyl-endblocked PDMS polymers with a molecular weight of about 63,000–140,000 Daltons, corresponding to a viscosity of about 10 Pa s to 100 Pa s.

© Woodhead Publishing Limited, 2010

### 4.4.2 Plasticizer (trimethylsiloxy-terminated PDMS polymer)

Owing to its excellent compatibility with the liquid siloxane polymer and the cured network, trimethylsiloxy-terminated PDMS polymer, often referred to as 'silicone fluid', is widely used as a plasticizer in silicone adhesives. The plasticizer can be selected either to lower the viscosity and/or to lower the modulus of the formulation. Most commercial silicone fluids have viscosities of 0.1–60 Pa s. These plasticizers have the same durability characteristics as the PDMS network. An interesting group of silicone fluids are the so-called 'reactive' plasticizers, in which a substantial fraction of the PDMS molecules are trimethylsiloxy-terminated at one end and silanol-terminated at the other end. These reactive fluids tie into the network during cure, forming loose polymer ends. By doing so, they plasticize the network internally. The benefit of these plasticizers is that they cannot migrate (bleed) from the cured formulation.

### 4.4.3 Cross-linkers

*RTV Condensation-cure*

Silane $R_{4-n}SiX_n$ cross linkers ($n = 3$) are used with one-part silicone cure systems. The reactivity of these cross-linkers is influenced by several factors, such as the number of hydrolyzable groups (X) attached per silicon atom, the number and type of organo-functional groups (R) attached to silicon and the substituents (R′) on the hydrolyzable group itself. A variety of these cross-linkers with different organic substituent R-groups and hydrolyzable leaving X-groups are commercially available. For instance, acetoxy cross-linkers are available with methyl, ethyl and vinyl R groups. Oxime cross-linkers can be purchased with methyl or vinyl R groups and methylethylketoxime (MEKO) or methyl-iso-butylketoxime (MIBKO) leaving groups, X. Blends of some of these cross-linkers are also commercially available. Standard blends are methyltriacetoxysilane (MTA) and ethyltriacetoxysilane (ETA), methyltrioximosilane (MTO) and vinyltrioximosilane (VTO), MTO and tetraoximosilane (TOS), and MTO, VTO, and TOS. These blends have tailored reaction rates, allowing an optimum balance of surface cure versus deep-section cure. The cross-linker is added at about 3.5–7.5% by weight based on the total formulation.

*RTV/LTV addition cure*

Both cyclic and linear silicon hydride cross-linkers are available. Linear trimethylsiloxy-endblocked poly[(hydrogenmethyl)(dimethyl)]siloxane cross-linkers are commercially available with viscosities between 0.005–0.1 Pa s

© Woodhead Publishing Limited, 2010

and molar hydrogen content between 0.7–1.5% by weight. The amount of cross-linker added to the formulation is adjusted based on its molar hydrogen content.

### 4.4.4 Catalysts

*Condensation-cure catalysts*

Commercially the most important condensation cure catalysts are dialkyl tin (IV) carboxylates, for example, dibutyltin dilaurate, dibutyltin dioctoate and dibutyltin diacetate[1] (commercially available, for example, as 'T-series catalysts' from Air Products and Chemicals, Allentown, PA, USA); tin (II) compounds, for example tin dioctoate and alkyl titanates, for example tetraisobutylorthotitanate, tetra-n-propyl titanate, titanium acetylacetonate and acetoacetic ester titanate (commercially available, for example, as Tyzor™, catalysts from Dupont, DuPont Building, 1007 Market Street, Wilmington, DE 19898, USA). The amount of catalyst added is typically in the range 0.05–0.2% for tin soaps and 0.5–2.0% for titanates, respectively, by weight based on the total formulation.

*Addition-cure catalysts*

A suitable catalyst for the hydrosilation addition-cure reaction is a metal of the platinum group in the periodic table, or a compound of such a metal. Platinum and palladium compounds are generally preferred based on their high activity. Platinum compounds are commercially the most important based on cost considerations. The platinum catalyst can exist in a variety of forms; more commonly used are chloroplatinic acid, $H_2PtCl_6$, and its complexes with vinyl-functional cyclic siloxanes, such as tetra (methylvinyl) cyclotetrasiloxane, or linear siloxanes, such as divinyltetramethyldisiloxane. The platinum–siloxane complexes have better compatibility with the siloxane medium and achieve similar cure rates at a lower addition level. The divinylsiloxane complexes in toluene are generally more active catalysts, while cyclic vinylsiloxanes provide a more moderate rate of cure. The platinum catalyst is generally used at a concentration of about 5–150 ppm based on the total formulation.

[1]Certain commercial products or equipments are described in this paper in order to specify adequately the experimental procedure. In no case does such identification imply recommendation or endorsement by the National Institute of Standards and Technology, nor does it imply that it is necessarily the best available for the purpose.

© Woodhead Publishing Limited, 2010

### 4.4.5 Adhesion promoters

Adhesion promoters are reactive silanes containing both organofunctional and hydrolyzable groups. These silanes are added at about 0.2–3% by weight, based on the total formulation in order to achieve self-priming adhesion characteristics. Upon cure, the adhesion promoter participates in the cross-linking reactions (Suzuki and Kasuya, 1989), but also establishes bonds between the silicone network and the substrate.

All the art and technology of a self-priming polymeric system resides in the choice and chemical design of the adhesion promoter molecules. Silane coupling agents are denoted by the general structure $RSiX_3$, where R is a reactive organofunctional group and X is a hydrolyzable group, such as a methoxy, ethoxy or acetoxy group. The variety of different organosilanes and their respective merits have been discussed in detail elsewhere (Plueddemann, 1982). Organosilanes are small, surface-active molecules, which easily can diffuse to the interface at the same time that cross-linking occurs in the bulk of the silicone composition. Once at the interface, they can improve adhesion through enhanced wetting and covalent bonding. Hydrolysis of the organosilane provides active silanol sites for hydrogen bonding. The silanol groups on the organosilane allow condensation reactions to occur, which result in the formation of Si–O–Si bonds between the silane molecule and the silicon-containing surface as well as the silicone network. It also is possible for the organofunctional group on the silane to react with chemical reactive groups present in the substrate surface. Silanes are particularly effective in the promotion of adhesion of silicones to metal, glass and siliceous surfaces in general. A recent study has shown that specific mixtures of silanes can provide better adhesive performance than the separate silanes and that an optimum composition is required (Van Ooij and Jayaseelan, 1999).

Suitable classes of adhesion promoters for condensation-cure RTV systems are functional silanes bearing aminoalkyl, mercaptoalkyl, epoxyalkyl, ureidoalkyl, acrylate and isocyanurate groups. Within these classes, the commercially most important adhesion promoters are aminopropyltriethoxysilane, aminoethylaminopropyltrimethoxysilane and glycidoxypropyltrimethoxysilane. Novel and more complex adhesion promoter systems are continually being developed to respond to the demands of emerging and future sealing and bonding technologies.

### 4.4.6 Fillers

Fillers are primarily added to adhesive formulations to improve their physical (viscoelastic) properties. Addition of fillers affects the rheological properties of the uncured material, such as extrusion rate, ‘body’, handling and tooling, as well as the elastomeric properties of the cured sealant, such as hardness,

© Woodhead Publishing Limited, 2010

modulus, elongation at break, tensile strength and abrasion resistance. The first type of filler is referred to as 'active' filler, the second as 'inactive' or 'extending' filler. Generally, a sealant formulation contains a combination of two or more active and inactive fillers. Surface area and energy (Wu *et al*., 1999), structure, density and availability of reactive surface groups influence the degree of interaction between fillers and the silicone rubber network.

Reinforcing fillers increase the tensile strength of the cured elastomer and reduce slump (sag) of the uncured material. Conventional reinforcing fillers are finely divided particulates that have a particle size of less than about 50 nm and include precipitated and fumed silicas (Brunauer, Emmett and Teller (BET) surface area of 150–300 $m^2\ g^{-1}$). Semi-reinforcing fillers have a primary particle size of between 50 nm and 500 nm, more typically between 70 nm and 150 nm, a BET surface area of about 20–80 $m^2\ g^{-1}$, and include fatty acid-treated precipitated calcium carbonates and calcium silicates (talc). Non-reinforcing fillers have a primary particle size of greater than 500 nm.

Non-reinforcing fillers interact very weakly with the silicone network. Examples include ground calcium carbonate (chalk), ground quartz, diatomaceous earth, mica, kaolin and bentonite clays, barium sulfate and aluminum hydroxide. In order to reduce the cost of the formulation on a per volume basis, low-density fillers, such as ceramic microspheres (commercially available, for example, as Z Light Spheres™, Zecosphere™ and Macrolite™ Ceramic Spheres from 3M Corporation, Saint Paul, MN, USA) and glass microbubbles may be added to the formulation. Filler content varies widely depending on the type of filler. Typical fumed silica content is in the 8–15% range, for ground calcium carbonate in the 15–45% range and for precipitated calcium carbonate in the 25–45% range (all ranges given as weight percent of the total formulation).

### 4.4.7 Special additives

*Heat stabilizers*

Iron oxides and carbon blacks are widely used as heat stabilizers in silicone sealants and adhesives. Iron carboxylate salts (Bayly, 1999), cerium hydrate, barium zirconate (Carlson and Glasbrenner, 1994), cerium and zirconium octoates (Lin, 1995), as well as porphyrins (Achenbach *et al*., 1998) are presented in the literature.

*Flame retardants*

Carbon black (Delatorre and Beers, 1978), hydrated aluminum hydroxide (Mitsuhashi and Tabei, 1997) and wollastonite (Alvarez and Shephard, 2001)

© Woodhead Publishing Limited, 2010

have been described in the patent literature as additives that improve the fire-resistance or self-extinguishing property of silicone adhesives. Platinum and platinum compounds also are known to improve the fire resistance of silicone compounds.

*Electrically conductive fillers*

Silicone adhesives have excellent dielectric properties, which make them good insulators. However, for some applications, such as electrically conductive adhesives, a substantial increase in electrical conductivity is highly desirable. This is achieved by adding electrically conductive fillers to the formulation. Conductivity is attained by the percolation of electricity through the silicone matrix via a network of conductive filler particles, where each conductive particle must be in contact with at least two other such particles for electricity to flow. This requires very high filler loadings; for instance, for metal particles up to 80% by weight of the formulation. Carbon black (see the following patent literature and prior art cited therein: Kobayashi and Mizuishi, 1986; Higuchi and Nakamura, 1990; Kroupa, 1990), silver particles (Lutz and Cole, 1989; see the following patent literature and prior art cited therein: Cole and Lutz, 1991; Cole *et al.*, 1993; Mine *et al.*, 1995; Kleyer and Lutz, 2002a, 2002b, 2003) or silver coated particles (see Getson and La Scola, 1988 and references cited therein), such as ceramic spheres, are the most frequently used electrically conductive fillers. Other electrically conductive metal fillers, such as copper, aluminum and nickel, have been described in the patent literature; however, these readily can oxidize to form an insulating metal oxide layer on the filler surface, which has a strong negative impact on the electrical conductivity of the silicone adhesive. Use of metal oxides in conductive silicone adhesives has been described as well (Adachi and Suganuma, 1993), although these oxides generally are not as suitable as metal particles, owing to their higher resistivity.

*Thermally conductive fillers*

Silicone adhesives have a very low thermal conductivity. However, for some applications, such as thermally conductive adhesives (TCA), a substantial increase in thermal conductivity is strongly desired. This is achieved by adding thermally conductive fillers to the formulation. Thermal conductivity is attained both by direct heat transfer via a conductive filler network as well as by indirect transfer via filler/polymer interfaces and, therefore, is a function of the filler volume loading (for a more detailed discussion of the mechanisms involved see the comprehensive review of methods used to predict the thermal conductivity of a filled system by Rogelhof *et al.*, 1976). Filler volume loading can be increased substantially by the use of mixtures of

© Woodhead Publishing Limited, 2010

different thermally conductive fillers with different particle sizes or shapes. Hence, formulations often include two or more thermally conductive fillers. The most commonly used thermally conductive filler, aluminum oxide ($Al_2O_3$), has a thermal conductivity of 35 W $(m \cdot K)^{-1}$, which is about 180 times the thermal conductivity of polydimethylsiloxane polymer. Other metal oxides have thermal conductivities similar to aluminum oxide. The exception to this rule is beryllium oxide, which has a substantially higher conductivity. However, this compound is highly toxic. Ceramic fillers, other than oxides, some of them with higher thermal conductivity than $Al_2O_3$, have been disclosed in recent patents (see Getson and Pate, 1986, and references cited therein). Often an increase in thermal conductivity is desirable for electronic applications, while low electrical conductivity is maintained. This is best achieved by use of ceramic fillers. Other applications demand a simultaneous increase in thermal and electrical conductivity. These compositions containing metal particles, for example silver flakes, or metal-coated fillers have been described in the patent literature (see Lewis *et al.*, 2003, and prior art cited herein).

## 4.5 Applications of silicone structural adhesives

Joining materials with structural silicone adhesives offers substantial benefits over mechanical methods of fixation. The silicone adhesive distributes the load over a larger area of the joint rather than concentrating it at one location, resulting in a more even distribution of stresses. The adhesively bonded joint is thus more resistant to flexural and vibrational movement than a mechanically fixed joint. A further important aspect is that the silicone adhesive forms a seal as well as a bond in a single processing step (dual functionality). Mechanically fixed (e.g. bolted or riveted) assemblies are often sealed in an additional process step. The hydrophobic silicone adhesive eliminates corrosion, which often occurs in a mechanically fastened joint. The capability to fill larger gaps with a structural silicone adhesive allows irregularly shaped surfaces to be joined more easily than does a mechanical fastener. Owing to the excellent self-adhesion of silicone adhesives, failed or serviced assemblies can be easily reassembled and resealed.

There is a wide range of silicone structural adhesive products available, including flame resistant, heat resistant, chemical resistant, oil resistant, as well as FDA (Food and Drug Administration) and aerospace specified products. Therefore, it is impossible to produce a definitive list of applications of silicone structural adhesives, as the versatility of these materials enables their use in almost every industry. Below is a list of a few examples that will be discussed in greater detail in this section:

- automotive – lamp bonding, 'under the hood' bonding applications, mirror mount adhesives
- aerospace – high temperature bonding, vibration protection

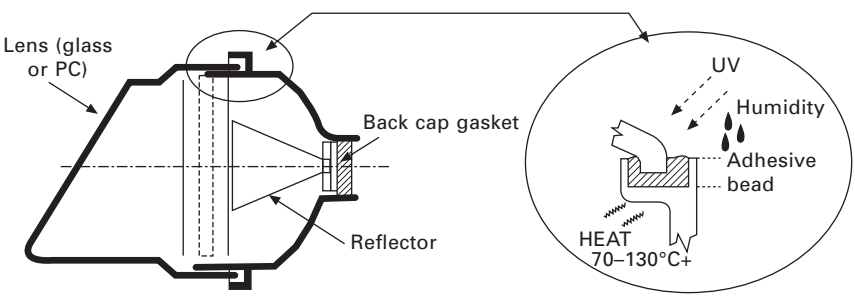
© Woodhead Publishing Limited, 2010

- construction – structural glazing, bonded windows, panel stiffeners, impact mitigation protection, mirror adhesives
- domestic appliances – attaching glass and door hinges to oven doors
- electronics – bonding electronic components and sub-assemblies
- solar/photovoltaic (PV) renewable energy industry – bonding PV modules into frames, attaching control boxes, bonding wind turbine rotor blades.

### 4.5.1 Automotive

Key requirements for the automotive industry in general include fast handling of components, rapid development of bond strength, adhesion to a wide range of materials, including many metals and plastics, such as polyamide (PA), poly(methyl methacrylate) (PMMA), polycarbonate (PC), poly(butylene terephthalate) (PBT), poly(ethylene terephthalate) (PET) and acrylonitrile-butadiene-styrene terpolymer (ABS), as well as excellent weathering, salt spray and heat resistance. Silicone adhesives meet these key requirements which fit them perfectly to automotive applications.

Structural silicone adhesives are used in the assembly of automotive head and fog lamps. One of the most important of these applications is the bonding of the lens, made either from glass or PC, to the reflector housing or body (Fig. 4.1). This application is done today almost exclusively using silicone adhesives. One reason for this is that flange space is rather constrained, limiting the use of compression gaskets. However, the primary reason is that the lens/reflector bond needs to be hermetically sealed against moisture, dirt and other engine fluids such that they do not penetrate into the reflector and impair its optical function. Silicone adhesives have been used with great success in this application since at least the 1980s. Lamp operating conditions are harsh, with operating temperatures ranging at the high end between 70 and 110°C for headlamps and 110–130°C for fog lamps. The inherent stability of silicones at high and low temperature extremes and




*4.1* The lamp bonding application.

© Woodhead Publishing Limited, 2010

their excellent adhesion characteristics make these materials well suited for this demanding application. The use of silicones in this application has an excellent track record of performance (Joseph, 2008).

The majority of the silicone adhesives used in this application are of the one- and two-component RTV condensation types (commonly alkoxy cures). Condensation cure silicone adhesives are preferred in this application over other silicone adhesives types, for example the addition cure types, because cure and especially adhesion can be tailored to proceed rapidly at room temperature. Durable adhesion is a key performance characteristic in this structural application (General Motors, 2006); adhesive failure of either the glass or the reflector body creates a path for moisture or other engine fluids into the lamp, leading to degradation of the optical performance. The lower shear modulus of a silicone structural adhesive results in lower stresses being induced at the interface by differential thermal expansion of the glass and the reflector housing. A further requirement for the silicone adhesive is low out-gassing at the high operational temperatures of the lamps. Proper functioning of automotive lamps demands that during operation the lens and reflector be kept absolutely free of any surface imperfections or deposits which impair lighting efficiency. Through careful research and development it is possible to formulate adhesives with reduced out-gassing and optimize joint design to reduce the fogging potential.

Furthermore, progress continues to be made in increasing the lighting power or brightness of (high brightness) light-emitting diodes (HBLEDs) with resultant higher power ratings. The first all-LED headlamps are already a reality. These LED headlamp units will generate even more heat than conventional halogen and xenon lights and the resulting temperatures in the lamp are expected to range from 105°C to ca. 160°C depending on design and size. These operating conditions will continue to necessitate the use of silicone adhesives, which are able to function in this environment.

The most recent development in automotive lamp assembly is the use of silicone reactive hot melt or warm melt adhesives. Hot or warm melt adhesives are applied to the substrates at elevated temperatures and make use of a rapid increase in viscosity during cooling to achieve a high level of ‘green strength’ or consistency. This green strength allows the adhesive to withstand moderate loads in the still uncured state and permits handling and manipulation of bonded parts. Hot or warm melts, in general, allow an increase in manufacturing productivity, owing to their instant green strength and absence of adhesive squeeze-out. Silicone hot or warm melts further offer the following performance advantages: good adhesion durability, no cold flow (creep), good elastic recovery, high joint movement capability, excellent temperature resistance and excellent resistance to UV light and humidity. Silicone reactive hot melt adhesives for automotive lamp assembly represent an exciting new development in adhesives. These products combine

© Woodhead Publishing Limited, 2010

the processing advantage associated with hot melt adhesives with the performance benefits of silicones.

Addition curing silicone structural adhesives frequently are used in automotive electronics that are placed 'under the hood' and exposed to high operational temperatures. These materials develop a high strength bond after a short heat cure cycle with lap shear strengths of more than 6 MPa on unprimed surfaces and can be exposed to more than 10,000 temperature cycles in the engine compartment, with a maximum service temperature of 200°C. Typical successful applications include engine management units in which the thermoplastic casing is adhered to the metal heat sink and semiconductor power modules in which stick cases are bonded to metal base plates.

Addition curing optically clear structural adhesives are used to attach rear view mirror mounts to windscreens of automobiles. The heat cure of the adhesive assembly takes place in the autoclave which is used to laminate the windscreens of the automobile. The silicone adhesive attaches a mounting plate to the glass so that a mirror can be fixed mechanically to the assembly. The UV resistance, heat resistance and vibration resistance of the silicone adhesive make it suitable for this application. This type of adhesive is also used to attach and protect optical sensors used to initiate windshield wipers during the rain. The optically clear nature of these special automotive adhesives gives them excellent performance in such applications.

### 4.5.2 Aviation and aerospace

Silicones are fundamental in many of the components used in aviation and aerospace, which, by their nature, place extreme demands on materials. Silicone semi-structural adhesives have been used in jet engines for more than 30 years where, for instance, they prevent bimetallic corrosion even at high temperatures. They are also used in electrical, electronic and optical assemblies and in the mounting of optics, resistors, connectors and other components. Additional benefits stemming from the use of silicone adhesives are a wide operating temperature range, easy repairability, good physical and electrical stability over a range of frequencies, temperatures and humidities, and the protection of components from temperature extremes, high humidity, radiation, thermal shock and mechanical vibration. Adhesives for aviation and aerospace applications must adhere to a wide range of substrates, including some difficult-to-bond plastics, such as PC, polyetherimide (PEI), PMMA and polyethersulfone (PES). In general, any material used in space must possess the following characteristics:

- excellent resistance to temperature extremes and microcracking during thermal cycling
- resistance to radiation degradation

© Woodhead Publishing Limited, 2010

- outstanding atomic oxygen resistance
- low out-gassing characteristics.

The special grades of silicone structural adhesives used in aerospace applications maintain adhesion and a good degree of flexibility over a wide range of operating temperatures, typically from –115°C to 200°C, where other materials would stiffen and crack. These special grades of silicone adhesives also possess excellent resistance to radiation. While silicone adhesives in space applications are not directly exposed to atomic oxygen, as they are encapsulated between two surfaces, the special aerospace grades show excellent resistance to this highly reactive form of oxygen which causes erosion of polymers (Banks *et al.*, 1996; Banks and Demko, 2002).

Silicone adhesives are able to dampen the effects of launch vibrations, to compensate for differential thermal expansion and to protect components from temperature extremes, high humidity, radiation, thermal shock and atomic oxygen. Silicone structural adhesives in space applications are often near or directly adjacent to electronic optical devices where contamination would be of major concern. Silicone adhesives, made by special formulation and processing techniques, meet or exceed the requirements set by American and European space agencies for low thermal vacuum out-gassing. Silicone structural adhesives are used in aerospace applications for bonding solar cells to substrates, cover glasses to solar cells and optical solar reflectors to substrates, as well as for the assembly of electronic sub-components and sub-assemblies, optical and other sensors, electronic components, modules, relays and connectors.

### 4.5.3 Construction

The primary use of silicone structural adhesives in the construction industry is in structural sealant glazing (SSG), in bonded windows and in protective impact-resistant glazing. SSG is the method of bonding glass, ceramic, metal, stone or composite panels to the frame of a building by utilizing the bond strength, movement capability and durability of a silicone structural adhesive. The total vision system (TVS) developed during the 1960s was an early version of SSG, as in this design the glass panes were structurally bonded to glass mullions by a silicone adhesive.

By the late 1960s, medium modulus silicone adhesives were also used to bond glass panes to aluminum support mullions. The design of the 37-story-high, 23,000 $m^2$ two-sided structural glazing façade of New York City's Park Avenue Tower, completed in 1983, established the SSG technique as an architectural landmark. After the completion of this building, SSG rapidly became the fastest growing form of curtain-wall construction in the USA because it allowed broader architectural flexibility and achieved dramatic

© Woodhead Publishing Limited, 2010

design accents in new construction or the renovation of old buildings. Today, SSG is one of the most versatile forms of curtain-wall construction in the commercial façade business. The silicone structural adhesive in all SSG designs carries repetitive intermittent wind loads. In some super-tall buildings exposed to hurricane-strength winds, the structural bond must resist very high wind loads. In more advanced SSG designs, the silicone structural adhesive also permanently carries the weight (dead load) of the glazing panel. Other advanced SSG designs use the silicone to transfer shear loads to the glazing so that the glass reinforces the aluminum framing to resist deflections.

The SSG designs offer a number of performance benefits:

- effective air- and weather-sealing of the façade
- improved thermal and sound insulation
- protection of the supporting structure from the elements by a durable glass skin
- increased rigidity and stability of the façade, resulting in the ability to withstand higher wind loads
- absorption of differential movements between glass and building frame, resulting in superior performance of SSG façades during seismic events
- aesthetically pleasing smooth glass façade free of mechanical interruptions
- reduced deflection of glass under wind loads compared to conventional glazing since the flexible rubber anchor resists loads in both shear and tension.

The SSG technique utilizes both the adhesive and sealing properties of structural silicone adhesives. Medium modulus, elastomeric properties and excellent, highly durable adhesion are needed to support the weight of glazed panels and to resist wind load, while simultaneously being able to absorb differential movements between dissimilar materials induced by thermal fluctuations, seismic loading or other forces. Because the interface between structural adhesive and glass is directly exposed to sunlight, the adhesive must be developed to be UV-stable in order to achieve an expected service life of 30 years to 50 years. Because of this requirement, only silicone adhesives are allowed for use in structural glazing applications by international standards and building code bodies. An excellent review of structural glazing history and the science and technology underpinning the building codes is available from ASTM (2008).

Knowledge of SSG systems performance has led naturally to the expanded use of silicone glazing in new high performance façade systems, in particular for protective, safety and security glazing systems for either hurricane glazing or bomb blast resistant façades. The unique characteristics of the continuous flexible rubber anchor resisting loads in both tension and shear,

© Woodhead Publishing Limited, 2010

designed into a safety glazing system with proper frame design, have superior performance unequalled by any other design. Bomb blasts generally are characterized by extremely high loads acting on the building over a short impact time.

Silicone adhesives display a very low glass transition temperature ($T_g$) owing to the flexibility of their siloxane polymer backbone. The time–temperature-equivalence principle developed by Williams, Landel and Ferry (Ferry, 1970) implies that a low $T_g$ means high flexibility of the polymer chains at high temperatures within very short time scales. The theory thus predicts particularly good performance for silicone adhesives when submitted to a sudden load condition, typical for bomb blast, hurricane or earthquake (Yarosh *et al.*, in 2009). Building codes in the USA for structures in the hurricane prone Gulf and Atlantic states require special design. Requirements for US government buildings that may be potential terrorist targets utilize a blast mitigation system for the glazing.

A remarkable extension of the structural glazing technology is the use of wet-applied RTV silicone structural adhesives in the manufacture of windows. This technology provides several key benefits for both window manufacturers and building owners. With the structural adhesive transferring loads between the frame and the insulating glass, the strength of the insulating glass unit contributes to the overall stability of the window. Obviously, the strength of the window then depends on the structural strength of the glass unit. However, glass has a good load bearing capability (stiffness) and can contribute considerably to the overall strength of the system. Therefore, structural bonding of the glass panes to the frame and the resulting load transfer between frame and glass result in a number of benefits:

- increased structural strength of window (load transfer between frame and glass, glass panes take on a role as a structural element)
- leaner and more slender frame designs (larger vision area – increased light transmission via window opening)
- increased window sizes with current standard frame cross-sections (steel inserts combined with bonding technology)
- elimination or reduction in size of steel reinforcement inserts in PVC windows
- improved thermal insulation (U-value) and seismic performance of window
- improved protective glazing properties (resistance to burglars, bomb blasts, hurricanes, earthquakes, avalanches, etc.)
- improved aesthetics (appearance of the window)
- reduced maintenance.

The bonding technology results in substantial productivity gains and cost savings for the manufacturer. For the building owner, improved thermal

© Woodhead Publishing Limited, 2010

performance, aesthetic benefits and lower maintenance costs, all associated with this glazing technique, are important considerations.

Silicone adhesives also may be employed in the structural bonding of other façade components. A well-known example is the European Commission's Berlaymont building, situated in Brussels, Belgium. The silicone structural adhesive is not only used to bond the glass to the façade sub-structure but also to join the glass louvers to the metal fixations. The computer-controlled 'living' façade employs in total 21,000 of these mobile glass louvers to maintain good lighting conditions and a constant temperature in the building throughout the year.

### 4.5.4 Domestic appliances

Silicone structural adhesives are used in domestic appliances where flexible bonding and resistance to harsh environments are important. For example, the metal base plate of a steam iron is bonded to the plastic water tank with silicone adhesives. In electric or gas ranges, silicone adhesives bond the glass pane to the metal door frame and often also the hinges to the door frame. Numerous other applications of silicone adhesives exist in domestic appliances where they function as durable dielectric insulation, barriers against environmental contaminants and stress-relieving shock and vibration absorbers over a wide temperature and humidity range. However, in these applications, silicones are used primarily as assembly adhesives and their application would not qualify as truly structural in nature.

### 4.5.5 Electronics

Silicone adhesives find extensive use in electrical and electronic applications where stable dielectric properties and resistance to harsh environments are important. The majority of these applications are not truly structural in nature; however, certain electric or electronic components in aerospace, automotive or military applications may be exposed to large acceleration or deceleration forces; therefore, the bonding must be capable of transferring considerable loads.

Silicone adhesives are used frequently in electronics as thermal and mechanical stress absorbers because of their flexibility, low ionic impurity, dielectric insulation properties, moisture resistance and wide operation temperature range. Specially formulated grades are available as low volatile silicone adhesives as well as adhesives with high electrical and/or thermal conductivity. The trend in electronics product development and design is toward ever-increasing density, complexity and power dissipation. This results in higher local heat flux and higher temperatures inside the modules or packaging. Interconnection of substrates having a mismatch of coefficients of

© Woodhead Publishing Limited, 2010

thermal expansion (CTE) can lead to failure upon thermal cycling owing to a build-up of mechanical stresses. In these applications, thermally conductive silicone adhesives are used in bonding of sensitive electronic components and sub-assemblies.

Thermally conductive adhesives eliminate the need for mechanical fasteners and clips, while providing an efficient method of thermal transfer between heat generating electronics devices and their heat sinks. In order to improve the thermal conductivity even further, these adhesives must be able to be applied in very thin bond lines. Silicone TCAs can be used to form thermal pathways in applications where the distance between a component and a heat sink is highly variable. A typical application would be printed circuit board components of different heights that need to be brought into contact with chassis or heat sink. Silicone TCAs are used, for example, in bonding large ceramic substrates to their heat sink in automobile microprocessor controlled ignition and fuel injection.

Continuing improvements in silicone adhesive technology have enabled these adhesives to replace solder in many electronic assembly applications. Whereas solder and most other electrically conductive adhesives would be too rigid to hold up against vibrations or impact loads, highly flexible and resilient silver-filled conductive silicones easily survive high-impact applications. Electrically conductive silicones help to protect devices from environmental hazards such as moisture and shield electromagnetic and radio frequency interference (EMI/RFI) emissions.

### 4.5.6 Solar/photovoltaic renewable energy industry

In solar applications, a silicone reactive hot-melt structural adhesive is used to bond the photovoltaic modules into the frames and to attach the polypropylene junction and control boxes to the solar modules. The key benefits of using silicones are the increased production rate in the assembly operation owing to fast bonding, use of substrates (plastics, glass, metals) without the need for priming or surface activation and the ability of the material to accommodate thermally induced movements in the joint. Silicone structural adhesives are also used in the integration of photovoltaic modules into curtain-wall façades and in bonding the giant rotor blades of wind turbines.

## 4.6 Conclusions

Silicone structural adhesives are highly durable, have excellent adhesion to a wide range of substrates, are capable of operating over a wide range of service temperatures and have long service lives even in very demanding environments. Furthermore, they can be formulated for either high or low electric and thermal conductivities. Silicone structural adhesives allow invisible

© Woodhead Publishing Limited, 2010

bonding of components, have the ability to join dissimilar substrates and fill gaps and, therefore, eliminate corrosion problems and vibration failures, and compensate for a mismatch in the coefficients of CTE. They allow reduction in manufacturing and assembly cost by providing dual functionality (bonding and sealing). Because of these unique properties, they are used in a wide range of electric, electronic, automotive, domestic appliance and construction applications.

## 4.7 Future trends

The continued desire and regulatory need for adhesives and sealants with low toxicity will be the way of the future for applications in occupied spaces such as automotive and building construction. The trend towards low volatile content or solventless adhesives will continue into the future, favoring silicone adhesives in general, but especially the reactive silicone hot-melts. The need for primerless adhesion will also continue to exist. More recent material trends that are likely to become even more important in future are reversible adhesion (in order to ease the recycling of bonded components) and command cure, that is, rapid cure initiated by external triggers. Silicone adhesives based on nanocomposite or copolymeric systems will provide novel or modified properties, such as lower gas permeability, higher strength, refractive index matching and even higher service temperature performance. Life cycle cost analysis of components and systems will favor silicone adhesives because of their greater durability and easy serviceability, both of which contribute to low overall maintenance costs. The need for lower total applied costs will continue to exist, requiring improved productivity and a reduction in components. This in turn will favor silicone adhesives that have high green strength, an automated application process and rapid cure processes. Changes in substrate type and surface modification, as well as increased utilization of dissimilar substrates in designs, will require silicone adhesives to adhere to an even broader range of substrate types, especially low surface energy substrates. Demand for adhesives with the ability to control thermal, sound and electrical energy will increase in all market sectors. This combination of tailored performance, longevity, durability and environmental friendliness will be the industry standard.

## 4.8 Sources of further information and advice

Further information on silicone adhesives and their applications may be obtained from some recent publications (Wolf, 1999; De Buyl, 2001; Brockmann *et al.*, 2008; Dunn, 2003).

© Woodhead Publishing Limited, 2010

## 4.9 References


Achenbach, F., Hechtl, W., Eberl, G., Egerter, N. and Schreyer, S. (1998), *Porphyrin-Containing Silicones Having Increased Thermal Stability*, US Patent 5,847,034.

Adachi, H. and Suganuma, N. (1993), *Electrically Conductive, Moisture-Curable Silicone Rubber Sealants Obtained by Blending Polyorganosiloxane with Silane or Siloxane Curing Agent and Blending the Mixture with Light-Coloured Electrically Conductive Metal Oxide Filler*, European Patent EP 0,558,044-B1.

Ahn, D. and Lutz, M.A. (2002), *Hydrosilylation Addition-Curable and Titanium or Zirconium Compounds-Containing Silicone Adhesive Compositions with Improved Adhesion*, European Patent Application 1,264,865.

Alvarez, K.E. and Shephard, K.L. (2001), *Fire Resistant Sealant Composition*, US Patent 6,271,299.

Anonymous (1967), *Pourable, Curable Elastomer-Forming Composition*, British Patent 1,090,958.

ASTM (2008), *ASTM Standards and Technical Articles Relating to Structural Glazing*, available from www.ASTM.org, viewed December 4, 2008.

Banks, B.A. and Demko, R. (2002), *Atomic Oxygen Protection of Materials in Low Earth Orbit*, NASA Technical Memorandum 211360, NASA, Washington DC.

Banks, B.A., de Groh, K.K., Rutledge, S.K. and DiFilippo, F.J. (1996), *Prediction of In-Space Durability of Protected Polymers Based on Ground Laboratory Thermal Energy Atomic Oxygen*, NASA Technical Memorandum 107209, NASA, Washington DC.

Bayly, B.P. (1999), *One Component Room Temperature Vulcanizable (RTV) Silicone Sealant with Improved High Temperature Adhesion*, US Patent 5,932,650.

Be, Al, Cai, Y. and Lower, L.D. (2004), *Continuous Process for Producing Hot Melt Adhesive Compositions*, PCT Patent Application WO 2004/037941 A2.

Beers, M.D. (1968), *Composition Containing Silanol Chain-Stopped Polydimethyl-Siloxane, Organosilicon Process Aid, and Curing Agent*, US Patent 3,382,205.

Beers, M.D. (1981), *Curable Compositions and Process*, US Patent 4,257,932.

Boissieras, J. and Ceyzeriat, L.F. (1969), *Organosilicon Compounds and Compositions Containing the Same*, US Patent 3,429,847.

Boissieras, J., Ceyzeriat, L.F. and Lefort, M.J.C. (1967), *Organosilicon Compounds and Their Use*, US Patent 3,359,237.

Brockmann, W., Geiß, P.L., Klingen, J., Schröder, K.B. and Mikhail, B. (Translator) (2008), *Adhesive Bonding: Materials, Applications and Technology*, Wiley, New York.

Brod, H.G. and Schweitzer, O. (1958), *Verfahren zur Herstellung von Formkoerpern und Ueberzuegen aus Elastomeren Organopolysiloxanen* (Translation: *Process for the Manufacture of Moldings and Coatings Based on Elastomeric Organopolysiloxanes)*, German Patent 1,035,358.

Brown, P.L. and Hyde, J.F. (1964), *Polyfunctional Alkoxy Endblocked Polysiloxanes and Their Cured Compositions*, US Patent 3,161,614.

Brummer, O., Carlson, E.D., Crevier, T., Giraud, Y., La Pointe, A-M. and Sterin, S. (2003), *Catalytic PGM Mixture for Hydrosilylation*, WO/2003/050174.

Bruner, L.B. (1962a), *Acyloxy-Endblocked Diorganopolysiloxane*, US Patent 3,032,532.

Bruner, L.B. (1962b), *Acyloxy Siloxanes and a Method of Using Them*, US Patent 3,035,016.

Carlson, B.W. and Glasbrenner, B.S. (1994), *High Temperature Sealant Containing Phenyl Silicone*, US Patent 5,310,588.


© Woodhead Publishing Limited, 2010

Ceyzeriat, L. (1964), *Room Temperature Curable Siloxane Compositions*, US Patent 3,133,891.

Chung, R.H. (1985), *End-Capping Catalysts for Forming Alkoxy-Functional One Component RTV Compositions*, US Patent 4,515,932.

Cifuentes, M.E., Brady, W.P., Fenton, W.N., Schmidt, R.G., Strong, M.R., Stickles, D.L. and VanWert, B. (1994), *Moisture-Curable Compositions Containing Aminoalkoxy-Functional Silicone*, US Patent 5,302,671.

Cifuentes, M.E., Strong, M.R., VanWert, B., Lutz, M.A. and Schmidt, R.G. (1996), *Moisture-Curable Hot Melt Silicone Pressure-Sensitive Adhesives*, US Patent 5,508,360.

Cifuentes, M.E., Brady, W.P., Schmidt, R.G., Schoenherr, W.J., Strong, M.R., VanWert, B. and Vincent, G.A. (1999), *Moisture-Curable Hot Melt Silicone Pressure-Sensitive Adhesives*, US Patent 5,905,123.

Cifuentes, M.E. Strong, M.R. VanWert, B. Lutz, M.A. and Schmidt, R.G. (2003), *Moisture-Curable Hot Melt Silicone Pressure-Sensitive Adhesives*, European Patent EP 0 735 103 B1.

Cole, R.L. and Lutz, M.A. (1991), *Electrically Conductive Silicone Compositions*, US Patent 5,075,038.

Cole, R.L., Fiori, J.E. and Lutz, M.A. (1993), *Organosiloxane Composition Curable to Electro-Conductive Material, Contains Silver-Particles Coated with Fatty Acid Ester*, European Patent EP 0,545,568-B1.

De Buyl, F. (2001), 'Silicone sealants and structural adhesives', *International Journal of Adhesion and Adhesives*, **21**, 411–22.

Delatorre, P. and Beers, M.D. (1978), *Self-Extinguishing Room Temperature Vulcanizable Silicone Rubber Compositions*, US Patent 4,102,852.

Dunn, D.J. (2003), *Adhesives and Sealants – Technology, Applications and Markets*, RAPRA Technology Limited, Shawbury, Shropshire, United Kingdom.

Dziark, J.J. (1983), *Scavengers for One-Component Alkoxy-Functional RTV Compositions and Processes*, US Patent 4,417,042.

Eckberg, R.P. (1982a), *Vinyl Gum Cure Accelerators for Addition-Cure Silicone*, US Patent 4,340,647.

Eckberg, R.P. (1982b), *Silicone Release Coatings and Inhibitors*, US Patent 4,347,346.

Evans, S.M., Lee, C.L. and Yeh, M.H. (1993), *Storage-Stable Heat-Curable Transparent Organosiloxane Compositions Containing a Microencapsulated Catalyst*, US Patent 5,194,460.

Ferry, J.D. (1970), *Viscoelastic Properties of Polymers*, 2nd edition, John Wiley & Sons, New York.

Fujiki, H. (1996), *Addition-Curable Silicone Rubber Adhesive Compositions*, Japan, Kokai Tokkyo Koho 08,291,254 A2.

General Motors (GM) (2006), *Engineering Standards, Material Specification: Adhesives (GMN11280), Performance Requirements of an Exterior Lighting Structural Adhesive*, General Motors Corporation (March 2006).

Getson, J.C. and La Scola, M.A. (1988), *Electrically Conductive, Cured Silicone Rubber Compounds, Made from Storage-Stable Compositions Based on Known Organopolysiloxane Composition Containing Silver-Coated Mica and Carbon Black Stabilizer*, US Patent 4,777,205.

Getson, J.C. and Pate, M. (1986), *Thermally Conductive Room Temperature Vulcanizable Silicone-Elastomer Containing Silicon Nitride Filler*, US Patent 4,584,336.

Goelitz, H.D., Damm, K. and Noll, W. (1968), *Organopolysiloxane Composition Convertible at Room Temperature*, US Patent 3,364,160.

© Woodhead Publishing Limited, 2010

Hara, H. (1999), *Addition Curing-Type Silicone Compositions Containing an Adhesion Promoter for Heat-Resistant Adhesives*, European Patent Application 0,934,981 A2.

Higuchi, K. and Nakamura, A. (1990), *Silicone Rubber Composition Containing Alkenyl Containing Polydiorganosiloxane, Including Carbon Black and Curing Agent, Having Stable and Narrow Variation of Volume Resistivity*, European Patent EP 0,392,262-B1.

Hittmair, P., Nitzsche, S., Wick, M. and Wohlfarth, E. (1968), *Room Temperature Vulcanizable Organopolysiloxane Elastomers*, US Patent 3,408,325.

Ikeno, M. and Fujiki, H. (1992), *Siloxane Compositions and Their Cured Products*, Japan, Kokai Tokkyo Koho 04,013,768 A2.

Israeli, Y., Phillipart, J.L., Cavezzan, J., Lacoste, J. and Lemaire, J. (1992a), 'Photo-oxidation of polydimethylsiloxane oils. Part I. Effect of silicon hydride groups', *Polym. Degrad. Stab.*, **36**, 179–85.

Israeli, Y., Cavezzan, J. and Lacoste, J. (1992b), Photo-oxidation of polydimethylsiloxane oils. Part II. Effect of vinyl groups', *Polym. Degrad. Stab.*, **37**, 201–8.

Israeli, Y., Cavezzan, J., Lacoste, J. and Lemaire, J. (1993), 'Photo-oxidation of polydimethylsiloxane oils. Part III. Effects of dimethylene groups', *Polym. Degrad. Stab.,* **42**, 267–79.

Israeli, Y., Lacoste, J., Cavezzan, J. and Lemaire, J. (1995), 'Photo-oxidation of polydimethylsiloxane oils and resins. IV. Effect of phenyl groups', *Polym. Degrad. Stab.,* **47**, 357–62.

Joseph, E.A. (2008), 'The role of silicone adhesives and sealing materials in the assembly of automotive exterior lighting components', *RAPRA Automotive Adhesives, Sealants and Coatings Conference*, Stuttgart, Germany, 10–11 June.

Kleyer, D.L. and Lutz, M.A. (2002a), '*Silicone Composition and Electrically Conductive Silicone Adhesive Formed Therefrom*, US Patent 6,361,716.

Kleyer, D.L. and Lutz, M.A. (2002b), *Electrically Conductive Hot-Melt Silicone Adhesive Composition*, US Patent 6,433,055.

Kleyer, D.L. and Lutz, M.A. (2003), *Silicone Composition and Electrically Conductive Silicone Adhesive Formed Therefrom*, US Patent 6,534,581.

Kobayashi, N. and Mizuishi, Y. (1986), *Electrically Conductive Silicon Rubber Composition Prepared by Mixing Silicone Rubber Base Material Containing Carbon Black with Ground Vulcanised Silicone Rubber*, Japanese Laid Open Patent Application JP 61,108,661.

Kroupa, L.N. (1990), *Electrically Conductive Silicone Compositions Containing Carbon Particles, Have Disilazane Compound or Hydroxyl Endblocked poly(methylphenyl) siloxane to Lower Resistivity*, European Patent EP 0,352,039-B1.

Kulpa, T.A. (1967), *Curable Organopolysiloxane*, US Patent 3,296,161.

Lewis, L.N., Gifford, S.K. and Rubinsztajn, S. (2003), *Curable Silicone Compositions, Methods and Articles made Therefrom*, US Patent 6,639,008.

Lin, S.B. (1995), 'High-temperature stability of silicone polymers and related pressure-sensitive adhesives', *High Temperature Properties and Applications of Polymeric Materials*, ACS Symposium Series, 603, 37–51.

Lucas, G.M. and Dziark, J.J. (1984), *Adhesion Promoters for One-Component RTV Silicone Compositions*, US Patent 4,483,973.

Lutz, M.A. and Cole, R.L. (1989), 'Flexible silicone adhesive with high electrical conductivity', *Proceedings of IEEE 39th Electronic Components Conference*, Houston, TX, 22–24 May 83–7.

© Woodhead Publishing Limited, 2010

Melancon, K.C. (1985), *Latently-Curable Organosilicone Release Coating Compositions*, US Patent 4,504,645.

Mine, K., Nakayoshi, K. and Tazawa, R. (1995), *Electrically Conductive, Curable Organosiloxane Composition Containing Ag Particles Treated with Organo-Si Compounds Containing Si-Bonded Alkoxy Groups*, European Patent EP 0,647,682-B1.

Mitsuhashi, K. and Tabei, H. (1997), *Fireproof, Fire-Retardant Silicone Rubber Composition*, Japanese Laid Open Patent Application JP 9,012,888.

Murphy, R.A. (1967), *Organopolysiloxane Compositions and a Method for Making Them*, US Patent 3,341,486.

Nishiwaki, N. and Urabe, T. (1994), *Storage-Stable Siloxane Compositions Curable by Addition Reaction*, Japan. Kokai Tokkyo Koho 06,345,969 A2.

Nitzsche, S. and Wick, M. (1962), *Silicone Elastomers*, US Patent 3,032,528.

Nitzsche, S., Kaiser, W., Wohlfarth, E. and Hittmair, P. (1972), *Room Temperature Vulcanizable Silicone Rubber Stocks*, US Patent 3,674,738.

Oldfield, D. and Symes, T. (1996), 'Long term natural aging of silicone elastomers', *Polym. Testing*, **15**, 115–28.

Pande, K.C. and Ridenour, R.E. (1969), *Aminoxysilanes*, US Patent 3,448,136.

Plueddemann, E.P. (1982), *Silane Coupling Agents*, Plenum, New York.

Polmanteer, K.E. (1960), *Siloxane Elastomers*, US Patent 2,927,907.

Rogelhof, R.C., Throne, J.L. and Ruetsch, R.R. (1976), 'Methods for predicting the thermal conductivity of composite systems: a review', *Polym. Eng. Sci.*, **16**(9), 615–25.

Sattlegger, H., Noll, W., Damm, K. and Golitz, H.D. (1968), *Organopolysiloxane Compositions Convertible into Elastomers*, Bayer AG, US Patent 3,378,520.

Smith, S.D. and Hamilton, Jr., S.B. (1972), *Curable Compositions*, US Patent 3,689,454.

Stein, J. (1994), *Addition-Curable Silicone Adhesive Compositions and N-Heterocyclic Silane Adhesion Promoters*, US Patent 5,362,781.

Stein, J. (1996), *Michael Addition Products as Adhesion Promoters for Addition-Curable Silicone Adhesive Compositions*, US Patent 5,569,689.

Stein, J. and Davis, M.W. (1995a), *Room Temperature Addition-Curable Silicone Adhesive Compositions and N-Heterocyclic Silane Adhesion Promoters*, US Patent 5,380,788.

Stein, J. and Davis, M.W. (1995b), *Room Temperature Addition-Curable Silicone Adhesive Compositions and N-Heterocyclic Silane Adhesion Promoters*, Cont.-in-part of US Patent 5,380,788.

Stein, J. and Eckberg, R.P. (1990), 'UV-curable silicone release coatings and controlled release additives', *J. Coated Fabrics*, **20**, 24–42.

Stein, J. and Rubinsztajn, S. (1995), *Addition-Curable Silicone Adhesive Compositions and Bis(trialkoxysilylalkylene)urea Adhesion Promoters*, US Patent 5,416,144.

Stein, J., King, J.A., Jr. and Caruso, A.J. (1994), *Addition-Curable Silicone Adhesive Compositions, and bis(trialkoxysilylalkyleneoxy-carbonylalkylene) Amine Adhesion Promoters*, US Patent 5,342,870.

Stein, J., Eichinger, B.E., Early, T. and Wood, C.D. (2002), *A New Class of Adhesion Promoters for Addition Curable Silicone Adhesives*, *Adhesive Joints: Formation, Characteristics and Testing*, (2nd International Symposium on Adhesive Joints: Formation, Characteristics and Testing), Newark, NJ, May 22–24, 2000, 89–100.

Strong, M.R., Cifuentes, M.E., VanWert, B. and Schoenherr, W.J. (1995), *Moisture-Curable Hot Melt Silicone Pressure-Sensitive Adhesives*, US Patent 5,473,026.

© Woodhead Publishing Limited, 2010

Suzuki, T. and Kasuya, A. (1989), 'Adhesion of addition-reaction type silicone elastomers', *J Adhesion Sci. Technol.*, **3**(6), 463–73.

Sweet, E. (1965), *Organosilicon Intermediates Containing Silicon-Bonded Oxime Radicals*, US Patent 3,189,576.

Takago, T. (1979), *Room Temperature Curable Organosiloxane Compositions*, US Patent 4,180,642.

Takago, T., Sato, T. and Aoki, H. (1974), *Room Temperature Vulcanizing Organopolysiloxane Compositions*, US Patent 3,819,563.

The European Parliament and the Council of the European Union (2007), Directive 2007/47/EC of The European Parliament and of the Council of 5 September 2007 amending Council Directive 90/385/EEC on the approximation of the laws of the Member States relating to active implantable medical devices, Council Directive 93/42/EEC concerning medical devices and Directive 98/8/EC concerning the placing of biocidal products on the market, *Official J. Europ. Union*, L 247, 21–55.

Van Ooij, W.J. and Jayaseelan, S.K. (1999), 'Bonding metals to rubber using functional and non-functional silanes', *Adhesion '99, Proceedings 7th International Conference on Adhesion and Adhesives*, Cambridge, UK, 15–17 September, 43–8.

Vincent, G.A., Brady, W.P., Cifuentes, M.E., Schoenherr, W.J. and Vincent, H.L. (1994), *Oxime-Functional Moisture-Curable Hot Melt Silicone Pressure-Sensitive Adhesives*, US Patent 5,340,887.

Weyenberg, D.R. (1967), *Method of Making One Component Room Temperature Curing Siloxane Rubbers*, US Patent 3,334,067.

White, M.A., Beers, M.D., Lucas, G.M., Smith, R.A. and Swiger, R.T. (1983), *One Package, Stable, Moisture Curable, Polyalkoxy-Terminated Organopolysiloxane Compositions and Method for Making*, US Patent 4,395,526.

Wolf, A. (1999), 'Durability of silicone sealants', in *Durability of Building Sealants – RILEM Report 21*, Wolf, A. (ed.), Cachan, France, RILEM Publications SARL, 253–74.

Wu, J.H., Chen, Y.K., Shen, Z., Huang, J.L. and Chen, N.S. (1999), 'Surface energy of mineral powders and interaction between silicone', *J. Mater. Sci. Lett.*, **18**(6), 461–2.

Yarosh, K., Wolf, A.T. and Sitte, S. (2009), 'Evaluation of silicone sealants at high movement rates relevant to bomb mitigating window and curtain wall design', *J. ASTM Int.*, **6**(2), paper ID JAI 101953.

© Woodhead Publishing Limited, 2010

# 5
# Advances in anaerobic and cyanoacrylate adhesives

P. KLEMARCZYK, Henkel Corporation, USA; and
J. GUTHRIE, Henkel Loctite RD&E, Ireland

**Abstract**: Anaerobic adhesives are one-part adhesives, which are stable at room temperature for an extended period of time and only polymerize when oxygen is excluded after assembly of a part with the adhesive. They are generally formulated with a mixture of monofunctional and multi-functional (meth)acrylate ester monomers and resins, a redox radical initiator system, stabilizers and different types of modifiers. Despite a number of studies which have investigated the redox initiation mechanism, it has still not been completely resolved. A proposed mechanism is reviewed. Recent advances in anaerobic adhesive technology, which include product development, use of new cure components, improvements in thermal resistance, improved cure speed and new applications, are also discussed. Cyanoacrylate adhesives are solvent free, rapid-curing 'one-part' adhesives based on alkyl-2-cyanoacrylate monomers. Cyanoacrylate adhesives are unique in that they bond rapidly and easily to a variety of substrates. Formulated instant adhesives consist of, essentially, pure monomer with relatively small amounts of property-modifying additives. The curing reaction is the result of anionic polymerization, initiated by traces of alkaline material present on most substrate surfaces in conjunction with low levels of surface moisture. Recent improvements in cyanoacrylate technology and its chemistry are discussed.

**Key words**: anaerobic adhesives, methacrylate monomers and resins, redox cure mechanism, cyanoacrylate, instant adhesives, anionic polymerization.

## 5.1 Introduction to anaerobic adhesives

Anaerobic adhesives are one-part, liquid or gel adhesives, which are stable at room temperature for an extended period of time. Polymerization of the adhesive only occurs when oxygen is excluded from the adhesive after the assembly of the bonded part. This paper will discuss one-component anaerobic adhesives, although much of what is written can also apply to two-component systems, which may include very active accelerators in a second component, especially for surfaces insensitive to the anaerobic cure system.

The history of this class of adhesives dates back to the late 1940s, when the first anaerobic adhesives were marketed by General Electric as 'Anaerobic Permafil' (Burnett and Nordlander, 1953). The liquid adhesive was manufactured by bubbling pure oxygen into a methacrylate monomer



© Woodhead Publishing Limited, 2010

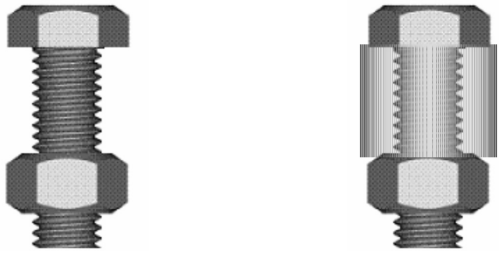
in the presence of an organic peroxide at elevated temperature to form a reactive 'oxygenated' monomer mixture. The resulting adhesive product was exceedingly unstable and required continuous oxygenation by bubbling air into it during shipment and storage to prevent rapid polymerization.

Eventually, GE eliminated 'Anaerobic Permafil' from its product line, because its difficulty in handling and poor long-term stability resulted in very limited sales. A GE employee, Robert 'Bob' Krieble, and his father, Vernon Krieble, a chemistry professor at Trinity College in Hartford, Connecticut obtained an exclusive license for the technology with the intention of modifying the manufacturing process and the formulation to yield a sufficiently stable product, which would not require the need for continuous oxygenation. Professor Krieble's research efforts were successful and in 1953 he formed the American Sealants Company, which sold its first 'Loctite' products in 1956 (Krieble, 1959; Krieble, 1965; Grant, 1983). Bob left a successful career at GE the same year to join his father in running the new company. As the Loctite line of products increasingly became a sales success, they decided to change the name of their company to Loctite Corporation in 1963 to strengthen the brand identification. The commercial success of this novel adhesive technology resulted in intense competition from other companies, such as Henkel KGaA, which acquired Loctite in 1997, 3M, Three Bond and ITW Devcon.

Anaerobic adhesives were initially used in threadlocking applications as a chemical locking agent to prevent the disassembly of steel nuts and bolts caused by the vibration of heavy machinery and automobiles during use over an extended period of time (Grant, 1983). Extensive modification of the original formulations has now expanded their use to structural applications and use on substrates, which are normally difficult to bond. From its humble beginnings, anaerobic adhesive technology has expanded into a multi-billion dollar line of products that are utilized in a large variety of industrial, aftermarket and consumer applications.

Anaerobic adhesives for threadlocking applications are tested with nut and bolt specimens of varying compositions, such as mild steel or stainless steel, and the torque strength required to break the adhesive bond is measured. There are two nut and bolt test specimen configurations, breakaway and breakloose, for measuring the torque adhesive strength according to ASTM Test D-5649. The breakaway test utilizes just the nut and the bolt specimen, which is not pretorqued. The breakloose test utilizes a steel spacer between the nut and the bolt, and the specimen is pretorqued to 5 N-m prior to aging. An illustration of the two test specimens is shown in Fig. 5.1. The assembled specimens are aged at ambient temperature or elevated temperature for a specified amount of time. After aging, the amount of torque strength required to break the adhesive bond is obtained on a mechanical torque tester.

© Woodhead Publishing Limited, 2010




*5.1* Configuration of nut and bolt test specimens for breakaway and breakloose testing.

Lapshear or block specimens are utilized for testing and evaluation of structural anaerobic adhesive applications. For lapshear testing, the test specimens consist of 10.16 cm × 2.54 cm × 1.6 mm lapshears with a variety of compositions, such as mild steel, galvanized steel or various plastics. The lapshear surface may be modified by treatment with solvent to remove grease, grit-blasting to create a more uniform surface, or both. The adhesive is applied to the two lapshears with a 1.27 cm overlap. They are then clamped and are aged either at ambient temperature or elevated temperature. After the specified aging period is completed, the adhesive strength of the assembled specimens is measured by ASTM test method D1002-05 in a mechanical tensile tester.

In general, blockshear testing is utilized for plastic substrates, which are easily deformed. For these tests, the adhesive is applied to two 2.54 cm × 2.54 cm × 1.27 cm blockshears with a variety of plastic or metal compositions, which may be cleaned with solvent, grit-blasted, or both. The two blockshears are assembled with a 1.27 cm overlap, clamped, and aged, either at ambient temperature or elevated temperature. After the specified aging period is completed, the adhesive strength of the assembled specimens is measured by ASTM test method D4501-01 in a mechanical tensile tester.

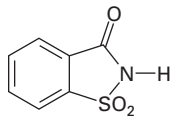
## 5.2 Chemistry of anaerobic adhesives

Anaerobic adhesives are generally formulated with a mixture of monofunctional and multifunctional (meth)acrylate ester monomers and resins, a redox radical initiator system, stabilizers and different types of modifiers. The physical properties of the earliest anaerobic adhesives were limited by the small number of available monomers for formulation. In contrast, relatively large numbers of raw materials with different chemical structures from a variety of suppliers, some of which are listed in Table 5.1, are now commercially available and permit the formulation of adhesives with a wide range of uncured and cured properties. These adhesives cure at room temperature after assembly in a part

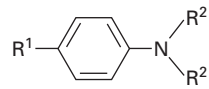
© Woodhead Publishing Limited, 2010

*Table 5.1* Monomer and resin suppliers

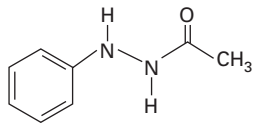
| Company | Location | Web address |
|---|---|---|
| Cognis | Düsseldorf, Germany | www.cognis.com |
| Evonik | Essen, Germany | corporate.evonik.com |
| San Esters | Tokyo, Japan/New York, NY | www.sanesters.com |
| Sartomer | Exton, PA | www.sartomer.com |



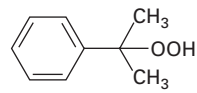

Saccharin (**1**)




*N,N*-Dialkyl arylamine (**2**)




Acetyl phenylhydrazine (**3**)




Cumene hydroperoxide (**4**)

with the use of a redox initiator system, which generates a flux of radicals *in situ* to initiate polymerization after air is excluded from the adhesive. The initiator system includes saccharin (benzosulfimide) (**1**), a reducing agent, such as an *N*,*N*-dialkyl arylamine, (**2**), or acetyl phenylhydrazine (APH), (**3**), and a stable peroxide, such as cumene hydroperoxide (CHP), (**4**).

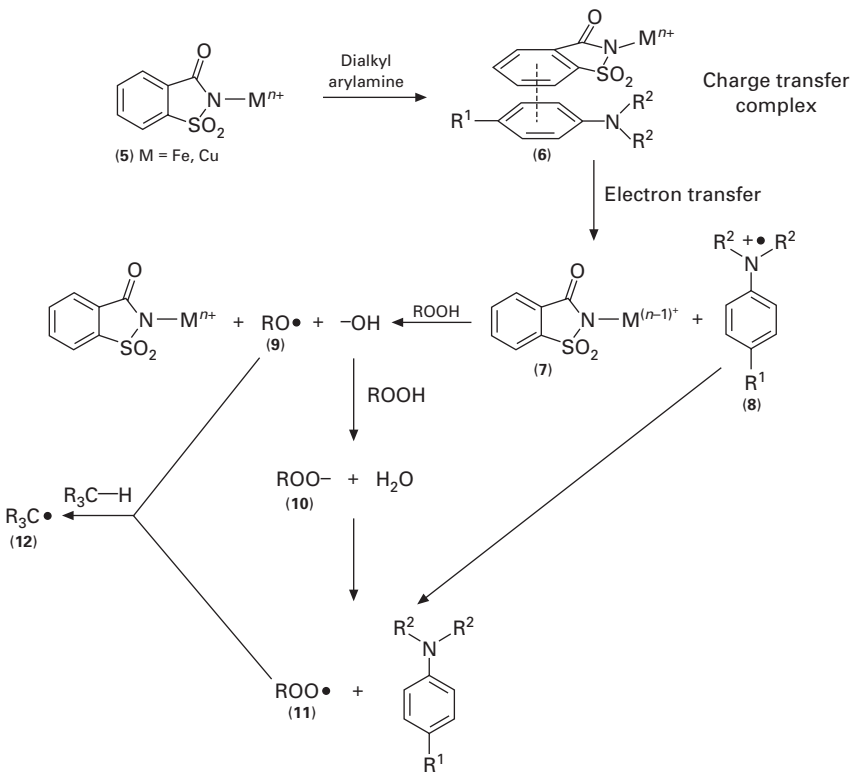
Despite a number of studies which investigated the redox initiation mechanism, it has still not been completely resolved (Beaunez *et al.*, 1994a, 1994b; Boerio *et al.*, 1990; George *et al.*, 1997, 1998a, 1998b, 2000; Humphreys, 1983; McGettrick *et al.*, 1994; Moane *et al.*, 1999; Okamoto, 1990a, 1990b; Raftery *et al.*, 1997a, 1997b; Smith, 1992; Wellmann and Brockmann, 1994). Although all of them agree that there is a complex interaction of the various cure components, there is no complete agreement on the specific details. A proposed mechanism is summarized in Scheme 5.1. The saccharin initially reacts with the metal surface to form the saccharide salt (**5**) and this salt forms a charge transfer complex (**6**) with the reducing agent amine. An electron transfer then occurs to produce the reduced metal salt (**7**) and a radical cation (**8**) which reacts with the hydroperoxide to form an alkoxy radical (**9**) and a hydroxyl anion. The hydroxyl anion reacts with a second mole of hydroperoxide to generate water and the peroxy anion (**10**), which reacts with the radical cation to form a peroxy radical (**11**). The alkoxy radical, RO•, can initiate polymerization or the two oxygen-centered radicals, RO• and ROO•, can abstract a hydrogen atom from a C–H bond to produce a

© Woodhead Publishing Limited, 2010

carbon-centered radical, $R_3C\bullet$ (**12**), that can also initiate the polymerization. The mechanism, outlined above, does not agree completely with some of the other proposals and may ultimately be displaced. The study of anaerobic cure mechanism is still a fertile area for scientific investigation.

Anaerobic adhesive cure is activated particularly well on copper and iron surfaces, while activation on tin surfaces also occurs but is less effective. All other metals either have no effect on anaerobic adhesive cure, or actually inhibit it. Part of the proposed redox catalytic cycle requires a metal$^{n+}$ to metal$^{(n-1)+}$ electron transfer, so the energy barrier for the electron transfer between the two oxidation states must be relatively low for a metal to promote anaerobic cure readily. Also, the metal cannot be too strong an oxidant or reductant, or the catalytic cycle would be suppressed. One measure of this energy barrier is the standard electrode potential between the two oxidation states of the metal.

Table 5.2 summarizes the standard electrode potential for several metals (Dean, 1985). The two metals, copper and iron, which are most effective in promoting anaerobic cure, have standard electrode potentials that are relatively low for a one electron transfer. While tin also has a low standard




Scheme 5.1

© Woodhead Publishing Limited, 2010

*Table 5.2* Standard electrode potential of some metals

| Metal ion | | | | Reduced metal ion | Standard electrode potential | |
|---|---|---|---|---|---|---|
| $Co^{3+}$ | + | $e^-$ | ⟷ | $Co^{2+}$ | 1.95 | Stronger oxidant |
| $Ce^{4+}$ | + | $e^-$ | ⟷ | $Ce^{3+}$ | 1.70 | |
| $Mn^{3+}$ | + | $e^-$ | ⟷ | $Mn^{2+}$ | 1.49 | |
| $Fe^{3+}$ | + | $e^-$ | ⟷ | $Fe^{2+}$ | 0.77 | |
| $Cu^{2+}$ | + | $e^-$ | ⟷ | $Cu^+$ | 0.17 | |
| $Sn^{4+}$ | + | $2e^-$ | ⟷ | $Sn^{2+}$ | 0.15 | |
| $Ni^{2+}$ | + | $2e^-$ | ⟷ | Ni | –0.26 | |
| $Cr^{3+}$ | + | $e^-$ | ⟷ | $Cr^{2+}$ | –0.41 | Stronger reductant |

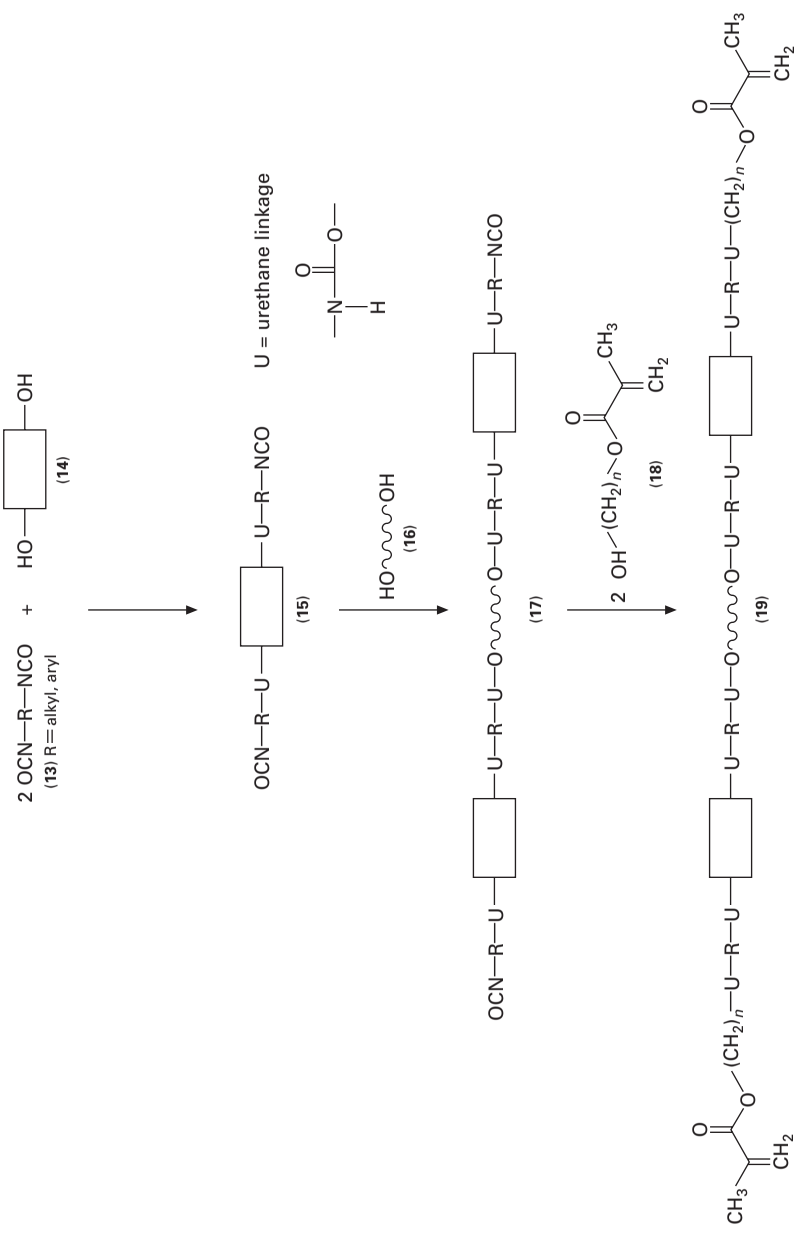
electrode potential, it involves a two electron transfer, which may not be as facile in the anaerobic cure system.

The anaerobic adhesives can still be utilized on metal substrates, which are less reactive toward anaerobic cure, or on plastics, which do not contain any metal, if a suitable primer is applied to the surface prior to the adhesive (Rich, 1994). Most primers contain either a strong reducing agent or a soluble copper salt, or both, to accelerate the adhesive cure on the surface of those less active substrates.

The addition of stabilizers is also essential for long term room temperature stability. A key stabilizer is atmospheric oxygen. The adhesives are packaged in polyolefin bottles, which are permeable to oxygen, but not moisture, and are only half filled to allow a sufficient headspace of air to assist in inhibiting premature polymerization. Additional chemical stabilizers include chelators, such as tetrasodium ethylenediamine tetraacetic acid ($Na_4$-EDTA), to scavenge extraneous metal ions, and radical inhibitors, such as hydroquinone (HQ) or naphthaquinone (NQ) (Rich, 1994).

The physical properties of the cured and uncured adhesives can also be modified by the addition of thickeners, fillers, rubber toughners, core-shell particles, elastomers and thixotropes to achieve products with a specific property profile (Rich, 1994). A particularly useful class of resins includes urethane block copolymers, which contain both rigid and flexible oligomeric segments and are terminated by a (meth)acrylate functionality. These resins were first introduced into anaerobic adhesive technology in the early 1980s (Baccei, 1981). Scheme 5.2 summarizes the preparation of these resins. In the initial reaction, two moles of a rigid aliphatic or aromatic diisocyanate (**13**), are treated with one mole of a rigid aliphatic diol (**14**). To the resulting rigid diisocyanate (**15**), is added half a mole of a flexible diol (**16**) to generate the block diisocyanate (**17**) with rigid and flexible segments. The block diisocyanate is capped by a hydroxyl (meth)acrylate ester (**18**) to form the methacrylate terminated block copolymer (**19**). The number and variety of diisocyanates, rigid diols and flexible diols has increased since

© Woodhead Publishing Limited, 2010




Scheme 5.2

© Woodhead Publishing Limited, 2010

these materials were first introduced. This has created a greater number of synthetic options and, subsequently, more formulating options for the product developers. These resins can dramatically increase the toughness and the adhesive strength of the anaerobic adhesive, which is especially important for structural applications (Attarwala *et al.*, 2004).

Because anaerobic adhesives are stable in the presence of oxygen, any extra adhesive that is present outside of the bond line will remain uncured. Therefore, there was a need to introduce a secondary polymerization mechanism to cure the unreacted adhesive, if this was a product requirement. The most widely used technology to fulfill this requirement is the addition of a photoinitiator to the formulation. The unreacted adhesive on the substrate can then be polymerized by exposure of the part to UV light after it has been assembled (Conway *et al.*, 1985).

## 5.3 Recent developments in anaerobic adhesive technology

### 5.3.1 Anaerobic adhesives in semi-solid form

Since the beginning of anaerobic adhesive technology, the products have been sold as liquids, pastes or gels. However, the containers may leak if they are punctured or if the cap is not put on with sufficient tightness. A liquid adhesive also has the potential to migrate into sensitive areas of an assembled part and cause problems in the performance of that part. More recently, anaerobic adhesives have been formulated into a convenient semi-solid (Attarwala *et al.*, 2006), which does not flow and is similar in appearance to the lower strength stick adhesives, which are sold for consumer applications. In contrast to the consumer adhesive, use of the anaerobic semi-solid in industrial applications provides ultimate adhesive strengths that are comparable to that of liquid anaerobic adhesives. The key ingredient in the new product is a polyamide thickener to increase the viscosity of the adhesive formulation into a semi-solid product without decreasing its long term stability.

Formulations for some of the stick adhesives, with and without the polyamide thickener, are provided in Table 5.3. These formulations were evaluated on mild steel nut and bolt specimens and were aged at ambient temperature for 24 hours. Figure 5.2 provides the breakaway and breakloose adhesive strength data for these adhesives. It is clear that the adhesive performance is unaffected by the addition of the polyamide thickener, regardless of the test method.

### 5.3.2 New anaerobic adhesive curatives

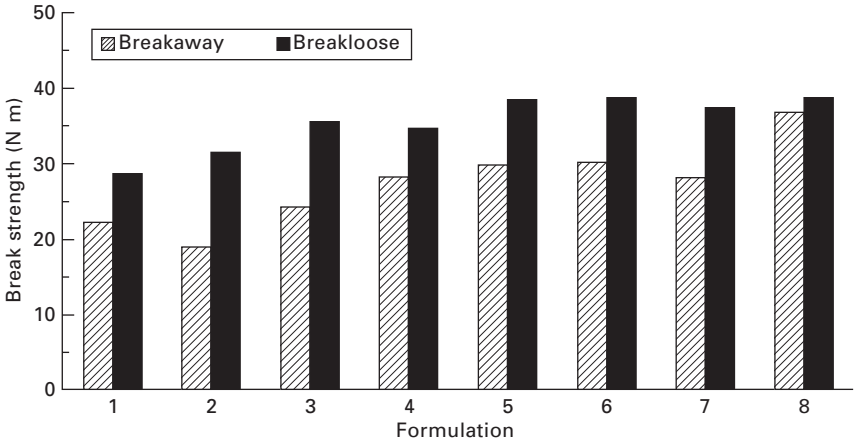
Another area of active research is the investigation into new anaerobic curative chemicals. As mentioned earlier, *N*,*N*-dialkyl arylamines and APH

© Woodhead Publishing Limited, 2010

*Table 5.3* Formulations for semi-solid anaerobic adhesives and controls

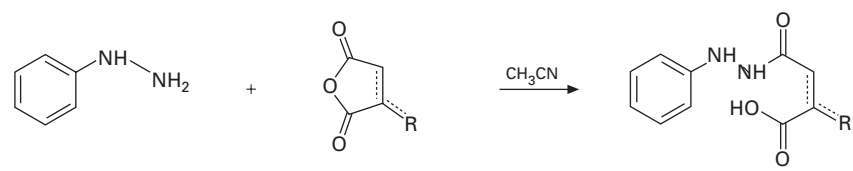
| Material | 1(wt%) | 2(wt%) | 3(wt%) | 4(wt%) | 5(wt%) | 6(wt%) | 7(wt%) | 8(wt%) |
|---|---|---|---|---|---|---|---|---|
| Polyethylene glycol dimethacrylate | 56.21 | 51.1 | 45.21 | 41.1 | 34.21 | 31.1 | 23.21 | 21.1 |
| $Na_4$-EDTA solution | 0.55 | 0.5 | 0.55 | 0.5 | 0.55 | 0.5 | 0.55 | 0.5 |
| Naphthaquinone solution | 0.55 | 0.5 | 0.55 | 0.5 | 0.55 | 0.5 | 0.55 | 0.5 |
| Ethoxylated bisphenol A dimethacrylate | 33 | 30 | 33 | 30 | 33 | 30 | 33 | 30 |
| 2-Methacryloxyethyl phenyl urethane | 0 | 0 | 11 | 10 | 22 | 20 | 33 | 30 |
| Fluoranthene | 0.022 | 0.02 | 0.022 | 0.02 | 0.022 | 0.02 | 0.022 | 0.02 |
| *N,N*-Diethyl-*p*-toluidine | 0.55 | 0.5 | 0.55 | 0.5 | 0.55 | 0.5 | 0.55 | 0.5 |
| *N,N*-Dimethyl-*o*-toluidine | 0.22 | 0.2 | 0.22 | 0.2 | 0.22 | 0.2 | 0.22 | 0.2 |
| BYK 410 | 0.55 | 0.5 | 0.55 | 0.5 | 0.55 | 0.5 | 0.55 | 0.5 |
| Saccharin | 1.65 | 1.5 | 1.65 | 1.5 | 1.65 | 1.5 | 1.65 | 1.5 |
| Polyethylene powder | 1.65 | 1.5 | 1.65 | 1.5 | 1.65 | 1.5 | 1.65 | 1.5 |
| Silica | 2.2 | 2 | 2.2 | 2 | 2.2 | 2 | 2.2 | 2 |
| Red dye solution | 0.198 | 0.18 | 0.198 | 0.18 | 0.198 | 0.18 | 0.198 | 0.18 |
| Cumene hydroperoxide | 2.2 | 2 | 2.2 | 2 | 2.2 | 2 | 2.2 | 2 |
| Polyamide wax | 0 | 10 | 0 | 10 | 0 | 10 | 0 | 10 |

© Woodhead Publishing Limited, 2010




*5.2* Breakaway and breakloose strength comparison of semi-solid anaerobic adhesives and controls after aging at ambient temperature for 24 hours.

have been utilized for many years as the reducing agents in the anaerobic cure system. Often, APH has been used with the addition of an organic acid to improve the cure speed of the adhesive. The reaction of phenylhydrazine (**20**) with cyclic anhydrides (**21**) produces novel APH analogs (**22**), in high yield and purity, as shown in Equation 5.1. These materials combine the hydrazine reactive portion of APH and the organic acid functional group into one molecule (Klemarczyk *et al*., 2004).




Phenylhydrazine (**20**) (**21**) R=H, $CH_3$, $CH_2$ (**22**)

[5.1]

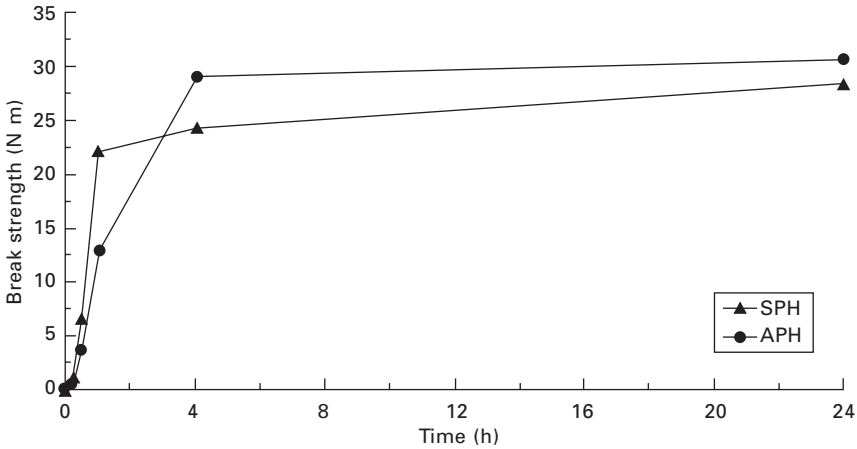
Table 5.4 summarizes the anhydrides, which were utilized as coreactants with phenylhydrazine, and the resulting reaction products. An example of the similarity in reactivity between APH and SPH is demonstrated in Fig. 5.3 for the development of breakaway adhesive strength from ASTM Test D-5649 over 24 hours for model adhesive formulations that contain the two different aromatic arylhydrazine curatives.

Additional reducing agents, which include a carboxylic acid functional group, are *N*-alkyl-*N*-phenyl glycines. For example, *N*-methyl-*N*-phenyl glycine (**23**), performs effectively as a replacement for *N*,*N*-dialkyl-*p*-toluidine in the anaerobic cure system (Klemarczyk and Brantl, 2005).

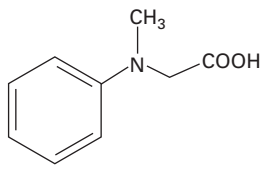
© Woodhead Publishing Limited, 2010

*Table 5.4* Anhydride coreactants with phenylhydrazine and the products

| Anhydride | Reaction product |
|---|---|
| Maleic anhydride | Maleic phenylhydrazine (MPH) |
| Itaconic anhydride | Itaconic phenylhydrazine (IPH) |
| Citraconic anhydride | Citraconic phenylhydrazine (CPH) |
| Succinic anhydride | Succinic phenylhydrazine (SPH) |




*5.3* Breakaway strength comparison of anaerobic formulations with APH and SPH over time.

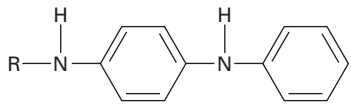



*N*-Methyl-*N*-phenylglycine (**23**)

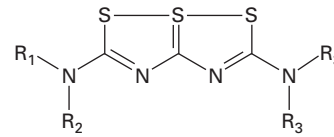
Two other classes of reducing agents, which have been investigated, include alkyl and aryl phenylene diamines (**24**) (Zhu and Attarwala, 2004) and substituted trithiadiazapentalenes (**25**) (McArdle and Barnes, 2003). Both classes of curatives are claimed to improve cure speed of the adhesive and the trithiadiazapentalenes are also claimed to reduce the effects of oxygen inhibition on the residual uncured adhesive on an assembled part.

Saccharin (benzosulfimide) has been used as a standard component in the anaerobic cure system as a cure accelerator since the earliest days of the technology. A series of linear saccharin analogs, di-*p*-toluylsulfonimide (**26**), t-butylbenzoyl toluylsulfonamide (**27**) methylbenzoyl toluylsulfonamide (**28**) and methoxybenzoyl toluylsulfonamide (**29**) were evaluated and were found

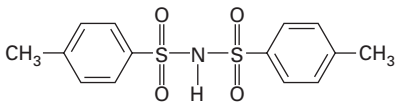
© Woodhead Publishing Limited, 2010



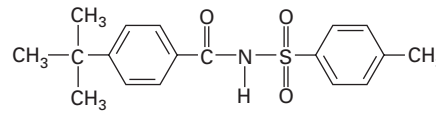
Alkyl and aryl phenylene diamines (**24**)



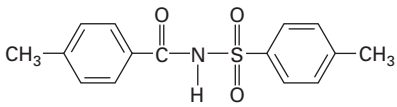
Alkyl trithiadiazapentalenes (**25**)



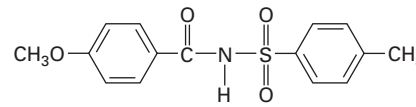
Di-*p*-toluylsulfonimide (**26**)



t-Butylbenzoyl toluylsulfonamide (**27**)



Methylbenzoyl toluylsulfonamide (**28**)



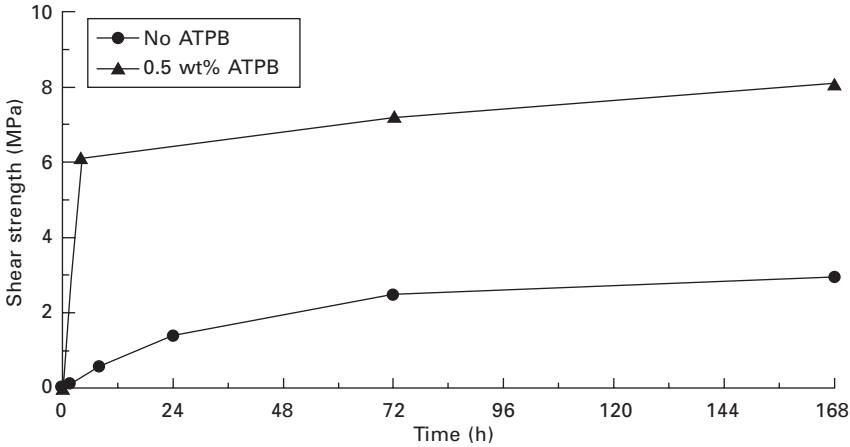
Methoxybenzoyl toluylsulfonamide (**29**)

to be acceptable replacements for saccharin in the anaerobic adhesive cure system (Klemarczyk *et al.*, 2005).

### 5.3.3 Surface insensitive anaerobic adhesives

As discussed earlier, anaerobic adhesives require the presence of metal ions, such as copper or iron, in the redox cure system to catalyze the polymerization of the adhesive. Because other metals, such as magnesium or nickel, or plastic surfaces do not catalyze the polymerization effectively, these surfaces must generally be treated with an activator to initiate anaerobic cure. Novel technology, which overcomes this limitation, particularly for magnesium substrates, was recently developed. It involves the addition of tetrasubstituted ammonium or tetrasubstituted phosphonium salts to the adhesive to overcome the limited activating capability of the surface (Woods *et al.*, 2006). A small amount, 0.5 wt%, of allyltriphenylphosphonium bromide (ATPB) was added to an anaerobic adhesive and these two formulations were evaluated in magnesium lapshear adhesion tests. The development of adhesive strength on the lapshears was monitored over seven days. Figure 5.4 demonstrates how effectively the addition of the phosphonium salt improves the speed of cure and the final adhesive tensile shear strength of the anaerobic adhesive on the relatively inactive surface.

© Woodhead Publishing Limited, 2010




*5.4* Tensile shear strength comparison of magnesium lapshear specimens assembled with anaerobic formulations with and without allyltriphenylphosphonium bromide (ATPB) over time.

### 5.3.4 Thermal resistance

Several recent investigations have demonstrated that the thermal resistance of anaerobic adhesives can be significantly improved by the addition of various additives and the use of specific methacrylate monomers. New technology for improving thermal resistance includes the use of allyl ethers of phenols, such as the diallyl ether of bisphenol A (DABPA) (**30**), in combination with a latent acid catalyst for this purpose (Woods *et al*., 2002). The data in Fig. 5.5 demonstrate the increase in adhesive strength after six weeks at 200°C for steel lapshear test specimens assembled with the modified adhesive. The combination of DABPA and latent acid clearly improves the thermal stability of the adhesive.

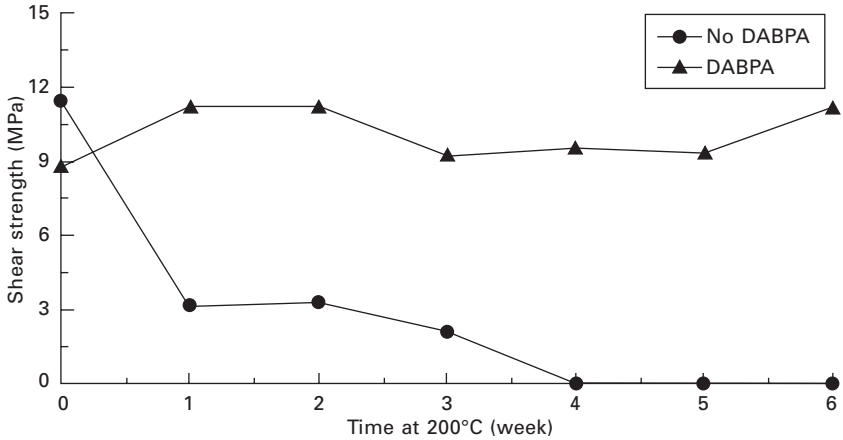
Unexpectedly, the addition of latent epoxy curing agents, such as Ajicure PN-23, which is an amine/epoxy adduct, can also significantly improve the thermal resistance of a cured anaerobic adhesive (Klemarczyk and Masterson, 2002). Figure 5.6 compares the effect of adding increasing amounts of Ajicure PN-23 to a control anaerobic adhesive formulation and aging the steel lapshear test specimens at 250°C for seven days.

Inclusion of oligomeric siloxanes, which contain methacrylate functional groups, in the anaerobic adhesive formulation has also been shown to improve the thermal resistance of the cured adhesives for extended periods of time at 200°C (Fujimoto *et al*., 1999; Attarwala *et al*., 2002).

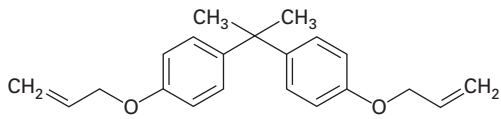
### 5.3.5 Accelerated cure speed

The addition of a metal methacrylate adhesion promoter, Chartwell B-545.1 increased the ultimate tensile adhesive shear strength of magnets bonded

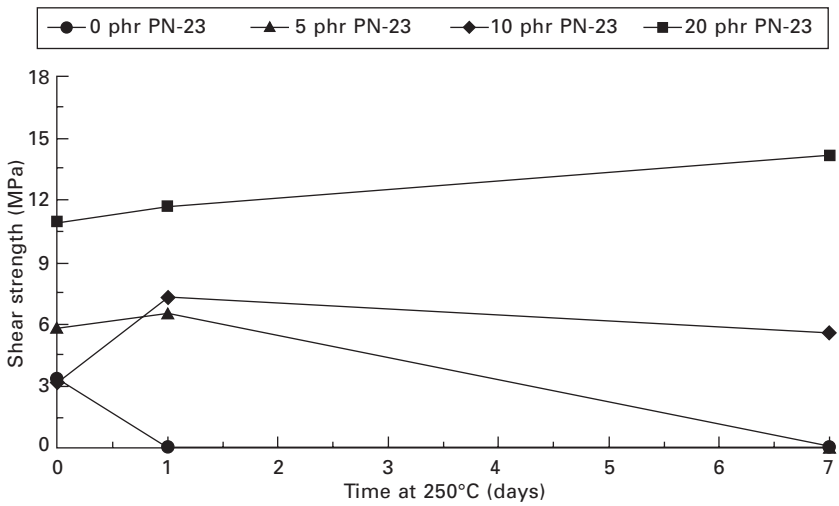
© Woodhead Publishing Limited, 2010




*5.5* Tensile shear strength comparison of steel lapshear specimens assembled with anaerobic formulations with and without the diallyl ether of bisphenol A (DABPA) and aged at 200°C for six weeks.

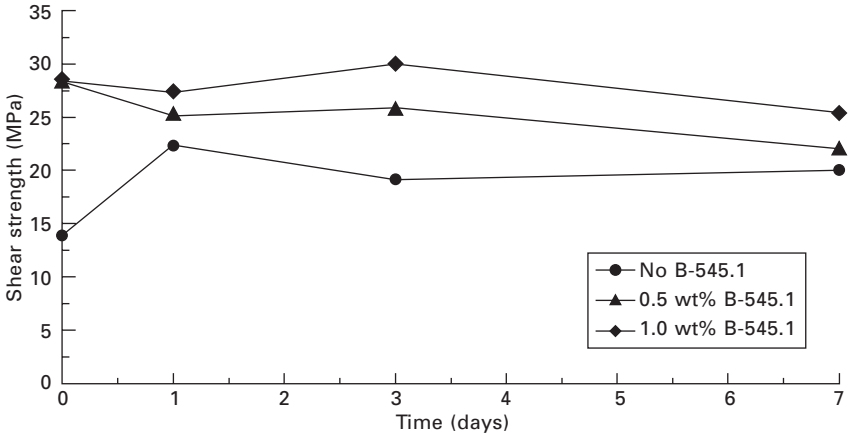



Diallyl ether of Bisphenol A (DABPA) (**30**)




*5.6* Tensile shear strength comparison of steel lapshear specimens assembled with anaerobic formulations with different concentrations of Ajicure PN-23 after aging at 250°C for one week.

© Woodhead Publishing Limited, 2010




*5.7* Tensile shear strength comparison of magnets bonded to epoxy coated steel with anaerobic formulations with two concentrations of Chartwell B545.1 after aging at ambient temperature for one week.

to epoxy coated steel, which were assembled with the modified anaerobic adhesives. In addition, it improved the cure speed of the formulations at ambient temperature (Newberth and Rachielles, 2003), as demonstrated in Fig. 5.7. The mechanism for this accelerated cure is still unclear.

### 5.3.6 Dental applications

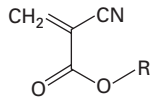
Because anaerobic adhesive products can be formulated with essentially 100% reactive ingredients, the cured adhesive contains a minimal amount of unreacted components. In addition, specific adhesive properties can be tailored to meet a product profile by formulating with the range of raw materials, which are available commercially. These features make them attractive candidates for dental applications, especially for temporarily bonding metal braces to teeth. The effective use of anaerobic adhesives has now been demonstrated both *in vitro* and *in vivo* for this specific application (Ireland and Sherriff, 2006). The optimal bonding occurred after the surface of the tooth was etched with a phosphoric acid/copper solution.

## 5.4 Introduction to cyanoacrylate adhesives

### 5.4.1 History

Cyanoacrylate adhesives are solvent free, rapid-curing 'one part' adhesives based on alkyl 2-cyanoacrylate monomers (**31**). The cure reaction associated with these adhesives is so rapid that they are referred to as 'instant adhesives' or 'superglue' (Lee, 1986). Cyanoacrylate adhesives are unique in that they bond rapidly and easily to a variety of substrates.

© Woodhead Publishing Limited, 2010



Alkyl 2-cyanoacrylate (**31**)

Cyanoacrylate adhesives were introduced in 1958 by Eastman Kodak but were not fully commercialized until the 1970s. The reason for this delay was related to the difficulty in manufacture and packaging of such reactive materials in a way that ensured that the product remained liquid. In the 1970s, Loctite and several Japanese companies entered the market with products that had sufficient shelf life to be commercially viable.

Cyanoacrylate adhesive products are usually based on the ethyl ester but methyl, n-butyl, allyl, β-methoxyethyl and β-ethoxyethyl are also important. Formulated adhesives, essentially, consist of pure monomer with relatively small amounts of property-modifying additives. The curing reaction is anionic polymerization, initiated by traces of alkaline material present on most substrate surfaces in conjunction with low levels of surface moisture. Cyanoacrylate adhesives will bond a wide variety of substrates with the exception of polyolefins (unless pre-treated), Teflon and highly acidic surfaces. Porous substrates such as wood, paper and leather require the use of products containing accelerators. Formulations are available which, when used in conjunction with a so-called primer, can give high bond strength on polyethylene and polypropylene. As with any adhesive, surface preparation is important. Pretreatment of metals is most easily achieved by solvent degreasing and grit-blasting. Pretreatment of polymers usually involves cleaning in a non-solvent and optional surface abrading. Glass and ceramics require surface cleaning and drying.

Some of the advantages and disadvantages of cyanoacrylate adhesives are shown in Table 5.5.

## 5.4.2 Chemistry

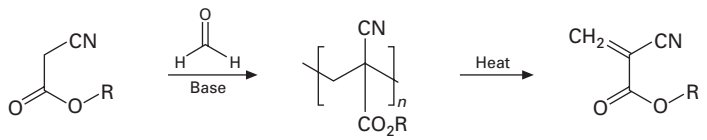
Alkyl 2-cyanoacrylate esters can be prepared by several synthetic procedures but the only method of commercial importance involves the Knoevenagel condensation of an alkyl cyanoacetate with formaldehyde. As this is a base-catalyzed reaction, the monomer is rapidly polymerized to give a low-molecular weight poly(alkyl-2-cyanoacrylate). The resulting polymer is depolymerized by heating under controlled conditions to yield monomeric cyanoacrylate, shown in equation 5.2.

Depolymerization is carried out under vacuum in the presence of an acid such as sulfur dioxide. The monomer which distills from the reaction mixture

© Woodhead Publishing Limited, 2010

*Table 5.5* Advantages and disadvantages of cyanoacrylate adhesives

| Advantages | Disadvantages |
|---|---|
| Excellent adhesion to many different substrates | Blooming – polymerized monomer vapor appears as a white deposit near to the bond line |
| Very rapid, one part room temperature cure | Slower times to achieve green strength in bond lines with a larger gap |
| Bond strength develops very quickly | Stress cracking can occur with some plastics |
| Can be used to bond polyolefins in combination with a primer | Cured adhesive is a thermoplastic with poor hot strength and solvent resistance |
| | Thermal and chemical stability are not as good as with other structural adhesives |
| | Low peel and impact strength |
| | Relatively high cost |
| | Pungent odor |
| | Bonds skin instantly |




[5.2]

is collected in a vessel containing radical and anionic polymerization inhibitors. The patent literature contains references to many different monomers, but only a limited group of monomers are actually used in commercial products. The structures of the most common monomers are shown in Table 5.6.

Cyanoacrylates can be polymerized by free radical and ionic initiators. In the context of adhesive curing, ionic polymerization is by far the most important mode of chain growth. The marked susceptibility of these monomers to initiation by anions and nucleophiles is responsible for their usefulness as adhesives. The cyanoacrylate π-electron system is under the influence of two strongly electron attracting groups. This results in a reduced electron density on the β-carbon and enhanced susceptibility to nucleophilic attack (Equation 5.3).

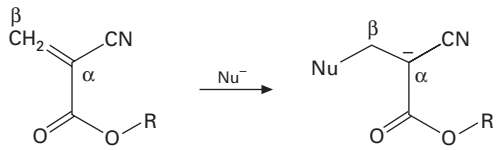
The carbanion formed at the α-carbon is stabilized by delocalization of the anionic charge by tautomeric structures I and II (Scheme 5.3).

The combination of a highly electrophilic β-carbon, a stable carbanion and an unhindered β-carbon confer on alkyl-2-cyanoacrylates their unique reactivity. When used as adhesives, polymerization or curing is brought about by nucleophilic species present on the substrate. The nucleophile can be an ion or a neutral molecule (amines, phosphines, alcohols). If the initiating species is an anion the polymerization proceeds by an anionic mechanism. If a neutral, nucleophilic molecule is involved, the reaction is referred to

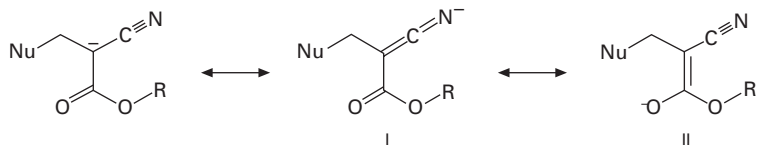
© Woodhead Publishing Limited, 2010

*Table 5.6* Chemical structures of different cyanoacrylate esters

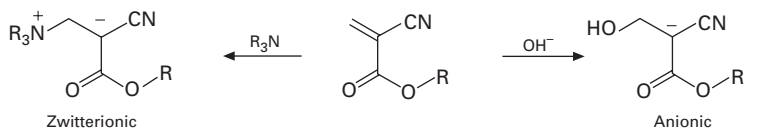
| Chemical structures of R | |
|---|---|
| Methyl | $CH_3$ |
| Ethyl | $CH_2CH_3$ |
| *n*-Butyl | $CH_2CH_2CH_2CH_3$ |
| Allyl | $CH_2CH{=}CH_2$ |
| β-Methoxyl | $CH_2CH_2OCH_3$ |
| β-Ethoxyl | $CH_2CH_2OCH_2CH_3$ |




[5.3]




Scheme 5.3




Scheme 5.4

as a zwitterionic polymerization (Pepper, 1978) (Scheme 5.4). A zwitterion from the reaction between an equimolar amount of ethyl cyanoacrylate and dimethyl phenylphosphine has actually been isolated and characterized spectroscopically (Klemarczyk, 2001). This zwitterion will initiate ethyl cyanoacrylate polymerization, if it is added to an excess of the cyanoacrylate monomer.

The nature of the polymerization, anionic or zwitterionic is dependent on the substrates involved. Both are extremely rapid, with overall rates much greater than radical polymerizations. Ionic polymerizations are normally sensitive to termination reactions, but in the case of cyanoacrylates only strong acids are capable of terminating the growing chain. Some chain-transfer reactions are believed to occur owing to the presence of carboxylic acids formed by monomer hydrolysis. A proton is transferred to the reactive carbanion at the terminus of the growing polymer chain to produce a 'dead'

© Woodhead Publishing Limited, 2010

*Table 5.7* Glass transition temperatures of poly(alkyl cyanoacrylates)

| Polymer | Glass transition (°C) |
|---|---|
| Methyl | 160 |
| Ethyl | 138 |
| *n*-Butyl | 90 |
| Allyl | 130 |
| β-Methoxyethyl | 85 |
| Octyl | 10 |

polymer. The weak acid anion is then capable of acting as an initiator and a new active center is generated by reaction with monomer.

### 5.4.3 Poly(alkyl cyanoacrylates)

Cured poly(alkyl cyanoacrylates) are clear thermoplastic polymers, very similar to poly(methyl methacrylate). The physical properties of the polymer are dependent on the nature of the ester side chain. The glass transition temperature of some of the more common polymers can be seen in Table 5.7 (Cheung *et al.*, 1987).

## 5.5 Cyanoacrylate adhesive formulations and adhesive types

### 5.5.1 Adhesive formulations

Formulated adhesives essentially consist of a pure monomer with relatively small amounts of additives that improve the performance profile of the product. They can be divided into two general groups:

1. those that modify the polymerization process
2. those that alter the properties of the final polymer.

*Polymerization process modifiers*

Stabilizers

The major difficulty associated with the manufacture of cyanoacrylate adhesives is ensuring a balance between stability (product life) of the product and cure speed. This problem has been solved by careful choice of anionic polymerization inhibitors. The materials employed are acidic compounds present at levels between 5 and 100 ppm: sulfur dioxide, sulfamides, sulfur trioxide, sulfonic acids, sulfones, cationic exchange resins, boric acid chelates.

These materials behave as strong acids. The mechanism of stabilization

© Woodhead Publishing Limited, 2010

is believed to involve protonation of the cyanoacrylate anion or zwitterion before any significant chain growth can occur. During storage, only small traces of initiating species will find their way into the formulations. The strong acid stabilizer will kill or deactivate any initiating species and the formulation will remain liquid and active for a period proportional to the concentration of strong acid. This strong acid has a profound influence on the cure characteristics of the adhesive. When an adhesive bond is formed and the film of liquid adhesive is compressed into a thin layer, the concentration of initiating species, after short period of time (seconds), overwhelms the strong acid stabilizers and a rapid polymerization occurs. The time between bond formation and polymerization is directly proportional to the concentration of strong acid. If too much strong acid is present, this induction period becomes very long and the adhesive ceases to appear to bond instantly. This is why a correct balance of stabilizer level and cure speed is essential. Free radical polymerization inhibitors are also added. These are phenolic compounds such as hydroquinone or hindered phenols.

### Accelerators

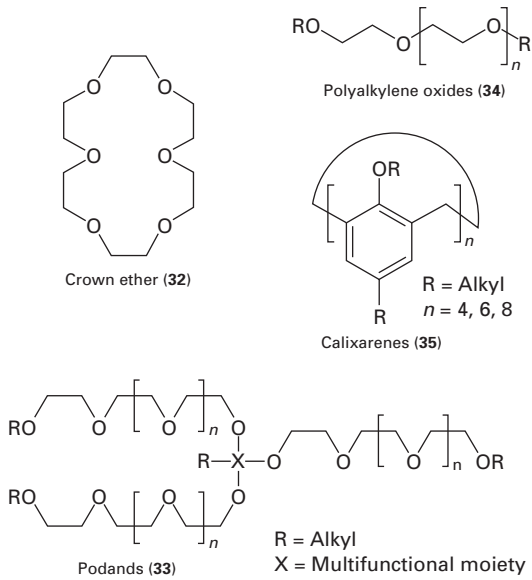
Accelerators increase the rate of polymerization. They are not polymerization initiators as they are not sufficiently nucleophilic to induce polymerization. One of the problems with early cyanoacrylate adhesives was that they were not capable of bonding porous substrates such as paper, wood and leather. Closer examination of the phenomenon revealed that the low viscosity liquid was rapidly absorbed by the porous substrate before polymerization occurred. Simple increases in the viscosity of the adhesive were not effective in promoting fixture. Several materials were identified and appeared in the patent literature (Motegi and Kimura, 1979, Motegi *et al*., 1980; Tomaschek and Berlinghof, 1981; Tomaschek and Reich, 1983; Tomaschek *et al*., 1984) that were claimed to promote cure on porous substrates. The compounds described have one common feature, namely they are all capable of sequestering alkali metal cations. The mechanism by which accelerators function is not clear, but it is believed to involve either increasing ion separation at the growing chain end or activation of anions on the substrate by cation sequestration to give so-called 'naked' anions in the liquid adhesive by a phase transfer process. Examples of compounds used as accelerators are crown ethers (**32**), podands (**33**), polyalkylene oxides (**34**), and calixarenes (**35**).

## *Polymer property modifiers*

### Adhesion promoters

The patent literature (Konig, 1976; Schoenberg, 1979; Schoenberg and Ray-Chaudhuri, 1979) describes the use of carboxylic acids and anhydrides as

© Woodhead Publishing Limited, 2010




adhesion promoters on metallic substrates. It is assumed that the carboxylic acid group is able to form a complex with the metal surface and that some degree of copolymerization takes place. There is, however, little or no experimental evidence to substantiate copolymerization. The addition of these acidic materials may also result in a reduction in cure speeds. Weak acids such as carboxylic acids are problematic materials in cyanoacrylate adhesives. These acids can terminate a growing anionic chain, but the carboxyl anion is sufficiently nucleophilic to initiate polymerization of the cyanoacrylate monomer. Weak acids, therefore, act as inhibitors in cyanoacrylate adhesives. Any acidic additive, designed to improve some aspect of the properties of the adhesive, may influence the cure speed of the adhesive. The monomer itself slowly hydrolyzes to produce cyanoacrylic acid. This is why many cyanoacrylate products may suffer a loss in activity on storage over long (years) periods of time.

## Plasticizers

Plasticizers are required to reduce the inherent brittleness of poly(alkyl-2-cyanoacrylates). This can be achieved by using non-copolymerizing plasticizers. Many materials have been suggested (Joyner and Coover, 1957; O'Sullivan and Bolger, 1972; Allies and Zimmerman, 1978; Brinkmann and Imoehl, 1976) or examined in this context: aliphatic esters of mono and

© Woodhead Publishing Limited, 2010

multi functional carboxylic acids. In practice only low levels (10–15%) of plasticizer are found in cyanoacrylate adhesives. Plasticizer concentrations greater than this can compromise the physical properties of the cured adhesive and the reactivity of the liquid adhesive. Higher alkyl cyanoacrylates that copolymerize with the basic adhesive monomer have also been investigated as internal plasticizers for cyanoacrylate adhesives (Klemarczyk, 1998).

### Toughers

Toughness properties can be improved by the inclusion of rubber toughening materials such as ABS (acrylonitrile-butadiene-styrene) or MBS (methacrylate-butadiene-styrene) copolymers (Kato *et al*., 1972; Gleave, 1978; O'Connor, 1984; Teramoto *et al*., 1982). Whichever approach is adopted, toughness is only achieved at the expense of reduced cure speed.

### Thermal stabilizers

Thermal stability can be improved by including additives in the formulation which give rise to a more thermally stable polymer. Examples of this approach are the use of biscyanoacrylate and bismaleimide cross-linking agents (Buck, 1976, 1977a, b, c, d, e). Loss in performance may also be attributed to a temperature-induced loss in adhesion. Phthalic anhydride is believed to act as a high-temperature adhesion promoter.

### Hydrophobic additives

Moisture resistance may be increased on metal and glass substrates by including cross-linking agents that may yield a more hydrolytically stable polymer or by using hydrophobic monomers such as fluorinated cyanoacrylates. Silane coupling agents also improve moisture durability. There is also evidence to suggest that inclusion of some of the anhydrides described above has a beneficial effect.

### Miscellaneous

Other modifications that can be made to cyanoacrylate adhesives include increasing the viscosity by the addition of thickeners such as polymethylmethacrylate, cellulose esters or hydrophobic silica fillers. Colour can be imparted to the product by using selected dyes and pigments.

© Woodhead Publishing Limited, 2010

## 5.5.2 Types of cyanoacrylate adhesives

Standard ethyl cyanoacrylate adhesives

A cyanoacrylate adhesive based on ethyl-2-cyanoacrylate that may be thickened. Thickening is usually accomplished by the addition of a carefully chosen grade of poly(methylmethacrylate).

Surface insensitive ethyl cyanoacrylate adhesives

Cyanoacrylates are cured by anions or nucleophiles on the substrate to be bonded. The inclusion of additives such as polyethyleneoxy compounds and, especially, crown ethers, gives rise to enhanced cure on porous substrates such as leather and wood.

Toughened ethyl cyanoacrylate adhesives

Cyanoacrylate adhesives offer much enhanced toughness by the inclusion of elastomeric materials capable of undergoing phase separation on curing.

Thermally resistant ethyl cyanoacrylate adhesives

Polymeric cyanoacrylates start to decompose thermally (unzipping) at temperatures approaching 140°C. However, the useful temperature limit on regular CA products is usually between 80 and 120°C. The higher values are obtained on flexible, base free substrates. Thermal bond strength enhancing additives are also added to 'toughened CAs' to offer multiple benefits.

UV curable ethyl cyanoacrylate adhesives

UV curable ethyl cyanoacrylate adhesives include low levels of materials that can undergo UV photo-generation of nucleophilic initiators. The fast UV cure means that the adhesives can be used on UV transparent substrates in thick bond lines.

Flexible cyanoacrylate adhesives

Flexible cyanoacrylate adhesives contain external plasticizers or are based on higher alkyl cyanoacrylate/ethyl cyanoacrylate/plasticizer mixtures. The distinctive feature is that the polymer formed remains flexible in the bond line indefinitely.

© Woodhead Publishing Limited, 2010

### Low 'bloom' cyanoacrylate adhesives

When bonds are prepared with ethyl cyanoacrylate-based adhesive, there is a tendency for the monomer vapor to polymerize on surfaces exterior to the bond line. This polymerized monomer forms a chalky white deposit referred to as 'blooming'. To avoid this effect a range of cyanoacrylate adhesives based on monomers with lower vapor pressure is available. The most commonly used are β-methoxyethyl and β-ethoxyethyl cyanoacrylates. These monomers were chosen because of their balance of low vapor pressure and cured polymer properties. Monomers with low vapor pressure such as hexyl or octyl CA are not used because the cured polymer is too soft and flexible for many adhesive applications. The low blooming adhesives also have the added advantage of being free of the irritating odor of simple ethyl cyanoacrylate-based adhesives.

### Cyanoacrylate adhesives for low surface energy substrates

Conventional cyanoacrylate adhesives will not bond low surface energy substrates such as polyethylene, polypropylene and polytetrafluoroethylene. Primer/adhesive systems have been developed (Kneafsey and McDonnell, 1989; Klemarczyk and Okamoto, 1993) that give very impressive performance when bonding polyolefins, particularly polypropylene. The substrate is treated with a dilute solution of strong nucleophile in a volatile solvent. When the solvent has evaporated, the adhesive is applied and the bond assembled in the normal way. Some typical adhesive tensile shear strength properties, which were obtained from lapshear or blockshear tests according to ASTM Method D1002-05 or ASTM D4501-01, respectively, for a wide variety of substrates are given in Table 5.8.

## 5.5.3 Durability of cyanoacrylate adhesive bonds

The durability or the behavior of an adhesive bond when exposed to a particular environment is one of the most important properties of an adhesive. One of the major disadvantages of cyanoacrylate adhesives is their poor performance under moderate to harsh environments. This is particularly apparent on metal and glass substrates. On plastics and flexible rubbers, durability is quite good. Bond failure on these materials is often due to substrate failure.

## 5.5.4 Thermal resistance

There are two main issues associated with the performance of cyanoacrylate adhesives at elevated temperature. The first is often referred to as 'hot strength'; the strength of the adhesive bond measured at an elevated

© Woodhead Publishing Limited, 2010

*Table 5.8* Typical tensile shear bond strengths achievable with cyanoacrylate adhesives

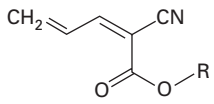
| Substrates | Bond strength (MPa) |
|---|---|
| Steel–steel | 22.8 |
| Aluminum–aluminum | 15.7 |
| Butyl rubber–butyl rubber | 1 |
| BR rubber–SBR rubber | 0.9 |
| Neoprene–neoprene | 0.7 |
| SBR rubber–phenolic | 0.7 |
| Phenolic–phenolic | 6.4 |
| Phenolic–aluminum | 6.3 |
| Aluminum–nylon | 6.6 |
| Nylon–nylon | 4.1 |
| Acrylic–acrylic | 5.5 |
| ABS–ABS | 4.9 |
| Polystyrene–polystyrene | 2.3 |
| Polycarbonate–polycarbonate | 6.6 |
| Polyester (GRP)–polyester (GRP) | 4.7 |

temperature. Polycyanoacrylates are thermoplastic materials and therefore soften and flow at temperatures above the glass transition temperature ($T_g$). In the case of polyethylcyanoacrylate the $T_g$ is in the region of 140–150°C. Clearly at temperatures close to or above these values the bond will exhibit low strength. In many cases, because the cure reaction is surface initiated, the polyethylcyanoacrylate polymer is plasticized with uncured monomer. This can often lead to poor hot strength at temperatures well below the theoretical $T_g$ of the fully cured polymer.

In most adhesive technologies, hot strength can be improved by the addition of cross-linking agents to the formulation. In the case of cyanoacrylates, this is very difficult to achieve because despite much research effort no practical cross-linking additives have been identified. Obviously a multifunction cyanoacrylate monomer would be capable of cross-linking a cyanoacrylate polymer. This has been clearly demonstrated (Buck, 1977a, b, c, d, e). The isolation of a pure difunctional cyanoacrylate ester has also been reported (Klemarczyk, 1996, 1998), but its addition to ethyl cyanoacrylate did not significantly affect the adhesive properties of the monomer, except for improved solvent resistance. Unfortunately there is no synthetic route for the preparation of multifunctional cyanoacrylates that can be used in a manufacturing/industrial context. There are many references in the patent and open literature describing the preparation and properties of multifunctional cyanoacrylates but no product containing such a material has ever been commercialized.

Alkyl 2-cyanopentadienoates (**36**) (Teramoto *et al.*, 1982; Millet, 1984) have also been claimed to improve the thermal properties of cyanoacrylate

© Woodhead Publishing Limited, 2010




Alkyl 2-cyanopentadienoate (**36**)

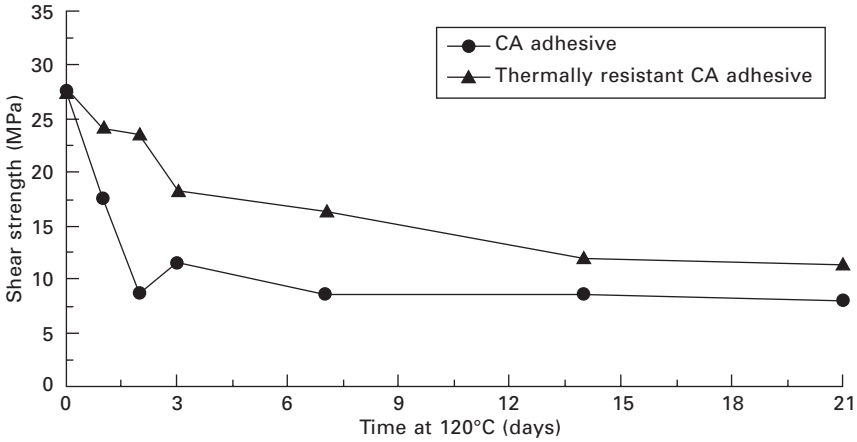
adhesives. These monomers can be polymerized by nucleophiles and anions in an analogous manner to cyanoacrylates but at a much slower rate. It is unlikely that any copolymerization takes place. Despite claims made in patents and research paper there are no commercial products containing these materials.

Allyl cyanoacrylate and other monomers that contain an unsaturated double bond in the ester side chain have been the subject of many studies (Kotzev *et al*., 1981) as potential cross-linking monomers for cyanoacrylate adhesives. Unfortunately the reactivity of these double bonds, compared to the activated cyanoacrylate double bond, is negligible. The allyl group can undergo thermally induced cross-linking by a free radical mechanism, but the temperature and time required are too great to give any improvements in hot strength.

The second aspect of thermal resistance is the response of the bond to long-term aging at high temperatures. Thermal durability is determined by exposing the adhesive bond to an elevated temperature for a period of time followed by cooling to room temperature and determining the bond strength. Simple standard ethyl cyanoacrylate adhesives show loss in strength at relatively moderate temperatures (80–100°C). This is believed to be partly due to simple physical effects resulting from a thermal post cure of uncured monomer. The conversion of the uncured monomer to polymer has the effect of increasing the brittleness of the cured adhesive. This can give rise to a reduction in tensile shear strength. In general, when metal substrates are bonded by ethyl cyanoacrylate based adhesives, rapid reductions in bond strength are observed at temperatures above 100°C. Typical behavior can be seen in Fig. 5.8 after mild steel lapshears are assembled using a typical ethyl cyanoacrylate adhesive and then aged at 120°C for three weeks. The bond strength drops dramatically over two days aging at 120°C and will fall eventually to zero.

Attempts have also been made to improve thermal durability by the addition of a difunctional cyanoacrylate ester monomer and copolymerizable electron deficient monomers (Klemarczyk, 1998) to the standard ethyl cyanoacrylate instant adhesive monomer. Again no products have appeared in the market place based on these developments. The reality of the situation is that no cost effective manufacturing technology for multifunctional cyanoacrylate monomers exists and that the benefits obtained by the inclusion of cyanopentadienoates or other electron deficient monomers is insufficient to warrant commercialization.

© Woodhead Publishing Limited, 2010




*5.8* Tensile shear strength comparison of steel lapshear specimens assembled using a typical instant adhesive and a thermally resistant instant adhesive after heating at 120°C for 21 days.

Some progress has been made in developing cyanoacrylate adhesives that show moderate improvements in thermal durability. The behavior of a typical thermally resistant cyanoacrylate adhesive can be seen in Fig. 5.8. This product shows improved performance over the standard ethyl cyanoacrylate product, but the effect is not very dramatic. These improvements are obtained by the use of additives (1–20%) that are claimed to improve the thermal stability of the cured polymer or act as adhesion promoters at higher temperatures. These additives include maleimide and bismaleimide resins in combination with acrylate monomers (Setsuda and Sugiyama, 1972). The inventors claim that the maleimides co-react with the cyanoacrylate during curing and the acrylate cross-links the resulting polymer.

A common group of additives found in thermally resistant cyanoacrylate adhesives are anhydrides. Maleic anhydride is effective in improving the thermal durability on mild steel. Anhydrides include itaconic, phthalic and benxophenonetetracarboxylic dianhydride. The reason why these additives are effective in this regard is not clear. Thermal durability consists of a complex set of phenomena: embrittlement, thermomechanical changes, polymer chain scission and depolymerization. A characteristic feature of additives that improve adhesion retention at elevated temperatures is that they are mostly acidic or potentially acidic.

When a bond is formed with a cyanoacrylate adhesive, polymerization commences at the metal oxide interface. The initiating species is believed to be the hydroxyl anion present in the moisture bound to the metal oxide surface. The rate of propagation in cyanoacrylate polymerization kinetics has been shown to be very high, much higher that the rate of initiation (Pepper, 1978). This results in the polymerization being complete before all the potential

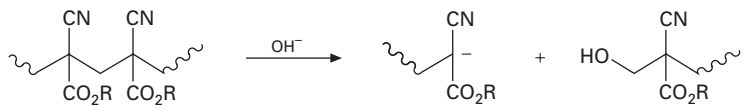
© Woodhead Publishing Limited, 2010

initiating species have been consumed. The solid polymer at the interface is in contact with a significant concentration of nucleophiles. It is believed that these basic species can induce thermal degradation/depolymerization at the interface and loss of adhesion. If the cured adhesive contains an acidic or potentially acidic material, it is possible that the basic materials can be neutralized and the potential for chemical degradation reduced. Anhydrides have the potential to generate carboxylic acid groups on heating in the presence of moisture trapped at the interface. Whatever the mechanism is, the improvements in thermal resistance are fairly modest. A truly thermally resistant cyanoacrylate adhesive remains to be developed.

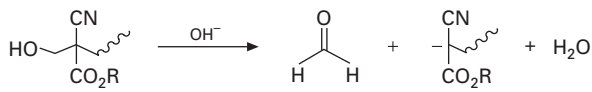
### 5.5.5 Moisture resistance

The moisture resistance of bonds created with cyanoacrylate adhesives on metals and glass is poor. It is well known that polycyanoacrylates are susceptible to hydrolysis in the presence of moisture. This degradation is very marked at pH greater than 7. In addition, on metal substrates, corrosion products may accelerate this hydrolysis process. It has been suggested (Drain *et al.*, 1984) that a combination of ingress of moisture at the metal oxide adhesive interface and ferric oxide catalyzed hydrolysis of the adhesive polymer at the interface is responsible for loss of adhesion when steel bonded with cyanoacrylate adhesives is exposed to high humidity. The observation that polycarbonate substrates bonded with cyanoacrylate adhesives have very high moisture resistance is further evidence that the metal oxide has a significant role in moisture durability.

The proposed mechanism for the hydrolytic degradation of the polymer is believed to involve hydrolytic chain scission (Leonard *et al.*, 1966), as seen in Equations 5.4 and 5.5. Production of formaldehyde has been reported (Drain *et al.*, 1984; Leonard *et al.*, 1966) and has been used as a means of monitoring the kinetics of polymer degradation in aqueous media.




[5.4]




[5.5]

Over the years researchers have approached the problem of moisture resistance by adopting a similar strategy for improving thermal resistance by the use of multifunctional cyanoacrylates, cyanopentadienoates and anhydrides (Korshak *et al.*, 1979).

© Woodhead Publishing Limited, 2010

Hydrophobic monomers capable of copolymerizing with cyanoacrylates are claimed to improve moisture resistance (Dyatlov and Katz, 1994). No manufacturer of cyanoacrylate has produced an adhesive that is claimed to have improved moisture resistance but it is well known that the thermally resistant products containing anhydrides show improved moisture resistance. This may be related to the ability of acidic residues from the anhydrides to suppress the base catalyzed degradation of the polymer at the substrate–adhesive interface.

## 5.6 Advances in cyanoacrylate technology

A survey of the total number of patents/patent applications for the period 2001–2006 shows that 1495 documents were published referring to cyanoacrylates. This number does not imply that there were 1495 individual inventions, as a single invention can give rise to several patent filings. The number provides an indication of patenting activity only.

The documents have been arbitrarily classified as shown in Table 5.9. Only 12% of the filings are related to cyanoacrylate adhesive compositions for industrial or consumer markets. The greatest area of activity has been in general applications where a cyanoacrylate has been used as part of an assembly or manufacturing process. This category covers a wide range of technologies. Some of the more unusual patents are associated with tire bonding applications (Bridgestone) and hair treatment products (L'Oreal). This major area of activity in new adhesive formulations is in tissue bonding and other medical/surgical procedures.

### 5.6.1 Industrial adhesive bonding

The most active companies during the period 2001–2006 were Henkel, Toagosei, Three Bond, Chemence, Alteco, Taoka and UHU. These companies

*Table 5.9* Patenting activity for cyanoacrylate adhesives 2001–2006

| Application | Comment | Number | % |
|---|---|---|---|
| General applications | Assorted applications using CAs | 423 | 28 |
| Medical/surgical applications | Surgical applications – not tissue bonding | 342 | 23 |
| Tissue bonding | Biomedical adhesives | 232 | 16 |
| Other applications | Other assorted CA applications | 204 | 14 |
| Cyanoacrylate adhesives | Instant adhesives | 181 | 12 |
| Polymers | Polymer synthesis | 56 | 4 |
| Encapsulation | | 23 | 1.5 |
| Dental | | 17 | 1 |
| Finger printing | | 10 | 0.7 |
| Finger nail bonding | | 7 | 0.5 |
| Total | | 1495 | |

© Woodhead Publishing Limited, 2010

accounted for 124 patent fillings relating to cyanoacrylate adhesive formulations in 2001–2006. The main areas of activity were in photocuring systems, primers/activators and toughness/flexibility (Ryan *et al.*, 2001; Misiak, 2003).

Photocuring cyanoacrylate adhesives (Wojciak and Attarwala, 2004) are relatively new developments. Ethyl cyanoacrylate monomer is formulated with a metallocene such as a ferrocene derivative and a photoinitiator that functions by hydrogen abstraction. The mechanism of the initiation process is not clear but it can be assumed the irradiation of the formula leads to the production of nucleophiles capable of initiating the polymerization of the cyanoacrylate monomer.

A patent assigned to Toagosei (Tajima and Sato, 2003) describes an adhesive formulation with improved cure speed in thick bond lines. The cyanoacrylate composition contains a haloacetate salt of metals such as aluminum, gallium, indium or thallium and a compound that has clathrating ability, such as a crown ether.

It has been shown (McDonnell *et al.*, 2006) that the addition of low levels of citric acid to ethyl cyanoacrylate adhesive greatly improves the shock resistance of metal–metal bonds. The addition of the citric acid also increases the bond strength on aluminum substrates. The shock resistance of bonded lap shear assemblies was determined by dropping bonded lap shear assemblies from a height of one meter onto a concrete surface. The assemblies were dropped repeatedly until failure was observed to occur through breakage of the bond. The number of times the bonded assembly was dropped and the bond survived were recorded as a measure of shock resistance. Typical results are shown in Table 5.10.

A solid cyanoacrylate adhesive composition has been patented (Kotzey, 2004) which can be applied to a substrate in solid form and which polymerizes into an adhesive polymer upon liquefying. The solid cyanoacrylate composition liquefies at temperatures slightly above room temperature and polymerizes upon liquefaction. ε-Caprolactones are used as a solidifying polymer with

*Table 5.10* Effect of adding various acids on the shock resistance of cyanoacrylate adhesives

| Acid | Shock resistance (number of drops) | | | |
|---|---|---|---|---|
| | Mild steel | | Aluminum | |
| | 48-hr cure | 168-hr cure | 48-hr cure | 168-hr cure |
| Pyruvic acid | 13 | 13 | >50 | >50 |
| 1,2,4-benzene tricarboxylic anhydride | 12 | 17 | 14 | 12 |
| 1,2,3-propane tricarboxylic acid | 12 | 9 | 50 | 21 |
| 1,2,4-benzene tricarboxylic acid | 16 | 17 | 17 | >70 |
| No acid | 1 | 1 | 1 | 1 |

© Woodhead Publishing Limited, 2010

cyanoacrylate monomers and other additives to form the solid cyanoacrylate adhesive composition.

A toughened cyanoacrylate adhesive composition is described (Woods and Morrill, 2004) which contains a cyanoacrylate monomer and an elastomeric copolymer soluble in the monomer. The elastomer is a copolymer of an olefin such as ethylene and methacrylate ester. The invention further discloses novel elastomeric copolymers that do not contain additives or functional groups which can interfere with the cure rate or stability of the adhesive composition in which they are included. Benefits of the copolymers include improved toughness of the cured adhesive composition.

### 5.6.2 Tissue bonding

Owing to their rapid curing and susceptibility to hydrolytic degradation, cyanoacrylate adhesives are used as alternative to sutures in what is referred to as tissue bonding. They were used extensively in the war in Vietnam by specially trained surgical teams who saved many lives by sealing severe wounds with cyanoacrylate adhesives prior to treatment by more conventional means. Modern cyanoacrylate tissue adhesives are based on butyl or octyl cyanoacrylate. The butyl ester is considered to be more suitable than the ethyl ester because poly(butyl cyanoacrylate) produces lower levels of formaldehyde when undergoing moisture induced degradation. Octyl cyanoacrylate has the added advantage of giving rise to a softer more flexible polymer than butyl cyanoacrylate. Octyl cyanoacrylate is difficult to prepare in high yield and purity. The octyl monomer is not as reactive as butyl cyanoacrylate and has to be used in conjunction with an activator. This has been an intense area of patent activity for the last ten years. Closure Medical is by far the most active company in this area.

## 5.7 Summary

Anaerobic adhesives continue to be utilized in a wide variety of industrial, aftermarket and consumer applications throughout the world. These one-part adhesives are easily dispensed by a variety of dispensing equipment and are capable of bonding a wide variety of substrates. In addition, they remain the focus of active research programs to improve their sustainability, physical properties and cure characteristics.

Cyanoacrylate adhesives or super glues are very successful and popular adhesives in the consumer market. They are used primarily for minor repairs where rapid fixture and high bond strength are required. There is however a large market for these adhesives in industrial applications. Cyanoacrylate adhesives are used where very rapid bonding or fixing is required. Dispensing equipment that can integrate the bonding process into an assembly line

© Woodhead Publishing Limited, 2010

production system is readily available. The number of applications where these adhesives are utilized is very diverse. It is often quite difficult for an adhesive manufacturer to ascertain in just what applications the products are being used because a large amount of cyanoacrylates is obtained by the customer through a distributor. The most commonly bonded substrates are plastics and rubbers. The most suitable applications are those where the bond is exposed to relatively low temperature, humidity and impact. Cyanoacrylates are being increasingly used in tissue bonding as alternative to sutures and in a wide range of surgical procedures.

## 5.8 Future trends

### 5.8.1 Sustainable products

The protection of the environment and chemical safety are serious concerns for the adhesive industry, in general, and for anaerobic adhesive products specifically. Future efforts will focus on the development of new resins, monomers, curatives, additives and processes, which will be even safer to use and result in a reduced environmental impact.

### 5.8.2 Products with improved physical properties

Continuous improvement of commercial products and the development of new, unique products are keys to the success of any business. The development of technology for new anaerobic and cyanoacrylate ester products with improved toughness, enhanced performance on less reactive surfaces and better resistance to adhesive strength degradation during high temperature exposure are highly desirable goals for the future investigations.

## 5.9 Acknowledgement

The authors wish to thank Henkel for its generous permission to publish this manuscript and Professor Rick Danheiser of the Massachusetts Institute of Technology for very helpful technical discussions.

## 5.10 References

Allies V and Zimmermann W (1978), *Debondable Cyanoacrylate Adhesive Composition*, UK patent 1,529,105, Loctite Corporation.

Attarwala S, Mazzella G, Chu H K, Luong D, Bennington L, Konarski M, Maandi E, Rich R, Li N, Newberth F and Levandoski S (2002), *High Temperature, Controlled Strength Anaerobic Compositions Curable under Ambient Environmental Conditions*, US patent 6,391,993, Loctite Corporation.

Attarwala S, Rich R and Li N (2004), *Anaerobic Compositions with Enhanced Toughness and Crack Resistance*, US patent 6,673,875, Henkel Loctite Corporation.

© Woodhead Publishing Limited, 2010

Attarwala S, Grismala R, Burdzy M and Zhu Q (2006), *Polymerizable Compositions in Non-Flowable Forms*, US patent 7,041,747, Henkel Corporation.

Baccei L (1981), *Curable Polybutadiene-Based Resins Having Improved Properties*, US patent 4,295,909, Loctite Corporation.

Beaunez P, Helary G and Sauvet G (1994a), 'Role of *N*,*N*-dimethyl-*p*-toluidine and saccharin in the radical polymerization of methyl methacrylate inititated by a redox system. I. cumene hydroperoxide/copper saccharinate', *J. Polym. Sci.: Part A: Polym. Chem.*, **32**, 1459–69.

Beaunez P, Helary G and Sauvet G (1994b), 'Role of *N*,*N*-dimethyl-*p*-toluidine and saccharin in the radical polymerization of methyl methacrylate inititated by a redox system. II. cumene hydroperoxide/iron saccharinate', *J. Polym. Sci.: Part A: Polym. Chem.*, **32**, 1471–80.

Boerio F J, Hong P, Clark P and Okamoto Y (1990), 'Surface-enhanced Raman scattering from model acrylic adhesive systems', *Langmuir*, **6**, 721–27.

Brinkmann B and Imoehl W (1976), *Cyanoacrylate Adhesives*, US patent 3,961,966, Sehering Aktiengesellschaff.

Buck C (1976), *Preparation of bis (2-Cyanoacrylate) Monomers*, US patent 3,975,422, Johnson & Johnson.

Buck C (1977a), *Blocked bis 2-Cyanoacrylate Monomers*, US patent 4,003,942, Johnson & Johnson.

Buck C (1977b), *Cyanoacrylic Acid Adducts*, US patent 4,013,703, Johnson & Johnson.

Buck C (1977c), *Modified Cyanoacrylate Monomers and Methods of Preparation*, US patent 4,041,061, Johnson & Johnson.

Buck C (1977d), *Modified Cyanoacrylate Monomers and Methods of Preparation*, US patent 4,041,062, Johnson & Johnson.

Buck C (1977e), *Modified Cyanoacrylate Monomers and Methods of Preparation*, US patent 4,041,063, Johnson & Johnson.

Burnett R and Nordlander B (1953), *Oxygenated Polymerizable Acrylic Acid Type Esters and Methods of Preparing and Polymerizing the Same*, US patent 2,628,178, General Electric Company.

Cheung K, Guthrie J, Otterburn M and Rooney J (1987), 'The dynamic mechanical properties of poly(alkyl 2-cyanoacrylates)', *Die Makromol. Chem.*, **188**(12), 3041–6.

Conway P, Melody D, Woods J, Casey J, Bolger B and Martin F (1985), *Radiation-Activatable Anaerobic Adhesive Composition*, US patent 4,533,446, Loctite (Ireland) Ltd.

Dean J (1985), *Lange's Handbook of Chemistry*, McGraw Hill, New York, pp 6-6–6-19 and private communication with Y Okamoto.

Drain K F, Guthrie J, Hung C, Martin F and Otterburn M (1984), 'Effect of moisture on the strength of steel–steel cyanoacrylate adhesive bonds', *J. Adhesion*, **17**(1), 71–81.

Dyatlov V and Katz G (1994), *Process for the Preparation of Esters of 2-Cyanoacrylate Esters and Use of the Esters so Prepared as Adhesives*, WO9415907, Eurotax Ltd.

Fujimoto T, Terada M and Endo I (1999), *Anaerobic Hardening Composition*, US patent 5,962,616, General Electric Co.

George B, Touyeras F, Grohens Y and Vebrel J (1997), 'Spectroscopic and mechanical evidence of the influence of the substrate on an anaerobic adhesive cure', *Int. J. Adhesion and Adhesives*, **17**(2), 121–6.

George B, Touyeras F, Grohens Y and Vebrel J (1998a), 'Analysis of curing mode

© Woodhead Publishing Limited, 2010

and mechanical properties of an anaerobic adhesive', *Eur. Polym. J.*, **34** (3/4), 399–404.

George B, Touyeras F, Grohens Y and Vebrel J (1998b), 'Calorimetric investigation of autoacceleration in the metal-catalyzed cure of anaerobic adhesives', *J. Adhesion Sci. Technol,* **12**(12), 1281–97.

George B, Grohens Y, Touyeras F and Vebrel J (2000), 'New elements for the understanding of the anaerobic adhesives reactivity', *Int. J. Adhesion and Adhesives*, **20**, 245–51.

Gleave E (1978), *Filled Cyanoacrylate Adhesive Compositions*, US patent 4,102,945, Loctite (Ireland) Ltd.

Grant E (1983), *Drop by Drop: The Loctite Story*, Loctite Corporation, Newington, CT.

Humphreys R (1983), 'Reaction of *N,N*-dimethylaniline derivatives with cumene hydroperoxide, oxazolidine formation via addition of α-aminomethyl radicals to formaldehyde', *J. Org. Chem.*, **48**, 1483–87.

Ireland A and Sherriff M (2006), 'An investigation into the use of an anaerobic adhesive with two commercially available orthodontic brackets', *Dental Mater.*, **22**(2), 112–18.

Joyner F and Coover H (1957), *Plasticized Monomeric Adhesive Compositions and Articles Prepared Therefrom*, US Patent 2,784,127, Eastman Kodak.

Kato K, Sasaki T and Narizawa H (1972), Japanese Patent Showa 47-51807, Denki Kaga Kogyo Kaisha.

Klemarczyk P (1996), *Synthesis of Cyanoacrylate Esters by Oxidation of Aromatic Selenyl Cyanopropionates*, US patent 5,504,252, Loctite Corporation.

Klemarczyk P (1998), 'A general synthesis of 1,1 disubstituted electron deficient olefins and their polymer properties', *Polymer*, **39**(1), 173–81.

Klemarczyk P (2001), 'The isolation of a zwitterionic initiating species for ethyl cyanoacrylate (ECA) polymerization and the identification of the reaction products between 1°, 2°, and 3° amines with ECA', *Polymer*, **42**(7), 2837–48.

Klemarczyk P and Brantl K (2005), *Cure Accelerators for Anaerobic Curable Compositions*, US patent 6,897,277, Henkel Corporation.

Klemarczyk P and Masterson M (2002), *Radical-Curable Adhesive Compositions, Reaction Products of which Demonstrate Superior Resistance to Thermal Degradation*, US patent 6,342,545, Loctite Corporation.

Klemarczyk P and Okamoto Y (1993), 'Primers for bonding polyolefin substrates with alkyl cyanoacrylate adhesive', *J. Adhesion*, **40**, 81–91.

Klemarczyk P, Brantl K and Jacobine A (2004), *Cure Accelerators for Anaerobic Curable Compositions*, US patent 6,835,762, Henkel Corporation.

Klemarczyk P, Brantl K and Messana A (2005), *Cure Accelerators for Anaerobic Curable Compositions*, US patent 6,958,368, Henkel Corporation.

Kneafsey B and McDonnell P (1989), *Diazabicyclo and Triazabicyclo Primer Compositions and Use Thereof in Bonding Non-Polar Substrates*, US patent 4,869,772, Loctite Corporation.

Konig E (1976), *Adhesive Compositions Containing a Cyanoacrylate and Itaconic Anhydride*, US Patent 3,948,794, USM Corporation.

Korshak V, Polyakova A, Suchkova M and Mager K (1979), *Adhesive Composition*, US patent 4,167,546.

Kotzev D, Ward T and Dwight D (1981), 'Assessment of the adhesive bond properties of allyl 2-cyanoacrylate', *J. Appl. Polym. Sci.,* **26**(6), 1941–9.

© Woodhead Publishing Limited, 2010

Kotzey D (2004), *Solid Cyanoacrylate Adhesive Composition and Method for its Use*, US patent 6,797,107, Chemence, Inc.

Krieble V (1959), *Compositions Containing Hydroperoxide Polymerization Catalyst and Acrylate Acid Diester*, US patent 2,895,950, American Sealants Company.

Krieble V (1965), *Accelerated Anaerobic Compositions and Method of Using Same*, US patent 3,218,305, Loctite Corporation.

Lee H (1986), *Cyanoacrylate Resins – The Instant Adhesives*, Pasadena Technology Press, Los Angeles.

Leonard F, Kulkarni R, Brandes G, Nelson J and Cameron J (1966), 'The degradation of n-butyl alpha-cyanoacrylate tissue adhesive', *J. Appl. Polym. Sci.* **10**, 259–65.

McArdle C and Barnes R (2003), *Curative for Anaerobic Adhesive Compositions*, US patent 6,583,289, Loctite (R&D) Ltd.

McDonnell P, Kelly R, Lambert R and Tierney F (2006), *Shock Resistant Cyanoacrylate Compositions*, WO2006048851A, Loctite (Ireland) Ltd.

McGettrick B, Vij J and McArdle C (1994), 'Investigations into the cure of model anaerobic adhesives using dielectric spectroscopy', *Polymer*, **35**(5), 939–48.

Millet G (1984), *Novel Cyanoacrylate Adhesive Compositions and Methods of Bonding*, US patent 4,425,471, 3M Company.

Misiak H (2003), *Cyanoacrylate Compositions Curable to Flexible Polymeric Materials*, EP1360257A1, Loctite R&D Ltd.

Moane S, Raftery D, Smyth M and Leonard R (1999), 'Decomposition of peroxides by transition metal ions in anaerobic adhesive cure chemistry', *Int. J. Adhesion and Adhesives*, **19**, 49–57.

Motegi A and Kimura K (1979), *Adhesive Composition*, US patent 4,170,585, Toagosei Chemical Industry Company.

Motegi A, Isowaa E and Kimura K (1980), *Alpha-Cyanoacrylate-Type Adhesive Composition*, US patent 4,171,416, Toagosei Chemical Industry.

Newberth F and Rachielles P (2003), *Structural Anaerobic Adhesive Compositions with Improved Cure Speed and Strength*, US patent 6,596,808, Henkel Loctite Corporation.

Okamoto Y (1990a), 'Anaerobic adhesive cure mechanism –I', *J. Adhesion*, **32**, 227–35.

Okamoto Y (1990b), 'Anaerobic adhesive cure mechanism –II', *J. Adhesion*, **32**, 237–44.

O'Connor J (1984), *Toughened Cyanoacrylates Containing Elastomeric Rubbers*, US patent 4,440,910, Loctite Corporation.

O'Sullivan D and Bolger B (1972), *Plasticized Cyanoacrylate Adhesive Compositions*, US Patent 3,699,127, Loctite (Ireland) Ltd.

Pepper D (1978), 'Kinetics and mechanisms of zwitterionic polymerizations of alkyl cyanoacrylates', *Polym. J.*, **12**(9), 629–37.

Raftery D, Smyth M, Leonard R and Heatley D (1997a), 'Effect of copper (II) and iron (III) on reactions undergone by the accelerator 1-acetyl-2-phenylhydrazine commonly used in anaerobic adhesives', *Int. J. Adhesion and Adhesives*, **17**(2), 151–3.

Raftery D, Smyth M and Leonard R (1997b), 'An electrochemical investigation on the role of saccharin in the cure chemistry of anaerobic adhesives', *J. Polym. Sci.: Part A: Polymer Chemistry*, **35**, 3327–9.

Rich R (1994), 'Anaerobic adhesives', in *Handbook of Adhesive Technology*, Pizzi A and Mittal K (eds), Marcel Dekker, New York, 467–79.

© Woodhead Publishing Limited, 2010

Ryan B, Houlihan J and McCann G (2001), *Activator Compositions for Cyanoacrylate Adhesives*, EP1280866A1, Loctite R&D Ltd.

Schoenberg J (1979), *2-Cyanoacrylate Adhesive Compositions Having Enhanced Bond Strength*, US patent 4,139,693, National Starch and Chemical Corporation.

Schoenberg J and Ray-Chaudhuri D (1979), *Adhesion Promoter for 2-Cyanoacrylate Adhesive Compositions*, US patent 4,125,494, National Starch and Chemical Corporation.

Setsuda K and Sugiyama I (1972), *Adhesive Composition Containing Alpha-Cyanoacrylate as its Main Ingredient*, US Patent 3,692,752, Matsumoto Seiyaku Kogyo Kabushiki Kaisha.

Smith J (1992), 'Kinetic studies on anaerobic initiated polymerization', *J. Appl. Polym. Sci.*, **45**, 1–15.

Tajima S and Sato M (2003), *Composition of 2-Cyanoacrylate, Lewis Acid Metal Salt and Clathrate*, US patent 6,547,985, Togosei Co. Ltd.

Teramoto T, ljuin N and Kotani T (1982), *Instant-Setting Adhesive Composition*, US patent 4,313,865, Japan Synthetic Rubber Co., Ltd.

Tomaschek H and Berlinghof P (1981), *Cyanoacrylate Adhesive Compositions*, UK patent application 2,069,512A, Teroson GmbH.

Tomaschek H and Reich K (1983), *Cyanoacrylate Adhesive Composition*, US Patent 4,386,193, Teroson GmbH.

Tomaschek H, Reich K and Busch G (1984), *Cyanoacrylate Adhesive Composition*, US Patent 4,424,327, Teroson GmbH.

Wellmann S and Brockmann H (1994), 'New aspects of the curing mechanism of anaerobic adhesives', *Int. J. Adhesion and Adhesives*, **14**, 47–55.

Wojciak S and Attarwala S (2004), *Radiation-Curable, Cyanoacrylate-Containing Compositions*, US patent 6,726,795, Henkel Corporation.

Woods J and Morrill S (2004), *Toughened Cyanoacrylate Adhesives Containing Alkene-Acrylate Copolymers and Method for Production*, US patent 6,822,052, Henkel Corporation.

Woods J, Morrill S and Jacobine A (2002), *Radical-Curable Adhesive Compositions, Reaction Products of which Demonstrate Superior Resistance to Thermal Degradation*, US patent 6,451,948, Loctite Corporation.

Woods J, Morrill S and Danheiser R (2006), *Adhesive Compositions for Bonding Passive Substrates*, US patent 7,115,676, Henkel Corporation.

Yamada A and Kimura K (1980), *Adhesive Composition*, US patent 4,196,271, Toagosei Chemical Industry Company.

Zhu Q and Attarwala S (2004), *Cure Accelerators for Anaerobic Adhesive Compositions*, US patent 6,723,763, Henkel Loctite Corporation.

© Woodhead Publishing Limited, 2010

# 6

# Advances in acrylic structural adhesives

P. C. BRIGGS, IPS Corporation, USA; and
G. L. JIALANELLA, The Dow Chemical Company, USA

**Abstract**: Acrylic adhesives as defined in this text are based on acrylate and methacrylate monomers and have been commercially used for more than 50 years. These products are supplied as two separate components that can be mixed prior to application or each component can be applied to separate surfaces. Traditionally, methacrylates are preferred over acrylates owing primarily to the odor of the acrylates. The most popular and most commercially successful structural acrylic adhesives in use today are polymerizable mixtures of polymers dispersed or dissolved in methyl methacrylate (MMA) monomer. These adhesive products are supplied as two separate components that are primarily mixed just prior to application. One component contains a peroxide compound (oxidizing agent) and the second component contains an amine or metal salt (reducing agent) that reacts with the peroxide component upon mixing to initiate the free-radical polymerization of the methyl methacrylate monomer. This chapter will review the historical evolution and cure systems of methacrylate adhesive systems. Also, it will review the first and second generation and advanced technology products as well as formulation variables, bondline properties and applications of methacrylate-based adhesive systems.

**Key words**: structural acrylic adhesives, acrylates, methacrylate, peroxide compound, oxidizing agent, tetrahydrofurfuryl methacrylate (THFMA), hydroxyethyl methacrylate (HEMA) hydroxypropyl methacrylate (HPMA).

## 6.1 Introduction

Acrylic adhesives as defined in this text are based on acrylate and methacrylate monomers and have been commercially used for more than 50 years. These products are supplied as two separate components that can be mixed prior to application or each component can be applied to separate surfaces. Traditionally, methacrylates are preferred over acrylates primarily because of the odor of the acrylates. This chapter will review the historical evolution and cure systems of methacrylate adhesive systems. Also, this chapter will review the first and second generation and advanced technology products as well as formulation variables, bondline properties and applications of methacrylate based adhesive systems.



© Woodhead Publishing Limited, 2010

### 6.1.1 Historical evolution

The most popular and most commercially successful structural acrylic adhesives in use today are polymerizable mixtures of polymers dispersed or dissolved in methyl methacrylate (MMA) monomer. As mentioned previously, these adhesive products are supplied as two separate components that are primarily mixed just prior to application. One component contains a peroxide compound (oxidizing agent) and the second component contains an amine or metal salt (reducing agent) that reacts with the peroxide component upon mixing to initiate the free radical polymerization of the methyl methacrylate monomer. Among the earliest examples of this type of adhesive were clear, colorless mil spec adhesives that first appeared in the 1950s as bonding agents for poly (MMA) sheet in applications such as aircraft canopies. In this most basic form, the polymerizable adhesive component consisted of poly (MMA) dissolved in MMA monomer with *N*,*N*-dimethyl aniline or a derivative as the amine component. A benzoyl peroxide initiator was supplied as either a powder or liquid solution.

In the 1960s, formulators began to use elastomers to supplement or replace the poly-MMA to provide toughness and provide improved bondability for a wider variety of substrates including metals, thermoplastics and thermosets (Owston, 1973). Functional monomers such as methacrylic acid and certain other additives were included for specific performance or application benefits. Today's high performance structural acrylic adhesives are the result of extensive evolutionary development of these basic systems by a number of companies who have tailored these products for increasingly demanding and sophisticated applications.

The MMA-based structural acrylics are distinctly different from other polymerizable acrylic adhesive technologies such as anaerobics, which are primarily used for narrow gap metal bonding, retaining and threadlocking, and the cyanoacrylates, which cure by an anionic mechanism. The latter are generally supplied as single component products that are catalyzed by metallic surfaces in the case of anaerobics and surface moisture in the case of cyanoacrylates. An accelerator is sometimes used to speed the cure on inactive surfaces. In addition to these reactive acrylic technologies, acrylic polymers are also found in solvent, emulsion and hot melt adhesives for a wide variety of applications. These adhesive classes have evolved concurrently over the past few decades, but this chapter will be limited to the evolution and development of the polymer-in-monomer-based structural acrylics.

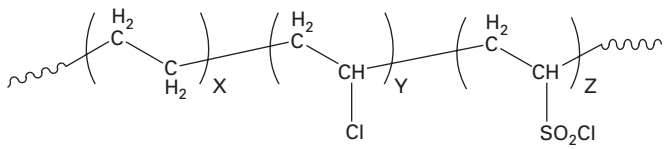
### 6.1.2 Cure systems

In the first 20 years of their development, the cure system of choice for structural acrylics most often consisted of benzoyl peroxide in combination

© Woodhead Publishing Limited, 2010

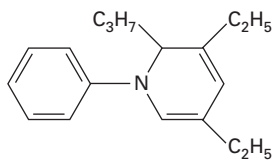
with a tertiary aromatic amine. In most cases, the amine compounds were included in the polymer-in-monomer portion, typically referred to as the adhesive component and the benzoyl peroxide was supplied as an activator or accelerator. The benzoyl peroxide was typically supplied as a paste in a plasticizer to facilitate mixing with the adhesive. Typical commercial formulations provide a working time of a few minutes, followed by rapid free radical exothermic polymerization that results in the very fast buildup of bond strength that characterizes these products. This fast cure differentiated these products from the epoxies that were gaining in popularity as well, but which take much longer to set and cure because of their kinetics of polymerization which provides a more gradual, linear buildup of strength. A convenient option for some applications involves applying the activator as a thin film from solution to one or both of the substrates to be bonded. This technique has limited utility because it is most effective in relatively thin bond gaps. Thick gaps require activation of both bonding surfaces and two-part mix-in application is generally more effective.

In the 1970s duPont introduced a new cure system for polymerizable methacrylate adhesives (Briggs, Jr. and Muschiatti, 1975). The adhesive composition comprised a solution of chlorosulfonated polyethylene, sold by duPont under the trade name Hypalon®, in a mixture of monomers and additives similar to the earlier methacrylates (Equation 6.1).




[6.1]

In the earliest embodiments, an aldehyde–amine reaction product was used as a surface activator to initiate the cure of the adhesive base when the substrates were mated. Among the many combinations of amine–aldehyde derivatives that are possible, the most effective were condensation products of butyraldehyde and aniline or butyl amine. Over the years, the butyraldehyde–aniline products have proved to be the most effective. The active ingredient is *N*-phenyl-3,5-diethyl-2,3-dihydropyridine, referred to as DHP or PDHP (Equation 6.2).




[6.2]

The original products were available as approximately 40% active unrefined condensation products. More recently, purified products containing up to 80–90% of the desired PDHP have become available (Melody *et al.*, 1984).

© Woodhead Publishing Limited, 2010

### 6.1.3 First and second generation

DuPont introduced the term 'second generation acrylic' or SGA to differentiate these products from the earlier products based on benzoyl peroxide and tertiary amines. The latter became referred to as 'first generation' products. Primary benefits of the SGAs were increased toughness and impact strength of metal to metal bonds, as well as the ability to bond metal surfaces, even oily metal surfaces, with little or no surface preparation. The products were also shown to be capable of effective performance as '100% solids' alternatives to solvent cements in applications such as plastic pipe bonding and decorative lamination of vinyl and high pressure laminates to metals and particle board. In this evolutionary stage during the 1970s and 1980s, the SGA products were promoted concurrently with development of improved waterborne systems to address looming threats against the use of flammable and toxic solvents. However, the two part nature of these products as well as other limitations prevented the SGAs from effectively competing with the simpler one part systems. Rather, the reactive methacrylate products have found a secure niche in a number of product assembly processes for which they provide unique benefits.

### 6.1.4 Advanced technologies

Several companies have approached these industries/markets in different ways as the products have evolved over the past two decades and this chapter will concentrate on that evolution to the present day status of these uniquely attractive products. The basic chemistry, along with the variety of basic cure systems employed in reactive acrylic adhesives, including those comprising the so-called first and second generation products, are discussed in great detail in a review article by Damico (1990). The review also includes a thorough overview of improvements that evolved during the 1980s in the durability and heat resistance of reactive acrylic adhesives, especially with respect to bonding metals. This chapter will focus on developments and improvements that have occurred over the past two decades in this field which have greatly broadened the popularity of acrylic adhesive products, especially in bonding thermoplastics, composites and combinations of these materials to metals. Along with improved substrate bonding capability and mechanical properties, significant improvements have been made in the application and handling characteristics of these products. As a result, the new reactive acrylics compete equally or better than epoxies and polyurethanes as the adhesives of choice for any challenging bonding application.

The earlier 'first generation' acrylics and the subsequent 'second generation' acrylics had certain limitations, especially in metal bonding capability owing to limitations in resistance to elevated temperature exposure and subsequent

© Woodhead Publishing Limited, 2010

resistance to harsh or corrosive environments. As reviewed by Damico (1990), the primary improvements in adhesives based on MMA monomer in the 1980s involved improvements in the ability of these products to bond as-received metals, especially aluminum steel and stainless steel, with little or no surface preparation. The primary enabling factor was the incorporation of phosphoric acid derivatives of methacrylate monomers which chemically interact with metal oxide surfaces to strengthen the normally weak interfacial layer between the adhesive and the base metal and to protect it from corrosive attack under harsh environmental conditions (Zalucha *et al*., 1980). Additional improvements in durability and resistance to elevated temperatures were obtained through the incorporation of epoxy resins in the compositions (Dawdy, 1984). Those containing relatively high levels of epoxy resin were considered to be hybrids of methacrylate and epoxy technology. The products were capable of withstanding repeated exposures to temperatures of 204°C (400°F) such as those encountered in paint baking ovens in the automotive industry.

In spite of the significant improvements in performance in niche metal fabrication and medical and electronic assembly, the use of reactive acrylates and methacrylates was still limited in the late 1980s. Damico estimates that the total annual volume used at the beginning of the 1990s was less than US$10 million globally. In the 1990s and later, challenging new bonding applications involving the use of plastics in the transportation and marine markets provided the impetus for additional opportunity for commercial development of further improved products that would finally spur the growth of these products in high volume applications. The following advances in capability have occurred sequentially from the late 1980s to the present, proving methacrylate technology to be uniquely suitable for the most challenging bonding applications:

- improvements in low temperature toughness and flexibility with retention of hot strength
- reduction of odor during application
- reduction and elimination of surface tackiness from air inhibition
- control of aggressive solvation of sensitive plastics
- regrind compatibility with thermoplastics
- improved bondability of composites
- extended open working time for application on large assemblies
- control of exotherm for reduced outgassing in thick bond cross-sections
- reduced print-through on show surfaces
- ability to bond low energy surfaces, including polyolefins.

These improvements can be best incorporated in a discussion of the various classifications of adhesives in use today.

© Woodhead Publishing Limited, 2010

## 6.2 Classification of acrylic structural adhesives

### 6.2.1 Elastomer modified methyl methacrylate-based adhesives

The early MMA-based adhesives, including first and second generation products, as well as most of the improved products reviewed by Damico (1990), generally employ a single elastomeric component as the primary toughening additive. Soluble thermoplastic additives such as poly-MMA or polystyrene are occasionally added to impart certain adhesive properties, but the elastomer is the dominant factor affecting adhesive rheology, bond characteristics and adhesion with single polymer modification. The single elastomer approach generally imposes the following limitations on adhesive characteristics.

- limited substrate compatibility, requiring multiple adhesives for different substrates;
- 'stringy' viscosity and Newtonian rheology characteristic of elastomer solutions;
- inorganic fillers required for improved rheology can negatively affect properties;
- lower $T_g$ of elastomer may reduce hot strength of adhesives.

The glass transition temperature, $T_g$, of unmodified poly(MMA) system is 100°C and the presence of the elastomer can have a significant impact on the $T_g$ of the cured adhesive depending on the resin/elastomer compatibility. As expected the $T_g$ of the cured poly(MMA) system is reduced when there is good compatibility between the poly(MMA)/elastomer, but is not affected when the elastomer forms discrete particles owing to the lack of compatibility. Achary *et al*. (1991) and Bianchi *et al*. (1991) have studied the affects of rubber modification of acrylic adhesives on the $T_g$ and adhesive strength properties and related these effects to bulk morphology.

Achary *et al*. (1991) studied the effect of hydroxyl terminated polybutadiene (HTPB) in a vinyl ester/methyl methacrylate base acrylic adhesive on the $T_g$ of the cured system using a differential scanning calorimeter (DSC). They showed two distinct $T_g$ values for the fully cured adhesive even though the HTPB was soluble in the monomer system. This finding indicates that phase separation of the HTPB (rubber) phase occurred during the curing cycle. They also showed that the cure profile and amount of HTPB affects the $T_g$ of the cured acrylic adhesive.

Room temperature cure showed a single depressed $T_g$ (120°C versus 138°C for the unmodified vinyl ester/methyl methacrylate system) with some residual exotherm on the second heating. The heat cured adhesives exhibited two distinct $T_g$ values, the main phase $T_g$ being similar to the unmodified system. They also showed that higher HTPB content (30% w/w) slightly depressed

© Woodhead Publishing Limited, 2010

the main phase $T_g$ to approximately 134°C, but intermediate levels of 15% w/w did not depress the main phase $T_g$. Lap shear and impact peel strengths were at maximum values when the HTPB levels were in the range 10–15% w/w and decreased with further increasing levels of HTPB.

Bianchi *et al*. (1991) also found that the bulk morphology in terms of resin/rubber compatibility of rubber modified acrylic adhesives significantly affects the $T_g$ as well as the strength properties. They found that the morphological features and resulting properties of the acrylic adhesive were dependent on rubber type was well. They found that better phase separation and improved strength properties were observed for butadiene–acrylonitrile rubbers and fluorinated rubbers compared to chlorosulfonated polyethylene.

### 6.2.2 Non-methyl methacrylate adhesives

When the SGA adhesives were introduced in the 1970s, the anticipation generated by their improvements caused increasing interest on the part of a number of formulating companies. This situation increased exposure and notoriety also exposed more potential users to the odor of methyl methacrylate monomer. Negative feedback regarding the odor problem, along with the flammability associated with the low molecular weight monomer, prompted additional development work directed at reducing volatility and related problems associated with it (Bachmann, 1996).

Commercial formulations have been introduced to the market, but their higher cost generally limits their use to specialized lower volume and high value applications.

The most commonly employed alternatives to MMA are tetrahydrofurfuryl methacrylate (THFMA), hydroxyethyl methacrylate (HEMA) and hydroxypropyl methacrylate (HPMA). THFMA has been used in conjunction with the phosphate and epoxy improvements noted above to make hybrid metal bonding products that are more readily accepted in the automotive assembly environment, where odor and flammability are decided deterrents to their use (Lord Corporation, 2005). This is one of the larger volume applications for the low volatility monomers. HEMA and HPMA have been used to prepare two part reactive and one part ultraviolet and visible light curable adhesives that can be used in the relatively clean environments used to assemble electronic and medical components (Friese and Bergmann, 2000). Other products of the 'anaerobic' type based on di- and polyfunctional acrylate and methacrylate monomers found limited use in high value metal and electronic assembly as an outgrowth of their use in threadlocking applications (Toback, 1971).

Because the higher methacrylates are generally produced by transesterification of methyl methacrylate with higher molecular weight alcohols, they are significantly more expensive than MMA. Many of the higher methacrylates are usually associated with lower odor than MMA and, owing to the lower

© Woodhead Publishing Limited, 2010

volatility, there is an increased tendency to incompletely cure at the surface because of air inhibition. In some cases, lingering odor can be a significant problem. This is especially true in the case of butyl methacrylate and 2-ethyl hexyl methacrylate, two of the more commonly available higher methacrylates. Another issue with adhesives, formulated with higher molecular weight monomers based on alcohols with $C_4$ and higher alkyl groups, is a reduced capability to bond polar substrates such as metals.

Among the more useful higher methacrylates are hydroxyl alkyl methacrylates such as hydroxyethyl and hydroxypropyl methacrylates (HEMA and HPMA) and tetrahydrofurfuryl methacrylate (THFMA). The influence of the hydroxyl group can impose limitations on polymer solubility characteristics and adhesive substrate compatibility, but some very commercially successful adhesives are available based on these materials. THFMA is probably the most versatile of the higher molecular weight alternatives to MMA but it is also quite expensive. Along with the higher cost and other limitations associated with the higher methacrylates, another performance limitation associated with them relates to the fact that the polymers derived from the higher methacrylates generally have lower glass transition temperatures than poly-MMA. While this can be a benefit in improving the toughness and flexibility of the cured adhesive, it generally reduces the high temperature capabilities of the products. This can be somewhat offset by increasing the cross-link density of the adhesive with difunctional and polyfunctional methacrylates, but this technique is limited by other compromises imposed by these monomers (Pelosi, 1980).

The simplest members of this group are the ethylene and polyethylene glycol dimethacrylates which, along with proliferation monomers of this type (Isobe, 1990), were originally used to formulate anaerobic adhesives for threadlocking. These highly cross-linked materials are generally very rigid and resistant to the effects of heat and chemicals. By adding small amounts, usually less than 5%, of these di- or poly-methacrylate monomers to any of the structural methacrylate adhesives, the formulator can impart these properties to the cured composition. Increasing amounts of cross-linking monomer imparts increasing rigidity and can eventually lead to embrittlement, thus negating a primary advantage of this class of products, which is toughness. The cross-linkers also generally increase the cure speed of the adhesive and can negatively impact shelf life and adhesion.

Numerous di- and polyfunctional acrylate and methacrylate monomers have become commercially available over the years and provide the formulator with many options for modifying and tailoring structural adhesive properties. In summary, unless the odor and flammability of MMA cannot be tolerated, the incentive to formulate high performance structural adhesives for typical high volume product assembly operations with higher methacrylates is very limited. Adhesive products utilizing higher molecular weight monomers do

© Woodhead Publishing Limited, 2010

have a place in specialized applications for which they are very successful, but MMA remains the monomer of choice for the highest performance and value.

### 6.2.3 Polymer blends as modifiers in methyl methacrylate-based adhesives

Certain polymer blends enable the formulator to take advantage of separate contributing factors derived from each individual polymer to develop combinations of properties that are not attainable from a single polymer. For example, one elastomer may provide excellent low temperature flexibility and toughness, but adhesion to specific substrates may be compromised. A second polymer can provide better wetting or compatibility with the desired bonding surfaces. The combination of available polymers, along with the ability to modify further formulations with different comonomers along with MMA, as well as the many other additives, is what makes the polymer-in-monomer technology so versatile with respect to tailoring adhesives for specific applications.

The low viscosity and high solvency of MMA and the numerous comonomers that can be blended with it allow the ready incorporation of high molecular weight polymers as toughers. Polymeric toughers include typical elastomers used in dry polymer applications, some of which, such as polychloroprene, acrylonitrile and styrene butadiene polymers, are available in solution grades for adhesives and coatings. Other polymeric additives include soluble thermoplastic polymers and core shell impact modifiers that disperse and swell in the monomers, but do not fully dissolve (Muggee and Zilley, 1990).

## 6.3 Advantages and disadvantages and unique characteristics of acrylic structural adhesives

As noted above, one of the great advantages of the reactive acrylic or methacrylate adhesives is their formulation versatility. Prior to discussing the advantages and disadvantages and unique characteristics of the group, it will be helpful to review additional formulation options and the characteristics they impart.

### 6.3.1 Formulation variables

All of the variables reviewed above provide an obviously infinite combination of adhesive properties for the engineer or production manager. The development of specific formulations to address all of the product characteristics and performance variables is highly proprietary to the formulating companies

© Woodhead Publishing Limited, 2010

that provide these products. A list of the generic components available to the formulator, along with the positive and negative impacts on handling and performance characteristics are presented below in Table 6.1 to illustrate the complexity involved in this technology. Specific examples of these formulas can be found in an article by Damico (1990).

The list of potential formulating variables and related effects is much more complex than commonly available or useful for formulating epoxies

*Table 6.1* Potential formulating variables of acrylic and methacrylate adhesives

| Type | Description | Positive effects | Potential negative effects |
|---|---|---|---|
| Primary monomer | MMA | Polymer solvent<br>Substrate solvation<br>High $T_g$ | Odor and flammability<br>May harm sensitive substrates<br>Rigid homopolymer |
| Secondary monomer | Higher MW monomer or MMA substitute | Reduced volatility<br>Increased flexibility | Increased cost<br>Lower $T_g$<br>Air inhibition |
| Primary polymer | Elastomer component | Toughness and flexibility | Viscosity and 'stringyness'<br>Heat resistance |
| Secondary polymer | Elastomer or thermoplastic | Improved adhesion<br>Increased $T_g$ | Increasing viscosity<br>Reduced toughnes |
| Acidic monomer | Functional monomer | Metal adhesion | Corrosive<br>Cure behavior, reduced shelf life |
| Cross-linking monomer | Di functional or higher functional monomer | Heat and solvent resistance | Cure behavior, reduced shelf life<br>Reduced toughness |
| Plasticizer | Plastic and rubber additives | Toughness and flexibility | Heat resistance<br>Reduced adhesion |
| Filler | Plastic and rubber additives | Cost reduction<br>Reduced shrinkage | Reduced toughness<br>Effects on adhesion |
| Thixotrope | Fumed silica, others | Reduced 'stringyness' | Same as fillers |
| Peroxide initiator or hydroperoxide | Acyl, dialkyl | Speed of cure | Reduced shelf life |
| Amine promoter or activator | Tertiary aromatic amine or derivative | Speed of cure | Discoloration of cured adhesive |
| Metallic additive | Organometallics | Speed of cure | Reduced shelf life |
| Boron additives | Organoboranes | Low energy surface bondability | Cost |
| Stabilizer or inhibitor | Phenolics | Shelf life<br>Increased working time | Reduced cure speed<br>Air inhibition |
| Pigments and colorants | Plastic and rubber additives | Mixing indicator<br>Color matching | May affect shelf life<br>Cost |

© Woodhead Publishing Limited, 2010

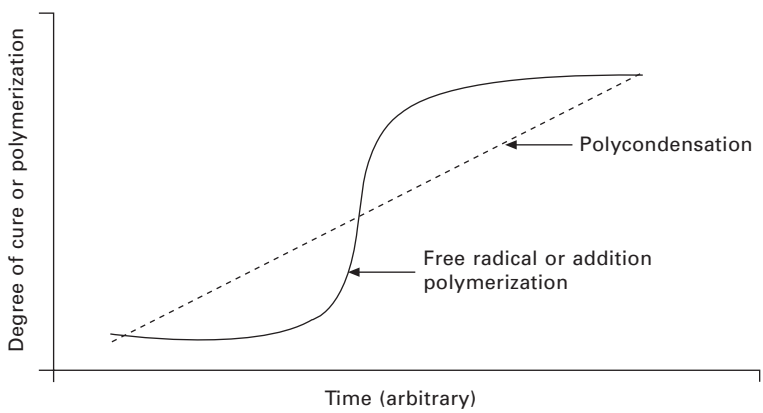
and polyurethanes. However, this list illustrates the many options to the formulator and end user with this class of products.

### 6.3.2 Advantages of structural methacrylates

*Cure profile*

One of the greatest advantages that the methacrylates exhibit relative to epoxies and polyurethanes is their cure profile and the ability to adjust the cure profile to provide a long open working time with the much desired 'snap cure' once parts are assembled. These characteristics are a result of the cure kinetics illustrated in Fig. 6.1 (Odian, 1991; Damico, 1990). Methacrylate adhesive systems cure via a free radical mechanism rather that the linear addition mechanism that characterizes the epoxies and polyurethanes. Epoxy and urethane adhesives (condensation polymers) exhibit a gradual cure with time. Acrylics (free radical addition polymers) on the other hand, exhibit a rapid cure after a given induction (delay) time. The unique aspect is that the delay time can be independently adjusted without compromising rapid curing. For example, the delay times can be quite large (1–3 hours) and exhibit a cure time of under 12 hours.

The strong solvency of MMA provides two significant advantages with respect to substrate bondability. First, it causes the adhesive to solvate the surface of many plastic substrates prior to completion of the curing process. The primary exceptions are polyolefins, fluorinated polymers, crystalline plastics such as polyamides and polyacetals, and highly cross-linked and post-cured thermosets such as epoxies and some polyesters and gel coats. Fortunately, the inherent inability of MMA to solvate certain plastics can be overcome with additive approaches that have been developed over the past




*6.1* Cure profile comparison of a free-radical cure adhesive with a polycondensation adhesive.

© Woodhead Publishing Limited, 2010

few years. As a last resort, typical surface preparation techniques that are used for epoxies and polyurethanes can also be used to improve the adhesion of methacrylates.

In addition to solvation of plastics, the solvency of MMA also reduces the sensitivity of adhesion and bondability to contaminants, particularly organic materials, on substrate surfaces. The MMA, and to some extent the polymers and additives in the methacrylates, dissolve and absorb many organic surface contaminants such as fingerprints, processing oils and release agents that normally interfere with bonding that uses epoxies and polyurethanes.

The breadth of substrate surface compatibility by the methacrylates is much greater than that of the epoxies and polyurethanes. Epoxies are most generally associated with bonding of metals and other inorganic materials, where the high polarity and hydrogen bonding capability of the resin and hardener components provide compatibility. Polyurethanes have been most successful in applications where increased flexibility is required, mostly with thermoplastics and thermosets such as the sheet molding compound (SMC) which is widely used in the transportation industry. The versatility of methacrylates to bond all of these materials has allowed them to capture an increasing market share in a variety of applications that can benefit from their superior processing and bonding characteristics.

### *Bondline properties*

Another unique advantage of the methacrylate class of products is the ability to formulate them with a broad range of bondline modulus characteristics which, in many cases, provide specific application or process advantages over epoxies. With specific exceptions for specific applications, epoxy adhesives have historically been considered to have the highest load bearing capability of the three classes of adhesives. This is especially true of the heat cured products of the type used to bond metal aircraft structures. When these products are formulated to impart increased peel and impact strength, great care is taken to preserve as much of the inherent load bearing capability as possible while reducing the brittle or glassy characteristics of the highly cross-linked epoxy matrix.

The most capable of these products have lap shear strengths of 35–40 MPa or higher, with peel strengths in excess of 10.5–12.5 N $mm^{-1}$, and are capable of maintaining a high degree of their strength over the temperature range of –55°C to 121°C required by the aerospace industry. These properties can be achieved by very careful formulation with proprietary toughening agents, mixed in precise quantities or provided as carefully formulated prepregs, coupled with high temperature curing which provides a near ideal (necessary) polymer morphology in the bondline. Epoxies that are formulated

© Woodhead Publishing Limited, 2010

to be mixed, applied and cured under more forgiving process conditions, typically lose a good measure of the high modulus that provides the highest load bearing capability.

When flexibilizers are added to maximize toughness and flexibility under these conditions, load bearing capability is compromised even more, especially at high temperatures. As a result, the methacrylates have become more competitive with epoxies where the compromises in performance required to achieve better application tolerance are a disadvantage for the epoxies.

An exception is the relatively new development of adhesively bonded metal frames and structural components in the automotive industry. While methacrylates and epoxies might both be considered, the combination of the reputation and history of epoxies in metal aircraft applications coupled with recent improvements in the ease of application and performance of the epoxies has proved to be an advantage for the epoxies in these applications (Okui and Shiokawa, 2001).

### 6.3.3 Disadvantages of structural methacrylate adhesives

In spite of all of the advantages of this class of products noted above, there are inherent drawbacks and limitations. First and foremost, the most cost effective monomer, which provides the highest performance products, is MMA, which, as noted above, is flammable and has a strong odor. In spite of its relatively low toxicity, misguided publicity stemming from the consumer cosmetic industry (finger nails) has cast a negative cloud over MMA. As also noted above, alternative monomers derived from MMA only add cost and reduce performance. This is the single most limiting fundamental drawback of the class. Another inherent disadvantage of the methacrylates is limited solvent resistance. The poly (MMA) matrix, as well as many of the additives used to modify the products, are soluble in polar and aromatic solvents such as ketones, toluene and solvent blends. However, they are reasonably resistant to petroleum lubricants and diesel fuel and are somewhat resistant to gasoline. Aqueous chemical resistance is generally good, although strong caustics, especially at high temperatures, can degrade performance.

The high temperature performance of highly toughened methacrylate structural adhesives is limited by the $T_g$ of MMA monomer, as well as the polymeric additives. Reducing elastomer toughener content and increasing cross-link density with multifunctional monomers can improve heat resistance as well as chemical resistance, but with a significant offset in physical properties. For such conditions, epoxy adhesives should be evaluated as alternatives.

© Woodhead Publishing Limited, 2010

## 6.4 Applications of acrylic structural adhesives

The emerging need for maximum toughness and flexibility for bonding applications, especially with the advent of composites in the transportation industry, provided an opportunity for polyurethane adhesives. They soon became much the same standard for bonding composites and treated metals in the transportation industry as epoxies were in the aerospace industry. Polyurethanes provide an excellent overall combination of load bearing strength and toughness over a broad temperature range, but are more limited in hot strength than the best epoxies and require significant surface strength to maximize adhesion and durability on metals.

A key opportunity for methacrylate adhesives resulted when a number of process and performance improvements evolved in the general area of plastic bonding and later with bonding combinations of plastics and metals. Four examples, presented chronologically, highlight the evolution of improved and unique methacrylate technology in concert with the emerging needs for which they were developed: thermoplastic automobile bumpers, composite stringer bonding in the marine industry, composite and metal bonding in heavy and light commercial trucks, and highly demanding metal bonding applications for school buses.

### 6.4.1 Thermoplastic bumpers

A large US automobile manufacturer had incorporated a two piece thermoplastic bumper in several high volume passenger car lines. The bumper consisted of a fascia component and a reinforcement that was mechanically attached to the automobile frame. The fascia and reinforcement, both injection molded with a polycarbonate/polyester alloy, were initially bonded with a highly elastic single component polyurethane adhesive that required a primer to bond the thermoplastic. Accelerated polyurethane adhesive systems with primers were selected because of their high elongation and flexibility. They enabled the bonded bumper assembly to pass a required low temperature impact test which simulated a 15 mile per hour barrier crash. In spite of the high level of performance provided by the polyurethane adhesive, the manufacturer began evaluating alternative adhesives to resolve two specific and limiting process issues for this very high volume application.

First, elimination of the primer application and flash off process would save time and increase available manufacture space. Second, a faster curing adhesive would eliminate a significant holding time required for the polyurethane adhesive to cure in order to enable required in-process quality control impact testing. A unique two part, highly flexibilized methacrylate adhesive that was specifically designed to pass the required high and low temperature performance requirements of the application and also to be compatible with the solvent sensitivity of the plastic without compromising

© Woodhead Publishing Limited, 2010

adhesion achieved the goals of the manufacturer. An added benefit was the ability of the manufacturer to recycle scrap parts directly without needing to cut out the bonded area, which represented significant savings in time, labor and materials.

### 6.4.2 Boat stringer bonding

A large manufacturer of high performance boats had decided to replace the traditional wooden stringer grid approach for hull reinforcement with molded stringer assemblies that could be bonded to the hull with an adhesive. The driving forces were:

- to eliminate the time and labor required to produce wooden stringers in the pattern shop;
- to eliminate manual lamination of the stringer grid in the hull with fiberglass and polyester resin – a significant reduction in time, labor and worker exposure to styrene monomer;
- to eliminate wood to provide environmental benefits and eliminate problems from wood rot as the boat aged and moisture penetrated the stringer grid;
- to increase overall production space and increase unit throughput as a result of reduced assembly and curing time;
- to increase performance and ride of the boat.

The manufacturer had initially chosen a two part polyurethane adhesive for this application because of the high performance demands, especially the ability to withstand the extreme flexing and impact loads imposed on a bonded hull for a high speed boat in choppy water. However, one aspect of the application process caused the manufacturer to evaluate a methacrylate adhesive. Boat hulls and stringers are typically fabricated by the 'open molded' laminating process wherein unsaturated polyester resin is either applied with successive layers of woven fiberglass or sprayed together with chopped glass fibers in a hull mold cavity until the desired laminate thickness is attained. When the resin cures, the molded hull is removed from the mold and moved to the stringer assembly process area.

The open or 'raw' surface to which the stringer is to be bonded can be difficult to bond using most adhesives unless the surface is abraded to remove the shiny resin surface which may contain incompletely cured resin and other components, such as barrier waxes, that reduce styrene emissions and reduce air inhibition of cure. This is especially true with epoxy and polyurethane adhesives. However, properly formulated methacrylate adhesives bond intimately to the unprepared open molded surface as a result of the solvating effect referred to earlier, as well as having inherent reactive compatibility between incompletely cured polyester resin and the polymerizing methacrylate

© Woodhead Publishing Limited, 2010

adhesive. Moreover, the ability of the methacrylates to have long open working time followed by the desired 'snap cure' can greatly expedite the stringer assembly process. Because of this, methacrylate adhesives that are formulated to have high tensile elongation and resistance to severe impact have experienced rapid growth in this market. In this case, the unique combination of processing and bonding characteristics of the methacrylates have virtually enabled a new manufacturing process.

### 6.4.3 Heavy truck assembly

Heavy trucks, more correctly named class 8 trucks, are the 'tractors' of large tractor-trailer trucks. Over the years, the preferred material for fabricating the cab portion has evolved from sheet metal to various composite materials, including SMC, resin transfer molding (RTM) and open molded fiberglass. Polyurethane adhesives became the bonding product of choice early in this transition, but as the transition proceeded, evolutionary changes challenged the capabilities of the polyurethane adhesive products to the point where alternatives were sought.

In SMC automotive component assembly, as well as in heavy truck assembly, heated fixtures are used to accelerate the cure of the Polyurethane (PUR) adhesive and to improve the quality of the bond. This permits a relatively long open working time allowing for application of the large amount of adhesive bead length required for the large truck components, with a relatively rapid cure cycle from the heat input from the bonding fixtures.

This approach is acceptable for large production runs which can justify the cost of the heated bonding fixtures. However, for smaller production runs and when dissimilar materials that include open molded parts, metal brackets and other attached parts are included in the assembly process, there is a need for adhesives with more versatility in bonding capability that do not require heated fixtures. To a limited extent, rapid curing polyurethane adhesives can be used, but in very hot and humid manufacturing environments, air conditioned assembly areas are required to prevent premature gelling and skinning of the PUR from the combined effects of heat and atmospheric moisture. Once again, the unique combination of problem-solving benefits provided by the methacrylates have opened this market for them and most class 8 manufacturing plants now employ a combination of PUR and methacrylate adhesives in their assembly operations (Illinois Tool Works (ITW), 2008).

### 6.4.4 School bus assembly

A large manufacturer of school buses embarked on an ambitious program to replace rivets, welds and mechanical fasteners in the assembly of school buses. The driving force for this drastic change in the assembly process was

© Woodhead Publishing Limited, 2010

to simplify the overall assembly process and improve the appearance of the finished bus with totally smooth exterior panels. Once again, there was a very challenging list of requirements for this application:

- Bond a variety of metallic surfaces including steel, aluminum and corrosion resistant alloys with minimum surface preparation
- Bond the surface of metals overcoated by a variety of corrosion-resistant organic coatings without damaging the coating or its bond to the metal surface
- Resist peeling and impact forces in potential crash situations
- Maintain performance after exposure to temperatures ranging from –40°C to +107°C. Methacrylate adhesives proved to be the only products that were capable of fulfilling all of these requirements and thus were selected for this application (Thomas Built Buses, 2005).

### 6.4.5 Thick gap bonding for marine and wind blade applications

As methacrylate adhesives have gained in popularity, their advantages in terms of their ability to bond composite structures with highly impact resistant and flexible bonds have become more widely recognized. As a result, they have been evaluated for applications that have required additional improvements in application properties. For example, when very large composite components are fabricated and bonded, additional demands related to larger bond gaps and open working time can become a factor. As part size increases, bonding gaps generally increase because of the nature of the molding process and more time is required to apply the beads of adhesive to the large structures. Two specific applications that illustrate this are large marine craft and windmill blades. As the boat stringer bonding application noted above is used to assemble larger and larger boats, bond gaps of 0.025 m or greater can be encountered (Gosiewski *et al*., 2002).

### 6.4.6 Bonding low energy surfaces

One of the most significant bonding challenges facing the adhesives industry has been the ability to bond low energy surfaces, particularly polyolefins, without the extensive and often prohibitive surface preparation required for conventional structural adhesives. Beginning in the 1990s, methacrylate adhesive formulators began to develop and commercialize products based on organoborane chemistry that had evolved from academic research. Once again, the methacrylate adhesive platform proved to be uniquely suited to exploiting this technology. Organoborane chemistry provides catalysts that initially create bondable sites on the surfaces of the low energy substrates. These systems are discussed thoroughly in Chapter 9.

© Woodhead Publishing Limited, 2010

## 6.5 Manufacturers

Structural acrylic adhesive manufacturers are fairly widespread and fragmented. So, it is extremely difficult to discuss all or even most of the different manufacturers in a single chapter. Therefore, the focus of this section will be to highlight a few of the major manufacturers. The order of the manufacturers is not a reflection of their size.

One of the largest suppliers of structural acrylic adhesives is ITW under the trade name of Plexus. They supply primarily methacrylate-based acrylic adhesives to the construction, industrial, marine and automotive markets. IPS is another large manufacturer and supplier of structural acrylic adhesive systems based on methyl methacrylate (MMA). Their application focus is primarily industrial and marine markets.

Lord Corporation is also a large manufacturer and supplier of structural acrylic adhesives which are methacrylate based. Their main focus is supplying the automotive original equipment manufacturer (OEM) and repair markets. Their methacrylate adhesive system exhibits good bonding to all types of metals, which include hot-dip galvanized, electro-galvanized and cold roll steels, and bare aluminum. Henkel AG & Co KGaA is another major manufacturer of methyl methacrylate (MMA)-based and non-MMA-based structural acrylic adhesives. Their penetration into the market place has been accomplished through three key acquisitions, Loctite Corporation, Dexter Corporation and, most recently, the adhesive division of National Starch and Chemical. The commercial focus of their products is in the areas of automotive OEM and aftermarket, electronics, home and office, do-it-yourself, craftsmen and construction and consumer markets. The uniqueness of Henkel's product line is that they manufacture and supply structural acrylic, thread lockers and anaerobic adhesive systems.

## 6.6 Future trends

As noted earlier, prior to the advanced evolution of methacrylate structural adhesives, epoxy and polyurethane adhesives dominated the structural adhesive market. Given this dominance, the newer methacrylates have made remarkable strides in gaining market share in spite of the inherent limitations noted earlier, particularly in the case of adhesives based on MMA monomer. This gain in market share is expected to continue in high volume, cost-sensitive applications with high performance demands. In such applications, the inherent advantages of cost effectiveness and performance of MMA-based methacrylate adhesives continue to make them competitive with epoxies and polyurethanes. Similarly, in low volume cartridge applications that involve limited exposure to MMA vapor, the products can be easily integrated into plant assembly processes provided that good local ventilation is employed.

© Woodhead Publishing Limited, 2010

The difficulty lies in middle volume or new applications, in manufacturing operations involving exposure of untrained or changing work forces, or in other situations with limited environmental controls. In such situations, the odor of the MMA monomer can give rise to concerns from sensitive work forces even though the actual health impact of exposure to levels of monomer below the threshold limit value (TLV) in air is minimal.

## 6.7 References


Achary, P S, Joseph, D and Ramaswamy, R (1991), 'Study on a vinyl ester/methyl methacrylate based reactive acrylic adhesive toughened by hydroxyl terminated polybutadiene', *J. Adhesion*, **34**, 121–36.

Bachmann, A G (1996), 'Advances in acrylic-adhesive technology', *Adhesives & Sealants Industry*, 36.

Bianchi, N, Garbassi, F, Pucciariello, R and Apicella, A (1991), 'Compositional influence on toughness of structural acrylic adhesives', *J Mater Sci*, **26**, 434–40.

Briggs, Jr., P C and Muschiagtti, L C (1975), *Novel Adhesive Compositions*, US Patent Office, 3,890,407.

Damico, D J (1990), 'Acrylics', *Engineered Materials Handbook*, Volume 3, ASTM International, 119–25.

Dawdy, T H (1984), *Epoxy Modified Structural Adhesives Having Improved Heat Resistance*, US Patent Office, 4,467,071.

Friese, C and Bergmann, F (2000), *Aerobically Curable Adhesive*, US Patent Office, 6,096,842.

Gosiewski, D, Loven, W E, Leeser, D L and Lambert, K A (2002), *Structural Adhesive*, US Patent Office, 6,462,126.

Illinois Tool Works (ITW), 2008.

Isobe, I (1990), *Adhesive Composition*, US Patent Office, 4,898,899.

Lord Corporation (2005), *VERSOLOK® Adhesive*, Technical Data and Material Data Sheets.

Melody D P, Grant S M and Martin F R (1984), *Two-part Composition with Activator Enriched with Dihdropyrdine Ingredients*, US Patent Office, 4,430,480.

Muggee, J M and Zilley, E L (1990), *Low Odor Adhesive Compositions and Bonding Method Employing Same*, US Patent Office, 4,945,006.

Odian, G (1991), *Principles of Polymerization*, John Wiley & Sons, New York.

Okui, K and Shiokawa, M (2001), *Method for Producing a Bonded Structure of Aluminum Alloy Pressed Plate*, US Patent Office, 6,176,965.

Owston, W J (1973), *Fast Curing Polychloroprene Acrylic Adhesive*, US Patent Office, 3,725,504.

Pelosi, L F (1980), *Reactive Fluid Adhesive Compositions*, US Patent Office, 4,226,954.

Thomas Built Buses (2005) *Technical Data Sheet*.

Toback, A S (1971), *Process for Bonding with Acrylate Polymerized by a Peroxy and a Condensation Product of Aldehyde and Primary or Secondary Amine*, US Patent Office, 3,616,040.

Zalucha, D J, Sexsmith, F H, Hornaman, E C and Dawdy, T H (1980), *Structural Adhesive Formulations*, US Patent Office, 4,223,115.


© Woodhead Publishing Limited, 2010

# 7

# Advances in nanoparticle reinforcement in structural adhesives

A. C. TAYLOR, Imperial College London, UK

**Abstract**: The increased commercial availability and the reduced prices of nanoparticles are leading to their incorporation in polymers and structural adhesives. This chapter outlines the principal types of nanoparticles and the methods that may be used to disperse the particles in a polymer matrix. It discusses how nanoparticles can alter the mechanical properties (e.g. stiffness), electrical properties (e.g. conductivity), functional properties (e.g. permeability, glass transition temperature) and fracture performance of thermoset polymers. The effect of nanoparticles on joint performance is also discussed. Sources of information on the application of nanoparticles are identified, and future trends in nanoparticle use in structural adhesives are proposed.

**Key words**: nanoparticle, dispersion, mechanical properties, electrical properties, fracture, fatigue, adhesive.

## 7.1 Introduction: opportunities and limitations in nanoparticle reinforcement

### 7.1.1 Nanotechnology

Nanotechnology is not new, in that the use of nanoparticles to alter the properties of materials is not a modern idea. The late Roman (4th century AD) Lycurgus cup is made of cut glass and is displayed in the British Museum in London. This cup looks green in reflected light, but appears red when light is shone through it. This effect is due to the colloidal dispersion of gold and silver nanoparticles, about 70 nm in diameter, in the glass which scatter the light. Another example is carbon black, used in millions of car tyres and printer cartridges per year, which is composed of particles of 20 nm and above. However, it was first produced as lamp black in China 3500 years ago.

Recently, nanotechnology has become a hot topic in science and engineering. One of the definitive points in the history of nanotechnology came in a lecture by Richard Feynman, in 1959, entitled ‘There is plenty of room at the bottom’ (Feynman, 1959). He highlighted the potential that working at a micro- or nanoscale has, and discussed the problem of manipulating and



© Woodhead Publishing Limited, 2010

controlling things on a small scale. He issued a challenge to scientists to work at this scale, a challenge that is now being taken up.

So what is nanotechnology? Nanotechnology could be defined as the combination of existing technologies with the ability to observe and manipulate at the nanometre ($10^{-9}$ m) scale (Harper, 2003; Hay and Shaw, 2001). The question is then, why is there so much interest in nanotechnology now? It is linked to the expanding ability to synthesise nanometre-scale materials, together with the availability of the tools which enable us to see at this scale. Hence, unlike the Romans, we can see how the nanoparticles are dispersed and start to understand why the effects we observe occur. As we approach the limits of the nanoscale, say less than 20 nm, different effects, such as quantum effects, become more significant.

One concern about the use of nanoparticles is the uncertainty over their toxicity. No-one wants to repeat the mistakes made over asbestos and its associated health problems. The fantastic stories, for example Michael Crichton's book *Prey* and Prince Charles' 'grey goo' speech have not helped public perception (Radford, 2003). Hence manufacturers are approaching new technology more cautiously. Studies are underway to assess the health effects and some results have been published (e.g. Warheit *et al*., 2004; Lam *et al*., 2004), but as yet there is no real agreement about the health effects. However, the nanoparticles used in adhesives are not free in the atmosphere, but are bound into a matrix. Current studies indicate that even during fracture of a nanoparticle-modified epoxy material, only a few nanoparticles are released into the atmosphere. In contrast, nanoparticles are produced in large quantities by the combustion of fossil fuels. Further, it must be borne in mind that millions of tonnes of nano- and submicrometre particles are already in use.

### 7.1.2 Nanoparticle reinforcement

Rothon and Hancock (1995) defined five basic characteristics of particulate fillers. These are true whether the particles are micro- or nanoparticles:

1. What properties are being sought?
2. What deleterious changes may also occur and can they be tolerated?
3. How easy is the filler to handle and how might it affect processing?
4. Are any special additives needed?
5. What is the true cost of using the filler, is it justifiable and are there more cost-effective alternatives?

Rothon and Hancock observed that it is widely assumed that fillers are cheap and that polymers are expensive. Conversely, for nanoparticles it is widely assumed that nanoparticles are expensive and that polymers are cheap. However, the nanoparticle manufacturing industry is expanding and some

© Woodhead Publishing Limited, 2010

nanoparticles are available in large (tonne) quantities. Even the price of expensive nanoparticles such as carbon nanotubes is being reduced. However, the price varies greatly with the type of nanoparticle as well as with the purity of the material. For example, silica nanoparticles supplied dispersed as a masterbatch in epoxy cost US$20 per kilogram (Nanoresins, 2008), and core-shell rubber nanoparticles similarly dispersed cost US$12 per kg (Kaneka, 2008). Nanoclays can cost as little as US$7 per kg (SigmaAldrich, 2008). However, a kilogram of carbon nanotubes cost between US$600 and US$95,000 in the spring of 2008 (CheapTubes, 2008).

## 7.2 Types of nanoparticles and their key attributes

### 7.2.1 Nanoparticles definition

The common definition of a nanoparticle is that it has at least one dimension in the nanometre range. Indeed, the term 'nano' has virtually replaced 'sub-micrometre', even when the latter is more appropriate. A search of the scientific literature published in the last 5 years yields 3,000 mentions of 'sub-micro', but 200,000 of 'nano'. Nanoparticles are characterised by a large surface area to volume ratio. They can be metallic (e.g. gold, silver), ceramic (e.g. silica, alumina, layered silicates, silicon carbide) or organic (e.g. carbon black, rubber particles, graphite, carbon nanotubes and nanofibres). Owing to their small size, the numbers of nanoparticles present in nanoparticle-modified materials are huge. For example, 1 kg of 20 nm silica nanoparticles will contain approximately $10^{17}$ individual particles.

As many nanoparticles are smaller than the wavelength of light (about 400–700 nm), they appear transparent when added to a transparent polymer. A consequence of this is that they are too small to be seen using optical microscopy, but can be imaged by high magnification microscopy, such as transmission electron microscopy (TEM), atomic force microscopy (AFM) and field emission gun scanning electron microscopy (FEGSEM). The characterisation of the structure of nanoparticles can also be achieved using X-ray diffraction or other techniques (Wang, 2001). Because the particles are so small, it is not normally possible to measure the mechanical properties and hence these are assumed to be the same as for the bulk material, or equal to those of a similar material.

As with micrometre-sized fillers, particle shape is important in determining the properties of the nanoparticle-modified materials, such as stiffness, flow characteristics, tensile strength and so on. The aggregation and dispersion of the particles are also important and may also affect the properties. We will start by looking at the three basic classes of nanoparticles, characterised by their shape: spherical, rod-like and plate-like.

© Woodhead Publishing Limited, 2010

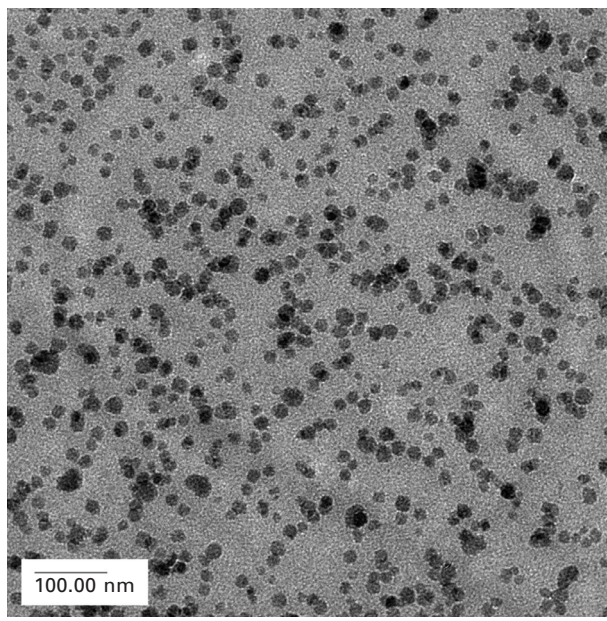
### 7.2.2 Equi-axed nanoparticles

Most equi-axed nanoparticles are spherical, but some irregular particles are available. The common particles are metallic (e.g. gold, silver), ceramic (e.g. silica, alumina, titania) or organic (e.g. rubber particles). Silica and alumina are the most commonly used with adhesives, see Fig. 7.1. The ceramic particles are typically prepared by sol-gel or flame-spraying methods. Rubber particles are typically core-shell particles, with a soft core and a hard shell.

### 7.2.3 Nanotubes and nanofibres

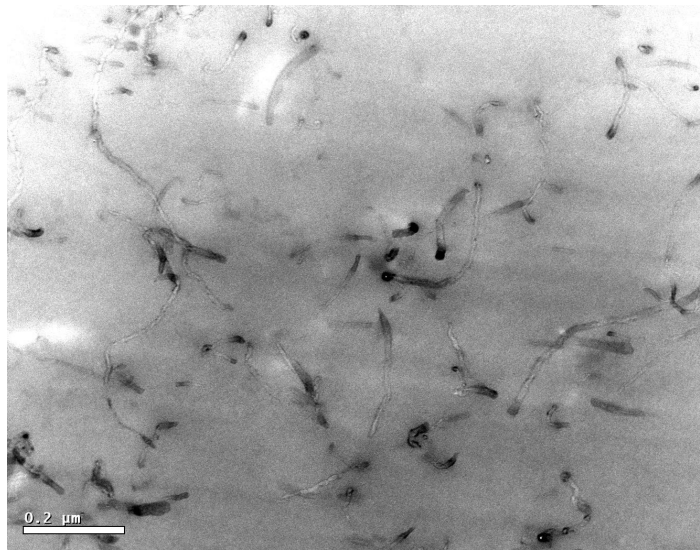
In the scientific literature, the most commonly discussed rod-like nanoparticles are carbon nanotubes. The larger diameter carbon nanofibres are also available, more cheaply and in much larger quantities than carbon nanotubes. Ceramic nanotubes (e.g. zirconia, tungsten disulfide) or whiskers (e.g. silicon nitride, silicon carbide, alumina) can also be used.

Carbon nanotubes were first reported by Iijima (Iijima, 1991; Iijima and Ichihashi, 1993) and are effectively sheets of graphite rolled into tubes, see Fig. 7.2. They are produced by chemical vapour deposition (CVD), electric arc or laser ablation methods. These techniques give nanotubes with different length, purity and degree of entanglement. The nanotubes require




*7.1* Transmission electron micrograph of silica nanoparticles in epoxy (courtesy S. Sprenger).

© Woodhead Publishing Limited, 2010




*7.2* Transmission electron micrograph of 0.25 wt% carbon nanotubes in an epoxy matrix (courtesy R. D. Brooker).

purification to remove the amorphous carbon that is also produced, typically by heating in a mixture of nitric and sulphuric acid (Gojny *et al.*, 2003). CVD is becoming the most popular method for producing relatively large quantities of nanotubes relatively cheaply. In this technique the nanotubes are grown on a ceramic substrate, rather like the bristles of a brush. The length of the nanotubes can be controlled and they have a relatively low degree of entanglement.

There are two types of carbon nanotubes. First, single-walled nanotubes (SWNT) have a single graphene layer rolled into a tube, with hemispherical end caps, typically 1–2 nm in diameter (Iijima and Ichihashi, 1993; Tjong, 2006). Second, multi-walled nanotubes (MWNT) comprise a number of co-axial graphene tubes, with end-caps. The outer diameter is typically 3–10 nm. Under tension, only the outer layer of a MWNT carries the load, as the van der Waals forces between the layers are too weak (Lau *et al.*, 2004). The length of nanotubes varies significantly, but they can be as long as several millimetres (Chakrabarti *et al.*, 2006). This gives very large aspect ratios. The modulus has been measured to be up to 1 TPa, with strengths of up to 150 MPa (Demczyk *et al.*, 2002). However, it is difficult to adhere the tubes to a matrix and hence surface treatments are used to activate the surface, which can weaken the tubes. The electrical properties of nanotubes vary from metallic to semi-conducting, depending on their chirality.

Vapour-grown carbon nanofibres do not have such a high aspect ratio as nanotubes and have more defects. However they are significantly cheaper

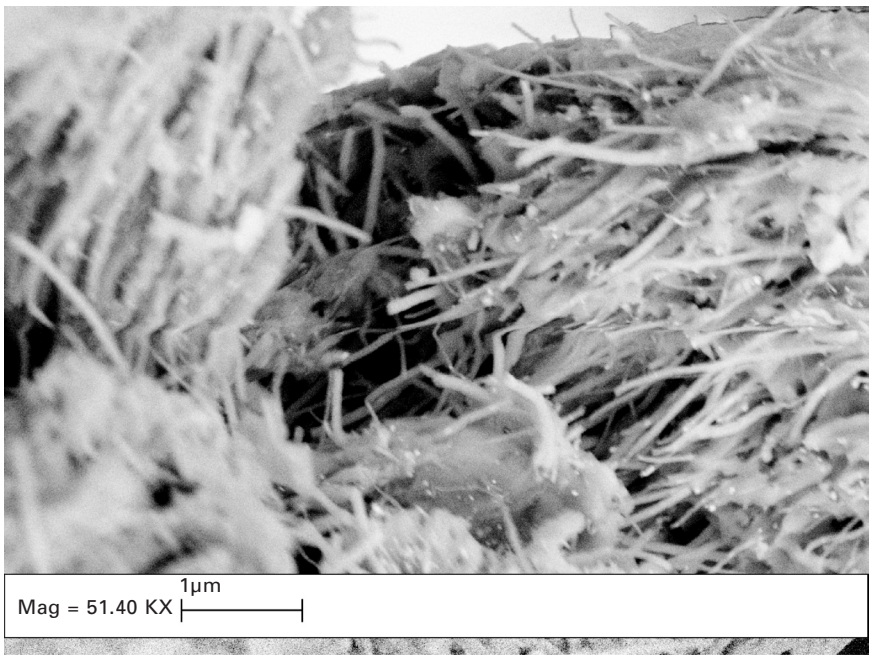
© Woodhead Publishing Limited, 2010

and available in much larger quantities. The nanofibres are typically 50–200 nm in diameter and 30–100 μm long (Zhou *et al*., 2007; Green *et al*., 2006), as shown in Fig. 7.3.

Ceramic whiskers have been produced for many years, as reported by Gordon (1978), although their use in epoxies seems to be limited. However, aluminium borate whiskers have been combined with thermoset polymer matrices by Liang and co-workers (Liang and Hu, 2004; Tang *et al*., 2007). Morisada *et al*. (2007) have produced ceramic nanotubes by coating carbon nanotubes with silicon carbide. Silicon carbide nanofibres have been produced by Zhu *et al*. (2002) and by Bechelany *et al*. (2007). The latter nanofibres were about 40 nm in diameter with lengths of up to several hundred micrometres.

### 7.2.4 Plate-like nanoparticles

A range of plate-like nanoparticles have been used with polymer matrices, including layered silicate nanoclays (e.g. montmorillonite), graphite and $\alpha$-zirconium phosphate. Generally these particles comprise stacks of platelets which are intercalated or exfoliated by the polymer during processing. This morphology is typically described as 'particulate' (or conventional), 'intercalated' or 'exfoliated', as identified by wide-angle X-ray scattering




*7.3* Scanning electron micrograph of carbon nanofibres in an epoxy matrix, showing fractured surface (courtesy J. H. Lee).

© Woodhead Publishing Limited, 2010

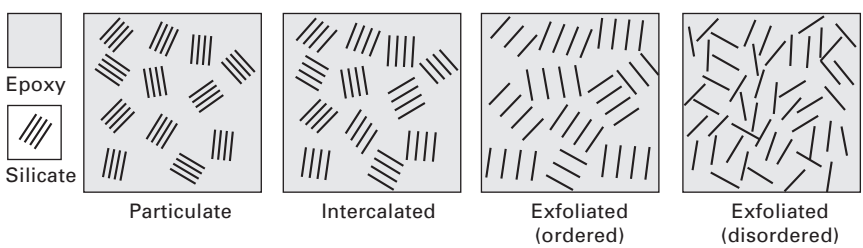
(WAXS). These microstructures are shown schematically in Fig. 7.4 for a nanoclay-modified polymer. In an intercalated nanocomposite, polymer chains enter the galleries between the platelets and increase the measured spacing. For an exfoliated structure, the platelets are pushed further apart and the spacing becomes too large to measure using WAXS. Note that an exfoliated structure may be ordered or disordered as shown in Fig. 7.4, but the fully disordered exfoliated structure is rarely seen in practice. For a particulate structure, the particles remain unchanged.

Nanoclays (e.g. montmorillonite, hectorite) are layered silicates which have a layered structure of stacked platelets similar to that of mica. The platelet thickness is around 1 nm and the lateral dimensions of the plates vary from 30 nm to tens of micrometres, and hence the platelets have a high aspect ratio. These layers have a regular van der Waals gap in-between, called the interlayer or the gallery (Alexandre and Dubois, 2000). These nanoclays are hydrophilic and hence are surface-treated using long-chain alkylammonium compounds to make them organophilic. The stacks of platelets can be readily delaminated by organic molecules to form an intercalated or exfoliated structure.

Natural graphite has also been used. A combination of chemical and thermal treatments can generate exfoliated graphite platelets with a thickness of 20–100 nm. Here the graphite is intercalated by an acid treatment, followed by exfoliation by a thermal shock at a temperature of around 600°C. The platelet diameter is in the order of 10 μm and hence these platelets have a high aspect ratio (Yasmin and Daniel, 2004; Yasmin *et al.*, 2006b).

### 7.2.5 Other nanoparticles

Carbon black is mostly an aciniform (grape-like cluster) particulate. It is produced by the incomplete combustion of oil. The current worldwide production is 8.1 million tonnes per year. It is very common as a pigment in inks and toners and as a functional filler in tyres and rubber products (International Carbon Black Association, 2008).




*7.4* Microstructures of nanoclay-modified polymers.

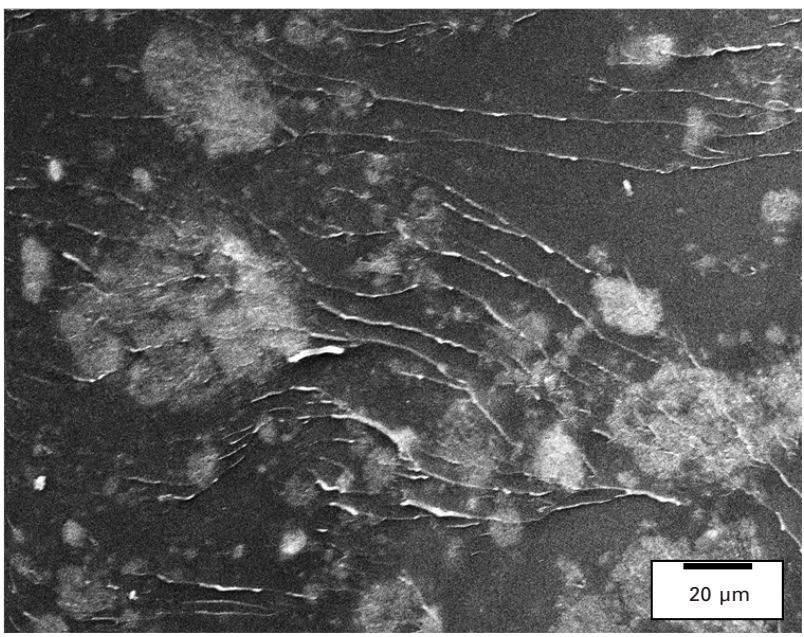
© Woodhead Publishing Limited, 2010

## 7.3 Methods of nanoparticle incorporation

### 7.3.1 Dispersion

To obtain the best properties from a nanoparticle-modified polymer, the nanoparticles should be well-dispersed and each particle should be wetted by the polymer. If this is not the case, as shown in Fig. 7.5 the agglomerates will act as defects resulting in a reduction in performance rather than any enhancement. This is a major challenge when preparing formulations.

The dispersion of nanoparticles is difficult owing to the high surface area and incompatability with the matrix polymer. Generally a surface treatment or compatabiliser is required. Once agglomeration occurs, it is very difficult to break up the agglomerates. Hence particles which are supplied predispersed in resin (e.g. Nanopox from Nanoresins, or the MX range of core-shell particles from Kaneka) are popular with formulators. However, there is no guarantee that this good dispersion will remain after subsequent processing. For example, in some systems the addition of a liquid rubber which phase-separates during curing will cause the nanoparticles to agglomerate (Mohammed, 2007). The mechanisms involved are the focus of several research programmes at present. It is normally assumed that good dispersion is required. However, small agglomerates do not necessarily adversely affect the performance.




*7.5* Scanning electron micrograph of the fracture surface of a cyanate ester polymer with 10 wt% titania nanoparticles, showing micrometre-sized agglomerates.

© Woodhead Publishing Limited, 2010

Assessing the quality of the dispersion is difficult, as techniques which can identify particles at the nanoscale such as AFM and TEM involve lengthy specimen preparation. Even then only a very small area of the sample is studied and the results may not be representative of the material as a whole. X-ray diffraction can analyse a larger volume, but tells us nothing about how well the particles are dispersed. It is normally suggested that dispersion is assessed on three size scales: optically, by scanning electron microscopy and by transmission electron microscopy. If the results from all three techniques indicate a good dispersion, then it is fairly safe to assume that this is the case. Quantitative methods of assessing dispersion, using the greyscale of images or by a quadrat method, are currently being researched (Brooker *et al.*, 2008).

It should be borne in mind that even small volume fractions of nanoparticles involve huge numbers of nanoparticles and very small interparticle distances. Shaffer and Kinloch (2004) point out that:

> One major difficulty with small diameter nanotubes is that they become increasingly difficult to wet. By trivial estimation, even a 1 vol% loading of single-walled nanotubes ensures that all of the polymer molecules are within one radius of gyration (say 5 nm) of a nanotube. This result implies that complete wetting of high loading fractions of single-walled nanotubes will be difficult, at least by conventional means, and that even more modest concentrations may be brittle and hard to process due to the constraint of the matrix.

Chemical functionalisation of the surface of the nanoparticles can improve dispersion, as it reduces agglomeration, and can also improve the bonding between the particle and the matrix (Gojny *et al.*, 2003; Kathi and Rhee, 2008).

### 7.3.2 Mixing

If nanoparticles are supplied well-dispersed in a polymer, then simple mixing is often enough to blend the particles into an adhesive formulation (e.g. Kinloch *et al.*, 2005). Low-shear mixing is also sufficient for well-compatabilised systems, as the thermodynamics of these materials can ensure a good dispersion. However, if nanoparticles are supplied as an untreated powder they will generally be agglomerated and these agglomerates need to be broken up. Simple low-shear mixing alone will not break up these agglomerates. High-power dispersion methods, such as high shear mixing and sonication, are the easiest to use to improve the dispersion of nanoparticles in polymers (Xie *et al.*, 2005).

In a multi-component system such as a structural adhesive, the polymer component into which the nanoparticles are introduced does not generally

© Woodhead Publishing Limited, 2010

cause a noticeable difference in the final morphology (Hackman and Hollaway, 2006; Brooker *et al*., 2008). However, the morphology is dependent on the cure time and temperature, together with the temperature, time and shear rate used for mixing.

Fiedler *et al*. (2006) report that the size and shape of the impeller and the mixing speed control the dispersion result for carbon nanotubes. Intensive stirring of MWNTs in epoxy resin can achieve a relatively good dispersion. Reagglomeration occurs owing to frictional contacts and elastic interlocking mechanisms (Schmid and Klingenberg, 2000). SWNTs have a greater tendency to reagglomerate than MWNTs, and hence higher shear forces are required to achieve a reasonable dispersion.

Hackman and Hollaway (2006) compared low-shear mixing to the use of a grinding media mill, filled with 2 mm diameter glass beads. Green *et al*. (2006) compared low-shear mixing to high-shear generated by extrusion of the nanoparticle-modified epoxy resin through a small orifice. In both cases the high-shear method gave better dispersion. Hackman and Hollaway found that the glass beads broke down the agglomerated nanoclay particles to form a uniform material. However, although neither work used microscopy to evaluate the dispersion at the nanometre-scale, differences could be seen at the micro-scale (Hackman and Hollaway, 2006). Many authors agree that using optical microscopy is useful in investigating the dispersion of nanoparticles as it highlights the presence of agglomerates (e.g. Hackman and Hollaway, 2006; Brooker *et al*., 2008), although individual nanoparticles will not be visible.

A three-roll mill (or calender) has been used by Yasmin *et al*. to disperse nanoclay in epoxy (Yasmin *et al*., 2003, 2006a) and by Gojny *et al*. (2004) to disperse nanotubes in epoxy. This is an established method, commonly used to disperse microparticles in polymers (Fiedler *et al*., 2006). As this is not a continuous process, the material from the apron was collected and fed back into the mill after each pass of the material. The authors assumed that the dispersion was achieved first by the shear forces generated between the rollers dispersing the particles as smaller tactoids and secondly by the combined shear and diffusion processes facilitating the separation and penetration of polymer between the clay (Yasmin *et al*., 2003, 2006a). This process requires a relatively viscous material and is thus suitable for higher loadings of nanoparticles. Fiedler *et al*. (2006) state that a major advantage of this method is that it allows the efficient manufacturing of larger quantities of nanocomposites, as the nanoparticle-modified polymer requires only minutes in the machine.

### 7.3.3 Sonication

Sonication uses an ultrasonic bath or probe to apply sound energy to a liquid containing particles. Many authors combine sonication and mixing,

© Woodhead Publishing Limited, 2010

especially when using probe sonicators, as the power is directed into a small volume and the low shear forces do not generally ensure that all the polymer passes through this volume. The combination of probe sonication with high-speed mixing has been reported to be a relatively successful way to disperse nanoparticles. This technique has been used for nanoclays in epoxy by Zunjarrao *et al.* (2006) and in polyimide by Gintert *et al.* (2007). Similarly, it has been used for carbon nanotubes in epoxy by Sandler *et al.* (1999).

However, this very localised introduction of energy from probe sonication leads to a considerable amount of damage, including buckling, bending, dislocations and rupture of carbon nanotubes (Lu *et al.*, 1996; Fiedler *et al.*, 2006). It will also cause local heating of the sample, so if sonication is undertaken in the presence of a curing agent it may be necessary to cool the sample to prevent premature curing (Lu *et al.*, 1996). The use of an ultrasonic bath reduces the energy density, alleviating some of these problems. However, the time taken to achieve a reasonable dispersion is much greater (Brooker *et al.*, 2008).

Lam *et al.* (2005) found that processing time affected the size of the nanoclay agglomerates. However, the d-spacing (the distance between the nanoclay platelets) was unaffected by the sonication time and hence exfoliation of the nanoclay could not be achieved using sonication. Gintert *et al.* (2007) also found that sonication was an important step in breaking up nanoclay agglomerates.

### 7.3.4 Alignment

The properties of composites are generally improved by alignment of the fibres, although this does produce an anisotropic material. It is also possible to align nanoparticles. This is generally achieved by physical means, for example by application of a force, cutting, extrusion or drawing (e.g. Ajayan *et al.*, 1994; Baik *et al.*, 2005). Additionally, alignment can be achieved by the application of magnetic or electric fields, with carbon nanotubes (e.g. Chen *et al.*, 2001; Martin *et al.*, 2005) and with layered silicates (e.g. Koerner *et al.*, 2005). For more information on alignment of carbon nanotubes and their dispersion, see the review by Xie *et al.* (2005).

## 7.4 Typical property variations available through nanoparticle reinforcement

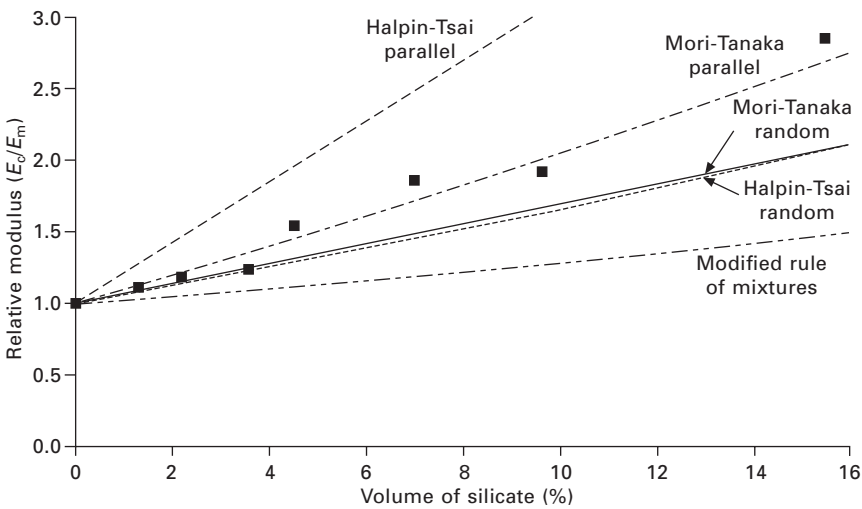
### 7.4.1 Mechanical properties

It is well known that the addition of stiff particles, that is those with a higher modulus than that of the polymer, increases the modulus of a polymeric

© Woodhead Publishing Limited, 2010

material. This is true whatever the particle size, although the stiffening effect may be higher for particles with larger aspect ratios. There are many theoretical models for predicting the modulus of particle-modified polymers, such as the Halpin-Tsai and Mori-Tanaka models (see Ahmed and Jones, 1990 for example). These models have been shown to apply broadly to nanoparticle-modified polymers (e.g. Kinloch and Taylor, 2006), see Fig. 7.6, although more accurate predictions can be obtained by finite element modelling (Sheng *et al*., 2004). The true aspect ratio of the particles, the degree of their alignment and some idea of the strength of the particle to matrix adhesion are required for accurate predictions. Note that the elastic properties of nanoparticles are almost unknown. This includes nanoclays such as montmorillonite, as discussed by Vanorio *et al*. (2003). This absence of modulus data is because the small grain size makes it impossible to perform reliable measurements on such small particles. Hence, most authors assume that the properties (e.g. modulus, density) of the nanoparticle are equal to that of the bulk material, or of a similar material.

Zhou *et al*. (2007) used an amine-cured epoxy polymer modified with carbon nanofibres (CNF) and showed a 19% increase in modulus when 3% CNF were added. This was accompanied by an increase in the tensile strength and a reduction in the strain to failure. These changes are typical of nanoparticle-modified epoxies. Generally the stiffness and the tensile strength are increased, while the strain to failure is reduced.




*7.6* Relative modulus (composite modulus divided by matrix modulus) of epoxy polymer modified with nanoclay. Experimental data are shown as points; predictions using various theoretical models are shown as lines (adapted from Kinloch and Taylor, 2006).

© Woodhead Publishing Limited, 2010

### 7.4.2 Functional properties

As plate-like nanoparticles have a high aspect ratio and low permeability, they should provide good barrier properties when aligned and incorporated into thin films. Here they make a tortuous path for diffusion (Hackman and Hollaway, 2006). Numerical predictions by Gusev and Lusti (2001) show that reduction in permeability is governed by the product $a.V_f$, where $a$ is the platelet aspect ratio and $V_f$ is the volume fraction. Epoxy films that were highly filled with nanoclay have been shown to have low oxygen permeability, up to three orders of magnitude lower than that of the unmodified epoxy (Triantafyllidis *et al*., 2006), see Table 7.1. The rate of diffusion of acetone into epoxy is also reduced by the addition of nanoclay, although the data did not reach saturation and so it is not possible to compare the equilibrium uptake (Chen and Curliss, 2001).

The fire resistance of nanoparticle-modified polymers has been studied, but most work has concentrated on thermoplastics. This has generally shown that the addition of nanoclays and nanotubes can improve the fire resistance (e.g. Gilman *et al*., 2000b; Gilman, 1999; Beyer, 2002). A significant amount of work has been performed by the National Institute of Standards and Technology (NIST) using various thermoset polymers modified by nanoclays, including epoxy, vinyl ester, cyanate ester and polyimide (e.g. Gilman *et al*., 1999a, 1999b, 2000a). These publications are available via the website of the Building and Fire Research Laboratory of NIST. Tests using cone calorimetry showed that the addition of 10% silicate reduced the peak heat release rate by up to 50% and increased the mass of char residue formed. However, the onset time was also often reduced, probably owing to the surface treatment.

The thermal degradation behaviour of nanoclay-modified epoxy has been studied and is closely linked to the fire performance. Brnardic *et al*. (2008) showed that the nanoclay has little effect on the behaviour and may even reduce the temperature at which degradation starts owing to the relative instability of the surface treatment. The addition of carbon nanofibres to an amine-cured epoxy polymer had no effect on the decomposition temperature of epoxy (Zhou *et al*., 2007), but single-walled nanotubes have been shown to degrade the thermal stability (Puglia *et al*., 2003).

*Table 7.1* Oxygen permeability data for films of epoxy and nanoclay-modified epoxy (adapted from Triantafyllidis *et al.,* 2006).

| Clay film composition | Clay film thickness (mm) | Epoxy-clay film thickness (mm) | $O_2$ permeability ($cm^3$ ml/$m^2$day) |
|---|---|---|---|
| Epoxy | – | 0.20 | 98.9 |
| Epoxy–montmorillonite | 0.060 | 0.11 | ≤0.1 |
| Epoxy–montmorillonite | 0.035 | 0.10 | 0.97 |
| Epoxy–fluoroectorite | 0.065 | 0.14 | 1.2 |

© Woodhead Publishing Limited, 2010

The glass transition temperature, $T_g$, of nanoparticle-modified polymers tends to shift to a higher temperature than that of the unmodified polymer, (e.g. Messersmith and Giannelis, 1994; Bugnicourt *et al*., 2007; Kinloch and Taylor, 2006). This can be explained by the interaction between the particles and the polymer, which may also locally change the properties of the polymer network. For example, Dodiuk *et al*. (2006) investigated the modification of a polyurethane (PU) adhesive using nanoclays and found that the $T_g$ of the PU increased from 32°C to 62°C with the addition of 5% of functionalised nanoclay. Where polymer chains are intercalated between silicate platelets, the silicate may constrain the polymer, increasing $T_g$ (Kinloch and Taylor, 2006). Bugnicourt *et al*. (2007) reported that $T_g$ increased from 161 up to 180°C for an amine-cured epoxy modified by silica nanoparticles. They also noted that the poorer the dispersion, the lower the impact of the addition of silica on the magnitude of the tan $\delta$ peak and $T_g$. However, tests on a rubbery epoxy, with a $T_g$ of –27°C, showed no effect of the addition of silica nanoparticles. Reductions in the glass transition temperature have also been reported (e.g. Kornmann, 1999). These reductions may be due to the surface treatment degrading during curing (Wang *et al*., 2000) or by enhanced free volume in the interphase between the particle and the matrix.

Carbon nanotubes have been shown to increase the rate of the curing reaction of epoxies by Puglia *et al*. (2003) and Yin *et al*. (1993). This effect arises from the surface chemistry of the nanotubes reported by Shaffer and Sandler (2006). However, barium titanate nanoparticles did not affect the curing behaviour of diamino diphenyl methare-cured epoxy (Chandradass and Bae, 2008).

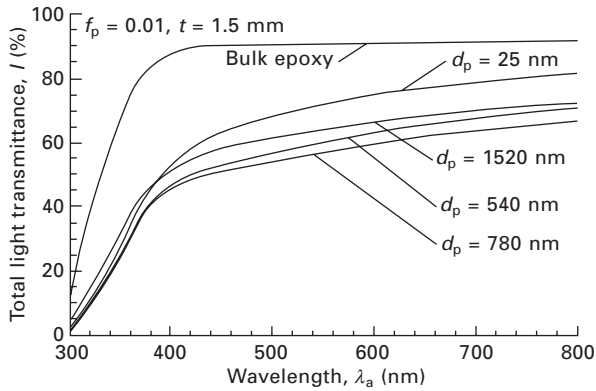
The use of nanoparticles with a diameter less than that of the wavelength of light allows transparent particle-modified materials to be produced. In practice, the particles do reduce the optical transparency compared to the unmodified matrix owing to differences in the respective refractive indices. For example, Naganuma and Kagawa (2002) showed that the light transmittance of epoxy modified with 25 nm diameter silica particles was greater than that for epoxy modified with particles of 540–1520 nm. However, using the smaller particles does give transmittance of 80–90% of the unmodified matrix value, see Fig. 7.7.

The addition of nanoclays to epoxy will also reduce the coefficient of thermal expansion (CTE) of the epoxy polymer, as the CTE of the ceramic particles is less than that of the polymer, as reported by Wang *et al*. (2000). For example, the CTE of epoxy below $T_g$ can be reduced from 77 to 63 $\mu m\ m^{-1}\ °C^{-1}$ by the addition of 3% of nanoclay (Chen and Curliss, 2001).

### 7.4.3 Electrical properties

AC impedence spectroscopy was used by Sandler *et al*. (2003) to measure the conductivity of an amine-cured epoxy modified with multiwalled carbon

© Woodhead Publishing Limited, 2010




*7.7* Wavelength dependence of normalized total light transmittance for silica particle-dispersed composite with particle diameter, $d_p$, of 25, 540, 780 and 1520 nm (reprinted from Naganuma and Kagawa, 2002, with permission from Elsevier).

nanotubes (MWNTs). The conductivity increased as a function of the MWNT weight fraction, see Fig. 7.8. There was an increase in conductivity of about two orders of magnitude, from $10^{-9}$ to $10^{-7}$ S m$^{-1}$, when 0.001 wt% of nanotubes was added. There was a further increase to above $10^{-3}$ S m$^{-1}$ for loading fractions greater than 0.005 wt%. This increase in conductivity suggests that an infinite network of percolated nanotubes starts forming above 0.001 wt%. The authors also state that comparison with the DC conductivity of the composites gave identical results. A similar transition in conductivity occurs for carbon black, but more than 1 wt% of carbon black is required (Sandler *et al*., 1999, 2003), see Fig. 7.8.

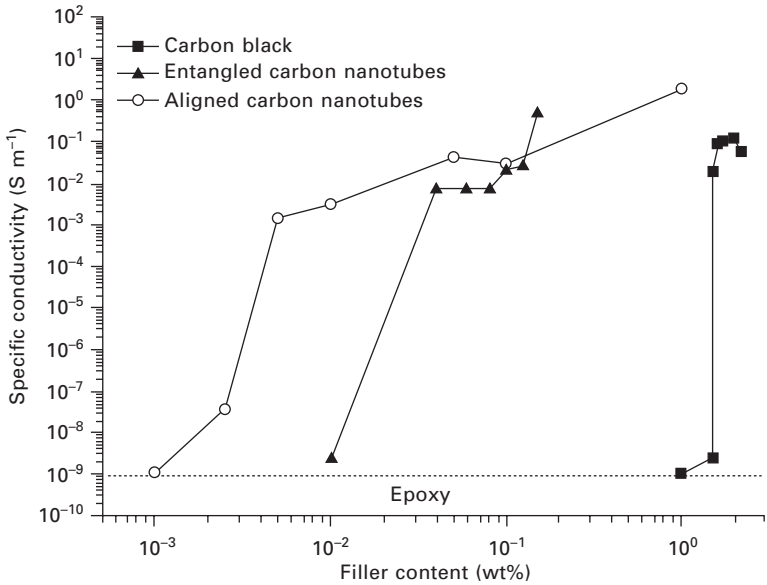
The thermal conductivity of epoxy modified with carbon nanotubes was investigated by Gojny *et al*. (2006). The authors reported that the thermal conductivity increased slightly with nanotube content. However, the changes are very small compared to the changes in electrical conductivity.

Montanari *et al*. (2005) have reported that the addition of layered silicates to epoxy resin improves the surface discharge endurance of the polymer, considerably increasing the time before electrical breakdown occurs. The addition of non-conducting silica or alumina nanoparticles will reduce the conductivity of the polymer (Cao *et al*., 2004). Layered silicates have been shown to increase the electrical breakdown strength and breakdown time (Imai *et al*., 2006), see Fig. 7.9. This indicates that these materials may have potential applications in electrical insulation materials.

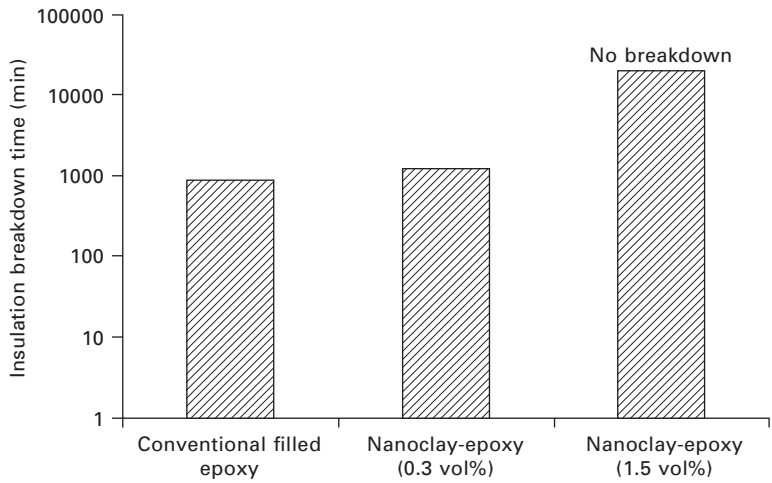
### 7.4.4 Fracture toughness

It is well-known that the addition of microparticles to thermoset polymers can increase their fracture toughness (e.g. Moloney *et al*., 1983; Kinloch and

© Woodhead Publishing Limited, 2010




*7.8* Conductivity versus filler content for aligned multi-walled carbon nanotubes, entangled nanotubes and carbon black particles in epoxy (reprinted from Sandler *et al.*, 2003, with permission from Elsevier).




*7.9* Insulation breakdown time for conventionally filled (50 vol% silica microparticles) epoxy and this epoxy with added nanoclay under constant AC voltage (10 kV, 1 kHz) (adapted from Imai *et al.*, 2006).

© Woodhead Publishing Limited, 2010

Taylor, 2002). Indeed, this is the basis of most structural adhesives, which have a rubber or thermoplastic particulate toughening phase. These particles may be preformed, or may be formed by phase separation of an initially soluble polymer during curing. Inorganic particles such as glass or mica also provide a toughening effect, although the increases in toughness are generally lower than for rubber toughening. In addition, hybrid formulations which combine rubber and glass particles have been shown to give high toughness.

Micrometre-sized rubber particles toughen thermoset polymers by cavitating, relieving the constraint in the plastic zone at the crack tip. Hence the matrix is able to deform, absorbing energy by dilation and shear banding, thus giving increased toughness. However, nanometre-sized rubber particles are thought not to cavitate, because the triaxial stresses required for cavitation are too high. Theoretical models predict that there is a minimum size below which rubber particles will not cavitate (Lazzeri and Bucknall, 1993; Dompas and Groeninckx, 1994). This diameter is predicted to be approximately 50 nm (Kody and Lesser, 1999). This lack of cavitation of small rubber particles has been observed experimentally. For example Chen and Jan (1992) observed no cavitation with carboxyl terminated butadiene acrylonitrile (CTBN) rubber particles which were 200 nm in diameter, but did see cavitation with micrometre-sized CTBN particles.

However, Azimi *et al*. (1996b) also used a piperidine-cured epoxy polymer, but observed cavitation using 200 nm diameter core-shell latex particles comprising a methacrylated butadiene-styrene copolymer (MBS) with a poly(methyl methacrylate) (PMMA) shell. Liang and Pearson (2008) also reported that nano-sized core-shell rubber particles increase toughness. They showed that the addition of 100 nm core-shell particles increased the fracture toughness of a piperidine-cured epoxy to 3.1 MPa $m^{1/2}$. Although no toughness was reported for the unmodified epoxy, similarly cured material has a fracture toughness of between 0.9 and 1.2 MPa $m^{1/2}$ (Kawaguchi and Pearson, 2003; Oba, 1999). In earlier work, Pearson and Yee (1991) compared 200 nm MBS core-shell particles to 1, 10 and 100 μm diameter CTBN particles. They reported that the fracture toughness was dependent on particle size and that small particles are more efficient at producing a toughening effect than large particles.

The addition of nanoclay particles to epoxy has been shown to increase the toughness. Karger-Kocsis *et al*. (2003) investigated vinylester/epoxy systems. They showed that the fracture energy of the systems containing 5 wt% nanoclay was increased more than two times compared to the unmodified resin. There was no significant effect of the type of the surface treatment used on the nanoclay. Increasing the amount of nanoclay above 5 wt% reduced both the fracture toughness and fracture energy. Kinloch and Taylor (2003 and 2006) compared the toughening effect caused by to the addition of layered silicate nanoparticles (nanoclays) with that due to similar microparticles, in

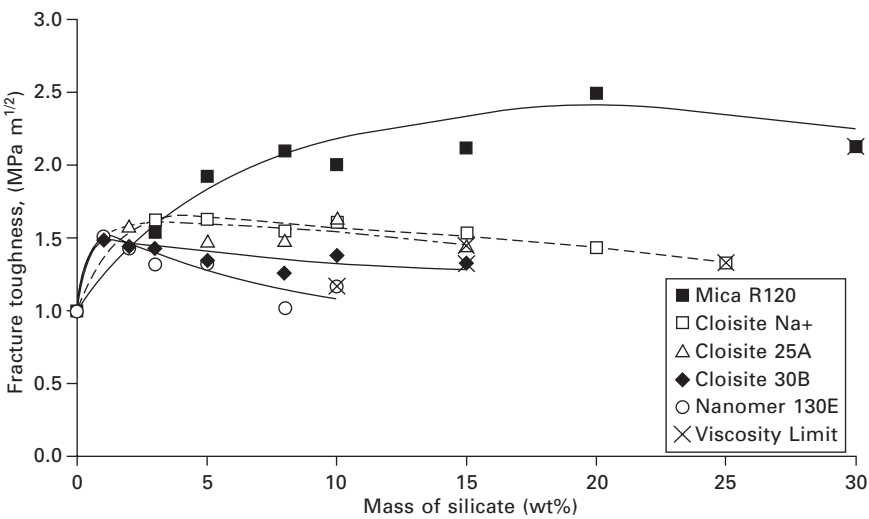
© Woodhead Publishing Limited, 2010

this case mica. They reported higher fracture toughness values for the mica microparticles than for the nanoclays, see Fig. 7.10.

They also showed that the fracture toughness was dependent on the weight fraction of nanoclay, with maximum toughness being achieved at between 1 and 5 wt% nanoclay. The fracture toughness was also dependent on the type of nanoclay used and, hence, on the surface treatment and the resulting morphology. The addition of layered silicates does not always increase the fracture toughness. For example, Tarrant (2004) found that the addition of nanoclay to thermoset acrylic systems reduced the fracture toughness.

Spherical nanoparticles have also been used to toughen epoxies. Ragosta *et al*. (2005) increased the fracture toughness, $K_C$, of tetrafunctional epoxy cured using 4,4-diaminodiphenyl sulfone (DDS) from 0.5 to 1.2 MPa $m^{1/2}$ using 10 wt% silica particles. The particles were between 10 and 15 nm in diameter. Wetzel *et al*. (2006) showed that the addition of 13-nm diameter alumina particles increased the fracture toughness of epoxy, cured using a cycloaliphatic amine, from 0.5 to 1.2 MPa $m^{1/2}$ using 11 vol% alumina. Similarly, the addition of 11 vol% 300-nm diameter titania particles increased $K_C$ to 0.85 MPa $m^{1/2}$.

Kinloch *et al*. (2005) showed that the addition of silica nanoparticles increased the fracture toughness of an anhydride-cured epoxy from 0.59 to 1.42 MPa $m^{1/2}$ when 20 wt% nanoparticles were added. These toughness values are equivalent to fracture energy, $G_C$, values of 100 and 460 J $m^{-2}$




*7.10* Fracture toughness of unmodified epoxy, mica microparticle-modified and nanoclay-modified epoxy versus content of layered silicate. Note 'viscosity limit' indicates maximum silicate content before the particle-modified resin becomes too viscous to cast (adapted from Kinloch and Taylor, 2006).

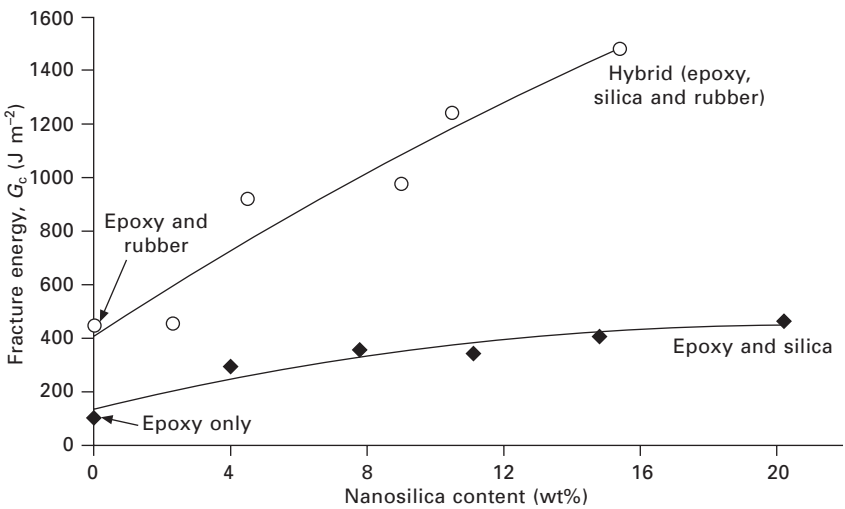
© Woodhead Publishing Limited, 2010

respectively, see Fig. 7.11. In addition, 4 wt% silica nanoparticles was sufficient almost to triple the fracture energy of the unmodified epoxy, to 290 J $m^{-2}$. The toughening mechanisms involved have been discussed by Johnsen *et al.* (2007). Zhang *et al.* (2006) and Rosso *et al.* (2006) also reported toughness increases owing to the addition of similarly-sized silica nanoparticles.

The largest increases in toughness have been reported for so-called 'hybrid' materials, which combine rubber and nanoparticle-modification of the epoxy. Kinloch *et al.* (2005) showed that the addition of silica nanoparticles to a rubber-toughened epoxy, using 9 wt% CTBN, increased the toughness from 1.11 to 2.19 MPa $m^{1/2}$ when 15 wt% nanoparticles were added. These toughness values are equivalent to fracture energy, $G_C$, values of 440 and 1480 J $m^{-2}$ respectively, see Fig. 7.11. A synergistic increase in fracture toughness has also been reported by Liang and Pearson (2008) and in impact strength by Zeng *et al.* (2007). Synergistic toughening has previously been reported for rubber-toughened epoxy with micrometre-sized glass beads, for example by Kinloch *et al.* (1985) and Azimi *et al.* (1996a). Increases in toughness have also been observed when nanoclay is added to rubber-modified epoxy, but there is not such a strong synergistic effect in this case (Liu *et al.*, 2004).

## 7.4.5 Fatigue performance

Wetzel *et al.* (2006) measured the fatigue crack propagation (FCP) rate, d*a*/d*N*, versus the stress intensity factor range, and showed that this relationship



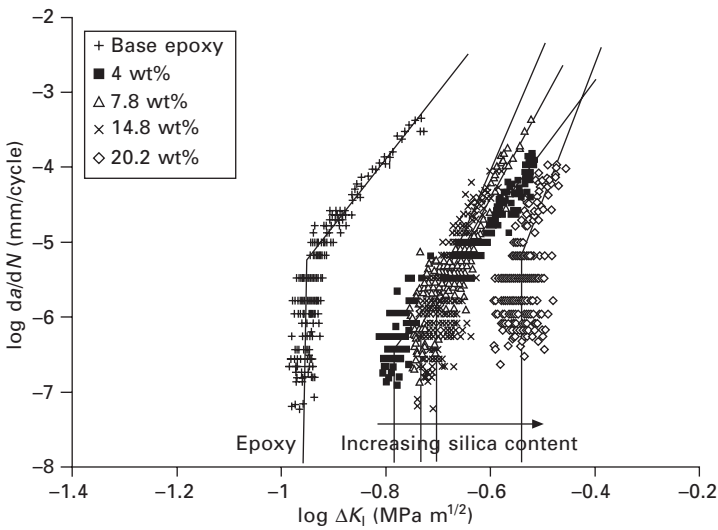

*7.11* Fracture energy versus content of silica nanoparticles in epoxy and rubber-toughened (9% CTBN) epoxy (adapted from Kinloch *et al.*, 2005).

© Woodhead Publishing Limited, 2010

follows the standard Paris–Erdogan law. These fatigue curves are shifted towards higher stress-intensity values as the nanoparticle content rises. At the same time, the gradient decreases. They report that the gain in FCP resistance of alumina-modified epoxy nanocomposites (10 vol%) is comparable to the reinforcement achieved by rubber particles in epoxy, as was demonstrated using small amounts of rubber (5–10 phr CTBN) (Karger-Kocsis and Friedrich, 1992) and is similar to that using 15–20 vol% of glass microspheres (Sautereau *et al.*, 1995). In contrast to such traditional modifiers, the authors point out that the benefits conferred by nanoparticles are neither at the expense of modulus nor of strength.

Blackman *et al.* (2007) showed that nano-silica particles significantly improved the cyclic fatigue behaviour of an anhydride-cured epoxy polymer, increasing the range of the applied stress intensity factor at threshold, $\Delta K_{th}$, see Fig. 7.12. The nanoparticles also increased the fracture toughness, $K_C$. The fatigue data followed the modified Paris law. Similarly, Azimi *et al.* (1996b) showed that 200-nm diameter rubber particles increase fracture toughness and improve fatigue resistance (Azimi *et al.*, 1996b). The fatigue data followed the classic Paris–Erdogan law. The use of 200 nm MBS particles in place of 1.5 μm CTBN particles resulted in about one order of magnitude improvement in fatigue resistance.

Zhou *et al.* (2007) measured the fatigue stress versus number of cycles to failure (S–N) curves of an amine-cured epoxy polymer modified with




*7.12* Logarithmic crack growth rate per cycle, d*a*/d*N*, versus logarithmic range of applied stress intensity factor from cyclic fatigue tests for unmodified epoxy and silica nanoparticle-modified epoxy (courtesy J. Sohn Lee).

© Woodhead Publishing Limited, 2010

carbon nanofibres (CNF). At the same stress level, the number of cycles to failure of the nano-modified epoxy was significantly higher than that of the unmodified epoxy. The fatigue life went through a maximum at 2 wt% CNF, although only two specimens were used for each combination of stress level and CNF loading.

Zhang *et al*. (2007) also showed a reduction in crack growth rate per cycle for an epoxy system with the addition of up to 0.5 wt% carbon nanotubes. The authors attributed this effect to pullout of the nanotubes that bridge across the crack opening. Although there are data available which show how nanoparticles can change the fatigue performance of adhesives, there are no data which quantify the durability (i.e. the resistance to an environment such as water) of these materials when used as adhesives.

### 7.4.6 Peel and lap shear performance

Modification of a polyurethane adhesive using nanoclays was tested by Dodiuk *et al*. (2006), using adhesive joints made with aluminium alloy adherends. The incorporation of functionalised nanoclays into PU improved the lap-shear strength by up to 195%. The functionalised nanoclays also gave higher peel strengths than the unmodified PU. Increases of up to 40% were measured, but one of the nanoclays gave almost no change in the peel strength.

The lap-shear strength of carbon fibre composites bonded using an epoxy adhesive increased by 45% with the addition of 5% MWNT (Hsiao *et al*., 2003). Note that in this case the locus of failure was altered from interfacial for the control specimens to cohesive for the nanotube-modified materials.

Gilbert *et al*. (2003) used a model rubber-toughened epoxy film adhesive, and modified this with 5 or 10 wt% of either 50-nm diameter alumina nanoparticles or alumina nanofibres with a diameter of 2–4 nm and an aspect ratio ranging from tens to hundreds. Climbing drum peel and lap shear tests were performed using aluminium alloy substrates. Both of the nano-modifiers increased the peel and shear strength. However, the most successful modification was the addition of 5% alumina nanoparticles, which increased the peel strength of the adhesive by 50% and the lap-shear strength by 15%.

Very soft acrylic adhesives modified by nanoclay or silica nanoparticles were developed by Patel *et al*. (2006). The lap shear and 180° peel test performance were improved by the addition of nanoparticles. Addition of 6 wt% nanoclay or 50 wt% silica increased the peel force by about 40%.

Sprenger and co-workers used a room-temperature curing rubber-toughened epoxy adhesive with a $T_g$ of 70°C (Sprenger *et al*., 2003, 2004; Kinloch *et al*., 2003). The addition of only 4 wt% of 20 nm diameter silica nanoparticles doubled the fracture energy from 1200 to 2300 J $m^{-2}$. The addition of the

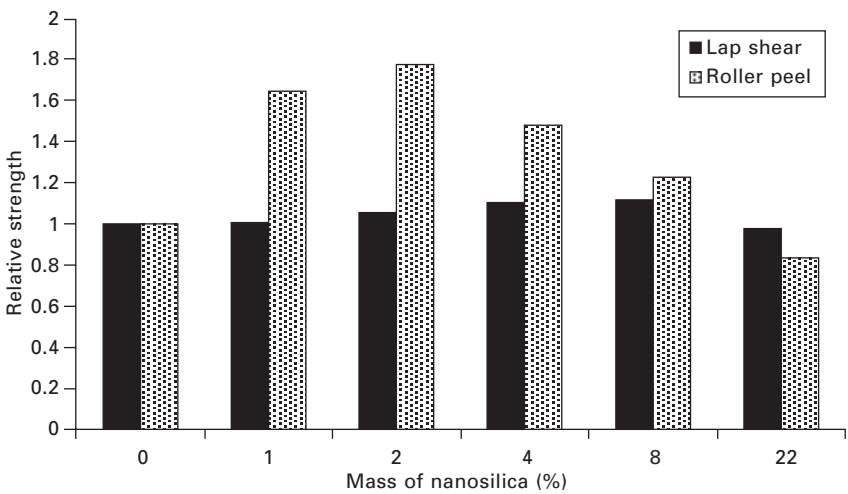
© Woodhead Publishing Limited, 2010

nanoparticles also increased both the lap-shear and peel strength, as shown in Fig. 7.13.

## 7.5 Future trends

Currently the addition of nanoparticles is often simply a marketing tool, as the performance benefit which they provide could be obtained using conventional fillers at a much lower cost. However, some successful applications have been shown, for example the addition of ceramic nanoparticles to transparent coatings gives improved scratch resistance without loss of transparency. The efficient use of nanoparticles and nanotubes as fillers will require optimisation of the surface treatment to ensure both dispersion and the require d degree of adhesion or coupling between the filler and the matrix (Endo *et al.*, 2004). They are most likely to be used as functional fillers, for example providing improved electrical properties or toughness, rather than as simple reinforcements for increasing the modulus of the polymer.

Nanoparticles have also been used in sporting goods, where a glass fibre composite with an anhydride-cured epoxy matrix modified with silica nanoparticles and rubber has been used for ski poles. Further combinations of micro and nanoparticles to achieve synergies will be a way to exploit nanoparticles, as improvements in performance may be achieved using relatively low volume fractions. Their use in composite materials will also be a growth area, as the nanoparticles can be used with low-cost resin infusion processes as they are small enough to flow between the fibres.

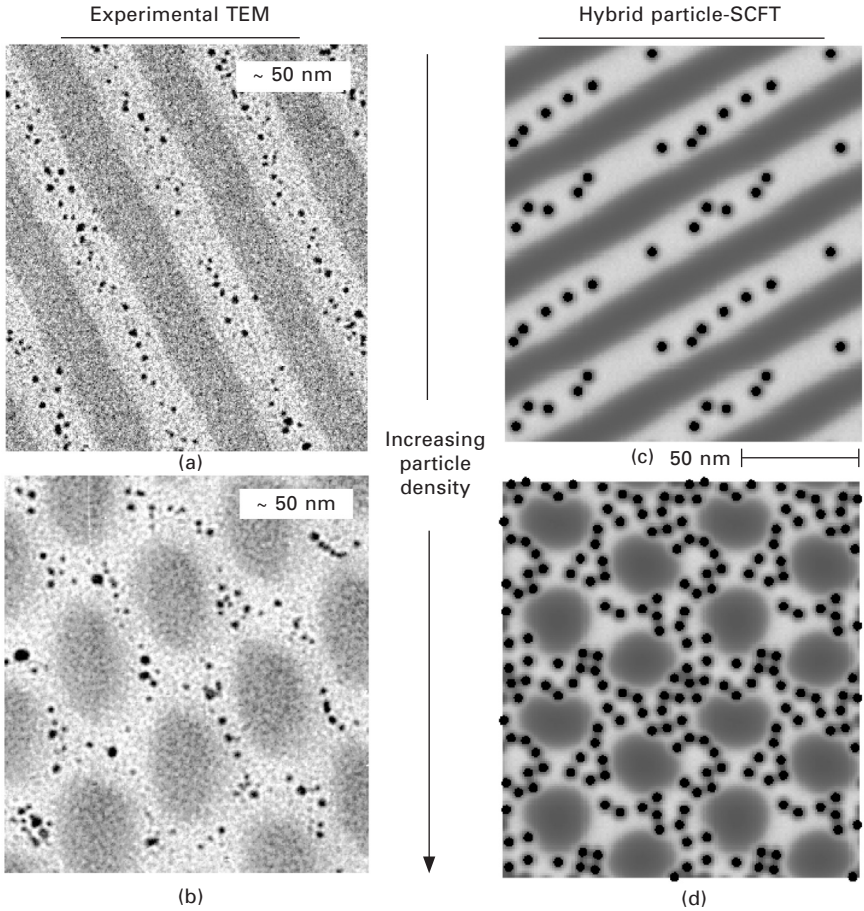



*7.13* Lap-shear and roller peel strength for hybrid (nanosilica and rubber-modified) epoxy (adapted from Kinloch *et al.*, 2003).

© Woodhead Publishing Limited, 2010

It is anticipated that hierarchical materials, with features that span a range of length scales, will become important. A current example is carbon fibres with nanotubes grown on the surface to improve the interaction between the fibre surface and the matrix (Qian *et al.*, 2008). This will be important for fibre composites, but the use of the same technology to produce fillers with nano-modified surfaces (e.g. short carbon fibres covered in nanotubes) will have an effect on structural adhesives.

In future, the use of nanoparticles will go beyond filled systems, to the use of regular or patterned structures (Vaia and Maguire, 2007). This can be




*7.14* Transmission electron micrographs (left column) of diblock polymer containing functionalized gold nanoparticles with a particle volume fraction of (a) 0.10 and (b) 0.35. Self-consistent field theory (SCFT) simulation results (right column) show the two blocks (light and dark), and nanoparticles (black) with a particle volume fraction of (c) 0.10 and (d) 0.35 (Sides *et al.*, 2006 (Copyright 2006 by the American Physical Society)).

© Woodhead Publishing Limited, 2010

achieved using directed patterning of nanoparticle dispersions or assembly of nanoparticles. Directed patterning can be achieved by magnetic or electric fields, mechanical deformation, spin coating and so on (e.g. Koerner *et al*., 2005; Park *et al*., 2005). Assembly of nanoparticles can be achieved using diblock polymers which will give a regular pattern of two separate nanometre-sized phases (Sides *et al*., 2006), see Fig. 7.14. Alternatively using core-shell particles which are sintered together enables all the particles to have an identical interparticle distance and prevents problems with agglomeration. These could be considered to be 'engineered, tailored or designed materials' (Vaia and Maguire, 2007).

Alternatively this method enables the formation of anisotropic materials, for example, allowing a graduation of properties through the thickness or along the length of an adhesive joint, to improve the stress distribution or enable the toughness to be modified. It is anticipated that nanoparticles will be increasingly used in structural adhesives. Their application will continue to expand as their availability increases and hence as their cost decreases.

## 7.6 Sources of further information and advice

*Review articles*

Alexandre M and Dubois P (2000), 'Polymer-layered silicate nanocomposites: Preparation, properties and uses of a new class of materials', *Mater. Sci. Eng. R*, **28**(12), 1–63.

Endo M, Hayashi T, Kim YA, Terrones M and Dresselhaus MS (2004), 'Applications of carbon nanotubes in the twenty-first century', *Phil. Trans. R. Soc. Lond. A*, **362**(1823), 2223–38.

Popov VN (2004), 'Carbon nanotubes: Properties and application', *Mater. Sci. Eng. R*, **43**(3), 61–102.

Ray SS and Okamoto M (2003), 'Polymer/layered silicate nanocomposites: A review from preparation to processing', *Progr. Polym. Sci*., **28**(11), 1539–641.

Tjong SC (2006), 'Structural and mechanical properties of polymer nanocomposites', *Mater. Sci. Eng. R*, **53**(3–4), 73–197.

Xie X-L, Mai Y-W and Zhou X-P (2005), 'Dispersion and alignment of carbon nanotubes in polymer matrix: A review', *Mater. Sci. Eng. R*, **49**(4), 89–112.

*Books*

Advani SG (ed.) (2006), *Processing and Properties of Nanocomposites,* World Scientific Publishing, Singapore.

Ajayan PM, Schadler LS and Braun PV (2003), *Nanocomposite Science and Technology*, Wiley-VCH, Weinheim.

© Woodhead Publishing Limited, 2010

Grim RE (1962), *Applied Clay Mineralogy*, McGraw-Hill, New York.
Krishnamoorti R and Vaia RA (eds) (2002), *Polymer Nanocomposites: Synthesis, Characterization and Modeling*, American Chemical Society, Washington.
Pinnavaia TJ and Beall GW (2000), *Polymer-clay Nanocomposites*, John Wiley & Sons, Chichester.
Rothon RN (ed.) (1995), *Particulate-filled Polymer Composites*, Longman Scientific & Technical, Harlow.
Utracki LA (2004a), *Clay-Containing Polymeric Nanocomposites Volume 1*, Rapra Technology, Shrewsbury.
Utracki LA (2004b), *Clay-containing Polymeric Nanocomposites Volume 2*, Rapra Technology, Shrewsbury.

*Reports*

DEFRA (2005), *Characterising the Risks Posed by Engineered Nanoparticles: A First UK Government Research Report*, Department for Environment, Food and Rural Affairs, London.
DEFRA (2006), *Characterising the Potential Risks Posed by Engineered Nanoparticles: UK Government Research: A Progress Report*, Department for Environment, Food and Rural Affairs, London.
Dowling A (2004), *Nanoscience and Nanotechnologies: Opportunities and Uncertainties*, The Royal Society and The Royal Academy of Engineering, London.

*Professional organisations and conferences*

The following professional organisations organise conferences or provide information and publications which have a significant content relevant to the use of nanoparticles in structural adhesives:

Institute of Nanotechnology at www.nano.org.uk
Society for Adhesion and Adhesives at www.uksaa.org
The Adhesion Society at www.adhesionsociety.org
Materials Research Society at www.mrs.org
Institute of Materials, Minerals & Mining at www.iom3.org
National Institute of Standards and Technology at www.nist.gov

## 7.7 Conclusions

Nanoparticle-modified polymers are being extensively researched, and a great deal of work has been done to produce nanoparticles. These nanoparticles are now commercially available in kilogram or tonne quantities, and at reasonable

© Woodhead Publishing Limited, 2010

prices (US$10 per kilogram). Hence, nanotechnology and nanoparticles are beginning to be applied in commercial products.

The dispersion of nanoparticles in polymer matrices can be difficult and agglomerates can remain even after aggressive processing. These may have a significant detrimental effect on the properties of the material. For this reason, pre-dispersed nanoparticles, available as a masterbatch in a polymer, are attractive. However, these particles can agglomerate during processing or curing, so there is no guarantee that a good dispersion will be obtained in the final material.

Nanoparticles have been shown to improve the structural and functional properties of thermoset polymers. However, in many cases similar increases can be obtained using micrometre-sized particles, especially for structural properties. High aspect ratio particles, such as carbon nanotubes or nanoclay, can give significant improvements in functional properties. Examples include electrical percolation at very low filler volume fractions and increases in barrier properties.

It is perhaps the synergistic effect of combining nanoparticles with existing technology based on micrometre-sized particles that is the most exciting area at present. For example, the fracture toughness and peel performance of adhesive joints can be improved by combining silica nanoparticles and rubber microparticles. Hierarchical materials like these and patterned arrays of nanoparticles, appear to be the next developments in this field.

## 7.8 References

Ahmed S and Jones FR (1990), 'A review of particulate reinforcement theories for polymer composites', *J. Mater. Sci.*, **25**(12), 4933–42.

Ajayan PM, Stephan O, Colliex C and Trauth D (1994), 'Aligned carbon nanotube arrays formed by cutting a polymer resin-nanotube composite', *Science*, **265**(5176), 1212–14.

Alexandre M and Dubois P (2000), 'Polymer-layered silicate nanocomposites: Preparation, properties and uses of a new class of materials', *Mater. Sci. Eng. R*, **28**(12), 1–63.

Azimi HR, Pearson RA and Hertzberg RW (1996a), 'Fatigue of hybrid epoxy composites: Epoxies containing rubber and hollow glass spheres', *Polym. Eng. Sci.*, **36**(18), 2352–65.

Azimi HR, Pearson RA and Hertzberg RW (1996b), 'Fatigue of rubber-modified epoxies: Effect of particle size and volume fraction', *J. Mater. Sci.*, **31**(14), 3777–89.

Baik Y, Lee S, Jang Y and Kim S (2005), 'Unidirectional alignment of carbon nano-sized fiber using drawing process', *J. Mater. Sci.*, **40**(22), 6037–9.

Bechelany M, Brioude A, Bernard S, Ferro G, Cornu D and Miele P (2007), 'Large-scale preparation of faceted $Si_3N_4$ nanorods from beta-SiC nanowires', *Nanotechnology*, **18**(33), 335305.

Beyer G (2002), 'Carbon nanotubes as flame retardants for polymers', *Fire Mater.*, **26**(6), 291–3.

Blackman BRK, Kinloch AJ, Sohn Lee J, Taylor AC, Agarwal R, Schueneman G and

© Woodhead Publishing Limited, 2010

Sprenger S (2007), 'The fracture and fatigue behaviour of nano-modified epoxy polymers', *J. Mater. Sci.*, **42**(16), 7049–51.

Brnardic I, Macan J, Ivankovic H and Ivankovic M (2008), 'Thermal degradation kinetics of epoxy/organically modified montmorillonite nanocomposites', *J. Appl. Polymer Sci.*, **107**(3), 1932–8.

Brooker RD, Blackman BRK, Taylor AC and Kinloch AJ (2008), 'Nano-reinforcement of epoxy/thermoplastic blends', *31st Annual Meeting of the Adhesion Society*, Austin, USA, Adhesion Society, Blacksburg, USA.

Bugnicourt E, Galy J, Gerard J-F and Barthel H (2007), 'Effect of sub-micron silica fillers on the mechanical performances of epoxy-based composites', *Polymer*, **48**(6), 1596–1605.

Cao Y, Irwin PC and Younsi K (2004), 'The future of nanodielectrics in the electrical power industry', *IEEE Trans. Dielectric Electrical Insul.*, **11**(5), 797–807.

Chakrabarti S, Nagasaka T, Yoshikawa Y, Pan LJ and Nakayama Y (2006), 'Growth of super long aligned brush-like carbon nanotubes', *Japan. J. Appl. Phys. 2 Lett & Expr. Lett.*, **45**(24–28), L720–L722.

Chandradass J and Bae D-S (2008), 'Preparation and properties of barium titanate nanopowder/epoxy composites', *Mater. Manuf. Process.*, **23**(2), 116–22.

CheapTubes (2008), http://www.cheaptubes.com.

Chen C and Curliss D (2001), 'Resin matrix composites: Organoclay-aerospace epoxy nanocomposites, part ii', *SAMPE J.*, **37**(5), 11–18.

Chen TK and Jan YH (1992), 'Fracture mechanism of toughened epoxy-resin with bimodal rubber-particle size distribution', *J. Mater. Sci.*, **27**(1), 111–21.

Chen XQ, Saito T, Yamada H and Matsushige K (2001), 'Aligning single-wall carbon nanotubes with an alternating-current electric field', *Appl. Phys. Lett.*, **78**(23), 3714–16.

Demczyk BG, Wang YM, Cumings J, Hetman M, Han W, Zettl A and Ritchie RO (2002), 'Direct mechanical measurement of the tensile strength and elastic modulus of multiwalled carbon nanotubes', *Mater. Sci. Eng. A*, **334**(1–2), 173–8.

Dodiuk H, Belinski I, Dotan A and Kenig S (2006), 'Polyurethane adhesives containing functionalized nanoclays', *J. Adhesion Sci. Tech.*, **20**(12), 1345–55.

Dompas D and Groeninckx G (1994), 'Toughening behavior of rubber-modified thermoplastic polymers involving very small rubber particles. 1. A criterion for internal rubber cavitation', *Polymer*, **35**(22), 4743–9.

Endo M, Hayashi T, Kim YA, Terrones M and Dresselhaus MS (2004), 'Applications of carbon nanotubes in the twenty-first century', *Phil. Trans. R. Soc. Lond. A*, **362**(1823), 2223–38.

Feynman RP (1959), *There's Plenty of Room at the Bottom – an Invitation to Enter a New Field of Physics*, http://www.zyvex.com/nanotech/feynman.html, American Physical Society at the California Institute of Technology (Caltech).

Fiedler B, Gojny FH, Wichmann MHG, Nolte MCM and Schulte K (2006), 'Fundamental aspects of nano-reinforced composites', *Composites Sci. Tech.,* **66**(16), 3115–25.

Gilbert EN, Hayes BS and Seferis JC (2003), 'Nano-alumina modified epoxy based film adhesives', *Polym. Eng. Sci.*, **43**(5), 1096–104.

Gilman JW (1999), 'Flammability and thermal stability studies of polymer layered-silicate (clay) nanocomposites', *Appl. Clay Sci.*, **15**(1–2), 31–49.

Gilman JW, Harris RH and Hunter D (1999a), 'Cyanate ester clay nanocomposites: Synthesis and flammability studies', *Evolving and Revolutionary Technologies for the New Millennium. 44th International SAMPE Symposium/Exhibition*, Society

© Woodhead Publishing Limited, 2010

for the Advancement of Material and Process Engineering (SAMPE), Long Beach, CA, USA.

Gilman JW, Kashiwagi T, Nyden M, Brown JET, Jackson CL, Lomakin S, Giannelis EP and Manias E (1999b), 'Flammability studies of polymer layered silicate nanocomposites: Polyolefin, epoxy and vinyl ester resins', in *Chemistry and Technology of Polymer Additives*, Ak-Malaika S, Golovoy A and Wilkie CA (eds), Blackwell Science, Malden, USA.

Gilman JW, Harris RH, Jackson CL, Morgan AB, Brassell LD and Hunter DL (2000a), 'Phenolic cyanate ester nanocomposites: Effect of ammonium ion structure on flammability and nano-dispersion', *Spring Meeting, Division of Polymeric Materials: Science and Engineering, American Chemical Society*, American Chemical Society, San Francisco, USA.

Gilman JW, Jackson CL, Morgan AB, Harris RH, Manias E, Giannelis EP, Wuthenow M, Hilton D and Phillips SH (2000b), 'Flammability properties of polymer-layered-silicate nanocomposites. Polypropylene and polystyrene nanocomposites', *Chem. Mater*., **12**(7), 1866–73.

Gintert MJ, Jana SC and Miller SG (2007), 'A novel strategy for nanoclay exfoliation in thermoset polyimide nanocomposite systems', *Polymer*, **48**(14), 4166–73.

Gojny FH, Nastalczyk J, Roslaniec Z and Schulte K (2003), 'Surface modified multi-walled carbon nanotubes in cnt/epoxy-composites', *Chem. Phys. Lett.,* **370**(5–6), 820–4.

Gojny FH, Wichmann MHG, Kopke U, Fiedler B and Schulte K (2004), 'Carbon nanotube-reinforced epoxy-composites: Enhanced stiffness and fracture toughness at low nanotube content', *Composites Sci. Tech.*, **64**(15), 2363–71.

Gojny FH, Wichmann MHG, Fiedler B, Kinloch IA, Bauhofer W, Windle AH and Schulte K (2006), 'Evaluation and identification of electrical and thermal conduction mechanisms in carbon nanotube/epoxy composites', *Polymer*, **47**(6), 2036–45.

Gordon JE (1978), *The New Science of Strong Materials or Why You Don't Fall Through the Floor*, Penguin Books, Harmondsworth.

Green K, Dean D, Abdalla M, Jose MV and Robinson P (2006), 'Aligned carbon nanofiber/epoxy nanocomposites', *Polym. Mater. Sci. Eng*., **94**, 53–4.

Gusev AA and Lusti HR (2001), 'Rational design of nanocomposites for barrier applications', *Adv. Mater.*, **13**(21), 1641–3.

Hackman I and Hollaway L (2006), 'Epoxy-layered silicate nanocomposites in civil engineering', *Composites Pt. A*, **37**(8), 1161–70.

Harper T (2003), 'What is nanotechnology?' *Nanotechnology,* **14**(1), U5–10.

Hay J and Shaw S (2001), 'Into the labyrinth', *Chemistry in Britain,* (November), 34–7.

Hsiao K-T, Alms J and Advani SG (2003), 'Use of epoxy/multiwalled carbon nanotubes as adhesives to join graphite fibre reinforced polymer composites', *Nanotechnology*, **14**(July), 791–3.

Iijima S (1991), 'Helical microtubules of graphitic carbon', *Nature*, **354**(6348), 56–8.

Iijima S and Ichihashi T (1993), 'Single-shell carbon nanotubes of 1-nm diameter', *Nature*, **363**(6430), 603–5.

Imai T, Sawa F, Nakano T, Ozaki T, Shimizu T, Kozako M and Tanaka T (2006), 'Effects of nano- and micro-filler mixture on electrical insulation properties of epoxy based composites', *IEEE Trans. Dielectric Electrical Insul.*, **13**(2), 319–26.

International Carbon Black Association (2008), http://www.carbon-black.org.

Johnsen BB, Kinloch AJ, Mohammed RD, Taylor AC and Sprenger S (2007), 'Toughening mechanisms of nanoparticle-modified epoxy polymers', *Polymer*, **48**(2), 530–41.

© Woodhead Publishing Limited, 2010

Kaneka (2008), http://www.kaneka.com.
Karger-Kocsis J and Friedrich K (1992), 'Fatigue crack-propagation and related failure in modified, anhydride-cured epoxy-resins', *Colloid Polym. Sci*., **270**(6), 549–62.
Karger-Kocsis J, Gryshchuk O, Frohlich J and Mulhaupt R (2003), 'Interpenetrating vinylester/epoxy resins modified with organophilic layered silicates', *Composites Sci. Tech*., **63**(14), 2045–54.
Kathi J and Rhee K (2008), 'Surface modification of multi-walled carbon nanotubes using 3-aminopropyltriethoxysilane', *J. Mater. Sci*., **43**(1), 33–7.
Kawaguchi T and Pearson RA (2003), 'The effect of particle-matrix adhesion on the mechanical behavior of glass filled epoxies. Part 2. A study on fracture toughness', *Polymer*, **44**(15), 4239–47.
Kinloch AJ and Taylor AC (2002), 'The toughening of cyanate-ester polymers. Part I: Physical modification using particles, fibres and woven-mats', *J. Mater. Sci*., **37**(3), 433–60.
Kinloch AJ and Taylor AC (2003), 'Mechanical and fracture properties of epoxy/inorganic micro- and nano-composites', *J. Mater. Sci. Lett*., **22**(20), 1439–41.
Kinloch AJ and Taylor AC (2006), 'The mechanical properties and fracture behaviour of epoxy-inorganic micro- and nano-composites', *J. Mater. Sci.,* **41**(11), 3271–97.
Kinloch AJ, Maxwell DL and Young RJ (1985), 'The fracture of hybrid-particulate composites', *J. Mater. Sci*., **20**(11), 4169–84.
Kinloch AJ, Lee JH, Taylor AC, Sprenger S, Eger C and Egan D (2003), 'Toughening structural adhesives via nano- and micro-phase inclusions', *J. Adhesion*, **79**(8–9), 867–73.
Kinloch AJ, Mohammed RD, Taylor AC, Eger C, Sprenger S and Egan D (2005), 'The effect of silica nano particles and rubber particles on the toughness of multiphase thermosetting epoxy polymers', *J. Mater. Sci*., **40**(18), 5083–6.
Kody RS and Lesser AJ (1999), 'Yield behavior and energy absorbing characteristics of rubber-modified epoxies subjected to biaxial stress states', *Polym. Composites*, **20**(2), 250–9.
Koerner H, Hampton E, Dean D, Turgut Z, Drummy L, Mirau P and Vaia R (2005), 'Generating triaxial reinforced epoxy/montmorillonite nanocomposites with uniaxial magnetic fields', *Chem. Mater.,* **17**(8), 1990–6.
Kornmann X (1999), *Synthesis and Characterisation of Thermoset-clay Nanocomoposites*, Licentiate, Thesis, University of Lulea.
Lam C-K, Lau K-T, Cheung H-Y and Ling H-Y (2005), 'Effect of ultrasound sonication in nanoclay clusters of nanoclay/epoxy composites', *Mater. Lett.,* **59**(11), 1369–72.
Lam C-W, James JT, McCluskey R and Hunter RL (2004), 'Pulmonary toxicity of single-wall carbon nanotubes in mice 7 and 90 days after intratracheal instillation', *Toxicol. Sci*., **77**(1), 126–34.
Lau K-T, Gu C, Gao G-H, Ling H-Y and Reid SR (2004), 'Stretching process of single- and multi-walled carbon nanotubes for nanocomposite applications', *Carbon*, **42**(2), 426–8.
Lazzeri A and Bucknall CB (1993), 'Dilatational bands in rubber-toughened polymers', *J. Mater. Sci*., **28**(24), 6799–808.
Liang G and Hu X (2004), 'Preparation and performance of aluminum borate whisker-reinforced epoxy composites. I. Effect of whiskers on processing, reactivity, and mechanical properties', *J. Appl. Polym. Sci*., **92**(3), 1950–4.
Liang YL and Pearson RA (2008), 'The role of nanosilica dispersion and particle size in hybrid epoxy-silica nanocomposites toughening mechanism', *31st Annual Meeting*

© Woodhead Publishing Limited, 2010

*of the Adhesion Society*, Austin, USA, Adhesion Society, Blacksburg, USA.
Liu WP, Hoa SV and Pugh M (2004), 'Morphology and performance of epoxy nanocomposites modified with organoclay and rubber', *Polym. Eng. Sci.*, **44**(6), 1178–86.
Lu KL, Lago RM, Chen YK, Green MLH, Harris PJF and Tsang SC (1996), 'Mechanical damage of carbon nanotubes by ultrasound', *Carbon*, **34**(6), 814–16.
Martin CA, Sandler JKW, Windle AH, Schwarz MK, Bauhofer W, Schulte K and Shaffer MSP (2005), 'Electric field-induced aligned multi-wall carbon nanotube networks in epoxy composites', *Polymer*, **46**(3), 877–86.
Messersmith PB and Giannelis EP (1994), 'Synthesis and characterisation of layered silicate-epoxy nanocomposites', *Chem. Mater.*, **6**(10), 1719–25.
Mohammed RD (2007), *Material Properties and Fracture Mechanisms of Epoxy Nano-Composites*, PhD Thesis, Imperial College London.
Moloney AC, Kausch HH and Stieger HR (1983), 'The fracture of particulate-filled epoxide resins', *J. Mater. Sci.*, **19**(4), 1125–30.
Montanari GC, Ciani F, Testa L, Guastavino F, Coletti G and Mulhaupt R (2005), 'Electric strength, space charge and surface discharge characterization of nanostructured epoxy-silicate insulating materials', *2005 International Symposium on Electrical Insulating Materials, Vols, 1-3*, Tokyo, Institute Electrical Engineers Japan.
Morisada Y, Miyamoto Y, Takaura Y, Hirota K and Tamari N (2007), 'Mechanical properties of SiC composites incorporating SiC-coated multi-walled carbon nanotubes', *Int. J. Refractory Metals and Hard Mater.*, **25**(4), 322–7.
Naganuma T and Kagawa Y (2002), 'Effect of particle size on the optically transparent nano meter-order glass particle-dispersed epoxy matrix composites', *Composites Sci. Tech.*, **62**(9), 1187–9.
Nanoresins (2008), http://www.nanoresins.com.
Oba T (1999), *The Fatigue Behaviour of Toughened Epoxy Polymers,* PhD Thesis, Imperial College of Science, Technology and Medicine, London.
Park SY, Cho YH and Vaia RA (2005), 'Three-dimensional structure of the zone-drawn film of the nylon-6/layered silicate nanocomposites', *Macromolecules*, **38**(5), 1729–35.
Patel S, Bandyopadhyay A, Ganguly A and Bhowmick AK (2006), 'Synthesis and properties of nanocomposite adhesives', *J. Adhesion Sci. Tech.*, **20**(4), 371–85.
Pearson RA and Yee AF (1991), 'Influence of particle-size and particle-size distribution on toughening mechanisms in rubber-modified epoxies', *J. Mater. Sci.*, **26**(14), 3828–44.
Puglia D, Valentini L and Kenny JM (2003), 'Analysis of the cure reaction of carbon nanotubes/epoxy resin composites through thermal analysis and raman spectroscopy', *J. Appl. Polymer Sci.*, **88**(2), 452–8.
Qian H, Bismarck A, Greenhalgh ES, Kalinka G and Shaffer MSP (2008), 'Hierarchical composites reinforced with carbon nanotube grafted fibers: The potential assessed at the single fiber level', *Chem. Mater.*, **20**(5), 1862–9.
Radford T (2003), 'Brave new world or miniature menace? Why Charles fears grey goo nightmare', *The Guardian*, London, 29 April 2003.
Ragosta G, Abbate M, Musto P, Scarinzi G and Mascia L (2005), 'Epoxy-silica particulate nanocomposites: Chemical interactions, reinforcement and fracture toughness', *Polymer*, **46**(23), 10506–16.
Rosso P, Ye L, Friedrich K and Sprenger S (2006), 'A toughened epoxy resin by silica nanoparticle reinforcement', *J. Appl. Polym. Sci.*, **100**(3), 1849–55.
Rothon RN and Hancock M (1995), 'General principles guiding selection and use of

© Woodhead Publishing Limited, 2010

particulate materials', in *Particulate-filled Polymer Composites*, Rothon RN (ed.), Longman Scientific & Technical, Harlow.

Sandler J, Shaffer MSP, Prasse T, Bauhofer W, Schulte K and Windle AH (1999), 'Development of a dispersion process for carbon nanotubes in an epoxy matrix and the resulting electrical properties', *Polymer*, **40**(21), 5967–71.

Sandler JKW, Kirk JE, Kinloch IA, Shaffer MSP and Windle AH (2003), 'Ultra-low electrical percolation threshold in carbon-nanotube-epoxy composites', *Polymer*, **44**(19), 5893–9.

Sautereau H, Maazouz A, Gerard JF and Trotignon JP (1995), 'Fatigue behavior of glass bead filled epoxy', *J. Mater. Sci.*, **30**(7), 1715–18.

Schmid CF and Klingenberg DJ (2000), 'Mechanical flocculation in flowing fiber suspensions', *Phys. Rev. Lett.*, **84**(2), 290–3.

Shaffer MSP and Kinloch IA (2004), 'Prospects for nanotube and nanofibre composites', *Composites Sci. Tech.*, **64**(15), 2281–2.

Shaffer MSP and Sandler JKW (2006), 'Carbon nanotube/nanofibre polymer composites', in *Processing and Properties of Nanocomposites*, Advani SG (ed.), World Scientific Publishing, Singapore.

Sheng N, Boyce MC, Parks DM, Rutledge GC, Abes JI and Cohen RE (2004), 'Multiscale micromechanical modeling of polymer/clay nanocomposites and the effective clay particle', *Polymer*, **45**(2), 487–506.

Sides SW, Kim BJ, Kramer EJ and Fredrickson GH (2006), 'Hybrid particle-field simulations of polymer nanocomposites', *Phys. Rev. Lett.*, **96**(25), 250601–4.

SigmaAldrich (2008), http://www.sigmaaldrich.com.

Sprenger S, Eger C, Kinloch AJ, Taylor AC, Lee JH and Egan D (2003), 'Nanoadhesives: Toughness and high strength', *Adhaesion, Kleben & Dichten*, **2003**(3), 24–8.

Sprenger S, Eger C, Kinloch AJ, Taylor AC, Lee JH and Egan D (2004), 'Nano-modified ambient temperature curing epoxy adhesives', *Adhaesion, Kleben & Dichten*, **2004**(3), 1–5.

Tang Y, Liang G, Zhang Z and Han J (2007), 'Performance of aluminum borate whisker reinforced cyanate ester resin', *J. Appl. Polymer Sci.*, **106**(6), 4131–7.

Tarrant AE (2004), *Thermoset-acrylic/layered-silicate Nanocomposites: Synthesis and Structure–Property Relationships*, PhD Thesis, Imperial College of Science, Technology and Medicine, London.

Tjong SC (2006), 'Structural and mechanical properties of polymer nanocomposites', *Mater. Sci. Eng. R*, **53**(3–4), 73–197.

Triantafyllidis KS, LeBaron PC, Park I and Pinnavaia TJ (2006), 'Epoxy-clay fabric film composites with unprecedented oxygen-barrier properties', *Chem. Mater.*, **18**(18), 4393–8.

Vaia RA and Maguire JF (2007), 'Polymer nanocomposites with prescribed morphology: Going beyond nanoparticle-filled polymers', *Chem. Mater.*, **19**(11), 2736–51.

Vanorio T, Prasad M and Nur A (2003), 'Elastic properties of dry clay mineral aggregates, suspensions and sandstones', *Geophysical J. Int.*, **155**(1), 319–26.

Wang ZL (ed.) (2001), *Characterization of Nanophase Materials*, Wiley-VCH Verlag, Weinheim.

Wang Z, Massam J and Pinnavaia TJ (2000), 'Epoxy-clay nanocomposites', in *Polymer-clay Nanocomposites*, Pinnavaia TJ and Beall GW (eds.), John Wiley & Sons, Chichester.

Warheit DB, Laurence BR, Reed KL, Roach DH, Reynolds GAM and Webb TR (2004), 'Comparative pulmonary toxicity assessment of single-wall carbon nanotubes in rats', *Toxicol. Sci.*, **77**(1), 117–25.

© Woodhead Publishing Limited, 2010

Wetzel B, Rosso P, Haupert F and Friedrich K (2006), 'Epoxy nanocomposites - fracture and toughening mechanisms', *Eng. Fract. Mech.*, **73**(16), 2375–98.

Xie X-L, Mai Y-W and Zhou X-P (2005), 'Dispersion and alignment of carbon nanotubes in polymer matrix: A review', *Mater. Sci. Eng. R*, **49**(4), 89–112.

Yasmin A and Daniel IM (2004), 'Mechanical and thermal properties of graphite platelet/epoxy composites', *Polymer*, **45**(24), 8211–19.

Yasmin A, Abot JL and Daniel IM (2003), 'Processing of clay/epoxy nanocomposites by shear mixing', *Scripta Materialia*, **49**(1), 81–6.

Yasmin A, Luo JJ, Abot JL and Daniel IM (2006a), 'Mechanical and thermal behavior of clay/epoxy nanocomposites', *Composites Sci. Tech.*, **66**(14), 2415–22.

Yasmin A, Luo JJ and Daniel IM (2006b), 'Processing of expanded graphite reinforced polymer nanocomposites', *Composites Sci. Tech.*, **66**(9), 1182–9.

Yin M, Koutsky JA, Barr TL, Rodriguez NM, Baker RTK and Klebanov L (1993), 'Characterization of carbon microfibers as reinforcement for epoxy resins', *Chem. Mater.*, **5**(7), 1024–31.

Zeng MF, Sun XD, Yao XD, Ji GZ, Chen N, Wang BY and Qi CZ (2007), 'Effects of $SiO_2$ nanoparticles on the performance of carboxyl-randomized liquid butadiene-acrylonitrile rubber modified epoxy nanocomposites', *J. Appl. Polym. Sci.*, **106**(2), 1347–52.

Zhang H, Zhang Z, Friedrich K and Eger C (2006), 'Property improvements of *in situ* epoxy nanocomposites with reduced interparticle distance at high nanosilica content', *Acta Mater.*, **54**(7), 1833–42.

Zhang W, Picu RC and Koratkar N (2007), 'Suppression of fatigue crack growth in carbon nanotube composites', *Appl. Phys. Lett.*, **91**(19), 193109.

Zhou Y, Pervin F and Jeelani S (2007), 'Effect vapor grown carbon nanofiber on thermal and mechanical properties of epoxy', *J. Mater. Sci.*, **42**(17), 7544–53.

Zhu YQ, Kroto HW, Walton DRM, Lange H and Huczko A (2002), 'A systematic study of ceramic nanostructures generated by arc discharge', *Chem. Phys. Lett.*, **365**(5–6), 457–63.

Zunjarrao S, Sriraman R and Singh R (2006), 'Effect of processing parameters and clay volume fraction on the mechanical properties of epoxy-clay nanocomposites', *J. Mater. Sci.*, **41**(8), 2219–28.

© Woodhead Publishing Limited, 2010

# 8

# Improvements in bonding metals (steel, aluminium)

A. KWAKERNAAK, J. HOFSTEDE, J. POULIS and R. BENEDICTUS, Delft University of Technology, The Netherlands

**Abstract**: This chapter discusses the developments in materials, processes and design, which make adhesive bonding an efficient and durable joining technology for metal structures. The chapter reviews the developments in adhesives and surface treatments for metal bonded joints, which have improved the mechanical properties and processing characteristics as well as significantly enhanced durability under humid or corrosive environments. Next developments in joint design are discussed, from simple lap joints to complex bonded metal laminates. Further improvements in modelling and testing techniques are reviewed, which have led to more accurate prediction and determination of joint strength and durability.

**Key words**: metal bonded joints, surface treatment of metallic substrates, durability, joint design, strength prediction.

## 8.1 Introduction: key problems in metal bonding

Adhesive bonding using natural materials was applied as a joining technology in ancient times. The first known application of adhesive is the use of bitumen (a natural substance that contains hydrocarbons found on the surface of the earth in tar or asphalt pits) about 36,000 years ago.[1] Various adhesive materials of animal or vegetable origin were used in ancient cultures.

With the development of synthetic polymeric materials, higher loaded joints in more demanding applications became possible. The first adhesive bonded joints between metal parts emerged in two different ways. In one they were developed from vibration damping structures, which used rubber layers vulcanized between the metal parts. In the other, Norman A. De Bruyne developed phenolic adhesives suitable for metal bonding based on the development of synthetic adhesives for bonding wood.[2]

The development of epoxy resins is another milestone in the history of metal bonding with the launch of epoxy adhesives into the market in 1946. Owing to the major advantages with regard to fatigue and damage tolerance and the inherent potential weight saving of a bonded metallic structure over a mechanical fastened one, the technology was rapidly adapted by the aircraft industry. Unfortunately, the operational experience of structures with



© Woodhead Publishing Limited, 2010

the first generation of epoxy adhesives in combination with etched surfaces showed limited durability. Only when chromic acid anodizing was applied as a surface treatment, as in the European aerospace industry, was sufficient long-term durability obtained.[3, 4] Also, when adhesive bonding is applied in other structural engineering applications, the rapid deterioration of the mechanical properties of the bonded joint upon exposure to environmental influences is often directly related to unstable interfacial durability. Evidently the durability of metal bonded joints under humid or corrosive environments depends on the surface treatment of the metallic substrate before bonding.

Over the years many surface treatments have been developed for various types of metallic materials with the objective of providing a durable adhesive bonded joint. Not all of these methods are environmentally friendly and some are highly toxic, so there is a need for continued development to replace these methods with safe alternatives. Manufacturing processes have been developed depending on the type of adhesive chemistry and the foreseen application.

In general thermosetting adhesives are used for structural metal bonding applications. The autoclave process has been developed to provide the elevated temperature and pressure required for curing one-component adhesives. Owing to the high capital cost and the long cure cycles related to the use of autoclaves, there is a need for development of out of autoclave technology, that is low temperature and low pressure processes. In the early days of structural bonding, simple analytical joint strength prediction techniques had already been developed. Although these analytical techniques have been further developed over the years they are generally limited to simple joint configurations. For complex joint geometries nowadays finite element models are used to predict bonded joint behaviour. However, the reliability of the joint strength prediction is not very high and a useful method of predicting long-term behaviour and durability is lacking.

## 8.2 Developments in the range of adhesives for metal

Structural bonding of metals became possible[2] with the development in 1942 of the modified phenol-formaldehyde adhesive Redux 775. The phenol-formaldehyde is toughened with a thermoplastic polyvinyl formal powder which is chemically bound to the phenolic network, providing a high strength adhesive material with excellent environmental resistance. This adhesive system was applied by coating the areas to be bonded with liquid resin and sprinkling the thermoplastic powder on top of it. Later on the liquid/powder adhesive system also became available as a more user-friendly film adhesive, ensuring a more constant quality of the applied adhesive layer.

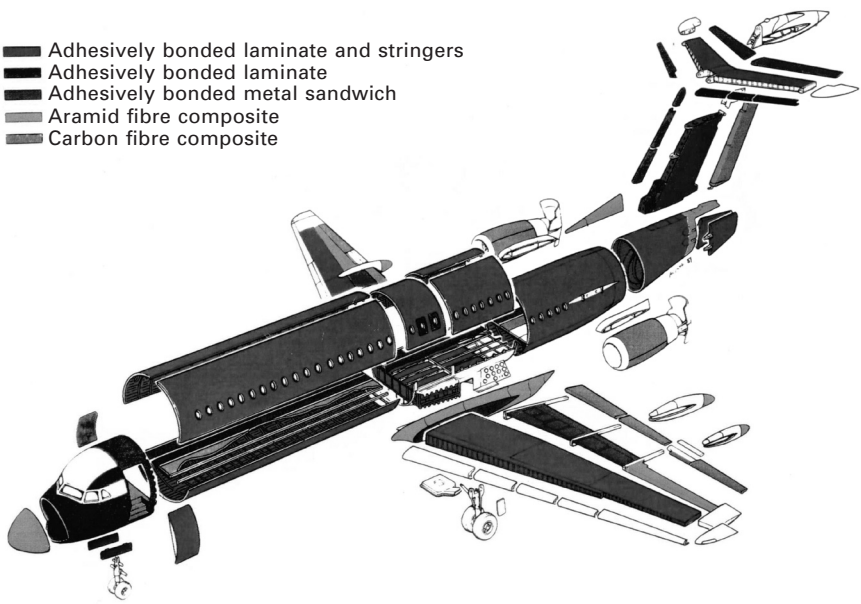
© Woodhead Publishing Limited, 2010

### 8.2.1 Modified phenolic adhesives

The modified phenolic adhesive Redux 775 was very successful in structural applications in the aircraft industry (see Fig. 8.1) and is still in use today.

Other adhesive suppliers followed with the development of phenolic adhesive systems. Similar to the polyvinyl formal, polyvinyl butyral is also used as a toughening agent.[5] Blending a phenolic resin with nitrile rubber produces nitrile–phenolic adhesive films. The ratio of nitrile rubber to the phenolic resin can be varied resulting in adhesives with different properties. Formulations with a relatively high rubber content have high flexibility and are used in vibration damping and acoustic fatigue applications. The flexible nitrile–phenolics with high peel strength are also used for seal bonding applications in aircraft integral fuel tanks. The nitrile–phenolic adhesives with lower rubber content have lower peel strength but improved high temperature characteristics. Types with operational temperatures up to 260°C are used to bond missile components.

Another adhesive type used for these high temperature applications is the epoxy–phenolic adhesives. These adhesives have good shear strength, but are more brittle, which is demonstrated in the relatively low peel strength. Although the phenolic adhesive shows very good durability, it does require high cure temperature and high pressure to prevent the formation of porous bondlines caused by water from the polycondensation cure reaction.




*8.1* Extent of adhesive bonding in the Fokker 100 aircraft. All metal laminate and stringers are bonded with Redux 775. Sandwich structures are bonded with toughened epoxy adhesives.

© Woodhead Publishing Limited, 2010

### 8.2.2 Epoxy adhesives

Since their introduction in the 1950s, epoxy adhesives have gained an increasingly strong foothold in the field of structural metal bonding. A wide range of epoxy resins and curing agents is available for formulating adhesives with specific properties for a specific application. Epoxies can be formulated as liquid or paste two-component systems that cure at room temperature, but also as premixed one-component systems which require heat to cure and form the adhesive bond. In general, epoxy bonds are rigid and of high strength and they fill gaps well with little shrinkage. To enhance their mechanical properties, epoxies are often modified to meet a wide variety of bonding needs. The major advantage of epoxy adhesives is that they are suitable for bonding metals and provide good adhesion to many plastics. In general, they have very high resistance to physical and chemical influences and show high long-term stability with a limited tendency to undergo creep. Epoxy adhesives can withstand continuous temperatures from –55°C to 100°C or, depending on the type, up to a maximum of 200°C.

*Modified epoxy adhesives*

Unmodified epoxies have good strength but low toughness. Introducing more flexibility into epoxy systems allows the adhesive to deform more under stress and distribute loads over a larger area. Furthermore, it increases the capability to compensate for differences in thermal expansion or elastic moduli of the substrates and will improve both the peel and the impact strength. Flexibility can be provided through the resin or hardener constituents by incorporating large groups in the molecular chain, which increase the distance between cross-links. Another method of increasing flexibility is by blending the primary epoxy resin with other, more elastic polymers (e.g. nylon or nitrile rubber). The disadvantage of increasing the flexibility is the negative influences on other properties, such as lower tensile strength, lower temperature resistance or less chemical and moisture resistance.[5–7]

The development of toughened epoxy systems has overcome this problem and resulted in epoxy adhesives with high impact and peel strength, while maintaining chemical, moisture and temperature resistance. Toughened epoxy adhesives generally have two distinct phases: the larger phase is the base resin and the other phase consists of small (in the order of one micrometre in diameter), distributed elastomeric entities. The addition of the second phase modifiers significantly improves fracture toughness by providing crack pinning and stress redistribution mechanisms within the material. A variety of toughening agents have been used to modify epoxy adhesives to improve peel and fracture toughness without significantly affecting other properties of the epoxy base resin. Epoxies are often modified by the addition of reactive liquid elastomers (e.g. carboxyl-terminated butadiene-acrylonitrile,

© Woodhead Publishing Limited, 2010

CTBN) or functionally terminated thermoplastics (e.g. polyether sulphone, PES).[6–8] Recent investigations have shown new ways of improving the toughness of epoxy adhesives by incorporation of additional functionalized nano particles in the epoxy matrix or by creating a flexible polymer structure that interpenetrates the epoxy network at nanoscale level.[9–11]

### *Out of autoclave curing methods*

In the early application of one-component structural adhesives, curing was performed using hot presses. This had the disadvantage that bonded components were limited in size and that special tooling was needed for curved parts and stringer bonding. By using an autoclave, a more flexible and less tool intensive manufacturing process was born. The high capital cost of large autoclaves and the long cure cycles have driven the development of out of autoclave technology.

Owing to their polyaddition cure mechanism, the epoxy adhesives need less pressure during cure than the phenolic type of adhesives. This makes it possible to use only vacuum to create sufficient pressure for simple components during the cure cycle. The assembly to be bonded is put together with the adhesive in a vacuum bag and the cure cycle can be performed in an oven at the required temperature. Care should be taken that the vacuum pressure is not too high because a small residue of solvents in the adhesive could lead to the formation of small voids in the adhesive bondline by the combination of vacuum and cure temperature. Generally a vacuum pressure of around 60 kPa with an adhesive free of solvents will give good results.

An alternative to this process is the use of the Quickstep™ technology,[12] which has been developed for out of autoclave curing of composite parts, but which can also be used for curing adhesive bonded parts. The Quickstep process involves using fluid-filled heated floating mould technology for curing. Flexible membranes separate the product and mould from a circulating liquid that transfers heat and provides pressure. Application of this technology is limited to the size of the tool needed and the complexity of the component to be bonded. Another alternative is the use of low viscosity adhesives and a liquid adhesive injection process like that used in composites technology (RTM: resin transfer molding or VARTM: vacuum assisted resin transfer molding). This is sometimes used for smaller parts with complex shapes.

### *Automotive bonding*

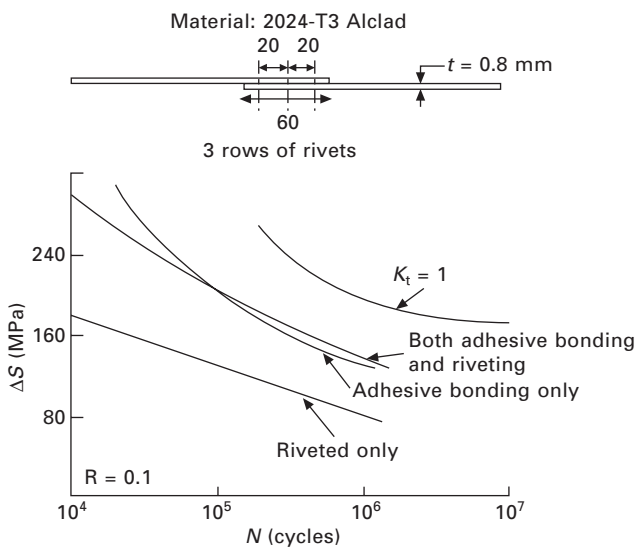
Special adhesives have been developed for use in automotive structures, which are capable of bonding to oily steel sheets without cleaning. In the automotive body, more and more adhesive beads are applied in order to increase structural stiffness and rigidity to reduce noise-vibration-harshness

© Woodhead Publishing Limited, 2010

(NVH) and increase final car body performance. Closure panels are generally adhesively bonded with hem flange adhesives. These automotive structures with uncured or partly cured adhesives are conveyed to the paint shop where surface oils are removed by degreasing, the steel is surface treated for corrosion protection and paint adhesion, followed by electrocoating by cataforesis. The adhesives are cured during the paint bake cycle.

*Assembly bonding*

Adhesive bonding is often applied in assembling components in combination with mechanical fastening. The advantage of this combination of joining methods is to lower the manufacturing costs by reducing the number of process steps. In fact, the adhesive can support the assembly when drilling holes and fastener installation are conducted after cure of the adhesive. This makes 'out-of-jig' drilling possible as well as the elimination of process steps (such as disassembly for deburring operations). Owing to the added strength of the bondline in the assembly-bonded joint, it is possible to reduce the number of fasteners, giving additional weight and cost savings. The added stiffness of the bondline also greatly reduces the stress concentrations near the rivet holes, thereby improving the life of fatigue critical joints considerably. One of the earliest applications of assembly bonding was in the aluminium alloy fuselage panel joints of the Fokker F28[13] and later also in the Fokker 100. The longitudinal splices between adhesive bonded fuselage panels were bonded with a RT-curing epoxy paste adhesive in assembly, cured and subsequently drilled and riveted. The effect of the assembly bonding of this critical joint is a dramatic improvement in fatigue life[14] (see Fig. 8.2) and a

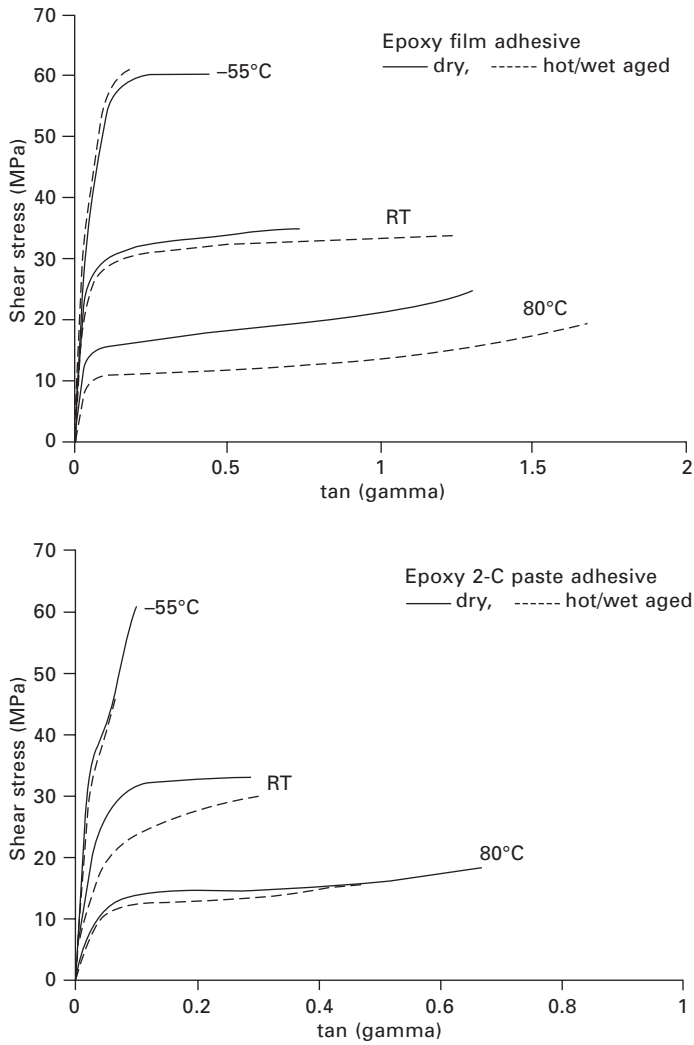



*8.2 S–N* curves of lap joints.

© Woodhead Publishing Limited, 2010

significant reduction of weight and manufacturing costs. Nowadays bond-assisted assembly is mostly applied to flaps, ailerons, rudders and the like for reasons of cost saving. This can effectively be applied both in metallic and in composite structures with cost savings of 10–20%.

The reduction of mechanical fasteners from the rivet-bonded joint is limited owing to the low temperature requirements of aircraft applications. The toughness of the two-component room temperature curing epoxy adhesives is less than that of the one-component film adhesives that cure at higher temperatures. Figure 8.3 shows a comparison of the shear stress–strain




*8.3* Shear stress–strain curves of epoxy film and 2-C room temperature curing epoxy adhesives.

© Woodhead Publishing Limited, 2010

characteristics of an epoxy film adhesive and a two-component epoxy paste adhesive. The curves tested at –55°C, RT and 80°C are shown both after manufacturing and after ageing for 30 days at 70°C and 95% RH. It is clear that the toughness of the film adhesive is considerably higher than the paste adhesive. This is even more evident in tests at low temperatures. Typically, at –55°C two-component epoxy paste adhesives do not have the peel strength that epoxy film adhesives have, so the use of fasteners to take up any peel loads remains essential in aircraft applications. Obviously, there is a need for further development in low temperature curing epoxy adhesives with high toughness to obtain similar properties to the high toughness epoxy films.

### 8.2.3 Polyurethane adhesives

Two-component polyurethanes are also used in industrial assembly. Curing in these adhesive systems is initiated by mixing together the resin (polyglycols or PUR (polyurethane) prepolymer with terminal OH groups) and the hardener (modified isocyanate). At room temperature curing can take from a few hours to several days. Heating can accelerate this process and also increases the strength of the bond. After curing, the adhesive ranges from tough and hard to rubber-like and flexible depending on the raw materials used. The strength of these adhesives is about one-third that of good epoxy adhesives. They have better low temperature strength than other adhesives; some types can be used for cryogenic applications. They have good chemical resistance, although generally not as good as epoxies or acrylics and their strength will drop considerably with moisture absorption. Their properties at elevated temperature drop off rapidly above 60°C. Two-component polyurethanes are used for large-surface adhesive bonds in land vehicle structures (semi-trailers and train sandwich structures), building elements (sandwich panels), ship building and container structures.

### 8.2.4 Methyl methacrylate adhesives

Another group of two-component adhesives whose strength is between the two component epoxies and polyurethanes are the methyl methacrylate adhesives. Two-component methyl methacrylate adhesives or reactive acrylic adhesives consist of two major ingredients, the monomer and the rubber toughener. Reactive acrylics are based mainly on monofunctional monomers, for example methyl methacrylate or cyclohexyl methacrylate, giving these adhesives their typical penetrating odour. Low-odour versions have been introduced by using higher molecular weight monomers. The reactive acrylic adhesives have good toughness with high impact and peel strengths because of the rubber component, generally a chlorosulphonated polyethylene rubber. These adhesives are used for a wide range of applications in the marine, automotive,

© Woodhead Publishing Limited, 2010

recreational vehicle, transportation and manufacturing industries. Applications include often dissimilar substrate bonding, for example engineering plastics, SMCs, and fibreglass to metal bonding, particularly when fast curing with limited surface preparation is required.

### 8.2.5 Adhesives with high flexibility

Next to the rigid one- and two-component adhesives, very flexible moisture curing one-component adhesives (polyurethane, MS-polymer, silicone) are also used in assembly. These flexible adhesives provide joints with a more uniform stress distribution and less of a difference between average and maximum stress. These adhesives distribute peel and shear stresses over a larger area, thereby improving joint efficiency. However, since adhesives with high flexibility and elongation typically have lower cohesive strength than more rigid adhesives, the advantage of flexibility and high elongation is usually compromised. In order to transfer the same load, a much larger overlap is needed, as shown in Fig. 8.4.

### 8.2.6 Improvements in temperature resistance of adhesives

All polymers are degraded to some extent by exposure to high temperature. Physical properties, like stiffness and strength, are lower at high temperatures (softening), but they also degrade during thermal ageing.

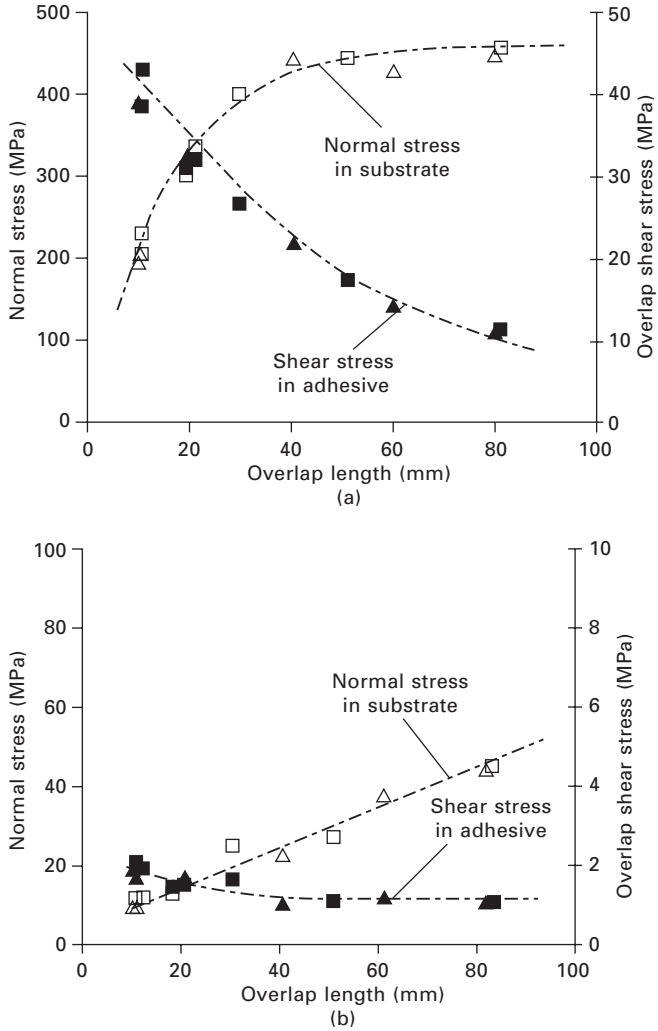
Adhesives that are resistant to high temperature usually have rigid polymeric structures, high softening temperatures and stable chemical groups. These same factors make the adhesive very difficult to process and they usually show low peel strength. Any form of added toughener generally increases the peel strength but lowers the temperature resistance. Addition of fillers, like aluminium powder, silica or ceramic material, can increase the temperature resistance, but at the expense of peel strength.

#### *Glass transition temperature*

An important parameter is the glass transition temperature ($T_g$), the temperature at which the resin begins to soften and its mechanical properties degrade.[15] For thermoset resins the upper service temperature for structural adhesives is typically limited by the resin modulus which falls off rapidly above the glass temperature, as depicted in Fig. 8.5. Therefore structural adhesives must have a $T_g$ higher than the maximum operating temperature to avoid a cohesively weak bond and creep problems.[15]

In Table 8.1 the typical glass transition temperatures of various thermoset adhesives are compared. The two-component toughened epoxies are limited

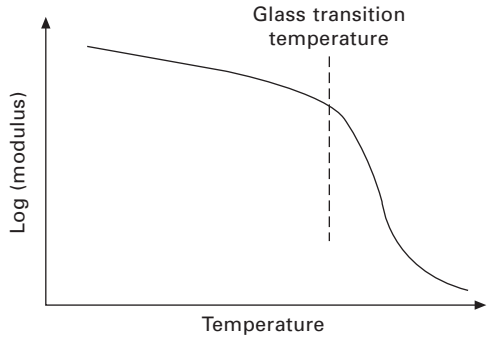
© Woodhead Publishing Limited, 2010




*8.4* Comparison between (a) epoxy (rigid) and (b) MS polymer (flexible) adhesive overlap joints.

to about 80°C. However, specific formulations of two-component epoxies exist that show higher $T_g$ typically at the expense of lower peel strength. The widely used toughened (nitrile) epoxy film adhesives have a $T_g$ up to 121°C and therefore are not feasible for application at higher temperatures. A higher $T_g$ is found for unmodified epoxies and nitrile–phenolic, epoxy–phenolic and other high temperature adhesives. Polyaromics (amongst others polyimides) show the highest thermal resistance of the organic adhesives. Only the ceramic (inorganic) adhesives perform better (up to 1000°C), but are very

© Woodhead Publishing Limited, 2010




*8.5* Decrease in the adhesive modulus with temperature, with indication of the glass transition temperature.

*Table 8.1* Range of typical glass transition temperatures for various structural adhesives

| Adhesive type | Glass transition temperature (°C) |
|---|---|
| Polyurethane | < 80 |
| Acrylate | < 80 |
| Toughened epoxy 2-C (RT cure) | 60–80 |
| Nitrile epoxy 1-C (120°C cure) | 90–120 |
| Modified epoxies 1-C (180°C cure) | 100–150 |
| Unmodified epoxies | 100–150 |
| Epoxy phenolic/nitrile phenolic | 150–200 |
| BMI | 200–300 |
| Cyanate-ester | 250–350 |
| Polyimide | 280–330 |

brittle. Under wet conditions the ingress of moisture softens the adhesive, which lowers $T_g$ (by about 20–30°C for toughened epoxy adhesives).

### *Overlap shear strength at elevated temperature*

Table 8.2 shows that at a service temperature of around 125°C, the standard structural adhesives, such as polyurethanes and rubber-modified epoxies have already lost most of their overlap shear strength. Stable mechanical properties between 125°C and 175°C are seen for the so-called high temperature structural adhesives, such as nitrile–phenolic, epoxy–phenolic, heat-resistant one part epoxy, bismaleimide (BMI) and polyimide. Despite the significant differences in overlap shear strength at room temperature (RT), it is found that most commercial high temperature adhesives have an overlap shear strength of around 20 MPa at 125°C. Bismaleimide and polyimide adhesives with a free standing post-cure will have a $T_g$ above 280°C and overlap shear strength values above 10 MPa at 280°C. The values in Table 8.2 are typical values obtained from static, short-term tests, whereas the applied loads

© Woodhead Publishing Limited, 2010

*Table 8.2* Strength of various adhesive types at high temperature

| Adhesive type | Overlap shear strength (MPa) at | | | |
|---|---|---|---|---|
| | RT | 125°C | 175°C | 200°C |
| Standard epoxy film 120°C cure | 42 | 10 | – | – |
| Elevated temperature epoxy 180°C cure | 35 | 28 | – | – |
| High temperature epoxy 180°C cure | 28 | 27 | 25 | 15 |
| Nitrile–phenolic 180°C cure | 25 | 21 | 16 | 8 |
| Epoxy–phenolic 180°C cure | 25 | 22 | 19 | 13 |
| Bismaleimide 180°C cure | 20 | 17 | 17 | 17 |
| Polyimide 180°C cure | 25 | 20 | 20 | 20 |

Note: Strength values depend on cure cycle, high temperature properties will need a post-cure.

may be continuous. The viscoelastic behaviour of the adhesive may result in creep failure under long-term sustained load, especially at temperatures near or above the $T_g$.

## 8.3 Developments in surface treatment techniques for metal

An adhesive bond consists of a layer of adhesive, which adheres to the contact areas of the surfaces of the parts that are joined. Therefore, the strength of the joint depends on the strength of the adhesive material (cohesion) and on the level of adhesion strength between the adhesive and the bonded surfaces (adhesion).

The adhesion strength is more complex and depends on the adherend surface adhesive interaction. The most common surface forces that originate at the adhesive–adherend interface are Van der Waals forces. In addition, covalent bonding, acid–base interactions and hydrogen bonds, generally considered a type of acid–base interaction, may also contribute to intrinsic adhesion forces.

Surface treatments are often required to provide maximum adhesion strength, not only to remove contaminants, but also to increase the difference in surface energy between adhesive and substrate, so good wetting and adsorption of the adhesive is obtained. The surface treatment should form surface layers with sufficient mechanical strength to transfer the loads through the bonded joint during the service life of that joint (durability).

### 8.3.1 Surface treatment of aluminium alloys

Aluminium alloys are generally considered to be ‘difficult to bond’. This is true in the sense that without proper surface treatment of the aluminium

© Woodhead Publishing Limited, 2010

surface before the bonding takes place, the strength and especially the retention of strength during the lifetime of the joint will be poor.

The aerospace industry recognized this in the early stages of the application of adhesives in metal bonded structures and this resulted in surface treatments that are very well adapted to the specific demands in this industry. By anodizing, long term durability of bonded structures is obtained, even under the extreme environmental and chemical exposures that the products are exposed to. In Table 8.3 a short overview is given of the most well-known and widely used surface treatments for metals.

A degreasing step is the basic step for all treatments and should be performed in all cases. This can be done either by wiping with a cloth or by immersing the material in a tank with an alkaline degreasing agent. The process may increase bond strength, but only degreasing is generally not enough to obtain good strength. The natural oxide layer that is still present on the surface mainly causes this. This layer has irregular properties and the mechanical strength can be relatively low. Good strength between the adhesive and the oxide can be obtained, but the bonded joint will often fail owing to failure of the oxide layer itself. There are some cases, when certain types of adhesives are used and when the adhesive bond will not be exposed to harsh environments, where only degreasing will suffice.

### *Etching processes for aluminium alloys*

In most cases, degreasing is not sufficient for good adhesion and more treatment is necessary. In the aerospace industry, an etching treatment is conducted which will remove the natural oxide layer of the aluminium, leaving only a very thin but closed oxide. When the adhesive bonding takes place soon after the etching treatment, good initial bond strength can be obtained. The process developed in Europe based on a mixture of chromic and sulphuric

*Table 8.3* Short overview of surface treatment methods for aluminium alloys

| Category | Surface treatment |
|---|---|
| Chemical and electrochemical | Degreasing<br>Etching/pickling (CSA/FPL)[a]<br>Anodizing (PAA/CAA/PSA)[a]<br>Conversion coatings (chromate, titanate, zirconate) |
| Mechanical | Grinding, scouring, brushing<br>Grit blasting with corundum (aluminium oxide) |
| Application of adhesion promotors | Application of silanes, sol–gels, primers |

[a] CSA = chromic and sulphuric acid, FPL = Forest Products Laboratory, PAA = phosphoric acid anodizing, CAA = Chromic acid anodizing, PSA = phosphoric–sulphuric acid anodizing.

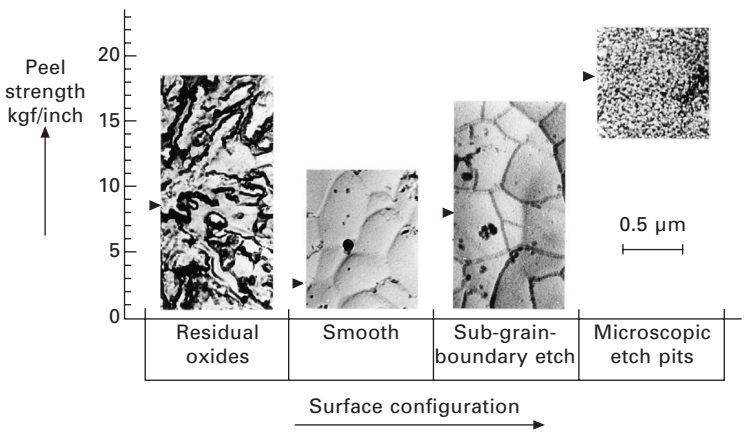
© Woodhead Publishing Limited, 2010

acid (CSA) was introduced in the 1940s[16] and used in combination with the early REDUX bonding. This CSA etch is used at 60–65°C and shows good initial adhesion and durability in combination with phenolic adhesives. A similar process mainly used in the USA became known as FPL etch, named after the Forest Products Laboratory which developed the process initially.[17] Based on research by Bethune,[18] the process is improved to become the 'optimized FPL etch', which is closer to the composition of the CSA etch. It is essential in these etching procedures to use process conditions to obtain good adhesion.

Figure 8.6 shows surface configurations and the adhesion quality measured by peel strength for various process conditions in sulphuric acid sodium dichromate solutions. It is clear that the microscopic etch pit surface morphology showed optimal adhesion. In both CSA and FPL, a good microstructure is obtained with a sufficient level of chromate ions and some solution ageing is present with Al and Cu ions.

Attempts have been made to replace the oxidizing power of the chromate ions by other oxidizing components. The application of ferric sulphate in sulphuric acid solution was successful.[19,23] This process, known as the P2 etch, shows a similar microscopic surface morphology as the CSA and optimized FPL etch.

Using a low anodic voltage in combination with sulphuric acid at 50°C[20] or phosphoric acid at room temperature will result in similar microstructures and good initial adhesion. However, the durability of the etched surfaces is limited in combination with epoxy adhesives. The etched surface treatments showed poor long-term durability with epoxy adhesives in aircraft operational use, especially on clad alloys. Alternative etching procedures based on acid or alkaline solutions can be used but will generally result in lower adhesion.




*8.6* Microscopic surface configuration after various etch process conditions in sulphuric acid–sodium dichromate solutions.

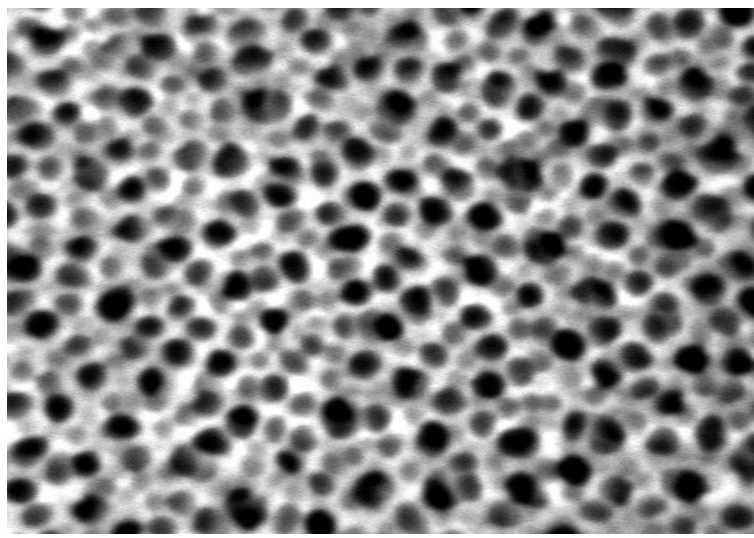
© Woodhead Publishing Limited, 2010

*Anodizing processes for aluminium alloys*

To improve durability the etching treatment has to be followed by an anodizing treatment. This is an electrochemical method for creating a surface structure suitable for adhesion. The created oxide layer consists of many pores (see Fig. 8.7) in which the adhesive is able to penetrate, before it cures completely. This results in so-called mechanical interlocking or hooking of the adhesive in the substrate. In addition, the total bonding area is enlarged by the porous structure.

Several different anodizing processes are available. The chromic acid anodizing process (CAA) is used extensively by the aerospace industry in Europe[21,22] and has a proven track record of long-term durability in combination with both clad and bare aluminium alloys. In the United States, another CAA process was used for adhesive bonding with partial sealing in a chromate containing rinse after anodizing.[23] After the durability problems with FPL etched and bonded components in the USA, the phosphoric acid anodizing (PAA) was adopted.[24] While the CAA coating is thicker, much less vulnerable and gives better corrosion protection than the PAA layer, it has one major disadvantage: in the process, hexavalent chromium is used, which is an environmentally unfriendly chemical.

The sulphuric acid anodizing (SAA) process widely used for corrosion protection of aluminium alloys is less suited for structural adhesive bonding with rigid adhesives. The pores are narrower (10 nm), so adhesives cannot fully penetrate resulting in relatively low strength interfaces. However, in



*8.7* Electron micrograph of CAA oxide (average pore diameter 30 nm).

© Woodhead Publishing Limited, 2010

industrial applications combined with flexible adhesives, thin sulphuric acid anodic layers are applied successfully.

The above-mentioned CAA and PAA anodizing treatments for aluminium generally result in good initial strength of the joint, as well as excellent durability (especially when an extra primer is applied to the surface, which acts as a corrosion inhibitor). The anodizing process of aluminium is however a relatively complex and expensive process. This has often led to the conclusion that adhesive bonding of aluminium is not economically viable in applications outside the aerospace industry. However, there are developments in surface treatment specifically aimed at reducing the cost, without sacrificing bond strength and durability too much. In this context, conversion coatings have to be mentioned.

*Conversion coatings for aluminium alloys*

Chromate conversion coatings are traditionally used in the corrosion protection and paint pretreating industries, with excellent results for corrosion protection. Because of the different loading situation on the adhesive compared to coatings, it is not possible to use these systems for adhesive bonding, especially when peel stresses are acting on the adhesive. The performance is relatively weak and low joint strengths are obtained when these traditional conversion coatings are used.

Much better results are found when more recent conversion coatings, based on titanate and/or zirconate, are used.[25, 26] The peel performance is enhanced and the durability of such systems is good.

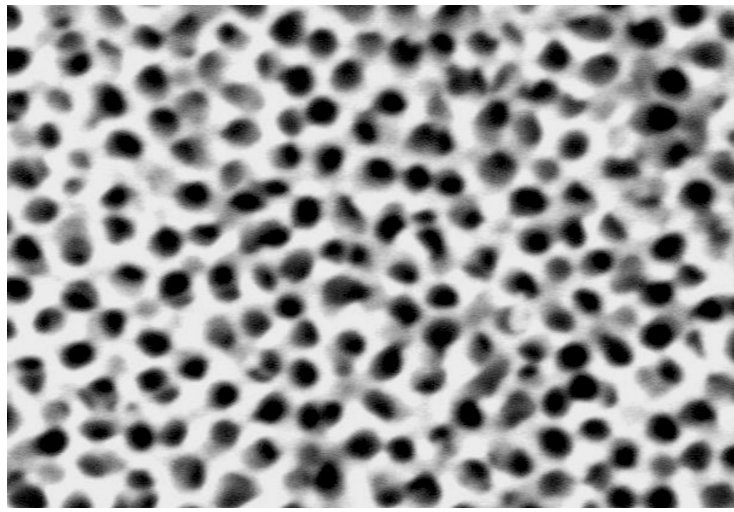
*Chromium-free anodizing treatments for aluminium*

As an alternative to the CAA and PAA treatments, a new process is currently under development, the phosphoric–sulphuric acid anodizing (PSA) treatment.[27, 28] This results in an oxide layer with the adhesion performance of the CAA treatment without the environmental penalty of the chromium. Current research aims to find the proper process parameters to obtain the optimal oxide layer for a wide range of aluminium alloys. Anodic layers with good adhesion and durability have been obtained in a PSA solution with 125 g $l^{-1}$ $H_3PO_4$ and 75 g $l^{-1}$ $H_2SO_4$ at 20–22°C and 18–20 volts for 20 minutes (see Fig. 8.8). Other reports[29] with other PSA process conditions also showed good adhesion and durability.

## 8.3.2 Surface treatment of steel and stainless steel

Steels are used in many automotive, shipbuilding and other industrial applications. In many applications steel is adhesive bonded instead of welded

© Woodhead Publishing Limited, 2010



*8.8* Electron micrograph of PSA oxide (average pore diameter 30 nm).

because of improved corrosion resistance, joining of dissimilar materials, increased joint stiffness and fatigue resistance, less heat distortion and, often, more cost effectiveness.

In the case where the adhesive bonded joint experiences no environmental or chemical exposure, a surface treatment for degreasing and cleaning thoroughly may be sufficient to provide a medium strength bonded joint.

### *Surface treatment of carbon steel*

Brockmann[30] suggests that, in contrast to aluminium and titanium alloys, where the surfaces are usually treated by chemical methods, etching procedures for the different types of steel are not recommended. Good bonding results are usually obtained by using abrasive or mechanical roughening techniques like grinding or grit blasting. The best results are obtained with 99.5% pure alumina grit ($Al_2O_3$, corundum) with a particle size between 150–250 μm. It has to be performed on a clean dry surface in order to prevent contamination of the grit-blasting medium with organic material. The grit blasting should be carried out with equipment provided with oil- and water-separators. After the grit blasting process, any dust on the surface has to be removed by blowing off the surface with dry and oil-free compressed air.

Abrasive treatments of thin sheet metal may result in warping. In which case an acid-etch solution might be preferred. A successful method is an etching technique in a nitric–phosphoric acid solution at room temperature for 5–7 minutes which produces a micro-rough surface morphology and

© Woodhead Publishing Limited, 2010

good adhesion and durability on carbon steels. The solution in deionized water contains 25 g $l^{-1}$ $H_3PO_4$ and 2 g $l^{-1}$ $HNO_3$ with a small addition of a suitable surfactant.[23]

As with corrosion-resistant conversion coating on steel, generally phosphate layers are used as a pretreatment for paint adhesion. These conversion coatings will result in good adhesion but in low strength in bonded joints. The cause is the low strength of the phosphate layer, which will fracture when the bonded joint is loaded.

### *Surface treatment of stainless steel*

Stainless or corrosion resistant steels (CRES) are steel alloys containing over 11% chromium. They are applied in various types of instruments and appliances, industrial equipment and as an automotive and aerospace structural alloy and construction materials in large buildings, for their decorative properties and chemical and corrosion resistance.

Abrasive treatments used as a surface treatment for adhesive bonding with carbon steels do not have good results with stainless steels. Grit blasting with alumina improves adhesion but it is also detrimental to the passive layer that protects the stainless steel against corrosion. It sometimes can be used for applications that are not exposed to moisture or a corrosive environment.

A number of chemical and electrochemical processes improve adhesion on stainless steels. Various strong acid etchants are sometimes used to improve adhesion, resulting in carbon smut layers on the surface of the stainless steel. By brushing off the black deposit or by desmutting in a passivation solution, high strength bonds can be obtained. However, the peel strength of passivated layers is sometimes low.

After degreasing, an oxalic (100 g $l^{-1}$)–sulphuric (100 g $l^{-1}$) acid mixture at 90°C can be used to etch the surface,[30, 5] followed by smut removal by brushing off the deposit. Another process often used to obtain good adhesion is a sulphuric acid etch followed by desmutting and passivating in a sulphuric acid sodium dichromate mixture.[5, 23, 31, 32] The etch process is best performed at 80°C for 10 minutes in a solution of 250 g $l^{-1}$ $H_2SO_4$, and the smut removal in a solution of 300 g $l^{-1}$ sulphuric acid and 30 g $l^{-1}$ sodium dichromate at 65°C for 5 minutes.

Good adhesion and durability results are also reported with a highly concentrated mixture of sulphuric acid and sodium dichromate at 80°C for 60 minutes.[31, 32] The toxicity of these chromate-containing etching mixtures is however a major drawback.

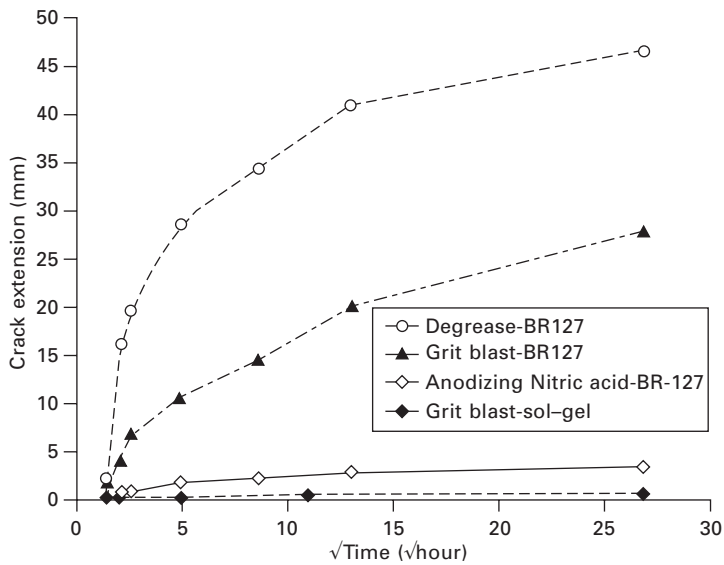
A surface treatment method that does not have this disadvantage is the nitric acid anodizing process.[31, 32] After degreasing, the anodizing is performed at a current density of 0.5 A $dm^{-2}$ in a 45–50 vol% nitric acid solution at 50°C for 60 minutes. The adhesion and durability of bonded

© Woodhead Publishing Limited, 2010

joints on surfaces formed in this process are excellent. The surface of the stainless steel has a microporous morphology and is chromium enriched. Figure 8.9 shows the results of wedge test specimens exposed in a salt spray cabinet (ASTM B117) up to 30 days. Four surface treatments are compared: alkaline cleaning; alkaline cleaning followed by grit-blasting with alumina and cleaning; alkaline cleaning and anodizing in nitric acid; cleaning, grit-blasting and cleaning followed by AC 130 sol-gel treatment (see Section 8.3.4). After surface treatment the specimens are primed with a corrosion inhibiting bond primer, except the sol–gel treated specimens. All specimens are bonded within two hours after surface treatment with an epoxy adhesive film and autoclave cured at 120°C. The anodized and the sol–gel treated specimens showed excellent durability with only cohesive and very limited crack growth. Although grit-blasting results in slower crack growth compared to only degreased specimens, both treatments resulted in interfacial delamination.

## 8.3.3 Surface treatment of titanium

Titanium and its alloys have been used in the aircraft industry because of their low density and good high temperature properties and nowadays in carbon composite structures as local reinforcement for improved bearing strength. Titanium is sometimes used in industrial and medical applications for its




*8.9* Crack extensions of wedge test specimens of stainless steel bonded with epoxy film adhesive after various surface treatments.

© Woodhead Publishing Limited, 2010

very good corrosion and chemical resistance. A range of surface treatments of titanium has been developed over the years.[5, 23, 33] Treatments that give the titanium surface macro and micro roughness show good results in initial adhesion and durability.

### *Etching and conversion treatments*

Early etching treatments based on nitric–hydrofluoric acid etching provided adequate initial adhesion but very poor durability. Phosphate–fluoride came in use as an etching and oxide conversion layer, but under hot wet exposure the durability results were poor. The oxide layer is made more stable by the modified phosphate fluoride process. Further improvements were made with commercial alkaline etchants Turco 5578, DAPCOtreat and acid treatment Pasajell 107, which provided more macro roughness to the surface of the titanium.

Titanium treated for 20 minutes in an alkaline peroxide etch, an oxidizing mixture of sodium hydroxide (2%) and hydrogen peroxide (2.2%) at 50–70°C results in micro roughness and good bond durability. The problem with this process is the instability of the hydrogen peroxide at the elevated temperature of the solution.

### *Anodizing surface treatments*

A number of anodizing treatments have been developed that outperform all other treatments. Generally an etching process is used to remove old oxide scales before anodizing.

Boeing developed a chromic acid anodizing process containing hydrofluoric acid.[34] Anodizing is performed in a solution of 50 g $l^{-1}$ chromic acid during 25 minutes at 5 V at room temperature. The hydrofluoric acid is added to obtain sufficient current density (0.2 A $dm^{-2}$) in the process. This process results in surfaces with a fine microstructure and good adhesion, and bonded joints show excellent durability.

Fokker uses a chromic acid solution (40 g $l^{-1}$) like that used for anodizing aluminium alloys without adding fluorides. Anodizing is performed at 50°C for 40 minutes at 15 V and bonded joints also show excellent durability.

Anodizing in alkaline peroxide solutions has also been used successfully as a surface treatment for durable bonded joints. Further research[35] indicates that anodizing in a solution of sodium hydroxide (200 g $l^{-1}$) without hydrogen peroxide showed excellent durability. The anodizing in this process is performed at 10 V at room temperature.

© Woodhead Publishing Limited, 2010

### 8.3.4 Development of sol–gel surface treatment for aluminium, steel, titanium

The increased continuation of the life of both military and civil aircraft resulted in a need for improved repair techniques. Conventionally, the structure is repaired by removing the cracked area and by riveting a patch on to the structure. However, the rivets act as stress concentrations and will limit the life of the repair. A more efficient method is the adhesively bonded patch repair (see Section 8.4.9).

In a bonded repair solution, surface treatment on the aged aircraft structure is critical in order to obtain good adhesion and durability of the repair.[36] The conventional approaches for preparing metal surfaces for bonding (etching and anodizing) are difficult to implement on existing structures. Mechanical abrasion of the metallic structure only is not sufficient for a durable bonded repair. *In situ* surface treatment processes have been developed to obtain sufficient chemical modification of the surface. By using chromic acid or phosphoric acid in gel form local area anodizing in a so-called brush anodizing process, thin anodic layers can be formed on aluminium alloys providing good adhesion and durability.

Good results are also obtained by a phosphoric acid anodizing containment system (PACS) using a double vacuum bag to contain the processing liquids.[37] These acid processes have a number of drawbacks like leakage, spillage and corrosion initiation in crevices and between dissimilar metals like fasteners. AMRL Melbourne developed the process often referred to as the grit-blast/silane (GBS) process.[38, 39] After cleaning, the area to be prepared is grit blasted with alumina. After removal of the blasting debris the surface is treated with an aqueous solution of an organo-functional silane-based coupling agent. The coupling agent found to be most suitable for epoxy adhesives is the epoxy-terminated silane, $\gamma$-GPS.[38] In combination with a corrosion-inhibiting bond primer and an epoxy film adhesive durable bonds to aluminium alloys, steel and titanium alloys are obtained.

A more recent process has been developed at Boeing based on sol–gel chemistry.[40] After cleaning, abrasion (either grit-blast or abrasive paper) and removal of abrasive residues the sol, which is prepared from a mixture of glycidoxyl functional silane and zirconium alkoxide, is applied. The thin film formed on the surface provides chemical bonds to the metal side and has active sites that bond during cure with an epoxy primer. Good durability results are obtained in combination with a water-based corrosion-inhibiting bond primer.[41, 42] The sol–gel material is commercially available as AC-130 from AC TECH, Inc. Figure 8.9 shows the excellent results of a wedge test durability experiment on the sol–gel treatment on stainless steel, even without a primer. The durability result is excellent on aluminium and titanium alloys and compares well with good anodizing treatment.

© Woodhead Publishing Limited, 2010

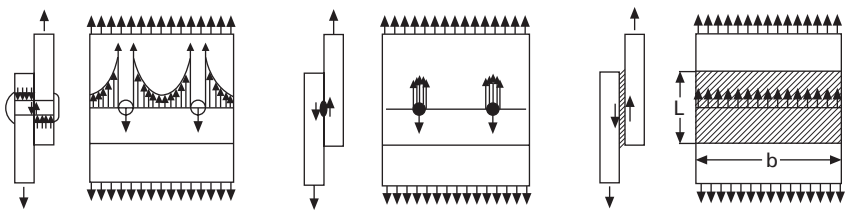
### 8.3.5 Developments in bonding primers

Adhesive primers generally function to conserve the surface of a material that has to be bonded in a later stage, thus providing more flexibility in the manufacturing process. Generally, adhesive primers can be considered to be a strongly (with organic solvent) diluted adhesive, often combined with a coupling agent such as a silane. They have the main function to wet the freshly prepared surface easily and, after drying or curing, to stabilize the surface until the adhesive is applied (which may take as long as a year). For structural bonding most primers are epoxy-based, available as a liquid and are sprayed onto the surface as a layer to a thickness of about 4–10 μm. One-component primers and two-component systems are both available. One-component primers have to be cured at elevated temperature, either precured or co-cured with an elevated-temperature curing adhesive. Two-component primers have to be mixed before application.

A corrosion-inhibiting compound, usually a chromate, is sometimes added to the adhesive primer formulation to protect the adherend against corrosion. To minimize production of volatile organic compounds, similar water-based versions have been developed. A steady change from solvent-based to water based-primers has taken place driven by ecological concern. In addition, the small amount of a hexavalent chromium salt in corrosion-inhibiting primers makes them environmentally unfriendly. Recently primers have been developed that are chromate free and contain other corrosion inhibitors.

## 8.4 Developments in joint design

In contrast to other joining methods, such as riveting and bolting, adhesive bonding has no adverse effect on the material characteristics of the surfaces to be joined, for example there are no holes which damage the joined parts and create stress concentrations. As can be seen in Fig. 8.10, the load transfer is uniformly distributed along the bonded joint. By preference, the load is transferred by shear stresses in the adhesive layer, whereas tensile, peel or cleavage loads should be avoided or minimized as much as possible. The strength of the joint not only depends on the shear strength of the adhesive



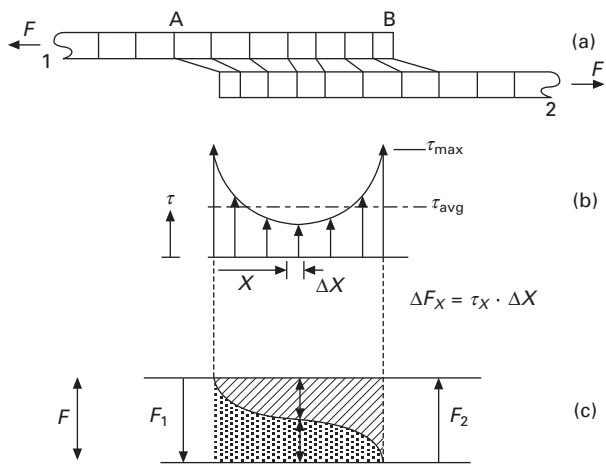

*8.10* Comparison of load transfer in various types of joints.

© Woodhead Publishing Limited, 2010

itself, but also on the shear and peel stress distribution along the length of the overlap.

### 8.4.1 Shear stress distribution of bonded overlap joints

The metal adherends are characterized by their stiffness, modulus of elasticity and can even show plastic deformation at high stress levels. Because of this finite stiffness the adherends will elongate under a load and this elongation (strain) is proportional to the applied load (Fig. 8.11(a)). As the adhesive transfers load along the overlap, the axial strain in one adherend is gradually reduced and increases in the other adherend. When both adherends have the same axial stiffness, in the middle of the overlap both adherends have the same strain, whereas at the ends a large difference exists. This causes the adhesive layer to deform additionally and the shear stress distribution shown in Fig. 8.11(b) is obtained. This mechanism is generally referred to as shear lag. The highly stressed ends of the overlap will transfer most of the load between the two adherends, whereas the lower stressed middle part contributes far less (see Fig. 8.11(c)). This explains why the non-uniform shear stress distribution has an unfavourable effect on the efficiency of the bonded joint. Joint failure is determined by the stress concentrations at the ends of the overlap, which depend on joint geometry, adherend material and type of adhesive.




*8.11* Elastic deformations of the adherends resulting in peak shear stresses in the adhesive. (a) Lap joint, (b) shear stress, (c) load transfer.

© Woodhead Publishing Limited, 2010

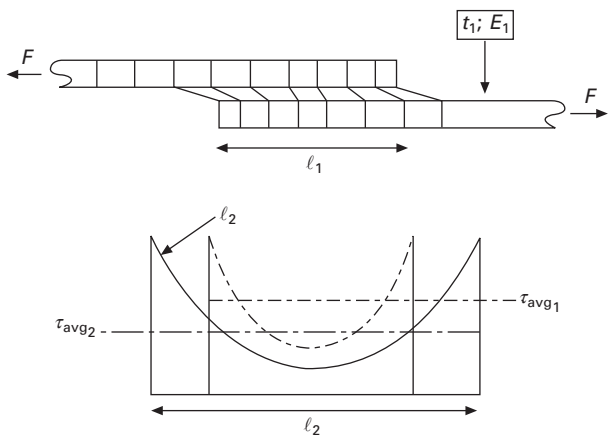
### 8.4.2 Effect of joint geometry, material and type of adhesive for lap joints

Following the principle of shear lag, an increase in adherend stiffness, either by more thickness or a higher Young's modulus, results in more uniform distribution of shear stresses along the overlap length accompanied by lower stress concentrations at the ends. Thus the joint efficiency is increased. At high load levels the yield stress of the adherend will be reached, thereby (locally) reducing its stiffness. The strains in the adhesive will increase more than proportionally with the increased load, which has a disadvantageous effect on the stress distribution and thus on the joint efficiency. Joint strength does not increase proportionally with the overlap length, since the middle part of the bonded joint becomes less and less effective in transferring load (see Fig. 8.12).

Joint efficiency decreases, as the average shear stress decreases, while the stress concentrations at the end of the overlap remain the same. More flexible adhesives provide joints with a more uniform stress distribution, that is higher joint efficiency, but stiffer adhesives generally provide greater strength by virtue of their higher degree of cross-linking. Asymmetrical lap joints in which the adherends are not of equal stiffness and show a non-symmetrical stress distribution in which the highest stresses are found at the side of the less stiff adherend owing to the higher axial strain (see Fig. 8.13). Obviously the joint efficiency is lower than for the equal stiffness lap joint.

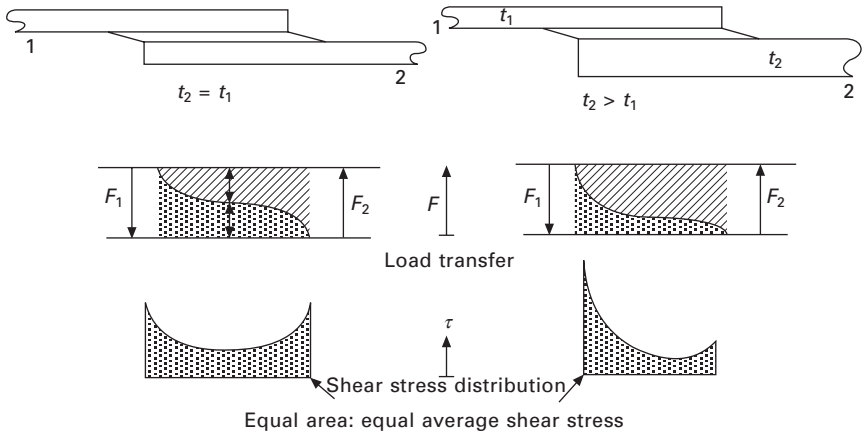
### 8.4.3 Eccentricity in overlap joints

Eccentricity of the loading forces on an overlap joint results in bending deformation of the joint, thereby introducing additional normal stresses in the




*8.12* Effect of the overlap length on the shear stress distribution.

© Woodhead Publishing Limited, 2010




*8.13* Effect of unequal axial stiffness adherends on the shear stress distribution.

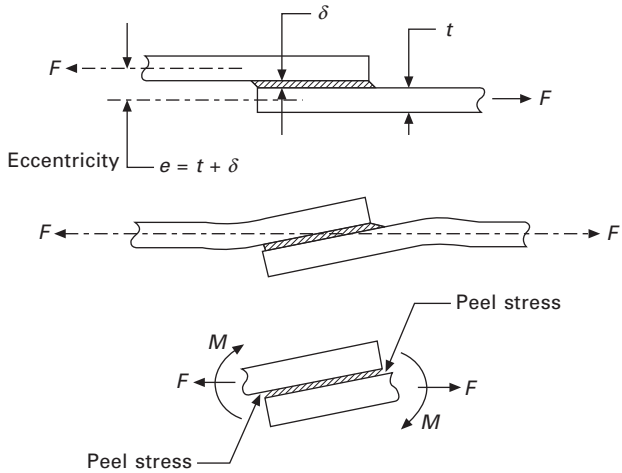
bondline. These stresses have the tendency to peel the two adherends apart (see Fig. 8.14). With increasing adherend thickness the eccentricity increases, that is slightly higher peel stresses are introduced, which partly counteract the positive effect that the larger adherend thickness has on the shear stress distribution. More importantly, the induced bending deformation also causes a stress concentration in the adherend just in front of the thickness change. This stress concentration, which increases with the thickness of the bonded doubler and the stiffness of the adhesive, can be detrimental to the fatigue strength of the structure.

### 8.4.4 Joint optimization

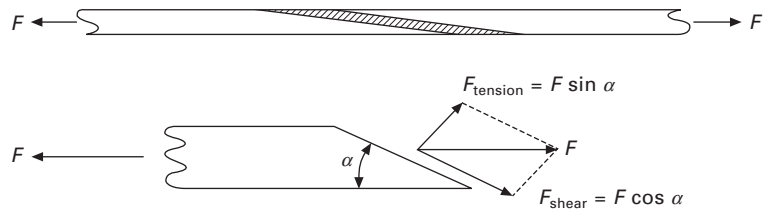
Joint design can be improved by adapting the geometry such that lower shear and peel stress peaks are obtained. Decreasing the eccentricity in the joint leads to lower bending moments at the end of the lap joint and thus lower peel stress. Replacing the single lap joint by a double lap joint or double strap joint can reduce this eccentricity. Designing adherends for constant elongation in the joint area will diminish the shear stress peaks and result in constant load transfer over the length of the lap joint. In order to obtain a constant deformation in the adherend over the length of the overlap, the axial stiffness of the adherend should decrease linearly. This can be effected by bevelling the adherend over the length of the joint from the undisturbed thickness to zero. The ideal lap joint is the result of a combination of tapering and bringing the adherends in line: the scarf joint (see Fig. 8.15).

The lack of eccentricity results in no bending moment induced peel stresses and the shear stress is constant owing to the linear decrease in thickness of the adherend. However the bondline remains loaded under a small tension

© Woodhead Publishing Limited, 2010




*8.14* Peel stresses at the edge of the bond layer caused by eccentricity in the joint.

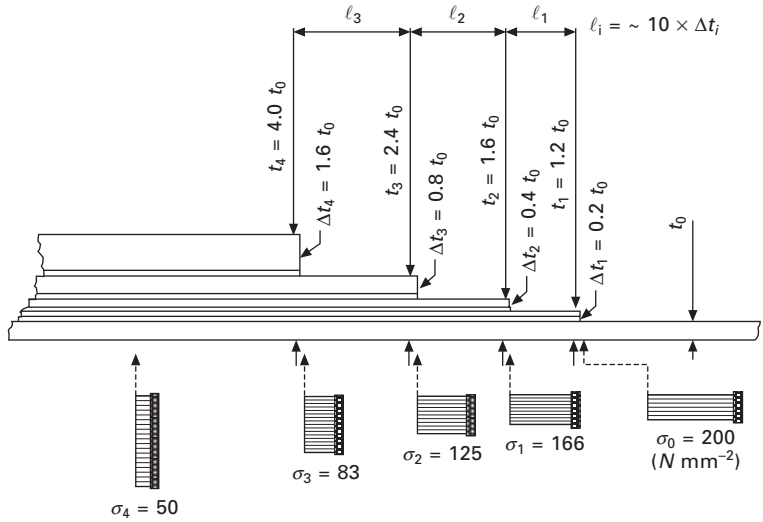



*8.15* The scarf joint.

stress due to the angle between the bondline and the adherends. This angle should be relatively small in order to limit the level of the tension stress in the adhesive. The application of tapered adherends is limited owing to manufacturing and cost constraints. Sometimes tapering is approximated by stepped adherend edges or stepped laminates.

In Fig. 8.16 an example is given of a bonded edge reinforcement for load introduction. An optimized step lamination is used to reduce the nominal stress from 200 MPa in the basic sheet down to 50 MPa at the edge. With a step thickness of the first doubler of 20% of the basic sheet, the secondary bending and the stress concentration are kept acceptably small. A similar effect can be obtained by doubling the doubler thickness at each next step. The resulting higher stress concentration is compensated by the reduced nominal stress caused by the increase in total thickness of the package. The minimum step length required to redistribute the stress evenly over the laminate thickness after the step has been determined by photo-elastic research.[43] For a stiff adhesive, the step length has to be at least ten times the added thickness step. In practice this step length generally is much longer for reasons of quality control, acceptable defects and reparability.

© Woodhead Publishing Limited, 2010



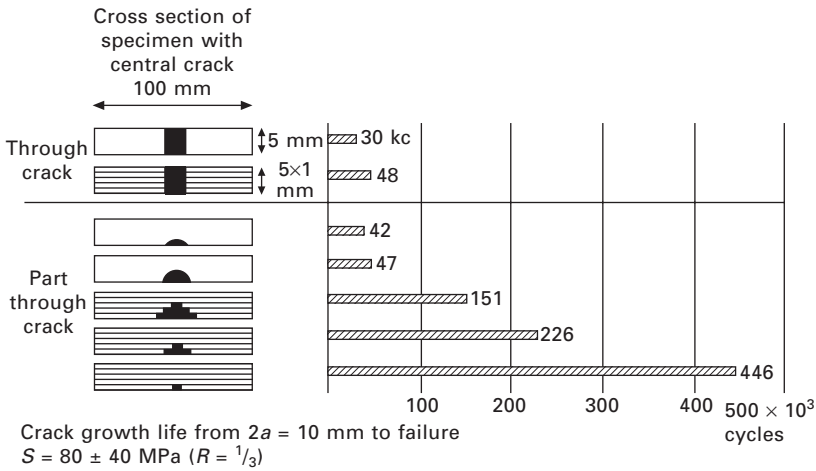

*8.16* Adhesive bonded stepped lamination with equal stress concentration at each step.

## 8.4.5 Adhesive bonded laminates

Adhesive bonding of thin layers of a material to build up a laminate has been used with various types of wood (plywood) for thousands of years. By laminating wood, the best properties can be obtained using the highest quality materials available; it reduces prices and improves the stability of structures. By combining laminated wood fibre orientations, properties could be tailored similar to those of advanced composites and hybrid laminates today. Also by bonding laminations in metal, better properties are obtained than for monolithic materials. Structural reinforcements can be placed where needed, optimizing both weight and component cost. This adhesively bonded build-up has a big advantage over integrally machined structures with regard to fatigue properties. A fatigue crack initiated in the skin will be retarded in its growth when it reaches a doubler or stringer flange. Further it will take time to initiate cracks in the doubler or the stringer flange. In integrally machined stiffened skins a crack will be retarded to some extent by thickness steps or stiffeners, but the panels will have a considerably larger weight when designed for the same inspection interval or fatigue life.

In metallic structures a bonded laminated skin benefits from the improved properties of a thin sheet compared to thick monolithic material. An aluminium laminate has better fatigue properties than a solid material of the same thickness. First, a metal laminate shows longer fatigue life because the thinner sheet material shows a lower crack growth rate. Second, a fatigue crack in an outer layer will not start a crack immediately in the next layer. There is crack arrest in the bond layer for part-through cracks (see Fig. 8.17).

© Woodhead Publishing Limited, 2010




*8.17* Fatigue crack growth life improvement of laminated specimens with full and partly through central cracks in comparison to solid specimens.[44]

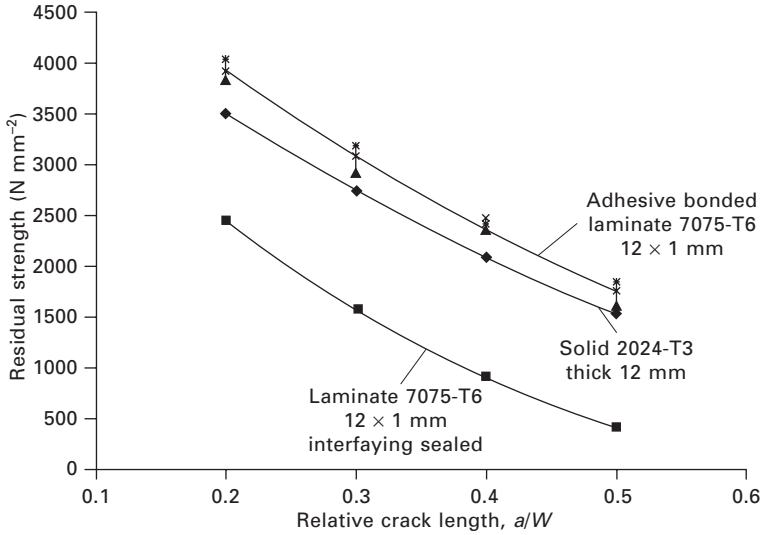
In thick monolithic material the plastic deformation at the crack tip is restricted because the surrounding material limits contraction in the thickness direction, that is plain strain condition, whereas in thin sheets this contraction is not limited, that is plane stress condition. The plain strain condition in thick material results in secondary stresses at the crack tip, which results in a higher crack growth rate at the same fatigue load as well as lower fracture toughness if compared to thin sheets. In a laminate the relatively low modulus adhesive material allows unrestricted contraction of the individual sheets and the laminate can benefit from the better properties of thinner sheets.

Figure 8.17 shows the difference in fatigue crack growth between solid 2024 T3 clad aluminium and laminated aluminium with through cracks. The improvement is far more significant for partly through cracks, i.e. only one, two or three layers with a through crack and the remaining layers intact.[44] This shows the advantage for laminated material, in the situation in which the fatigue crack has to be initiated in every layer. In a 'damage-tolerant' design, the behaviour in the cracked condition is also important. The higher fracture thoughness of thin sheets results in higher residual strength for laminated material.[45]

Figure 8.18 shows favourable results for laminates in AA 7075-T6 in compact tension specimen tests compared to monolithic more damage-tolerant AA 2024 T3 material. This advantageous effect is independent of the type of adhesive. Only in the case of a very low stiffness bond, like by an interfaying sealant, the separate lamellae are allowed to buckle, resulting in lower toughness values.

The fracture of a cracked bonded laminate clearly shows the ductile

© Woodhead Publishing Limited, 2010



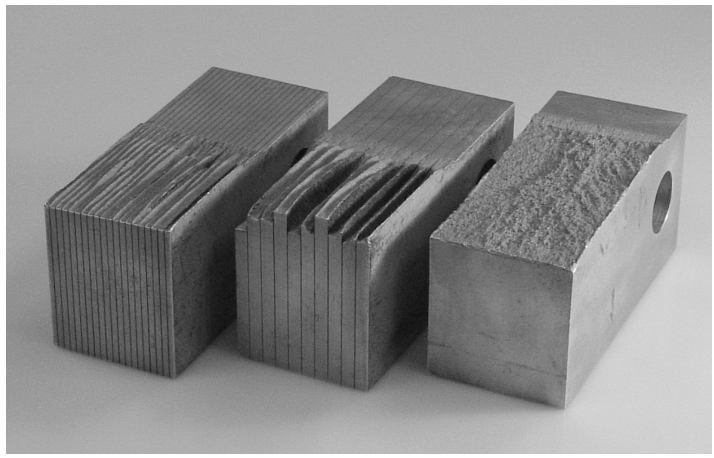

*8.18* Residual strength of laminated AA 7075-T6 material with three adhesives (▲, FM123-5; × EC2216; × FM 1000) compared with solid AA 2024-T3 specimens, where *a* is the crack length and *W* is the width of the test specimen.

behaviour, while the solid specimen shows a flat brittle fracture surface (see Fig. 8.19). The wing skins of Fokker and SAAB aircraft have this laminated structure with the advantage of improved fatigue and damage tolerance in the highly loaded area of the wing box. Figure 8.20 shows an example of a lower wing skin cross-section near the root of the outer wing. Although laminates provide the stated improvement in fatigue crack initiation and high resistance to fracture, the fatigue crack growth behaviour of laminates in through cracks is only slightly improved compared to monolithic plate. The fatigue and fracture toughness properties are further improved by incorporating high strength fibres into the adhesive layers.

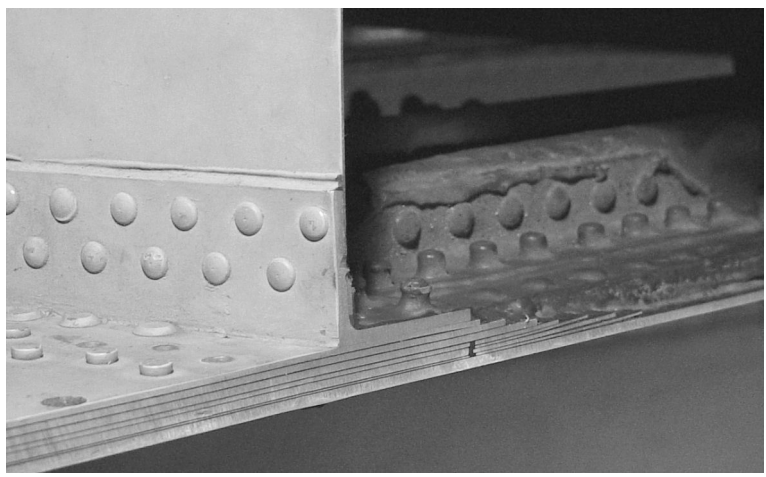
### 8.4.6 Fibre metal laminates (FMLs)

Research at Delft University of Technology further optimized bonded laminates by incorporating high strength fibres for fatigue and damage tolerance properties. ARALL, Aramid Reinforced ALuminium Laminates was the first material developed targeted primarily for wing applications, having all fibres in the spanwise direction. A potential weight saving of 30% can be achieved for the lower wing skin panel compared to a bonded wing design.[46] An application of ARALL in the C-17 cargo door skin showed a weight saving of 26%.[47] The development of ARALL was followed by the development of GLARE® (GLAss fibre REinforced aluminium laminate),

© Woodhead Publishing Limited, 2010



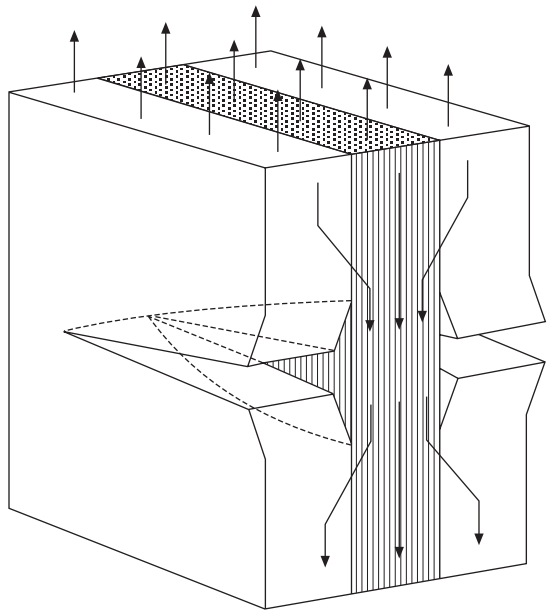
*8.19* Fracture surface of bonded aluminium alloy laminate compared with solid aluminium alloy specimen.



*8.20* Detail of cross-section of Fokker F28 outer wing skin.

which further improved the properties with the use of high strength S2 glass fibres. For fuselage applications a dedicated variant was developed, called Glare 3, with biaxial fibre layers. The excellent fatigue properties of an FML are due to the fact that the high strength fibres 'bridge' the crack. Loads from the cracking metal layer are transmitted via the adhesive to the fibre, unloading the metal layer and slowing down crack growth (see Fig. 8.21). Fatigue loading causes adhesive delamination to occur around the crack, preventing the fibres from breaking. Generally FMLs consist of thin metal layers (0.2–0.5 mm) that allow more fibre layers in order to reduce the shear stress in the adhesive between the fibres and the metal. This controls the delamination and subsequently the crack growth characteristics.

© Woodhead Publishing Limited, 2010



*8.21* Bridging fatigue cracks with high strength fibres.

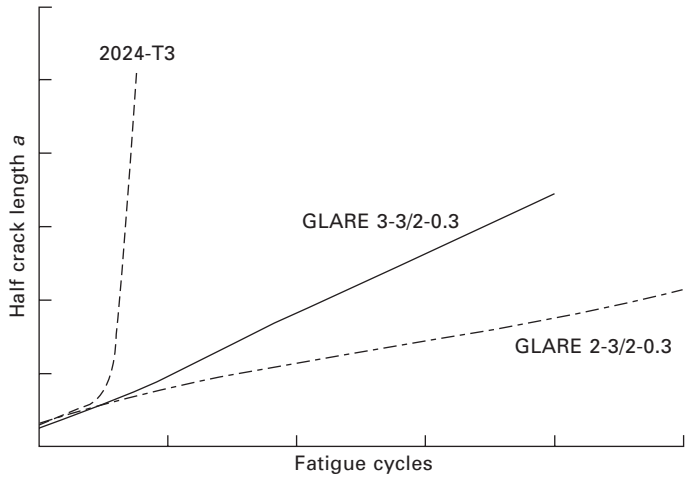
Figure 8.22 shows the fatigue crack growth characteristics of two types of GLARE® laminates compared with AA 2024-T3. All the fibres of Glare 2 are in one direction perpendicular to the crack and Glare 3 has cross-ply fibre layers. In addition to good fatigue and residual strength properties, very good impact properties are also found compared to solid aluminium owing to the fibres supporting the metal.

The stress–strain curve (see Fig. 8.23) shows considerable capability to transform energy into plastic deformation (area under the stress–strain curve). With the development of GLARE® and improvements in manufacturing technology[48, 49] the first large-scale application of FML material in a civil aircraft, the Airbus A380, was realized. Manufacture of these larger panels was made possible by the introduction of splices in the panel to overcome the limitations of thin sheet width dimensions. The high strength glass fibre-reinforced adhesive layer is continuous in the splice area, while the thin metal sheets are joined by overlaps.

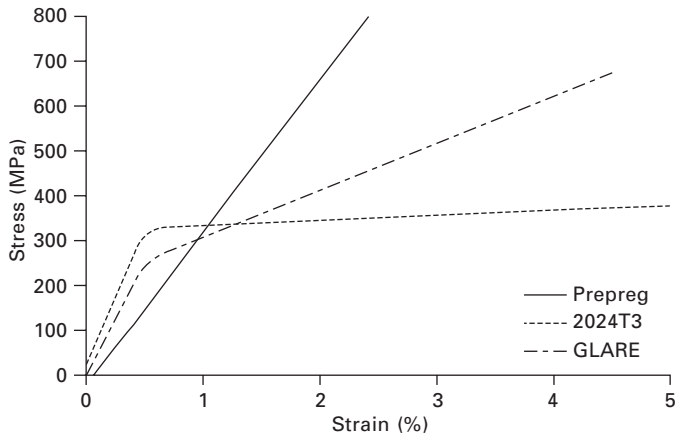
Figure 8.24 shows a fuselage panel with the bonded fibre metal laminate GLARE®, reinforcing doublers around the door cut-out and adhesive bonded stringers. Next to these large fuselage panels; the leading edges of the vertical and horizontal tail plane are also made of the FML material, because of its good impact properties[50, 51] and protection against bird strikes.

Figure 8.25(a) shows one of the GLARE® leading edges of the vertical tail plane with cut-outs for the location of antennas. Figure 8.25(b) shows the result of a bird strike test on a typical leading edge laminate.

© Woodhead Publishing Limited, 2010




*8.22* Fatigue crack growth of GLARE® compared to AA 2024-T3.

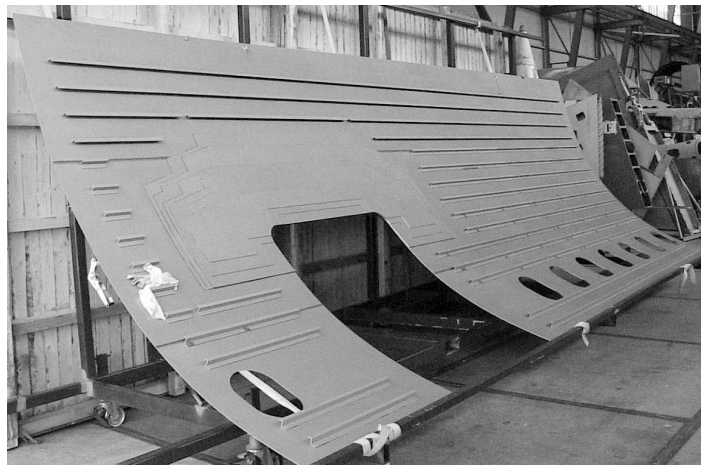



*8.23* Stress–strain curve of GLARE®.

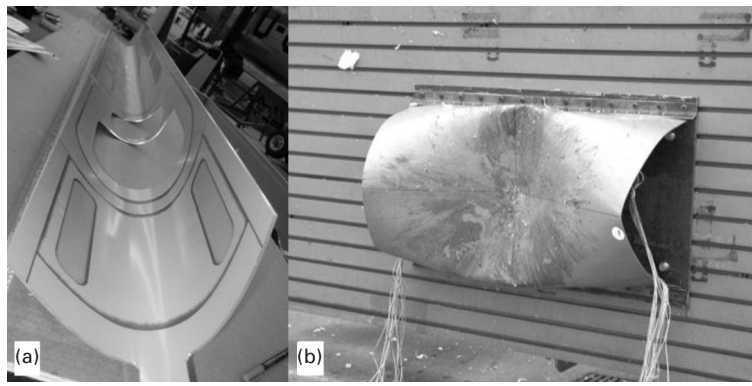
## 8.4.7 Weight and cost reduction

Weight and cost reductions can be obtained in advanced designs owing to the improved properties of adhesive bonded laminates and fibre metal laminates compared to conventionally riveted monolithic structures. Cost can be reduced for designs in GLARE® by integrating local reinforcements, doublers, splices and thickness steps into a one-shot cured large panel. Automation of lay-up of thin aluminium sheets and adhesive prepreg will further reduce costs. No preforming of thin sheets is needed as the lay-up will follow the contour of the mould and take on the (compound) curvature of the mould after consolidation. This integrated manufacturing approach leads to a decrease in

© Woodhead Publishing Limited, 2010



*8.24* Large fuselage panel with spliced GLARE® skin with bonded doublers and stringers.




*8.25* VTP leading edge. (a) One of the LE sections, (b) bird strike test result.

manufacturing costs. The higher price of the constituent materials is balanced by this manufacturing efficiency and by the weight saving. Weight savings between 12 and 26% are mentioned[47, 48, 52] owing to the higher allowable design stress, integrated splices and efficient designs.

### 8.4.8 Sandwich structures

A sandwich is built up from two face sheets with high mechanical properties, which are bonded to a low-density core generally of aluminium honeycomb or foam. This type of structure has a high bending stiffness in the longitudinal and, in contrast to a stringer-sheet panel structure, also in the transverse

© Woodhead Publishing Limited, 2010

direction. The relatively thin sandwich skins are perfectly supported by the core so that local buckling of these skins under compressive loads is prevented. These favourable stiffness properties make the sandwich structure especially effective for compression panels. The application of sandwich panels in aircraft is nowadays mainly restricted to secondary applications, owing to problems for highly loaded sandwiches caused by the complexity of panel coupling and attachments to sandwich panels and durability problems of some of the bonded metallic sandwiches.

Sandwich structures are often used in control surface applications. The use of thin, lightweight skin-sheets bonded to low weight core materials, enables a structure to be obtained that has a high bending and torsion stiffness that maintains accurately the aerodynamic shape under load, thanks to the perfect stabilization of the skin against buckling. Other aircraft parts, which are usually built in the sandwich structure, are the trailing edge panels of the wing box and cabin interior parts and floor panels. Most of these parts nowadays are no longer metal structures, but composite panels with a Nomex® honeycomb core. In space applications, like satellite and solar array structures, sandwiches provide the stiffness required, originally in thin skin metallic sandwiches, but nowadays in aluminium honeycomb cores with carbon fibre composite skins.

In other industries many sandwich applications can be found as walls and panels in semi-trailers, trains, building and construction, ship building and container structures. Sandwiches are sometimes also applied as energy absorbing structures.

### 8.4.9 Bonded repairs

Ageing aircraft structures require safe, damage tolerant and cost-effective repair techniques. Fatigue and corrosion problems become an important topic in maintenance owing to the intensive use and long life of aircraft. Compared to conventional riveted repairs, bonded patch repairs have the advantage of providing more uniform and efficient load transfer.[53] They do not have high stress concentrations at the mechanical fasteners, which nucleate new fatigue cracks leading to even larger repairs. Further, the much higher joint stiffness allows bonded patches, unlike riveted ones, to restrain crack opening and stop the fatigue crack from growing further. The bridging of the crack reduces the stress intensity at the crack tip similar to the mechanism seen for FMLs. The patch is designed such that the repaired stress intensity factor ($K$) at the crack tip is below the threshold value and that stresses and strains in the bondline, skin and patch are not critical.

Design procedures developed by the RAAF (Royal Australian Air Force and USAF mostly use the analytical model developed by Rose and co-workers,[54] which is a two-dimensional continuum analysis based on the

© Woodhead Publishing Limited, 2010

theory of elasticity. It considers an infinitely wide centre-cracked isotropic plate with a one-sided bonded orthotropic plate remotely loaded by a biaxial system. First the repair is modelled as an equivalent inclusion to calculate the stress redistribution in the plate caused by the bonded doubler. Then the crack is introduced and the stress intensity factor $K$ at the crack tip is calculated.

The Rose model has been further extended to include bending caused by eccentricity of a one-sided patch and to include thermal stresses induced by curing the adhesive.[54, 55] Owing to the shift in neutral axis, single-sided patches inevitably induce bending stresses, which can be as high as 50% of the stresses at the critical locations.[53] The calculation of secondary bending requires (geometrically) non-linear analysis, since linear analysis largely overestimates bending stresses.

The neutral line method (NLM) provides a geometrically non-linear closed form solution. Secondary bending stresses can be reduced by gradually changing the neutral axis, that is by tapering or stepping the edge of the patch. The difference in coefficient of thermal expansion (CTE) between patch material and parent material plays a crucial role in patch effectiveness considering that temperature differences between cure and operating temperatures can become as high as 180°C. Thermal residual stresses for low CTE patches are compressive in nature in the patch and in the skin near the patch edge, but are tensile in nature in the skin at the crack tip. The latter lowers the crack tip stress intensity factor reduction and the patch becomes less effective at lower operating temperatures.[53] Since only the repair area is locally heated, the surrounding structure restrains its expansion, which has been modelled by Fredell[55] using fully clamped edges of the patch area and by Wang/Rose (see page 137 in Reference 54) with a distribution of springs.

A complex analytical model is available in specially developed software packages, such as CalcuRep or CRAS, which calculate the critical design parameters:

- the repaired stress intensity factor ($K$) at the crack tip
- the maximum stress in the patch (at the crack)
- the maximum skin stress (at the patch tip)
- the maximum shear strain in the adhesive
- the load transfer length in the bondline
- thermal residual stresses from curing
- bending stresses caused by eccentricity.

The patch material and geometry can quickly be optimized using an iterative design procedure based on conservative engineering guidelines and past experience. This allows non-specialists, such as maintenance engineers, to design safe and damage-tolerant bonded repairs quickly. The crack patching bonding technique was first applied to the fatigue critical D6AC steel wing

© Woodhead Publishing Limited, 2010

pivot fitting of the F-111 bomber and later to many other aircraft, such as the C-141, C-5A, F-16, F-18, Mirage and Lockheed Tristar.[54] Repair materials mainly studied and used by the RAAF and USAF are carbon- and boron-reinforced epoxy, since their high stiffness makes thin patches possible. The application of bonded GLARE patches has been extensively investigated in a joint cooperation between the USAF and Delft University of Technology, as this repair material has a much lower CTE mismatch from the parent (metal) structure.[53, 56]

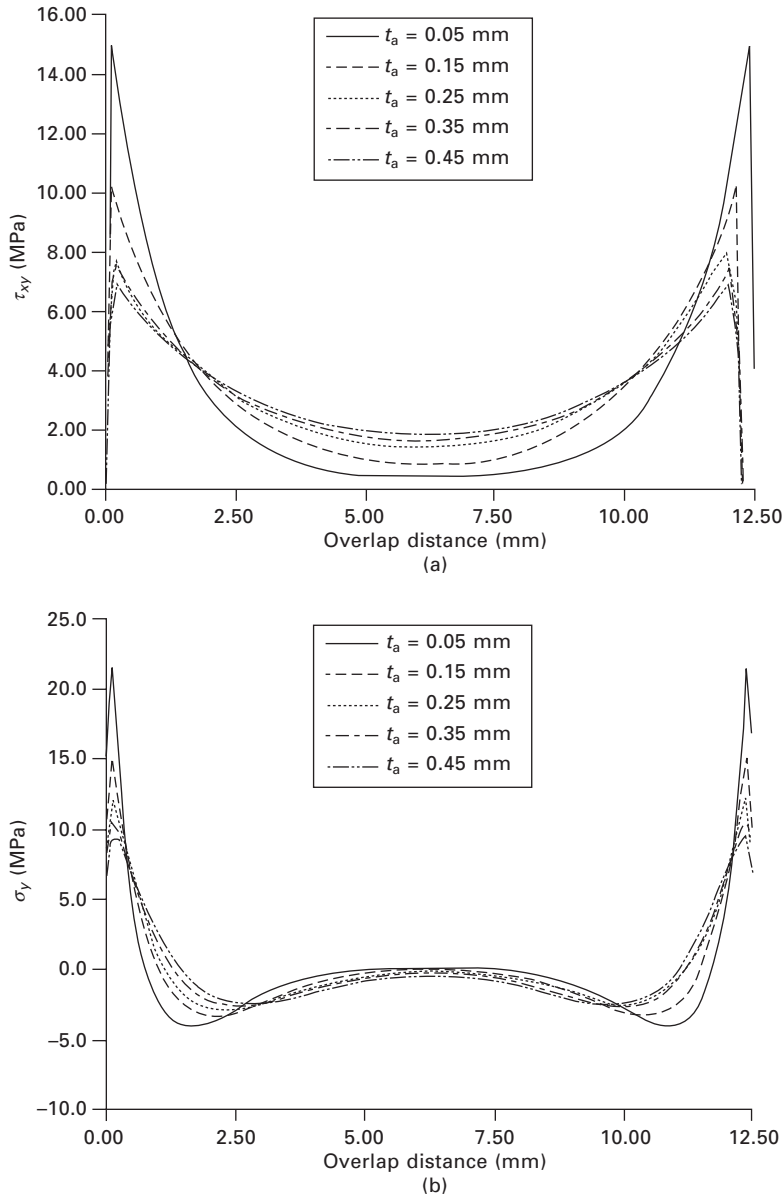
### 8.4.10 Bonded window frames

Passenger windows require adequate reinforcement around the edge of the cut-out, which is in a highly loaded area of the fuselage. In a typical conventional design a window pan (T-shaped forged frame) is riveted to the skin using about one hundred fasteners per frame. It is obvious that drilling so many holes in such a heavily loaded area weakens the skin significantly with the danger of fatigue crack initiation at the rivet holes. With dozens of windows one can imagine the costs and effort required in drilling, deburring and rivet installation, as well as inspection of every rivet hole during maintenance. Bonded window frames do not require mechanical fasteners, therefore drastically reducing the amount of potential fatigue crack initiation locations in the skin and window frame. Combining the bonding of components such as skins, doublers, window frames and stringers offers a cost effective way of manufacturing large fuselage shells. The higher joint efficiency makes the window pan a more effective edge reinforcement, allowing reduced frame cross-section and thinner skins. Bonded window reinforcements were first applied in the SAAB 2000 aircraft and are now in production for the Airbus A380.

## 8.5 Developments in modelling and testing the effectiveness of adhesive bonded metal joints

The shear lag theory, first used by Volkersen[57] and later extended by Goland and Reissner[58] to include peel stresses, showed that the stress distribution in a bonded overlap joint is highly non-linear. As shown in Fig. 8.26, high shear and peel stresses are found at the overlap ends and low stresses in the middle, which means that almost all load is carried by the first few millimetres from the edges.[59, 60] The fact that high strain gradients are present in relatively small areas makes it most difficult to model accurately or determine experimentally the stresses and strains inside the bondline and in the adherends.

© Woodhead Publishing Limited, 2010




*8.26* Typical shear (a) and peel (b) stresses in a bonded lap joint.

## 8.5.1 Analytical solutions

The governing differential equations for the stresses in bonded joints can be derived based on simplifying assumptions concerning the behavior of the adherends and the adhesive. Many different solutions are available which

© Woodhead Publishing Limited, 2010

deviate with respect to the assumptions made to simplify the problem and the boundary conditions applied. Analytical closed form solutions are possible for simple, linear geometries and linear material behaviour (Gleich,[61] van Ingen,[62] Adams and Wake,[63] Kinloch[15]). The shear lag theory published by Volkersen in 1938[57] assumes that the adherends only carry tensile stresses and the adhesive only shear stresses. Adhesive stresses are assumed to be constant through the thickness. Peel stresses are not taken into account nor is eccentricity. The use of the Volkersen method therefore is very limited, yet it does give important insight in the basic understanding that the shear stress distribution in a bonded overlap joint is highly non-linear. Peak stresses arise near the ends of an overlap, whereas low shear stresses are found in the mid-section. This is accompanied by a variation of the normal stress in the adherend.

Goland and Reisner in 1944[58] included peel stresses in their solution as well as the effect of the load eccentricity. Eccentricity results in additional shear and bending loads, which depend on the actual loading condition caused by the bending rotation of the joint. Hart-Smith[64] used a similar approach and included adhesive plasticity in shear. The adhesive is assumed to behave as a perfect elastic–plastic material and to be plastic only in small zones at the overlap edges. In these plastic zones the shear stress has a constant value, but the shear strain varies.

Ojalvo and Eidinoff[65] developed a theory in 1978 which allows for linear variation of the shear stress over the bondline thickness. The analysis for asymmetrical joints was modelled by Williams[66] in 1975 and Bigwood and Crocombe in 1989.[67] Transverse shear effects in the adherend have been included by Delale *et al.*[68] and Yuceoglu and Updike.[69] The latter was developed for symmetrical configurations, the former for dissimilar adherends. The zero stress condition in the adhesive at the edge of the overlap has been taken into account by Allman,[70] Du Chen[71] and Renton and Vinson.[72] More recently, analysis methods for three-dimensional (3D) problems under more general loading conditions were developed, for instance, by extending the Goland and Reissner model.[73] Mortensen developed a unified approach for which good agreement is found in comparison with Erdogan's analysis and with the finite element model (FEM) (Zhang).[74]

### 8.5.2 Numerical tools

For complex geometries or non-linear analysis a closed form analytical solution will be difficult or impossible to find. The governing differential equations can then be solved numerically by the finite difference method (FDM).[61] Herewith it should be noted that it is only the solving method that is different. The governing equations are still derived based on simplifying assumptions, so similar limitations as for the closed form solutions apply.[62]

© Woodhead Publishing Limited, 2010

Implementation in, for instance Matlab or equivalent software programs, makes FDM a powerful tool for linear elastic analysis and, as such, an excellent engineering design tool.[75]

The finite element model (FEM) approach divides the joint into smaller building blocks, called finite elements, each with their own (simplified) governing differential equations. Together they describe the behaviour of the joint. This opens up the possibility of analysing complex joint geometries, like spew fillet, adherend tapering and 3D, and of including geometrical and material non-linear behaviour. However, the method is time-consuming and not easily applicable to routine design work.[62] The thin bondline and the high strain gradients at the edges require a large number of small elements to obtain sufficiently accurate results. Different approaches to modelling the bonded joints have been reported (Jones,[76] Carver and Wooley,[77] Adams,[63] NASA,[78] Barut,[73] Goncalves[79]):

- 2D finite element model: using plate/shell elements for substrate and adhesive
- Shear spring method: 3D plate/shell element for the adherend + 1D spring, bar or beam elements for the adhesive
- Three layer method: the adherends and adhesive are modelled as 3D plate/shell layers rigidly connected
- Full 3D model: adherends and adhesives are modelled as 3D solids.

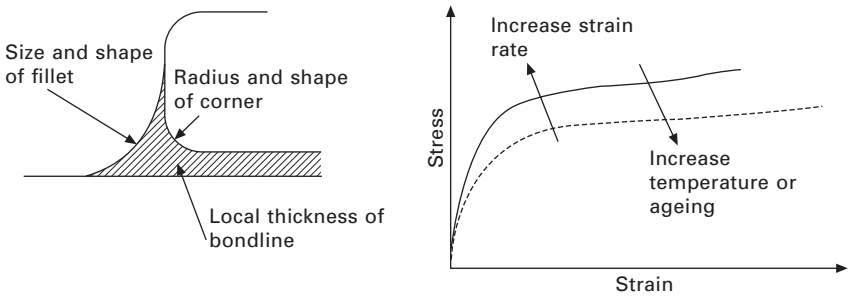
To limit the number of elements the following approaches are used (Jones,[76] Zhu and Kedward,[80] Engelstadt,[81] Cornec[82]):

- a coarse global model with a fine local model for detailed stress analysis
- FE codes which use higher degree polynomial (p-based);
- specific interface elements representing the bondline (e.g. cohesive zone model)

### 8.5.3 Failure load prediction

The prediction of joint failure depends highly on the accuracy of the calculated stresses and strains in combination with a suitable failure criterion. Strength predictions based on linear elastic analysis are inadequate, as this is not the case at the moment of failure. Both material and geometrical non-linear behaviour should be taken into account. The accuracy of the calculated stresses and strains in the bondline is sensitive to variations in material properties and small changes in local geometry (see Fig. 8.27). On the one hand it is very difficult to determine accurately the stress–strain properties for the adhesive materials. And on the other hand the stress field at the edge of the joint is strongly influenced by local geometrical parameters. Two distinct approaches to strength predictions can be identified:[83]

© Woodhead Publishing Limited, 2010




*8.27* Several parameters that influence calculated stresses and strains.

1. maximum value criteria
2. fracture mechanics

The use of maximum value criteria was advocated in non-linear stress analysis and good correlation with experimental results was reported for specific cases. However, this approach could not be generalized to other joint strength predictions, although it was shown that for adhesive joints the fracture energy is not independent of the joint geometry and as such cannot be treated as an adhesive property.[83] Many failure criteria have been proposed by various authors and good agreement with test results is reported, yet only for specific cases (Gleich,[61] Odi and Friend[83]). So far, none of the below was found to be universally applicable:

- maximum stress/strain
- elastic–plastic curve with maximum strain (Hart-Smith)[60, 84]
- modified Von Mises (Zhu and Kedward)[80]
- yield criteria, e.g. Tresca (Wang and Chalkley[85], Ignjatovic[86])
- linear elastic fracture mechanics (LEFM)
- stress singularity (Gleich,[61] Zhu and Kedward[80])
- strain energy density (Hart-Smith)[84]
- strain invariant failure (SIFT) (Engelstadt)[81]
- cohesive zone model (Cornec).[82]

A good failure criterion should predict both failure mode as well as failure load.[61] To date, however, the accurate prediction of bond strength has been limited by the lack of a suitable, universally applicable failure criterion and insufficient accuracy in calculating bondline stresses and strains.

### 8.5.4 Fracture mechanics approach

The principle of fracture mechanics predicts failure propagation based on the assumption of a pre-existing crack (or delamination) in the bonded joint

© Woodhead Publishing Limited, 2010

at the most critical location, usually the highly loaded edges. The strain energy release rate $G$ or the stress intensity factor $K$ is checked against a critical value, that is $G_c$ or $K_c$ respectively, in order to check for further crack growth or failure (Broughton,[87] Kinloch,[15] Groth[88]). Applied to bonded joint durability, that is fatigue and environmental effects (Johnson *et al.*),[89] the virtual crack closure technique (VCCT) predicts the delamination growth on the basis of the work required to close a virtual crack.[90] VCCT is available in commercially available FE code.[91] An interface fracture finite element for predicting the delamination propagation, damage tolerance and residual strength is reported by Engelstadt.[81] The use of a traction-separation law for the decohesion is the fundamental idea of cohesive zone models (CZM). In this way, the unrealistic continuum mechanics stress singularity at the crack tip is avoided.[82]

### 8.5.5 Improved analytical methods for fatigue crack growth prediction in FML

During crack growth in a FML, like Glare®, the fibres transfer part of the load around the crack tip in the aluminium layers, thereby reducing crack growth. This is accompanied by delamination at the interface between the aluminium and glass fibre/adhesive layers, in which size and shape play an important role in fibre bridging effectiveness. An accurate analytical prediction model was developed by Alderliesten,[92] which accounts for delamination growth and fibre bridging. Similar to models developed for monolithic aluminium, the stress intensity at the crack tip in the metal layers is taken as the factor determining the extension of that crack under cyclic loading. The stress intensity factor consists of a crack opening contribution caused by far field stresses in the aluminium layers and a crack closing contribution of the intact fibres in the wake of the crack. The stresses in these fibre layers determine the delamination growth. The stress intensity factor is described by LEFM, including the contribution of the fibre layers and the with crack growth associated delamination behaviour in the prepreg layers in the wake of the propagating crack.

The bridging stress along the crack length is calculated on the basis of the crack opening relations for the individual mechanisms. It is then used to calculate the delamination extension, using a correlation between the delamination growth rate and the energy release rate. Once the stress intensity factor at the crack tip in the aluminium layers is known, the fatigue crack growth rate can be calculated using an empirical Paris relation. A good correlation between predicted and experimental crack growth rates, crack opening contours and delamination shapes has been obtained using a wide range of test data.

© Woodhead Publishing Limited, 2010

### 8.5.6 Testing adhesive bonded joints

Most test methods and specimens used for adhesive bonding are coupon tests related to the quality evaluation of either the adhesive material or the surface pretreatment (see Table 8.4).

Others are used for the determination of adhesive mechanical properties, that is shear stress–strain curve or fracture energy (Minford,[93] Kinloch,[15] deVries and Anderson,[94] ASTM[95] or ISO/EN standards). These coupon tests, however, are less useful for design purpose or tool validation.[60] Most case studies on stress analysis of bonded joints use the single or double overlap test specimen. This choice, however, is driven by the fact that results are widely available and the simplicity of the test itself.[62] A major difficulty is that the test results depend highly on factors like substrate and bondline thickness, surface treatment and overlap length and that the failure mode is a combination of peel and shear. With the absence of a suitable failure criterion[61] the one-test result, that is failure load, cannot be linked directly to the analysis results.

Any comparison reported between test and analysis is based on indirect results like deflection of the specimen or strains measured on the substrate's outer surface. Until recently local strains inside the bondline simply could not be measured accurately, although digital optical methods supported by image correlation software can now be used for exactly that purpose. As simple coupon tests are unsuitable, the validation of calculation tools requires specially developed specimens. Typical examples are doubler run-out, cracked lap-shear specimen (CLS) or stringer run-out specimens.[81] Their principle is based on crack initiation and growth in relation to fracture energy, both static and dynamic. By changing geometrical parameters the load on the joint can be varied. Scaling up is severely limited,[60] since all dimensions of a bonded joint can be scaled up, yet bondline thickness cannot. Further, the strength of the substrate is proportional to its thickness, whereas bond strength is proportional to the square root of the substrate thickness.

*Table 8.4* Overview of some of the most used test methods for adhesive bonding

| Description | Tested item | Specification | |
|---|---|---|---|
| Single overlap shear test | Quality control | ASTM D1002 | EN 2243-1 |
| Floating roller peel test | Surface treatment | ASTM D3167 | EN 2243-2 |
| Climbing drum peel test | Surface treatment | ASTM D1781 | EN 2243-3 |
| Wedge test | Surface treatment | ASTM D3762 | |
| Thick adherend test | Shear stress–strain curve | ASTM D5656 | EN 2243-6 |
| Double cantilever beam | Fracture energy | ASTM D3807 | ASTM D3433 |

© Woodhead Publishing Limited, 2010

### 8.5.7 Determination of bondline strains by fibre optic sensors

Fibre optic sensors are currently used as transducers for various physical phenomena. The embedding of fibre optic sensors in structural materials presents the possibility of structural health monitoring. In adhesive bonded joints they can be used to monitor changes in strains in the bondline and the onset of delamination.[96] Various types of fibre optic sensors are available on the market. Fibre Bragg gratings (FBG) are mostly applied in monitoring composite structures and adhesive bondlines. Most applications are used in the area of bonded composite repair patches, where the change in the stress field is monitored to detect cracks propagating beneath the patch.[97, 98]

The measured wavelength shift in a Bragg grating sensor is proportional to the linear combination of the principle strains and the temperature. Furthermore the effect of the fibre coating, adhesion quality between coating and adhesive material, and effect of the fibre diameter hinder the accuracy of the strain measurement. Commonly the fibres have a diameter between 50 and 100 μm, while the adhesive bondline thickness of a structural joint is between 0.1 and 0.2 mm. This makes it likely that fibres embedded in the adhesive layer influence the strain distribution in the bonded joint and influence the failure behaviour.

### 8.5.8 Development of optical digital videomicroscopy to measure bondline strains

Strain fields in bonded joints are characterized by high gradients and local concentrations inside thin bondlines, which for a long time prohibited accurate measurement. The development of high-resolution optical measurement systems together with sophisticated image correlation software makes detailed material behaviour visible and can provide detailed local information about the strain field without the need for physical contact with the specimen.[99] Thick adherend tests are typically used for the determination of adhesive mechanical properties under shear loading. In the test, the relative displacement of the substrates with respect to each other needs to be measured to obtain the shear angle. For some time, the standard method is based on the work by Krieger,[100] in which a specially developed type of mechanical extensometer is attached to both sides of the specimen. Pins are positioned on the substrates as close as possible to the bondline. The accuracy of the measurements is lowered owing to the following difficulties with the mechanical extensometers:[101]

- rotation of the bondline caused by secondary bending;
- pins are located some distance away from the interface, so the shear deformation of the aluminium adherend needs to be filtered;
- slippage of the pins results in inaccurate readings.

© Woodhead Publishing Limited, 2010

By using a non-contact optical method these drawbacks are eliminated, as the bondline deformation is measured directly. Slippage does not occur and adherend deformation and rotation do not influence the measurements. Further it is possible to measure local strain fields, whereas an extensometer only measures the average strain over a large gauge length. High accuracy is possible, although it is dependent on the quality of the images, the pattern of the surface and the light used. Digital image correlation (DIC) is the analysis of a large number of images taken from a test specimen during the test, in which one specific part of the first image is correlated to each consecutive image to establish the displacement of one or more points of the image. By using higher degree polynomial interpolation, sub pixel accuracy of down to 0.01 pixels can be obtained. Following the relative displacement of multiple points, the local strain field (or any other deformation related property) is calculated. For the thick adherend test the shear angle is obtained from the relative displacement of both substrates, which is determined for multiple points on the adhesive–substrate interface. Each image is linked to the load data recorded by the tensile machine and subsequently the shear stress–strain curve is plotted. Similar optical methods are used for Mode I crack propagation tests using double cantilever beam (DCB) specimens or for the determination of the strain field around a crack tip.[99] By zooming out, the strain field around bonded doublers can be determined to verify design calculations, where out-of-plane deformation (3D) can be determined by using two cameras simultaneously.

## 8.6 Future trends

In the development of adhesive bonded structures long term durability and reliability of bonded joints is a continued area of attention. The requirements for strength and durability of the total system, the combination of adherend material, surface treatment, primer and adhesive, are of continued concern. The need for environmentally safe materials and processes will result in further development of low volatile organic components (VOC), chromate-free adhesive materials and surface treatments. The search for more toughness in high strength structural adhesive systems is a challenge, especially in RT or moderate temperature curing adhesives. The developments in nano-structured materials may further increase adhesive toughness. These improved adhesives should enable the curing of large structures without the use of an autoclave while the structural joint characteristics at both low as well as high temperatures are maintained. Developments in nano materials may also lead to improved high temperature adhesive materials and even to adhesives with improved fire properties.

Structural development in bonded laminates and FMLs will result in new applications. Recently a new FML called CentrAl (centrally reinforced

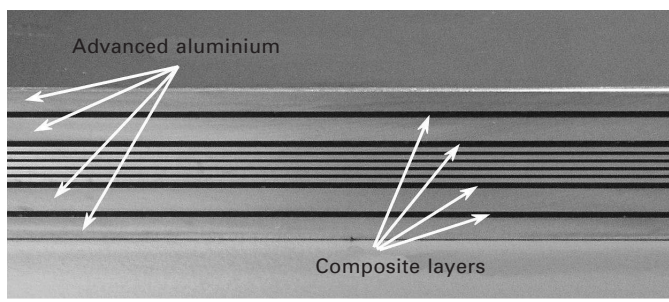
© Woodhead Publishing Limited, 2010

aluminium) was introduced for application in aircraft wings.[102–104] The CentrAl concept comprises a central layer of FML (GLARE), sandwiched between one or more thick layers of new generation damage-tolerant aluminium alloys (see Fig. 8.28). Fibre-reinforced adhesive layers called bondpreg™, also bond the outer layers in this concept. This creates a robust structural material, which is not only exceptionally strong, but also insensitive to fatigue. Because the hybrid material is practically immune to fatigue, wing panels can be designed which do not need frequent inspection and repair of cracks during the life of the aircraft, in other words they have a 'care-free' economic life. The new CentrAl structures are stronger than carbon fibre-reinforced plastic (CFRP) structures.[102] CentrAl allows higher stress levels and by using it in lower wing structures, the weight can be reduced by 20% compared to CFRP structures. The application of CentrAl will result in considerably lower manufacturing and maintenance costs.

Rapid developments in sophisticated computer hard- and software will result in more accurate strength prediction models and will boost the development of digital optical methods for strain measurements, which can then be used for model validation. This will result in more reliable design methods for adhesively bonded metal joints.

## 8.7 Sources of further information and advice

Many references have been given in this chapter, but the most important sources of further information are summarized below. A general review of the multi-disciplined subject of adhesion and adhesives is given by A.J. Kinloch in *Adhesion and Adhesives – Science and Technology*,[15] which covers the first principles of surface chemistry, physics and adhesive chemistry up to the engineering design of joints and the service life considerations. The terminology most used in the field of adhesive bonding is described in the *Handbook of Adhesion*,[105] which provides a basic understanding via short, self-contained articles on scientific, engineering and industrial aspects of adhesion.




*8.28* The CentrAl concept.

© Woodhead Publishing Limited, 2010

A true landmark reference, which reviews more than 4500 articles, is a comprehensive discussion on every important aspect of aluminium bonding by J.D. Minford in *Handbook of Aluminum Bonding Technology and Data*.[93] The wide variety of different adhesive types, their properties and applications, as well as the many surface treatments available for various substrates is described by A.H. Landrock in the *Adhesives Technology Handbook*.[5] *Structural Adhesive Joints in Engineering* by R.D. Adams[63] provides basic engineering design knowledge, with the focus on understanding the way stresses are transferred from one member to another.

The most important way to ensure long-term durability of structural adhesive joints is discussed in *Durability of Structural Adhesives* by A.J. Kinloch.[106] Included is the kinetics and mechanism of environmental attack, as well as the durability of aluminium, steel and titanium bonded substrates. The mechanical testing of adhesives and bonded joints, as well as stress analysis and failure mechanisms is described in *Adhesively Bonded Joints: testing, analysis and design*'.[107] E.W. Thrall and R.W. Shannon collected in *Adhesive Bonding of Aluminum Alloys* the lessons learned during the PABST programme about adhesives, surface treatments, mechanical properties, environmental durability, structural analysis and tooling design for adhesively bonded primary aircraft structures.[108]

An overview of all essential aspects of bonded patch repair, including materials and processes, design of repairs, certification issues and many example cases, is given in *Advances in the Bonded Composite Repair of Metallic Aircraft Structures* compiled by A.A. Baker, L.R.F. Rose and R. Jones.[54] To learn more about the development of FMLs and their static, fatigue and impact properties, as well as design, production and maintenance of FML-based aircraft structures, the reader is referred to the book edited by J.W. Gunnink and A. Vlot called *Fibre Metal Laminates: an introduction*.[109]

## 8.8 References

1. Boëda, E., Connan, J., Dessort, D., Muhesen, S., Mercier, N., Valladas, M. and Tisnerat, N. (1996). 'Bitumen as hafting material on Middle Palaeolithic artefacts', *Nature*, **380**, 336–8.
2. Bishopp, J.A. (1997). 'The history of Redux® and the Redux bonding process', *Int. J. Adhesion and Adhesives*, **17**, 287–301.
3. Schliekelmann, R.J. (1979). 'Operational experience with adhesive bonded structures', in *AGARD-LS-102, Bonded Joints and Preparation for Bonding*. AGARD-NATO, Paris, 1-1–1-30.
4. Kwakernaak, A. (1994). 'More than 40 years experience with primary adhesive bonded structures', in *50 Years of Advanced Materials or 'Back to the Future'*. J. Hognat, R. Pinzelli and E. Gillard (eds), SAMPE Europe, Switzerland, 67–78.
5. Landrock, A.H. (1985). *Adhesives Technology Handbook*, Noyes Publications, Park Ridge, NJ.

© Woodhead Publishing Limited, 2010

6. Garnish, E.W. (1977). 'Advances in epoxy adhesive technology', in *Developments in Adhesives-1*, W.C. Wake (ed.), Applied Science Publishers, London.
7. Kinloch, A.J. (2003). 'Toughening epoxy adhesives to meet today's challenges', *MRS Bulletin*, June, 445–8.
8. Bishopp, J.A. (1992). 'The chemistry and properties of a new generation of toughened epoxy matrices', *Int. J. Adhesion and Adhesives*, **12**, 178–84.
9. Kinloch, A.J., Lee, J.H., Taylor, A.C., Sprenger, S., Eger, C. and Egan, D. (2004). 'Toughening structural adhesives using nano- and micro-phase inclusions', in: *27th Annual Meeting of the Adhesion Society*, Chaudhury, M.K. (ed.), Adhesion Society, Wilmington, NC, 96–8.
10. Brooker, R.D., Blackman, B.R.K., Kinloch, A.J. and Taylor, A.C. (2008). 'Nano-reinforcement of epoxy/thermoplastic blends', in *31st Annual Meeting of The Adhesion Society*, Gregory Anderson (ed.), Adhesion Society, Austin, TX, 250–2.
11. Barsotti, R., Inoubli, R., Schmidt, S., Macy, N., Magnet, S., Fine, T., Navarro, C. and Wells, M. (2008). 'Block copolymers for epoxy toughening', in *SAMPE Fall Technical Conference Proceedings: Multifunctional Materials: Working Smart Together*, Memphis, TN, September 8–11, Society for the Advancement of Material and Process Engineering, Covina, CA, USA, CD-ROM-8 pp.
12. Noble, N., Brosius, D. and Schlimbach, J. (2008). 'An advanced out-of-autoclave curing technology for prepregs and resin infusion', in *SAMPE Asia Conference 2008 Proceedings*, Bangkok, Thailand, 11–13 February, 2008, Society for the Advancement of Material and Process Engineering, Covina, CA, USA, CD-ROM-10 pp.
13. Schliekelmann, R.J. (1973). *Adhesive Bonding in the Fokker-VFW F-28 'Fellowship'*, Fokker report K-67, NTIS A06-99-028392.
14. Hartman, A. (1966). *Fatigue Tests on Single Lap Joints in Clad 2024-T3 Aluminium Alloy Manufactured by a Combination of Riveting and Adhesive Bonding*, NLR, Report M.2170.
15. Kinloch, A.J. (1987). *Adhesion and Adhesives: Science and Technology*, Chapman & Hall, London.
16. Anon. (1941). *Process for Cleaning Aluminium Alloy Plating Prior to Painting*, Process Specification DTD 915, UK Ministry of Aircraft Production.
17. Eickner, H.W. and Schowalter, N.E. (1950). *A Study of Methods for Preparing Clad 24S-T3 Aluminum Alloy Sheet Surfaces for Adhesive Bonding*, Forest Products Laboratory Report No. 1813.
18. Bethune, A.W. (1975). 'Durability of bonded aluminum structure', *SAMPE J.*, **11**(3), 4–10.
19. Russel, W.J. and Garnis, E.A. (1981). 'A chromate-free low toxicity method of preparing aluminium surfaces for adhesive bonding', *SAMPE J.*, **17**(3), 19–23.
20. Bijlmer, P.F.A. (1977). *Pickling Aluminium*, US patent 4042475.
21. Anon. (2008). *Chromic Acid Anodising of Aluminium and Aluminium Alloys*, Process Specification Def Stan 03-24, iss. 5, UK Ministry of Defence, Defence Standard.
22. Bijlmer, P.F.A. (1972). 'Adhesive bonding on anodised aluminium', *Metal Finishing*, **70**(4), 30–34.
23. Wegman, R.F. (1989). *Surface Preparation Techniques for Adhesive Bonding*, Noyes Publications, Park Ridge, NJ.
24. McMillan, J.C., Davis, R.A. and Quinlivan, J.T. (1976). 'Phosphoric acid anodizing of aluminium for structural bonding', *SAMPE Quart*, **7**(3), 13–18.
25. Kwakernaak, A. and van den Berg, A. (2002). 'Adhesive bonded joints in aluminium structures', *Acta Technica Belgica Metallurgie*, **42**(1–2), 103–8.

© Woodhead Publishing Limited, 2010

26. van den Berg, A. and Kwakernaak, A. (2002). 'Conversion coating as a pretreatment for adhesive bonding', *Proceedings 10th International Symposium Swiss Bonding*, 27–29 May, 2002, Rapperswil, Swibotech, Switzerland.
27. Kock, E., Muss, V., Matz, C. and De Wit, F. (1993). *Verfahren zur anodischen Oxidation*, Patent EP0607579 A1, 16 December 1993.
28. Kwakernaak, A. (2004). 'The importance of anodic oxide morphology in relation to adhesion and durability of bonded joints', in *Workshop in Bremen*: *Anodisation in the Aircraft Manufacturing Industry*, 15 April 2004, IFAM, Bremen, Germany.
29. Critchlow, G. (2006). 'Alternatives to chromic acid anodizing for structural bonding applications', Symposium, *Disruptive Technologies for Light Metals*, IOM3, London, UK.
30. Brockmann W. (1987). 'Steel adherends', in *Durability of Structural Adhesives*, A.J. Kinloch (ed.), Elsevier Applied Science, London, Chapter 7, 306.
31. Haak, R.P. and Smith, T. (1983). 'Surface treatment of AM355 stainless steel for adhesive bonding', *Int. J. Adhesion and Adhesives*, **3**, 15–23.
32. Bouquet, F., Cuntz, J.M. and Coddet, C. (1992). 'Influence of surface treatment on the durability of stainless steel sheets bonded with epoxy', *J. Adhesion Sci. Technol.*, **6**(2) 233–242.
33. Mahoon, A. (1987). 'Titanium adherends', in *Durability of Structural Adhesives*, Elsevier Applied Science, London.
34. Locke, M.C., Harriman, K.M. and Arnold, D.B. (1980). 'Optimization of chromic acid – fluoride anodizing for titanium prebond surface treatment', *Proceedings 25th National SAMPE Symposium*, San Diego, CA, USA, 6–8 May, 1980, 1–12, Society for the Advancement of Material and Process Engineering, Covina, CA, USA.
35. Kennedy, A.C., Kohler, R. and Poole, P. (1983). 'A sodium hydroxide anodize surface pretreatment for the adhesive bonding of titanium alloys', *Int. J. Adhesion and Adhesives*, **3**(2), 133–139.
36. Arnott, D., Rider, A. and Mazza, J. (2002). 'Surface treatment and repair bonding', in *Advances in the bonded composite repairs of metallic aircraft structure*, A.A. Baker, L.R.F. Rose and R. Jones (eds.), Elsevier Science Oxford.
37. Bergan, L. (1999). 'On-aircraft phosphoric acid anodising', *Int. J. of Adhesion and Adhesives*, **19**, 199–204.
38. Baker, A.A. and Chester, R.J. (1992). 'Minimum surface treatments for adhesively bonded repairs', *Int. J. Adhesion and Adhesives*, **121**(2), 73–8.
39. Kuhbander R.J. and Mazza, J.J. (1993). 'Understanding the Australian silane surface treatment', *Proceedings of 38th International SAMPE Symposium and Exhibition*, Anaheim, CA. Society for the Advancement of Material and Process Engineering, Covina, CA, USA.
40. Blohowiak, K.Y., Osborne, J.H. and Krienke, K.A. (1998–2000). *Sol for Bonding Epoxies to Aluminum or Titanium Alloys*, US Patent 6,037,060 (2000); *Sol–gel Coated Metal*, US Patent 5,958,578 (1999); *Sol–gel Coated Metal*, US Patent 5,939,197 (1999); *Surface Pretreatment for Sol Coating of Metals*, US Patent 5,869,141 (1999); *Surface Pretreatment of Metals to Activate the Surface for Sol–gel Coating*, US Patent 5,869,140 (1999); *Sol Coating of Metals*, US Patent 5,849,110 (1998); *Sol for Coating Metals*, US Patent 5,814,137 (1998).
41. McCray, D.B. and Mazza, J.J. (2000). 'Optimization of sol–gel surface preparations for repair bonding of aluminum alloys'. *Proceedings of 45th International SAMPE Symposium and Exhibition*, Long Beach CA, May, 53–4, Society for the Advancement of Material and Process Engineering, Covina, CA, USA.

© Woodhead Publishing Limited, 2010

42. Blohowiak, K.Y., Grob, J., Grace, W.B., Cejka, N. and Berg, D. (2007). 'Improvements in sol–gel surface preparation methods for metal bonding applications', *Proceedings of 39th International SAMPE Tech. Conference*, Cincinnati, OH, Society for the Advancement of Material and Process Engineering, Covina, CA, USA, CD-ROM-15 pp.
43. Harteveld, C.D.H. (1971). *Optimal Adhesive Bonded Panel Edge Configurations Determined by Photoelastic Investigation* (in Dutch), Fokker report R-1429.
44. Schijve, J. (1978). *Fatigue Properties of Adhesive Bonded Laminated Sheet Material of Aluminium Alloys*, TU Delft, Aerospace Engineering, Report LR-276.
45. Bijlmer, P.F.A. (1978). 'Fracture toughness of multiply layer adhesive aluminium alloy sheets', *Proceedings 11th ICAS Conference*, Lisbon, 1978, 544–54.
46. van Veggel, L.H., Jongebreur, A.A. and Gunnink, J.W. (1987). 'Damage tolerance aspects of an experimental ARALL F27 lower wing skin panel', *Proceedings 14th ICAF Conference*, Ottawa.
47. Matway, T.J. (1991). 'Producibility and cost effectiveness of ARALL laminates, C17 aft cargo door skin: a case study', *Proceedings 12th European SAMPE Conference*, Maastricht, 373–9.
48. Gunnink, J.W. and Vogelesang, L.B. (1994). 'Fibre metal laminates and the very large civil transport', *Proceedings 15th International SAMPE Europe Conference*, Toulouse, 93–102.
49. Hooijmeijer, P.A. (2003). 'Cost reduction of Glare components', *Proceedings 35th International SAMPE Technical Conference*, Dayton OH, Society for the Advancement of Material and Process Engineering, Covina, CA, USA, CD-ROM, 10 pp.
50. Hooijmeijer, P.A. (2005). 'Impact on Glare fibre metal laminates', *Proceedings 26th International SAMPE Europe Conference*, Paris, 482–7.
51. Poston, K., Mattousch, A.C. and Matway, T.J. (1994). 'Impact properties and related applications of fiber metal laminates', *Proceedings 15th International SAMPE Europe Conference*, Toulouse, 103–13.
52. Schmidt, H.-J., Schmidt-Brandecker, B. and Tober, G. (1998). 'Design of modern aircraft structure and the role of NDI', *Proceedings 7th European Conference on Non-Destructive Testing*, Copenhagen, www.NDT.net, June 1999, Vol. 4 No. 6.
53. Woerden H.J.M., Mortier, W.J., Guijt, C.B. and Verhoeven, S. (2001). 'Bonded repair patches', in *Fibre Metal Laminates: an Introduction*, A. Vlot and J.W. Gunnink (eds), Kluwer Academic, Dordrecht, Netherland, 451–75.
54. Baker, A.A., Jones, R. and Rose, L.R.F. (eds) (2002), *Advances in the Bonded Composite Repair of Metallic Aircraft Structures*, Elsevier Science, Oxford, UK.
55. Fredell, R.S. (1994), *Damage Tolerant Repair Techniques for Pressurized Aircraft Fuselages*, PhD thesis, Delft University of Technology.
56. Vlot, A., Verhoeven, S., Ipenburg, G., Simpersad, D.R.C., Woerden, H.J.M. (2000). 'Stress concentrations around bonded repairs', *Fatigue and Fracture of Engineering Materials and Structures*, **23**(3), 263–76.
57. Volkersen, O. (1938). 'Die Nietkraft verteiling in zugbeanspruchten Nietverbindungen mit konstanten laschen Querschnitten', *Luftfahrtforschung*, **15**, 41–7.
58. Goland, M. and Reissner E. (1944). 'The stresses in cemented joints', *J. Appl. Mech.* A17–A27.
59. Vlot, A., Verhoeven, S., Nijssen, P.J.M. (1998). *Bonded Repairs for Aircraft Fuselages*, Series 07 Aerospace Materials, TU Delft.
60. Hart-Smith, L.J. (2006). 'The design of adhesively bonded joints', in *Symposium on Innovations in Bonded Structures*, Adhesion Institute TU Delft, April 2006.

© Woodhead Publishing Limited, 2010

61. Gleich, D. (2002). *Stress Analysis of Structural Bonded Joints*, PhD thesis, TU Delft.
62. van Ingen, J.W. and Vlot, A. (1993). *Stress Analysis of Adhesively Bonded Single Lap Joints*, Report LR-740, TU Delft.
63. Adams, R.D. and Wake, W.C. (1984). *Structural Adhesive Joints in Engineering*, Elsevier Applied Science, London, UK.
64. Hart-Smith, L.J. (1973). *Adhesive-bonded Single Lap Joints*, NASA Report CR 112236.
65. Ojalvo, I.U. and Eidinoff, H.L. (1978). 'Bond thickness effects upon stresses in single lap adhesive joints', *AIAA J.*, **16**(3), 204–11.
66. Williams, J.H. (1975). 'Stresses in adhesives between dissimilar adherends', *J. Adhesion*, **7**, 97–107.
67. Bigwood, D.A. and Crocombe, A.D. (1989). 'Elastic analysis and engineering design formulae for bonded joints', *Int. J. Adhesion and Adhesives*, **9**(4), 229–42.
68. Delale, F., Erdogan, F. and Aydinoglu M.N. (1981). 'Stresses in adhesively bonded joints: A closed form solution', *J. Composite Materials*, **15**, 249–71.
69. Yuceoglu, U and Updike, D.P. (1981). 'Bending and shear deformation effects in lap joints', *J. Engineering Mech. Division*, ASCE, **107**(1), 55–76.
70. Allman, D.J. (1977). 'A theory for elastic stresses in adhesive bonded lap joints', *Q. J. Mech. Appl. Math.*, **30**, 415–36.
71. Chen, D. and Cheng S. (1983). 'An analysis of adhesive-bonded single-lap joints', *J. Appl. Mech.*, **50**, 109–15.
72. Renton, W.J. and Vinson, J.R. (1977). 'Analysis of adhesively bonded joints between panels of composite materials', *J. Appl. Mech.*, **44**, 101–6.
73. Barut, A., Hanauska, J., Modeni, E. and Anbur, D.R. (2002). 'Analysis method for bonded patch repair of a skin with a cut-out', *Composite Structures*, **55**, 277–94.
74. Zhang, J., Bednarcyk, B.A., Collier, C., Yarrington, P., Bansal, Y. and Pindera, M-.J. (2005). '3D stress analysis of adhesively bonded composite joints', *49th AIAA/ASME/ASCE/AHS/ASC Structures, Structural Dynamics & Materials Conference*, Published by AIAA on a CD-ROM, Vol. 10, No. 6–7, 2005–21, 35 pp.
75. Roza, Z.C. and van Tooren, M.J.L. (1998). *Finite Difference Methods for Stress Analysis of Adhesive Bonded Joints. The Design of a MATLAB Adhesive Toolbox*, Aerospace Materials Series 07, No.10, TU Delft.
76. Jones, R. (2002). 'Numerical analysis and design', in *Advances in the Bonded Composite Repair of Metallic Aircraft Structures*, A. Baker, F. Rose and R. Jones (eds), Volume 1, Elsevier Science, Oxford, UK.
77. Carver, D.R. and Wooley, G.R. (1971). 'Stress concentration factors for bonded lap joints', *Journal of Aircraft*, **8**, 817–20.
78. http://femci.gsfc.nasa.gov/
79. Goncalves, J.P.M., De Moura, M.F.S.F. and De Castro, P.M.S.T. (2002). 'A three dimensional finite element model for stress analysis of adhesive joints', *Int. J. of Adhesion and Adhesives*, **22**, 357–65.
80. Zhu, Y. and Kedward, K. (2005). *Methods of Analysis and Failure Prediction for Adhesively Bonded Joints of Uniform and Variable Bondline Thickness*, DOT/FAA/AR-05/12, US Department of Transportation, Federal Aviation Administration.
81. Engelstadt, S.P., Berry, O.T., Renieri, G.D., Deobald, L.R., Mabson, G.E. and Dopker, B. (2005). 'High fidelity composite bonded joint analysis validation study – part 1 analysis', *49th AIAA/ASME/ASCE/AHS/ASC Structures, Structural Dynamics & Materials Conference*, Published by AIAA on a CD-ROM, Vol. 10, No. 6–7, 2005–2166, 16 pp.

© Woodhead Publishing Limited, 2010

82. Cornec, A., Scheider, I. and Schwalbe, K.H. (2003). 'On the practical application of the cohesive model', *Engineering Fracture Mechanics*, **70**(14), 1963–87.
83. Odi, R.A. and Friend, C.M. (2004). 'An improved 2D model for bonded composite joints', *Int. J. Adhesion and Adhesives*, **24**(5), 389–405.
84. Hart-Smith, L.J. (1987). 'Design of adhesively bonded joints', in *Joining Fibre-Reinforced Plastics*, F.L. Matthews (ed.), Elsevier Applied Science, London, UK.
85. Wang, C.H. and Chalkley, P. (2000). 'Plastic yielding of a film adhesive under multiaxial stresses', *Int. J. Adhesion and Adhesives*, **20**(2), 155–64.
86. Ignjatovic, M., Chalkley, P. and Wang, C. (1998). *The Yield Behaviour of a Structural Adhesive Under Complex Loading*, Report DSTO-TR-0728, DSTO, Australia.
87. Broughton, W.R., Crocker, L.E. and Gower, M.R.L. (2002). *Design Requirements for Bonded and Bolted Composite Structures*, NPL report MATC(A)65, NPL, UK.
88. Groth, H.L. (1988). 'Stress singularities and fracture at interface corners in bonded joints', *Int. J. Adhesion and Adhesives*, **8**(2), 107–13.
89. Johnson, W.S., Butkus, L.M. and Valentin, R.V. (1998). *Applications of Fracture Mechanics to the Durability of Bonded Composite Joints*, DOT/FAA/AR-97/56, US Department of Transportation, Federal Aviation Administration.
90. Kreuger, R. (2004). 'Virtual crack closure technique: history, approach and applications', *Appl. Mech. Rev.*, **57**(2), 109–43.
91. *ABAQUS Technology Brief*, TB-05-VCCT-1, Oct 2005.
92. Alderliesten, R.C. (2005). *Fatigue Crack Propagation and Delamination Growth in Glare*, PhD Thesis, TU Delft.
93. Minford, J.D. (1993). *Handbook of Aluminum Bonding Technology and Data*, Marcel Dekker, New York.
94. deVries, K.L. and Anderson, G.P. (1979). 'Analysis and design of adhesive bonded joints', in *Bonded Joints and Preparation for Bonding*, AGARD LS 102, NATO.
95. Anonymous, (2009). *Annual Book of ASTM Standards – Section 15 – General Products, Chemical Specialities, and End Use Products – Volume 15.06 Adhesives*, ASTM International.
96. Schulz, W.L., Udd, E., Seim, J.M., Perez, I. and Trego, A. (2000). 'Progress on monitoring of adhesive joints using multi-axis fiber grating sensors', *Proceedings of SPIE*, **3991**, 52.
97. Baker, W., McKenzie, I. and Jones, R. (2004). 'Development of life extension strategies for Australian military aircraft, using structural health monitoring of composite repairs and joints', *Composite Structures*, **66**, 133–43.
98. Mckenzie, I., Jones, R., Marshall, I.H. and Galea, S. (2000). 'Optical fibre sensors for health monitoring of bonded repair systems', *Composite Structures*, **50**, 405–16.
99. Lemmen, H.J.K., Alderliesten, R.C., Benedictus, R., Hofstede, J.C.J. and Rodi, R. (2008). 'The power of digital image correlation for detailed elastic–plastic strain measurements', in *Proceedings EMESEG 2008*, *New Aspects of Engineering Mechanics, Structures, Engineering Geology*, Heraklion, Crete Island, Greece, July 22–24 WSEAS Press, 73–89.
100. Krieger, R.B. (1988). 'Stress analysis concepts for adhesive bonding of aircraft primary structure', in *Adhesive Bonded Joints: Testing, analysis and design*, W.S. Johnson (ed.), American Society of Testing and Materials, 264–75.
101. Yang, C., Hyang, H., Tomblin, J.S. and Oplinger, D.W. (2001). 'Evaluation and adjustment for ASTM D-5656 standard test method for thick-adherend metal lap shear joints for determination of the stress strain behaviour of adhesives in shear by tensile loading', *J. Testing and Evaluation*, **29**(1), 36–43.

© Woodhead Publishing Limited, 2010

102. Bucci, R.J. (2006). 'Advanced metallic and hybrid structural concepts', *Proceedings USAF Structural Integrity Program Conference (ASIP 2006)*, San Antonio, TX.
103. Roebroeks, G.H.J.J., Hooijmeijer, P., Kroon, E. and Heinimann, M.B. (2007). 'The development of CentrAl', *Proceedings First International Conference on Damage Tolerance of Aircraft Structures*, TU Delft.
104. Fredell, R.S., Gunnink, J.W., Bucci, R.J. and Hinrichsen, J. (2007). '"Care-free" hybrid wing structures for aging USAF transports', *Proceedings First International Conference on Damage Tolerance of Aircraft Structures*, TU Delft.
105. D.E. Packham (ed.) (2006). *Handbook of Adhesion*, second edition, John Wiley & Sons, Hoboken, USA.
106. A.J. Kinloch (ed.) (1986), *Durability of Structural Adhesives*, Elsevier Applied Science, London, UK.
107. W.S. Johnson (ed.) (1988). *Adhesively Bonded Joints: Testing, Analysis, and Design*, ASTM Special Technical Publications STP 981, American Society for Testing and Materials ASTM, Philadelphia, USA.
108. E.W. Thrall and R.W. Shannon (eds) (1985). *Adhesive Bonding of Aluminum Alloys*, Marcel Dekker, New York.
109. A. Vlot and J.W. Gunnink (eds) (2001). *Fibre Metal Laminates: an Introduction*, Kluwer Academic Publishers, Dordrecht, Netherlands.

© Woodhead Publishing Limited, 2010

# 9
# Advances in bonding plastics

G. L. JIALANELLA, The Dow Chemical Company, USA

**Abstract**: There are many different approaches to adhesive bonding of plastics depending on the type of plastic. Difficult to bond plastics usually exhibit two characteristics, surface crystal structure or low surface energy. The surface energy can vary quite significantly depending on the chemistry of the plastic surface and is one of the main factors that determine wetting characteristics of the adhesive on the solid substrate or adherend. The bonding characteristics of low surface energy plastic are usually quite poor with conventional adhesives. Either surface treatments or self priming adhesives are generally used to circumvent these adverse surface effects. Although there are many surface treatments for plastics, the main emphasis for future direction is the use of self priming adhesive systems (organoboron catalyzed acrylic adhesives). The emphasis of this chapter is to discuss bonding techniques used for adhesive bonding of difficult to bond plastics.

**Key words**: surface energy, surface treatments, adhesion mechanisms, mechanical interlocking theory, electronic theory, adsorption theory, diffusion theory, plastics, adhesion, adhesives, primers, self priming

## 9.1 Introduction

The two basic requirements of adhesive bonding of plastic joints are the same as the requirements of metal or glass bonding. First, the adhesive must form intimate contact with the substrate. Second, bond formation between adhesive and substrate must occur. The result of fulfilling these requirements is the formation of an adhesive bond or intrinsic adhesion. The term adhesion is usually defined as the attractive forces between substances. It is very difficult to measure adhesion or the level of adhesion operating across an interface using mechanical tests. Therefore, experimentalists usually measure a macroscopic unit referred to as adhesive performance. The expression 'adhesion performance' is used because it is dependent on many aspects of the adhesive system and application. There are four factors on which adhesive performance is strongly dependent: (1) surface characteristics, (2) rheology, (3) material properties and (4) service life. When designing adhesive systems for plastics these four factors are crucial. This chapter will focus on primarily surface characteristics with a minor discussion of wetting.

As mentioned above, a crucial requirement for developing strong adhesive bonds is that intimate contact between the adhesive and substrate is established.



© Woodhead Publishing Limited, 2010

This means that the adhesive or primers (if one is used) must readily spread on the surface of the substrate. In doing so, the adhesive must displace air or surface contaminants. The ability of the adhesive to spread spontaneously on the surface of the substrate is a function of two parameters: (1) surface characteristics and (2) rheology.

## 9.2 Adhesion mechanisms in bonding plastics

The previous section discussed the two essential requirements for adhesion, intimate contact of the adhesive with the substrate and bond formation. The bond formation is an essential process in attaining good joint performance. For practical adhesives, the bonds between the adhesive and substrate should be stronger than the cohesive strength of the adhesive. Otherwise, the adhesive/substrate interface will be the weak link and the joint will fail at this interface. Typically, this type of failure is unacceptable to the end user. Therefore, the adhesive design must account for developing these forces across the interface and producing intrinsic adhesion. Significant work has focused on trying to measure bond forces across the adhesive/substrate interface (intrinsic adhesion), but success has not been forthcoming. The main reason for the lack of success is that tests measure the strength of the joint and this strength is a function of many factors such as loading rates, joint dimensions, rheology of the adhesive, and material properties of the joint. Thus, adhesive performance tests are not designed to measure intrinsic adhesion independently of the contributions of the joint or even a small contribution from the adhesive properties.

Although intrinsic adhesion cannot be easily measured, it significantly influences joint strength. There are a number of techniques that can be used to develop effective bonds across the adhesive/substrate interface (intrinsic adhesion forces) and theories as a result of these techniques are usually referred to as mechanisms of adhesion. As outlined by Kinloch (1987), the four mechanisms of adhesion are (1) mechanical interlocking, (2) electronic, (3) adsorption theories and (4) diffusion. These theories explain the development of the adhesive force on a microscopic basis and in some cases on a molecular level. The theories have wide applicability, especially in plastic bonding, but none individually can explain all adhesive interactions. As pointed out in the subsequent discussion, the various mechanisms of adhesion apply to specific types of adhesives and adherends.

### 9.2.1 Mechanical interlocking theory

Mechanical interlocking theory is a macroscopic theory, which can be used to explain intrinsic adhesion, but not on a molecular level. The best example of the use of mechanical interlocking is in dentistry. The cavity is shaped

© Woodhead Publishing Limited, 2010

so that the area inside the tooth is larger than the area close to the surface of the tooth. The filling is held in the tooth by the larger portion below the surface of the tooth. This approach is used because the adhesion between the tooth and the amalgam filling is poor.

Plating of plastics is another example where mechanical interlocking may improve the intrinsic adhesion. In this case, a chemical pretreatment is used to treat the surface of the plastic prior to the metal plating. The effect of the chemical treatment has been debated. Kato (1967, 1968) showed that the improved adhesion is a result of the surface roughening of the plastic. However, some researchers believe that the increased oxidation has a greater impact on the adhesion than the increased roughening from the chemical treatment. Although this work is not related to plastic bonding, Jennings (1972) studied the effect of surface roughness of aluminum and stainless steel substrates with epoxy and silicone adhesives. The joint strengths (butt and shear joints) were higher with increased surface roughness. He also found that chromate etch afforded stronger bonds, but usually much less than when the surfaces were mechanically abraded. The improvements in butt tensile strength are shown in Tables 9.1 and 9.2 (Jennings, 1972).

In all cases, the adhesive system consisted of D.E.R.™ 332 epoxy resin (trademark of The Dow Chemical Company) and Versamide 140 curing agent which is a diglycidyl ether of bisphenol-A and a polyamide curing agent, respectively. The five groups in Table 9.1 were all solvent cleaned and chromate etched prior to applying the adhesive in order to keep a consistent surface preparation. The data clearly shows that the butt tensile strengths increased with increased abrasion. Sandblasted surfaces gave the highest strengths, followed by sandpaper. The data in Table 9.2 shows the effects of surface roughening for aluminum (6061) and for stainless steel (304) in which the surfaces were polished or sandblasted. The sandblasted surfaces showed higher strengths. In some cases, joint strengths were higher than the strength of the bulk adhesive. The fracture occurred on a plane across the ridges, but the epoxy remained in the valleys of the surface of the metal.

*Table 9.1* Joint strengths with abraded and chromate etched 6061 Al adherends and DER™ 332 epoxy resin (trademark of The Dow Chemical Company) and Versamide 140 (60/40) curing agent (Jennings, 1972)

| Adherend surface | Butt tensile strength (MPa) |
|---|---|
| A. Polished, 1μm diamond dust | 28.8 ± 7.0 |
| B. Abraded through 600 paper | 30.9 ± 7.7 |
| C. Abraded through 280 paper | 39.0 ± 6.8 |
| D. Abraded through 180 paper | 36.7 ± 7.5 |
| E. Sandblasted (40–50 grit) | 48.5 ± 7.0 |

Note: Five groups, A through E, were each solvent cleaned, chromate etched, bonded and cured (Jennings, 1972). Reprinted with permission of Taylor & Francis.

© Woodhead Publishing Limited, 2010

*Table 9.2* Effect of surface geometry on butt tensile strength of DER™ 332- (trademark of The Dow Chemical Company) Versamide 140 (60/40) epoxy joints cured for 16 hours at 74°C. Adherend surfaces were chromate etched (Jennings, 1972)

| Adherend | | Adherend surface | Butt tensile strength (MPa) |
|---|---|---|---|
| 6061 | Al | Polished | 32.5 ± 6.9 |
| 6061 | Al | 0.005 inch groves, negative bondline[a] | 34.8 ± 5.2 |
| 6061 | Al | 0.005 inch grooves | 44.3 ± 3.4 |
| 6061 | Al | 0.005 inch grooves, sandblasted | 48.4 ± 7.7 |
| 6061 | Al | Sandblasted (40–50 grit) | 54.6 ± 3.7 |
| 6061 | Al | Sandblasted (10–20 grit) | 53.0 ± 3.6 |
| 304 | SS | Polished | 27.8 ± 5.79 |
| 304 | SS | Lapped to $2\lambda$[b] | 32.5 ± 5.9 |
| 304 | SS | 0.010 inch grooves, negative bondline | 34.9 ± 2.3 |
| 304 | SS | 0.010 inch grooves | 35.2 ± 7.0 |
| 304 | SS | 0.010 inch grooves, sandblasted | 38.0 ± 5.3 |
| 304 | SS | Sandblasted (40–50 grit) | 53.4 ± 5.8 |
| 304 | SS | Sandblasted (10–20 grit) | 62.9 ± 3.2 |

Note: [a] Grooves meshed: all other joints had an 0.005 inch bondline.
[b] Surface not polished
Source: Jennings, 1972. Reprinted with permission of Taylor & Francis.

### 9.2.2 Electronic theory

The electronic theory was studied extensively by Weaver (1972, 1975). This theory has little application to plastic bonding and thus, will not be discussed in this chapter.

### 9.2.3 Adsorption theory

The adsorption theory deals with the intermolecular interaction between the adhesive and surface of the substrate. Specifically, the forces of attraction between the atoms of the molecules in the adhesive and the atoms of the molecules on the surface of the substrate form intermolecular bonds. This intermolecular bond formation results in adhesion. Intermolecular bond formation can be divided into two categories: (1) primary bond formation and (2) secondary bond formation. Primary bond formation is the result of a covalent or ionic bond acting between two functional groups across the bond interface. Secondary bond formation is a result of the common intermolecular interaction such as van der Waals forces of attraction. The adsorption theory is the most widely applicable to adhesive applications. It has been successfully used to describe adhesive bonding to metals, glass and other non-polymeric materials. Ahagon and Gent (1976), Chang and Gent (1981b) and Gent (1981) have documented the formation of primary

© Woodhead Publishing Limited, 2010

bonds in adhesive joints consisting of two elastomers. This bonding process is particularly important when bonding elastomers that will be subsequently vulcanized.

### *Primary bond formation*

As mentioned above, primary bond formation is a result of primary bonds forming across the adhesive–substrate interface. Also, primary bond formation is either ionic or covalent. Most of the plastic bonding examples in the literature are examples of covalent bond formation. A typical example of an ionic bond occurs when a polymer with carboxylic acid bonds to a metal such as zinc. Since this chapter deals with plastic bonding, these examples will not be discussed.

Chang and Gent (1981b) have extensively studied covalent bond formation between elastomer adhesives and a substrate of similar chemical composition and dissimilar chemical composition (Chang and Gent, 1981a). In the case when the adherend has a similar composition, the effect of interfacial bond strength was evaluated by measuring the tearing energy or work of detachment as a function of cross-link density of the elastomers. The degree of cross-linking was varied from zero, when the two fully reacted sheets were joined, up to levels characteristic of those found in the bulk of the elastomer. Chang and Gent found that the tearing energy increased with increased cross-link density at the interface.

Similar results were found for the case of dissimilar adherends (Chang and Gent, 1981a). This type of adhesion is extremely important in the manufacture of rubber goods, especially tires. Tires are made of numerous plies of compatible and incompatible rubber. These plies are required to adhere during the vulcanization process. For example, plies of polystyrene-co-polybutadiene (SBR) are required to adhere to other plies of SBR and are required to adhere to plies of butyl rubber. In these cases, the mechanism of adhesion is primary bonding between the adhesive layers.

### *Secondary bond formation*

Adhesion resulting from secondary bond formation forms from intermolecular forces of attraction usually referred to as van der Waals forces. These attractive forces are a result of the interaction of neighboring molecules and there are three types of interaction: (1) dipole interactions, (2) hydrogen bonding interactions and (3) molecule–molecule interactions (London dispersion forces). As stated previously, the adsorption theory is the most applicable to adhesive bonding and, particularly, secondary bond formation has the most applicability. It has extensive applicability in metal bonding as well as plastic bonding.

© Woodhead Publishing Limited, 2010

Owens (1975) examined the mechanism of self adhesion for corona-treated polyethylene (PE) film. The adhesive joints were prepared by corona treating the polyethylene films followed by contacting the films at 75°C and 0.17 MPa. The corona treatment significantly increased joint strength. Peel strengths ranged from zero for the untreated films up to 77.2 N $m^{-1}$ for the corona treated films. This ascertained the nature of the bonds by examining the effect of thermal and chemical treatments on joint strength.

Thermal treatment dramatically affected joint strength as shown in Table 9.3 (Owens, 1975). As these data show, the joint strength significantly decreased from 48.3 N $m^{-1}$ at 60°C to 3.86 N $m^{-1}$ at 80°C.

Similarly, as shown in Table 9.4 (Owens, 1975), chemical treatments can dramatically affect joint strength depending on the chemical nature of the treatment. When the joints were exposed to acetyl chloride, bond strength decreased from 63.7 to 11.6 N $m^{-1}$. However, when the joints were exposed to heptane, the joint strength was unaffected by this treatment. The authors explained this behavior based on the chemical nature of the adhesive bond. They claimed that the adhesive bonds from corona treatments should be a result of hydrogen bonding by the polar functional groups formed from the treatment. If this is the case, then thermal treatment at around 80°C should have an impact on the strength because this temperature provides kinetic

*Table 9.3* Effect of heating corona-treated PE film prior to bond formation (Owens, 1975). Reprinted with permission of John Wiley & Sons

| Heating temperature (°C) | Bond strength (N $m^{-1}$) |
|---|---|
| 60 | 48.3 |
| 65 | 27.0 |
| 70 | 13.5 |
| 80 | 3.9 |

*Table 9.4* Effect of chemical treatments on bond strength of corona-treated PE film (Owens, 1975). Reprinted with permission of John Wiley & Sons

| Treatment | Conditions | Bond strength (N $m^{-1}$) |
|---|---|---|
| None | Control | 63.7 |
| Acetyl chloride | 20% in heptane, 50°C, 10 min | 11.6 |
| Acetic acid | 20% in heptane, 50°C, 10 min | 73.4 |
| Heptane | 20% in heptane, 50°C, 10 min | 63.7 |
| Bromine water | 20°C, 10 min | 0 |
| $HNO_2$ | 0°C, 10 min | 3.86 |
| $HNO_3$ (2N) | 20°C, 10 min | 50.2 |
| HCl (2N) | 20°C, 10 min | 57.9 |
| $H_2SO_4$ (2N) | 20°C, 10 min | 59.8 |
| NaOH (2%) | 20°C, 10 min | 61.8 |
| Phenylhydrazine | 40°C, 10 min | 7.7 |

© Woodhead Publishing Limited, 2010

energy greater than the energy of hydrogen bonding. Thus, the hydrogen bonds should break, thereby reducing joint strength. The chemical treatment would affect the joint strength more for compounds that can prevent hydrogen bonding as is the case for the acetyl chloride but is not the case for heptane. These effects were observed experimentally. Therefore, the authors claim the functional groups on the surface of the polyethylene films form hydrogen bonds (secondary bonds) and not covalent or ionic bonds.

McLaren (1948), McLaren and Sieler (1949) and McLaren *et al*. (1951) have studied factors affecting adhesion to numerous substrates including plastics. They were the first to identify that adhesion of polymers involves an intricate composite of physicochemical factors including surface tension, wetting absorption, intermolecular forces and numerous material properties. Primarily, adhesion of polymers to cellulose was examined. This work showed that tack, dielectronic properties, and the dipole moment of the polymers are extremely significant. Their conclusion was that adhesion is strongest when the dipole moments of the adhesive and substrate polymer are equal. This conclusion indicates that intermolecular forces provide the adhesive forces.

### 9.2.4 Diffusion theory

The diffusion theory states that adhesion between polymers is a result of mutual diffusion across the interface and has some applicability to plastic bonding. In fact, one way of getting an adhesive to bond to a plastic substrate is to have a component in the adhesive system which can promote dissolution of the plastic substrate. This theory was originally proposed by several Russian researchers as a mechanism of adhesion for elastomers above the glass transition temperature, $T_g$ (Allen, 2003). Voyutskii (1956), Voyutskii and Vakula (1963) and Voyutskii *et al*. (1965) originally proposed this theory and have studied it extensively. They used the concepts from this theory to solve adhesion problems and to identify adhesion performance. Their work was to identify the role of diffusion phenomena and provide specific evidence to identify the mechanism of adhesion in polymer as polymer adhesion.

In many cases depending on the type of polymer, adhesion of polymers is dependent on the interdiffusion of the polymers. Voyutskii and co-workers claimed that this was especially true for non-polar polymers such as polyolefins, polybutadiene and polyisoprene. In these cases, polymer entanglement must be the primary factor which promotes adhesion because of the lack of polar functional groups. Their findings showed that temperature, contact time, polymer type and molecular weight, and viscosity strongly affected diffusion of the adhesive polymer and substrate polymer and ultimately affected the adhesive strength. The following is a list of observations they claimed substantiated the diffusion theory.

© Woodhead Publishing Limited, 2010

The first observation is contact time. Voyutskii and co-workers claimed that contact time between the adhesive and adherend is one of the most substantial proofs of the diffusion theory. They observed that the adhesive strength increased with increasing contact time and reached a limiting value for a solvent-based butadiene-acrylonitrile copolymer.

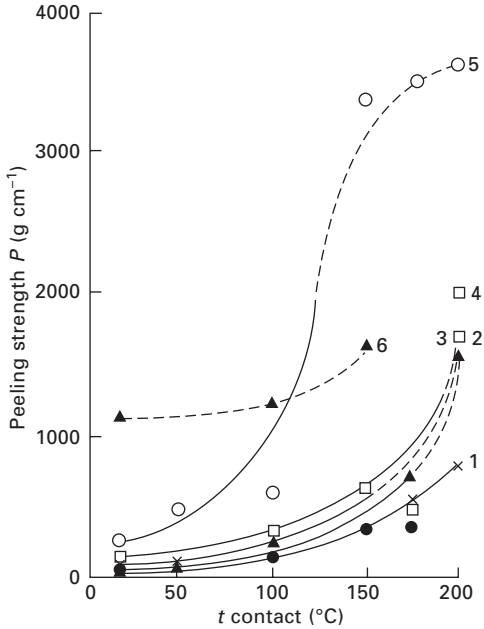
Second, the effect of thermal treatment of the bondline was examined for a solvent-based butadiene-acrylonitrile copolymer bonded to cellophane. The results of these experiments showed that the adhesive performance increased with thermal treatment. These results were explained by the fact that polymer diffusion is temperature dependent. As the Brownian motion of molecules increase with temperature, the mobility and diffusion of polymers is also increased.

Third, the effect of polarity of the solvent-based butadiene-acrylonitrile copolymer bonded to polyamide substrate was examined by varying the acrylonitrile content. The results clearly showed that the copolymers with the lower acrylonitrile content (10–22% w/w) exhibited better adhesion than the copolymers with a higher acrylonitrile content (40% w/w). The rational for these results is that the polarity does not have the impact on adhesion that might be expected. However, the amount of acrylonitrile does have an impact on diffusion because of the lower solubility of acrylonitrile containing polymers. Thus, diffusion is the main driver for adhesive performance in this system.

Finally, Voyutskii and Vakula (1963) discuss the effect of molecular weight fractions of a butadiene-acrylonitrile copolymer on adhesive performance when bonded to a polyamide. Figure 9.1 (Voyutskii and Vakula, 1963) shows that the molecular weight fraction of 100,000 g $mol^{-1}$ exhibits the best adhesion performance. Their claim is that the molecular weight dependence on adhesive performance clearly illustrates the dependence on diffusion between the adhesive polymer and adherend polymer. Thus, this work supports the diffusion theory as a main theory explaining polymer–polymer adhesion.

Lee (1967) recognized that the adsorption and diffusion theories of adhesion have limitations and do not have broad applicability. In understanding these limitations, a classification system was developed to restrict application of these theories. These classifications were designed to identify three distinct types of polymer adhesion on the basis of the physical state of the adhesive and adherend, (1) rubber polymer–rubber polymer (R–R adhesion), (2) rubbery polymer–glassy polymer (R–G adhesion) and (3) rubber polymer–non-polar polymer (R–S adhesion). They found by defining the physical state that many of the discrepancies can be eliminated when applying the diffusion and adsorption theories of adhesion. They found that diffusion of polymer molecules can greatly be affected by the physical state of the polymers as predicted by the Bueche–Cashin–Debye equation (Bueche *et al.*, 1952):

© Woodhead Publishing Limited, 2010




*9.1* Peeling strength *P* of the bonded samples of polyamide with different fractions of butadiene-acrylonitrile copolymer with 42% nitrile vs. temperature of thermal treatment of the bonded samples (1) Fraction with molecular weight 550,000; (2) fraction with molecular weight 524,000; (3) molecular weight 278,000; (4) molecular weight 266,000; (5) molecular weight 100,000; (6) molecular weight 20,000 (Voyutskii and Vakula, 1963). Reprinted with permission from John Wiley & Sons.

$$D_n/p = (AkT/36)(R^2/M) \quad [9.1]$$

where $A$ is Avagadro's numbr, $k$ is Boltzmann's constant, $T$ is the absolute temperature, $R^2$ is the mean square end-to-end distance of a single polymer chain and $M$ is the molecular weight. Using this equation, Lee (1967) calculated diffusion coefficients below and above the glass transition temperatures ($T_g$). Lee (1967) found that below the polymer's $T_g$, the diffusion of polymers is so slow at room temperature that it becomes insignificant.

Vasenin (1965) examined diffusion theory and developed models for quantitative predictions of adhesion. From these models he concluded that various theories of adhesion, adsorption, diffusion, electronic and mechanical theories have been proposed, but none of these theories can explain all of the facts of adhesion phenomena. The applicability of each theory is limited based on the adhesive type and adherend type. Moreover, it is very difficult to study applicability owing to the complexity of adhesion phenomena and the large number of factors involved. For example, the mechanical theory of

© Woodhead Publishing Limited, 2010

adhesion can only predict adhesion for highly structured surfaces when the rheology of the systems allows wetting of the highly structured surfaces. So time, rheology and temperature can be additional factors affecting wetting and ultimately adhesion.

The electronic theory of adhesion works for adhesive/adherend systems where a charge is capable of being developed. Adsorption theory works for only polar adhesive/adherend systems. Although this theory has some applicability in describing adhesion to polymer adherends (plastics), it has virtually no applicability for non-polar adherends.

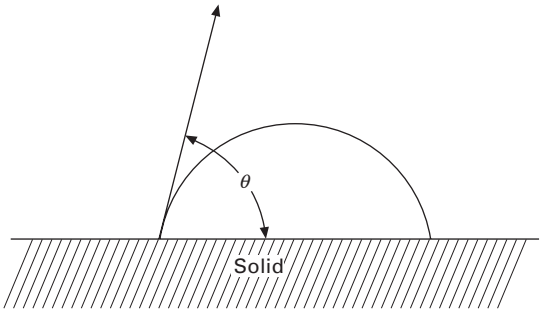
The diffusion theory of adhesion appears to have the broadest range of applicability for adhesion to polymers (plastics). However, certain limitations do exist. This theory can only describe adhesion when the adhesive and adherend exhibit mutual solubility or miscibility. It cannot be used to describe adhesion to cross-linked rubbers or plastics or crystalline plastics. The author of this chapter believes that these theories of adhesion have good utility, but are system dependent.

## 9.3 Surface characteristics affecting plastic bonding

The surface energy of a solid is one of the most important and fundamental properties of an adherend. The surface energy can vary significantly depending on the chemistry of the particular solid. For adhesive bonding, surface energy is one of the main factors that determine the wetting characteristics of the adhesive on the solid substrate or adherend. Certainly, the rheology of the adhesive is another property which significantly affects the wetting or flow properties of the adhesive. However, this topic will not be covered in this chapter.

As discussed earlier in this chapter, adhesive bonds can only form after the adhesive has thoroughly wetted the surface and displaced any contaminants. Ideally, the surface energy of the adherend should be of significant magnitude to overcome the surface tension of the individual droplets of the adhesive. The capability of a liquid to wet a solid can be measured by the contact angle. Typically, the contact angle of the adhesive is not measured, but the contact angle is measured for the solid surface with a number of conventional liquids. These liquids are placed on the solid surface and will form a droplet, as illustrated in Fig. 9.2. When theta is small, the surface tension of the liquid is overcome by the attractive forces of the surface energy of the solid and the liquid spreads out or wets the solid. Conversely, when theta is large, the attractive forces of the solid are not strong enough to overcome the surface tension of the adhesive. Thus, the adhesive forms discrete droplets on the surface of the solid. This contact angle is an extremely powerful analytical tool for ascertaining the type of chemistry on the surface of a

© Woodhead Publishing Limited, 2010




*9.2* Liquid droplet on a solid surface demonstrating the contact angle $\theta$.

solid. Experimentally, these contact angle measurements are completed for a prescribed set of liquid types and surface energy is calculated.

Typical data for surface energies of a number of different solids are shown in Table 9.5 (Adhesive and Sealant Council). There is a very broad range of surface energies depending on the chemical composition of the solid. Aluminum has the highest surface energy, 850 mJ $m^{-2}$, of any material in this table.

It is well known that most typical adhesive systems can easily wet and in most cases bond to aluminum. Interestingly, plastics have a much lower surface energy by more than an order of magnitude compared to aluminum. Nylon, polyvinyl chloride (PVC), polymethyl methacrylate (PMMA), polyethylene terephthalate (PET) and acrylonitrile-butadiene-styrene copolymers (ABS) exhibit surface energies above 40 mJ $m^{-2}$.

Finally, the hydrocarbon, fluorocarbon and silicone solids, polyethylene, polypropylene (PP), Teflon and polydimethylsiloxane have the lowest surface energy. As a general rule, if the surface energy is above 40 mJ $m^{-2}$, then this surface energy is sufficiently large to overcome the surface tension of the adhesive. However, attainment of this requirement does not ensure good adhesion. Other surface characteristics such as crystal domains, low molecular weight species and contaminants may prevent bond formation between the adhesive and adherend. Surface energy is a prerequisite for adhesion and should be considered when developing an adhesive system. However, it is not a guarantee of good bond formation.

## 9.4 Surface treatments used in bonding plastics

### 9.4.1 Introduction

Surface treatments can be an essential part of adhesive bonding depending on the type of substrate. As in the case of high energy surfaces, such as metals,

© Woodhead Publishing Limited, 2010

*Table 9.5* Surface energies of common adherends (Adhesive and Sealant Council)

| Substrate | Surface energy (mJ $m^{-2}$) |
|---|---|
| Aluminum | 850 |
| Kapton (R) | 50 |
| Nylon 6,6 | 46 |
| Acrylonitrile butadiene styrene | 42–55 |
| Polyethylene terephthalate | 47 |
| Polyethylene | 31 |
| Teflon/polydimethyl siloxane PDMS | 20 |
| Polypropylene | 30 |
| Poly(methyl methacrylate) | 41 |

surface treatments may not be used. However, this is often not the case for plastics. As was shown in Table 9.5, plastics generally have a much lower surface energy than metals, albeit the lower surface energy alone does not prevent good bond formation. From a surface chemistry point of view, there are three factors that affect adhesive performance. As mentioned previously, the magnitude of surface energy of the adherend must be sufficient to overcome the surface tension and impart wetting to the adhesive. The quantity (if any) of crystalline domains and a loose boundary layer residing on the surface of the adherend can have a significant impact on adhesive performance. Surface treatments are generally used to circumvent these adverse surface effects.

### 9.4.2 Solvent treatment

Solvent as a wipe is mostly used to remove any contaminants residing on the surface as a result of the manufacturing of the component. These contaminants are typically mold release agents and low molecular weight species from the bulk polymer. This type of cleaning can be used for either high-energy or low-energy surfaces. Solvents have also been used to promote adhesion by placing them in the adhesive formulation or by solvent soaking the substrate prior to bonding. Cements based on solvent/polymer systems have been used extensively for bonding thermoplastic adherends. The primary example of a solvent-based adhesive is used for assembling polyvinyl chloride (PVC) components. This type of adhesion is referred to as solvent welding. Solvent-based adhesive systems have been used extensively in the aerospace, automotive, construction, furniture and general manufacturing.

The use of solvents for surface modification of plastics has been extensively studied for paint adhesion. Schuman and Thames (2005) studied the effect of a variety of solvent types on adhesion of coatings to PP and ethylene–styrene copolymers. They found that the chemical nature of the solvent in the coating had a strong impact on the adhesion of the coating. Interestingly, the affinity

© Woodhead Publishing Limited, 2010

of the solvent with a higher solubility character for the adherend as defined by the Flory interaction parameter was not a good indicator of the resultant adhesive character of the coating. In other words, the ability of a solvent to swell the adherend usually was not indicative of its ability to promote adhesion. Additionally, coating solvents that gave moderate or slow rather than fast swelling rates appeared to afford the greatest topographical changes. Thus, the change in surface topography was the main driver for improved coating adhesion.

As expected, Schuman and Thames found that surface crystalline domains had an impact on adhesion. Crystalline domains reduce the ability of the solvent to alter the topography of the adherend and thus reduce coating adhesion. However, alteration of the surface topography through solvent exposure also improved adhesion even with higher surface crystallinity. Schuman and Thames (2004) also showed that altering the surface topography of the adherend exhibited the most significant impact on adhesion. This work clearly indicates that since enhancing the surface topography improved adhesion, this adhesion improvement can be explained by a mechanical interlocking mechanism.

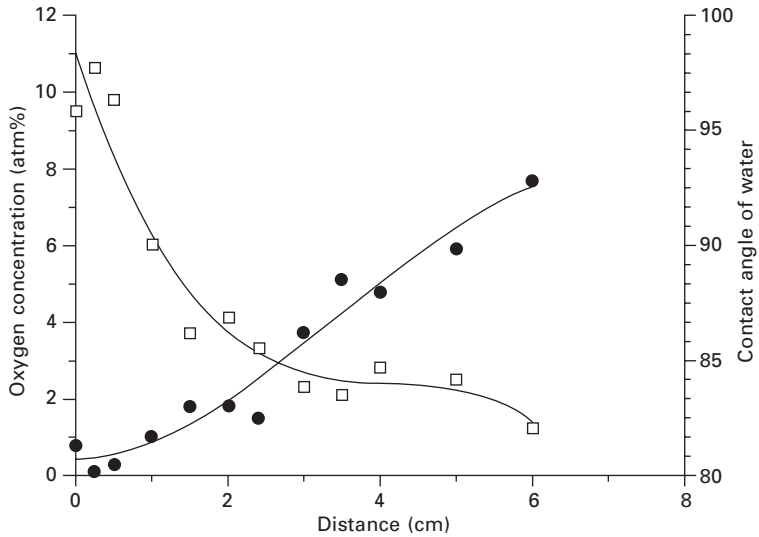
### 9.4.3 Flame treatment

The use of flame treatment to modify polypropylene substrate (Sutherland *et al.*, 1991; Green *et al.*, 2002), rubber modified polypropylene (Sutherland *et al.*, 1994) and polyethylene (Sutherland *et al.*, 1994) has been studied using X-ray photoelectron spectroscopy (XPS), contact angle measurements and adhesion tests. These studies focused on evaluating the surface chemistry and comparing the changes in surface chemistry with changes in adhesive performance.

Sutherland *et al.* (1991) studied the effect of air-to-gas ratio, flow rate, distance from inner core of the flame and contact time of the flame on the amount of surface oxygen content measured by XPS. The air-to-gas ratio and flow rates of the gas exhibited lower critical concentrations of 10% air and 25 l $min^{-1}$, respectively. Values above these numbers did not show an improvement in surface oxygen content and contact angle. The distance from the inner core of the flame strongly affected the surface oxygen content and contact angle. Once the distance exceeded 1 cm, the contact angle increased and the surface oxygen content decreased rapidly, as shown in Figure 9.3 (Sutherland *et al.*, 1991). Surprisingly, the flame contact time had little effect on surface oxygen content and contact angle.

The data in Table 9.6 (Sutherland, 1991) show tensile strength of a polyurethane paint on a polypropylene plastic as a function of air-to-gas ratio, total flow rate and distance from the inner core of the flame. The tensile strength using a butt joint did not show a dependence on the air-to-

© Woodhead Publishing Limited, 2010




*9.3* Effect of changing the distance between the inner tip and the polypropylene surface. The total flow rate was held constant at 24 l $min^{-1}$ and the air-to-gas ratio held at 11:1 (Sutherland *et al.*, 1991). Reprinted with permission of John Wiley & Sons (open squares correspond to contact angle, filled circles correspond to oxygen concentration).

*Table 9.6* Tensile strength of polyurethane-painted polypropylene (Sutherland *et al.*, 1991). Reprinted with permission of John Wiley & Sons

| | | Tensile strength (MPa) | Standard deviation (MPa) | Locus of failure |
|---|---|---|---|---|
| Air-to gas ratio[a] | 16:2 | 24.7 | 3.6 | Complex |
| | 18:2 | 25.4 | 2.5 | Complex |
| | 22:2 | 26.4 | 2.6 | Complex |
| | 26:2 | 26.7 | 2.3 | Complex |
| | 28:2 | 25.8 | 3.0 | Complex |
| Total flow rate[b] (l $min^{-1}$) | 12 | 26.0 | 2.0 | Paint/polymer interface |
| | 18 | 25.6 | 2.1 | Complex |
| | 24 | 26.4 | 2.6 | Complex |
| | 36 | 27.2 | 1.2 | Complex |
| | 48 | 24.0 | 3.0 | Complex |
| Distance from inner cone tip[c] (cm) | 0.25 | 22.8 | 2.9 | Complex |
| | 1.0 | 26.4 | 2.6 | Complex |
| | 2.0 | 22.1 | 1.7 | Complex |
| | 4.0 | 6.5 | 1.6 | Paint/polymer interface |
| | 6.0 | 4.2 | 0.5 | Paint/polymer interface |

[a] Total flow rate 24 l $min^{-1}$; distance 1 cm
[b] Air-to-gas ratio 11:1; distance 1 cm
[c] Air-to-gas ratio 11:1; total flow rate 24 l $min^{-1}$ (Sutherland *et al.*, 1991).

© Woodhead Publishing Limited, 2010

gas ratio and total flow rate because these values were measured above the minimum critical values. However, the distance from the inner core resulted in a decrease in tensile strength at about 2 cm.

### 9.4.4 Ionizing environments

Ionizing environments have been used to modify the physical and chemical states of plastics. One method is called a plasma treatment. A plasma treatment is a gas generated by an electric field under reduced pressure or in a vacuum. Provided that the electric field is sufficiently strong, the atoms of the gas will lose an electron and become ionized. When this ionized gas is accelerated through the electric field, the electrons and ions will bombard the surface of a material, induce reactivity and cause chemical changes. When air at atmospheric pressures is used as the ionizing gas, this process is called corona discharge and when air is used under reduced pressures, this process is called glow discharge. Primarily, the desired effect of exposing a plastic to these ionizing environments is to improve adhesion.

### 9.4.5 Plasma treatments

Plasma treatment has been used extensively to induce chemical and physical changes in PP, PET, polyamide, (PA) and high density polyethylene (HDPE) (Noeske *et al.*, 2004; Stewart *et al.*, 2005). Extensive studies examined the effects of polybutylene terephthalate (PBT) (Anagreh and Dorn, 2005) and polyetheretherketone (PEEK) (Comyn *et al.*, 1996b).

The work of Noeske *et al.* (2004) consisted of exposing the plastic to plasma and measuring the changes in contact angle, surface functionality and adhesion. The lap shear strength and surface energy results are shown in Table 9.7 (Noeske *et al.*, 2004) for HDPE, PP, PVDF, PET and PA6.

In all cases, there was a significant increase in lap shear strength and surface energy when the plasma treatment was applied to the substrate prior to bonding. Also, the failure modes were either substrate breakage or cohesive failure for the pretreated substrate compared to adhesive failure for untreated substrates. As expected, the oxygen and nitrogen content on the surface of the polymer measured by XPS increased with plasma treatment. Adhesion was also affected by topography changes in the adherend. Influential factors such as contact area, unfilled volumes between the adherend and microscopic roughness can lead to improved adhesive performance. The surface topographies of PET and PVDF were studied using atomic force microscopy (AFM). The AFM images for the PET and PVDF are shown in Figs. 9.4 and 9.5 (Noeske *et al.*, 2004).

The initial surface characteristics of the PET and the PVDF are different whether examined on a 10 μm or 30 μm scale. The PET surfaces are mostly

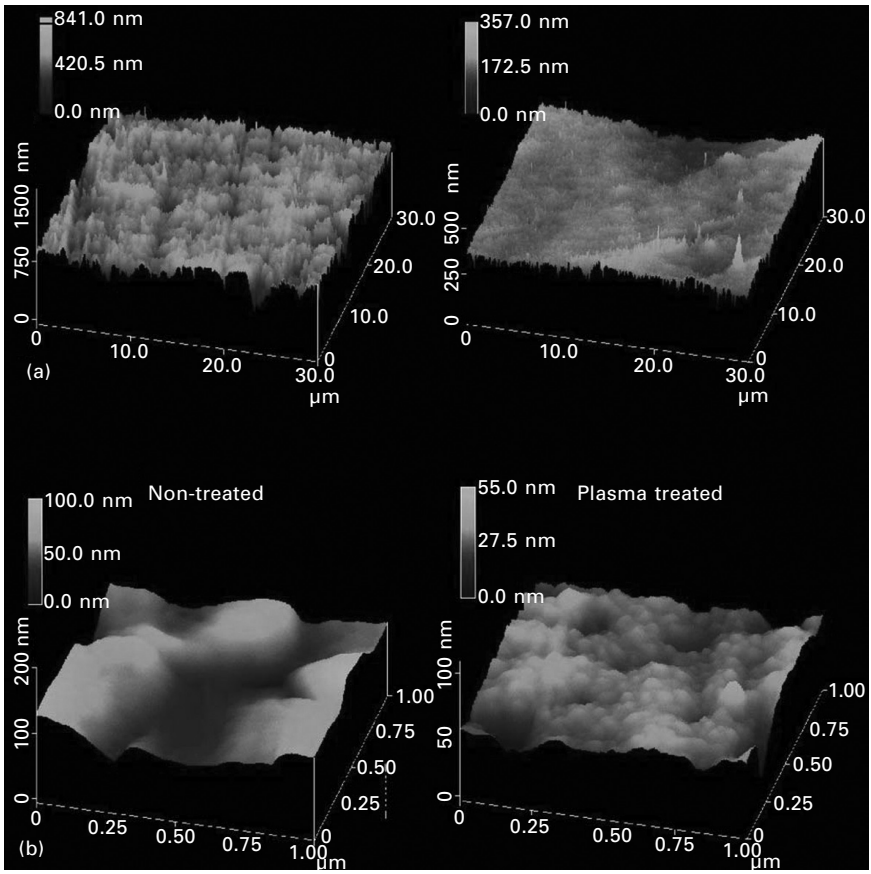
© Woodhead Publishing Limited, 2010

*Table 9.7* Adhesion and surface properties of the polymers studied (Noeske *et al.*, 2004). Reprinted with permission of Elsevier Limited

| | | HD-PE | | PP | | PVDF | | PET | | PA6 | |
|---|---|---|---|---|---|---|---|---|---|---|---|
| | | Ref. | Plasma | Ref. | Plasma | Ref. | Plasma | Ref. | Plasma | Ref. | Plasma |
| Lap shear strength (MPa) | | 0.3 | 4.6[a] | 0.2 | 3.7[b] | 0.6 | 8.9[b] | 1.6 | 4.8[a] | 1.9 | 7.8[a] |
| Surface energy (mN $m^{-1}$) | | 28 | 60 | 27 | 52 | 35 | 42 | 35 | 63 | 35 | 62 |
| Atmospheric concentration (%) | O | 2.0 | 24.4 | 3.1 | 8.7 | 3.1 | 6.8 | 15.2 | 32.4 | 11.9 | 23.8 |
| | C | 98.0 | 71.5 | 96.2 | 91.3 | 54.6 | 49.5 | 84.5 | 65.3 | 76.6 | 64.1 |
| | N | — | 3.4 | — | 0.3 | 41.7[c] | 42.3[c] | 0.3 | 1.7 | 10.5 | 12.1 |

[a] Substrate failure mode
[b] Cohesive failure mode
[c] Atmospheric concentrations of fluorine (Noeske *et al.*, 2004)

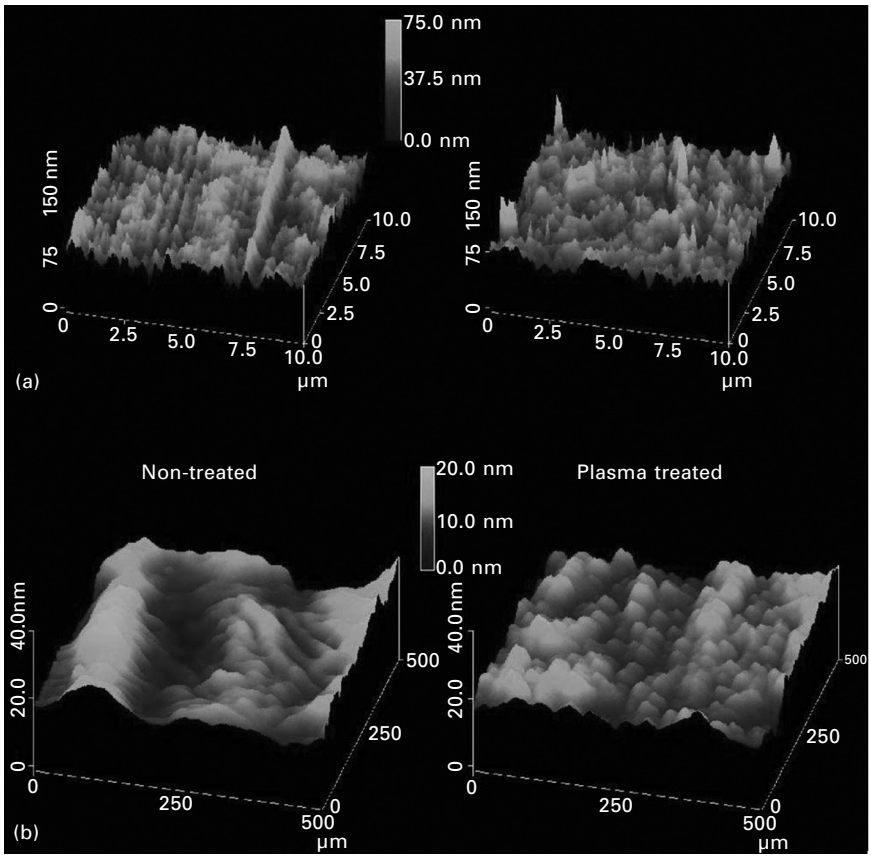
© Woodhead Publishing Limited, 2010




*9.4* AFM images of PET before (left) and after (right) plasma treatment for an analyzed area of (a) 30 × 30 μm and (b) 1 × 1 μm. Please note the different height scales between images. The surface roughness (RMS) changes from 81 to 26 nm, and from 16 to 6 nm on the 30 μm and 1 μm *xy* (horizontal plane) scale, respectively (Noeske *et al.*, 2004). Reprinted with permission of Elsevier Limited.

smooth and the PVDF surfaces are much rougher. However, where the PET surface became smoother after plasma treatment, the PVDF maintained nearly the same roughness on the 30 μm scale. On the 0.5 or 1 μm scale, the surfaces of both polymers show common bump-like features. It was hypothesized that the topographical changes could be a result of thermal or chemical changes on the surface resulting from the plasma environment. Noeske and co-workers' work showed that plasma treatment at atmospheric pressure has been successfully used to enhance the bondability of five polymers. The failure modes were either cohesive failure or substrate break after plasma treatment, compared with adhesive failure for the untreated specimens.

© Woodhead Publishing Limited, 2010




*9.5* AFM images of PVDF before (left) and after (right) plasma treatment for an analyzed area of (a) 10 × 10 μm and (b) 0.5 × 0.5 μm. Please note the different height scales between the images. The roughness (RMS) changes from 10 to 8 nm, and is 3 nm on the 10 and 0.5 μm *xy* (horizontal plane) scale, respectively (Noeske *et al.*, 2004). Reprinted with premission of Elsevier Limited.

Comyn *et al*. (1996b) studied the effect of air, argon, ammonia and oxygen plasma treatment of the surface of PEEK on adhesive bonding at pressures of 40 MPa. They found that adhesion was enhanced to the same level regardless of the type of gas used. Lap shear joints failed at around 33 MPa either by rupturing the epoxy film adhesive or PEEK. Although the adhesion was enhanced, the topography of the surface of PEEK remained smooth and was not roughened by the plasma treatment. XPS measurements showed that the surface developed the –COO– functional groups after oxygen plasma treatment. These treated PEEK surfaces could be stored for 90 days at room temperature without any loss of adhesion. However, the heat treated surfaces at 180°C or solvent wiped PEEK surface after plasma treatment

© Woodhead Publishing Limited, 2010

experienced a loss of adhesion when treated substrate was stored prior to bonding.

### 9.4.6 Corona discharge

The effect of corona discharge on adhesion has been studied using a variety of polymers, including polypropylene (Green *et al*., 2002), ethylene-vinyl acetate copolymers (Martinez-Garcia *et al*., 2007) and PEEK (Comyn *et al*., 1996a). Green *et al*. (2002) showed that corona discharge treatment can significantly improve the adhesion to polypropylene with BETASEAL™ 1780 polyurethane adhesive (trademark of The Dow Chemical Company). Shear stress increased from 0.07 MPa for untreated specimens to 2.72 MPa for the pretreated specimens.

Comyn *et al*. (1996a) studied the effects of corona treatment on the surface of PEEK prior to adhesive bonding. Their study included the use of air as well as other gases such as oxygen, argon and ammonia. These gases were fed into the electrode gap of a Tanec model HV 95-2 corona discharge apparatus. For air-treated PEEK, lap shear strengths significantly increased from 17 MPa to 28–29 MPa. The failure mode changed from a combination of interfacial and cohesive to primarily material failure of the PEEK. However, varying the treatment level by changing the energy of the corona treatment from 0.05 to 2.0 J $mm^{-1}$ did not affect the joint strength. The surface topography was not affected either. The contact angle with three solvents, water, ethanediol and dimethylsulfoxide, was significantly reduced by corona discharge treatment.

### 9.4.7 Chemical treatments

Chemical treatments in the form of acid etch primers or solvent-based primers have been used extensively to enhance adhesion to a number of different plastics, although most of this work has focused on paint adhesion. Chromic acid and sulfuric acid are the most prevalent acid etch primers. The efficacy of these primers exhibits a varied performance depending on the type of plastic and the type of adhesive or paint. There has been a debate about the level of surface modification caused by these primers. Briggs *et al*. (1976) have shown that for polyethylene and polypropylene, the level of surface modification and the depth of modification are strongly dependent on the etching time. The bonded joints using polyethylene or polypropylene exhibited excellent strength and this strength was not dependent on exposure time.

Solvent primers based on chlorinated polyolefins or chlorinated maleated polyolefins have been studied extensively, although most of this work has focused on paint adhesion. Jialanella (1998) clearly showed that the chemical composition of the maleated olefin can have a significant impact on the

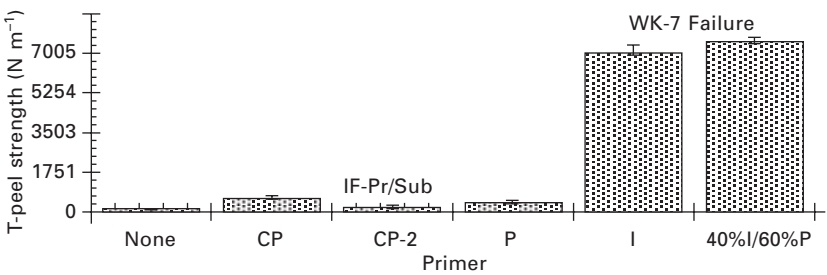
© Woodhead Publishing Limited, 2010

joint strength. In this study, copolymers of ethylene–octene copolymers were primed with maleic anhydride modified ethylene–octene copolymers, polyethylene and polypropylene and bonded with an epoxy adhesive. The results in Fig. 9.6 (Jialanella, 1998) clearly show that the maleic anhydride modified ethylene–octene copolymers exhibited excellent adhesion only to the ethylene–octene copolymer adherends.

## 9.5 Uses of organoboron chemistry in plastic bonding

Organoboron compounds have been used extensively in organic synthesis. Most recent attention has focused primarily at the pharmaceutical industry, but they also find applications in adhesives. Zharov and Krasnov (1996) disclosed the use of an initiating system for a two-part acrylic adhesive composition comprising an organoborane–amine complex in one part and an acid decomplexer in the second part. More importantly, they were the first to describe the use of such compositions for bonding low energy substrates. This discovery emphasized the full utility of organoborane initiated acrylic adhesives. These systems can be used to adhere a variety of plastic substrates including polyethylene and polypropylene.

It is believed that the alkyl borane/borate initiating systems impart adhesion to low energy substrates without any surface pretreatment. The systems described are two-part acrylic adhesive systems. Owing to the pyrophoric nature of alkyl borane/borate initiators, they must possess a blocking agent or be tetravalent. The blocking agent must be removed prior to curing the adhesive. Pocius and co-workers (1997–2000) described the use of numerous agents to remove the blocking agent which include acids, acid chlorides, aldehyde, anhydrides, epoxies, polyisocyanates and sulfonyl chloride.

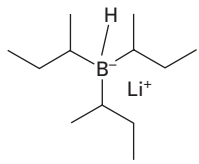



*9.6* Effect of primer type on the T-peel strength of metallocene polyolefin using an epoxy adhesive. CP - chlorinated polypropylene-g-MAH; CP-2 - chlorinated polyethylene-g-MAH; P - PRIMACOR™ 3460 Adhesive Polymer, trademark of The Dow Chemical Company; I - INSITE™ Technology, ethylene-octene copolymer-g-MAH, trademark of The Dow Chemical Company.

© Woodhead Publishing Limited, 2010

Their initiating systems comprised an alkyl borane or borate compound for use in acrylic adhesives with polyamine, with or without polyols as the complexing agent. Their preferred polyamine is a primary diamine based on polyoxyalkylenepolyamine under the trade name of Jeffamine. There has been a substantial amount of work using hexamethylene diamine as the polyamine. However, they have also done some work examining aziridines and polyaziridines. Their work has shown that these systems exhibit excellent adhesion to polyethylene and polypropylene.

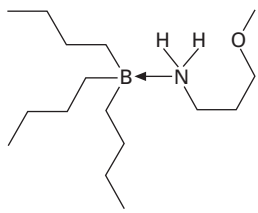
Kneafsey *et al.* (2005) have developed a family of metal alkyl borohydrides, like lithium tri-sec-butyl borohydride (L-selectride) (**1**) shown below.




(**1**) Lithium tri-sec-butyl borohydride (L-selectride)

This family of compounds has been used very effectively as initiators in methacrylate adhesives to bond low energy substrates. Kendall *et al.* (2003) described a unique class of internally blocked borates which are useful for curing acrylic adhesives. The internal block refers to the presence of boron as part of an internal ring structure bridged across at least two of the four boron coordinates or valences. It is claimed that this catalyst exhibits good air stability and promotes adhesion to low energy substrates when unblocked in an acrylic adhesive.

Sonnenschein *et al.* (2004a–c) developed a series of organoborane/amine complexes, TnBB-MOPA complex (2) for example, which exhibited good air stability.




(**2**) TnBB-MOPA complex

In addition to the development of alkyl borane blocking agents, other advancements were reported based on this technology. Webb and Sonnenschein (2004) showed that higher temperature strength performance can be attained when isocyanates are used as deblockers. Sonnenschein *et al.* (2007) also disclosed the use of a two-phase (heterophase) system in which one phase is cured by free radical polymerization via the alkyl borane and the second phase

© Woodhead Publishing Limited, 2010

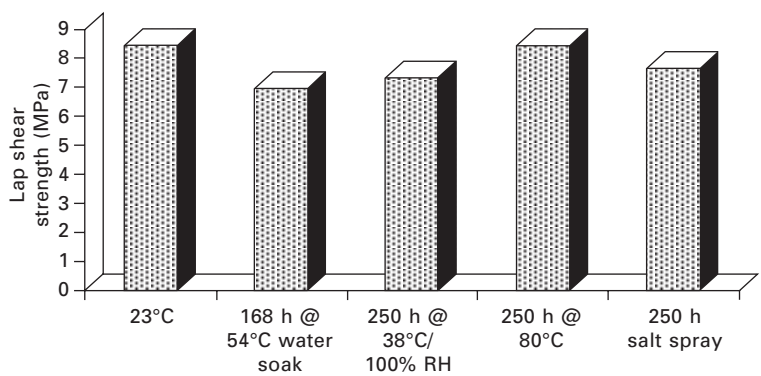
is cured by ring opening polymerization. Additionally, a dual cure system comprising a cured organoborane and olefinic monomers and monomers/oligomers with a siloxane backbone, which are capable of polycondensation polymerization, has also been reported. Lastly an example focusing upon coating applications has also been reported. This catalyst type has been used in acrylic and silicone hybrid adhesive systems. In all cases, excellent adhesion to most plastics has been reported including substrates with low energy surfaces such as polyethylene (PE) and PP.

Jialanella *et al.* (2007) reported that the commercial product using the above catalyst structure, BETAMATE™ LESA Adhesive (trademark of The Dow Chemical Company), exhibited excellent adhesion to glass filled PP. The results in Fig. 9.7 (Jialanella, 2007) show the adhesive performance initially and after environmental aging. In these series of experiments, the strengths after environmental exposure were similar to the initial high strength of 12.4 MPa. The locus of failure for all samples was in the PP substrate.

## 9.6 Limitations of plastic bonding

### 9.6.1 Durability of treatments

The durability of the surface treatments has been studied utilizing two techniques: heat aging and solvent wiping. Morra *et al.* (1990) have extensively studied durability in terms of heat aging of oxygen plasma treated PE and PP prior to adhesive bonding with an epoxy adhesive. They studied the effect of room-temperature aging on treated PE and PP surfaces utilizing contact angle of water, X-ray photoelectron spectroscopy (XPS) and bond strengths. Advancing and receding contact angle measurements for PE and PP as a function of time at room temperature are shown in Table 9.8 (Morra *et al.*, 1990).




*9.7* Lap shear strength of BETAMATE™ LESA adhesive (trademark of The Dow Chemical Company) on glass filled polypropylene (Jialanella, 2007).

© Woodhead Publishing Limited, 2010

*Table 9.8* Water advancing and receding angles (both in degrees), static secondary ion mass spectrometry (SSIMS) $CH^-/^{18}O^-$ ratios and XPS O/C ratios for selected aging conditions (Morra *et al.*, 1990). Reprinted with permission of Taylor & Francis

| Aging conditions | Advancing contact angle (°) | Receding contact angle (°) | SSIMS $CH^-/^{18}O^-$ | XPS O/C |
|---|---|---|---|---|
| PE | | | | |
| Untreated | 93 | 78 | | 0.04 |
| Just-treated | 12 | 7 | | 0.32 |
| 24 h, 293 K | 16 | 7 | | 0.33 |
| 375 h, 293 K | 24 | 12 | | 0.30 |
| 8 h, 393 K | 24 | 13 | | 0.30 |
| PP | | | | |
| Untreated | 95 | 80 | – | 0.02 |
| Just-treated | 24 | 10 | – | 0.19 |
| 16 h, 293 K | 54 | 11 | 0.7 | 0.18 |
| 148 h, 293 K | 81 | 13 | 1.3 | |
| 175 h, 293 K | 8 | 15 | 1.7 | 0.19 |
| 3 h, 333 K, 44 h, 293K | 92 | 30 | 2.9 | 0.18 |
| 2 h, 393 K, 23 h, 293 K | 94 | 50 | 4.5 | |
| 8 h, 393 K | 94 | 49 | | 0.19 |

In both cases, the contact angle results for the untreated surfaces are similar to published results. The treated surfaces show a significant reduction in advancing and receding contact angle measurements. Interestingly, the PE surfaces exhibit a larger reduction in advancing contact angle results than the PP surfaces. The receding contact angle results were comparable for the PE and PP surfaces after treatment. As expected, the XPS results show an increase in the oxygen/carbon (O/C) ratio. Here again, the PE surfaces show a significantly higher oxygen/carbon ratio. These results seem to indicate that PE surfaces accept oxygen plasma more than PP surfaces. After aging, the treated PE surfaces show only a small change in contact angle results, but the PP surfaces show a significant change in contact angle results. In fact, the PP surfaces revert back to the same contact angle results as the untreated PP surfaces after only 9 days aging at room temperature.

The bond strengths with an epoxy adhesive were evaluated using a lap shear test and a stud pull off test in Table 9.9 and Table 9.10 (Morra *et al.*, 1990), respectively. The shear strengths and pull off strengths improved significantly after oxygen plasma pretreatment of the surfaces of PE and PP.

These shear strengths did not change after room temperature aging as shown in Table 9.9. The pull off bond strengths remained the same for PE after aging, but the pull off bond strengths decreased significantly after aging for PP as shown in Table 9.10. These results clearly show that the treated PP surface exhibits a strong aging dependency as predicted by contact angle

© Woodhead Publishing Limited, 2010

*Table 9.9* Results of shear testing of PP and PE/epoxy bonds (Morra *et al.*, 1990). Reprinted with permission of Taylor & Francis

| Sample | Bond strength (MPa) |
|---|---|
| PE | |
| Untreated | 0.3 ± 0.04 |
| Just-treated | 3.4 ± 0.7 |
| Aged (8 h, 393 K) | 3.2 ± 0.6 |
| PP | |
| Untreated | 0.2 ± 0.01 |
| Just-treated | 1.4 ± 0.5 |
| Aged (8 h, 393 K) | 1.3 ± 0.2 |

*Table 9.10* Results of stud pull off testing of PP and PE/epoxy bonds (Morra *et al.*, 1990). Reprinted with permission of Taylor & Francis

| Sample | Bond strength (MPa) |
|---|---|
| PE | |
| Untreated | Not measurable |
| Just-treated | 17.7 ± 2.0 |
| Aged (8 h, 393 K) | 17.5 ± 1.7 |
| PP | |
| Untreated | Not measurable |
| Just-treated | 3.9 ± 0.98 |
| Aged (8 h, 393 K) | 0.69 ± 0.39 |

measurements. Interestingly, the initial bond strengths for the pretreated PP surface were less than half of the bond strengths for the pretreated PE. Also, the oxygen/carbon ratio for PP is less than half of the oxygen/carbon ratio for PE. This certainly suggests that PP does accept the oxygen plasma treatment, but differently from PE. Also, close examination of the failure modes by XPS reflect this opinion. The failure modes were classified as substrate break for the pretreated PP and PE specimens. The PP specimens were in the bulk PP, but close to the surface or close to the modified layer. This suggests that PP fails in a weaker section of the bulk PP.

Carter (1981) illustrated the importance of the adhesive when evaluating bond strength of flame pretreated PE. In one set of experiments, flame pretreated PE was bonded with a two-part urethane adhesive and a solvent-based one-part urethane adhesive. The peel strengths of the two-part urethane were approximately 3 N $mm^{-1}$ whereas the bond strengths of the solvent-based one-part adhesive were approximately 0.6 N $mm^{-1}$. The explanation for these results was that the two-part urethane adhesive had excess isocyanate groups to react with the functionality provided by the flame treatment. However, the solvent-based adhesive did not provide isocyanate functionality for reaction with the surface of the PE. Carter (1981) also showed that excellent bond

© Woodhead Publishing Limited, 2010

strengths could be achieved with the solvent-based urethane adhesive by applying a methylene diphenyl disocyanate (MDI) solution to the flame treated PE surfaces.

Comyn *et al*. (1996b) showed that oxygen and air plasma treatment of PEEK was not durable after solvent wiping with acetone. They showed that acetone wiping the PEEK adherends with oxygen and air plasma pretreatments had a significant impact on the peel strengths when bonded by an epoxy film adhesive. The peel strengths of the specimens with the plasma pretreatment were in the range of 4 kN $m^{-1}$ and were essentially reduced to zero when the treated specimens were wiped with acetone prior to adhesive bonding. They also found that heat treatment reduced the lap shear strength of plasma pretreated lap shear strips by 50% when heated to about 180°C prior to bonding. The strengths did not decrease when heated to less than 180°C. This temperature seems to be a threshold temperature.

### 9.6.2 Versatility of treatments

Green *et al*. (2002) have examined seven different pretreatments for PP. They were corona discharge, flame, fluorination, low-pressure vacuum plasma, atmospheric plasma, infrared (IR) laser and chromic acid. The results are shown in Table 9.11 (Green *et al*., 2002). The results show that the most effective treatments were corona discharge, flame fluorination and vacuum plasma. All of these treatments afforded bond strengths of 2.72–3.47 MPa. The air plasma did improve the bond strength from 0.07 to 1.97 MPa. The IR laser and the chromic acid treatments showed little or no efficacy.

## 9.7 Future trends

There are many different approaches to adhesive bonding of plastics depending on the type of plastics. The emphasis of this chapter was to discuss bonding

*Table 9.11* Lap shear test values for pretreated homopolymer, HF 135M, polypropylene bonded with a polyurethane adhesive (Betaseal™ 1780, trademark of The Dow Chemical Company) (Green *et al*., 2002). Reprinted with permission of Taylor & Francis

| Pre-treatment | Shear stress (MPa) |
|---|---|
| Untreated | 0.07 |
| Corona discharge | 2.72 |
| Flame | 3.47 |
| Fluorination | 2.96 |
| Vacuum plasma | 3.35 |
| Agrodyn™ plasma | 1.97 |
| IR laser | 0 |
| Chromic acid | 0.26 |

© Woodhead Publishing Limited, 2010

techniques used for adhesive bonding of difficult to bond plastics. Difficult to bond plastics with conventional adhesives usually exhibit two characteristics, surface crystal structure or low surface energy. Although there are many approaches to bonding these types of plastic, the main emphasis for the future is the use of self-priming adhesive systems (organoboron catalyzed acrylic adhesives). This capability provides the customer with tremendous flexibility in designing their plant conditions. The other extremely important benefit of organoboron catalyzed acrylic adhesives is that there is no concern about the shelf life of the pretreatment. The BETAMATE™ LESA adhesive (trademark of The Dow Chemical Company) is the first commercial product in the automotive original equipment manufactures (OEM) market. It is currently used to assemble automobile components for numerous vehicle platforms.

## 9.8 References

Ahagon A and Gent A N (1976), 'Effect of interfacial bonding on the strength of adhesion', *J Polym Sci Polymer Phys*, **13**, 1285–1300.

Allen K W (2003), 'At forty commeth understanding: A review of some basics of adhesion over the past four decades', *Int J Adhesion and Adhesives*, **23**(2), 87–93.

Anagreh N and Dorn L (2005), 'Influence of low-pressure plasma treatment on adhesive bonding between polybutylene terephthalate (PBT) and aluminum', *Int J Adhesion and Adhesives*, **25**, 165–72.

Briggs D, Brewis D M and Konieczko M B (1976), 'Etching of a low-density polyethylene film by fuming nitric acid', *J Mater Sci*, **11**, 1270–7.

Bueche F, Cashin W and Debye P (1952), 'The measurement of self-diffusion in solid polymers', *J Chem Phys*, **20**(12), 1956–8.

Carter, A R (1981), 'Adhesion to polyolefins with flexible adhesives', *J Adhesion*, **12**, 37–49.

Chang R J and Gent A N (1981a), 'Effect of interfacial bonding on the strength of adhesion of elastomers. II. Dissimilar adherends', *J Polym Sci Phs Ed*, **19**, 1619–33.

Chang R J and Gent A N (1981b), 'Effect of interfacial bonding on the strength of adhesion of elastomers. I. self adhesion', *J Polym Sci Phs Ed,* **19**, 1635–40.

Comyn J, Mascia L and Xiao G (1996a), 'Corona-discharge treatment of polyetheretherketone (PEEK) for adhesive bonding', *Int J Adhesion and Adhesives*, **16**, 301–4.

Comyn J, Mascia L and Xiao G (1996b), 'Plasma-treatment of polyetheretherketone (PEEK) for adhesive bonding', *Int J Adhesion and Adhesives*, **16**, 97–104.

Gent A N (1981), 'The role of chemical bonding in the adhesion of elastomers', *Int J Adhesion Adhesives*, **1**(4), 175–80.

Green M D, Guild F J and Adams R D (2002), 'Characterisation and comparison of industrially pre-treated homopolymer polypropylene, HF 135 M', *Int J Adhesion and Adhesives*, **22**, 82–90.

Jennings C W (1972), 'Surface roughness and bond strength of adhesives', *J Adhesion*, **4**, 25–38.

Jialanella G L (1998), *Adhesion Promoter for a Laminate Comprising a Substantially Linear Polyolefin*, US 5,741,594.

© Woodhead Publishing Limited, 2010

Jialanella G L, Ristoski T and Cawley A C (2007), 'Recent developments in novel stabilization chemistry for low energy surface adhesive (LESA) cured with alkyl boranes', *Adhesion Society Meeting*, **30**, 1–5.

Kato K (1967), 'ABS mouldings for electroplating – An electron microscope study', *Polymer*, **8**, 33–9.

Kato K (1968), 'Electron microscope studies on etching of ABS mouldings for electroplating', *Polymer*, **9**, 419–24.

Kendall J L, Righettini R F and Abbey K J (2003), 'Internally blocked organoborate initiators and adhesives therefrom', US 6,630,555B2.

Kendall J L and Caster K C (2004), 'Metathesis polymerization adhesives and coatings', US 6,800,170B2.

Kendall J L, Righettini R F and Abbey K J (2005), 'Internally blocked organoborate initiators and adhesives therefrom', US 6,841,635B2.

Kinloch A J (1987), A*dhesion and Adhesives*, Chapman Hall, New York.

Kneafsey B J and Coughlan G (2005), *Metal Alkyl Borphydride Polymerisation Initiators, Polymerisable Compositions and Uses Therof*', US 6,844,080B2.

Kneafsey B J and Maandi E (2005), '*Non-flammable and Non-combustible Bonding Systems Having Adherence to Low Energy Surfaces*', US 6,867,271B1.

Lee L H (1967), 'Adhesion of high polymers, I. influence of diffusion, adsorption, and physical state on polymer adhesion', *J Polym Sci A-2*, **5**, 751–60.

Martinez-Garcia A, Sanchez-Reche A, Gisbert-Soler S, Cepeda-Jimenez C, Torregrosa-Macia R and Martin-Martinez J (2007), 'Corona discharge treatment of EVAs with different vinyl acetate contents', *J Adhesion Sci Technol*, **21**(5–6), 441–63.

McLaren A D (1948), 'Adhesion of high polymers to cellulose. Influence of structure, polarity, and tack temperature', *J Polym Sci*, **3**, 552–62.

McLaren A D and Sieler C J (1949), 'Adhesion III. Adhesion of polymers to cellulose and aluminum', *J Polym Sci*, **4**, 63–74.

McLaren A D, Li T T, Rager R and Mark H (1951), 'Adhesion IV. The meaning of tack temperature', *J Poly Sci*, **7**, 463–70.

Morra M, Occhiello E, Gila L and Garbassi F (1990), 'Surface dynamics vs. adhesion in oxygen plasma treated polyolefins', *J Adhesion*, **33**, 77–88.

Noeske M, Degenhardt J, Strudthoff S and Lommatzsch U (2004), 'Plasma jet treatment of five polymers at atmoshpheic pressure: surface modifications and the relevance for adhesion', *Int J Adhesion and Adhesives*, **24**, 171–7.

Owens D K (1975), 'Mechanism of corona-induced self-adhesion of polyethylene film', *J Appl Polym Sci*, **19**, 265–71.

Pocius A V (1997), *Organoborane Polyoxyalkylenepolyamine Complexes and Adhesive Compositions Made Therewith*, US 5,621,143.

Pocius A V (1997), *Organoborane Polyoxyalkylenepolyamine Complexes and Adhesive Compositions Made Therewith*, US 5,681,910.

Pocius A V (1998), *Organoborane Polyoxyalkylenepolyamine Complexes and Adhesive Compositions Made Therewith*, US 5,718,977.

Pocius A V (1999), *Organoborane Polyamine Complex Initiator Systems and Polymerizable Compositions Made Therewith*, US 5,994,484.

Pocius A V (1999), *Organoborane Polyamine Complex Initiator Systems and Polymerizable Compositions Made Therewith*, US 6,008,308.

Pocius A V (2000), *Organoborane Polyamine Complex Initiator Systems and Polymerizable Compositions Made Therewith*, US 6,093,778.

Pocius A V and Nigatu T G (1997), *Organoborane Polyamine Complexes and Adhesive Composition Made Therewith*, US 5,616,796.

© Woodhead Publishing Limited, 2010

Pocius A V and Nigatu T G (1997), *Organoborane Polyamine Complexes and Adhesive Compositions Made Therewith*, US 5,684,102.

Pocius A V and Nigatu T G (1998), *Organoborane Polyamine Complexes and Adhesive Compositions Made Therewith*, US 5,795,657.

Ryunge M L and Dreyfuss P (1979), 'Effect of interfacial chemical bonding on the strength of adhesion of grlass-polybutadiene joints', *J Polym Sci*, **17**, 1067–72.

Schuman T P and Thames S F (2004), 'Image of a bitten molded polymer surface: solvent-induced adhesion', *Proceedings of the Annual Meeting Program of the FSCT*, **82**, 73/1–73/21.

Schuman T and Thames S F (2005), 'Coating solvent effects producing adhesion to mold plastic parts', *J Adhesion Sci Technol*, **19**(13–14), 1207–35.

Sheng E, Sutherland I, Brewis D M, Heath R J and Bradley R H (1994), 'Surface studies of polyethylene modified by flame treatment', *J Mater Chem*, **4**, 487–90.

Sonnenschein M F, Webb S P and Rondan N G (2004a), *Amine Organoborane Complex Polymerization Initiators and Polymerizable Compositions*, US 6,706,831B2.

Sonnenschein M F, Webb S P and Rondan N G (2004b), *Amine Organoborane Complex Polymerization Initiators and Polymerizable Compositions*, US 6,730,759B2.

Sonnenschein M F, Webb S P and Rondan N G (2004c), *Amine Organoborane Complex Polymerization Initiators and Polymerizable Compositions*, US 6,806,330B1.

Sonnenschein M F, Webb S P Cieslinkski R C and Wendt B L (2007), 'Poly(acrylate/epoxy) hybrid adhesive for low-surface-energy plastic adhesion', *J Polym Chem Part A*, **45**(6), 989–98.

Stewart R, Goodship V, Guild F, Green M and Farrow J (2005), 'Investigation and demonstration of the durability of air plasma pre-treatment on polypropylene automotive bumpers', *Int J Adhesion and Adhesives*, **25**, 93–9.

Sutherland I, Brewis D M, Heath R J and Sheng E (1991), 'Modification of polypropylene surfaces by flame treatment', *Surf Interface Anal*, **17**, 505–10.

Sutherland I, Sheng E, Brewis D M and Heath R J (1994), 'Flame treatment and surface characterization of rubber modified polypropylene', *J Adhesion*, **44**(1–2), 17–27.

Vasenin R M (1965), 'Adhesion of high polymers part II: Predicting adhesion', *Adhesive Age*, **8**(6), 30–5.

Voyutskii S S (1956), 'The diffusion theory of adhesion', *Colloid J USSR*, June, 748–56.

Voyutskii S S and Vakula V L (1963), 'The role of diffusion phenomena in polymer to polymer adhesion', **7**, 475–91.

Voyutskii S S, Markin Y I, Gorchakova V M and Gul V E (1965), 'Adhesion of polymer to metals', *Adhesives Age*, **8**(11), 24–8.

Weaver C (1972), 'Adhesion of metals to polymers', *Faraday Special Discussions*, **2**, 18–24.

Weaver C (1975), 'Adhesion of thin films', *J. Vac. Sci. Technol.,* **12**(1), 18–25.

Webb S P and Sonnenschein M F (2004), *Organoborane Amine Complex Polymerization Initiators and Polymerizable Compositions*, US 6,740,716B2.

Zharov J V and Krasnov J N (1996), *Polymerizable Compositions made with Polymerization Initiator Systems based on Organoborane Amine Complexes*, US 5,539,070.

© Woodhead Publishing Limited, 2010

# 10
# Bonding of polymer matrix composites

K. D. FERNHOLZ, Ford Motor Company, USA

**Abstract**: This chapter discusses the drivers of and developments in structural adhesive bonding of composites by comparing and contrasting composite bonding within the aerospace and automotive industries. The chapter addresses composite pretreatment and surface characterization, composite joint design, modeling and testing of composite joints, and future trends. For each topic, the considerations that drive manufacturer's decisions are reviewed. Recent developments in the area are then discussed.

**Key words**: adhesive bonding, aerospace, automotive, polymer matrix composites.

## 10.1 Introduction

Polymer matrix composite (PMC) structures may be used as an alternative to metal structures for many reasons. The four most common reasons that manufacturers choose to use PMCs over metals are (1) to reduce the weight of the structure, (2) to reduce the cost of tooling required to produce the structure, (3) to reduce the number of individual parts that must be fabricated (i.e. 'parts consolidation') and (4) to improve the durability of the structure by eliminating corrosion. Adhesive bonding is an attractive method of joining composite and composite–metal hybrid structures since composites cannot be welded. In addition, using mechanical fastening in composite structures can reduce the structure's long term durability because the addition of holes needed for mechanical fastening can produce stress concentrations in the composite.

The materials and methods for bonding composite materials are largely determined by the polymer chosen for the matrix, the structural requirements of the joint and manufacturing considerations. In all industries, a primary driver in the design and manufacture of composite joints is the need to produce reliable and durable joints. Other requirements, and their relative importance, are determined by the factors that are most important in a particular application. Well-established details regarding the basics of composite bonding are summarized in US Department of Defense (DoD) *Composite Materials Handbook, Military Handbook 17 (MIL-HDBK-17) Volume 3* and *ASM Handbook Volume 21, Composites*. This chapter will discuss the drivers of and recent developments in structural adhesive bonding



© Woodhead Publishing Limited, 2010

of composites by comparing and contrasting composite bonding within the aerospace and automotive industries.

### 10.1.1 Common requirements in composite bonding

While the relative importance of factors that determine the choice of materials and joint design is different in the aerospace and automotive industries, there are also many similarities. First, and most important, adhesives are used in both aerospace and automotive applications to improve the structural durability of joints. The durability of a structure is a critical design parameter in all industries. By either adding adhesive to a mechanically fastened joint or replacing mechanical fasteners with adhesive, the load can be distributed over a larger area, reducing stress concentrations and improving the life of a structure.

One of the most important factors in the successful implementation and continued use of bonded-only composite joints is the design of the joint. Joints must be designed not only to meet structural requirements but also to minimize the likelihood of creating a defect when the joint is manufactured. Since a disbond of an adhesively bonded joint often initiates from a defect, it is critical that both the joint design and joint manufacturing process minimize the chance that a defect will be created in the bond. In both industries, the design of a joint is influenced by manufacturability considerations. The joint design should improve the likelihood that the manufacturing process can reliably produce joints meeting design intent.

While manufacturers work to ensure that joints are well designed and that their manufacturing processes are robust, it is not possible to eliminate all sources of variability and contamination from a process cost-effectively. There is, therefore, always a possibility that the manufactured joint may not meet design intent. Of particular concern are so-called 'kissing bonds', that is, bonds in which the adhesive is present but adhesion to one or both of the substrates is poor. The inability to reliably identify the presence of this type of bond as part of the manufacturing process is a concern in both the aerospace and automotive industries. While non-destructive detection of these types of bonds is difficult in metals (Adams and Drinkwater, 1999; Nagy, 1991), detection of these defects in composites is further complicated by the need to use lower frequency signals to penetrate the composite substrate. Although research in this area continues (Brotherhood *et al.*, 2003), additional development work is required before kissing bonds can reliably be identified in composite substrates.

One way to alleviate concerns about the strength of the bond and to reduce the impact that bonding defects have on joint performance, is to add secondary mechanical fasteners to the joint. While adding mechanical fasteners adds weight to the structure and complexity to the manufacturing

© Woodhead Publishing Limited, 2010

process, both industries rely upon mechanical fastening to prevent catastrophic peel in a joint and to improve confidence in the joint's long-term structural performance. Aerospace manufacturers are more willing to use bonded-only joints in some applications since they perform non-destructive evaluation (NDE) or non-destructive inspection (NDI) on 100% of their joints. They typically use hybrid joints (i.e. joints with both adhesive and mechanical fasteners), however, for joints that are 'safety critical' or that carry out-of-plane loads.

Automotive manufacturing cycle times make universal NDE/NDI to validate the quality of every joint in high volume applications unfeasible; therefore, adhesive bonding is almost always used in conjunction with mechanical fasteners in high volume applications. There are, however, exceptions to this rule. One exception is the bonding of spare wheel wells into the rear floor pan. An example of a spare wheel well is shown in Fig. 10.1.

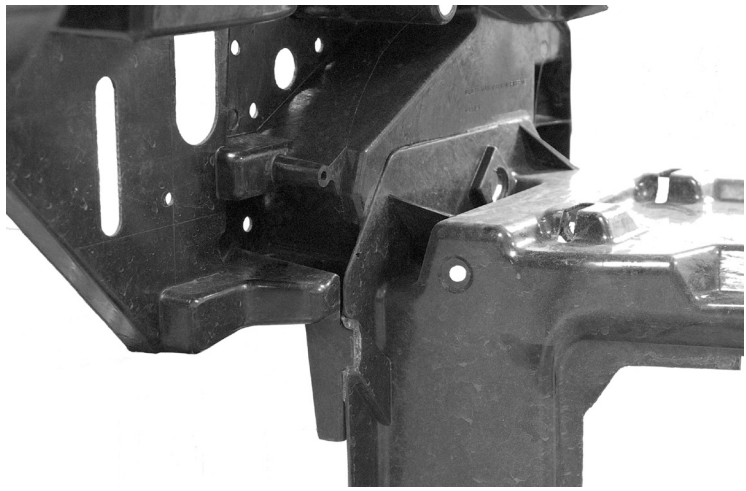
Spare wheel wells are a unique application in which the joint need only retain the well in a crash event and where the design of the joint allows the weight of the well itself to hold the part in place in the assembly plant while the adhesive cures. Bonded-only joints may also be used in some low volume automotive applications. An example of this type of application is the Dodge Viper headlamp support-to-fender support joint. This joint is shown in Fig. 10.2. In this case, the components are molded and bonded at the component supplier and sent to the assembly plant as a sub-assembly.

The requirement that design and manufacturing engineers have high confidence in the initial and long-term strength of the joints can be an



*10.1* Example of a glass fiber-polypropylene composite spare wheel well (photograph courtesy of Ford Motor Company).

© Woodhead Publishing Limited, 2010



*10.2* Bonded-only joint in the Dodge Viper: the headlamp support-to-fender support joint (photograph courtesy of Meridian Automotive Systems).

impediment in both industries to the implementation of new adhesives and processes. This is true even though manufacturers in both industries are increasingly likely to use composites in composite–metal hybrid structures. While adhesive bonding can enable manufacture of mixed material structures, manufacturers, particularly those in the automotive industry, generally prefer to use adhesives with which they have many years of experience. This becomes a complication in composite bonding as the majority of adhesives with a long service history are those developed for metals. Implementation of new adhesives can also be complicated by the fact that manufacturers would prefer new adhesive materials to bond equally well to both composite and metal substrates.

The final common desire of manufacturers in the aerospace and automotive industries is to minimize the need for surface treatment of the substrate prior to bonding. Surface treatment in the automotive industry has historically been limited by cycle time and cost considerations to wiping of the surface or, when necessary, scuff sanding. In contrast, the aerospace industry has historically relied upon multi-step sanding processes to achieve clean, chemically active bonding surfaces. Aerospace and automotive manufacturers alike, however, would like to eliminate the need for surface preparation while maintaining high confidence in the resultant joint strength. Manufacturers would prefer to eliminate surface preparation processes since it is difficult to apply traditional processes consistently over large surfaces and long production runs. Nevertheless, there are a number of contaminants, including mold releases, oils, dust and debris, with which manufacturers must contend.

© Woodhead Publishing Limited, 2010

Consequently, manufacturers in both industries take part in research into processes that can reduce the amount of surface preparation required or that can validate the chemical makeup of the surface after treatment as part of the manufacturing process.

### 10.1.2 Unique requirements for bonding in aerospace applications

A principal driver of differences in adhesive bonding approaches and materials used by the aerospace and automotive industries is their choice of composite. In aerospace applications, structural performance and temperature requirements are the primary considerations in resin selection. As a result, the most commonly used resins are epoxy, bismaleimide (BMI), polyetheretherketone (PEEK) and polyphenylene sulfide (PPS). Aerospace manufacturers are far more likely to use carbon fiber as the reinforcement than automotive manufacturers. In general, however, the choice of reinforcement has more of an impact on substrate properties than on adhesion properties since manufacturers prefer to bond to a resin-rich surface rather than to bare fibers. In fact, since adhesion to bare fibers is generally poor, surface treatments are intended to clean and chemically activate the polymer matrix (Davis and Bond, 1999) rather than to expose bare fibers.

In aerospace applications, design decisions are frequently driven by the need to minimize the weight of the structure. Use of an adhesively bonded joint can result in significant weight savings in comparison with a mechanically fastened or bonded/bolted hybrid joint. Furthermore, manufacturing and life cycle costs can often be reduced through the use of adhesively bonded joints. Nevertheless, not all aerospace joints will be adhesively bonded since there are applications where the joint must carry out-of-plane loads or where the ease of disassembly of a mechanically fastened joint is beneficial.

While automotive structures are also designed to ensure that the structures will perform as designed throughout their lifetime, in aerospace applications 'disbond arrestment' requirements are dictated by Federal Aviation Regulation (FAR) Part 25, Section 571 (FAA, 1998). Disbond arrestment requirements specifically address concerns about the behavior of joints when subjected to peel loads. The intent of the regulations contained in FAR Part 25, Section 571 is to 'show that catastrophic failure due to fatigue, corrosion, manufacturing defects, or accidental damage, will be avoided throughout the operational life of the airplane'. As a result, these regulations can have a significant impact on the design of joints in aerospace structures.

Finally, as mentioned earlier, NDE/NDI is an integral part of the manufacturing plan for all bonded structures in the aerospace industry. Aerospace product development processes require that a quality control process utilizing NDE/NDI be established for all bonded joints. Load-bearing

© Woodhead Publishing Limited, 2010

bonded structures must be evaluated specifically with through-transmission ultrasonic NDE/NDI. While the use of NDE/NDI provides a level of confidence in the quality of the joint, the quality control plan for the structure must be established early in the design process since the need to be able to inspect all the joints can influence the joint design.

### 10.1.3 Unique requirements for bonding in automotive applications

In the automotive industry cost and processing time are of primary importance when choosing materials and processes; consequently, the most commonly used resins in automotive composite applications are polypropylene (PP), nylon and polyester. Vinyl esters and epoxies are used in limited applications as well. While carbon fiber may be used in low volume specialty applications, glass fiber is the preferred reinforcement in high volume applications.

In automotive applications, design decisions are driven by durability and total cost (material and manufacturing costs) considerations. The need to reduce the cost of structures has generated increasing interest in new applications of PP-based composites. Unfortunately, PP has a low surface energy; therefore, creating strong, durable adhesive bonds to this material can be difficult. As the number of potential PP–composite applications grows, manufacturers would like to have higher confidence in the strength of bonds in PP-based components. As a result, there is significant interest in the automotive industry in surface treatments that can enable bonding to PP with commonly used adhesives while maintaining a sufficient level of confidence in the strength and durability of the joint.

Another requirement specific to the automotive industry is the need for fast cycle times. To maximize efficiency and minimize costs, assembly plants that build high volume, mass market vehicles generally aim to produce vehicles at the rate of one vehicle per minute. This means that the processes used to manufacture automotive components cannot substantially exceed that cycle time and still be cost effective. Because of this cycle time requirement, many of the processes that are used in aerospace applications to produce strong joints reliably simply take too long to be used in high volume automotive applications.

Finally, again because of the cycle time requirements of the automotive industry, 100% inspection of adhesively bonded joints is not feasible. Consequently, the materials and processes used to manufacture adhesive joints in automotive applications must be robust to both manufacturing variability (including component variation stack-up and adhesive dispensing variability) and contamination. Process robustness is an important enough factor in the automotive industry for the robustness of a process in the manufacturing environment to influence the selection of material and processes as much as the structural requirements of the joint.

© Woodhead Publishing Limited, 2010

## 10.2 Pretreatment and surface characterization in composite bonding

The surface preparation method used to treat a substrate, whether it be metal or composite, is critical to the strength and durability of the joint. Since the effect a surface treatment has on a substrate cannot currently be validated as part of the manufacturing process, both aerospace and automotive manufacturers generally try to minimize the need for pretreatment of composite substrates prior to bonding. The ability to validate the chemistry of a surface after surface treatment has been and continues to be of great importance (Bossi and Nerenberg, 2000). Inability to verify the effectiveness of a surface treatment can be a barrier to implementation of new treatment processes because manufacturers must have confidence that every bonded joint manufactured meets design intent. Until a reliable methodology exists to validate the actual chemistry of a surface immediately prior to bonding for each and every component, the need to minimize sources of variability in the manufacturing process will be likely to dominate the selection process for surface treatments. Furthermore, the need for high reliability and robustness in the manufacturing process drives manufacturers to choose highly automated processes whenever possible.

The US Federal Aviation Administration (FAA) has periodically hosted workshops on adhesive bonding in the aerospace industry. The information presented at these workshops provides a good overview of the state of the art in aerospace bonding. Presentations from past workshops have been available on the internet. Historically, the primary surface preparation used for composites in the aerospace industry has been manual multi-step sanding (i.e. dry sanding, followed by wet sanding and final cleaning with a powdered cleanser and steel wool or scouring pad). Assessment of the effect of this process on the chemical make-up of the surface on individual parts was then validated by a 'water break test'. This 'test' applied water to the surface to see if the water formed a uniform sheet across the surface rather than beading up. While this process was still being used extensively in the aerospace industry as recently as 2004, there is a significant desire within the aerospace industry to eliminate sanding as a surface treatment process, particularly for critical, highly loaded structures. Many manufacturers do not have confidence in this process since it relies upon workers to consistently create a properly prepared surface, often over very large areas.

Grit blasting is often the preferred alternative to sanding (Boerio *et al.*, 2006) as it can be automated more easily than sanding and it is better suited to removing material in the small impressions on the surface left by the weave of peel plies. Peel plies are a woven fabric manufacturing aid, often made from nylon, which are commonly used in the manufacture of aerospace composites. Davis and Bond (1999) make a strong case for preparing surfaces

© Woodhead Publishing Limited, 2010

for bonding using grit blasting. Excessive grit blasting, however, can remove too much resin, leaving behind bare fibers and resulting in a poorly bonded joint. Consequently, aerospace manufacturers would like to have surface preparation options other than sanding and grit blasting because of the limitations of these processes.

Manufacturers in the automotive industry generally prefer that no surface preparation be required prior to bonding. Some composite component suppliers may be allowed to wipe the surface with a dry rag or with isopropyl alcohol (IPA). A dry rag wipe obviously does not necessarily remove all contamination from the surface, although it can remove gross contamination. Manufacturers would prefer instead that the source of the contamination be eliminated. Whether the surface wipe is dry or uses IPA, the surface can be left more highly contaminated after wiping than before if the wiping rags are not changed often enough. This is a primary reason that automotive manufacturers try to minimize the need for wiping.

There are applications in which automotive part suppliers may scuff sand a surface prior to bonding. Scuff sanding in the automotive industry, however, suffers from the same repeatability and reproducibility limitations as sanding in the aerospace industry. Nevertheless, it is commonly used in the manufacture of semi-structural composite components for low volume, high performance vehicles such as the Dodge Viper, Chevrolet Corvette and Aston Martin Vanquish. Semi-structural applications are structures that are not required to absorb energy or transmit loads in a crash. A description of bonding in the Aston Martin Vanquish can be found in Hill (2003). Scuff sanding is also typically required when using a room temperature adhesive to bond exterior class 'A' closure panel assemblies (i.e. hoods, decklids and doors) molded from sheet molding compound (SMC). Automotive class 'A' surfaces are the highly visible surfaces of a vehicle. Class 'A' SMC assemblies are used by many automotive manufacturers in medium and low volume (60,000 units per year or less) mass-market vehicle applications worldwide. The bonded joints in these assemblies, however, are non-structural.

### 10.2.1 New surface treatments for aerospace applications

The ability to use peel plies to provide a clean, chemically active surface for bonding is of significant interest to aerospace manufacturers (Flinn and Phariss, 2006; Phariss *et al.*, 2005). In the past, the use of peel plies as part of the composite manufacturing process has resulted in poorly bonded joints (Hart-Smith *et al.*, 1996). Some peel plies, particularly those coated with silicone or Teflon, can leave a residue on the composite surface which must be removed prior to bonding. While the peel plies that historically caused the most problems are no longer used, even materials that do not necessarily

© Woodhead Publishing Limited, 2010

transfer chemical groups to the surface may still leave behind a slick, inert bonding surface.

Since peel plies are generally used as part of the composite manufacturing process in the aerospace industry, there is great interest in modifying these materials so that they leave behind the clean, chemically active surface needed for bonding when they are removed from the composite. Since the choice of peel ply affects the chemistry of the bonding sites on the composite surface, the composite, peel ply and adhesive must be selected as a system. Manufacturers would prefer to use of one of these materials systems in lieu of other surface preparation techniques since simply removing a peel ply reduces the number of steps in the manufacturing process and should also reduce the opportunity for part-to-part variability resulting from inconsistent application of other surface treatments. Recent research has identified composite/peel ply/adhesive systems for some combinations of composites and adhesives. Research into the factors affecting adhesion in these systems and development of other composite/peel ply/adhesive systems for new materials continues in both industry and academia.

Since use of a peel ply does not always provide an ideal surface for bonding, there is interest in using various types of plasma to modify composite surfaces in a consistent, reliable way. One of the most promising surface treatment methods is atmospheric plasma (Kim *et al.*, 2003). This is an attractive surface treatment for aerospace applications because it can be automated, used on large parts and works well for low energy polymeric surfaces. Unfortunately, plasma in any form has yet to be implemented in aerospace applications largely owing to (1) the existence of functioning peel ply systems for existing materials and (2) the capital investment required to implement it on large parts. As new materials are qualified for aerospace applications, however, it becomes more likely that manufacturers will develop plasma treatment processes for use with these materials rather than developing new peel plies, given the inherent limitations of peel plies.

Equally important for both the aerospace and automotive industries is the development of a methodology for validating that the application of a surface treatment in production that resulted in the expected change in surface chemistry over the entire bonding surface on each and every part. As mentioned earlier, there is currently no way to confirm this as a part of a production process. Far too often an in-service failure in aerospace applications has been found to be the result of improper surface preparation (Davis and Tomblin, 2007).

Unfortunately, research at the University of Washington (Phariss *et al.*, 2005), as well as unpublished work completed within Ford Motor Company, has found that surface energy measurements alone are not sufficient to predict the strength of a bonded joint. A concise discussion of the problem faced by manufacturers in validating the quality of bonds can be found in

© Woodhead Publishing Limited, 2010

the literature (Hart-Smith, 2006). This inability to determine if a surface was prepared properly can result in a kissing bond that is not detectable by NDE/NDI. A structure built with a kissing bond in a joint may not meet design intent throughout its design life. Consequently, development of a tool that can validate the effect of a surface treatment as part of the manufacturing process is important to both industries. Aerospace manufacturers were sponsoring research to develop such a tool (Zhou *et al.*, 2008) at the time this book was written.

### 10.2.2 New surface treatments for automotive applications

The use of PP-matrix composites is expanding in automotive semi-structural applications. The difficultly in bonding PP-based materials has generated considerable interest in applying various types of plasma and flame treatments for these PP composite applications. Flame treatment has historically been used to increase the surface energy of the PP composite in spare wheel well applications in Europe (Kurcz *et al.*, 2004). As more manufacturers hope to implement PP-matrix composites in spare wheel wells, flame treatment may be replaced with atmospheric plasma treatment. Most of the documented work on both flame treatment and atmospheric plasma in the automotive industry has focused on non-structural PP-based bumper fascia applications (Pijpers and Meier, 2001; Carrino *et al.*, 2003, 2004; Staudigel *et al.*, 1999). Fortunately, most of the work on non-structural PP should be applicable to PP composite applications. There is increasing interest in the industry in bonding PP-based composites to metals in semi-structural applications. Regrettably, as of this writing, there is very little published information about the surface treatment processes used for PP–metal bonding.

Another potential surface treatment of some interest to automotive manufacturers is sulfonation. As in the case of PP–metal bonding, there is relatively little information available in the literature regarding sulfonation of PP (Erickson *et al.*, 1997; Asthana *et al.*, 1997). A description of the process being considered is available in US Patent 6,758,910 (Schmoyer, 2004). While initial evaluations of this process appear promising, much work still must be done to verify the long-term durability of joints in materials modified using this surface treatment and to verify the robustness of this treatment in the automotive manufacturing environment.

## 10.3 Composite joint design considerations

Good overviews of basic design considerations for composites joints are available in the *ASM Handbook* (Hart-Smith, 2001, Campbell, 2001) and *Adhesion Science and Engineering I: The Mechanics of Adhesion* (Hart-Smith,

© Woodhead Publishing Limited, 2010

2002). The reader should be aware that adherend thickness determines the most appropriate joint design. Adherend thickness is relatively thin in most automotive applications; as a result, single lap-type joints are common. Adherend thicknesses in aerospace applications are much more variable so joint designs are more varied as well. While strength and stiffness are often perceived to be the primary factors that determine the design of a joint, manufacturability, fatigue performance and weight can be just as important.

While the use of composite materials in primary structures continues to increase in the aerospace industry, composite applications in the automotive industry are currently restricted to those applications that do not carry crash loads during a collision. This is because vehicle development timelines require that the crash performance of the vehicle be predicted prior to the availability of prototype vehicles. While there are on-going efforts to develop finite element modeling methods that can predict the crash performance of composites (Gal and Fish, 2008; Pan *et al*., 2008; Bazant *et al*., 2008; Song *et al*., 2007; Xie *et al*., 2007), these models cannot currently predict composite behavior in crash events with the degree of accuracy required for primary structure analysis in high-volume vehicle programs. As a result, structural composite applications in the automotive industry are limited to very low volume specialty vehicle applications or to semi-structural or non-structural applications in high volume vehicles.

Automotive manufacturers are increasing their use of PP-based composites in semi-structural applications to consolidate parts and reduce costs. Unfortunately, PP cannot survive the oven temperatures used to cure the polymeric coating (the 'electrocoat' or 'e-coat') applied to steel to prevent corrosion. E-coat is applied by an electrophoretic deposition process and is the first step in the painting process. To cure the e-coat, the vehicle travels through long, high temperature ovens after coating has been deposited. This exposes the vehicle to temperatures of 360–400°F (180–205°C) for 20–30 minutes. Since PP-based materials will not maintain their structural integrity when exposed to those conditions, PP-based components must be assembled into the vehicle after the painting process. Installation after paint in most applications requires that mechanical fasteners be used to hold the components in place while the adhesive cures; therefore, these components are typically assembled using either mechanically fastened or hybrid (bolted and bonded) joints.

### 10.3.1 Developments in joint designs for aerospace applications

A recent development in aerospace composite joint design and manufacture is the incorporation of 'z-pins' into the joint. Z-pins are small diameter

© Woodhead Publishing Limited, 2010

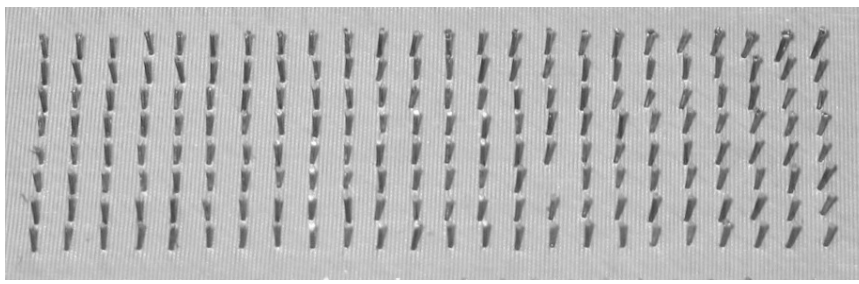
carbon rods that are ultrasonically inserted through composite laminates in the *z*-direction to provide extra resistance to crack growth and delamination (Clarke *et al.*, 2003). A photograph of a composite laminate with embedded z-pins is shown in Fig. 10.3.

Z-pins can be inserted into a composite-to-composite joint as part of either a co-curing or a co-bonding process. In a 'co-bonding' process, one of the detail parts is cured prior to the assembly of the joint and the mating part is cured simultaneously with the adhesive. Clay and Pommer (2006) have shown that the addition of z-pins improves joint toughness, as measured by average strain energy release rate. With more development, z-pins could potentially be used in some applications as a replacement for mechanical fasteners.

### 10.3.2 Developments in joint designs for automotive applications

As mentioned earlier, manufacturability has a strong influence on the design of composite joints in automotive applications. To accommodate the one minute cycle time needed for high volume applications, manufacturers would prefer to use a joining method that can meet this cycle time requirement without having to resort to the use of multiple bonding fixtures in the assembly plant.

At the time of writing, the Automotive Composites Consortium (ACC) is developing a concept for a fully structural composite underbody (Fuchs, 2008; Berger *et al.*, 2008). The ACC is a research partnership between Chrysler LLC, Ford Motor Company and General Motors and is part of the US Consortium for Automotive Research (USCAR). Funding for research conducted by the ACC is provided by the Department of Energy (DOE) National Energy Technology Laboratory under Award Number DE-FC26-02OR22910. A new joint concept (Fuchs *et al.*, 2008) was invented as part of this development program. This joint concept will allow a composite structure



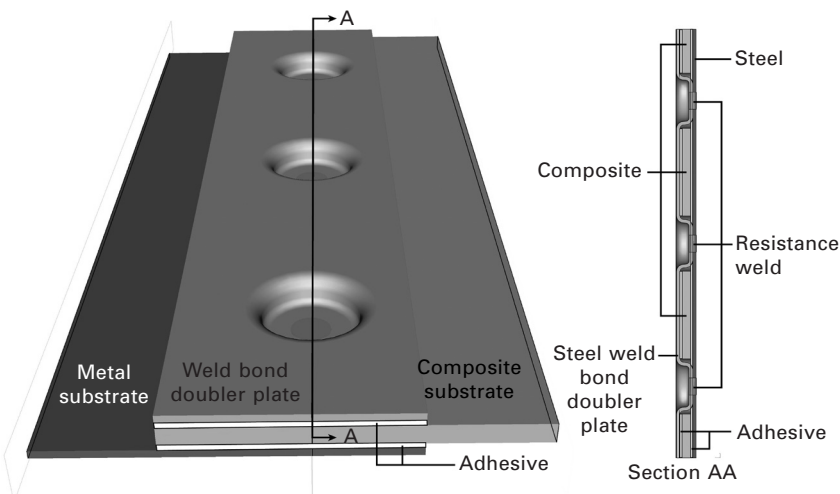
*10.3* Z-pin stubble in a composite substrate (photograph courtesy of the US Air Force Research Laboratory).

© Woodhead Publishing Limited, 2010

made from glass fabric reinforced SMC to be joined to a metal structure using traditional automotive body shop processes. A schematic of this joint concept is shown in Fig. 10.4. The basic concept of this joint design is that holes are drilled in the composite and a metal strip, termed a 'weld-bond doubler', is bonded to the composite. The weld-bond doubler is a strip of steel that has been stamped with depressions that fit into the corresponding holes in the composite. The composite component with the bonded metal doubler is then welded to the mating metal structure through the stamped depressions in the metal doubler using a conventional metal weld-bonding adhesive (e.g. Dow BETAMATE™ 1484 or Henkel Terokal® 5087-02P) and process. This joint design not only enables a composite structure to be joined to a metal one with no change in the assembly plant body shop, but the welds also act as 'peel stoppers' in the joint improving durability of the joint. As the time of writing, a project at Oak Ridge National Lab is currently underway to assess the durability of this joint design.

## 10.4 Modeling and testing of composite joints

Aerospace and automotive manufacturers conduct a significant amount of testing to characterize and validate the performance of both materials and joint concepts. Testing at the coupon and element level is used to qualify materials and to generate the material data necessary for finite element modeling of components and vehicles. Testing at the component and vehicle level is used to validate the performance of a structure.




*10.4* Schematic of the weld–bond joint concept developed for the Automotive Composites Consortium Underbody (schematic courtesy of the Automotive Composites Consortium).

© Woodhead Publishing Limited, 2010

One major difference between the aerospace and automotive industries is the willingness to complete developmental testing. Automotive manufacturers avoid developmental testing (i.e. testing conducted to develop a design rather than simply to validate the performance of the design) whenever possible. This is particularly true for high volume, mass market vehicle programs because this type of testing would significantly slow the introduction of new vehicles. Conversely, developmental testing is an expected and accepted part of aircraft development programs and can be accommodated by the longer product life cycle typical of this industry. Given the expense associated with comprehensive testing programs, manufacturers in both industries would benefit from, and therefore sponsor development of, better modeling techniques to minimize the amount of testing required.

### 10.4.1 Modeling adhesively bonded composite joints

Structural modeling (i.e. modeling of strength and stiffness) of composites and bonded joints is well established and is commonly used in both industries. While this eliminates the need for some testing, major deficiencies remain in the modeling of composite fatigue and crash performance. This is, unfortunately, true of both the composite substrate as well as the joints.

In order to predict the durability and crash performance of composite joints accurately, the ability to accurately predict the performance of the composite itself must first be developed. The US DOE, through the ACC, has funded a number of projects to improve predictive modeling of composite crash performance; however, the available models still fall short of the goal of true predictive capability. Additional development work in this area continues within several research groups (Gal and Fish, 2008; Pan *et al.*, 2008; Bazant *et al.*, 2008; Song *et al.*, 2007; Xie *et al.*, 2007).

After the ability to predict the performance of the composite has been developed, a similarly substantial effort will be required to develop the ability to predict the durability and crash performance of adhesively bonded composite joints. Radice and Vinson (2006) provide an excellent overview of developments in modeling of adhesively bonded structures. Their work went on to evaluate a number of issues related to adhesive bonding of mixed material structures and also evaluated the effect of mesh density on the predicted deflection of a cantilevered beam. Their analysis of the effect of mesh density illustrates one of the primary issues with modeling adhesively bonded structures in automotive and aerospace applications: the relatively small element size needed to predict the performance of adhesives is generally incompatible with the coarse mesh sizes needed to model large structures efficiently.

While a relatively simple model compatible with vehicle-level modeling mesh sizes has been developed for metal substrates (Faruque *et al.*, 2006), in

© Woodhead Publishing Limited, 2010

practice the adhesive is still typically omitted from durability and crash models in automotive vehicle development programs. Furthermore, this simplified model has not yet, to the author's knowledge, been successfully validated in conjunction with composite substrates. It is possible that reliable prediction of the durability and crash performance of adhesively bonded structures at the vehicle level may not be possible until computational resources allow efficient modeling of large models incorporating fine mesh densities for bonded joints within a larger, more coarse, vehicle level model.

Predictive modeling of the performance of adhesively bonded joints is also hampered by the strain-rate sensitivity of adhesive material properties. This is of particular concern in the automotive industry because of the high strain rates to which materials may be subjected during crash events. Strain rate sensitivity is also, unfortunately, an issue when predicting the performance of composite substrates. There is significant interest in characterizing polymers, adhesives and polymer composite material properties as a function of strain rate, but standardized test methods have not yet been agreed upon (Pinnell *et al.*, 2006). Development of appropriate test methods to obtain the necessary material property data is a critical first step in the development of finite element models capable of reliably predicting the structural performance of bonded composite structures in crash events.

While the capability of modeling 'ideal' adhesive bonds continues to improve, predictive modeling will not be truly dependable until manufacturers understand and can model joint performance as a function of substrate surface properties and interfaces. At present there appears to be relatively little information in the literature about the relationship between polymer and composite processing conditions and surface morphology in either unreinforced polymers or polymer composites. The surface morphology of the material, however, can have an impact on its bonding characteristics. The information available (Tomasetti *et al.*, 1999; Feuillade *et al.*, 2006) supports internal work completed at Ford Motor Company showing that molding process conditions have an impact on the surface characteristics of polymers and that these process-induced changes in the surface affect the long-term durability of bonding to the surface. These interface issues may be further complicated when mixed material (i.e. composite/metal) structures are considered. Addition of metal substrates into the system is likely to require incorporation of corrosion prediction into the finite element models.

Another potential limitation of existing models is their inability to predict the impact of manufacturing defects and of the evolution of the interface during service on the long-term performance of the joint. Manufacturing defects can act as disbond initiators, but the location and size of a defect will determine its ultimate impact on the properties of the structure. Similarly, migration of moisture to the composite/adhesive interface can degrade the properties of the joint (Campbell, 2001). Development of models capable of

© Woodhead Publishing Limited, 2010

predicting the impact of both of these factors on long-term joint performance is of particular interest to aerospace manufacturers since aerospace structures are generally required to carry higher loads and to function over longer time frames than automotive structures.

### 10.4.2 Testing adhesively bonded composite joints

Testing adhesively bonded joints is typically completed at different structural scales to fully characterize the performance of the joint. Manufacturers and their suppliers first characterize the basic performance of the materials and joints at a coupon or element level using standardized test methods. This type of testing is well established and details of typical test programs for basic material and joint characterization can be found in *Military Handbook MIL-HDBK-17, Volume 1* and the *ASM Handbook, Volume 21*, Testing and Certification section. A joint is classified as an 'element' in both *Military Handbook MIL-HDBK-17* and the *ASM Handbook*.

The performance with which aerospace and automotive manufacturers are concerned, however, is the performance of the vehicle. Thus, a considerable amount of testing in both the aerospace and automotive industries is completed on components and structures. Testing of these larger structural components, however, is design specific so there are no standardized test methods for this type of testing. The reader should note that while the MIL-HDBK-17 specifications for test plan development specify that the strength-critical failure modes should be used to identify the test matrix (MIL-HDBK-17-1F, p. 2-1), this may not in fact be the appropriate strategy for all applications. In the ACC composite underbody project discussed in Section 10.3.2, the design of that component was determined to be strain-limited rather than strength-limited owing to manufacturer-specific fuel-fed fire requirements (i.e. the vehicle must prevent smoke and flames from entering the passenger compartment for a certain amount of time to allow the occupants to escape from a vehicle after a collision). Consequently, the test program for that particular component must be developed around those application-specific requirements.

The testing a joint element, rather than a structure, is generally completed only to validate a material or process. In the aerospace industry this type of testing may be completed to establish 'design allowables' for a joint design, material or process. The cost of collecting sufficient data to establish these allowables, however, is often prohibitive. Accordingly, aerospace manufacturers may simply choose an older established material system or process to avoid the testing required to validate a new material or process.

Testing joint elements in the automotive industry is also generally done only to qualify new materials. It is likely that considerably more joint element testing will be completed in the future by automotive manufacturers

© Woodhead Publishing Limited, 2010

and suppliers to characterize adhesive and joint properties at high strain rates as standardized test methods for high strain rate testing are developed and as better finite element models for predicting the crash performance of adhesively bonded structures become available.

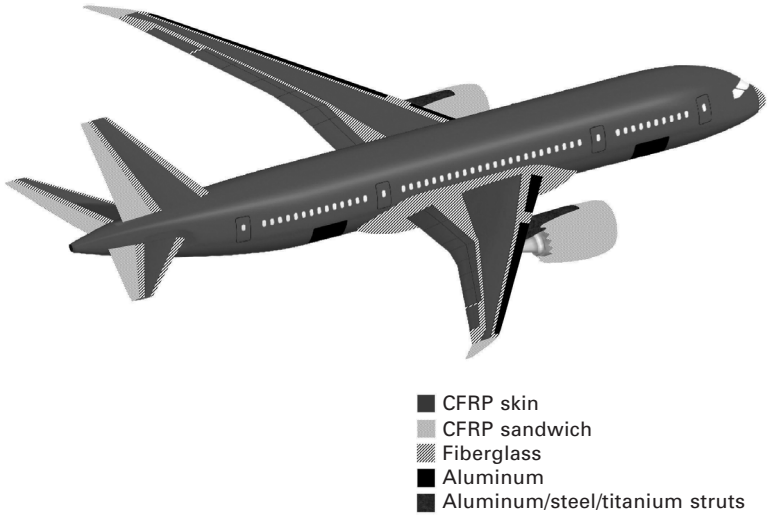
Testing larger sub-structural components may be completed in limited circumstances, but establishing both the loading mode and appropriate load levels to apply to a 'generic' joint in a sub-structure is often difficult. The type of loading and the loads to apply can be estimated by computer aided engineering (CAE) modeling; however, the limitations in modeling of composites discussed earlier reduce the confidence in information derived from existing models. It should be noted that one must be careful when applying testing methodologies developed for metal substrates to composite structures because composite materials may be substantially more compliant than metals. As a result, the loading mode in a composite structure may not be equivalent to that in a metal structure.

Since the strength and stiffness of structures can be modeled with a high degree of confidence, the bulk of vehicle-level testing completed by manufacturers is used to evaluate the properties for which modeling results are suspect (i.e. the durability or crash worthiness of a structure). Unfortunately, since durability and crash testing generally must be completed at the vehicle level, those tests are quite expensive. Given the expense incurred to complete these tests, companies try to minimize the amount of testing required to validate the performance of a structure. Nevertheless, there is no substitute for full-scale structural testing. Regardless of the improvement in predictive modeling capabilities, manufacturers will always rely upon full vehicle (aircraft or automobile) testing to validate the performance of a structure prior to the introduction of a new product. This is true for metal structures as well as composite structures.

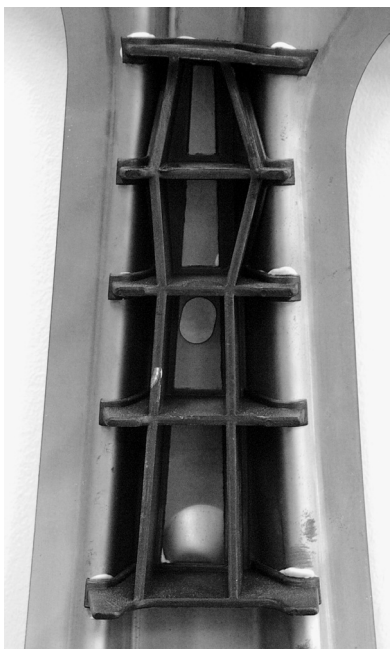
## 10.5 Future trends in aerospace and automotive composites

One trend likely to accelerate in both the aerospace and automotive industries is the use of mixed material (i.e. composite/metal hybrid) structures. The composition of the Boeing 787 aircraft is probably the most well known example of a composite/metal hybrid structure. The apportionment of composite and metal components in this aircraft is illustrated in Fig. 10.5. Structural hybrid material concepts are being explored in the automotive industry as well. Figure 10.6 shows a concept for reinforcing a metal structure with a bonded composite stiffener to use the sectional characteristics of the design more efficiently. In both industries the trend toward hybrid material structures is being driven by the increasing importance of fuel efficiency. As fuel efficiency becomes more important to customers, customers become

© Woodhead Publishing Limited, 2010




*10.5* Composite and metal usage in the Boeing 787 primary structure (schematic courtesy of The Boeing Company).



*10.6* Concept for reinforcing metal with a bonded polymer composite stiffener (photograph courtesy of Ford Motor Company).

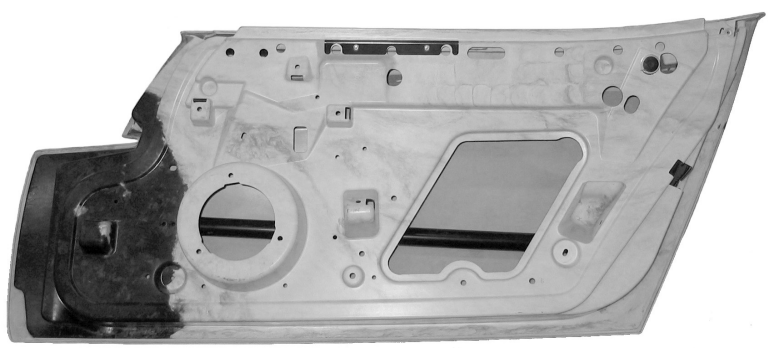
© Woodhead Publishing Limited, 2010

more likely to value lighter weight, but more expensive, vehicles. This means that manufacturers will be able to establish a business case for using composite materials in their vehicles more often. There will, however, always be applications for which metals are more appropriate than composites. Consequently, future designs are more likely to utilize composite/metal hybrid structures than entirely composite structures.

In the near term, implementation of composite/metal hybrid structures in the automotive industry is likely to continue to be limited to SMC and PP-composites in semi-structural applications. For example, SMC will continue to be used for fender supports and closure assembly inner panels. The carbon fiber SMC fender support, including the bonded headlamp support, for the Dodge Viper is shown in Fig. 10.7. The glass/carbon hybrid SMC door inner panel for the Dodge Viper is shown in Fig. 10.8. This component is a good example of the use of multiple materials to achieve an efficient



*10.7* Dodge Viper carbon fiber SMC fender support (photograph courtesy of Meridian Automotive Systems).



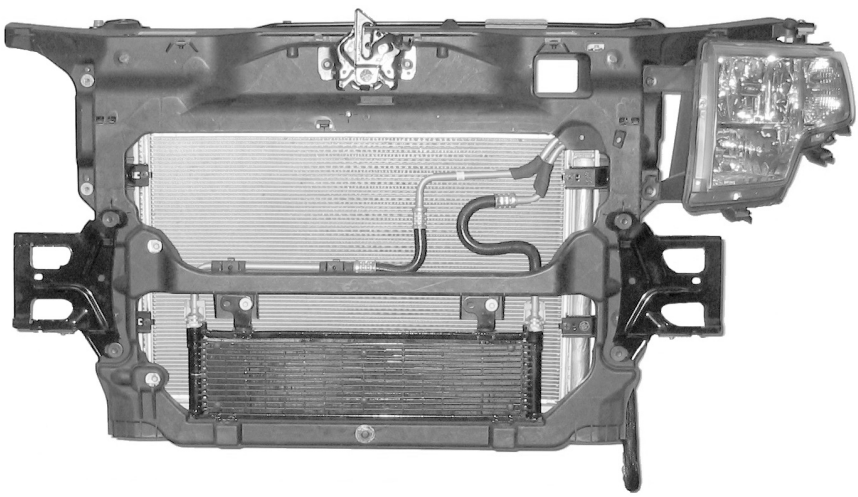
*10.8* Dodge Viper glass/carbon hybrid SMC door inner panel (photograph courtesy of Meridian Automotive Systems).

© Woodhead Publishing Limited, 2010

structure. Metal reinforcements are always used at attachments points in SMC components, but in this case a carbon fiber SMC patch was co-molded into a primarily glass fiber inner panel so that the size and metal thickness of the metal hinge reinforcement could be reduced.

The two most common PP-composite applications today are spare wheel wells (Kurcz *et al.*, 2004) and front end modules (Anon, 1998; Mapleston, 2000). A typical spare wheel well was illustrated in Fig. 10.1. A partially assembled front end module is illustrated in Fig. 10.9. In addition, there are also new concepts in thermoplastic overcoating of metals (Gruijcic *et al.*, 2008a and b; Li and Maj, 2008) which could also be used in future vehicle programs. These composite applications are unlikely to result in increased use of purely adhesively bonded joint designs in the automotive industry owing to the temperature limitations of thermoplastics and assembly plant manufacturing limitations which make curing adhesively bonded joints within typical automotive cycle times difficult. Development of composite-metal hybrid structural designs (i.e. the ACC composite underbody concept discussed in Section 10.3.2) may find their way into high volume automotive vehicle primary structures once CAE models capable of predicting the crash performance of composites and adhesively bonded joints have been developed.

Research into improved durability and crash performance modeling for both composites and adhesively bonded joints will continue. Much of this work will continue to be sponsored by the US DOE and the ACC. The ACC has created a roadmap for developing the tools necessary to be able to predict, rather than simply simulate, crash performance of composites by 2013. The



*10.9* An example of an automotive front end module (partially assembled) (photograph courtesy of Meridian Automotive Systems).

© Woodhead Publishing Limited, 2010

intent is to then validate these tools by building and testing a vehicle with a composite front crash structure. Development and validation of these tools is necessary prior to implementation of truly structural composites in high volume, mass market automotive applications.

Research into methodologies to make adhesive bonding more robust in the manufacturing environment will continue to be of interest to both industries. In the automotive industry, much of this work is concentrated on bonding to metal substrates. This work will also be directly applicable to composite applications, particularly composite/metal hybrid applications. In the aerospace industry, improving both the reproducibility and robustness of processes is of equal importance.

An area of considerable interest to the aerospace industry for composite bonding is so-called 'out-of-autoclave bonding'. Currently, all bonded primary structures are bonded using an autoclave, generally using film adhesives. Autoclave bonding is used to improve part fit-up and to ensure wet-out of the substrate surfaces. Using an autoclave improves wet-out by allowing use of adhesives that reach a low viscosity during processing and by creating high pressure during adhesive cure. These two factors are particularly important when bonding to the surface left behind after removal of a peel ply. As composite structures become larger, however, the cost of building larger autoclaves to manufacture these parts becomes prohibitive. Consequently, development of materials and processes for out-of-autoclave bonding which can create bonded joints with the same strength and durability as joints created in an autoclave becomes more important.

While development of new adhesives that cure at room temperature is the most obvious path to out-of-autoclave bonding, development of adhesives that use alternate curing mechanisms could also create a path to reliable and reproducible out-of-autoclave bonding. Alternate curing methods include e-beam, UV, microwave and induction curing. Hay and O'Gara (2006) provide a good overview of the strengths and weaknesses of e-beam, UV and microwave processing of polymer composites. The limitations noted for curing composite using these methods are likely to apply to composite bonding as well.

E-beam curing is not necessarily a good option because it can be difficult to apply pressure during the process. To make e-beam cure of adhesives an option for composite bonding in aerospace applications, new adhesive systems that can properly wet-out the surface at low pressures would have to be developed. UV curing can only be used with optically transparent materials, so this curing method is not likely to be a practical option for composite bonding. Microwave curing of adhesives has been studied as a process for completing field repairs of aircraft (Zhang and Dai, 2006). While the particular material and process studied may not necessarily meet the requirements for new structures, this work demonstrates the basic applicability

© Woodhead Publishing Limited, 2010

of the concept. Induction curing (Madhi *et al.*, 2003; Sands *et al.*, 2001) is another potential option, although work on this process has, up to now, also been focused only on repair applications.

While adhesives that cure using alternate mechanisms could become important in the aerospace industry, implementation of these types of adhesives is less likely in the automotive industry. During conventional painting processes in automotive assembly plants, vehicles (and therefore automotive structural joints) are exposed to temperatures that will heat cure standard one-component adhesives. This allows the use of relatively low cost conventional adhesives in automotive manufacturing processes. Use of secondary mechanical fasteners to 'fixture' semi-structural components, while the adhesive cures, eliminates the need for bonding fixtures in assembly plants so there is also no strong incentive to find alternative adhesives for these applications.

In addition to interest in new adhesives that do not require heat to cure, aerospace manufacturers would also like to see development of new adhesives that have a smaller environmental impact or that reduce health and safety concerns, both as part of the manufacturing process and while in service. These types of materials are also of interest to the automotive industry, particularly because of increasingly stringent emissions limitations in many regions. For example, the annual production of an automotive assembly plant can be restricted by the emissions produced by manufacturing processes in the plant. While total emission levels in an assembly plant are driven primarily by emissions from the paint shop, reduction in emissions from other manufacturing processes could allow manufacturers to increase the number of vehicles produced at a plant.

Since weight is such a critical design criterion in aerospace applications, there is considerable interest in 'multifunctional' adhesives and composites among aerospace manufacturers. In this context multifunctional refers to materials that can provide other functions in addition to their primary function. For example, a structural adhesive might also be electrically conductive, thermally dissipative, and so on. The goal is to improve the overall system capability while reducing weight and manufacturing complexity by decreasing the number of additional functional layers that one has to manufacture and assemble. Aerospace manufacturers are also following developments in nanomaterials to see what benefits these materials might bring to their products. Of particular interest are nano-scale reinforcements in adhesives that would allow for the construction of smaller, lighter weight joints, especially in highly loaded applications. While the automotive industry tracks developments in these areas, these types of material are less likely to be implemented in the near term in the automotive industry because of the high sensitivity of automotive vehicle programs to cost. To establish a sound business case for the application of these specialty materials in high

© Woodhead Publishing Limited, 2010

volume automotive applications, any increase in material cost would have to be offset by improvements in manufacturing efficiencies.

Finally, economic and competitive stresses in both industries, although particularly in the automotive industry, compel all manufacturers continually to look for technologies that will reduce the cost of building structures. To have the greatest likelihood of being implemented, technologies must reduce the total cost (materials, production, assembly, and maintenance/service) of the structure. Adhesive bonding can be a good alternative for lower cost structures; however, to see greater use of exclusively bonded assemblies in structural applications, technologies are also needed to improve confidence in the robustness of the bonding process as the joint is being manufactured. Developments in NDE/NDI will contribute to improved confidence, but in-line systems that evaluate the substrate and adhesive conditions at the time of bonding are necessary to foster the most increased confidence in, and therefore the most expanded use of, exclusively bonded assemblies in structural applications.

## 10.6 Sources of further information and advice

For more details on the fundamentals of composite joint design, bonding and testing:

US Department of Defense, *Military Handbook – MIL-HDBK-17-1F: Composite Materials Handbook, Volume 1: Polymer Matrix Composites Guidelines for Characterization of Structural Materials* (http://knovel.com/web/portal/browse/display?_EXT_KNOVEL_DISPLAY_bookid=721&VerticalID=0)

US Department of Defense, *Military Handbook - MIL-HDBK-17-3F: Composite Materials Handbook, Volume 3: Polymer Matrix Composites Materials Usage, Design, and Analysis* (http://knovel.com/web/portal/browse/display?_EXT_KNOVEL_DISPLAY_bookid=720&VerticalID=0)

*ASM Handbook Volume 21, Composites* (http://products.asminternational.org/matinfo/index.jsp)

For more information on the latest developments in bonding of aerospace composites:

Joint Advanced Materials & Structures Annual Technical Review Meetings (http://www.jams-coe.org/mx/hm.asp?id=home)

Federal Aviation Administration Adhesive Bonding Workshop Presentations: https://www.niar.wichita.edu/niarworkshops/Workshops/AdhesiveBondingWorkshop2004/tabid/104/Default.aspx

Information on Oak Ridge National Lab's assessment of the ACC Weld Bond Joint's durability can be found at: http://www1.eere.energy.gov/

© Woodhead Publishing Limited, 2010

vehiclesandfuels/technologies/materials/index.html. The project is funded by agreement number 18528, project number 17241.

An overview of NDE techniques for composites can be found at NetComposites: http://www.netcomposites.com/composite-tools.asp

## 10.7 Acknowledgements

The author would like to thank Kay Blohowiak and Will Grace at the Boeing Company for their clarification of current aerospace bonding practices, their assistance in identifying useful aerospace references and websites and in obtaining the 787 schematic included in this publication.

The author would also like to thank Kim Lazarz, Ann Straccia and Ari Caliskan at Ford Motor Company. Kim Lazarz provided much of the information on NDE of kissing bonds and verified the typical modeling practices for adhesive joints in automotive applications. Ann Straccia provided much of the information regarding surface treatments in automotive applications. Ari Caliskan graciously provided much of the information on the most recent developments in composite-metal hybrid structures and the photograph of the prototype spare tire tub.

The author would like to thank Hannes Fuchs at Multimatic for many useful discussions on modeling of composites and adhesively bonded structures as well as for providing the illustration of the weld-bond joint.

The author thanks Michael Hunt and David Dyke at Meridian Automotive Systems for their assistance in obtaining photographs of Meridian production parts.

Finally, the author would like to thank David Biernat at The Chrysler Corporation and Jessica Schroeder at General Motors for their input regarding common bonding practices and applications at their respective companies.

## 10.8 References

Adams R and Drinkwater B (1999), 'Non-destructive testing of adhesively bonded joints', *Int. J. Mater. Product Technol.*, **14**, 385–98.

Anon (1998), 'Metal/plastic composite for automotive front end', *Plastics News International*, April. 1998, page 6.

Asthana H, Erickson B and Drzal L (1997), 'Sulfonation of polymer surfaces - II. Chemical changes on polypropylene and polystyrene surfaces after gas phase sulfonation', *J. Adhesion Sci. Tech.*, **11**, 1269–88.

Bazant Z, Caner F and Hoover C (2008), 'Mesomechanical multiscale elastic-fracturing model for braided polymer composites', *49th AIAA/ASME/ASCE/AHS/ASC Structures, Structural Dynamics & Materials Conference*, Schaumburg, IL, AIAA Paper 2008-1932.

Berger L, Banks E and Wlosinski R (2008), 'Materials and processes for a structural composites underbody', *2008 SAMPE Technical Conference*, Memphis, TN.

© Woodhead Publishing Limited, 2010

Boerio F, Roby B, Dillingham R, Bossi R and Crane H (2006), 'Effect of grit-blasting on the surface energy of graphite/epoxy composites', *J. Adhesion*, **82**, 19–37.

Bossi R and Nerenberg R (2000), 'Quality assurance for composite bonding', *45th International SAMPE Symposium and Exhibition*, Long Beach, CA, 1787–99.

Brotherhood C, Drinkwater B and Dixon S (2003), 'The detectability of kissing bonds in adhesive joints using ultrasonic techniques', *Ultrasonics,* **41**, 521–9.

Campbell F (2001), 'Secondary adhesive bonding of polymer-matrix composites', in *ASM Handbook, Volume 21 Composites*, Miracle D and Donaldson S (eds), ASM International, Materials Park, OH, 620–32.

Carrino L, Polini W and Sorrentino L (2003), 'Adhesion of polypropylene surfaces treated by cold plasma', *SAE Transactions: J. Mater. Manufacturing*, **111**, 949–57.

Carrino L, Polini W and Sorrentino L (2004), 'Ageing time of wettability on polypropylene surfaces processed by cold plasma', *J. Mater. Processing Technol.*, 153–4, 519–25.

Clarke A, Greenhalgh E, Meeks C and Jones C (2003), 'Enhanced structural damage tolerance of CFRP primary structures by z-pin reinforcement,' *Proceedings 44th AIAA/ASME/ASCE/AHS Structures, Structural Dynamics, and Materials Conference*, Norfolk, VA.

Clay S and Pommer A (2006), 'Co-bonded composite joints using z-fiber stubble', *47th AIAA/ASME/ASCE/AHS/ASC Structures, Structural Dynamics, and Materials Conference*, Newport, RI, AIAA Paper 2006-1958.

Davis M and Bond D (1999), 'Principles and practices of adhesive bonded structural joints and repairs', *Int. J. Adhesion and Adhesives*, **19**, 91–105.

Davis M and Tomblin (2007), 'Best practice in adhesive bonded structures and repairs', *STAR*, 45.

Erickson B, Asthana H and Drzal L (1997), 'Sulfonation of polymer surfaces - I. Improving adhesion of polypropylene and polystyrene to epoxy adhesives via gas phase sulfonation', *J. Adhesion Sci. Tech.*, **11**, 1249–67.

Faruque O, Hill J, Bonnen J, Lazarz K, Ward S and Guimberteau T (2006) 'Adhesive modeling in crash simulation', *2006 SAE World Congress*, Detroit, MI, SAE Paper 2006-01-0955.

Federal Aviation Administration (United States) (1998), 'Fatigue evaluation of structure', *Federal Aviation Regulation FAA-FAR25.571*, Federal Register Volume 63, Number 61, pg 15707. http://rgl.faa.gov/REGULATORY_AND_GUIDANCE_LIBRARY/RGFAR.NSF/0/7385FBFAE1D21F328525667200503E10?OpenDocument

Feuillade V, Bergeret A, Quantin J-C and Crespy A (2006), 'Relationships between the glass fibre sizing composition and the surface quality of sheet moulding compounds (SMC) body panels', *Composites Sci. Tech.*, **66**, 115–27.

Flinn B and Phariss M (2006), 'Effect of peel-ply surface preparation variables on bond quality', *STAR*, V44, Report Number 20060047667.

Fuchs H (2008) 'Initial design of the Automotive Composites Consortium structural composite underbody', *2008 SAMPE Technical Conference*, Memphis, TN.

Fuchs H, Fickes J, Banks E and Berger E (2008), *Automotive Structural Joint and Method of Making Same*', US Patent Application 12119084.

Gal E and Fish J (2008), 'Anisotropic micromechanical creep damage model for composite materials: a reduced-order approach', *Int. J. Multiscale Computational Eng.*, **6**, 113–21.

Grujicic M, Sellappan V, Omar M, Seyr N, Obieglo A, Erdmann M and Holzleitner J (2008a), 'An overview of the polymer-to-metal direct-adhesion hybrid technologies

© Woodhead Publishing Limited, 2010

for load bearing automotive components', *J. Mater. Processing Technol.*, **197**, 363–73.

Grujicic M, Sellappan V, Mears L, Xuan X, Seyr N, Erdmann M and Holzleitner J (2008b), 'Selection of the spraying technologies for over-coating of metal-stampings with thermoplastics for use in direct-adhesion polymer metal hybrid load-bearing components', *J. Mater. Processing Technol.*, **198**, 300–12.

Hart-Smith L (2001), 'Bolted and Bonded Joints', in *ASM Handbook, Volume 21 Composites*, Miracle D and Donaldson S (eds), ASM International, Materials Park, OH, 271–89.

Hart-Smith L (2002), 'The design of adhesively bonded joints', in *Adhesion Science and Engineering I: The Mechanics of Adhesion*, Dillard D and Pocius A (eds), Elsevier, Amsterdam, 725–77.

Hart-Smith L (2006), 'An engineer asks: is it really more important that paint stays stuck on the outside of an aircraft than that glue stays stuck on the inside?', *J. Adhesion*, **82**, 181–214.

Hart-Smith L, Redmond G and Davis M (1996), 'The curse of the nylon peel ply', *Materials and Process Challenges: Aging Systems, Affordability, Alternative Applications*, **41-I**, 303–17.

Hay J and O'Gara P (2006), 'Recent developments in thermoset cure methods', *Proceedings IMechE, Part G: J. Aerospace Engineering*, **220**, 187–95.

Hill J (2003) 'Adhesively bonded structural composites for Aston Martin vehicles', *3rd Annual SPE Automotive Composites Conference*, Troy, MI.

Kim J, Kim H and Lee D (2003), *Effects of Plasma Surface Treatments on the Carbon/Epoxy Composite*', SME Technical Paper EM03-313.

Kurcz M, Baser B, Dittmar H, Sengbusch J and Phister H (2004), 'A case for replacing steel with glass mat thermoplastic composites in spare wheel well applications', *4th Annual SPE Automotive Composites Conference and Exposition*, Troy, MI.

Li N and Maj M (2008), *Lightweight Integral Corrosion-Resistant Front-end Structure for a Vehicle*, US Patent 7,374,233.

Mahdi S, Kim H-J, Gama B, Yarlagadda S and Gillespie Jr. J (2003) 'A comparison of oven-cured and induction-cured adhesively bonded composite joints', *J. Composite Mater.*, **37**, 519–42.

Mapleston P (2000), 'Modular front-end systems to reshape auto production', *Modern Plastics*, **77**, 24–5.

Nagy P (1991), 'Ultrasonic detection of kissing bonds at adhesive interfaces', *J. Adhesion Sci. Tech.*, **5**, 619–30.

Pan Y, Iorga L and Pelegri A (2008), 'Numerical generation of a random chopped fiber composite RVE and its elastic properties', *Composites Sci Tech.*, **68**, 2792–8.

Phariss M, Flinn B, Ballien B, Grace W and VanVoast P (2005), 'Evaluation of peel-ply materials on composite bond quality', *SAMPE 2005 Fall Technical Conference*, Seattle, WA.

Pijpers A and Meier R (2001), 'Adhesion behavior of polypropylenes after flame treatment determined by XPS(ESCA) spectral analysis', *J. Electron Spectrosc. Related Phenomena*, **121**, 299–313.

Pinnell M, Hill S and Minch A (2006), 'Special concerns in high strain rate tensile testing of polymers', *SAE 2006 World Congress & Exhibition*, Detroit, MI, SAE Paper 2006-01-0121.

Radice J and Vinson J (2006), 'On the use of quasi-dynamic modeling for composite

© Woodhead Publishing Limited, 2010

material structures: Analysis of adhesively bonded joints with midplane asymmetry and transverse shear deformation', *Composites Sci. Technol.*, **66**, 2528–47.

Sands J, Wetzel E and Yungwirth C (2001), 'Induction processed adhesives for military applications', *Proceedings of the 33rd International SAMPE Technical Conference*, Seattle, WA, 383–92.

Schmoyer T (2004), *Apparatus and Method for Sulfonating an Article and Articles Made Therefrom*, US Patent 6,758,910.

Song S, Waas A, Shahwan K, Xiao Z and Faruque O (2007), 'Braided textile composites under compressive loads: modeling the response, strength and degradation', *Composites Sci. Technol.*, **67**, 3059–70.

Staudigel G, Suchentrunk R and Gleich H (1999), 'Surface treatment of plastics using plasma processes', *Galvanotechnik*, **90**, 2816–21.

Tomasetti E, Nysten B, Rouxhet P, Poleunis C, Bertrand P and Legras R (1999), 'Surface characterization of polypropylene/(ethylene-propylene) copolymer blends (PP/EP): application to injection-moulded systems', *Surface Interface Anal.*, **27**, 735–42.

Xie D, Salvi A, Sun C, Waas A and Caliskan A (2007), 'Discrete cohesive zone model to simulate static fracture in 2D triaxially braided carbon fiber composites', *J. Composite Mater.*, **10**, 2025–46.

Zhang J and Dai Y (2006), 'Microwave curing and its applications to aircraft structure repair', *Key Engineering Mater.*, 326–8, 1725–8.

Zhou X, Zhang W, McDaniel D and Burton R (2008), 'Identification and validation of analytical chemistry methods for detecting composite surface contamination and moisture', presentation at the *Joint Advanced Materials & Structures 4th Annual Technical Review Meeting*, (http://www.jams-coe.org/mx/hm.asp?id=home).

© Woodhead Publishing Limited, 2010

# 11

# Selecting the right joint design and fabrication techniques

K. DILGER, Technical University Braunschweig, Germany

**Abstract**: Almost any modern product is put together with various components using a variety of joining techniques. The joining technique affects the properties of the product significantly and vice versa. Hence, the joining technique and additionally the whole correlated joining process must be considered during an early stage of the design process. Adhesive joints must fulfill certain properties depending on the parts' applications. Having this in mind when designing a joint, one has to differentiate between the various classes of materials and the variety of applications which are related to the range of loads and environments. Owing to their technical and economic importance, this chapter focuses on light metals, steel, plastics, fiber-reinforced plastics and sandwich materials. This chapter provides examples of vehicles and civil infrastructure applications.

**Key words**: bonding strength, design optimization, fabrication techniques, joint design, stiffness.

## 11.1 Introduction

Adhesive bonding is used as a joining technique to create complex parts from substructures. The joint must fulfill certain properties depending on the parts' applications. In most cases these properties can be deduced from the substrate material. The design engineer selects this material and chooses the dimensions of the part in order to fulfill given requirements. Additionally, an adhesive binding layer can introduce desirable properties that cannot be obtained by substructure materials, such as noise damping and electrical isolation. Having this in mind when designing a joint, one has to differentiate between the various classes of materials and the variety of applications which are related to the range of loads and environments. Owing to their technical and economic importance, this chapter focuses on light metals, steel, plastics, fiber-reinforced plastics and sandwich materials. Examples of vehicles and civil infrastructure applications are provided in this chapter.

A primary topic of concern for all materials and most applications is the environmental impact on the adhesively bonded joint properties. Environmental effects such as humidity, solvents, temperature extremes, thermal cycling and so on may cause either a reversible weakening or irreversible damage to the adhesive bonding. Effects on the different areas of the bonded joint have to be taken into account. Depending on adherend material, surface



© Woodhead Publishing Limited, 2010

treatment, adhesive, curing conditions, and so on, weakening can appear in the boundary layer of the adherend (both sides of the joint), in the boundary layer of the adhesive (both sides of the joint) and in the bulk material of the adhesive. For correct joint design, all these constraints need to be taken into account.

Almost any modern product is put together with various components using a variety of joining techniques. As discussed above, the joining technique affects the properties of the product significantly and vice versa. Hence, the joining technique and additionally the whole correlated joining process must be considered during an early stage of the design process.

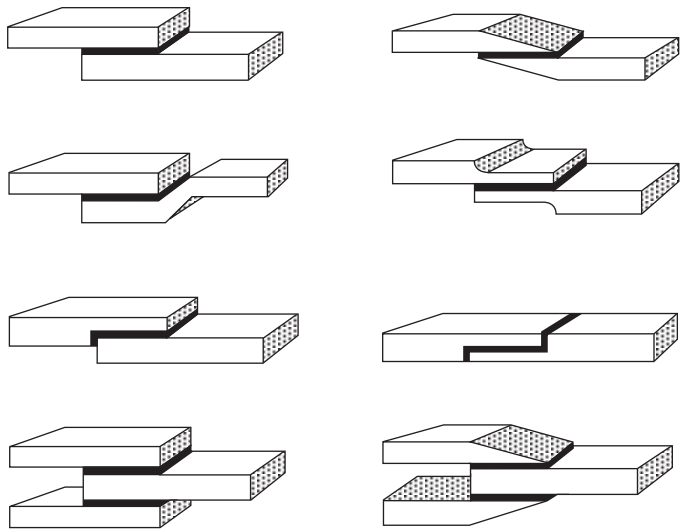
## 11.2 Basics

The design and the correlating calculation for adhesive joints to optimize the properties of bonded parts have been published frequently over the last 50 years. Hence, in this chapter, only some basics which are necessary to understand these particular applications and new results will be described. For further information, please refer to the listed references. In many cases the strength and the stiffness of the adhesive is much lower than the strength and the stiffness of the substrate. Common adhesives have a range in nominal shear strength from about 1–40 MPa, depending on different factors like joint geometry, temperature and so on. Young's modulus varies from 1 to 10,000 MPa. Compared to common steels with a material strength of about 350–2000 MPa and a Young's modulus of 200 GPa, there is a factor of roughly 10–1000 in strength and 1–100 in stiffness.

To compensate for these differences it is necessary to apply the right joint geometry. To bond mild steel with a high strength epoxy adhesive, the bonding area must be about ten times the sheet thickness in order to exploit the substrate material to the full (due to the factor of about ten between the strength of the steel and the strength of the adhesive). This example shows that the lower strength of adhesives has to be compensated by a larger bonding area. Depending on the different requirements given by the global design and the load cases, many sample solutions are described in the literature. Some design possibilities are shown in Fig. 11.1. Further details can be taken from Chamis and Murthy (1991), Baldan (2004), Apalak *et al*. (1995), Fuhrmann and Hinterwaldner (1984), Heitz (1971), Moulds (2006), Ulmer and Hennig (1962), Käufer (1984) and Marques and da Silva (2008).

The geometries shown in Fig. 11.1 are based on a longitudinal connection of plane structures. Here different kinds of overlap geometries as well as butt joints have to be taken into account. Because of the difference in strength and stiffness described above, overlap joints normally have better performance than butt joints. For elastic materials and massive geometries, butt joints may be advantageous. The tapers and steps decrease the stress concentration

© Woodhead Publishing Limited, 2010



*11.1* Possible geometries to enhance the bonding area, and/or to reduce stress concentrations caused by moments and edge effects.

at the edges. The other designs are used to increase the bonding area (double overlap) and/or to avoid moments caused by centric force transmission (Fig. 11.1).

The situation is similar for cylindrical geometries and closed profiles. Here overlap and butt joints are also possible. The static overdetermination is an additional problem when joining closed profiles. Owing to part tolerances, the gap between these parts varies from zero to a couple of millimeters depending on the dimensions of the parts. If the gap is too small, no adhesive can be applied, or the adhesive may be pushed away during joining. The displaced adhesives cause contamination of the parts, which leads to high cleaning costs. The bonding strength can be reduced because insufficient adhesive remains in the gap. Joining closed profiles is of great importance in modern vehicle designs; therefore possible solutions are discussed later.

A third basic geometry variant given by the global part geometry is the T-joint. Here two (or more) parts have to be joined at an angle of, for example, 90°. In this case there is a high probability of cleavage loads caused by moments. Therefore, the design of these joints is of great importance for the properties of the whole part (strength, stiffness). Design variants for T-joints are shown in Lees (1986), Käufer (1984), Ulmer and Hennig (1962), Hashim *et al*. (1990), Stuart and Crouch (1992), To *et al*. (2009) and Davies and Khalil (1990).

Because of the described causal relationship the load case is also very important. Peel and cleaving loads cause high stress concentrations at the beginning of the overlap, which may result in a crack initiation at this point

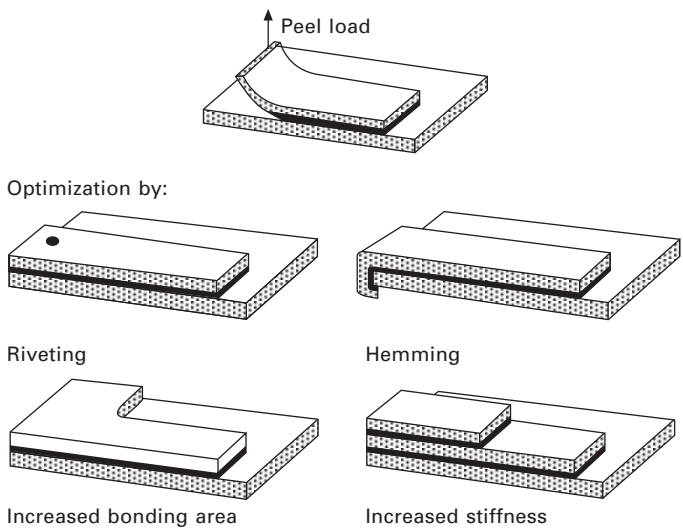
© Woodhead Publishing Limited, 2010

(Kinloch *et al.*, 2000). A uniform load distribution, resulting from tension, shear or compressive loads, results in high exploitation of the adhesive layer. This leads to a higher (nominal) bonding strength. In Fig. 11.2 design optimizations are shown for the reduction of local stress concentrations caused by peel loads.

Various methods are suitable to reduce the stress intensity. One approach is to enlarge the bonding area at the end of the overlap. Another approach is to enhance the stiffness of the parts in order to activate a larger section of the adhesive layer. A very simple method to reduce stress concentrations caused by peel or cleavage is to combine the adhesive bonding with additional joining techniques such as riveting or hemming.

The stress state and the resulting nominal strength of an adhesive bond are highly dependent on the geometry of the joint. Single overlaps lead to a bending moment, which results in a stress concentration at the end of the overlap. The elongation of the adherends under load leads to an additional stress in the adhesive layer. Because of this, very stiff substrates cause uniform stress in the adhesive layer, which increases the nominal bonding strength. Flexible substrates will reduce the strength of the joint. This is a well known and often published phenomenon (Goglio *et al.*, 2008; Straalen and Tooren, 2005).

A high stress concentration at the ends of the overlap can be avoided by varying the stiffness of the parts over the length of the overlap. A suitable technique for achieving this is to use of a scarf joint. In principle, a scarf joint will improve the properties of almost any joint and is mechanically one




*11.2* Design optimization to reduce stress concentration caused by peel loads. Adapted from Habenicht (2005).

© Woodhead Publishing Limited, 2010

of the best designs possible. Practically, the production of the scarf geometry is only sensible for particular applications, for example bonding composites where different components have to be activated.

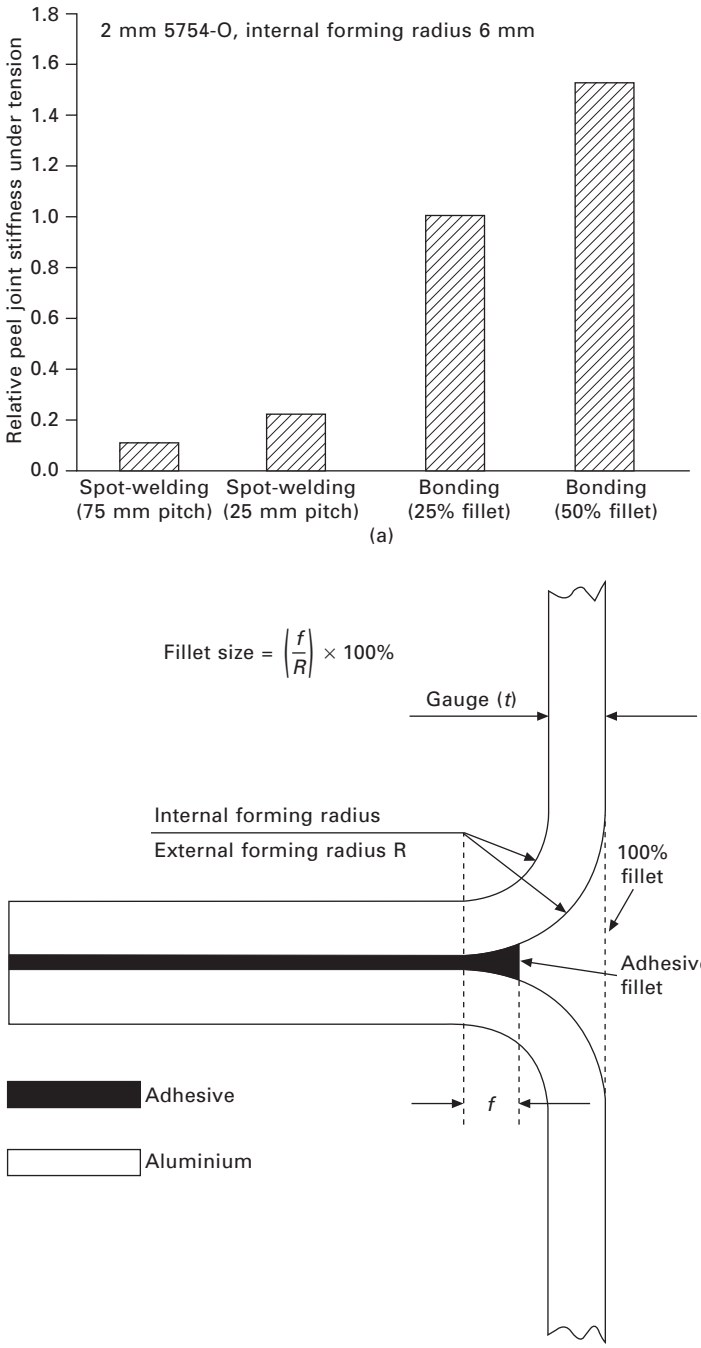
Another geometric influence on the bonding strength comes from the degree of gap filling at the end of the overlap. If excess adhesive is applied, the adhesive is squeezed out. This squeeze out leads to adhesive spew and an enlargement of the bonding area by wetting the edges of the adherends. Additionally fatigue properties are improved through the optimized stiffness gradient at the edges. Improved durability is observed, since the diffusion paths of water are longer and the humidity is not retained by capillary attraction. A possible disadvantage of the excess adhesive application is, as mentioned above, contamination of the part's surface. This can be avoided through an optimal dosage, which results in a fillet with comparable properties (Fig. 11.3a and b). Under dosage shows up gap sections lacking adhesive, which behave similarly to a sharp notch or a crack in reducing the static strength as well as the dynamic strength and durability. This suggests that under dosage should be avoided in order to assure the defined properties. In an industrial process, it is difficult to guarantee the right amount of adhesive and the correct shape of the part. Because of this, under and over dosage may appear (e.g. by tolerances of the gap width). Therefore the design should be robust enough that certain voids are tolerable.

## 11.3 Selecting the right joint design

As pointed out above, selection of the right joint design depends on a wide range of parameters. An adequate joint design ensures durable transmission of the applied loads during the entire service life of the part. The relatively low strength of the adhesive layer has to be compensated by a large bonding area. Stress concentrations in the bond line should be reduced. Thus peel and cleavage loads have to be minimized by the right design of the part. This can be done by positioning the joints in areas where only low stresses occur or mostly shear and compressive stresses are present. Peel and cleavage loads can also be reduced by special joint designs. A high stiffness of the joint, additional fixation by spot welding, riveting or clinching and a 100% adhesive fillet reduce the stress concentration and therefore enhance the bonding strength (Hunter *et al.*, 1998). Elongation of the adherends in the area of the bonding causes an increase in the local stresses in the adhesive layer. Therefore elastic deformation should be minimized and plastic deformation should be avoided. To reduce stress concentrations at the end of the overlap, the substrates can be tapered (Adams, 2005). Thus deviation of the local adhesive's von Mises stresses from average values is minimized.

To enhance the durability of a bonded part it must be ensured that water (and other critical substances) does not continuously interact with the bond

© Woodhead Publishing Limited, 2010




*11.3* (a) Stiffness of joints with various fillets. Adapted from Hunter *et al*. (1998). (b) Joint geometry. Adapted from Hunter *et al*. (1998).

© Woodhead Publishing Limited, 2010

line. Methods of achieving this are the selection of the right position of the joint or an additional sealing bead.

## 11.4 Fabrication techniques

To produce an adhesively bonded joint that fulfills all the demands in terms of service and production, adequate methods must be selected for surface pretreatment, adhesive application, assembling and curing. As these methods are complex and described in a multitude of publications only specialties correlating with the joint design are presented in this chapter. Higher strength and/or good durability of a bonded joint often can only be obtained using an adequate surface pretreatment. Polyolefines have to be pretreated by flaming, corona or plasma treatment, and metals by sand blasting (corundum), etching or anodizing.

New methods that can easily be established in the industrial process chain are laser pretreatment (Stammen *et al.*, 2007) and atmospheric plasma pretreatment. Both are suitable for metals and plastics. Using these methods it is possible to treat the bonding area locally in an automated process with almost no impact on the environment. Other promising techniques for local pretreatment are dry ice blasting, where solid carbon dioxide pellets (dry ice) are used in an impingement process to clean the surface, and Pyrosil™ treatment, where a silane is applied under the oxidizing conditions of an open flame (Hunter *et al.*, 1998).

Viscous adhesive is traditionally applied in a robot dispensing process where a (round) bead of adhesive is extruded onto the panels. This technique features a low entry cost and is used for processes with long dispense times. A more recent development is the application of even high viscous materials in a streaming process, where the adhesive can also be swirled (dispensed in a circular pattern). During the process, the material temperature and the material flow are controlled. These techniques greatly affect the performance of the operation and improve the automation process (Mandeville, 1999). New application tools even give the possibility of achieving a consistent bead diameter, which is velocity independent (Hellmanns *et al.*, 2006).

After applying the adhesive, the two parts have to be assembled. In most cases, an additional (hybrid) joining process like clinching is applied. During assembly and/or hybrid joining the gap must be filled up completely, not too much adhesive should be squeezed out and the parts must not be deformed by the applied mating forces. Processing a two-part adhesive curing results from the reaction of the two components where elevated temperatures often are applied to accelerate the cross-linking. Cross-linking a one-part adhesive may be initiated by the presence of moisture (e.g. one-part polyurethane) or by heating up the adhesive layer to temperatures of 125°C or 180°C (one-part epoxy).

© Woodhead Publishing Limited, 2010

In new applications the adhesive is often cured by inductive heating. When using two-part adhesives partial heating may be preferred to reduce distortions. Recent publications describe a method for heating up the adhesive itself using an induction process. For this reason so-called nano ferrites are added to the adhesive. This allows curing of adhesive bonds in non-metallic parts using this fast and economic method (Frauenhofer *et al.*, 2007).

## 11.5 Joints for different materials

As aforementioned, the design of joints is highly dependent on the adherend properties. Various materials and various applications suggest particular designs. In the following different designs are discussed, focusing on material dependence. Subsequently particular applications are described.

### 11.5.1 Bonding sheet metals

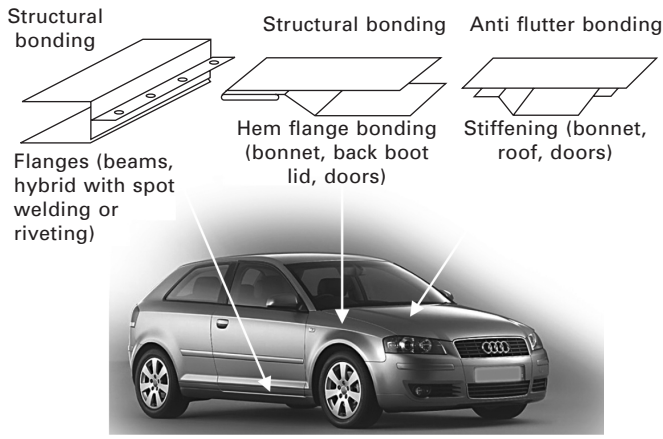
Sheet metals are used widely in the transportation and consumer (white goods) industries as well as in construction. Classic materials that have to be bonded include mild steel, modern high strength steels and light metals like aluminium, magnesium and titanium. These materials have a wide range in stiffness and strength, but they have in common strengths that are about 10 to 100 times higher than that of typical adhesives. On the other hand, the sheets have a small thickness compared to their other dimensions. An overlap of 10 to 100 times the sheet thickness may be needed for efficient load transfer. This is necessary for all kinds of connections such as longitudinal joints, T-Joints and so on. To realize the overlap, the flanges are normally formed in the pressing process of the part, so that no additional forming to construct the flange like hemming or bending is necessary. Figure 11.4 shows typical geometries for these flanges.

Since the use of clamps, jigs, and so on to fix the parts to be bonded is difficult and expensive, often additional joining techniques are used to provide handling strength in a so-called hybrid process. Here hemming, spot welding, clinching, riveting and screwing are common methods. Spot weld bonding is the preferred technique for joining steel sheets.

Here the welding electrodes apply a certain pressure to the sheet. This pressure causes the adhesive to be squeezed out and ensures metallic contact between the sheets. The electric current causes, in combination with the local resistance, a common melting zone between the two sheets. The spot weld is formed under increased pressure. The heat arising leads to a degradation of the polymer (Ghosh and Sambasivarao, 1998).

It must be ensured that the generated decomposition products do not cause corrosion. The dust accruing from this process needs to be removed. Using riveting and screwing suggests higher costs but avoids decomposition

© Woodhead Publishing Limited, 2010




*11.4* Typical flanges for joining sheet metals. Adapted from Friedrich and Kötting (1994).

of the polymer. All hybrid technologies have in common that the adhesive is pressed out of the area of the spot. Consequently, there is a weakening of the area near the spot resulting in adhesive pockets in between the spots. The discontinuity in stiffness may cause a decrease in fatigue behaviour. In automobile production the adhesive is cured at the same time as the E-coat after the coating process. This means that the uncured adhesive has to pass the washing and phosphatization procedures. Here the adhesive will be washed out if the viscosity is too low. Therefore, very high viscosity products are used for this application, which additionally complicates the hybrid process. Another method of avoiding washing out the adhesive is to use two-part-adhesives, which cure before the washing process without additional heat input.

Immediate handling strength can also be obtained through quick curing the adhesive. Inductive heating the sheets is a good way to achieve curing within seconds. The adhesive layer may be cured completely in this way, in combination with a two-part reaction or through oven curing.

Because corrosion is of great importance in terms of bonding sheet metals, it must be ensured that the flanges are completely filled up with adhesive or that an additional sealer is applied to prevent water from penetrating into the joint. For hem flange joints, it is almost impossible to fill the joint completely, because during the hemming process the adhesive is squeezed out of the joint. This leads to contamination of the pressing tools. After opening the pressing tool, the flange unclenches owing to elastic spring back. The bonding area is often decreased, as tool cleaning is expensive and hazardous because of the solvents required. This results in portions of the flange which are not filled with adhesive. Water can penetrate into this gap and cause corrosion. Therefore a sealer bead has to be applied. When the

© Woodhead Publishing Limited, 2010

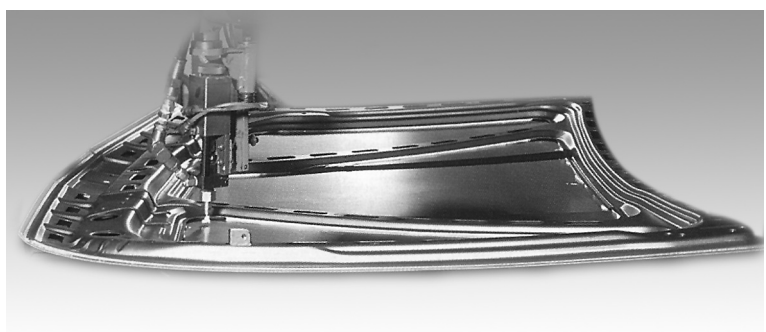
adhesive and the sealer are cured in an oven, the air in the flange expands and the sealing bead is perforated.

A suitable solution to this problem is to apply the sealer to the heated flange. Here the air expands and both the sealer and the hem flange adhesive are cured so that in the following processes, the integrity of the bond is maintained. Heating may lead to a distortion of the part. Here partial curing of the adhesive (so called 'spot curing') offers the possibility of avoiding the distortion and yet provide adequate handling strength. To avoid or to reduce squeeze out, the adhesive may be filled with glass beads to ensure a defined gap. The glass beads are pressed in between the sheets during the hemming process and provide additional initial strength because of the friction between the substrates and the beads. Another particularity is the appearance of optical irregularities on the surface of thin sheets caused by the shrinkage of the material. In Fig. 11.5 typical anti-flutter bonding of an automobile bonnet is shown. Here the requested class A surface may not be achieved because of the distortion of the sheets owing to chemical and thermal shrinkage (Vollertsen *et al.*, 2000).

This problem is intensified by the use of thin high strength steel sheets for the outer panels in a light weight design. To avoid these optical irregularities the design and processing have to be selected properly.

### 11.5.2 Bonding fiber-reinforced plastics (FRP)

Fiber-reinforced plastics (FRP), especially carbon reinforced plastics (CRP), are used in modern lightweight designs because of their extremely high strength and stiffness. This high strength and stiffness results from the fibers, which have a Young's modulus of up to 600 GPa and a tensile strength of up to 6000 MPa (carbon fibers). The matrix material, commonly epoxy, has a Young's modulus of about 10 GPa and a strength of about 50 MPa. These



*11.5* Anti-flutter bonding of an automobile bonnet. Adapted from Teroson (2001).

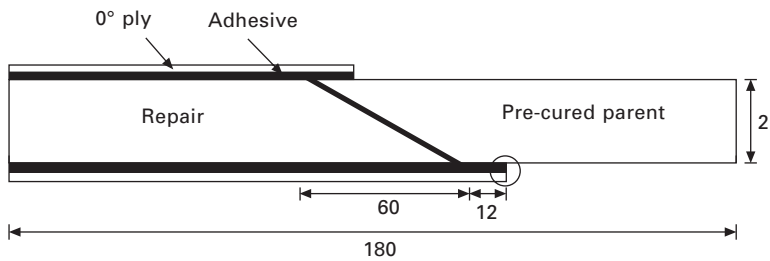
© Woodhead Publishing Limited, 2010

values suggest that the properties result from fibers embedded in the matrix in the primary load directions. To retain the basic material properties in a bonded structure it is necessary, besides having good adhesion to the substrate, to introduce the load into the fibers. If two sheets of FRP are bonded in a single lap shear configuration, delamination occurs when a higher load is applied. FRP can be better exploited when the adhesive introduces the load into the complete cross-section and/or penetrates the fiber layers. A commonly used approach is the application of scarf joints with very low scarf angles. Figure 11.6 shows typical geometry in the repair of a fiber-reinforced structure. To obtain suitable mechanical properties, a scarf angle of about 2° is used and a 0°-ply is bonded on either side of the sheet.

Another method of activating more volume is to include mold embedded elements into the FRP. In this case, it is important that the elements are integrated into the structure before it is cured. Thus, the fibers can be arranged continuously around the bolt. If the mechanical elements are inserted later by drilling, the fibers are destroyed and the structure is weakened (Fig. 11.7) (Karpov, 2006)

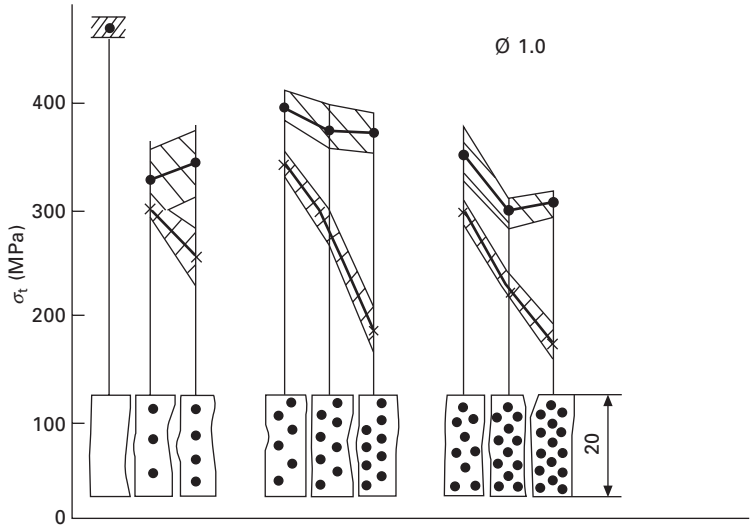
The activation of more fibers or layers in a FRP can be reached by using additional 'inter-adherend-fibers'. In this case, fibers both in and out of the joint plane direction are placed in order to strengthen the joint and to activate the complete sheet (Fig. 11.8) (Matsuzaki *et al.*, 2008). If two FRP sheets are being joined, sewing (stitching) is a common method of employing the additional fibers. The geometry of the fillet significantly affects the stress distribution in the adhesive layer and the adherend. Flat fillets with a large radius lead to a higher strength bond.

Another method of reducing stress concentration at the end of the overlap and enhancing the performance of the bonding is to use various adhesives in different areas of the overlap. A combination of a high strength and high modulus adhesive in the inner section and a low strength and low modulus adhesive in the outer sections provides more uniform stress distribution and improved load bearing capacity for the bond.

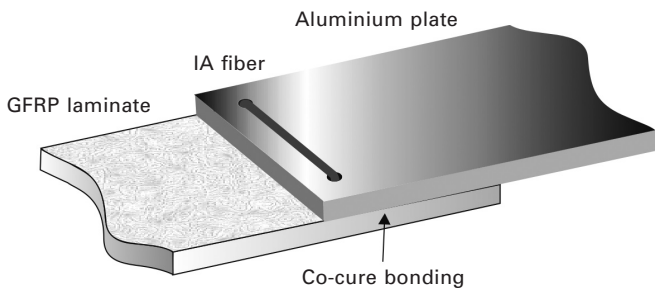



*11.6* Repair joint in a CRP sample. Adapted from Charalambides *et al.* (1998).

© Woodhead Publishing Limited, 2010




*11.7* Experimental values for the strength degradation: •, mold-embedded elements; ×, micro elements inserted into drilled holes. Adapted from Karpov (2006).




*11.8* Schematic illustration of an inter-adherend-fiber joint. Adapted from Matsuzaki *et al.* (2008).

## 11.5.3 Bonding sandwich structures

Applying a load to a sandwich structure is even more problematic than in a fiber-reinforced material. Sandwich materials are designed for load application over greater areas. If the load is applied at a point, the weaker inner parts of the sandwich (often polymeric foam or honeycomb) are destroyed locally. In this case, joints must be designed that introduce the load into the complete volume of the sandwich structure. This can be achieved through various anchor systems. A typical method that allows the application of point loads in sandwich structures is the introduction of anchor elements (metal or plastic), fixed by mechanical blocking, friction and/or an adhesive. Another

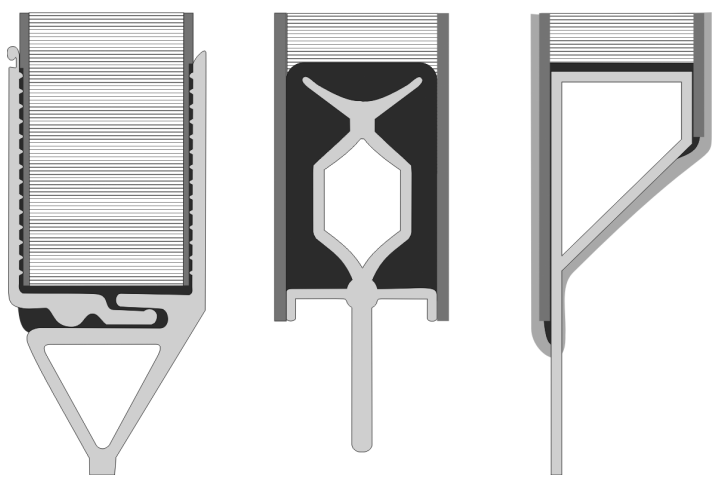
© Woodhead Publishing Limited, 2010

suitable method is the injection of adhesive into the hole or the structure to attain a 'polymeric anchor'.

Joining sandwiches is a comparable challenge. The load flow from each component of one sandwich panel to the other must be assured, otherwise the joint will be weaker and less stiff than the panels. Therefore, the joints must be placed in areas with low stress or a joining geometry must be selected that is suitable for the particular application. Figure 11.9 shows possible joining geometries of sandwich panel.

### 11.5.4 Bonding closed profiles

The state-of-the-art involves joining tubes made from steel or FRP by means of adhesive bonding. Recently further applications have arisen, such as the joining of tubular structures in automobiles and in civil engineering. A concern regarding bonding such structures is static over-determination. The reproducibility of a gap in the adhesive cannot be assured owing to tolerances. When using flat structures such as metal sheets, the joining precedure should be carried out in a rectangular fashion to avoid pushing the adhesive bead. Closed profiles have to be joined coaxially through a translational movement. One profile is pushed into the other, thus a certain amount of adhesive is pushed off depending on the resulting gap. This leads to contamination of the outer parts of the profile by adhesive and prevents the adhesive from filling up the gap completely. One possibility for avoiding this is to use a third component to guarantee overlap. Thus, additional preformed sheets can be bonded to the outside of the structure. Simple sheets can be used if the profile has more or less plane areas like a rectangular box beam.



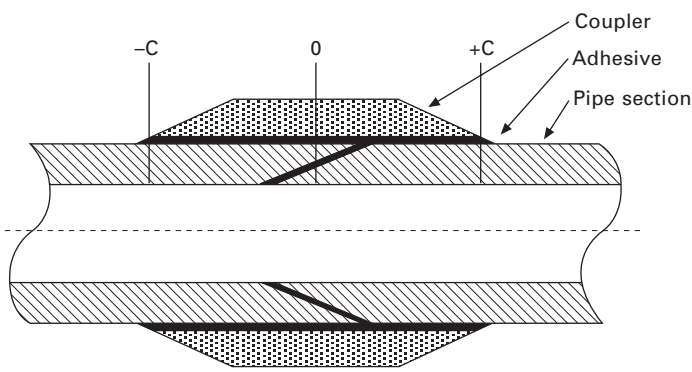
*11.9* Suitable joints for sandwich panels. Adapted from Hentinen *et al.* (1997).

© Woodhead Publishing Limited, 2010

The joining process is easy, because a linear, roughly rectangular joining movement can be realized. Cylindrical tubes can be backed by half shells. A problem here is that the radius of the tubes and the shell must fit very well. Otherwise an undefined adhesive layer, a loss of strength and residual stresses may result.

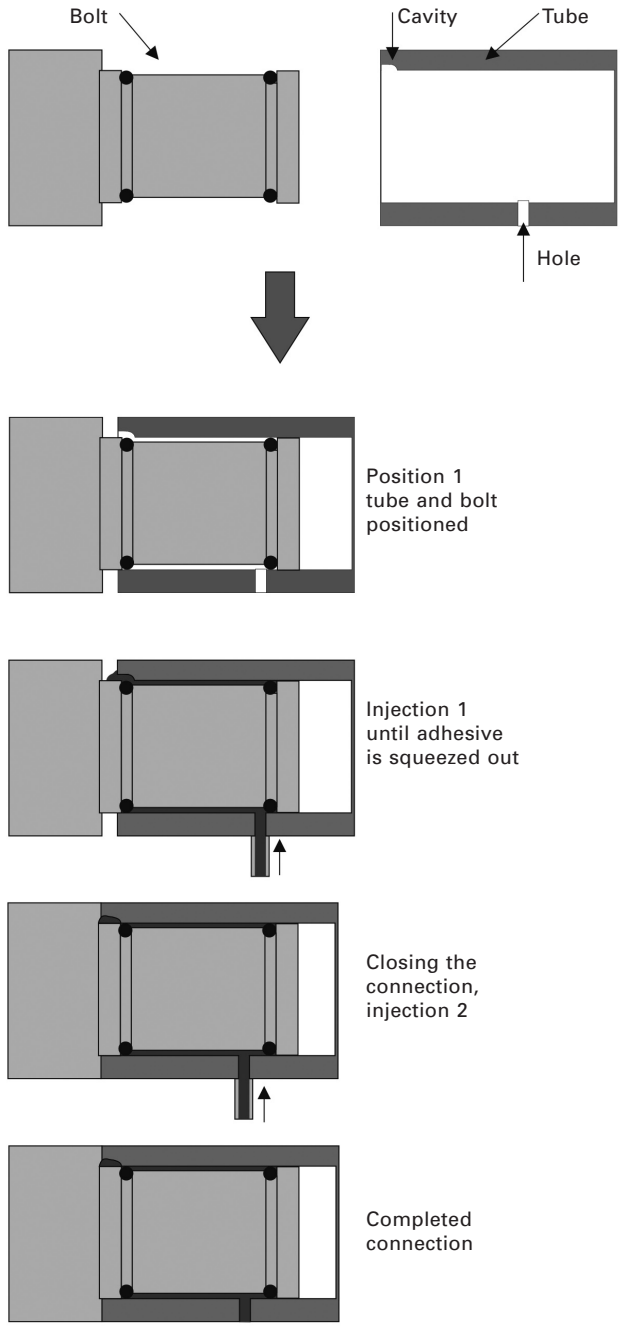
For profiles with more complex geometries and in order to avoid problems caused by tolerances, the backing could be formed *in situ*. This can be carried out by winding a steel sheet over the bonding area, or by laminating several layers of FRP around the tube. The thickness of the steel sheet is limited owing to the bending forces. By forming the coupler through lamination one can adapt the thickness to the necessary load transmission. Bonding can be carried out using an additional adhesive or by an FRP matrix resin. The stress distribution in the adhesive bonding can be improved by applying a scarf configuration (Pelekh *et al.*, 1992; Siebert and Schlimmer, 2005) (Fig. 11.10).

Another technique for bonding tubes and other closed profiles is injection bonding. In this process, the adhesive is pressed into the gap after joining. This allows compensation for the tolerances without great technical and economical effort. The adhesive is injected through a hole in the area of the joint. Filling the gap can be controlled by another, diametrically opposed hole. This hole facilitates exhaust of the air from the gap. To assure uniform filling it may be necessary to include gaskets or seams in the joint. These elements are also beneficial in guaranteeing the minimum gap width necessary to ensure adequate adhesive flow. Another advantage of this technology is that additional joining methods such as welding or riveting that provide handling strength can be carried out beforehand. This prevents the joining process being obstructed by the adhesive. A suitable geometry for injection bonding is shown in Fig. 11.11.




*11.10* Joint configuration for an optimized pipe joint. Adapted from Mertiny and Ellyin (2006).

© Woodhead Publishing Limited, 2010




*11.11* Injection bonding set up. Adapted from Siebert and Schlimmer (2005).

© Woodhead Publishing Limited, 2010

### 11.5.5 Reinforcement of concrete structures

A relatively new application of adhesive bonding is the use of bonded steel plates or bonded carbon fiber layers to reinforce buildings and other civil infrastructures. The reinforcing elements are adhesively bonded onto the tensile area of the structure with complete overlap. In newer applications the carbon fibers are prestressed and bonded onto the concrete surface using a two-part epoxy adhesive. The bonded structures show good environmental resistance. If steel sheets are used as reinforcing elements, corrosion inhibition of these elements, especially at the bondline, becomes a great challenge. For outdoor applications the steel plates need to be painted and primed and the bonding area has to be sealed (Ummenhofer *et al.*, 2007; Schmidt *et al.*, 2007; Arenas and Guillamón, 2007; Kessler *et al.*, 2004; Si Larbi *et al.*, 2009). The weakest layer in both reinforcement designs is the boundary layer of the concrete. Owing to its porous state there is good adhesion because the adhesive penetrates into this porous layer (Freisinger *et al.*, 2008). The reduced cross-section in the deeper zones of the boundary layer may lead to failure in this area under load. Therefore, to improve the strength of the adhesive bonding, it is necessary to improve the strength of the boundary layer of the concrete. This can be carried out by applying a very low viscosity primer to the concrete part, which easily penetrates deep into the boundary layer and, once cured, reinforces this layer.

## 11.6 Graphic representation of adhesive joints in engineering drawings

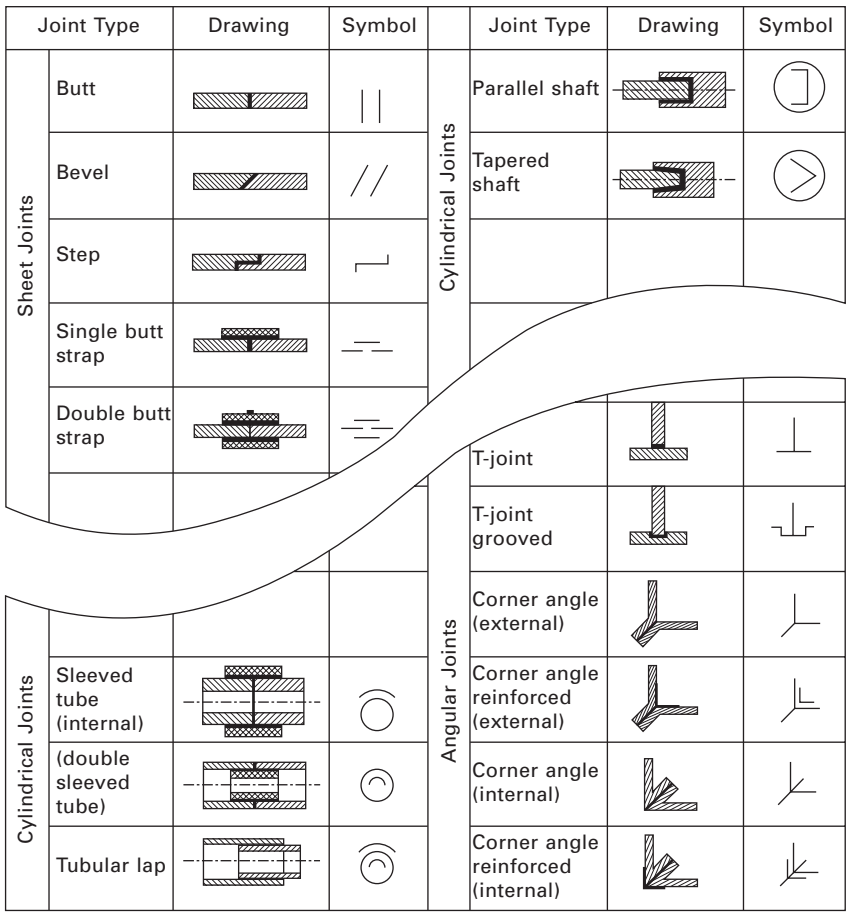
For various joining processes, there are graphic standards for including the relevant information in an engineering drawing. The graphic standard characteristics for welded joints are included in the EN 22553 standard. In this standard, the most important technical and geometrical welded joint parameters are defined precisely and two drawing methods are established: graphic and symbolic (Arenas and Guillamón, 2007).

Arenas and Guillamon present a proposal for a graphic standard that represents the information in a drawing. Similar to welded joints, a differentiation is made between a graphic and a symbolic representation. Figure 11.12 shows the symbols for different joint geometries.

The required information for adhesive bonding is included in a graphic symbol. Listed next to the geometry (A), the type of adhesive (B), the service loading (C), the priming of the substrate (D), the curing method (E), adhesive dimensions (F) and joint dimensions (G) are listed. Figure 11.13(a) shows the suggested symbols.

The secondary technical factors such as the adhesive application method, the type of assembly and the test standards are described in 11.13(b) An

© Woodhead Publishing Limited, 2010



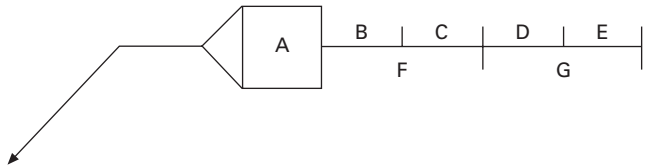

*11.12* Graphic symbols indicate the geometry of the adhesive joint. Adapted from Arenas and Guillamón (2007).

example for the use of this methodology in an engineering drawing is given in Fig. 11.14.

## 11.7 Conclusions and outlook

An adhesive joint has to be designed so that the properties of the bonded part are not affected negatively. Therefore the applied loads, the environmental conditions and the material properties of the adherends and the adhesives must be considered. It is necessary first to assure that there is a sufficient bonding area and then to minimize local stress concentrations, for example caused by high stiffness gradients. Hence, joint geometries are adapted to generate a more or less uniform stress distribution. This can be achieved by using, for example, certain fillet geometries or tapered joints.

© Woodhead Publishing Limited, 2010

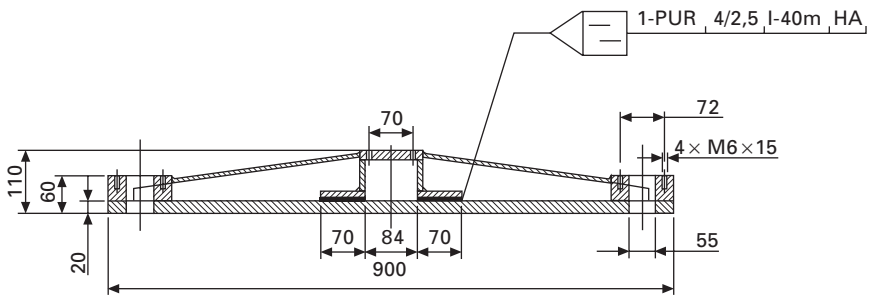



(a)

| | Dates of Application Assembly and Tests | |
|---|---|---|
| Application | Application way<br>Application temperature | ES<br>15–35°C |
| Assembly | Setting time<br>Service time | 4 h<br>12 h |
| Tests | Tension<br>Shear | UNE 26922<br>UNE 1465 |

(b)

*11.13* (a) Graphic symbol for adhesive joints, (b) Secondary technical factors. Adapted from Arenas and Guillamón (2007).




*11.14* Graphic representation of adhesive joints in an engineering drawing.

The application of the load into the material cross-section is particularly important for composite materials. Different approaches to this have been tried, but a really satisfying method that also meets the requirements of the production process has still to be established. Nowadays finite element analysis of the adhesive connection is an appropriate means of optimizing joint geometries. This method has not been discussed in this chapter as it is included in other chapters.

The focus of the actual research into fabrication techniques is on the rapid curing of adhesives, for example to achieve a handling strength within one working cycle in a production flow. Here inductive and UV-curing are established as suitable methods. In future there will be an effort to optimize the properties of the adhesive layer after curing especially in terms of crash behaviour. Additionally, methods for debonding have to be investigated.

© Woodhead Publishing Limited, 2010

## 11.8 References


Adams, R. D. (2005). *Adhesive Bonding*, *Science*, *Technology and Applications*, CRC Press, Boca Raton.

Apalak, M. K., Davies, R. and Apalak, Z. G. (1995). 'Analysis and design of adhesively-bonded double-containment corner joints'. *Journal of Adhesion Science and Technology*, **9**, 267–94.

Arenas, J. M. and Guillamón, A. (2007). 'Proposal for the graphic representation of structural adhesive joints in engineering drawings and their integration in a computer-assisted designing system'. *International Journal of Adhesion and Adhesives*, **27**, 122–8.

Baldan, A. (2004). 'Adhesively-bonded joints in metallic alloys, polymers and composite materials: Mechanical and environmental durability performance'. *Journal of Materials Science*, **39**, 4729–97.

Chamis, C. C. and Murthy, P. L. N. (1991). 'Simplified procedures for designing adhesively bonded composite joints'. *Journal of Reinforced Plastics and Composites*, **10**, 29–41.

Charalambides, M. N., Hardouin, R., Kinloch, A. J. and Matthews, F. L. (1998). 'Adhesively-bonded repairs to fibre-composite materials I. Experimental'. *Composites Part A: Applied Science and Manufacturing*, **29**, 1371–81.

Davies, R. and Khalil, A. A. (1990). 'Design and analysis of bonded double containment corner joints'. *International Journal of Adhesion and Adhesives*, **10**, 25–30.

Frauenhofer, M., Dilger, K. and Böhm, S. (2007). 'Influence of particle coating on nanoparticulate ferrites for electromagnetic adhesive curing on the adhesive properties'. *Proceeding of the 30th Annual Meeting of the Adhesion Society*, Tampa Bay/Florida, 18–21.02.07.

Freisinger, S., Wisner, G., Krelaus, R., Schmidt, M., Boehm, S. and Dilger, K. (2008). 'Structural and semi-structural adhesive bonding of UHPC by modifying the surface and close to surface layers'. *Ultra High Performance Concrete (UHPC) Proceedings of the Second International Symposium on Ultra High Performance Concrete*, March 5–7, 2008, Kassel, Germany, Schriftenreihe Baustoffe und Massivbau/Structural Materials and Engineering Series **10**, 275–82, Kassel University Press.

Friedrich, M. and Kötting, G. (1994). 'Geklebte Bauteile aus konstruktiver Sicht: Teil I geht auf die Ermittlung der mechanischen Klebstoffeigenschaften ein'. *Kleben und dichten*, **38**, 11–16.

Fuhrmann, U. and Hinterwaldner, R. (1984). 'Konstruktionskatalog fuer Klebeverbindungen tragender Elemente'. *Adhäsion – Kleben und Dichten*, **28**, 26–9.

Ghosh, P. K. and Sambasivarao, N. (1998). 'Weldbonding of thin sheet aluminium'. *International Journal for the Joining of Materials (JOM)*, **10**, 45–53.

Goglio, L., Rossetto, M. and Dragoni, E. (2008). 'Design of adhesive joints based on peak elastic stresses. *International Journal of Adhesion and Adhesives*, **28**, 427–35.

Habenicht, G. (2005). 'Konstruktive Gestaltung von Klebungen'. *Kleben – Grundlagen, Technologien Anwendungen*, Springer, Berlin, 529–37.

Hashim, S. A., Cowling, M. J. and Winkle, I. E. (1990). 'Design and assessment methodologies for adhesively bonded structural connections'. *International Journal of Adhesion and Adhesives*, **10**, 139–45.

Heitz, E. (1971). 'Konstruktive Gestaltung in Der Klebetechnik'. *Industrieanzeiger*, **93**, 2185–9.

Hellmanns, M., Böhm, S. and Dilger, K. (2006). 'Implementation of a velocity controlled manual applicator for adhesives and sealants in the automotive industry in consideration


© Woodhead Publishing Limited, 2010

of quality control'. *29th Annual Meeting of the Adhesion Society*. Jacksonville, Fl, USA, The Adhesion Society.

Hentinen, M., Hildebrand, M. and Visuri, M. (1997). 'Adhesively bonded joints between FRP sandwich and metal. Different concepts and their strength behaviour'. *VTT Research Notes; 1862*. Valtion Teknillinen Tutkimuskeskus, Espoo.

Hunter, J. A., Nardini, D., Gao, Y. and Ricks, R. A. (1998). 'Design and production of adhesively bonded aluminium automotive structures'. *Proceedings ISATA*, *International Symposium on Automotive Technology and Automation*, Düsseldorf, DE, Jun 2–5, 1998.

Karpov, Y. (2006). 'Jointing of high-loaded composite structural components. Part 3. An experimental study of strength of joints with transverse fastening microelements'. *Strength of Materials*, **38**, 575–85.

Käufer, H. (1984). 'Design of constructive adhesive joints for the optimization of manufacture and strength'. *Konstruktion*, **36**, 371–7.

Kessler, J., Lesko, J. and Cousins, T. (2004). 'Rehabilitation design and evaluation of the Hawthorne Street Bridge FRP deck installation'. *Advanced Polymer Composites for Structural Applications in Construction. Proceedings of the Second International Conference*. University of Surrey, Guildford, UK on 20–22 April 2004, 738–46, Holloway L.C. (ed.), Woodhead Publishing, Cambridge, UK.

Kinloch, A. J., Hadavinia, H., Blackman, B. R. K., Ring-Groth, M., Williams, J. G. and Busso, E. P. (2000). 'The peel behavior of adhesive joints'. *Adhesion Science for the 21st Century: Proceedings of the 23rd Annual Meeting*, Anderson G. L. (ed.), Adhesion Society, Myrtle Beach, South Carolina, February 20–23.

Lees, W. A. (1986). 'Bonding composites'. *International Journal of Adhesion and Adhesives*, **6**, 171–80.

Mandeville, D. C. (1999). 'Adhesives and sealants application (Zur Anwendung von Klebstoffen und Dichtmitteln)'. *Automotive Engineering International*, **107**, 42, 44, 46–7.

Marques, E. A. S. and Da Silva, L. F. M. (2008). 'Joint strength optimization of adhesively bonded patches'. *The Journal of Adhesion*, **84**, 915–34.

Matsuzaki, R., Shibata, M. and Todoroki, A. (2008). 'Reinforcing an aluminum/GFRP co-cured single lap joint using inter-adherend fiber'. *Applied Science and Manufacturing*, 786–95.

Mertiny, P. and Ellyin, F. (2006). 'Joining of fiber-reinforced polymer tubes for high-pressure applications'. *Polymer Composites*, **27**, 99–109.

Moulds, R. J. (2006). 'Design and stress calculations for bonded joints'. *Adhesives and Sealants: General Knowledge, Application Techniques, New Curing Techniques*, Cognard, P. (ed.), Versailles, France, Elsevier, Amsterdam, 2, 197.

Pelekh, B. L., Marchuk, M. V. and Kogut, I. S. (1992). 'Strength and design of adhesive joints in cylindrical elements made of metal and reinforced polymeric materials'. *Mechanics of Composite Materials*, **28**, 259–63.

Schmidt, M., Schlimmer, M. and Dilger, K. (2007). 'Kleben von Bauteilen aus ultra-hochfestem Beton'. *7. Kolloquium Gemeinsame Forschung in der Klebtechnik*. 27 und 28 Februar 2007, DECHEMA-Haus, Frankfurt/Main.

Si Larbi, A., Ferrier, E. and Hamelin, P. (2009). 'Concrete to steel lap joint failure criteria under combined shear and peeling stress'. *Journal of Constructional Steel Research*, **65**, 386–94.

Siebert, M. and Schlimmer, M. (2005). 'Prozesssicheres Kleben von Rundsteckverbindungen aus metallischen Werkstoffen unter rauen Fertigungsbedingungen'. *5. Kolloquium*

© Woodhead Publishing Limited, 2010

*Gemeinsame Forschung in der Klebtechnik*. Düsseldorf, DE, 15–16 Feb, 2005.

Stammen, E., Dilger, K., Böhm, S. and Hose, R. (2007). 'Surface modification with laser: pretreatment of aluminium alloys for adhesive bonding'. *Plasma Processes and Polymers*, **4**, S39–S43.

Straalen, D. I. J. V. and Tooren, M. V. (2005). 'Building and construction – steel and aluminium'. *Adhesive Bonding. Science, Technology and Applications*. CRC Press, Boca Raton.

Stuart, T. P. and Crouch, I. G. (1992). 'The design, testing and evaluation of adhesively bonded, interlocking, tapered joints between thick aluminium alloy plates'. *International Journal of Adhesion and Adhesives*, **12**, 3–8.

Teroson (2001). *High-Tech Industrial Adhesives*, Verlag Moderne Industrie, Landsberg/Lech.

To, Q. D., He, Q. C., Cossavella, M., Morcant, K. and Panait, A. (2009). 'Stress analysis of the adhesive resin layer in a reinforced pin-loaded joint used in glass structures'. *International Journal of Adhesion and Adhesives*, **29**, 91–7.

Ulmer, K. and Hennig, G. (1962). 'Die konstruktive Gestaltung der Metallklebverbindung'. *Mitt. Forsch. Ges. Blechverarb*., **23–24**, 320–8.

Ummenhofer, T., Medgenberg, J., Geiß, P. L., Dilger, K., Feldmann, M. and Pasternak, H. (2007). 'Klebeverbindungen im Stahlbau'. *Bauen mit innovativen Werkstoffen. Tagung Leonberg,* 19. und 20. März 2007/VDI-Gesellschaft Bautechnik VDI-Verl., Düsseldorf.

Vollertsen, F., Hahn, O., Herrmann, K. and Maier, H. J. (2000). 'Near Final Property Forming, Manufacturing and Component Testing'. *Congress Report. EndForm2000 on 3 and 4 May 2000, Paderborn,* [IPW, Institut für Prozess- und Werkstofftechnik]. Shaker, Aachen.

© Woodhead Publishing Limited, 2010

# 12

# Life prediction for bonded joints in composite material based on actual fatigue damage

G. MENEGHETTI, M. QUARESIMIN and M. RICOTTA, University of Padova, Italy

**Abstract**: After presenting an overview of fatigue behaviour and damage mechanics in single lap composite bonded joints, this chapter illustrates a model which describes the fatigue life of the joint as the sum of initiation and propagation up to failure of an average crack. Life to crack initiation is calculated by using a stress intensity factor approach and life spent in the propagation phase by the integration of a crack growth power law. Details of the analytical and numerical tools required by the model, the procedure for its application and the validation against experimental results are discussed.

**Key words**: bonded joints, composite materials, damage mechanics, fatigue, life assessment.

## 12.1 Introduction

Failures of bonded joints in composite material under fatigue loading occur, as in many other cases in engineering, when one or more cracks that were previously nucleated at the critical locations in the joint grow to a length that reduces the strength of the joint to a value lower than the applied cyclic stress. This damage scenario has been reported by several authors for both metallic and composite bonded joints.[1–8]

The relative contributions of the crack initiation and propagation phases to the total fatigue life depend on several geometric and design parameters of the joint, such as the type of adhesive and adherend material, the overall and corner geometry, the stress level and the presence of porosity and defects in the bondline, just to mention a few. In the authors' experience,[7–10] the crack nucleation phase can take from 10–90% of the total fatigue life, usually being higher in the case of spew fillet joints. It is therefore clear that an accurate lifetime assessment can be made only by taking into account and modelling both the life spent in nucleating the cracks and that spent in their propagation up to the critical length. To achieve this, a model for the life prediction of bonded joints in composite material, suitable for describing nucleation and propagation phases, has already been presented by the authors.[9,10] The nucleation phase is described by assuming that the generalised intensity of



© Woodhead Publishing Limited, 2010

the local stress field is a suitable parameter for rationalising the fatigue life to crack initiation. The life spent in the propagation phase is obtained by the integration of a power law relating the strain energy release rate (SERR) to the crack growth rate.

In this chapter, the model is discussed and further validated in the light of the results of a recent experimental programme[8] geared towards investigating the possible influence of the adherend stacking sequence and the interface ply orientation on the fatigue behaviour of single lap joints made by bonding carbon epoxy laminates with an epoxy adhesive.

The adherend stacking sequence and the orientation of the laminate ply in contact with the adhesive layer are among the variables the designer can adjust to control the overall behaviour of the joint[11,12] or the stress distributions near the singular locations at the end of the bonded overlap.[13–15] Their choices eventually affect the static and fatigue properties of the joint.

There is very little literature on research into this subject and results reported about the influence of ply orientation at the adhesive/adherend interface on static and fatigue strength are sometimes contradictory. A limited effect of interface ply orientation on the static strength was reported by Renton and Vinson[16] when testing glass/epoxy single lap joints with all 0° or 45°/0°/45°/0° unidirectional (UD) laminate adherends. The high cycle fatigue strength of the angle-ply joint was, however, 20–40% lower than that of all 0° joints.

Matthews and Tester[11] tested carbon/epoxy single lap joints made from UD laminates with several combinations of 0°, 45° and –45° layers. The static strength of the joints was found to increase with the proportion of 0° plies. The failure mode was found to be influenced by both lay-up and the overlap length, with the stiffer joints usually failing in the adhesive.

The influence of the interface ply orientation on fatigue damage was explicitly analysed by Johnson and Mall[17] for carbon/epoxy cracked lap shear joints made with three different lay-ups, namely $[0/\pm45/90]_s/[0/\pm45/90]_{2s}$, $[\pm45/0/90]_{2s}/[\pm45/0/90]_{2s}$ and $[90/\pm45/0]_{2s}/[90/\pm45/0]_{2s}$. Thus, 0/0, 45/45 and 90/90 interface conditions were investigated. Results indicated that 0/0 and 45/45 interfaces exhibited similar values of the total strain energy release rate at the threshold of crack propagation. However, the threshold for 45/45 interface joints was slightly higher (about 10%) than that for 0/0 interface joints. The 45/45 interfaces were also found to be stronger than the 90/90 interfaces.

An average decrease of about 30% in the fatigue shear strength for woven glass/polypropylene single lap joints was reported by Ferreira *et al.*[18] with respect to joints with $[0]_7$ adherends. As result of an extensive literature investigation, De Goeij *et al.*[19] reported that interface ply orientation had a negligible influence on static strength, but under fatigue loading, all 0° joints behaved better than those with 45° and 90° oriented ply at the interface.

© Woodhead Publishing Limited, 2010

From the brief survey above, it seems difficult to find evidence of improvements in the structural properties of composite bonded joints derived from changes in the interface ply orientation or lay-up. However, the extensive discussion on damage evolution under fatigue, reported by Johnson and Mall,[17] suggests that a possible strengthening mechanism could be the more complicated crack paths which occur when the orientation at the adhesive/adherend interface is different from 0/0. In an attempt to clarify the subject further, recent results for the fatigue strength of single lap bonded joints are discussed in this chapter, together with an extensive overview of fatigue damage mechanics observed during fatigue testing. The life prediction model is then briefly outlined and the data for its application are derived. Finally, the validation of the model is presented using the fatigue results for the new joint configuration.

## 12.2 Recent results for fatigue behaviour of single lap bonded joints

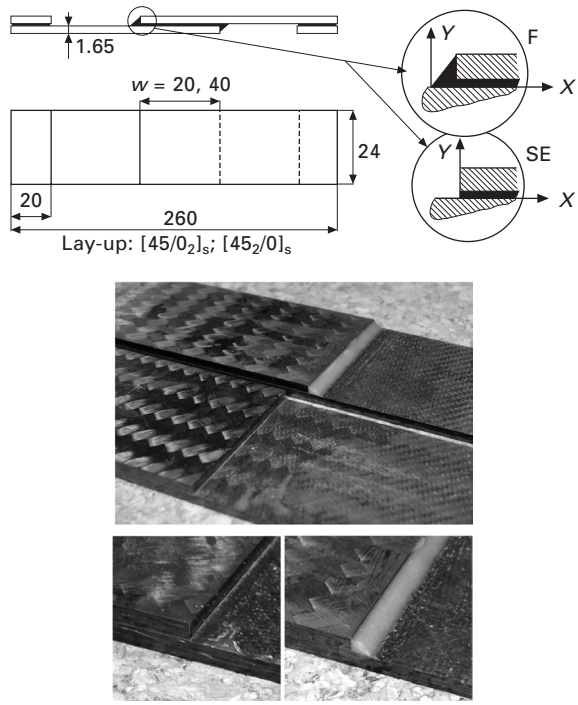
As mentioned above, the fatigue life of bonded joints can be split into two main phases: nucleation and propagation. This is also confirmed by our last experimental programme, extensively discussed by Meneghetti *et al*.[8,20] The geometry, dimensions and details of the corner geometry for the single lap joints tested are shown in Fig. 12.1. The joint geometry, adherend material and adhesive are the same as those investigated previously.[7,9,10]

Two overlap lengths (20 and 40 mm), two corner geometries (square edge SE and spew fillet F) and two laminate lay-ups ($[45/0_2]_s$ and $[45_2/0]_s$) were investigated under tension–tension loading. The joints were obtained, using the procedure presented by Quaresimin and Ricotta,[7] from autoclave-moulded laminates (Seal Texipreg® CC206, T300 twill $2 \times 2$ carbon fibre fabric/ET442 toughened epoxy matrix) and bonded with the two-part epoxy adhesive 9323 B/A by 3M.

An MTS 858 servo-hydraulic testing device equipped with a 15 kN load cell was used for the experimental programme. The nominal load ratio during fatigue testing was set to 0.05 and the test frequency was kept in the range from 5–15 Hz. To investigate damage evolution during the fatigue life and assess the fraction of life spent for crack nucleation and propagation, joints were subjected to repeated blocks of fatigue loading at constant amplitude up to failure. Damage evolution was monitored by measuring the stiffness drop and via periodical inspection by the naked eye and using an optical microscope (magnification 50× or 100×) of the polished edges of the joint. Fracture surfaces were investigated by scanning electron microscope (SEM) analysis. The properties of the joints under static loading are presented and discussed by Meneghetti *et al*.[8]

Let us now consider the fatigue data produced using the classical stress–life

© Woodhead Publishing Limited, 2010

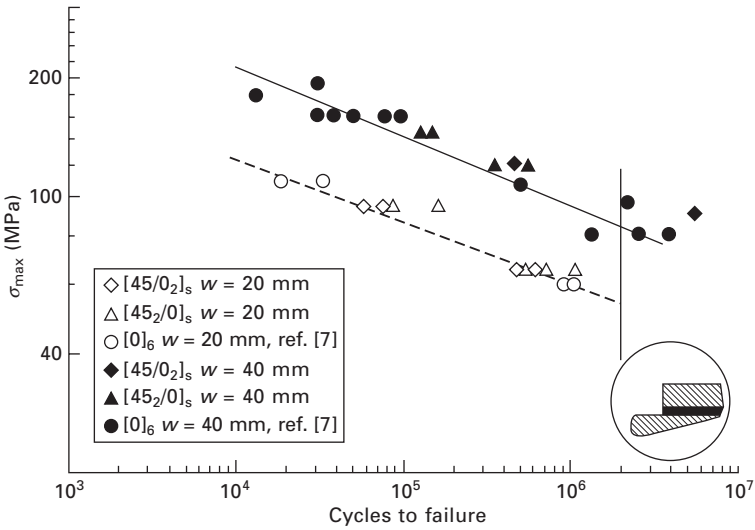



*12.1* Geometry of the single lap bonded joint ($w$ = 20 and 40 mm) and details of the corner geometry (SE = square edge joint; F = fillet joint); bondline thickness is 0.15 mm.

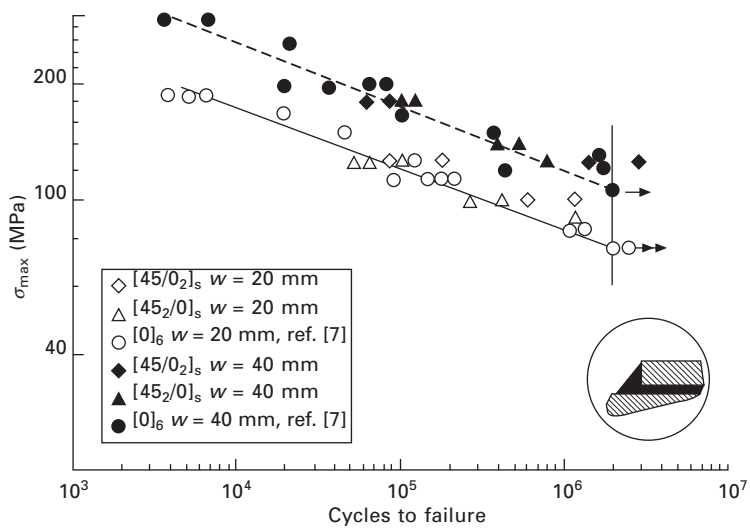
approach. Figures 12.2 and 12.3 show the fatigue data for the different series in terms of maximum nominal stress, $\sigma_{max}$, versus the number of cycles to failure. Stresses are calculated by simply dividing the applied load by the cross-section of one of the adherends. The results are compared to those obtained from previous work on $[0]_6$ single lap joints.[7] The available data were also statistically analysed to provide design fatigue curves, under the hypothesis of a log-normal distribution of the number of cycles to failure. Reference stress values at $2 \times 10^6$ cycles, $\sigma_{MAX,50\%}$, the inverse slope of the S–N curve, $k$, and the scatter index $T_\sigma$ ($\sigma_{MAX,10\%}/\sigma_{MAX,90\%}$) are listed in Table 12.1 for each of the series tested.

From the analysis of the results reported, it appears that only in the case of square edge joints does the 45° interface result in a limited improvement in the fatigue strength. On the other hand, changing the overlap length from 20 to 40 mm leads to a significant improvement of the cyclic load-bearing capability of the joint. Moreover, a comparison of the results in Figs 12.2 and 12.3 shows the life extension at the same stress level, deriving from the presence of the spew fillet at the end of the overlap region and independent of the adherend lay-up.

© Woodhead Publishing Limited, 2010




*12.2* Experimental fatigue data for square edge joints (fatigue lines are for $[0]_6$ joints)




*12.3* Experimental fatigue data for spew fillet joints (fatigue lines are for $[0]_6$ joints)

It can therefore be concluded that, from the design standpoint, the influence of overlap length and corner geometry on the fatigue strength of these joints is far more important than that of the stacking sequence of the laminates and the orientation of the plies at the adhesive–adherend interface.

© Woodhead Publishing Limited, 2010

*Table 12.1* Results of the statistical analysis on experimental fatigue data (reference fatigue strength at $2 \times 10^6$ cycles)

| Lay-up | Corner geometry | Overlap (mm) | $\sigma_{MAX,50\%}$ (MPa) | $\sigma_{MAX,90\%}$ (MPa) | $k$ | $T_\sigma$ | No. of data |
|---|---|---|---|---|---|---|---|
| $[45/0_2]_s$ | Square edge | 20 | 51.3 | 46.5 | 5.47 | 1.215 | 4 |
| | | 40 | 101.5 | – | 8.38 | – | 2 |
| | Fillet | 20 | 89.8 | 73.9 | 8.07 | 1.479 | 4 |
| | | 40 | 125.5 | 110.1 | 9.08 | 1.300 | 4 |
| $[45_2/0]_s$ | Square edge | 20 | 52.8 | 42.2 | 4.77 | 1.646 | 5 |
| | | 40 | 94.2 | 82.8 | 6.15 | 1.295 | 4 |
| | Fillet | 20 | 79.4 | 71.3 | 7.31 | 1.240 | 6 |
| | | 40 | 107.0 | 97.5 | 5.62 | 1.204 | 5 |

Another detail of practical design interest may be the strength reduction of a structure associated with the presence of a bonded joint, which is in some ways representative of the 'structural efficiency' of the connection. In fact, although a well-balanced bonded joint can fail under static loading outside the bonded area (see Quaresimin and co-workers[7,8] for several examples), the presence of the bondline will always result in a significant reduction of its load-bearing capability in fatigue. This reduction can be quantified by calculating the ratio between the reference fatigue strength of the joints and the static strength of the adherends (defined fatigue strength reduction factor) and then making a comparison with the fatigue ratio of the adherends under the same load ratio in order to identify the fatigue strength reduction that is solely caused by the fatigue damage process in the laminates. These two ratios can be calculated by the following equations

$$\text{fatigue strength reduction factor} = \frac{\sigma_{MAX,50\%} \text{ of the joint}}{\sigma_{UTS} \text{ of the adherend}}$$

$$\text{fatigue ratio} = \frac{\sigma_{MAX,50\%} \text{ of the adherend}}{\sigma_{UTS} \text{ of the adherend}}$$

Tensile strength values for the laminates used in preparing the adherends are reported by Meneghetti *et al.*[8] and are equal to 500 MPa (coefficient of variation, c.o.v. 12%) for $[45/0_2]_s$ laminates and 350 MPa (c.o.v. 4%) for $[45_2/0]_s$ laminates. The fatigue strength reduction factor caused by the bondline can be easily calculated using the reference fatigue strength at $2 \times 10^6$ cycles (Table 12.1). It ranges from 0.10, for the $[45/0_2]_s$ SE joints with an overlap $w = 20$ mm, up to 0.31, for the $[45_2/0]_s$ spew fillet joints with an overlap $w = 40$ mm. Joints made by bonding $[0]_6$ laminates,[7] are characterised by even lower values, in the range 0.09 to 0.17.

The fatigue ratios under tension–tension loading for laminates of the same material, but with lay-up $[0]_{10}$ and $[45]_{10}$, have been quantified[21] and

© Woodhead Publishing Limited, 2010

are equal to 0.77 and 0.49, respectively. It is therefore clear that most of the significant loss in fatigue strength that should be taken into account is solely due to the bonding.

Although the stress–life approach is useful in practical design problems, Figs. 12.2 and 12.3 demonstrate that it is not suitable for combining data for joints of different geometry and consequently for providing a model of general validity. Moreover, independent of the layer orientation at the adhesive–adherend interface and adherend stacking sequence, the ratio between the average fatigue strength at 2 million cycles for joints with overlap length of 40 mm and 20 mm is not equal to two, which is the ratio one would expect if the mean shear stress calculated with reference to the overlap area were used as the unifying parameter. This situation confirms the need to use alternative approaches to the development of effective prediction methods. The idea of a model based on actual damage evolution, suitable for describing the fatigue life of the joint from a physical point of view, was presented Quaresimin and co-workers.[7, 9, 10] Before describing it and for a better understanding of the model hypothesis, it is worth illustrating and clarifying the mechanics of the fatigue damage evolution observed during the experimental programme.

## 12.3 Overview and analysis of fatigue damage mechanics (nucleation and propagation)

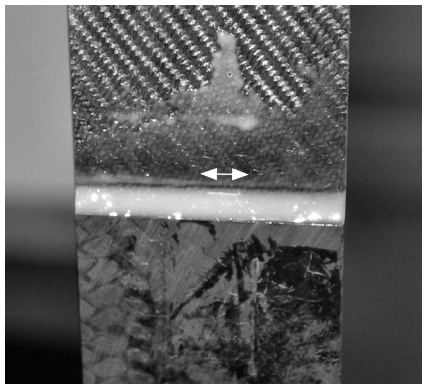
As mentioned at the beginning of the chapter, the typical damage scenario under fatigue loading consists of the nucleation of one or more cracks at critical locations and their growth up to the joint's failure.

To illustrate the whole phenomenon better, we can take as a representative example the damage evolution observed in a spew fillet joint that failed at a high number of cycles. The joint had a lay-up of $[45/0_2]_s$ and was loaded with a maximum tensile cyclic stress (measured on the section of one adherend) equal to 100 MPa. Figure 12.4 shows the typical sequence of crack nucleation and early propagation observed on the free surface of the adhesive fillet (adhesive whitening indicating the onset of a crack could be easily observed by the naked eye). In this case, the onset of the first crack was observed at about 310,000 cycles. As shown, this crack took some further 700,000 cycles to reach the joint edges. Then, the crack front grew in the longitudinal direction for several cycles, as illustrated by the side view of the crack patterns in Figures 12.5(a) and 12.5(b). The joint eventually failed at 1,163,120 cycles.

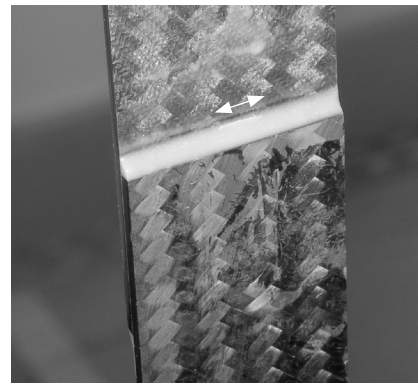
Crack lengths, measured at the overlap corners, versus the normalised fatigue life are reported in Fig. 12.6 and the morphology of the fracture surface obtained from SEM analysis is shown in Fig. 12.7.

Figure 12.6 clearly illustrates the non-symmetric propagation of the crack

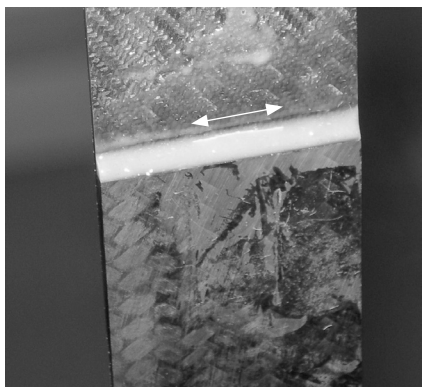
© Woodhead Publishing Limited, 2010



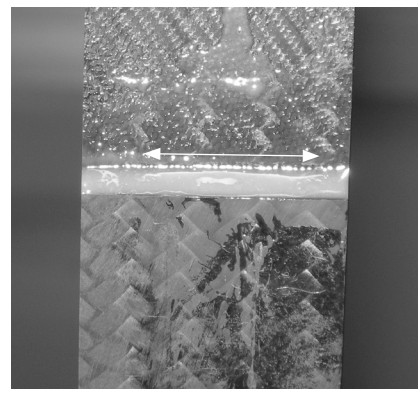
410 kcycles



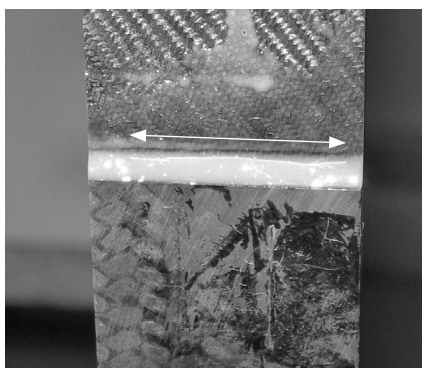
500 kcycles



600 kcycles



800 kcycles

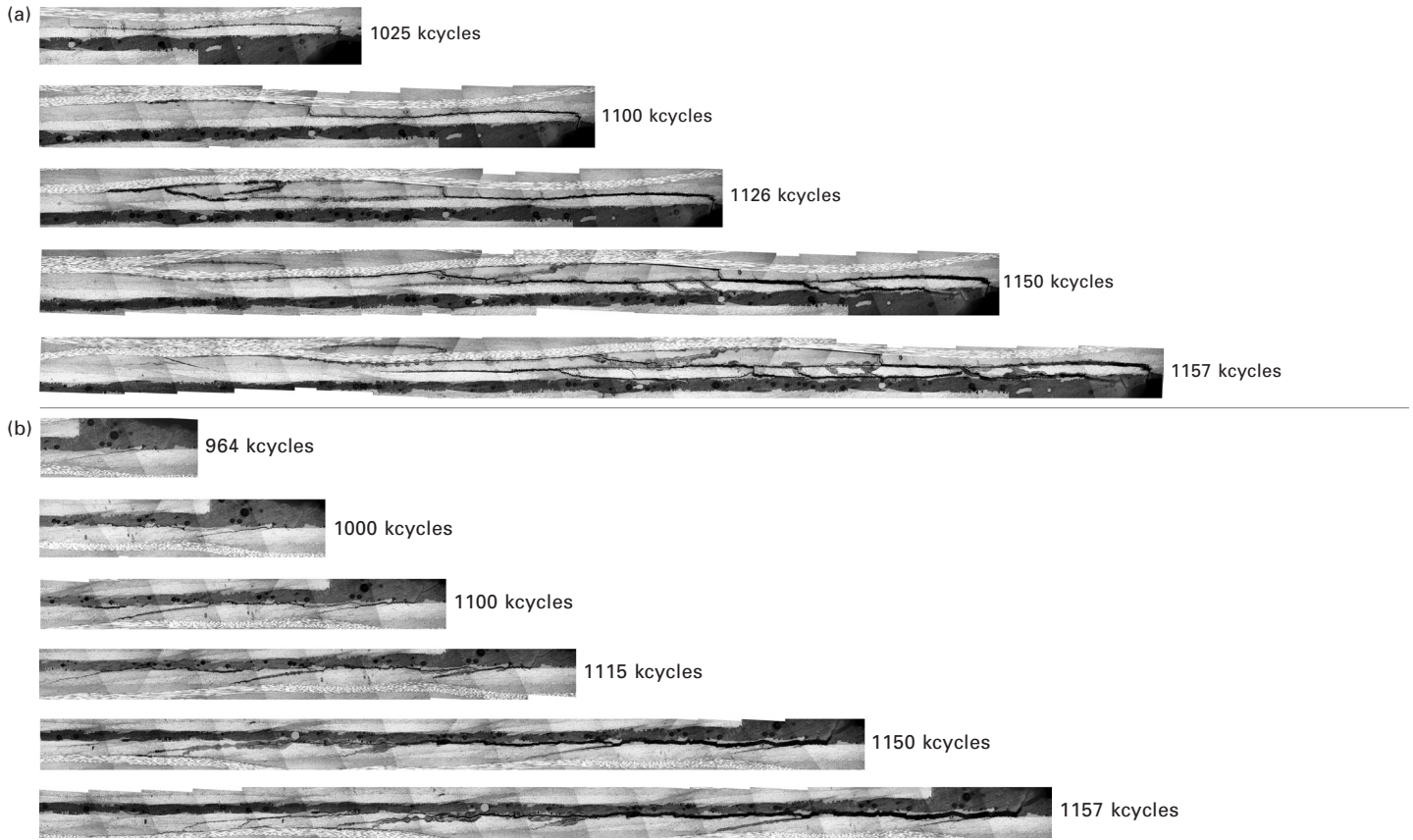


900 kcycles

*12.4* Crack initiation in the fillet (identified by adhesive whitening) of a spew fillet joint (lay-up $[45/0_2]_s$; $\sigma_{max}$ = 100 MPa, $w$ = 20 mm, $N_{it}$ = 310,000 cycles, $N_i$ = 980,000 cycles, $N_f$ = 1163,120 cycles).

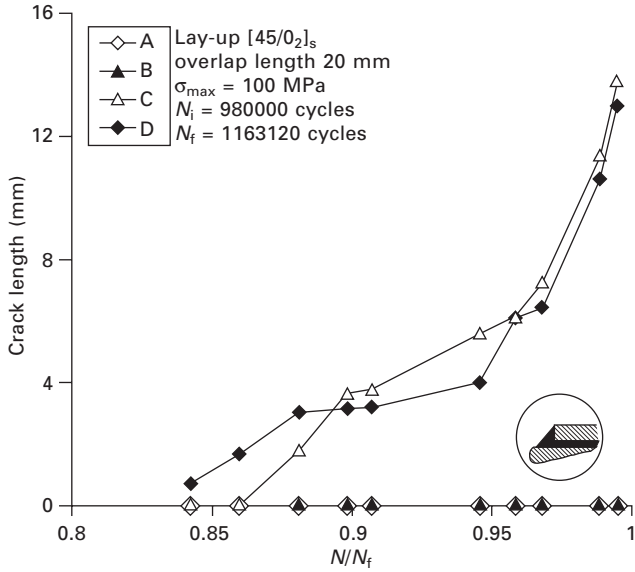
front from the two fillets, since corners A and B were not affected by crack propagation. This example makes evident the complexity of the damage mechanics observed and helps us to describe the onset and growth process of the fatigue damage.

© Woodhead Publishing Limited, 2010

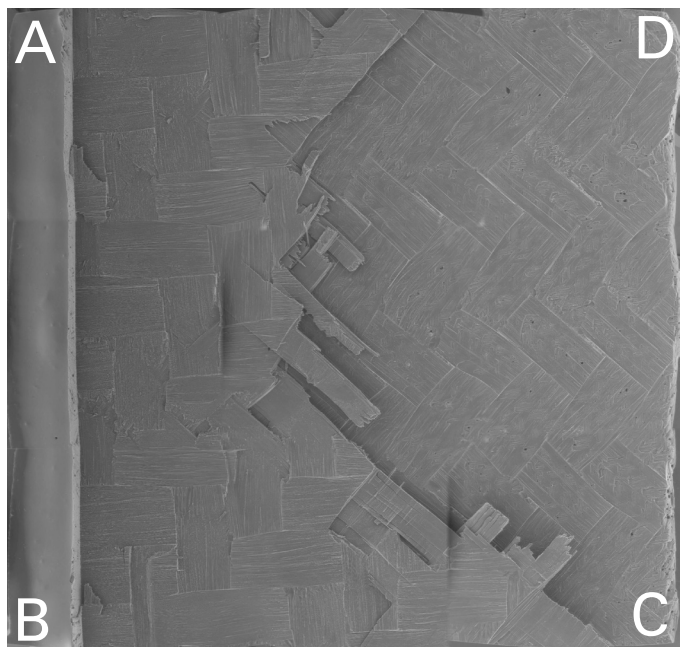



*12.5* (a) Crack patterns from C corner; (b) crack patterns from D corner, for the same joint as in Fig 12.4. See Fig. 12.12 for corner locations.

© Woodhead Publishing Limited, 2010




*12.6* Crack length evolution from the four overlap corners plotted against normalised fatigue life (see Fig. 12.12 for corner locations).

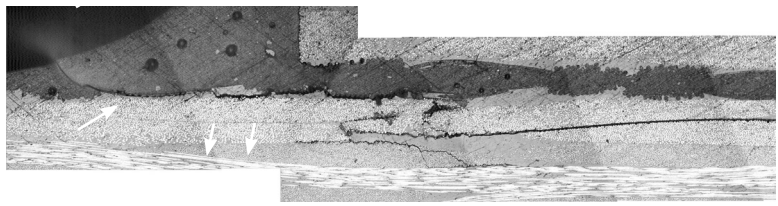



*12.7* SEM of fracture surface morphology over the entire overlap length for the same joint as in Fig. 12.4. See Fig. 12.12 for corner locations.

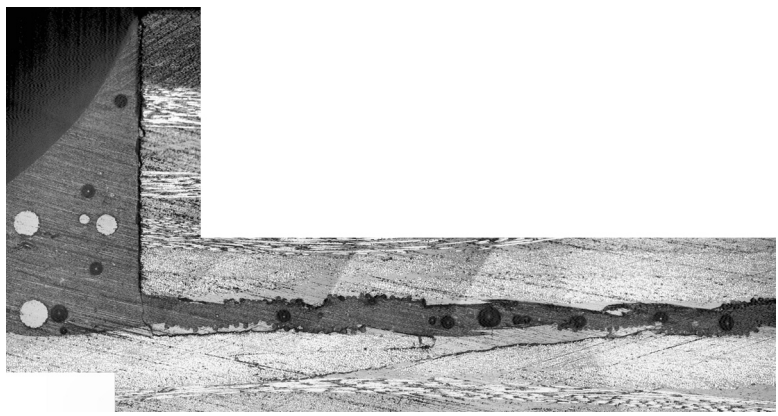
© Woodhead Publishing Limited, 2010

As illustrated above, cracks in the spew fillet joints were seen to nucleate (or at least became visible) mainly near the toe of the fillet, in a central position with respect to the joint width. The number of cycles corresponding to this crack onset was defined as $N_{it}$. Less frequently, cracks were seen to nucleate in the upper corner of the fillet (see Fig. 12.8(b)). Cracks then propagated toward the joint edges as shown in Fig. 12.4.

From this point, rather complicated damage patterns were observed, with crack propagation occurring either as inter–intralaminar delaminations inside the adherends (Fig. 12.5 and Fig. 12.9) or at the adhesive–adherend interface (Fig. 12.10). In previous research on 0° interface joints,[7] crack propagation occurred mainly at the adherend–adhesive interface (Fig. 12.11). It must be

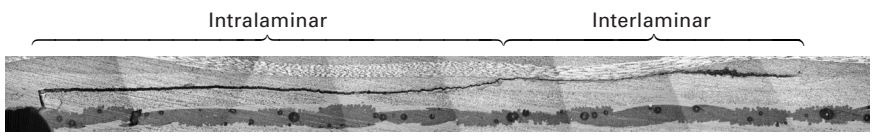


(a)



(b)

*12.8* Side views of cracks nucleated at (a) the fillet toe and at (b) the fillet upper corner.

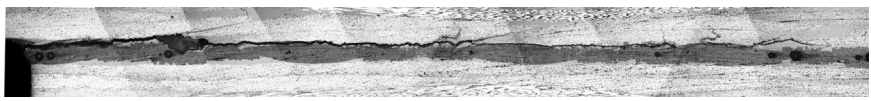



*12.9* Crack initiation and intralaminar/interlaminar crack path in a square edge joint (lay-up $[45/0_2]_s$; $w$ = 20 mm, $\sigma_{max}$ = 95 MPa, $N_f$ = 78,209 cycles).

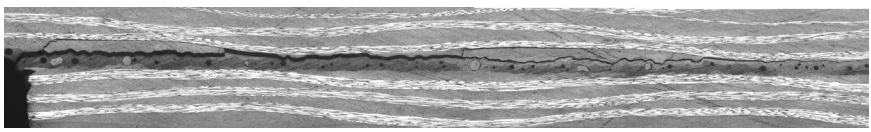
© Woodhead Publishing Limited, 2010

noted that Figs. 12.9, 12.10 and 12.11 refer to square edge joints: however, once the cracks reached the joint edges, the mechanics of the damage evolution and damage patterns during propagation were similar, independent of the corner geometry.

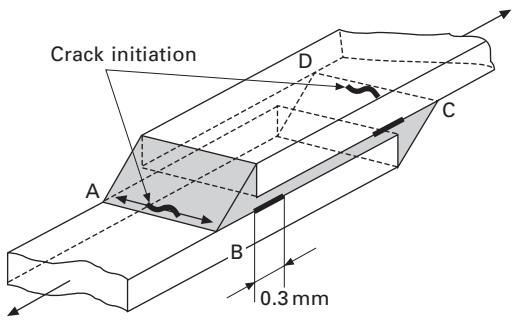
It is worth noting that owing to the reduced thickness of the adhesive layer, it was very difficult to identify the true crack nucleation for square edge joints. Therefore, as already reported,[7–9] the 'technical' crack nucleation was identified when the largest crack, measured on the joint edges, reached 0.3 mm in length (used as a practical measurable length via an optical microscope), according to the scheme illustrated in Fig. 12.12. The number of cycles corresponding to the 'technical' crack detection was defined as the 'number of cycles to crack initiation' $N_i$. The remaining part of the fatigue life spent in propagating a crack up to final fatigue failure was then calculated as the difference between the total life ($N_f$) and the life to 'technical' crack initiation $N_i$. The number of cycles for crack propagation was identified as $N_p$.



*12.10* Interface crack initiation and propagation path in a square edge joint (lay-up $[45/0_2]_s$; $w$ = 20 mm, $\sigma_{max}$ = 65 MPa, $N_f$ = 588,737 cycles).



*12.11* Interface crack initiation and propagation path in a square edge joint (lay-up $[0]_6$; $w$ = 40 mm, $\sigma_{max}$ = 160 MPa, $N_f$ = 32,146 cycles).




*12.12* Corner locations and definition of the 'technical' crack for the evaluation of the number of cycles to crack initiation, $N_i$, for square edge and fillet joints.

© Woodhead Publishing Limited, 2010

Apart from the technical problems in measuring the actual crack onset for square edge joints, the choice of using $N_i$ and not $N_{it}$ as life to crack initiation is justified by considering that the propagation from the nucleation site in the centre of the joint to its edges (in terms of the number of cycles: propagation from $N_{it}$ to $N_i$) occurs in a region completely controlled by the intensity of the local stress field, which is the parameter assumed by the authors to be suitable for unifying the life to crack initiation. Therefore, the assumption that the crack initiation phase is completed when the crack has propagated up to the joint edges is consistent with both experimental observations and local stress analysis.

To quantify the crack growth during the propagation phase, the lengths of the cracks emanating from each overlap corner were monitored. For all the joints tested, cracks were measured by projecting the observed crack paths onto the interface adhesive–adherend plane: the resulting projected lengths, including interface cracks and/or delamination, were referred to as 'nominal' cracks (see Fig. 12.12).

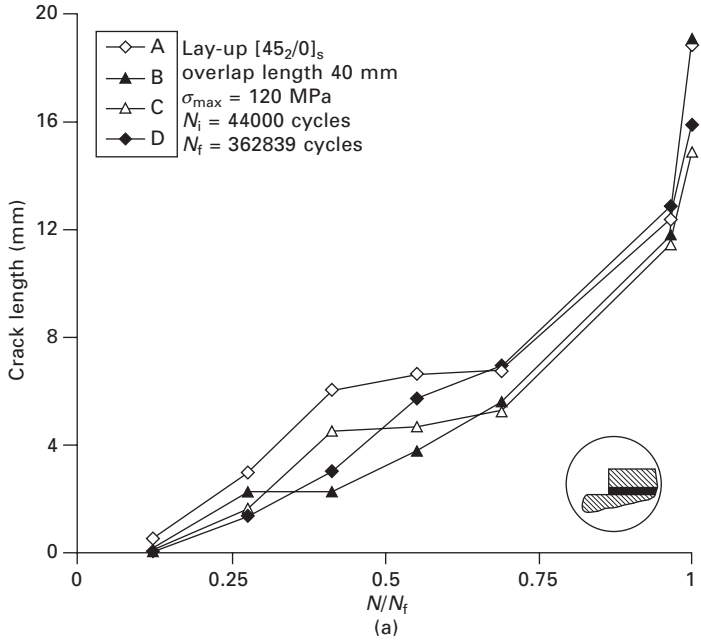
Independent of the corner geometry and overlap length, crack fronts were seen to propagate either from one side of the joint only as shown previously in Fig. 12.6 or, more frequently, uniformly from both sides of the overlap, as illustrated in Fig. 12.13 for a square edge joint. The resulting fracture surface morphology is also shown in the same figure.

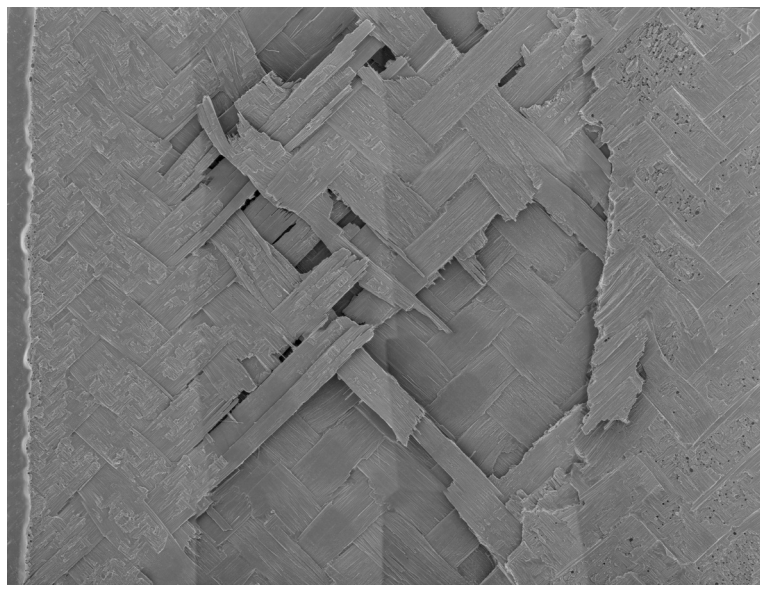
As a further example, Fig. 12.14 compares the crack length evolution for two joints, a square edge and a spew fillet, characterised by similar fatigue lives. In spite of being in the presence of a symmetric propagation of the crack front from both sides of the overlap, nucleation does not occur simultaneously at the different corners, thus making the damage pattern rather complicated. Moreover, the presence of a fillet delays the crack nucleation in comparison with the square edge configuration. This tendency is confirmed by an overall analysis of the crack/delamination evolution measured on several joints. On the other hand, the influence of the stacking sequence and stress level on the fraction of life spent for crack nucleation was seen to be almost negligible.

The increase in the life to crack initiation for the spew fillet joint compared with the square edge can also be observed in Fig. 12.15, while the life spent in propagating the crack/delamination up to failure is more or less the same, independent of the corner geometry (Fig. 12.16).

The improvement in crack initiation life can be justified by the reduced values of both the strength of singularity $s$ and the generalised stress intensity factor $H_0$ calculated for the spew fillet joints, as explained later. However, the overlap length can influence both the initiation and propagation phases, with joints with an overlap length equal to 40 mm being characterised by a longer life to crack onset and also by a longer propagation phase (Figs. 12.17 and 12.18). Even in this case, results are consistent with local stress analysis.

© Woodhead Publishing Limited, 2010

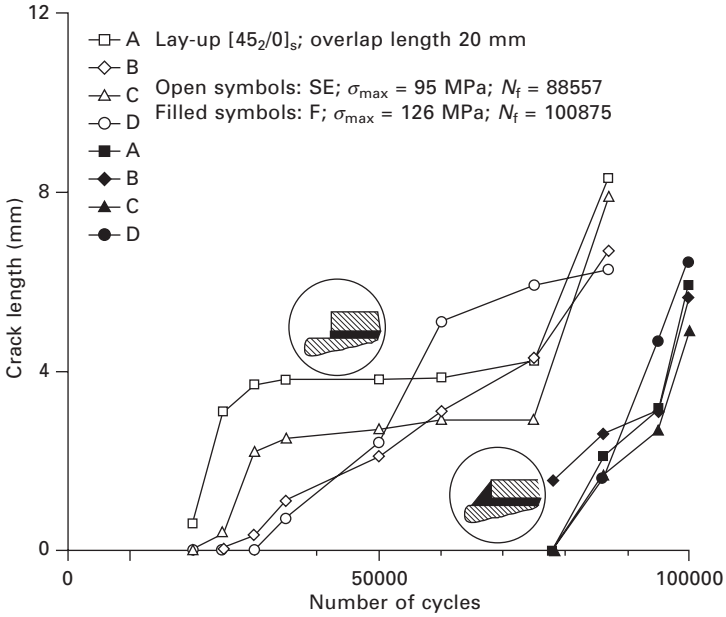


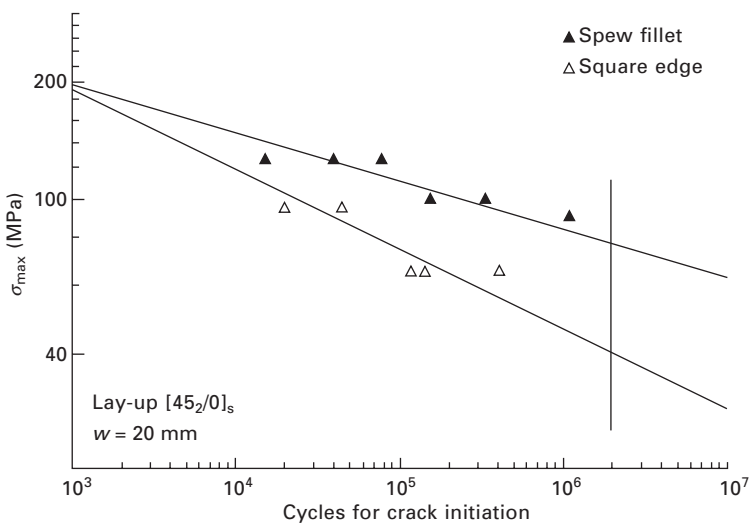
(b)

*12.13* (a) Crack length versus normalised fatigue life and (b) fracture surface morphology for a square edge joint $[45_2/0]_s$; $\sigma_{max}$ = 120 MPa, $w$ = 40 mm, $N_i$ = 44,000 $N_f$ = 362,839 cycles).

© Woodhead Publishing Limited, 2010

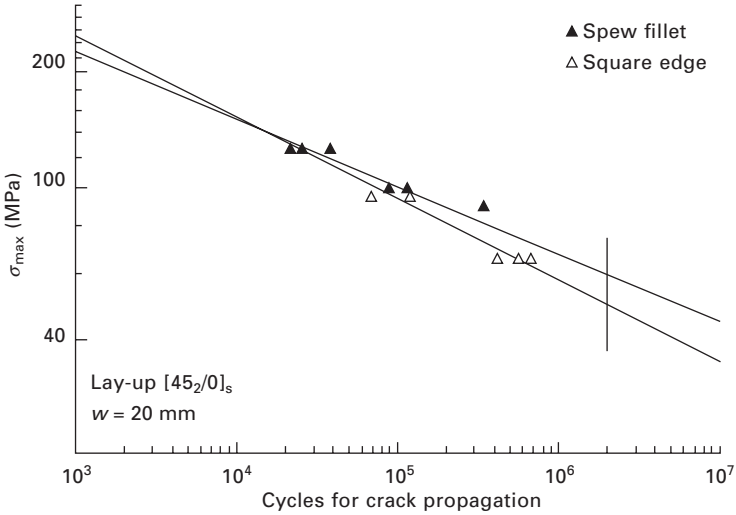



*12.14* Comparison of the crack propagation phase for a square edge (SE) and a spew fillet joint (F) with similar fatigue lives.

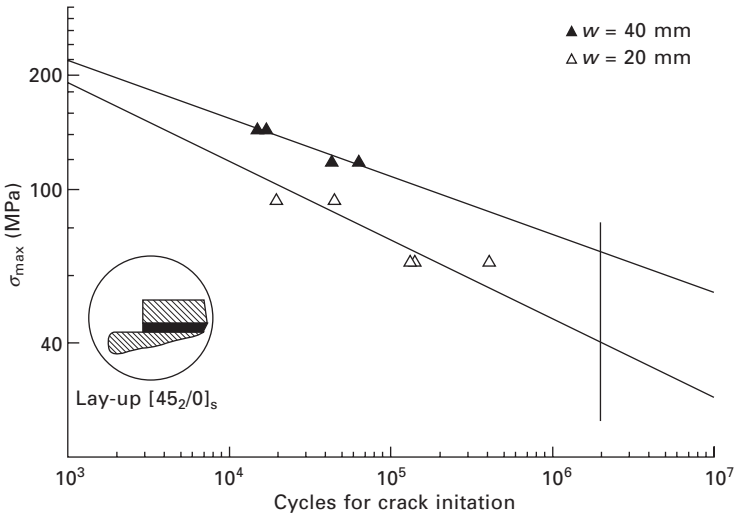



*12.15* Influence of corner geometry on crack initiation.

© Woodhead Publishing Limited, 2010



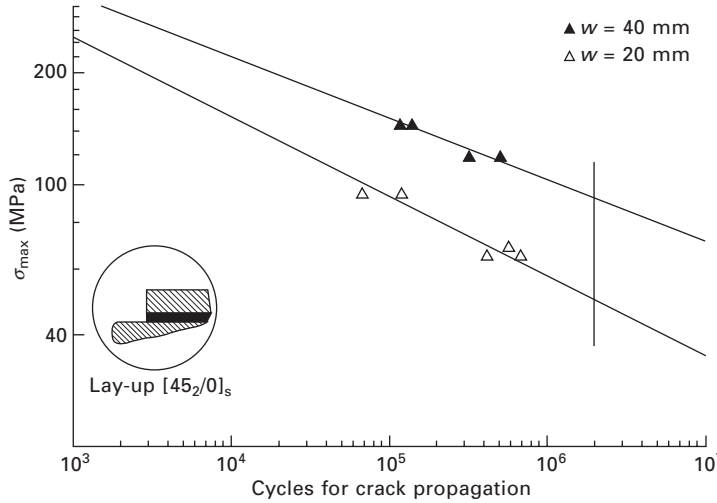

*12.16* Influence of corner geometry on crack propagation.




*12.17* Influence of overlap length on crack initiation.

The normalised value of the generalised stress intensity factor calculated for 40 mm joints is lower than that for 20 mm joints, thus justifying the longer life to crack onset. Moreover, the strain energy release rate calculated for a 40 mm joint is about half that of a 20 mm joint (at the same stress level and crack length) and therefore the propagation phase is extended. Results presented in Figs. 12.15–12.18 are valid for joints with $[45_2/0]_s$ lay-up, but similar trends were observed for $[45/0_2]_s$ joints.

© Woodhead Publishing Limited, 2010




*12.18* Influence of overlap length on crack propagation.

*Table 12.2* Fraction of fatigue life to crack initiation for several joint configurations

| Lay-up | Corner geometry | $N_i/N_f$ range |
|---|---|---|
| $[45/0_2]_s$ | Square edge | 0.2–0.4 |
| $[45/0_2]_s$ | Fillet | 0.6–0.9 |
| $[45_2/0]_s$ | Square edge | 0.1–0.4 |
| $[45_2/0]_s$ | Fillet | 0.25–0.8 |
| $[0]_6$, ref. [7] | Square edge | 0.2–0.7 |
| $[0]_6$, ref. [7] | Fillet | 0.25–0.75 |

Full details of the fatigue data are reported in Meneghetti *et al.*;[8] the available results are summarised here in terms of fraction of life to crack initiation and reported in Table 12.2. Previous results for $[0]_6$ joints are included for comparison.

It is clear that a significant fraction of the fatigue life of a joint is spent initiating a crack or a delamination of measurable size, according to the definition given in Fig. 12.12. Therefore, the need for fatigue models capable of taking into account and describing both the initiation and the propagation phases is justified.

## 12.4 The life prediction model

The model for the life assessment of bonded joints in composite material has already been presented and discussed.[9, 10] The model is based on the actual mechanics of the damage evolution and describes the joint lifetime as a sequence of initiation and propagation phases. According to the schematic

© Woodhead Publishing Limited, 2010

shown in Fig. 12.19, the life spent in nucleating a 'technical' crack is described using a generalised stress intensity factor (SIF) approach, which is suitable for summarising the fatigue life to crack initiation. The extension of the propagation phase is calculated, as is usually reported in the literature, by the integration of a power law relating the strain energy release rate (SERR) to the rate of crack growth. The total fatigue life is then obtained by the sum of the two contributions.

An extensive discussion on the alternative models and approaches available in the technical literature for the fatigue design of bonded connections is given by Quaresimin and co-workers.[9, 10] It is important to recall here that the nucleation phase is usually ignored on the assumption that this choice is on the conservative side and that the fatigue life of the joints is dominated by the propagation phase. The former assumption is definitely reasonable and acceptable from a design viewpoint. On the other hand, a large body of experimental evidence indicates that the latter assumption is quite inconsistent: apart from the results reported above, the reader can refer to the data presented in references 1–7, the literature analysis presented by Hadavinia *et al.*[22] and the discussion on this subject reported in a couple of interesting papers by Abdel Wahab *et al.*[23, 24]

Therefore, in all the (frequent) cases when the crack nucleation takes a significant fraction of the joint life time, a predictive model not incorporating and describing this phase runs the risk of greatly underestimating the life of the connection, eventually leading to an overdesigned structure.

## 12.5 Generalised stress intensity factor (SIF) approach and assessment of the life to crack initiation

In a bonded joint, under the hypothesis of linear elastic behaviour of the facing materials, the stress field near the corners at the end of the overlap becomes singular owing to the combined contributions of the geometric singularity associated with the corner and the constitutive singularity caused by a mismatch of the elastic properties of the facing materials.

The asymptotic stress fields at the singular locations of the joints can be expressed[25] by a stress expansion, in variable separable form, which describes analytically the entire stress distribution:




*12.19* Schematic model of the two phases in the joint fatigue life.[9,10]

© Woodhead Publishing Limited, 2010

$$\sigma_{ij}(r, \theta) = \sum_{k=0}^{\infty} T_{ij}^{k}(\theta) \cdot r^{\lambda_k} + \overline{T}(\theta) \quad [12.1]$$

where $T_{ij}^{k}(\theta)$ are functions dependent on $\theta$, load and geometry, $r$ is the distance from the singular point and $\lambda_k$ are eigenvalues.

In many cases of practical interest, the stress expansion can be conveniently truncated at the first term[13] and rewritten in the form:

$$\sigma_{ij}(r, \theta) = H_0 r^s f_{ij}^{(0)}(\theta) \quad [12.2]$$

where $H_0$ is the generalised stress intensity factor, $s$ is the first eigenvalue, $f_{ij}^{(0)}(\theta)$ is the angular function and $r$ is the distance from the singular point.

The generalised stress intensity factor, denoted by $H_0$, is associated with the first term of the stress expansion and depends on the boundary conditions and joint configuration; the relevant associated singularity power is denoted by $s$ and depends on both the local geometry and the elastic properties of the matching materials.

The generalised stress intensity factor has been successfully used in the past to predict the static properties of connections bonded by brittle adhesives, and more recently was suggested as being the controlling and unifying parameter for fatigue crack onset in bonded connections made of isotropic material.[13, 25] For comprehensive coverage of literature on the generalised stress intensity factor approach and the theoretical basis of the subject, the reader is referred to references 13, 14 and 25.

The evaluation of the generalised stress intensity factor $H_0$, for the various configurations analysed, can be performed numerically or by using more general and elegant analytical–numerical procedures like those proposed by Lazzarin *et al.*[13] for isotropic adherends and by Barroso *et al.*[14] for anisotropic adherends.

According to previous research,[15] linear elastic plane-strain models of the joints were defined in the Ansys® 11.0 finite element (FE) environment. Eight-node PLANE82 anisotropic finite elements were used in the model's definition and the elastic properties of the adherends and adhesive used as input data are listed in Table 12.3.

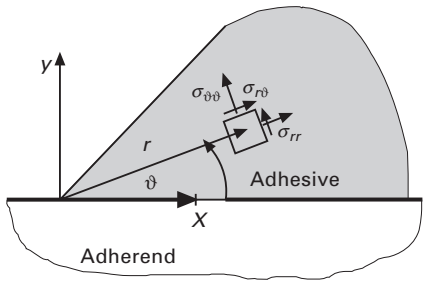
*Table 12.3* Properties of adherends and adhesive used as input for FE models

| Woven composite lamina | | | | | | | | |
|---|---|---|---|---|---|---|---|---|
| $E_X$ (MPa) | $E_Y$ (MPa) | $E_Z$ (MPa) | $G_{XY}$ (MPa) | $G_{YZ}$ (MPa) | $G_{XZ}$ (MPa) | $\nu_{XY}$ | $\nu_{YZ}$ | $\nu_{XZ}$ |
| 58050 | 6000 | 58650 | 500 | 500 | 3300 | 0.27 | 0.27 | 0.06 |

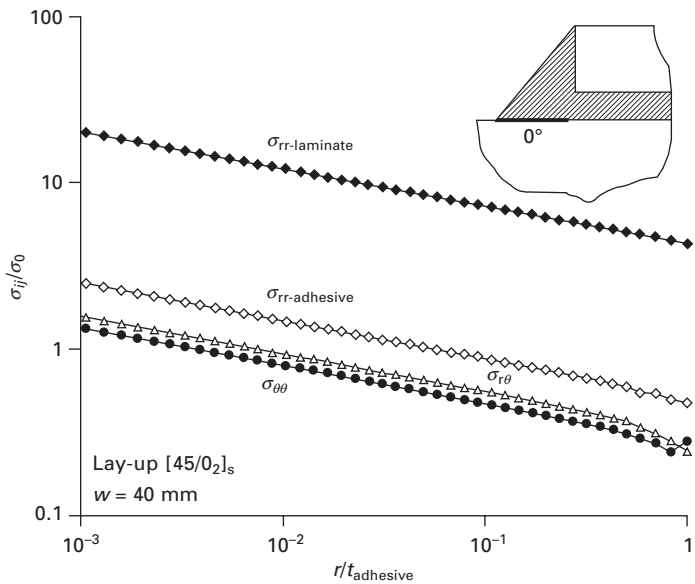
| Scotch weld 9323 B/A adhesive | | |
|---|---|---|
| $E$ (MPa) | $G$ (MPa) | $\nu$ |
| 2870 | 1050 | 0.37 |

© Woodhead Publishing Limited, 2010

Figure 12.20 shows the frame of reference (in polar coordinates) adopted for the stress analysis, while examples of the stress distribution near the singular location at the adhesive–adherend interface of a spew fillet joint are plotted in Fig. 12.21.




*12.20* Local frame of reference adopted for FE models.




*12.21* Normalised asymptotic stress distributions at adhesive–adherend interface for a spew fillet joint.

© Woodhead Publishing Limited, 2010

Values for the generalised stress intensity factor $H_0$ and associated eigenvalue $s$, representative of the degree of singularity of the local stress field, can be calculated by fitting the stress distributions obtained from the finite element analyses for each lay-up and overlap length. A summary of the results is presented in Table 12.4. $H_0$ values are normalised to the applied nominal stress $\sigma_0$, since linear elastic behaviour was assumed, and therefore the results are proportional to the applied stress level. The limit of applicability of linear elastic analysis for calculating the singular stress fields and generalised stress intensity factor $H_0$ in the case of joints with $[45/0_2]_s$ and $[45_2/0]_s$ lay-up was discussed by Quaresimin.[9] However, by considering that the out-of-plane displacements in the uncracked joint are limited and taking advantage of a significant saving in calculation time, it was decided to use linear elastic analyses to investigate the stress field in the uncracked joint geometry.

Data reported in Table 12.4 justify the experimental trend of the fatigue data for crack initiation and, in particular, those presented in Figs. 12.15 and 12.17. Lower values for both the normalised stress parameter $H_0/\sigma_0$ and the singularity degree are typical for the spew fillet joints when compared with the square edge joints and this fact is believed to be the cause of the significant delay in crack onset. Life to crack initiation was seen to increase for joints with longer overlap lengths and this is in agreement with the corresponding decreases in the $H_0/\sigma_0$ values.

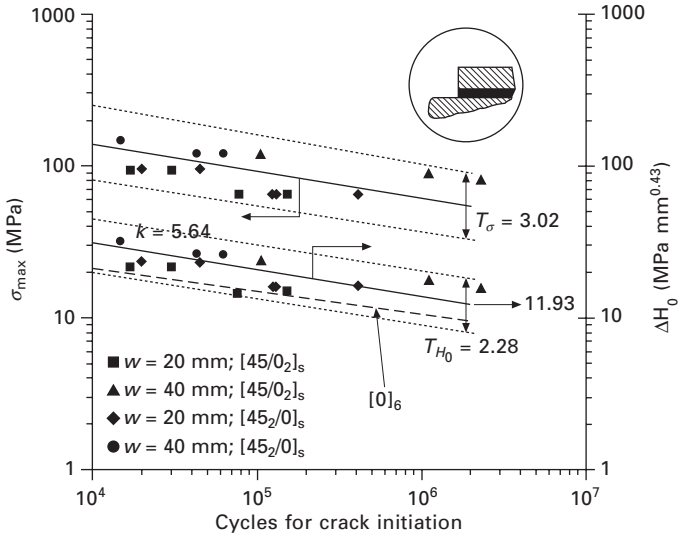
Dependent only on the elastic properties of the interface materials and corner geometry, the singularity degree, quantified by the exponent $s$, is not influenced by the lay-up. Hence, when summarising the fatigue life to crack initiation, only two sets of homogeneous data have to be defined: the square edge and spew fillet joints, respectively.

The available fatigue data to crack initiation are thus plotted in Figs. 12.22 and 12.23 in terms of the range of variation of $H_0$, $\Delta H_0$, for square edge and spew fillet joints, respectively. Scatter bands are defined in both

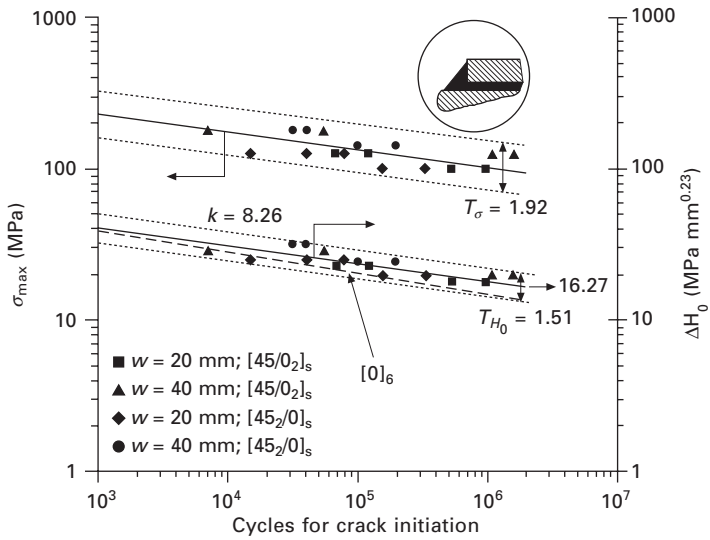
*Table 12.4* Strength of singularity $s$ and normalised values of generalised stress intensity factor $H_0$

| | Square edge | | Fillet | |
|---|---|---|---|---|
| | $[45/0_2]_s$ | $[45_2/0]_s$ | $[45/0_2]_s$ | $[45_2/0]_s$ |
| | $s = -0.432$ | $s = -0.432$ | $s = -0.226$ | $s = -0.226$ |
| w (mm) | $H_0/\sigma_0$ (mm$^{-s}$) | $H_0/\sigma_0$ (mm$^{-s}$) | $H_0/\sigma_0$ (mm$^{-s}$) | $H_0/\sigma_0$ (mm$^{-s}$) |
| 20 | 0.2374 | 0.2585 | 0.1900 | 0.2076 |
| 40 | 0.2091 | 0.2268 | 0.1664 | 0.1816 |
| Data for $[0]_6$ joints, from ref. [15] | | | | |
| | $s = -0.423$ | | $s = -0.199$ | |
| w (mm) | $H_0/\sigma_0$ (mm$^{-s}$) | | $H_0/\sigma_0$ (mm$^{-s}$) | |
| 20 | 0.1713 | | 0.1683 | |
| 40 | 0.1577 | | 0.1493 | |

© Woodhead Publishing Limited, 2010




*12.22* Scatter bands for fatigue to crack initiation for square edge joints (S–N and local approach).




*12.23* Scatter bands for fatigue to crack initiation for spew fillet joints (S–N and local approach).

cases for a survival probability of 10% and 90%, respectively, with a confidence level of 95%. In order to appreciate the unifying capability of $H_0$, the same data are also plotted in terms of nominal stresses. Both figures highlight that the scatter of the life to crack initiation is significantly

© Woodhead Publishing Limited, 2010

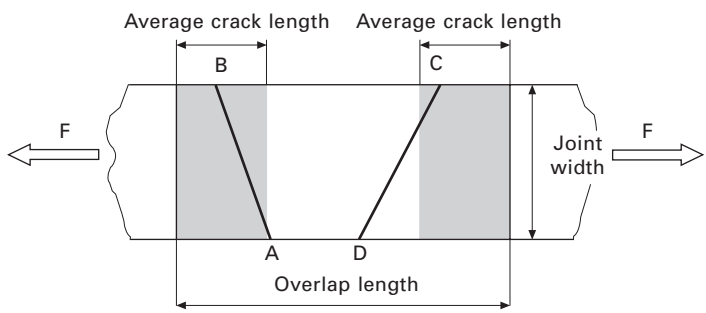
reduced if the local rather than the nominal stress approach is adopted, as shown by the reduced values of the $T_{H_0}$ scatter index with respect to those of $T_\sigma$.

For a direct comparison with the results previously obtained on $[0]_6$ joints [7], the relevant $H_0$-based fatigue curve with a survival probability of 50% is included in Figs. 12.22 and 12.23. A maximum difference of about 10% can be observed between the previous and present curves for crack initiation. Care should be taken, however, when doing this comparison, since it is not formally correct owing to the difference in the degree of the singularity at the 0° and 45° degree interfaces (see Table 12.4). Nevertheless, for this specific case, this difference is greatly reduced and therefore the $H_0$-based fatigue curves can be directly compared, at least from an engineering standpoint.

## 12.6 The crack propagation phase

As previously illustrated, damage patterns during the crack propagation phase are rather complicated because the propagation of the crack front occurs either at the adhesive–adherend interface or as multiple and/or inter/intralaminar delamination paths (see Figs. 12.5, 12.9–12.11).

For all the joints tested, crack growth was monitored at the four corners of the overlap. In order to make the measurements feasible from a practical point of view, the length of a 'nominal' crack at each corner was measured by projecting the observed crack paths, including the interface crack and/or delaminations, onto the adhesive–adherend interface, as schematically illustrated in Fig. 12.12. The results of this process are presented in Figs. 12.6, 12.13 and 12.14. The difficulty in modelling this complex and variable damage scenario can be easily appreciated. Therefore, to reduce the amount of data to be dealt with, it was decided to assume straight crack fronts and symmetrical crack propagation from both sides of the overlap, as already suggested.[15] A schematic of the crack length averaging procedure is presented in Fig. 12.24

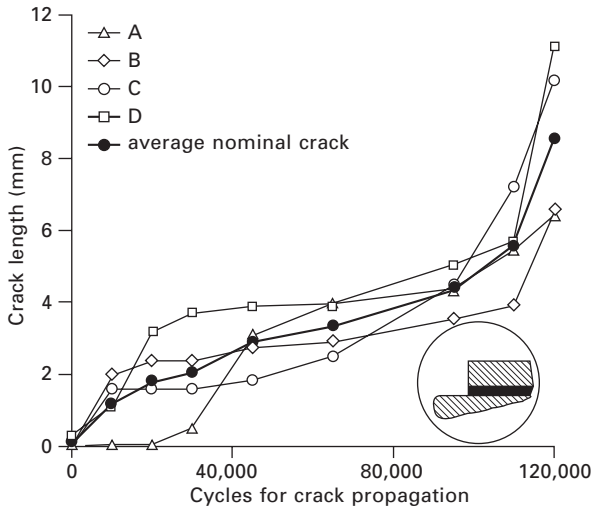



*12.24* Schematic of the crack length averaging (the sum of the length of the cracks running from the four corners, divided by four).

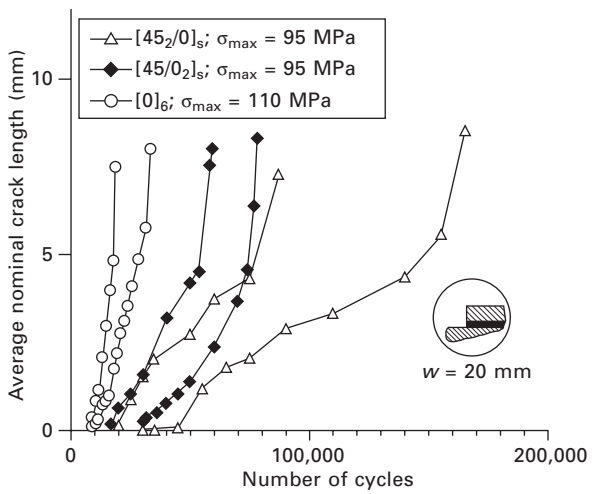
© Woodhead Publishing Limited, 2010

and a comparison between the actual and average crack length is shown in Fig. 12.25. Further examples of average crack length versus the number of cycles measured on some square edge joints are presented in Fig. 12.26.

Crack growth rates were then calculated for all the joints tested, starting from the values of the average crack, using the incremental polynomial method (IPM) proposed in the ASTM 647-00[26] and fitting crack growth data using piecewise second-order polynomials. The results obtained for




*12.25* Comparison between nominal crack lengths measured at the four corners and average 'nominal' crack length for a square edge joint (lay-up $[45_2/0]_s$; $\sigma_{max}$ = 95 MPa, $w$ = 20 mm, $N_p$ = 120,262 cycles, $N_f$ = 165,262 cycles).




*12.26* Crack length evolution for square edge joints.

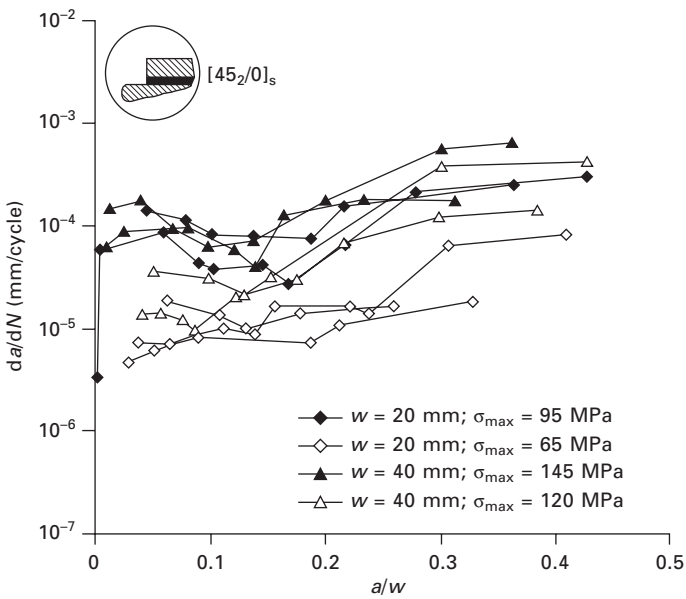
© Woodhead Publishing Limited, 2010

$[45_2/0]_s$ square edge joints are shown in Fig. 12.27. For an easier comparison, the crack growth rate is plotted versus the average nominal crack length $a$, normalised to the overlap length $w$.

As discussed in the introduction, the driving force for crack propagation was assumed to be the strain energy release rate (SERR). Calculation of the SERR components at the crack tip, given the applied load and the crack length, was performed using the virtual crack closure technique (VCTT),[27] according to the procedure reported in detail by Quaresimin and Ricotta.[15]

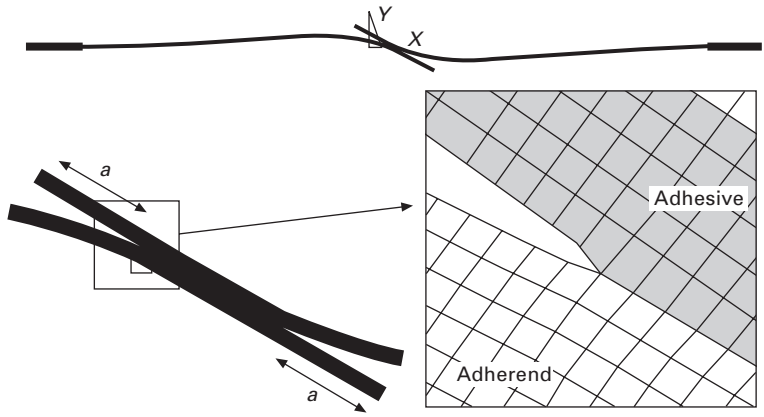
Even in this case, bidimensional plane strain finite element models were defined in the Ansys environment, using as input data the material properties listed in Table 12.3. According to the averaging procedure adopted when processing the experimental data (see Fig. 12.24), cracks were always supposed to propagate symmetrically along the adhesive–adherend interface. A schematic of the model adopted and details of the mesh close to the interface crack are shown in Fig. 12.28. On the basis of the extensive investigation reported by Quaresimin and Ricotta,[15] the adopted mesh density was carefully calibrated to avoid the problems associated with the oscillating stress field near the interface crack tip. This required an element size in the order of 0.03 mm, the adhesive layer being 0.15 mm thick.

As illustrated above, stress distributions near the singular locations of the joint were calculated by running geometrically linear analyses on the uncracked joint geometry. Under this condition, out-of-plane displacements were considered




*12.27* Crack growth rates versus normalised crack length measured on $[45_2/0]_s$ square edge joints with different overlap lengths.

© Woodhead Publishing Limited, 2010




*12.28* Deformed shape of a cracked joint and details of the FE model at the interface crack.[10,15]

to have a reduced influence on the calculated values of the generalised stress intensity factor. The situation is different when modelling the propagation phase because the bending compliance of the cracked joint increases as the crack propagates and therefore linear elastic analyses are no longer appropriate to describe the global deformed shape of the joint and the stress distributions near the crack tip location. Therefore, geometrically non-linear analyses were performed when modelling the crack propagation phase.

Typical results of the analyses were the SERR components at different crack lengths as shown in Fig. 12.29, where the mode I and mode II components, together with their sum, the total SERR, are reported for 12.20 mm overlap joints. The influence of the stacking sequence is illustrated and the trends for $[0]_6$ joints, calculated by Quaresimin and Ricotta,[15] are also included. The SERR trends obtained, like those plotted in Fig. 12.29, are valid for both square edge and spew fillet joints since, once a technical crack is identified on the joint edge, no more differences exist between the two types of joint.

Rates of crack growth and SERR trends were used to calculate and draw the scatter band of the crack propagation data. The interpolating power law was, conventionally, expressed in the form:

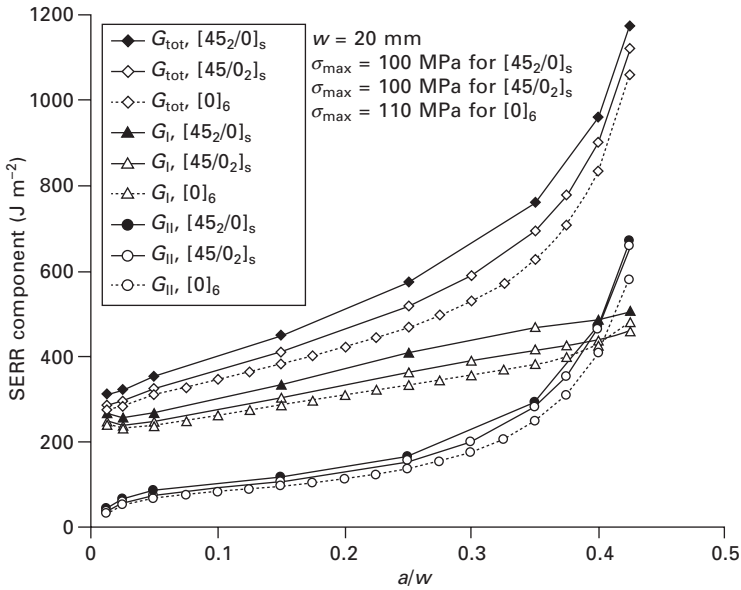
$$\frac{da}{dN} = D \cdot (\Delta G_{eqv})^n \qquad [12.3]$$

where $\Delta G_{eqv} = (G_{eqv,max} - G_{eqv,min})$ is the range of equivalent SERR values, defined by Quaresimin and Ricotta which represents one possible formulation that accounts for the combined presence of mode I and mode II loading (opening and sliding modes at the crack tip) and for the variation in the mode mixity during the fatigue life, and $D$ and $n$ are the curve parameters derived from fitting the experimental data. The expression of the equivalent SERR, already proposed by the authors,[15] is:

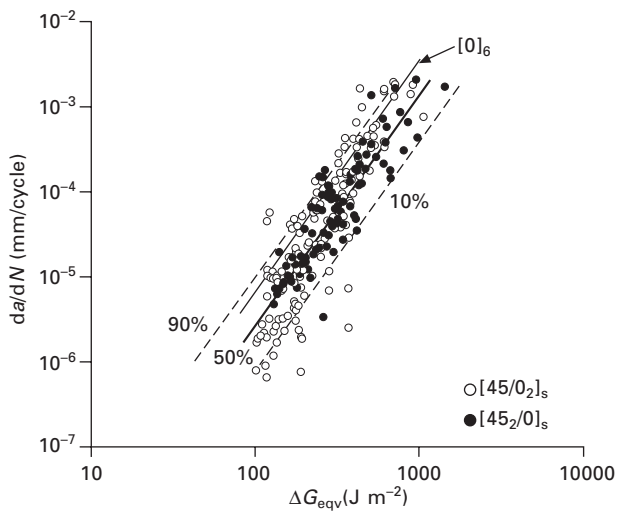
© Woodhead Publishing Limited, 2010

$$G_{eqv}(a) = G_I(a) + \frac{G_{II}(a)}{G_I(a) + G_{II}(a)} \cdot G_{II}(a) \qquad [12.4]$$

Available crack growth data, for joints with different overlap length, corner geometry and applied stress level, are plotted together in Fig. 12.30, where the relevant 10–90% crack propagation scatter band is also plotted.




*12.29* Trends in SERR components and influence of adherend stacking sequence.




*12.30* Crack propagation scatter band for all the joints tested.

© Woodhead Publishing Limited, 2010

The average curve reported[9, 10] for joints with $[0]_6$ lay-up is included for comparison.

Characteristic parameters of the power law interpolating the experimental data at different survival probabilities are listed in Table 12.5. Figure 12.30 shows that the 45° interface is characterised by a greater resistance to crack propagation than the 0° interface. A reason for this might be the much more complicated damage patterns observed in the 45° interface joints with respect to those with a 0° interface that were investigated previously. Table 12.5 lists also the $D$ and $n$ parameters characteristic of the crack propagation curve calculated by using the total SERR, given as the sum of mode I and mode II components, rather than the equivalent SERR. However, it has been shown that the use of $\Delta G_{eqv}$ or $\Delta G_{tot}$ parameters leads to similar estimations of crack propagation life.[10]

## 12.7 Life prediction procedure and application

The procedure for applying the model for fatigue life assessment was comprehensively presented by Quaresimin and co-workers[9, 10] and is schematically shown in Fig. 12.31. The first step is to estimate the number of cycles needed to nucleate a technical crack. For this, stress distributions and the relevant generalised SIF $H_0$ can be obtained for the uncracked joint model from FE analysis. As the analysis in this case is linear elastic, it only has to be performed once to obtain a normalised value of $H_0$ for each geometry investigated. Then the life to crack initiation can be calculated by taking advantage of scatter bands $\Delta H_0$–$N_i$ similar to those reported in Figs 12.22 and 12.23. Depending on the design requirements, an appropriate survival probability can be adopted at this stage.

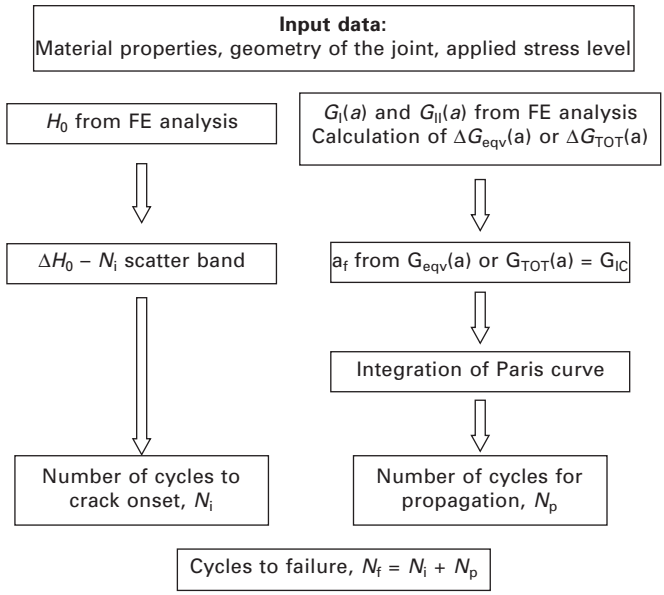
It is important to note that a new reference scatter band should be defined if corner geometry or material properties change, because of their

*Table 12.5* Paris curve data calculated for different survival probabilities

| | Data for $[45/0_2]_s$ and $[45_2/0]_s$ joints (analysed together) | |
|---|---|---|
| | $\Delta G_{eqv}$ (J m$^{-2}$) | $\Delta G_{tot}$ (J m$^{-2}$) |
| 50% PS | $D = 1.17 \times 10^{-11}$ | $D = 4.77 \times 10^{-12}$ |
| | $n = 2.69$ | $n = 2.73$ |
| 90% PS | $D = 4.06 \times 10^{-11}$ | $D = 1.66 \times 10^{-11}$ |
| | $n = 2.69$ | $n = 2.73$ |
| | Data for $[0]_6$ joints, from refs 9 and 10 | |
| | $\Delta G_{eqv}$ (J m$^{-2}$) | $\Delta G_{tot}$ (J m$^{-2}$) |
| 50% PS | $D = 2.42 \times 10^{-11}$ | $D = 1.35 \times 10^{-11}$ |
| | $n = 2.72$ | $n = 2.73$ |
| 90% PS | $D = 9.66 \times 10^{-11}$ | $D = 5.23 \times 10^{-11}$ |
| | $n = 2.72$ | $n = 2.73$ |

PS is the probability of survival.

© Woodhead Publishing Limited, 2010




*12.31* Flow chart of the life prediction procedure.[9,10]

direct influence on the singularity degree of the local stress distributions. An assessment of the number of cycles required to propagate a crack up to the joint failure can be made by integration of the crack propagation curve reported in Equation 12.3:

$$N_p = \int_0^{N_p} dN = \int_{a_i}^{a_f} \frac{da}{D[\Delta G(a)]^n} \qquad [12.5]$$

where $\Delta G$ can be either $\Delta G_{eqv}$ or $\Delta G_{tot}$.

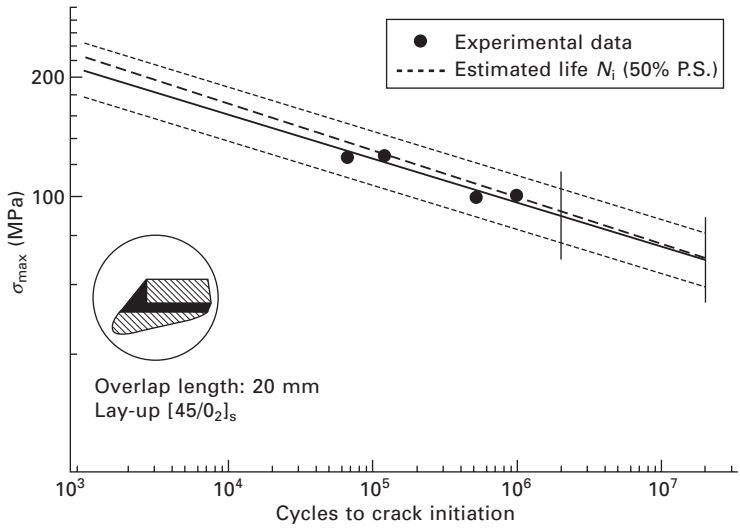
The lower and upper limits of the integration, that is the crack lengths $a_i$ and $a_f$, are defined as follows: $a_i$ corresponds to the 'technical' crack length and is equal to 0.3 mm, while the crack length at failure $a_f$ is defined using a static fracture criterion and equating the equivalent SERR $G_{eqv}$ or, alternatively, its total value $G_{tot}$ to the mode I adhesive fracture toughness $G_{IC}$ (900 J m$^{-2}$ in this case). Calculated and measured values of the final crack length have been compared,[10] indicating good agreement. The equivalent SERR as a function of the crack length '$a$' is obtained from non-linear finite element analyses (see, as an example, Fig. 12.29). Hence, the calculation effort can be quite significant, the results being dependent on both the applied stress level and the crack length. The characteristic parameters $D$ and $n$ of the crack propagation curve are reported in Table 12.5.

Finally, the number of cycles to failure is obtained by the sum of the two contributions just calculated. The procedure was applied to all the fatigue data made available by the recent research programme. Experimental fatigue

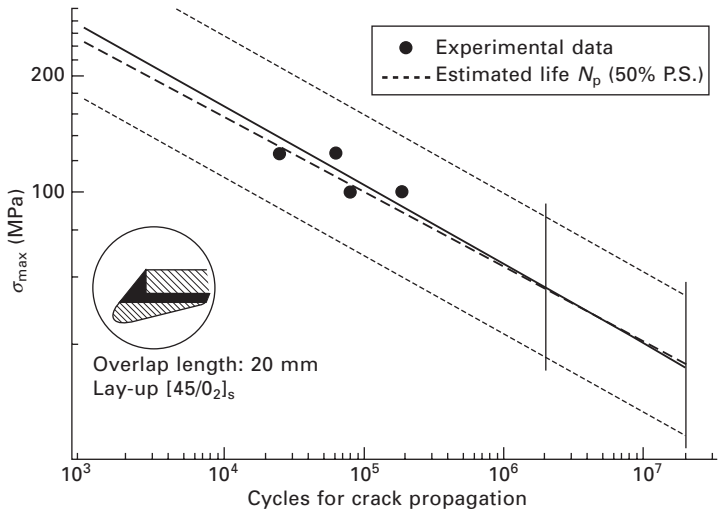
© Woodhead Publishing Limited, 2010

data and scatter bands were compared with the model prediction at 50% probability of survival.

Representative comparisons are presented in Figs. 12.32–12.34 for life to crack initiation, life to crack propagation and total life, respectively. In spite of the reduced amount of experimental data, good agreement can generally

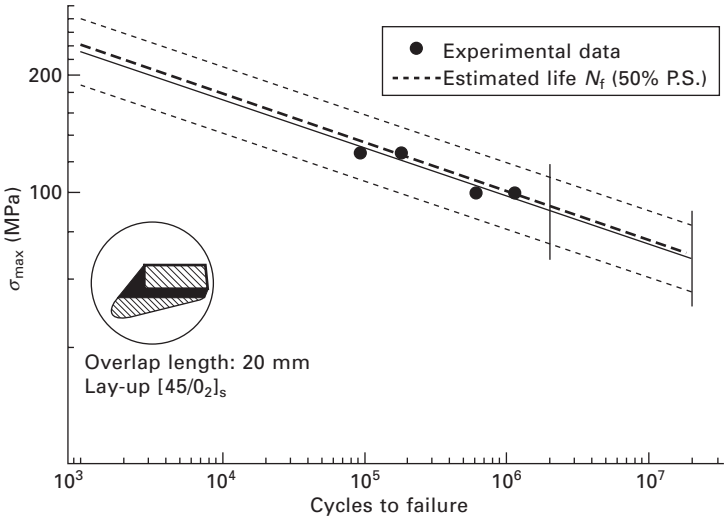



*12.32* Experimental 10–90% scatter band of the life to crack initiation for $[45/0_2]_s$ fillet joints (overlap 20 mm) compared with model predictions.

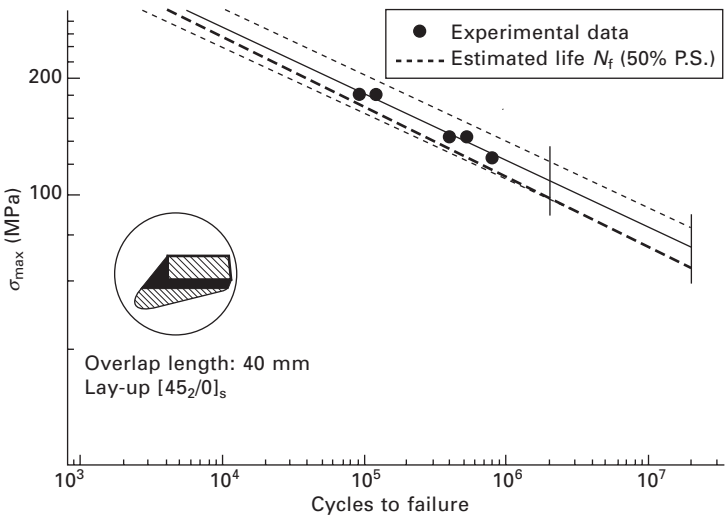



*12.33* Experimental 10–90% scatter band of the life for crack propagation for $[45/0_2]_s$ fillet joints (overlap 20 mm) compared with model predictions.

© Woodhead Publishing Limited, 2010




*12.34* Experimental 10–90% scatter band of the fatigue data at failure for $[45/0_2]_s$ fillet joints (overlap 20 mm) compared with model predictions.




*12.35* Experimental 10–90% scatter band of the fatigue data at failure for $[45_2/0]_s$ fillet joints (overlap 40 mm) compared with model predictions.

be observed. The worst case obtained is presented in Fig. 12.35. Here the predicted total life curve is still inside the 10–90% P.S. experimental scatter band and, even more important for design purposes, the prediction is on the conservative side.

© Woodhead Publishing Limited, 2010

## 12.8 Discussion and conclusions

The results discussed in the previous section, in particular the good agreement between experimental and estimated fatigue life data, proves the reliability of the model for fatigue life assessment proposed by the authors.[9,10] This is important with regard to implementing the proposed approach in practical design tools. In this chapter and in the previous validations, the model was used to assess the fatigue life of joints with simple geometry. However, the proposed approach can easily be applied to real bonded structures by keeping the same conceptual framework. The difference is likely to be the need to develop full three-dimensional FE models, instead of the plane strain models discussed here, to account for the actual more complex geometry of the structure to be designed and to calculate the stress/energy parameters required by the model.

The experimental data required to assess the procedure are also the same. In particular, a $\Delta H_0$–$N_i$ scatter band is required for each material/corner geometry combination; at first glance, this seems to represent a limitation of the proposed approach. However, standardizing both the materials and bonding procedures can help to reduce experimental efforts. Instead, a single crack growth rate curve is needed for each adherend/adhesive/interface combination.

With reference to recent experimental results discussed in this chapter:

- It is confirmed that the onset of fatigue damage, in the form of crack nucleation, can take up a significant part of the joint life.
- Limited benefits, in terms of fatigue strength, can be obtained by changing the orientation of the composite layer at its interface with the adhesive or by changing the stacking sequence of the composite adherends.
- On the other hand, resistance to crack propagation is significantly increased by the presence of a 45° interface in comparison with previous $[0]_6$ joints. This can be justified by the more complicated damage scenario observed during the analysis of damage evolution under fatigue loading: after nucleation near the adhesive toe, interface cracks and/or multiple intra/interlaminar delamination paths were observed in most of the tested joints; the increase in crack propagation life due to the 45° interface, however, has a limited effect on the total fatigue life.
- From the design point of view, improvements in fatigue strength derived from the appropriate choice of corner geometry and overlap length are far more significant than those introduced by changing the interface ply orientation.

In conclusion, it is worth mentioning that in the past few decades, significant efforts have been dedicated by the scientific community to the study of structural bonded connections under fatigue loading. A fairly large body of

© Woodhead Publishing Limited, 2010

experimental results, a reasonably good understanding of the problem and reliable predictive models have been produced. However, in the authors' opinion, much work remains to be done. In particular, the mechanics of crack nucleation needs to be further investigated for an improved and deeper understanding of the damage mechanisms and associated driving and controlling parameters. The mixed-mode loading condition always associated with crack evolution in the joints of real structures is another matter which requires significant attention. New research in this area should be the basis for developing predictive models that are suitable for estimating propagation under mixed-mode loading from pure mode I and mode II crack growth data. Finally, variable amplitude fatigue and multi-axial loading conditions should be additional areas of paramount design importance where research efforts should be concentrated in the next few years.

## 12.9 References

1. Zhang Z, Shang J K and Lawrence F V, 'Backface strain technique for detecting fatigue crack initiation in adhesive joints', *J Adhesion*, 1995, **49**, 23–36.
2. Dessureault M and Spelt J K, 'Observations of fatigue crack initiation and propagation in an epoxy adhesive', *Int J Adhes Adhes,* 1997, **17**, 183–95.
3. Crocombe A D and Richardson G, 'Assessing stress state and mean load effects on the fatigue response of adhesively bonded joints', *Int J Adhes Adhes*, 1999, **19**, 19–27.
4. Ishii K, Imanaka M, Nakayama H and Kodama H, 'Evaluation of the fatigue strength of adhesively bonded CFRP/metal single and single-step double-lap joints', *Compos Sci Technol*, 1999, **59**, 1675–83.
5. Ashcroft I A, Abdel Wahab M M, Crocombe A D, Hughes D J and Shaw S J, 'The effect of environment on the fatigue of bonded composite joints. Part 1: testing and fractography', *Compos Part A-Appl S*, 2001, **32**, 45–58.
6. Potter K D, Guild F J, Harvey H J, Wisnom M R and Adams R D, 'Understanding and control of adhesive crack propagation in bonded joints between carbon fibre composite adherends I. Experimental', *Int J Adhes Adhes*, 2001, **21**, 435–43.
7. Quaresimin M and Ricotta M, 'Fatigue behaviour and damage evolution of single lap bonded joints in composite material', *Compos Sci Technol*, 2006, **66**, 176–87.
8. Meneghetti G, Quaresimin M and Ricotta M, 'Influence of the interface ply orientation on the fatigue behaviour of bonded joints in composite materials', *Int J Fatigue*, 2010, **32**, 82–93.
9. Quaresimin M, 'Modelling the fatigue behaviour of bonded joints in composite materials', in *Multi-scale Modelling of Composite Material Systems – the Art of Predictive Damage Modelling*, P. Beaumont and C. Soutis (eds), Woodhead Publishing, Abington, Cambridge UK, 2005, 469–94.
10. Quaresimin M and Ricotta M, 'Life prediction of bonded joints in composite materials', *Int J Fatigue*, 2006, **28**, 1166–76.
11. Matthews F L and Tester T T, 'The influence of stacking sequence on the strength of bonded CFRP single lap joints', *Int J Adhes Adhes*, 1985, **5**, 13–18.
12. Boss J N, Ganesh V K and Lim C T, 'Modulus grading versus geometrical grading

© Woodhead Publishing Limited, 2010

of composite adherends in single-lap bonded joints', *Compos Struct*, 2003, **62**, 113–21.
13. Lazzarin P, Quaresimin M and Ferro P, 'A two terms stress function approach to evaluate stress distributions in bonded joints of different geometry', *J Strain Anal Eng*, 2002, **37**, 385–98.
14. Barroso A, Mantic V and Paris F, 'General solution for anisotropic multimaterial corners', *Int J Fract*, 2003, **119**, 1–23.
15. Quaresimin M and Ricotta M, 'Stress intensity factors and strain energy release rates in single lap bonded joints in composite materials', *Compos Sci Technol*, 2006, **66**, 647–56.
16. Renton W J and Vinson J R, 'Fatigue behavior of bonded joints in composite material structures', *J Aircraft*, 1975, **12**, 442–7.
17. Johnson WS and Mall S, 'Influence of interface ply orientation on fatigue damage of adhesively bonded composite joints', *J Compos Tech Res*, 1986, **8**, 3–7.
18. Ferreira J A M, Reis P N, Costa J D M and Richardson M O W, 'Fatigue behaviour of composite adhesive lap joints', *Compos Sci Technol*, 2002, **62**, 1373**–**9.
19. De Goeij W C, Van Tooren M J L and Beukers A, 'Composite adhesive joints under cyclic loading', *Mater Design*, 1999, **20**, 213–21.
20. Meneghetti G, Quaresimin M and Ricotta M, 'Damage mechanisms in composite bonded joints under fatigue loading', to appear.
21. Quaresimin M, 'Fatigue of woven composite laminates under tensile and compressive loading', *Proceedings of ECCM10, 10th European Conference on Composite Materials*, June 3–7, 2002, Brugge, Belgium.
22. Hadavinia H, Kinloch A J, Little M S G and Taylor A C, 'The prediction of crack growth in bonded joints under cyclic-fatigue loading I. Experimental studies', *Int J Adhes Adhes*, 2003, **23**, 449–61.
23. Abdel Wahab M M, Ashcroft I A, Crocombe A D and Shaw S J, 'Prediction of fatigue thresholds in adhesively bonded joints using damage mechanics and fracture mechanics', *J Adhes Sci Technol*, 2001, **15**, 763–81.
24. Abdel Wahab M M, Ashcroft I A, Crocombe A D and Smith P A, 'Finite element prediction of fatigue crack propagation lifetime in composite bonded joints', *Compos Part A-Appl S*, 2004, **35**, 213–22.
25. Lefebvre D R and Dillard D A, 'A stress singularity approach for the prediction of fatigue crack initiation in adhesive bonds. Part I: theory', *J Adhesion*, 1999, **70**, 119–38.
26. ASTM E 647-00. *Standard Test Method for Measurement of Fatigue Crack Growth Rates*, American Society for Testing and Materials, 2000.
27. Krueger R, 'Virtual crack closure technique: History, approach, and applications', *Appl Mech Rev*, 2004, **57**, 109–43.

© Woodhead Publishing Limited, 2010

# 13

# Improving adhesive joint design using fracture mechanics

DAVID A. DILLARD, Virginia Polytechnic Institute and State University, USA

**Abstract**: This chapter provides an overview of applications of fracture mechanics to the design of adhesive joints, establishing the relative merits of fracture over more traditional strength-based design approaches and reviewing some of the design approaches that have been used to incorporate fracture mechanics into design. Applications for predicting critical and subcritical fracture are discussed, including the effects of fatigue, environments and viscoelastic behavior. Insights into the effects of mode mixity and the resulting locus of failure are discussed, illustrating the importance of characterizing failure envelopes across a range of fracture mode mixities. The effects of rate and temperature are reviewed in relation to viscoelastic adhesives, suggesting that underlying molecular mobility as measured in dynamic mechanical analysis tests can provide useful insights into fracture of adhesives and bonded joints. Finally, a review of several numerical approaches for analyzing structural components for fracture-based design are discussed.

**Key words**: fracture mechanics, strength-based design, fracture-based design, time dependence, rate dependence, temperature dependence, cohesive zone model, virtual crack closure technique, *J*-integral, mode mixity effects, locus of failure, viscoelasticity, fatigue, life prediction.

## 13.1 Introduction

Engineering design has a rich history filled with great strides and accomplishments, erroneous twists and turns, and a number of failures, some spectacular and catastrophic (Petroski, 1985). Developing efficient and reliable adhesively bonded structures highlights some of the complexities of the design process, where joining multiple materials that have very different properties poses special engineering challenges. Structural adhesives have become an essential and cost effective means of joining dissimilar or damage-prone materials; to offer energy dissipation capabilities to reduce noise, vibration, and harshness in automobiles; to improve the stiffness and durability of transportation vehicles; to combine the unique properties of different materials; and simply to make larger structures than can be fabricated, transported or installed in one piece.

The design process for adhesive bonds can involve many decisions, including the geometric configuration of the joint, the thickness of the bondline, the



© Woodhead Publishing Limited, 2010

option to incorporate mechanical fasteners in the design, and selection from myriads of surface pretreatments, adhesive formulations, and fixturing and curing procedures. There are basically two approaches to structural analysis that accompanies the design process, both of which have been widely used for adhesive joints: strength and fracture mechanics.

Galileo is often cited for his contributions to design from a strength standpoint through his estimates of stresses within a cantilever beam and comparisons of these with the uniaxial strength of the material. Had his expressions for stresses been correct, he should, in principle, have been able to predict the strength of a beam by knowing the breaking strength of the material measured using a very different geometry (Timoshenko, 1953).

The idea that basic material properties can be obtained from one test configuration and used to predict the stiffness, strength, or performance of an engineering component or structure remains at the heart of structural design and these concepts have been widely used in many fields, including adhesive bonding. One should avoid the assumption that one can base predictions of adhesive joint behavior solely on the properties of the adhesive, however, as the choice of adherends, surface pretreatment, processing conditions and even the configuration of the joint can affect the properties of a bonded joint, which represent a material system rather than a single material. Although bulk material properties can be useful for assessing constitutive properties, time and temperature dependence and some environmental trends, tests of actual bonded joints fabricated with the same procedures are recommended when considering strength, fracture resistance and other joint integrity and performance metrics.

The strength approach to designing adhesive bonds has been successfully used in many applications, although generous margins of safety have often been employed to account for uncertainties as adhesive applications have expanded. Application of strength-based design approaches to adhesive joints, however, is complicated by several factors associated with determining stresses in proposed designs accurately and comparing them with meaningful strength metrics which are, in themselves, often difficult to obtain. In engineering design of monolithic materials, one often measures yield, ultimate or other strength quantities of simple specimens in which stresses are uniform within the gage section, allowing simple determination of the appropriate strength. Because these often involve a simple stress mode, yield or failure criteria have been proposed, some with widespread acceptance, allowing extensions to the multi-axial stress states often encountered in engineering design (Seely and Smith, 1952).

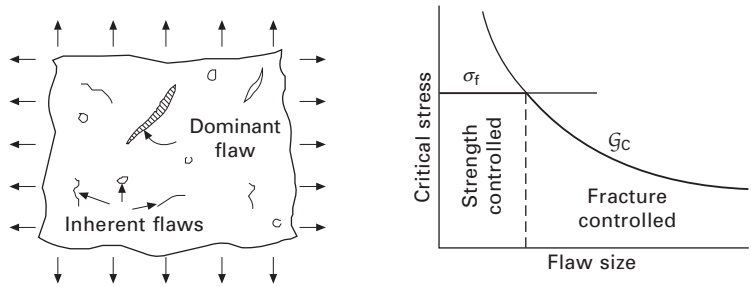
In essence then, one tests a material by exposing it to a uniform stress state, thereby characterizing the relevant strength metric, which is then used to design a more complex structure involving what is typically a non-uniform, multi-axial stress state. Such approaches often assume continuity

© Woodhead Publishing Limited, 2010

of the material being tested. The presence of voids, cracks or other flaws can significantly reduce the measured strengths. If the size and distributions of such flaws are consistent in test specimens and engineering structures in which the material is incorporated, these inherent flaws result in an allowable strength that may be successfully used for design. In many situations, however, the growth of pre-existing or induced flaws in engineering structures over time can lead to catastrophic failures not anticipated by the strength-based design approaches applied to a continuum.

Figure 13.1 schematically illustrates the insensitivity of continuum-based strength criteria to the size of an assumed dominant flaw. The results are in pronounced contrast to the fracture mechanics approach, which depends directly on the size of the dominant flaw. Although very simplistic, the bounding envelope, controlled by a strength criterion (based on some failure strength $\sigma_f$) on the left, when the largest flaws are comparable to the inherent flaw size, and controlled by a fracture criterion ($\mathcal{G}_c$) when a dominant flaw exists, provides a useful insight into the regions of applicability and limitations of each approach as they apply to design. It is only when the dominant flaw (actual or potential) is of the order of the inherent flaws within the material system that a continuum-based strength approach is applicable. Where larger flaws may exist or develop during service, fracture mechanics offers an alternative design approach that can avoid failures not anticipated by a simple continuum strength analysis.

The design of multi-material systems, such as adhesive joints, adds several complications to the strength approach, in that the stresses within an adhesive joint test specimen are almost never uniform and, in fact, can display large gradients in the regions which will ultimately control the performance and durability of the bond. In essence every adhesive joint, including the bonded test specimens from which material properties are sought, becomes a structure, which must first be analyzed before meaningful strength metrics can be ascertained. In addition, adhesively bonded joints are inherently multi-




*13.1* Illustration of how flaw size determines direct applicability of either a strength or fracture-based design approach.

© Woodhead Publishing Limited, 2010

material systems, involving different materials with different properties of the adhesive, adherends and other layers that might be present. Strength metrics may vary depending on the locus of failure, rate of loading, temperature, hygrothermal history and residual stresses in the composite system. Finally, cracks, bimaterial corners and other singular regions can result in very large stresses and strains, much larger than predicted by mechanics of materials level analyses. Although captured properly by elasticity solutions for simple configurations of linear elastic materials, these singular stress regions are often problematic for numerical procedures such as the finite element method because the peak stresses obtained depend strongly on the mesh refinement (Adams and Harris 1987). Applications of the strength approach, along with the means to address some of the complications mentioned above, can be found in Chapters 14 and 15 in this volume.

The strength-based approach remains a common tool for adhesive joint design, in part because it builds on the basic design approaches taught at the undergraduate level in most engineering programs (Adams and Peppiatt, 1974, 1977; Adams, *et al.*, 1997). A number of techniques have been examined to adapt stress or strain criteria to adhesive joints. Success has been achieved in a variety of design approaches that recognize the singular stress region, including the maximum principal stress or strain, usually at some specified distance from the singularity or averaged over some region, or related energy metrics (Adams and Harris, 1987). The ability to predict engineering design loads without considering the stress singularity remains particularly appealing for simplicity, such methods often utilize mechanics of materials level solutions (Taylor and Dillard, 1994; Wahab *et al.*, 2004; Goglio *et al.*, 2008), but it is uncertain whether these models can be extended to other adhesive systems and significantly different joint configurations. Weibull statistics have been employed to account for the fact that the strength of vanishingly small volumes of material near singularities and the stress distributions in these regions combine to give finite strength (Towse *et al.*, 1999). This is an interesting concept for linear elastic materials.

Thus, although the strength approach has been commonly used for adhesive bonds and remains an area of active research, shortcomings have encouraged many researchers and designers to consider alternative approaches to joint design. Fracture mechanics offers an alternate design approach which is able to incorporate the influence of such defects in the material being tested as well as the structure being designed and has become a powerful tool for augmenting and, in some cases, replacing strength-based design approaches in many engineering applications. The remainder of this chapter will provide a background to this topic, along with some recent developments and current challenges in the use of this approach in engineering design.

© Woodhead Publishing Limited, 2010

## 13.2 Fracture mechanics overview

Developed over the past century, fracture mechanics has become an essential approach for understanding and avoiding failures through proper design of a wide range of structures and engineering components (Anderson, 1995). Recognizing that virtually all materials and fabricated structures contain flaws, the field of fracture mechanics seeks to quantify the driving forces available for crack propagation and compare them with the material's resistance to crack growth. Adhesively bonded joints in assembled structures typically fail when a significant flaw or debond propagates (Anderson *et al.*, 1977; Kinloch, 1987). Debond propagation may occur rapidly owing to rapid crack growth during so-called critical fracture, or more slowly in response to environmental degradation, viscoelastic behavior or fatigue. When such subcritical debonding occurs under load-controlled scenarios, the strain energy release rate (SERR) available to drive the crack forward will often increase as the crack lengthens, thereby accelerating the debond rate. Unless these debonds are detected in time, they may reach critical size, at which point rapid or catastrophic failure can occur. An important part of the design process for adhesive joints is to determine whether an existing or assumed flaw will propagate and whether it can reach a critical size that will allow catastrophic debonding. This design process requires a thorough understanding of the fracture resistance of the adhesive joint, often over a range of loading conditions and environmental exposure histories, along with the size and location of possible debonds.

Although a fracture test specimen may be designed for effective testing purposes, engineering structures are not typically designed intentionally to contain a flaw or debond. Some design engineers often have more limited training and experience in applications of fracture mechanics and may have concerns with designing a structure based on a crack or debond that is not seen in the manufactured component. In fact, steps are typically taken in manufacturing to try to prevent such defects from forming. Nonetheless, the possibility that such defects can occur, either through improper or non-uniform surface treatment or adhesive placement and cure, or through unexpected loading conditions, environmental degradation, or other events, requires that structural bonds must resist fracture. In essence, fracture mechanics in design is an analysis of what will happen if things go wrong.

Traditional fracture mechanics assumes that flaws exist, either resulting from the manufacturing process or initiated by a specific service event and seeks to determine if a dominant flaw will propagate under the imposed loading conditions. Both the stress intensity factor and the SERR approaches to fracture mechanics have been successfully used in modeling behavior in adhesive joints, although the energy release rate approach is often most convenient for evaluating the global state of a debond propagating within a

© Woodhead Publishing Limited, 2010

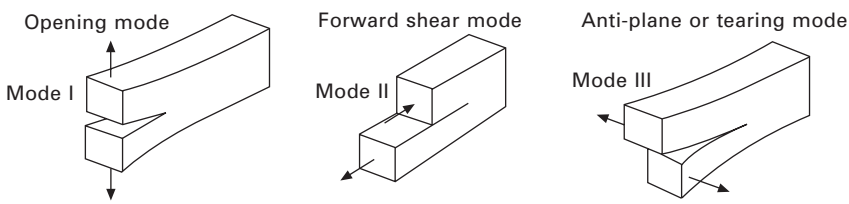
bonded joint and thus will be the focus of this chapter. Debonds propagating within the adhesive layer are often analyzed locally as a crack within a homogeneous material. If the crack propagates at an interface, however, interfacial fracture mechanics is needed to model the resulting behavior, which is complicated by coupled opening and shear fracture modes and oscillatory stresses and displacements (Rice, 1988; Liechti, 2002). A global analysis of debonds, rather than a local analysis, is often employed in the design process. In doing so, however, it is critical to recognize that resistance to debond propagation may be strongly dependent on the locus of failure, whether cohesive within the adhesive layer, interfacial (also referred to as adhesive failure) or within certain types of adherends such as wood and laminated composites (Dillard *et al.*, 2009).

Fracture may occur in a pure mode or in some combination of the three propagation modes: mode I (opening), mode II (forward shear) and mode III (tearing or out-of-plane), illustrated in Fig. 13.2. Using the SERR approach, critical fracture is assumed to occur when the crack driving force or applied SERR, $\mathcal{G}$, reaches the critical SERR, $\mathcal{G}_c$, for the bonded system. For subcritical fracture, the rate of crack propagation depends on several factors, including the available energy release rate, the viscoelastic properties of the materials, the environmental conditions, and the fracture mode.

Griffith laid the foundations for the SERR approach in 1921 (Griffith, 1921), several decades prior to Irwin's introduction of the stress intensity factor (Irwin, 1958). The applied energy release rate is the amount of energy per unit crack area imposed by the loading conditions and available to drive a growing crack, a relationship that is often expressed as:

$$\mathcal{G} = \frac{\partial(W - U)}{\partial A} \qquad [13.1]$$

for systems in which dissipation is limited to the crack tip region. Here $W$ is the external work, $U$ is the stored elastic energy and $A$ is the crack area. The resulting failure criteria, in the simplest form, state that the crack will propagate when this applied energy release rate reaches the critical value, $\mathcal{G}_c$, also known as the fracture energy, of the material or bonded system. Characterized as the amount of energy available or required to propagate




*13.2* The three fracture modes.

© Woodhead Publishing Limited, 2010

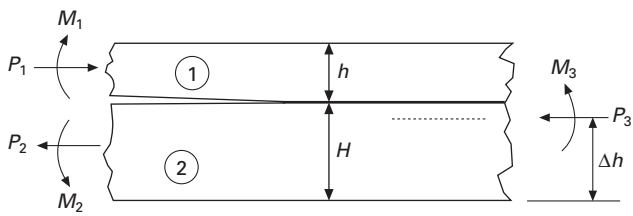
a crack per unit area, the SERR approach is quite intuitive from a physical standpoint and has found widespread applications, including to bonded systems. The stress intensity factor approach and the energy release rate approach can be shown to be equivalent for homogeneous materials (Broek, 1978; Anderson, 1995) and are often more convenient, such as for analyzing bimaterial interfaces (Rice, 1988).

One of the key advantages of using fracture mechanics to analyze cracked material systems is how easily the energy release rate can be estimated for many bonded configurations. For systems in which the generalized load and deflection are linearly related, the energy release rate can be shown to be simply (Broek, 1978):

$$\mathcal{G} = \frac{1}{2} P^2 \frac{\mathrm{d}C}{\mathrm{d}A} \qquad [13.2]$$

where $P$ represents the generalized force (e.g. force, moment or pressure), $C$ is the compliance of the system, relating the generalized displacement (e.g. linear displacement, rotation or displaced volume, respectively) to the generalized force and $A$ is the crack area. This covers many practical adhesion tests, although non-linear forms are sometimes encountered, such as in cases involving membrane stretching or peel tests and alternative forms of Equation 13.2 are needed (Williams, 1984). These simple formulae allow the energy release rate of many geometries to be readily determined; good approximations can often be determined with relatively simple and brief derivations, although numerical procedures are often needed for more comprehensive solutions.

Several authors (Williams, 1988; Davidson and Schapery, 1990; Suo and Hutchinson, 1990) have introduced relationships for determining the energy release rate and phase angle of arbitrary loading of a general bilayer beam (plane stress) or plate (plane strain), such as illustrated in Figure 13.3. Applications of these relationships readily provide energy release rates and mode mixities for a variety of specimen configurations and loading modes of adhesive joints (Lai and Dillard, 1997; Thouless and Yang, 2002) and coatings (Lai and Dillard, 1994; Papini and Spelt, 2002).




*13.3* Illustration of general loading for a cracked bilayer.

© Woodhead Publishing Limited, 2010

Where large scale plasticity is involved, linear elastic fracture mechanics (LEFM), wherein inelastic behavior is confined to the crack tip region, may not be applicable and the *J*-integral approach, introduced by Rice (Rice, 1968) may be used. For limited amounts of plasticity, the *J*-integral simplifies to $\mathcal{G}$ as appropriate for LEFM. The *J*-integral and other path independent criteria have been used to account for inelastic behavior (Anderson, 1995), see also chapter 16.

One of the complications and arguments against using fracture mechanics is the need to analyze an actual or assumed crack. By maintaining good quality control of the surface preparation and bonding process during manufacture, initial flaws can be minimized and are difficult or impossible to detect. In essence, one cannot conduct a classical fracture mechanics analysis without a crack, resulting in approaches that have separately considered the initiation (Zhang *et al.*, 1995; Lefebvre and Dillard, 1999; Lefebvre *et al.*, 1999, 2002) and propagation (Kinloch and Osiyemi, 1993) of cracks. This problem was circumvented by the development of the cohesive zone method (CZM), which can accommodate the progression of damage from initiation through crack propagation, as will be discussed later on in this chapter.

## 13.3 Measuring adhesion fracture energies

### 13.3.1 Measured fracture energies

For perfectly brittle materials, the critical energy release rate, $\mathcal{G}_c$, should simply be the energy required to create new surfaces. For this idealized thermodynamically reversible situation, the energy release rate for crack propagation in a monolithic material would be twice $\gamma$, the surface energy of the material, since there are two crack faces. For debonding at an interface between two materials, the thermodynamic work of adhesion is given by $W_{adh} = \gamma_1 + \gamma_2 - \gamma_{12}$, where, $\gamma_1$, $\gamma_2$ and $\gamma_{12}$ are the surface energies of materials 1 and 2 and the interface, respectively. The thermodynamic work of adhesion, often measured by contact angle techniques or the JKR (Johnson *et al.*, 1971) method, arises from dispersion or other physisorption forces and is usually in the order of several tens of millijoules per square meter (mJ $m^{-2}$). Although these thermodynamic energies are extremely useful in establishing the thermodynamics of wetting for an adhesive on a substrate, they are only a very small fraction of the practical adhesion, as measured by a debonding test.

The practical work of adhesion, or the apparent fracture energy, is often 3–6 orders of magnitude larger than the thermodynamic surface energy (for cohesive failures) or work of adhesion (for adhesion failures), implying that significant energy is being dissipated through other mechanisms, including plastic or viscoelastic deformation or microcracking of the adhesive. In

© Woodhead Publishing Limited, 2010

some geometries such as peel specimens (Moidu *et al.*, 1998; Kinloch and Williams, 2002), significant dissipation within the adherends can occur as well, increasing the practical adhesion by as much as a hundredfold (Kim and Kim, 1988). Because polymeric adhesives are viscoelastic, the fracture energy can depend strongly on time, rate and temperature.

Fracture energy has been observed to correlate with tan $\delta$, the ratio of the viscoelastic loss to storage moduli, in polymers and adhesive joints (Xu and Dillard, 2003; Pohlit *et al.*, 2008). Fracture energies are large in transition regions, but smaller at very slow propagation rates, where viscous processes are negligible, and at very fast propagation, where molecular mobility is insufficient to effectively dissipate energy. Thus, if fracture tests could be carried out at an infinitesimally slow rate or, in recognition of the time-temperature superposition principle (Ferry, 1980), at elevated temperatures, the practical work of adhesion should be reduced substantially. These tests have been conducted with elastomeric adhesives and the limiting fracture energies are referred to as the intrinsic adhesion (Gent and Kinloch, 1971), $\mathcal{G}_0$. This intrinsic adhesion value is still measured to be several orders of magnitude larger than the thermodynamic work of adhesion owing to other mechanisms, such as dissipation associated with chain stretching and rupture (Lake and Thomas, 1967). In turn, the fracture energy or practical work of adhesion, measured at typical test speeds, is often several orders of magnitude larger than the intrinsic adhesion.

Even though the intrinsic and practical work of adhesion are much larger than the thermodynamic surface energy or work of adhesion, they may be strongly dependent on these values. If an adhesive does not wet the surface well, for example, that bond is likely to have poor practical adhesion, even if the adhesive itself is capable of dissipating considerable energy through plastic or viscoelastic deformation. Empirically, this dependence has been expressed in multiplicative forms such as one of the following:

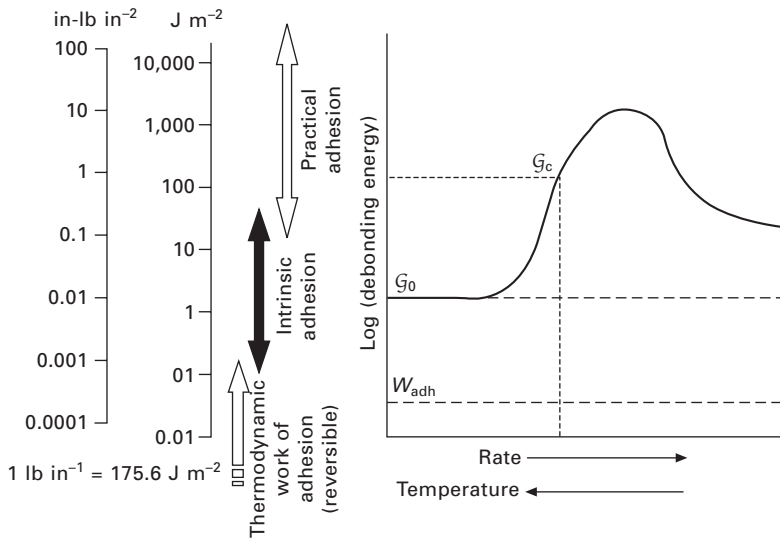
$$\mathcal{G}_c = W_{adh}(1 + \psi(\dot{a}, T, \ldots)) \qquad [13.3]$$

$$\mathcal{G}_c = \mathcal{G}_0(1 + \Psi(\dot{a}, T, \ldots))$$

where $\mathcal{G}_c$ for a given condition will depend on either $\psi$ or $\Psi$, which are appropriate dissipation functions depending on debond rate, temperature and perhaps other factors.

Extensions of such relationships to structural adhesives are more tenuous, but may be qualitatively useful. Figure 13.4 schematically illustrates the relationship between thermodynamic, intrinsic and practical adhesion, along with representative magnitudes of these quantities, suggesting that the measured $\mathcal{G}_c$ is strongly dependent on rate of debonding and temperature. In using measured fracture energies, it is important to characterize them at appropriate growth rates and temperatures, and not to confound the dissipation

© Woodhead Publishing Limited, 2010




*13.4* Illustration of thermodynamic, intrinsic and practical adhesion.

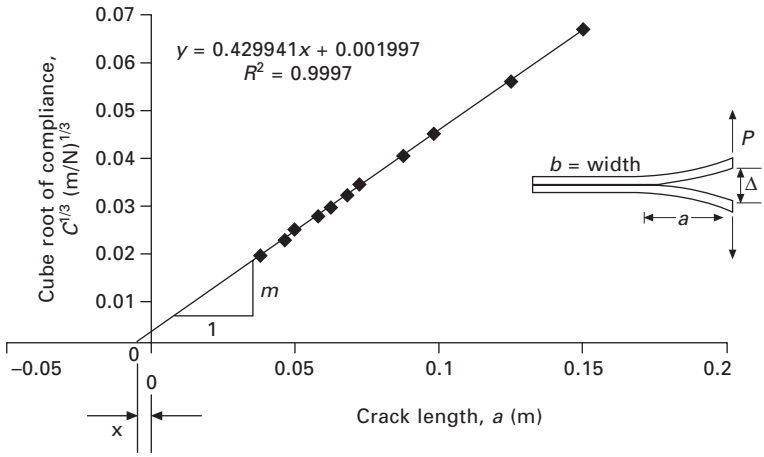
within the adhesive layer by dissipation in the test specimen adherends that may not be present in the structures being designed. Thus, it is important to separate out the energy attributable to the adhesive fracture process when attempting to design structures in which dissipation outside the adhesive layer can occur.

## 13.3.2 Characterizing fracture energies

A number of test methods have been developed or adapted to characterize the fracture energies of adhesive bonds. In relation to structural adhesives, the double cantilever beam (DCB) specimen and related beam-type specimens have been widely used (Blackman and Kinloch 2001). The basics of the DCB specimen have been outlined in Chapter 14 of this volume using analytical expressions that have traditionally been employed to calculate relevant fracture energies from experimental data (ASTM-D3433-99, 2001). Alternate analysis procedures have been developed, however, and are becoming increasingly popular, offering improved accuracy, consistency and robustness(Blackman *et al.*, 1991; Blackman *et al.*, 2003).

Examples of these methods include corrected beam theory, in which the experimentally measured beam compliances are incorporated, along with corrections that include an effective crack length. This method involves plots of the cube root (this arises because the deflection of a cantilevered beam subjected to a concentrated load is proportional to the cube of the length of the beam) of the specimen compliance versus the observed crack length, as illustrated in Fig. 13.5.

© Woodhead Publishing Limited, 2010




*13.5* Illustration of the application of the corrected beam theory to evaluate fracture energy of a DCB specimen.

The slope of a linear line effectively captures the measured compliance of the specimen and the negative value of the abscissa intercept, x, provides the crack length correction. This latter term is important for several reasons, accounting for the crack length variations across the specimen width (often manifested as thumbnail crack patterns); crack tip displacement and rotation, terms arising from the beam on elastic foundation nature of the bonded portion of the beam; and systematic variations in crack lengths reported by different observers. Another approach is to make plots of the log of the compliance versus the log of the crack length. Known as the experimental compliance method, this approach does not assume beam theory, but uses a best fit of the data to determine the fracture energy. The merits of these and other approaches have been addressed (Blackman *et al.*, 1991; Blackman, *et al.*, 2003) and recommended procedures codified (Blackman and Kinloch, 2001).

## 13.4 Designing to resist fracture

### 13.4.1 Designing to resist critical debonding

If the critical energy release rate or fracture energy, $\mathcal{G}_c$, can be thought of as a constant, bonded structure design can proceed directly. (Complications will be addressed in the following sections, including the common dependence of fracture energy on cyclic loading, debond rate, temperature, environmental exposure and mode mixity.) Whereas strength criteria typically involve comparing a calculated applied stress with a known material strength, fracture mechanics adds a third quantity, a characteristic length, to the

© Woodhead Publishing Limited, 2010

design process. For monolithic structures, this length is usually the size of the crack. For structural adhesive applications, the relevant length is typically the crack length as well, although exceptions exist, especially for relatively soft adhesives bonded to relatively rigid adherends. In such cases, the thickness of the adhesive layer may be the relevant length dimension (Gent 1974; Anderson, *et al.*, 1977). Whereas adhesive layer thickness may be a known quantity, the size of a potential crack can range from a nearly undetectable flaw to a significant fraction of the bonded area and obviously can change significantly over the life of a bonded component. Especially for components subjected to prescribed loads, debonding in adhesive joints often leads to increasing applied energy release rate values, suggesting that a crack is unlikely to arrest, thereby leading to catastrophic failures. Crack stoppers of various sorts have been employed in many applications, including spot welds, rivets, bolts, and even the use of more ductile adhesives in strips along the bond length.

Because of this dependence on crack length, fracture mechanics design and analysis often go hand in hand with non-destructive evaluation (NDE) techniques used to determine the crack length in as-fabricated or fielded structures. Adhesive bonds in critical applications such as the aerospace field often must be inspected individually with techniques such as ultrasound scans, leaky Lamb waves, thermal imaging, X-ray inspection or other techniques. Although details are beyond the scope of this chapter, readers are referred to the growing body of literature in this area (Rose, 1999, 2002). Determining the location, size and, in some cases, orientation of initial or service-induced flaws allows flaws to be identified and decisions to be made to repair or replace bonded joints deemed unsafe according to the design and maintenance procedures in place.

### 13.4.2 Designing to resist subcritical debonding

Fracture mechanics has proven to be particularly useful in estimating the time-dependent flaw growth within adhesive bonds, often known as subcritical fracture or debonding. Subcritical debonding may result from cyclic fatigue loading, commonly imposed by either cyclic mechanical or hygrothermal loading scenarios; from time-dependent crack propagation within a viscoelastic adhesive or interphase; or from degradation of the adhesive or interphase caused by environmental exposure and the resulting degradation of the interface, adhesive or both.

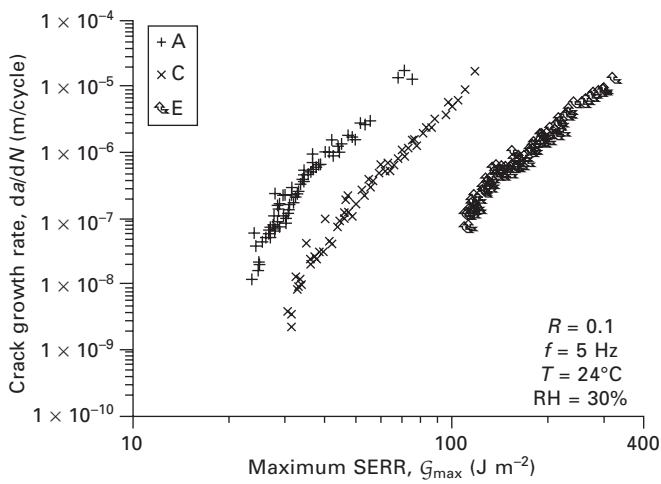
#### *Cyclic fatigue debonding*

The deleterious effects of fatigue on structural materials have been known for nearly two centuries, although the mechanisms were poorly understood

© Woodhead Publishing Limited, 2010

initially (Broek, 1978). Traditional design approaches to account for fatigue centered around so-called *S–N* plots, in which applied stress is plotted against the log of the number of cycles to failure. Linear fits to experimental data were often, and continue to be, used for design. Mean stress, surface finish, stress gradients, and other issues can affect fatigue life, so their effects often need to be considered. Furthermore, the extension of *S–N* results obtained at constant amplitude loading to more realistic fatigue profiles often requires the use of empirical cumulative damage methods, often refinements of the Palmgren–Miner rule (Miner, 1945), with varying degrees of success. Although the *S–N* design approach has been widely used, extensions to adhesive joints, with the significant stress gradients that often appear, is problematic. Fatigue life predictions for bonded joints may require fatigue life data on joints that are very similar to the intended joints, thus complicating the design process.

Paris and his coworkers first proposed the use of fracture mechanics to characterize the influence of cyclic loading on structural materials (Paris *et al.*, 1961). They proposed what they considered to be a rational approach to fatigue, relating the rate of crack growth to the amplitude of applied cyclic stress intensity factor. Often over a significant range, such data can be represented by a power law relationship that is referred to as the Paris law. Although his approach was not initially accepted, it has become an important part of modern fatigue design. Paris' initial work was applied to metals, but the approach has subsequently been applied to many other materials, including polymers and adhesive bonds. Figure 13.6 illustrates fatigue crack growth rates for a model epoxy system containing several different amounts




*13.6* Effect of adding rubber toughening component on fatigue resistance of a model epoxy.

© Woodhead Publishing Limited, 2010

of rubber toughener; growth rates in the epoxy containing the highest rubber toughener content system (E) are nearly three orders of magnitude slower than for the unmodified epoxy (A) (Rakestraw *et al.*, 1995; Vrana *et al.*, 1995). In adhesive joint design, the rate of debond growth is related to the applied SERR. Kinloch and his coworkers have used a relationship like Equation 13.4 (Kinloch and Osiyemi 1993; Hadavinia *et al.*, 2003):

$$\frac{\mathrm{d}a}{\mathrm{d}N} = D\mathcal{G}_{\max}^{n}\left[\frac{1-\left(\frac{\mathcal{G}_{\mathrm{th}}}{\mathcal{G}_{\max}}\right)^{n_1}}{1-\left(\frac{\mathcal{G}_{\max}}{\mathcal{G}_{\mathrm{c}}}\right)^{n_2}}\right] \qquad [13.4]$$

where $a$ is the crack length, $N$ the number of cycles, $\mathcal{G}_{\max}$ the maximum applied energy release rate during a given cycle, $\mathcal{G}_{\mathrm{th}}$ the threshold fracture energy below which crack growth is not observed, $\mathcal{G}_{\mathrm{c}}$ the critical fracture energy at which rapid cracking occurs, and $D$, $n$, $n_1$ and $n_2$ are determined from experimental results obtained in the relevant material system. This approach has been used by several authors in this volume to predict joint performance, see Chapters 12, 16 and 19 in this volume.

Several approaches may be considered for use in design. One approach is to operate at stress levels that induce applied energy release rates below $\mathcal{G}_{\mathrm{th}}$, thereby supposedly assuring that cracks or debonds cannot grow. In the safe-life approach, the structure is designed so that although the crack can grow over time, the growth will be small enough that the crack never reaches critical size, $a_{\mathrm{c}}$, where catastrophic failure would occur. To use this approach, one can measure the initial flaw size and location, infer it from strength measurements of as produced joints, or assume that it is in the most critical location and equal in size to the detection limit of NDE techniques that may be used to detect debonds or other damage. This initial flaw size, $a_0$, becomes the starting point for crack growth over the life of the bonded structure. Equation 13.4 can then be integrated to obtain the number of cycles to failure, $N_{\mathrm{f}}$ (Kinloch and Osiyemi, 1993). Crack stoppers of various types, as mentioned earlier, can be sometimes employed to arrest growing cracks giving damage tolerant designs.

It should be cautioned that because of the time, temperature and often environmental sensitivity of polymers and their bonded joints, care should be used in extending this equation to conditions other than those used to collect crack growth data (Johnson and Butkus, 1998). Some of these issues are addressed in the next sections.

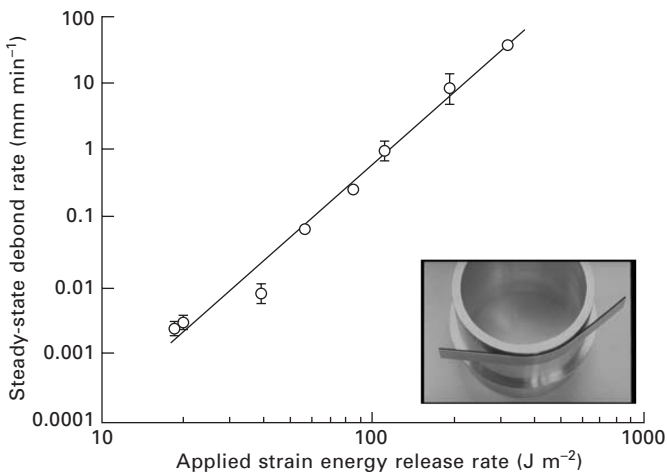
© Woodhead Publishing Limited, 2010

*Time-dependent debonding*

Another form of subcritical crack growth can arise because of the viscoelastic nature of polymeric adhesives, whose time dependence is especially significant when used near their transition temperatures. The term 'static fatigue' is sometimes used to distinguish such behavior from cyclic fatigue loading, implying that damage or crack growth can occur even under constant stress amplitudes. In principle, a modified form of the Paris law can be used, in which the time rate of crack growth replaces the cyclic rate. Additional details can be found in Chapter 16 in this volume.

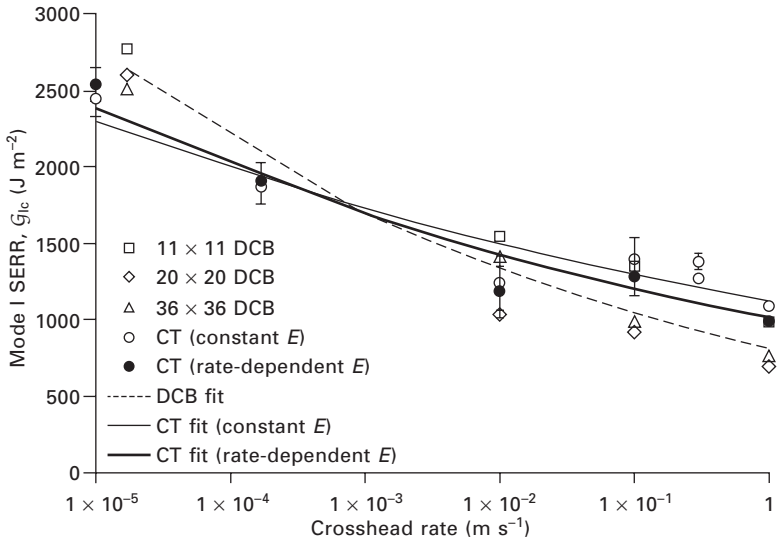
An example of time-dependent debonding is presented for an acrylic foam tape of the type that is often used for semi-structural applications. Here, an inexpensive, self-loading curvature mismatch specimen (Dillard, 1988) was used to gather rate-dependent debond data. Figure 13.7 illustrates the debonding behavior obtained by characterizing the debond rate as a function of the applied energy release rate, which was varied by changing the mandrel radius or flexible adherend thickness. Being elastomeric at the rates tested, the results suggest that increasing debond rates require higher amounts of input energy, placing it on the left side of the schematic diagram in Fig. 13.4.

On the other hand, when on the glassy side of the response curve, the opposite behavior can be seen, as illustrated in Fig. 13.8 for an epoxy adhesive used to bond 11, 20, or 36 ply composite adherends (Pohlit *et al.*, 2008). Here, the fracture energy drops with increasing debond rate, as less viscoelastic dissipation is able to occur at the crack tip. It is important to




*13.7* Illustration of debond rate data collected at several different $\mathcal{G}$ values for an acrylic foam tape in a curvature mismatch specimen.

© Woodhead Publishing Limited, 2010




*13.8* Illustration of rate dependence of an epoxy adhesive tested on neat compact tension (CT) and bonded composite DCB specimens.

recognize that these two figures represent only limited ranges of debond rate obtained at a single temperature. Rate-dependent processes in polymers, including debonding, are often strongly affected by temperature. Application of the time–temperature superposition principle (TTSP) can permit a wider range of effective or reduced debond rates to be studied (Bitner *et al.*, 1981), often resulting in fracture energy master curves similar to that schematically shown in Fig. 13.4. Depending on the loading times and environments of interest, fracture data over narrow ranges of debond rate may be appropriate for design, although in other cases, a more complete understanding of the broader response will be required.

### *Environmental exposure debonding*

Environmental exposure of adhesive joints can involve a number of phenomena, see Chapter 19, including an acceleration of subcritical debonding. Considering an almost ubiquitous environmental factor, moisture, for example, one recognizes that several mechanisms may be involved, however. Water sorbed by the polymeric adhesive can plasticize the material, depressing the glass transition temperature significantly. If this were the only affect, the presence of moisture might be modeled through an effective acceleration, a hygral shift factor that is similar to the thermal shift factors so widely used in the time–temperature superposition principle (TTSP). Some success

© Woodhead Publishing Limited, 2010

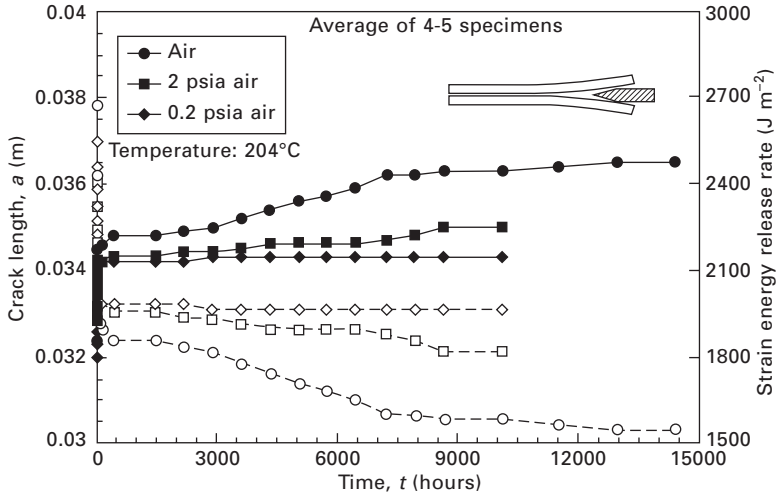
has been demonstrated with doubly shifted master curves using the time–temperature–moisture superposition principle (TTMSP) (Shephard, 1995). Unfortunately, the effects of moisture or other environmental factors are not always limited to a simple acceleration of a known rate process. In some cases other degradation mechanisms may occur, such as an interaction with the substrate interface or the interphase region.

Since many metallic and ceramic substrates have high surface energies, polar diluents such as water are often strongly attracted to the interface, where they may disrupt the interactions with the substrate. This may lower the fracture energy threshold and increase the debond rate at any given applied energy release rate level. In principle, such behavior, if characterized, could be used to estimate the lifetime of a bonded component. In some cases, the surface of the substrate is changed by the water, as the oxide layer becomes hydrated. Other environmental effects can also occur, including environmental stress cracking, in which the presence of the environment can substantially lower the fracture energy of the polymer. Thermoplastic adhesives, which lack cross-links, are often more susceptible to this type of problem (Dillard *et al.*, 1994; Dillard *et al.*, 1995; Parvatareddy *et al.*, 1999).

Care should be used when characterizing the rate dependence of failure processes associated with diluent diffusion because of the time that can be required. For example, characterizing the rate dependent fracture in straight-sided bonded beam specimens is complicated by the fact that the diluents will diffuse from the sides of the specimen as well as the growing debond tip. Comyn has provided analysis of the two-dimensional diffusion problem that is common in adhesives bonding impervious substrates (Comyn 1983). Axisymmetric specimens, such as the blister test, may avoid some of these problems because the diffusion front is perpendicular to the debond tip. Recognizing that dramatic loss in adhesion can occur owing to diffused diluents, Gledhill *et al.* (Gledhill *et al.*, 1980) assumed that the bond was essentially destroyed once a critical amount of sorbed moisture was present in the bond (Lefebvre *et al.*, 1991; Tan *et al.*, 2008). Thus Fickian diffusion models have been successfully used to estimate the effective crack size, from which breaking load or life could be predicted.

Another example of environmental effects are due to the physical and chemical aging (in the presence of oxygen) of a polyimide adhesive used to bond titanium adherends intended for supersonic aircraft (Parvatareddy *et al.*, 1998). The polyimide adhesive, with a glass transition temperature, $T_g$, of about 250°C, was required to offer good durability over a multiple of the intended life of the aircraft at temperatures that could reach as high as 204°C. The use of inexpensive self-loading specimens, such as wedge tests, can be well suited to gathering relevant data for such designs, as was used to obtain the results shown in Fig. 13.9.

© Woodhead Publishing Limited, 2010




*13.9* Crack length and fracture energy values for chromic acid anodized titanium adherends bonded with a polyimide adhesive and aged at 204°C. (Filled symbols correspond to crack length and open symbols correspond to SERR.)

Here a series of wedge tests were performed at 204°C in ambient air and at reduced pressures of 13.8 kPa (2 psia), which was expected at the service altitude, and 1.38 kPa (0.2 psia), which represented only a tenth of the oxygen level expected at the service altitude. By recording the crack length as a function of time in these environments and then determining the SERR (Cognard, 1987) from the known wedge thickness, adherend properties and dimensions, and crack length, insight is gained into the rate of crack growth as well as a potential thresholds for the fracture energy, both of which can be useful in design approaches. Interestingly, if these specimens were reheated to 300°C for 2 hours, physical aging (Struik, 1978) effects could be eliminated through rejuvenation. Specimens exposed to higher oxygen content environments showed the greatest crack growth and correspondingly lowest fracture energy. They also showed little benefit from rejuvenation, suggesting that the reduced fracture energies resulted primarily from chemical aging effects. This is in contrast to the specimens tested in reduced oxygen environments, which exhibited less degradation and more benefit from thermal rejuvenation (Parvatareddy *et al.*, 1998).

## 13.5 Issues related to mixed mode fracture

Fracture can occur in any one of the three modes previously discussed (pure mode) or in combinations (mixed mode) of these loading conditions. For monolithic materials, cracks grow in mode I and will turn or kink to maintain propagation in this fashion (Erdogan and Sih, 1963; Goldstein and

© Woodhead Publishing Limited, 2010

Salganik, 1974; Palaniswamy and Knauss, 1978; Cotterell and Rice, 1980). As such, most fracture tests on monolithic materials are conducted in opening mode. The situation becomes more complex with layered materials, such as adhesively bonded joints or laminated composite materials, however, because the growing crack is often constrained to grow within the adhesive layer. Because of this, comprehensive fracture studies of layered materials often require control of and examination of the applied fracture mode. If the fracture energy were not a function of the applied fracture mode, characterization of fracture by any mode would be appropriate and sufficient.

This simple idealization is attractive, as it assumes that the energy required to break an interface is independent of the mode. Although this should be true for the thermodynamic surface energy of a monolithic material or the work of adhesion for fracture at an interface, significant variations of fracture energy with mode mixity have been seen in many real systems. Mode I fracture energies are often smaller than fracture energies measured for other modes and can arise from several sources, including enhanced plasticity which often results in shear loading, the longer and more tortuous crack paths that often result in shear loading and frictional effects (Liechti and Chai, 1992). In addition to these mechanisms, the locus of failure may also depend on mode mixity and sometimes this can result in a very different dependence on mode mixity. For example, shear loading an adhesive bond tends to drive the crack towards the interface, as cracks tend to grow perpendicular to the largest tensile stress in monolithic materials. This may drive the crack away from the center of the adhesive layer, where enhanced energy dissipation caused by the presence of a scrim layer (Parvatareddy and Dillard, 1999), the presence of rubber toughening particles (Chen *et al.*, 2001a; Chen and Dillard, 2002), or large scale plasticity during crack arrest (Simón *et al.*, 2005; Pohlit *et al.*, 2008) can occur. Mixed mode fracture energies of adhesive joints as small as 25% of the mode I fracture energy have been reported (Dillard *et al.*, 2009).

The in-plane modes, I and II, are usually believed to be the most common or important (or lead to more conservative designs) and have been the subject of the majority of fracture tests and analyses of adhesive bonds. The mode mixity, which is useful for characterizing in-plane fracture problems involving cohesive fracture, is given by:

$$\psi = \tan^{-1}\left[\frac{K_{II}}{K_I}\right] = \tan^{-1}\left[\sqrt{\frac{\mathcal{G}_{II}}{\mathcal{G}_I}}\right] \qquad [13.5]$$

Mixed mode fracture energy results may be presented in several ways, including as plots of total fracture energy as a function of mode mixity and as fracture envelopes in which either stress intensity factors ($K$) or SERRs ($\mathcal{G}$) for mode I and mode II loading are plotted on the abscissa and ordinate

© Woodhead Publishing Limited, 2010

axes, respectively. Functional forms have been used to express the fracture energy criteria such as (Russel and Street, 1985):

$$\left[\frac{(\mathcal{G}_{\mathrm{I}})_{\mathrm{c}}}{\mathcal{G}_{\mathrm{Ic}}}\right]^{\alpha} + \left[\frac{(\mathcal{G}_{\mathrm{II}})_{\mathrm{c}}}{\mathcal{G}_{\mathrm{IIc}}}\right]^{\beta} = 1 \qquad [13.6]$$

where $(\mathcal{G}_{\mathrm{I}})_{\mathrm{c}}$ and $(\mathcal{G}_{\mathrm{II}})_{\mathrm{c}}$ are the mode I and mode II components of the SERR rate at fracture, $\mathcal{G}_{\mathrm{Ic}}$ and $\mathcal{G}_{\mathrm{IIc}}$ are the critical fracture energies for pure modes, and $\alpha$ and $\beta$ are exponents. The exponents may be chosen to form the best fit of experimental data or may be prescribed based on some assumed relationship. For example, if the critical fracture energy is assumed to depend only on the total fracture energy ($\mathcal{G}_{\mathrm{T}} = \mathcal{G}_{\mathrm{I}} + \mathcal{G}_{\mathrm{II}}$) and not the mode mixity, $\alpha = \beta = 1$ and $\mathcal{G}_{\mathrm{Ic}} = \mathcal{G}_{\mathrm{IIc}}$; if $\alpha$ and $\beta$ are both greater than or equal to unity, the resulting criterion implies that the mixed mode fracture energies will be larger than the minimum of $\mathcal{G}_{\mathrm{Ic}}$ and $\mathcal{G}_{\mathrm{IIc}}$. In that case, the use of the minimum pure mode fracture energy (Min($\mathcal{G}_{\mathrm{Ic}}$, $\mathcal{G}_{\mathrm{IIc}}$)) would be conservative for design purposes (Choupani, 2008). On the other hand, if $\alpha$ is less than unity, mixed mode fracture energies could be smaller than $\mathcal{G}_{\mathrm{Ic}}$, which is often the smallest pure mode fracture energy. Alternate forms of fracture envelope criteria have also been proposed (Kinloch, 1987; Charalambides *et al.*, 1992), including (Hashemi *et al.*, 1989):

$$\left(\frac{\mathcal{G}_{\mathrm{I}}}{\mathcal{G}_{\mathrm{Ic}}} - 1\right)\left(\frac{\mathcal{G}_{\mathrm{II}}}{\mathcal{G}_{\mathrm{IIc}}} - 1\right) - I_{\mathrm{i}}\left(\frac{\mathcal{G}_{\mathrm{I}}}{\mathcal{G}_{\mathrm{Ic}}}\right)\left(\frac{\mathcal{G}_{\mathrm{II}}}{\mathcal{G}_{\mathrm{IIc}}}\right) = 0 \qquad [13.7]$$

This relationship involves a single interaction factor, $I_{\mathrm{i}}$, which is zero if there is no interaction ($\mathcal{G}_{\mathrm{I}}/\mathcal{G}_{\mathrm{Ic}} = 1$ or $\mathcal{G}_{\mathrm{II}}/\mathcal{G}_{\mathrm{IIc}} = 1$, corresponding to $\alpha \to \infty$ and $\beta \to \infty$) and unity if there is a simple addition ($\mathcal{G}_{\mathrm{I}}/\mathcal{G}_{\mathrm{Ic}} + \mathcal{G}_{\mathrm{II}}/\mathcal{G}_{\mathrm{IIc}} = 1$, corresponding to $\alpha = \beta = 1$) such that the total energy release rate controls the fracture.

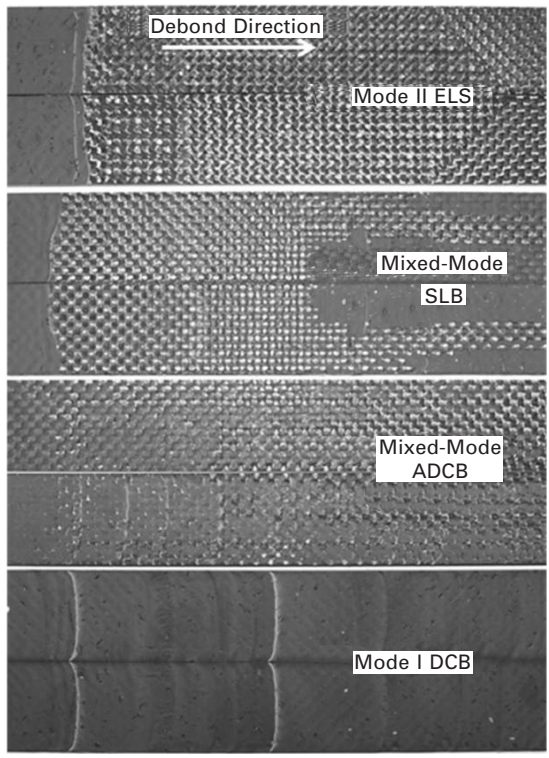
In real bonds, criteria such as given above may be used to model fracture envelopes, but because they are phenomenological in nature, they typically cannot accurately represent results when changes in locus or type of fracture process occur. Mechanistically, shear stresses tend to drive cracks away from a path that is parallel to the bond planes, potentially steering cracks into regions of the material system where the energy dissipation associated with crack advance can change significantly (Chai, 1992; Chen *et al.*, 2002). In some cases, the direction of the shear stress state in relation to the growing crack can steer the crack towards interfaces that are 'weaker', allowing the crack to propagate with less energy dissipation. In other cases, however, the crack can actually be steered to regions where greater energy dissipation occurs because of an improved interface (Chen *et al.*, 2001a) or other reasons.

To understand the role that shear stress plays in determining the mode of

© Woodhead Publishing Limited, 2010

failure, note that in homogeneous isotropic materials, cracks tend to propagate perpendicular to the direction of maximum tensile stress. In an adhesive joint subjected to a shear state, cracks within the adhesive layer have a tendency to grow toward one interface. Shear-dominated loading often results in interfacial failures or failures with less adhesive left on an interface (Chen and Dillard, 2001a and b; Chen *et al*., 2001a; Chen *et al*., 2001b; Chen *et al*., 2002), although more complex hackle pattern failures have also been reported (Chai, 1986). Also, some adhesive fracture envelopes are relatively smooth, permitting reasonable fits with phenomenological criteria, such as cited above. Where changes in failure mode occur, however, the fracture envelopes may take on distorted shapes. For example, consider the fracture surfaces shown for the case of fiber-reinforced composite adherends bonded with an epoxy adhesive, as shown in Fig. 13.10.

Under mode I loading, the locus of failure is cohesive within the adhesive layer, resulting in large fracture energies caused by localized plasticity (shown as stress whitening in the figure). As increasing amounts of mode II loading are introduced, the locus of failure is directed towards the adhesive/




*13.10* Effect of specimen type and fracture mode on locus of failure for epoxy-bonded composite specimens.

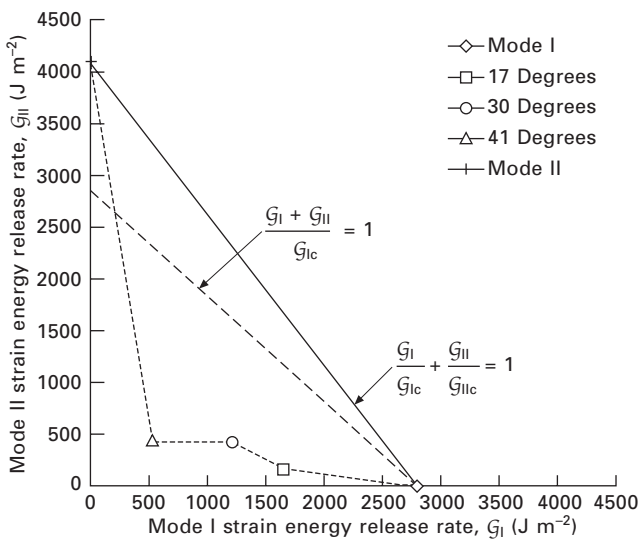
© Woodhead Publishing Limited, 2010

composite interface, where the measured fracture energies drop considerably because local plastic dissipation is reduced. Under mode II conditions, the failure is directed through the interface and propagates within the composite adherend. The fracture energies associated with these various failure modes are shown in the fracture envelope illustrated in Fig. 13.11.

### 13.5.1 Mode mixity effects

To evaluate the fracture energies over a range of mode mixities, a number of specimens have been developed, primarily for testing adhesively bonded joints and laminated composites. With symmetric adherends, common fracture specimens such as the double cantilever beam (DCB) and tapered DCB specimens are widely used for mode I testing, the single leg bend specimen (SLB) provides $\mathcal{G}_{IIc}/\mathcal{G}_{Ic}$ = 3/4 for mixed mode fracture, and the end load split (ELS) or end notch flex (ENF) specimens are used for mode II loading. By varying the adherend thickness, one can achieve modest deviations from these three fixed mode tests, as predicted by (Suo and Hutchinson, 1990). However, the compliance of the adhesive layer often reduces the local mode mixity from what is predicted by these equations (Park and Dillard, 2007), which only provide the global mode mixity.

Fracture of other mode mixities can be achieved through the use of special fixtures that alter the bending ratios in the adherends (Reeder and Crews,




*13.11* Fracture energies for epoxy-bonded composite specimens tested under several mode mixities, along with common fracture energy envelope equations.

© Woodhead Publishing Limited, 2010

1990, 1992; Fernlund and Spelt, 1994a and b), vary the thickness ratio of the adherends (Park and Dillard, 2007), or incorporate a second degree of actuation, such as a dual actuator load frame for testing DCB-type specimens (Dillard *et al.*, 2006; Singh *et al.*, 2006, 2008). The out-of-plane fracture mode (III) is less commonly evaluated because of the particular difficulty it poses experimentally, although several test methods have been proposed.

### 13.5.2 Locus of failure

The measured fracture energy of a test specimen and the energy required to grow a debond in an adhesively bonded structure can depend on the debond propagation path. Careful imaging or chemical analysis of the locus of failure can provide important insights into the cause of failure in test specimens as well as conducting autopsies on field failures of adhesive joints. Caution is needed however, for several reasons. First, because final fracture often occurs rapidly, the initiation of fracture, rather than its propagation, may provide answers for the cause of failure. Changes in surface preparation may affect the load at which failure is initiated without influencing the locus of a rapidly growing crack, which may remain cohesive (Anderson, 1988). This may require determining and analyzing the region in which failure initiated. Second, many have assumed that failure always occurs at the 'weakest link' location, a concept that works well for discrete systems such as chains, but which can lead to erroneous conclusions in continuous systems, where a spatially varying stress state interacts with a spatially varying resistance to fracture. Third, the path of the fracture may depend on other factors, such as the orientation of the grain in bonded wood specimens.

During the design process, prototype components and structures are often developed and tested to failure to evaluate the effectiveness of the design. In examining these failures, as well as failures that may occur in service of fielded systems, fracture mechanics can provide valuable insights to aid in accurately evaluating the causes of failure. Keeping in mind the effect that shear stresses have on crack direction, for example, one can often gain insights into the type of loading that precipitated failure. Surface analysis techniques can provide valuable tools for isolating the locus and cause of failure, and are recommended for use in the design and evaluation process, as well as in examining failures from fielded structures.

## 13.6 Design insights from fracture mechanics

### 13.6.1 Adherend flexibility

When work is done on cracked structures with linear load deflection relationships, half of the energy is stored and the other half is available to

© Woodhead Publishing Limited, 2010

drive the crack. For load controlled scenarios (i.e. structures that must hold a given force, such as a wing bonded on an aircraft), the ability to store energy is linearly dependent on the compliance of the structure. More flexible structures can store more energy and equivalently apply more energy to a growing crack. Thus for load-controlled structures, increasing the stiffness can increase the resistance to debonding failures. For displacement-controlled applications (i.e. structures in which the adhesive is forced to prescribed strain levels, such as the sealant in a highway joint), the energy available to drive a debond comes from the energy relieved by the growing crack. For these situations, the stored energy is linearly dependent on the stiffness of the adhesive, so stiffer adhesives require greater fracture energies to survive. For structural adhesives that are relatively thin and stiff, greater structure flexibility generally requires less load for joint failure.

It is interesting how the stress analysis and strength approach closely parallel this line of reasoning based on an energy or fracture mechanics perspective. For example, in Volkersen's classic development of the shear lag model (Volkersen, 1938), increased adherend flexibility leads to greater differential straining in the adherends and hence larger shear stresses. In fact, the fracture and strength analyses provide the same results for a cracked lap shear joint, a lap joint with a propagating crack (Anderson *et al.*, 1977).

### 13.6.2 Adhesive thickness effects

The bondline thickness in an adhesive joint is controlled by a number of factors, including the viscosity of the adhesive, the pressure applied, the tolerance and fit of the adherends, the presence of scrim or carrier layers in the case of film adhesives and, in some cases, spacers that are added to the adhesive or designed into the joint. The structural performance of a joint will often depend on bondline thickness, in some cases quite dramatically. The optimal thickness for structural integrity depends on a number of factors, including:

- Nature of the loading: joints subject to displacement controlled loading often benefit more from thicker bondlines than do joints subjected to load controlled situations.
- Type of the joint: lap shear joints may benefit from slightly larger bondline thicknesses because these reduce the stresses, whereas butt joint configurations perform better with thin bondlines (Reedy, 1990, 2002; Reedy and Guess, 1995).
- Properties of the adhesive: more ductile adhesives often provide more fracture resistance in moderately thicker bondlines than do brittle adhesives and these optimal thicknesses change with temperature and loading rate because of their effect on plastic zone size (Kinloch, 1987).

© Woodhead Publishing Limited, 2010

### 13.6.3 Rate and temperature effects

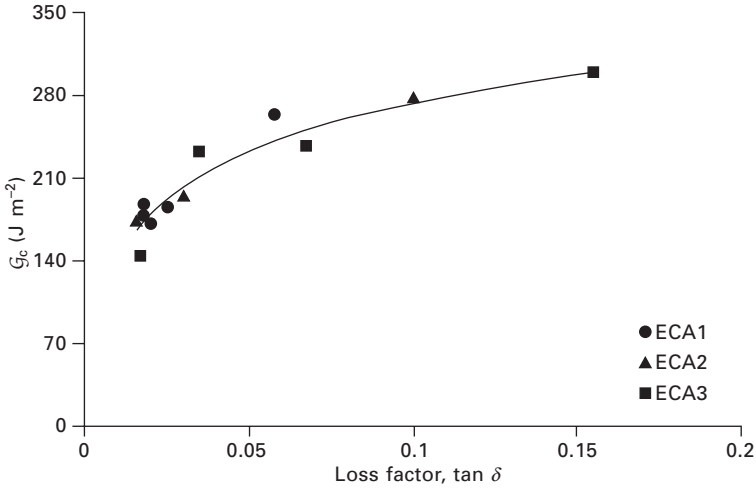
Polymeric adhesives are viscoelastic, exhibiting significant time and temperature dependence. The time–temperature superposition principle (TTSP) has been widely used to predict how materials would perform on shorter and longer time scales than experimentally accessible. Based on the assumption that increased temperature accelerates the same molecular motions that would occur more slowly at lower temperatures, this principle has become an important foundation in physical polymer chemistry and the mechanics of time-dependent materials. Mechanical properties obtained over a range of test temperatures can often be shifted to form a smooth master curve spanning many decades in time, much shorter than could readily be measured experimentally or much longer than experimental patience would permit. The shift factor required to form the master curve is as function of temperature in TTSP, although other accelerating quantities such as moisture or solvent content or stress can be used, sometimes in combination with temperature to obtain doubly shifted master curves.

Although most widely employed for constitutive properties such as stress relaxation moduli, creep compliance and dynamic moduli, TTSP is also widely used for time-dependent strength and fracture as well. In fact, assuming that the same deformations are being accelerated, the shift factors that may accurately be obtained for constitutive properties are often appropriate for predicting the effect of temperature on crack initiation as a function of loading rate or the rate of crack propagation in subcritical crack growth.

Working within the TTSP construct, the fracture resistance can be viewed as a function of time and temperature. When fracture resistance is plotted versus the logarithm of the reduced rate of crack growth, one often obtains plots such as illustrated in Fig. 13.4.

As noted earlier, fracture energy often correlates with tan $\delta$, reflecting the fact that molecular mobility and dissipation responsible for increases in the loss tangent in polymers may also control time-dependent cohesive fracture or even adhesive fracture in some bonded joints (Xu and Dillard, 2003; Pohlit *et al.*, 2008). Although the applicability of this correlation may not be universal, the ease of measuring tan $\delta$ over a range of temperatures and frequencies makes this an attractive technique to gain insights into an adhesive's likely fracture dependence on rate and temperature. Figure 13.12, for example, shows a plot of the fracture energies measured in a falling wedge test (Xu and Dillard, 2003) as a function of the tan $\delta$ measured using a dynamic mechanical analyzer (DMA). Both tests were conducted over a range of temperatures and the tan $\delta$ values were selected at frequencies to correspond with the effective loading time of the fracture tests. Good correlation is seen between the fracture energy and tan $\delta$ values for a series of three conductive adhesive formulations which have significantly different

© Woodhead Publishing Limited, 2010




*13.12* Illustration of the correlation between measured fracture energy and the tan δ value at the corresponding temperature and effective rate for three variations of a model epoxy system.

glass transition temperatures. The correlation between the DMA results at very small strain levels (e.g. 0.5%) and fracture involving considerable plastic dissipation results from the fact that both measurements depend on the molecular mobility of the adhesive being tested.

## 13.7 Design implications of other singularities

Although fracture mechanics specifically addresses crack-like flaws in materials, the underlying mathematics behind classical linear elastic fracture mechanics also applies to other geometric features. The stresses surrounding a singularity may be represented by:

$$\sigma_{ij}(r, \theta) = Qr^{\lambda} f_{ij}(\theta) + \ldots \quad [13.8]$$

where for the case of a sharp-tipped crack, $Q$, the generalized stress intensity factor becomes $K$, the stress intensity factor and $\lambda$ takes on a value of –½. (Here only a single term is suggested to be dominant, as is appropriate for monolithic and interfacial failure. Additional terms may be important for certain geometric and material scenarios.) For re-entrant angles in monolithic materials, the eigenvalue, $\lambda$, varies with the angle. For cracks at an interface between dissimilar materials, the eigenvalue, $\lambda$, becomes complex, suggesting oscillating displacements. For more general wedges of dissimilar materials, a range of real and complex eigenvalues can result depending on the material properties and the geometric angles (Erdogan and Ozturk, 2008).

© Woodhead Publishing Limited, 2010

While a discussion of these general singularities is beyond the scope of this chapter, the insights gained from extension of the singular stress fields surrounding a crack to bimaterial interfaces for a range of angles has many applications in the field of adhesive joining. This generalized stress intensity factor approach has been used as a failure criterion for microelectronic adhesion problems (Hattori *et al*., 1989), for a wide range of bonded joints (Reedy and Guess, 2001; Reedy, 2002), for effects of varying bondline thickness (Gleich *et al*., 2001; Van Tooren *et al*., 2004), and as a means of evaluating the effects of adhesive spew on initiation of fatigue cracks in adhesive bonds (Lefebvre and Dillard, 1999; Lefebvre *et al*., 1999, 2002).

This extension of fracture mechanics to other singularities has proven to be a useful means of characterizing and quantifying the manner in which damage initiates (Sheng and Chernenkoff, 1996; Lefebvre and Dillard, 1999; Lefebvre *et al*., 2002; see also Chapter 12 in this volume) or propagates (Johnson and Butkus, 1998) under cyclic loading conditions. Once a defined crack occurs, durability can be predicted knowing the rate of debond propagation as a function of the applied energy release rates.

## 13.8 Numerical analysis

Although analytical solutions of varying complexity are adequate to analyze debonding configurations, including common fracture test specimens, engineering components will often require the use of numerical procedures to account properly for the complex materials, joint configurations, boundary conditions and loading scenarios. To analyze crack growth, the proposed directions of increments in the crack can be obtained and the crack allowed to increment. This allows determination of the crack path and may be done manually or in an automated fashion (Bittencourt *et al*., 1996; James and Swenson, 1999), such as provided in FRANC2D (Ingraffea and Wawrzynek, 1995; Chen *et al*., 1997), FRANC3D (Carter *et al*., 2000), ABAQUS, GENOA and other packages that incorporate special features that facilitate analysis of cracked structures. Fracture calculations have been based on several approaches, including those discussed briefly herein. Improved accuracy with relatively coarse meshes can often be obtained using special elements that capture the crack tip singularity.

### 13.8.1 Virtual crack closure method

Early approaches for characterizing fracture parameters focused on the virtual crack closure technique (VCCT) (Rybicki and Kanninen, 1977) in which the applied energy release rate method is determined by evaluating the energy per unit area required to close a small increment of crack length. In two

© Woodhead Publishing Limited, 2010

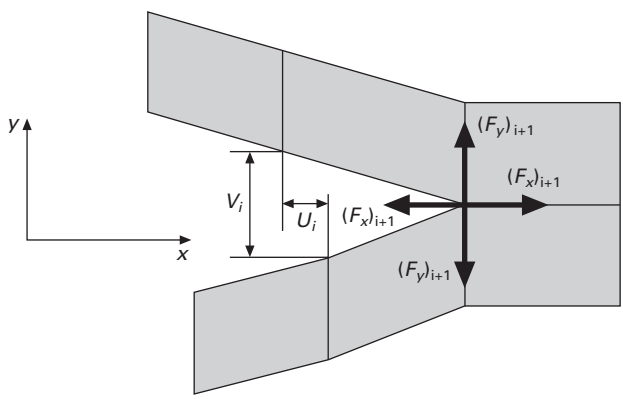
dimensions, the components of the energy release rate can be determined as:

$$\mathcal{G}_{\mathrm{I}} = \frac{1}{2b \cdot \Delta a} F_x \cdot \Delta u$$
$$\mathcal{G}_{\mathrm{II}} = \frac{1}{2b \cdot \Delta a} F_y \cdot \Delta v \qquad [13.9]$$

where $b$ is the width, $\Delta a$ is the increment in crack length between two successive runs, $F_x$ and $F_y$ are the nodal force components at an intact node, and $\Delta u$ and $\Delta v$ are the nodal displacement components in the second run after the nodes are released. Alternatively, based on the modified VCCT illustrated in Fig. 13.13, good estimates can be obtained by using the tractions at the bonded node and the separations at the first debonded nodes of the same solution, provided the mesh is sufficiently small. The VCCT may easily be extended to three dimensions and has been a popular approach because of its ease of use and ability to partition the SERR into the various modes (Krueger, 2002).

### 13.8.2 *J*-integral method

The *J*-integral (Rice, 1968) offers a path-independent fracture parameter that can be used for inelastic fracture problems and simplifies to the energy release rate, $\mathcal{G}$, for linear elastic fracture mechanics. This method is easily implemented in finite element analysis by computing the value of $J$ around several closed paths available by the mesh discretization, as illustrated in Figure 13.14, using:




*13.13* Illustration of nodal forces and displacements used with modified VCCT.

© Woodhead Publishing Limited, 2010

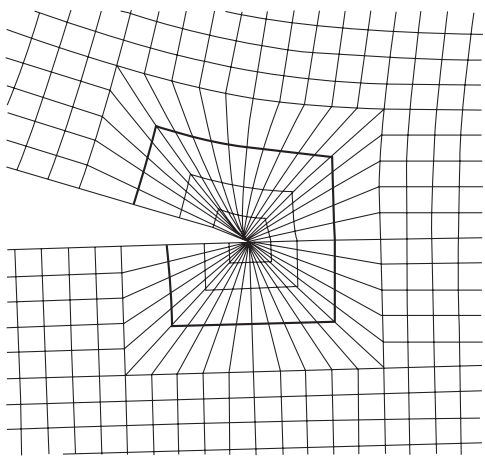
$$J = \int_{\Gamma} \left( W \cdot \mathrm{d}y - \mathbf{T} \cdot \frac{\partial \mathbf{u}}{\partial x} \mathrm{d}s \right) \qquad [13.10]$$

where $W$ is the strain energy density, $\mathbf{T} = \mathbf{n} \cdot \boldsymbol{\sigma}$ is an outward directed traction vector, where $\mathbf{n}$ is a unit normal vector to the contour and $\boldsymbol{\sigma}$ is the stress tensor, and d$s$ is a counterclockwise increment around the contour $\Gamma$.

### 13.8.3 Cohesive zone models

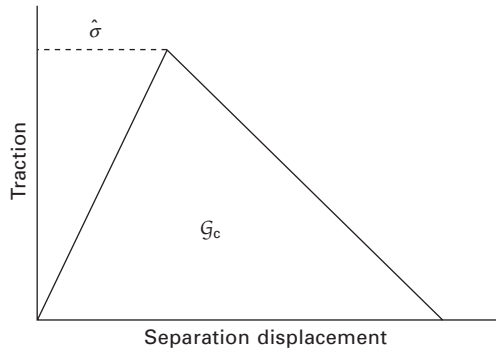
Traditionally, the strength and fracture mechanics approaches to characterizing materials have been quite separate approaches, using very different formulations to address two different understandings of the mechanisms of failure, resulting in the distinct envelopes shown in Fig. 13.1 Proponents of each method have argued their cases, but have been forced to deal with complications. For strength advocates, the singular stress fields present at crack tips and bimaterial corners present many problems. Designers using this approach, focused on continuous media, often ignore the idea of flaws or cracks and this can lead to unanticipated failures. When promoting fracture mechanics with the exclusion of strength criteria, proponents of this approach often assume that a well-defined crack exists, regardless of how physically tenuous this may be, especially in seemingly well-made components. Engineering designers are often less familiar with this approach and are forced to assume the existence of a flaw in order to conduct an analysis.

The relationship between fracture and strength criteria can be seen in the pioneering work of Dugdale (Dugdale, 1960) and Barenblatt (Barenblatt, 1962), in which they included a yielded zone at the tip of a crack to eliminate



*13.14* Illustration of a deformed mesh, showing a potential contour about which the *J*-integral can be evaluated.

© Woodhead Publishing Limited, 2010




*13.15* Illustration of a traction plotted against separation distance description for use with CZM.

the stress singularity. Extending this approach more recently (Tvergaard and Hutchinson, 1993, 1996; Xu and Needleman, 1994), the cohesive zone model (CZM) offers to bridge this chasm. By invoking a strength criterion and an energy dissipation criterion, this method allows both aspects of failure to be included in a single model. Instead of considering a single fracture parameter, the fracture energy, this approach adds a cohesive strength, $\hat{\sigma}$, as well. To implement the procedure, traction separation laws, such as shown in Fig. 13.15 are invoked numerically.

CZMs have been used in many applications including finite element analysis of fracture in concrete, a computational model of polymer decohesion in a double cantilever beam (DCB) specimen, mixed mode interfacial fracture of bimaterial systems and mode I and mode II crack propagation of adhesively bonded beam-type specimens (Yang *et al*., 1999, 2001; Yang and Thouless, 2001). This method is becoming increasingly popular (Kafkalidis and Thouless, 2002; Georgiou *et al*., 2003; Yang *et al*., 2004; De Moura *et al*., 2008a and b; de Moura, 2008) and, when implemented with special elements, can result in cracks or debonds initiating where no flaw exists and propagation in realistic directions (Goyal *et al*., 2004a and b). The CZM approach is gaining in popularity in that it combines aspects of both strength- and fracture-based approaches, including initiation as well as propagation of debonds. Continued work is needed to simplify the design process and allow extension to a range of debonding rates (time dependent to impact conditions), environments and loading modes.

## 13.9 Future trends

Failure of adhesive bonds involving structural adhesives still occurs, suggesting the need for improved understanding of materials, the bonding process and the design of joints. The 2006 ceiling collapse of a tunnel in Boston's Big

© Woodhead Publishing Limited, 2010

Dig project underscores the increasingly crucial role that adhesives play in modern engineering components and structures, along with the potentially devastating consequences when failure occurs. Undergraduate engineering curricula, at least in the United States, typically offer many students little exposure to engineering polymers or adhesives and the special nature of these time-, temperature- and environmental-dependent materials. Fracture mechanics, as a design tool, also often receives minimal attention. Clearly, as engineering plastics and polymeric adhesives find increasing applicability in lightweight transportation vehicles, in corrosion-resistant or reinforced infrastructure, and in microelectronic and biomedical devices, more exposure of students to these materials and appropriate design methodologies are needed. In some materials, such as fiber-reinforced plastic composites, the reinforcing fibers limit crack growth, resulting in extensive damage zones that are less appropriate for fracture mechanics treatments. On the other hand, adhesively bonded components can often fail by propagation of a crack-like debond growing between the adherends. Such configurations are often well suited to fracture mechanics analyses. Clearly, more educational opportunities should be provided.

On a technical level, fracture mechanics will continue to be used to characterize adhesives and adhesion, but further improvements are needed. Several challenges remain in the experimental characterization of fracture properties of bonded joints. The effect of mode mixity on measured fracture energy is still poorly understood, especially in practical engineering adhesives. Whereas mode I toughness is critical in monolithic materials and in some adhesives, these results may not always be conservative. Additional information is needed to ensure conservative designs. The effect of impact loading is important, especially stick–slip behavior, which can result when viscoelastic deformation can blunt slowly moving cracks, increasing the energy required for propagation. Environmental exposure can still be quite detrimental to some adhesively bonded joints and incorporating these effects into structural analysis remain complex for both strength and fracture-based design approaches. Finally, although the CZM approach offers potential to apply fracture mechanics design criteria to bonded components that may not initially contain flaws, challenges remain in extending this technique to routine engineering design methodology.

## 13.10 Conclusions

Fracture mechanics offers a powerful tool for characterizing failure of both monolithic materials and bonded systems. Based on the concept that all real material systems contain (or may develop) flaws that can significantly alter the resulting stress state, fracture mechanics has proven uniquely appropriate for characterizing the structural integrity of a wide array of materials and

© Woodhead Publishing Limited, 2010

structures. Fracture mechanics has been applied to adhesive joints with good success in characterizing the critical and subcritical debonding of structural adhesives used in the aerospace, construction, automotive, microelectronic, biomedical and other fields. Fracture test methods differ from those used for strength-based specimens in that sharp-tipped debonds are intentionally introduced. The propagation of these debonds under quasi-static, creep, impact and fatigue loading conditions may be studied to determine material properties that are useful in selecting appropriate adhesive systems and ultimately in the design of bonded joints.

## 13.11 References


Adams, R. D. and Harris, J. A. (1987). 'The influence of local geometry on the strength of adhesive joints'. *International Journal of Adhesion and Adhesives*, **7**(2), 69–80.

Adams, R. D. and Peppiatt, N. A. (1974). 'Stress analysis of adhesively bonded lap joints'. *Journal of Strain Analysis for Engineering Design*, **9**, 185–96.

Adams, R. D. and Peppiatt, N. A. (1977). 'Stress analysis of adhesive bonded tubular lap joints'. *Journal of Adhesion*, **9**, 1–18.

Adams, R. D., Comyn, J. and Wake, W. C. (1997). *Structural Adhesive Joints in Engineering*, Chapman and Hall, London.

Anderson, G. P. (1988). Personal communication.

Anderson, T. L. (1995). *Fracture Mechanics*, *Fundamentals and Applications*, CRC Press, Boca Raton.

Anderson, G. P., Bennett, S. J. and DeVries, K. L. (1977). *Analysis and Testing of Adhesive Bonds*, Academic Press, New York.

ASTM-D3433-99 (2001). 'Standard test method for fracture strength in cleavage of adhesives in bonded metal joints'. *Annual Book of ASTM Standards*. ASTM, West Conshohocken **15.06**, 225–31.

Barenblatt, G. I. (1962). 'The mathematical theory of equilibrium cracks in brittle fracture'. *Advances in Applied Mechanics*, **7**, 55–129.

Bitner, J. L., Rushford, J. L., Rose, W. S., Hunston, D. L. and Riew, C. K. (1981). 'Viscoelastic fracture of structural adhesives'. *Journal of Adhesion*, **13**(1), 3–28.

Bittencourt, T. N., Wawrzynek, P. A., Ingraffea, A. R. and Sousa, J. L. (1996). 'Quasi-automatic simulation of crack propagation for 2D LEFM problems'. *Engineering Fracture Mechanics*, **55**(2), 321–34.

Blackman, B. R. K. and Kinloch, A. J. (2001). 'Fracture tests for structural adhesive joints'. in *Fracture Mechanics Testing Methods for Polymers*, *Adhesives and Composites*. A. Pavan, D. R. Moore and J. G. Williams (eds). Elsevier, Amsterdam, 225–67.

Blackman, B., Dear, J. P., Kinloch, A. J. and Osiyemi, S. (1991). 'The calculation of adhesive fracture energies from double-cantilever beam test specimens'. *Journal of Materials Science Letters*, **10**(5), 253–6.

Blackman, B. R. K., Kinloch, A. J., Paraschi, M. and Teo, W. S. (2003). 'Measuring the mode I adhesive fracture energy, G(IC), of structural adhesive joints: the results of an international round-robin'. *International Journal of Adhesion and Adhesives*, **23**(4), 293–305.

Broek, D. (1978). *Elementary Engineering Fracture Mechanics*. Sijthoff & Noordhoff, Alphen aan den Rijn.


© Woodhead Publishing Limited, 2010

Carter, B. J., Wawrzynek, P. A. and Ingraffea, A. R. (2000). 'Automated 3-D crack growth simulation'. *International Journal for Numerical Methods in Engineering*, **47**(1–3), 229–53.

Chai, H. (1986). 'A note on crack trajectory in an elastic strip bounded by rigid substrates'. *International Journal of Fracture*, **32**(3), 211–13.

Chai, H. (1992). 'Experimental evaluation of mixed-mode fracture in adhesive bonds'. *Experimental Mechanics*, **32**(4), 296–303.

Charalambides, M., Kinloch, A. J. Wang, Y. and Williams, J. G. (1992). 'On the analysis of mixed-mode failure'. *International Journal of Fracture*, **54**(3), 269–91.

Chen, B. and Dillard, D. A. (2001a). 'The effect of the T-stress on crack path selection in adhesively bonded joints'. *International Journal of Adhesion and Adhesives*, **21**(5), 357–68.

Chen, B. and Dillard, D. A. (2001b). 'Numerical analysis of directionally unstable crack propagation in adhesively bonded joints'. *International Journal of Solids and Structures*, **38**(38–39), 6907–24.

Chen, B. and Dillard, D. A. (2002). *Crack Path Selection in Adhesively Bonded Joints*. D. A. Dillard and A. V. Pocius (eds), Adhesion Science and Engineering - I: The Mechanics of Adhesion. Elsevier Science, Amsterdam.

Chen, C. S., Wawrzynek, P. A. and Ingraffea, A. R. (1997). 'A methodology for fatigue crack growth and residual strength prediction with applications to aircraft fuselages'. *Computational Mechanics*, **19**(6), 527–32.

Chen, B., Dillard, D. A., Dillard, J. G. and Clark, R. L. (2001a). 'Crack path selection in adhesively-bonded joints: The role of material properties'. *Journal of Adhesion*, **75**(4), 405–34.

Chen, C. S., Krause, R., Pettit, R. G., Banks-Sills, L. and Ingraffea, A. R. (2001b). 'Numerical assessment of T-stress computation using a p-version finite element method'. *International Journal of Fracture*, **107**(2), 177–99.

Chen, B., Dillard, D. A., Dillard, J. G. and Clark, R. L. (2002). 'Crack path selection in adhesively bonded joints, the roles of external loads and specimen geometry'. *International Journal of Fracture*, **114**(2), 167–90.

Choupani, N. (2008). 'Mixed-mode cohesive fracture of adhesive joints: Experimental and numerical studies'. *Engineering Fracture Mechanics*, **75**(15), 4363–82.

Cognard, J. (1987). 'Quantitative measurement of the energy of fracture of an adhesive joint using the wedge-test'. *Journal of Adhesion*, **22**(2), 97–108.

Comyn, J. (1983). 'Kinetics and mechanism of environmental attack'. in *Durability of Structural Adhesives*, A. J. Kinloch (ed.). Applied Science Publishers, London.

Cotterell, B. and Rice, J. R. (1980). 'Slightly curved or kinked cracks'. *International Journal of Fracture*, **16**, 155–69.

Davidson, B. D. and Schapery, R. A. (1990). 'A technique for predicting mode-i energy-release rates using a 1st-order shear deformable plate-theory'. *Engineering Fracture Mechanics*, **36**(1), 157–65.

De Moura, M. F. S. F. (2008). 'Progressive damage modelling'. *Modeling of Adhesively Bonded Joints*. L. da Silva and A. Oschner (eds), Springer, 155–82.

De Moura, M., Campilho, R. and Goncalves, J. P. M. (2008a). 'Crack equivalent concept applied to the fracture characterization of bonded joints under pure mode I loading'. *Composites Science and Technology*, **68**(10–11), 2224–30.

De Moura, M., Goncalves, J. P. M., Chousal, J. A. G. and Campilho, R. (2008b). 'Cohesive and continuum mixed-mode damage models applied to the simulation of the mechanical behaviour of bonded joints'. *International Journal of Adhesion and Adhesives*, **28**(8), 419–26.

© Woodhead Publishing Limited, 2010

Dillard, D. A. (1988). 'Stresses between adherends with different curvatures'. *Journal of Adhesion*, **26**(1), 59–69.

Dillard, D. A., Hinkley, J. A., Johnson, W. S. and Clair, T. L. S. (1994). 'Spiral tunneling cracks induced by environmental-stress cracking in LARC(tm)-TPI adhesives'. *Journal of Adhesion*, **44**(1–2), 51–67.

Dillard, D., Parvatareddy, H. and Clifton, A. P. (1995). 'Environmental stress cracking in high performance adhesives and composites'. *Antec 95 – the Plastics Challenger, a Revolution in Education, Conference Proceedings, Vols I-Iii – Vol I, Processing; Vol Ii, Materials; Vol Iii, Special Areas*, 3971–5.

Dillard, D. A., Singh, H. K., Park, S., Ohanehi, D. and McGaw, M. A. (2006). *A Dual-actuator Load Frame for Mixed-mode Fracture of Laminated or Adhesively Bonded Specimens*, Society for Experimental Mechanics, St. Louis.

Dillard, D. A., Singh, H. K., Pohlit, D. J. and Starbuck, J. M. (2009). 'Observations on reduced fracture toughness for mixed-mode fracture testing of adhesively bonded joint'. *Journal of Adhesion Science and Technology*, **23**, 1515–30.

Dugdale, D. S. (1960). 'Yielding in steel sheets containing slits'. *Journal of the Mechanics and Physics of Solids*, **8**, 100–4.

Erdogan, F. and Ozturk, M. (2008). 'On the singularities in fracture and contact mechanics'. *Journal of Applied Mechanics–Transactions of the ASME*, **75**(5), 051111–23.

Erdogan, V. F. and Sih, G. C. (1963). 'On crack extension in plates under plane loading and transverse shear'. *Transactions of the ASME Journal of Basic Engineering*, **85**, 519–27.

Fernlund, G. and Spelt, J. K. (1994a). 'Mixed-mode energy-release rates for adhesively bonded beam specimens'. *Journal of Composites Technology & Research*, **16**(3), 234–43.

Fernlund, G. and Spelt, J. K. (1994b). 'Mixed-mode fracture characterization of adhesive joints'. *Composites Science and Technology*, **50**(4), 441–9.

Ferry, J. D. (1980). *Viscoelastic Properties of Polymers*, New York, Wiley.

Gent, A. N. (1974). 'Fracture mechanics of adhesive bonds'. *Rubber Chemistry and Technology*, **47**, 202–12.

Gent, A. N. and Kinloch, A. J. (1971). 'Adhesion of viscoelastic materials to rigid substrates. III. Energy criterion for failure'. *Journal of Polymer Science, Polymer Physics Edition*, **9**(4), 659–68.

Georgiou, I., Hadavinia, H., Ivankovic, A., Kinloch, A. J., Tropsa, V. and Williams, J. G. (2003). 'Cohesive zone models and the plastically deforming peel test'. *Journal of Adhesion*, **79**(3), 239–65.

Gledhill, R. A., Kinloch, A. J. and Shaw, S. J. (1980). 'A model for predicting joint durability'. *Journal of Adhesion*, **11**(1), 3–15.

Gleich, D. M., Van Tooren, M. J. L. and Beukers, A. (2001). 'A stress singularity approach to failure initiation in a bonded joint with varying bondline thickness'. *Journal of Adhesion Science and Technology*, **15**(10), 1247–59.

Goglio, L., Rossetto, M. and Dragoni, E. (2008). 'Design of adhesive joints based on peak elastic stresses'. *International Journal of Adhesion and Adhesives*, **28**(8), 427–35.

Goldstein, R. V. and Salganik, R. L. (1974). 'Brittle fracture of solids with arbitrary cracks'. *International Journal of Fracture*, **10**(4), 507–27.

Goyal, V. K., Jaunky, N. R., Johnson, E. R. and Ambur, D. R. (2004a). 'Intralaminar and interlaminar progressive failure analyses of composite panels with circular cutouts'. *Composite Structures*, **64**(1), 91–105.

Goyal, V. K., Johnson, E. R. and Davila, C. G. (2004b). 'Irreversible constitutive law for

© Woodhead Publishing Limited, 2010

modeling the delamination process using interfacial surface discontinuities'. *Composite Structures*, **65**(3–4), 289–305.

Griffith, A. A. (1921). 'The phenomena of rupture and flow in solids'. *Philosophical Transactions of the Royal Society*, **A221**, 163–98.

Hadavinia, H., Kinloch, A. J., Little, M. S. G. and Taylor, A. C. (2003). 'The prediction of crack growth in bonded joints under cyclic-fatigue loading II. Analytical and finite element studies'. *International Journal of Adhesion and Adhesives*, **23**(6), 463–71.

Hashemi, S., Kinloch, A. J. and Williams, J. G. (1989). 'Corrections needed in double-cantilever beam tests for assessing the interlaminar failure of fibre-composites'. *Journal of Materials Science Letters*, **8**(2), 125–9.

Hattori, T., Sakata, S. and Murakami, G. (1989). 'A stress singularity parameter approach for evaluating the interfacial reliability of plastic encapsulated LSI devices'. *Journal of Electronic Packaging*, **111**, 243–8.

Ingraffea, A. R. and Wawrzynek, P. A. (1995). 'FRANC2D: A case study in transfer of software technology'. *Research Transformed into Practice*, *Implementations of NSF Research*. J. Colville and A. Amde, (eds). New York, ASCE Press, 233–44.

Irwin, G. R. (1958). *Handbuch der Physik*. S. Flügge (ed.), Springer-Verlag, Berlin-Heidelberg, Volume 6, 551–90.

James, M. A. and Swenson, D. (1998). *A Software Framework for two-Dimensional Mixed Mode I/II Elastic-Plastic Fracture*, Symposium on Mixed-Mode Crack Behavior, Atlanta, Ga.

James, M. and Swenson, D. (1999). *FRANC2D/L: A Crack Propagation simulator for Plane Layered Structures*, Kansas State University, Manhattan, KS.

Johnson, W. S. and Butkus, L. M. (1998). 'Considering environmental conditions in the design of bonded structures: A fracture mechanics approach'. *Fatigue & Fracture of Engineering Materials & Structures*, **21**(4), 465–78.

Johnson, K. L., Kendall, K. and Roberts, A. D. (1971). 'Surface energy and the contact of elastic solids'. *Proceedings Royal Society London A*, **324**, 301–13.

Kafkalidis, M. S. and Thouless, M. D. (2002). 'The effects of geometry and material properties on the fracture of single lap-shear joints'. *International Journal of Solids and Structures*, **39**(17), 4367–83.

Kim, K. S. and Kim, J. (1988). 'Elasto-plastic analysis of the peel test for thin-film adhesion'. *Journal of Engineering Materials and Technology–Transactions of the ASME*, **110**(3), 266–73.

Kinloch, A. J. (1987). *Adhesion and Adhesives*, *Science and Technology*, Chapman and Hall, London.

Kinloch, A. J. and Osiyemi, S. O. (1993). 'Predicting the fatigue life of adhesively-bonded joints'. *Journal of Adhesion*, **43**(1–2), 79–90.

Kinloch, A. J. and Williams, J. G. (2002). 'The mechanics of peel tests'. *The Mechanics of Adhesion*. D. A. Dillard and A. V. Pocius (eds). Elsevier, Amsterdam Volume 1, 273–302.

Krueger, R. (2004). *The Virtual Crack Closure Technique, History, Approach and Applications*, Applied Mechanics Review, **57**(2), 109–4.

Lai, Y. H. and Dillard, D. A. (1994). 'A study of the fracture efficiency parameter of blister tests for films and coatings'. *Journal of Adhesion Science and Technology*, **8**(6), 663–78.

Lai, Y. H. and Dillard, D. A. (1997). 'Using the fracture efficiency to compare adhesion tests'. *International Journal of Solids and Structures*, **34**(4), 509–25.

Lake, G. J. and Thomas, A. G. (1967). 'The strength of highly elastic materials'.

© Woodhead Publishing Limited, 2010

*Proceedings of the Royal Society of London. Series A. Mathematical and Physical Sciences*, **300**(1460), 108–19.

Lefebvre, D. R. and Dillard, D. A. (1999). 'A stress singularity approach for the prediction of fatigue crack initiation in adhesive bonds. Part 1: Theory'. *Journal of Adhesion*, **70**(1–2), 119–38.

Lefebvre, D. R., Takahashi, K. M., Muller, A. J. and Raju, V. R. (1991). 'Degradation of epoxy coatings in humid environments – the critical relative humidity for adhesion loss'. *Journal of Adhesion Science and Technology*, **5**(3), 201–27.

Lefebvre, D. R., Dillard, D. A. and Dillard, J. G. (1999). 'A stress singularity approach for the prediction of fatigue crack initiation in adhesive bonds. Part 2: Experimental'. *Journal of Adhesion*, **70**(1–2), 139–54.

Lefebvre, D. R., Ahn, B. K., Dillard, D. A. and Dillard, J. G. (2002). 'The effect of surface treatments on interfacial fatigue crack initiation in aluminum/epoxy bonds'. *International Journal of Fracture*, **114**(2), 191–202.

Liechti, K. M. (2002). 'Fracture mechanics and singularities in bonded systems'. in *Adhesion Science and Engineering I*, *The Mechanics of Adhesion*, D. A. Dillard and A. V. Pocius (eds), Elsevier, 45–76.

Liechti, K. M. and Chai, Y. S. (1992). 'Asymmetric shielding in interfacial fracture under inplane shear'. *Journal of Applied Mechanics–Transactions of the ASME*, **59**(2), 295–304.

Miner, M. A. (1945). 'Cumulative damage in fatigue'. *Journal of Applied Mechanics*, **12**, A159–A164.

Moidu, A. K., Sinclair, A. N. and Spelt, J. K. (1998). 'On the determination of fracture energy using the peel test'. *Journal of Testing and Evaluation*, **26**(3), 247–54.

Palaniswamy, K. and Knauss, W. G. (1978). 'On the problem of crack extension in brittle solids under general loading'. *Mechanics Today*, **4**, 87–148.

Papini, M. and Spelt, J. K. (2002). 'The mechanics of coatings'. *The Mechanics of Adhesion*, D. A. Dillard and A. V. Pocius (eds), Elsevier, Amsterdam, Volume 1, 303–50.

Paris, P. C., Gomez, M. P. and Anderson, W. E. (1961). 'A rational analytic theory of fatigue'. *The Trend in Engineering*, **13**, 9–14.

Park, S. and Dillard, D. A. (2007). 'Development of a simple mixed-mode fracture test and the resulting fracture energy envelope for an adhesive bond'. *International Journal of Fracture*, **148**(3), 261–71.

Parvatareddy, H. and Dillard, D. A. (1999). 'Effect of mode-mixity on the fracture toughness of Ti-6Al-4V/FM-5 adhesive joints'. *International Journal of Fracture*, **96**(3), 215–28.

Parvatareddy, H., Dillard, J. G., McGrath, J. E. and Dillard, D. A. (1998). 'Environmental aging of the Ti-6Al-4V/FM-5 polyimide adhesive bonded system: implications of physical and chemical aging on durability'. *Journal of Adhesion Science and Technology*, **12**(6), 615–37.

Parvatareddy, H., Dillard, J. G., McGrath, J. E. and Dillard, D. A. (1999). 'Solvent effects on high temperature polyimides and their bonded joints'. *Journal of Adhesion*, **69**(1–2), 83–98.

Petroski, H. (1985). *To Engineer is Human*, *The Role of Failure in Successful Design*. St. Martin's Press, New York.

Pohlit, D. J., Dillard, D. A., Jacob, G. C. and Starbuck, J. M. (2008). 'Evaluating the rate-dependent fracture toughness of an automotive adhesive'. *Journal of Adhesion*, **84**(2), 143–63.

Rakestraw, M. D., Taylor, M. W., Dillard, D. A. and Chang, T. (1995). 'Time dependent

© Woodhead Publishing Limited, 2010

crack growth and loading rate effects on interfacial and cohesive fracture of adhesive joints'. *Journal of Adhesion*, **55**(1–2), 123–49.

Reeder, J. R. and Crews, J. H. (1990). 'Mixed-mode bending method for delamination testing'. *AIAA Journal*, **28**(7), 1270–6.

Reeder, J. R. and Crews, J. H. (1992). 'Redesign of the mixed-mode bending delamination test to reduce nonlinear effects'. *Journal of Composites Technology & Research*, **14**(1), 12–19.

Reedy, E. D. (1990). 'Intensity of the stress singularity at the interface corner between a bonded elastic and rigid layer'. *Engineering Fracture Mechanics*, **36**(4), 575–83.

Reedy, E. D. (2002). 'Strength of butt and sharp-cornered joints'. *Adhesion Science and Engineering - I, The Mechanics of Adhesion*. D. A. Dillard and A. V. Pocius, (eds). Elsevier Science, Amsterdam, 145–92.

Reedy, E. D. and Guess, T. R. (1995). 'Butt-joint tensile-strength – interface corner stress intensity factor prediction'. *Journal of Adhesion Science and Technology*, **9**(2), 237–51.

Reedy, E. D. and Guess, T. R. (2001). 'Rigid square inclusion embedded within an epoxy disk, asymptotic stress analysis'. *International Journal of Solids and Structures*, **38**(8), 1281–93.

Rice, J. R. (1968). 'A path independent integral and the approximate analysis of strain concentrations by notches and cracks'. *Journal of Applied Mechanics*, **35**, 379–86.

Rice, J. R. (1988). 'Elastic fracture-mechanics concepts for interfacial cracks'. *Journal of Applied Mechanics–Transactions of the ASME*, **55**(1), 98–103.

Rose, J. L. (1999). *Ultrasonic Waves in Solid Media*. Cambridge University Press, Cambridge.

Rose, J. L. (2002). 'Ultrasonic inspection of adhesive bonds'. *The Mechanics of Adhesion*. D. A. Dillard and A. V. Pocius (eds). Amsterdam, Elsevier, 699–724.

Russel, A. J. and Street, K. N. (1985). 'Moisture and temperature effects on the mixed mond delamination fracture of unidirectional graphite/epoxy'. in *STP 876 Delamination and Debonding of Materials*, W. S. Johnson (ed.), ASTM, Philadelphia, 349–70.

Rybicki, E. F. and Kanninen, M. F. (1977). 'A finite element calculation of stress intensity factors by a modified crack closure integral'. *Engineering Fracture Mechanics*, **9**, 931–8.

Seely, F. B. and Smith, J. O. (1952). *Advanced Mechanics of Materials*, John Wiley & Sons, New York.

Sheng, J. K. and Chernenkoff, R. A. (1996). SAE *International Congress and Exposition*, Detroit, MI, SAE Technical Paper Series 960575.

Shephard, N. (1995). *Measuring and Predicting Sealant Adhesion. Materials Engineering Science*, PhD Thesis, Virginia Tech, Blacksburg.

Simón , J. C., Johnson, E. and Dillard, D. A. (2005). 'Characterizing dynamic fracture behavior of adhesive joints under quasi-static and impact loading'. *Journal of ASTM International*, **2**, 53–71.

Singh, H. K., Park, S., Ohanehi, D. and Dillard D. A. (2006). 'A design space for a novel dual-actuator mixed-mode test frame'. *The 29th Annual Meeting of the Adhesion Society*, February 19–22, Jacksonville, FL, The Adhesion Society.

Singh, H. K., Chakraborty, A., Frazier, C. E. and Dillard, D. A. (2008). 'Mixed mode fracture testing of adhesively-bonded wood specimens using a dual actuator load frame'. *31st Annual Meeting of the Adhesion Society*, Austin, TX, The Adhesion Society.

© Woodhead Publishing Limited, 2010

Singh, H. K., Chakraborty, A., Frazier, C. and Dillard, D. A. (in press). 'Mixed mode fracture testing of adhesively-bonded wood using a novel dual actuator load frame'.

Struik, L. C. E. (1978). *Physical Aging in Amorphous Polymers and Other Materials*. Elsevier Scientific, New York, NY and Amsterdam.

Suo, Z. G. and Hutchinson, J. W. (1990). 'Interface crack between two elastic layers'. *International Journal of Fracture*, **43**(1), 1–18.

Tan, K. T., White, C. C., Hunston, D. L., Clerici, C., Steffens, K. L., Goldman, J. and Vogt, B. D. (2008). 'Fundamentals of adhesion failure for a model adhesive (PMMA/glass) joint in humid environments'. *Journal of Adhesion*, **84**(4), 339–67.

Taylor, M. W. and Dillard, D. A. (1994). 'Simple 2-dimensional and 3-dimensional finite elements for modelling the adhesive in bonded joints and crack-patching configurations'. *Adhesion Society – Proceedings of the Seventeenth Annual Meeting and the Symposium on Particle Adhesion*, Orlando, Florida, 168–70.

Thouless, M. D. and Yang, Q. D. (2002). 'Measurement and analysis of the fracture properties of adhesive joints'. *The Mechanics of Adhesion*, D. A. Dillard and A. V. Pocius (eds). Elsevier, Amsterdam, Volume 1, 235–72.

Timoshenko, S. P. (1953). *History of Strength of Materials*, McGraw-Hill, New York.

Towse, A., Potter, K. D., Wisnom, M. R. and Adams, R. D. (1999). 'The sensitivity of a Weibull failure criterion to singularity strength and local geometry variations'. *International Journal of Adhesion and Adhesives*, **19**(1), 71–82.

Tvergaard, V. and Hutchinson, J. W. (1993). 'The influence of plasticity on mixed-mode interface toughness'. *Journal of the Mechanics and Physics of Solids*, **41**(6), 1119–35.

Tvergaard, V. and Hutchinson, J. W. (1996). 'On the toughness of ductile adhesive joints'. *Journal of the Mechanics and Physics of Solids*, **44**(5), 789–800.

Van Tooren, M. J. L., Gleich, D. M. and Beukers, A. (2004). 'Experimental verification of a stress singularity model to predict the effect of bondline thickness on joint strength'. *Journal of Adhesion Science and Technology*, **18**(4), 395–412.

Volkersen, O. (1938). 'Die Nietkraft Verteilung in zugbeanspruchten Nietverbindungen mit konstanten Laschenquerschnitten'. *Luftfahrtforschung*, **15**, 41–7.

Vrana, M. A., Dillard, J. G., Ward, T. C., Rakestraw, M. D. and Dillard, D. A. (1995). 'The influence of curing agent content on the mechanical and adhesive properties of dicyandiamide cured epoxy systems'. *Journal of Adhesion*, **55**(1–2), 31–42.

Wahab, M. M. A., Ashcroft, I. A. and Crocombe, A. D. (2004). 'A comparison of failure prediction methods for an adhesively bonded composite beam'. *Journal of Strain Analysis for Engineering Design*, **39**(2), 173–85.

Williams, J. G. (1984). *Fracture Mechanics of Polymers*, Ellis Horwood, Chichester.

Williams, J. G. (1988). 'On the calculation of energy-release rates for cracked laminates'. *International Journal of Fracture*, **36**(2), 101–19.

Xu, S. Y. and Dillard, D. A. (2003). 'Determining the impact resistance of electrically conductive adhesives using a falling wedge test'. *IEEE Transactions on Components and Packaging Technologies*, **26**(3), 554–62.

Xu, X. P. and Needleman, A. (1994). 'Numerical Simulations of Fast Crack-Growth in Brittle Solids', *Journal of the Mechanics and Physics of Solids*, **42**(9), 1397–434.

Yang, Q. D. and Thouless, M. D. (2001). 'Mixed-mode fracture analyses of plastically-deforming adhesive joints'. *International Journal of Fracture*, **110**(2), 175–87.

Yang, Q. D., Thouless, M. D. and Ward, S. M. (1999). 'Numerical simulations of adhesively-bonded beams failing with extensive plastic deformation'. *Journal of the Mechanics and Physics of Solids*, **47**(6), 1337–53.

© Woodhead Publishing Limited, 2010

Yang, Q. D., Thouless, M. D. and Ward, S. M. (2001). 'Elastic-plastic mode-II fracture of adhesive joints'. *International Journal of Solids and Structures*, **38**(18), 3251–62.

Yang, C. D., Huang, H., Tomblin, J. S. and Sun, W. J. (2004). 'Elastic-plastic model of adhesive-bonded single-lap composite joints'. *Journal of Composite Materials*, **38**(4), 293–309.

Zhang, Z. H., Shang, J. K. and Lawrence, F. V. (1995). 'A backface strain technique for detecting fatigue-crack initiation in adhesive joints'. *Journal of Adhesion*, **49**(1–2), 23–36.

© Woodhead Publishing Limited, 2010

# 14

# Developments in testing adhesive joints

BRUCE DUNCAN, National Physical Laboratory, UK

**Abstract**: This chapter covers the large and varied field of adhesive joint testing and focuses on the applications of joint testing for load-bearing structural applications, including quality control, material/process screening and design (data acquisition and verification) and developments in testing. The emphasis is on factors that affect the accuracy, relevance and reliability of the test data delivered by the joint test. The tests described were generally developed for rigid, structural adhesives, such as epoxies and acrylics, but most can also be applied to flexible adhesives. Case studies demonstrating the use of adhesive joint testing are provided.

**Key words**: design, fracture, quality assurance, shear, specimen preparation, strain measurement, tension.

## 14.1 Introduction

### 14.1.1 Role of testing

Adhesive joint testing is critical for ensuring the reliability of any bonded system or component. Tests are carried out for many different purposes, including materials selection, acquisition of data for design, validation, environmental durability assessment and quality control. Many different test methods are available and it is important that the method used is fit for purpose and can be applied in a repeatable manner. For further information on adhesives and adhesion the reader is encouraged to consult general textbooks, such as Adams, *et al*. (1997), Bikerman (1968) and Kinloch (1987), and numerous industry specific publications, for example Weitzenböck and McGeorge (shipbuilding) (2005), Clarke (composites) (1996), European Space Agency (1990), Construction Industry Research and Information Association (1997) and The Institution of Structural Engineers (1999).

There is an extensive range of test methods available as national and international standards. These are generally those methods with long histories of use that are widely used and accepted in different industries. Key standards published by the International Organisation for Standardization (ISO) and ASTM International are listed at the end of this chapter under sources of further information and advice. However, there are also many national, industry and company specific standards for joint tests. Standard tests may not necessarily be the most accurate tests or the most appropriate tests for many purposes. Most of these tests, like the ubiquitous single lap shear test,



© Woodhead Publishing Limited, 2010

can only be used effectively for qualitative or comparative measurements, for example checking the effectiveness of different surface preparations or ranking strengths of different adhesive systems. Only a few standard test methods, such as the thick adherend shear test, are suitable to generate engineering data in order to design adhesively bonded structures that are subject to loading and environmental effects.

### *Quality assurance*

Quality assurance (QA) testing is undertaken to ensure the reliability of the bonding process. Well-designed quality assurance test protocols should be able to reveal:

- Problems with the process
  - surface cleanliness/contamination
  - consistency of application
  - mixing or curing
- changes in supplied materials (adhesive or adherends)
  - surface properties affecting bonding
  - mechanical strength of the adhesive or adherends.

However, QA tests cannot be relied upon to reveal inadequacies in the design or materials selected for the structure.

Effective QA joint specimens should mimic the bonded system as closely as possible within the economic constraints of manufacturing and testing. Specimens should be prepared in the production environment using the same materials and processes as the bonded system. Often large numbers of test specimens may be needed and for this reason it is quite usual for simple test systems, such as lap shear or T-peel, to be chosen.

QA tests should have well-defined criteria for pass or failure. Sometimes requesting a cohesive mode of failure can be sufficient. Where a strength criterion is required, this should be consistent with the design requirements of the structural joint and take into account the different stress distributions likely to exist in the QA test specimen compared to the actual structure.

### *Process and materials screening*

Screening tests are undertaken in advance of detailed design calculations, to select or eliminate substrates, adhesives, surface treatments and preparation methods. The requirements for process and material screening tests are similar to those for QA tests. The screening test needs to replicate the critical performance requirements of the application. If environmental conditioning is included in the test programme, economic factors will tend to favour test specimens such as the lap shear test, which are quick to prepare and test.

© Woodhead Publishing Limited, 2010

*Design and verification*

Good quality materials property data are required to model accurately the performance of an adhesive joint in design calculations. The amount of validated materials properties data, which are suitable for design calculations, published for adhesives, is extremely low relative to the wide range of adhesives that a design engineer may wish to consider. Therefore, it is most likely that design data will need to be obtained. Generating good quality data is time consuming and expensive. Hence, screening tests should be used to minimise the number of adhesives requiring a full test programme. The most accurate method of measuring design properties, such as modulus, Poisson's ratio and yield/ultimate strengths is generally through bulk specimen tests (e.g. tensile testing as described in ISO 527-4). This is usually straightforward for substrate materials and many adhesives can be cast as bulk specimens. Recommended procedures for the preparation of bulk specimens of adhesives are given in ISO 15166.

Complex materials models that fully describe non-linear plastic behaviour have extensive data requirements, Dean *et al*. (2004). Bulk specimen tests (Dean and Duncan, 1998) that provide a combination of tensile, shear and compression data can be used to determine yield and flow parameters. Joint tests, such as lap shear, butt tension and scarf joint, provide validation of the predicted multi-axial yield functions and help evaluate failure criteria.

It is not always possible or convenient to make representative bulk samples of an adhesive. Joint tests are then the only option for obtaining data. Adhesive joint tests to determine the mechanical properties of the adhesive need to:

- Produce well-controlled stress states in the adhesive layer; the adhesive should sustain a state of stress that is principally tension, shear or compression.
- Take account of adherend effects, in particular minimise or correct for deformation of the adherends.
- Ensure that the adhesive material in the test joint is representative of the material within the actual bond layer.
- Include a means of determining strain within the adhesive layer, which will require suitable extensometry.

Obtaining data suitable for design from joint tests will generally require an approach that combines data from different types of joint. Even for the simplest elastic model, two input constants (Young's modulus and Poisson's ratio) need to be determined. If bulk specimen tests are not possible, the determination of elastic properties will normally require two or more different types of test, most often the thick adherend shear and butt tension tests.

© Woodhead Publishing Limited, 2010

Verification or proof tests, undertaken to test the reliability of structural joint designs, need to replicate design operation condition closely and, therefore, are often considerably more complex to carry out than QA or screening tests. The quantities measured in validation tests need to be meaningful to evaluate the design and may include measurement of:

- failure strength – from the applied load
- joint stiffness – from applied load and measured deflections
- non-linear yielding and hardening curves – from applied force and measured deflections
- locus of failure initiation – from post-failure examination or photography of the joint during testing
- rate of crack growth – from crack opening gauges or video images.

## 14.2 Current and emerging types of testing

Adhesive testing has a long history and traditionally joint testing has emphasised failure load (e.g. ultimate load or continuous peeling load) and mode of failure (degree of adhesive or cohesive failure) as the key parameters. The introduction of modern tough adhesives and the growing use of design stress analyses using finite element (FE) methods has increased the demands for data from joint testing. The growing need to provide quantitative predictions of long-term performance, for example in harsh environments or sustaining long-term static (creep) or cyclical (fatigue) loads, requires accurate and reliable data for model inputs. Measurement of properties of the adhesive like modulus, strain to failure, yield stresses or fracture toughness is increasingly an objective of joint tests. The validation of structural designs or development of new material models for adhesives generates new requirements for test methods and new demands for accuracy.

Accompanying the increased demand for sophisticated joint testing are new measurement technologies, for example non-contact strain mapping and analysis tools that allow the collection of data that were previously impossible to obtain. FE modelling provides a valuable tool for analysing the results of joint tests and, by providing detailed information on stress and strain states within substrates and the bond, is able to improve the interpretation of results. Understanding the stress concentrations within joints enables improved comparison between data generated from different specimen types.

Test results depend on the type of joint test performed and the equipment and procedures used to make the measurements. In addition to the specimen manufacture issues outlined in Section 14.3, test factors such as machine alignment, extensometers, displacement rate and test temperature, discussed in Section 14.4 will affect the results.

© Woodhead Publishing Limited, 2010

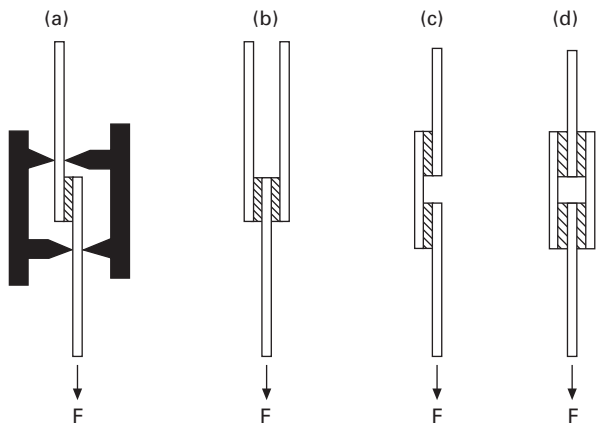
### 14.2.1 Shear tests

Lap shear tests (including single lap, double lap, lap-strap and thick adherend shear tests) are commonly used in adhesive testing. The mean shear stress, $\tau$, in the adhesive layer is the applied load divided by the area of the bonded overlap. Some typical test joints are illustrated in Fig. 14.1. Single lap shear strength (shear stress at failure) is usually quoted on adhesive data sheets. Failure can be defined in different ways, for example, as the yield stress, the point of maximum load, the start of failure (first drop in load) or the point where catastrophic failure occurs, see Fig. 14.2. Safety factors in structures are often based on the yield stress (the departure of the stress–strain curve from linearity) but data sheets often provide strengths based on maximum load.

Although shear strength is commonly quoted, this can be misleading when extrapolating the result to other joint types or structures, as the quantity quoted is a mean shear stress. The actual distribution of stress in shear test joints is multi-axial and non-uniform, varying with position in the bondline, and depends on factors such as the bond layer thickness, adherend thickness, size and shape of fillets, and mechanical properties (stiffness) of the adhesive and adherends. The ends of the bond layer experience significant peel stress components that are normally the cause of failure. The shear stress component peaks at the end of the joint and is comparatively low in the centre.

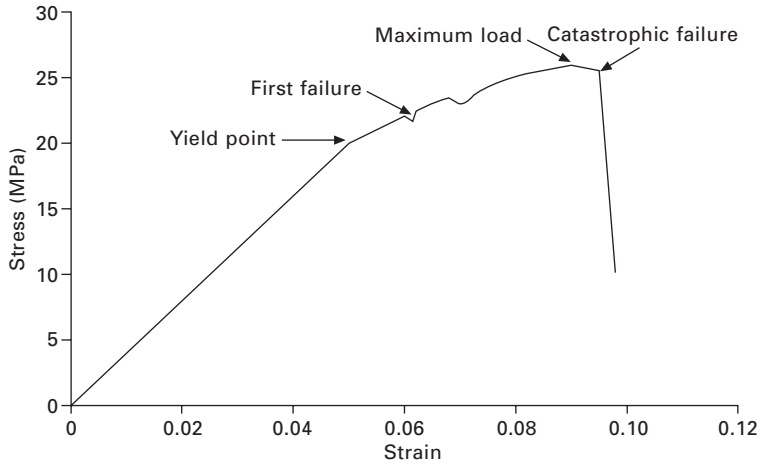
#### *Single lap shear*

The single lap shear test, Fig. 14.1(a) is also known as the thin lap shear test and is the most widely used method of producing data on adhesively bonded




*14.1* Schematic of typical lap joint configurations: (a) single lap shear with extensometers straddling the bondline, (b) double lap, (c) lap strap, (d) double lap strap.

© Woodhead Publishing Limited, 2010




*14.2* Stress–strain curve illustrating potential points of 'failure' during a joint test.

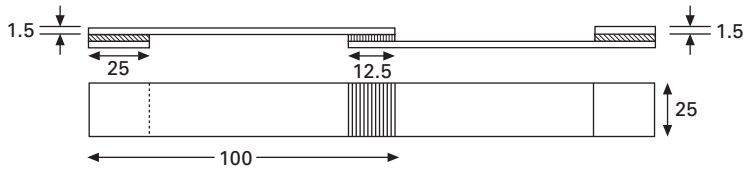
joints. Variants of this test are described in many standards, for example ISO 4587 and ASTM D 1002. Results from these tests carried out to these standards are widely quoted in adhesive data sheets. The simplicity and low costs associated with specimen manufacture, testing and data analysis has contributed to the widespread use of this method of quality assurance and to the assessment of chemical or fatigue resistance. Testing is conducted using standard tension/compression mechanical test equipment with a suitable pair of self-aligning (manual or servo hydraulic wedge-action) grips to hold the specimen.

The single lap test (Fig. 14.3) consists of two rectangular adherends, typically 25 mm wide, 100 mm long and 1.5 to 2.0 mm thick, bonded together, with an overlap length ranging from 12.5 to 25 mm. End tabs, cut from the same material as the adherend sections, are often adhesively bonded to the specimen to reduce (not eliminate) the eccentricity of the load path which causes out-of-plane bending moments and consequently high peel stresses and non-uniform shear stresses in the adhesive layer. The long axis of the specimen coincides with the direction of the applied force through the centre line of the grip assembly.

If the purpose of the test is to assess adhesive properties or bond quality then it is undesirable to exceed the yield point of the adherend in tension. Hence the overlap length should be chosen to ensure adhesive failure occurs before the adherend yields.

The maximum permissible length $L$, which is a function of thickness and stiffness of the adherend, can be estimated:

© Woodhead Publishing Limited, 2010




*14.3* Thin-lap shear specimen with dimensions specified by standards, the end tabs are not specified by standards but reduce out-of-plane bending.

$$L < \frac{\sigma_Y t}{1.5\tau}$$

where $\sigma_Y$ is the yield stress of the adherend, $\tau$ the expected average shear strength of the adhesive and $t$ the adherend thickness.

Results obtained from the single lap joint test have a significant dependence on the mechanical stiffness of the adherends since this influences the peel stress concentrations at the end of the joint. Increasing the modulus or thickness of the adherends will, if failure is cohesive, lead to an increase in the apparent strength of the bond.

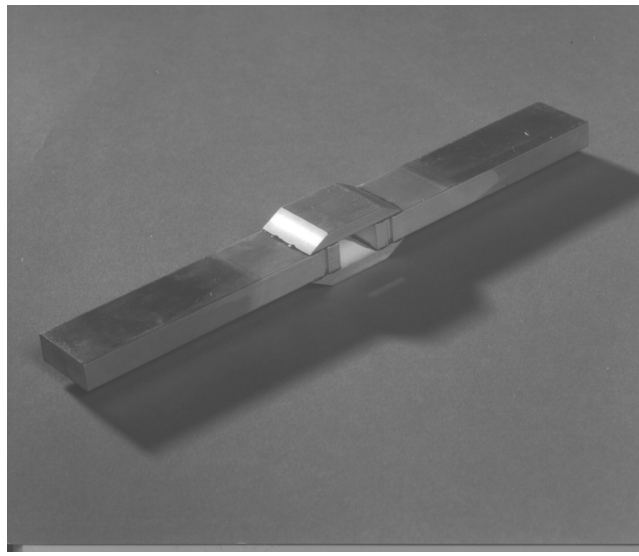
### *Double lap*

Owing to load eccentricity, single lap joint adherends bend during loading and, as the joint is unsymmetrical, the plane of the bond can rotate, introducing large peel stresses at the ends of the adhesive layer. This can lead to premature failure and an underestimate of the shear capacity of the adhesive. The double lap joint, ASTM D 3528 (Fig. 14.1(b)), is symmetrical about the mid-plane of the specimen. Bond rotation, and hence the amount of peel stress, is considerably reduced compared to an equivalent single lap joint made with the same adherends.

### *Lap strap*

Lap strap joints are common in practical applications (such as repairs). The lap strap configuration is used to provide tests results relevant to these applications. They also provide an alternative lap shear configuration to generate data. Although the single lap strap joint (Fig. 14.1(c)) will suffer from peel, the double lap strap joint (Fig. 14.1(d)) provides a reasonably uniform shear stress within the bond layer. Using thick straps with tapered ends can further reduce peel stresses. The double lap strap joint with tapered straps, Fig. 14.4, is an alternative to the thick adherend shear test for measuring mechanical properties for design purposes. Shear displacements

© Woodhead Publishing Limited, 2010



*14.4* Double-lap strap joint with tapered adherends that reduce stress concentrations at the end of the bondlines. The adherends are notched to provide improved location points for knife-edged extensometers.

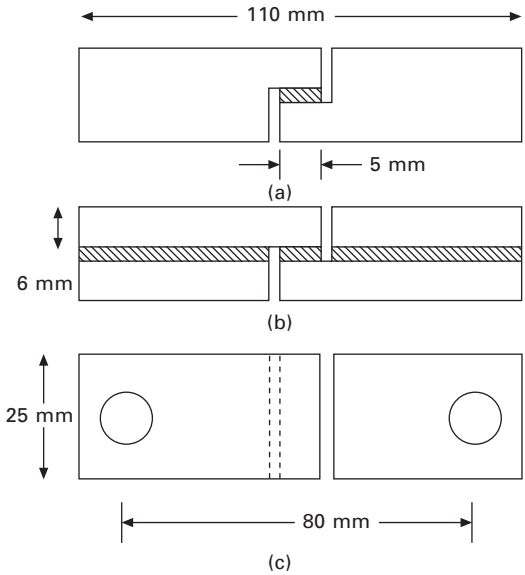
can be determined using general-purpose extensometers that bridge the gap between the central adherends.

### *Thick adherend shear*

Thick-adherend shear tests (TAST), ISO 11003-2 and ASTM D 5656, are common joint-specimen tests used to measure material properties (shear modulus and shear strength). The thick adherends reduce the peel stress and produce more uniform shear stress and strain distributions in the adhesive than are generated in the single lap shear test.

ISO and ASTM standards specify different sample geometries so care should be taken when comparing results produced using different standards. ISO 11003-2 specifies a specimen with an overall length of 110 mm, a width of 25 mm and overlap length of 5 mm. The ISO standard recommends an adherend thickness of 6 mm and a bondline thickness of 0.5 mm. Samples can be made either using single piece adherends pre-cut to shape and bonded (Fig. 14.5(a)) or by cutting and slotting from bonded plates (Fig. 14.5(b)). Pre-cut adherends are preferred as they are more rigid, leading to lower peel stresses. Slots should be 1.5 mm wide. Load is introduced to the specimen via two 12.7 mm diameter bolt holes with centres 80 mm apart (Fig. 14.5(c)), although grips can also be used. Holes should be accurately drilled in the

© Woodhead Publishing Limited, 2010



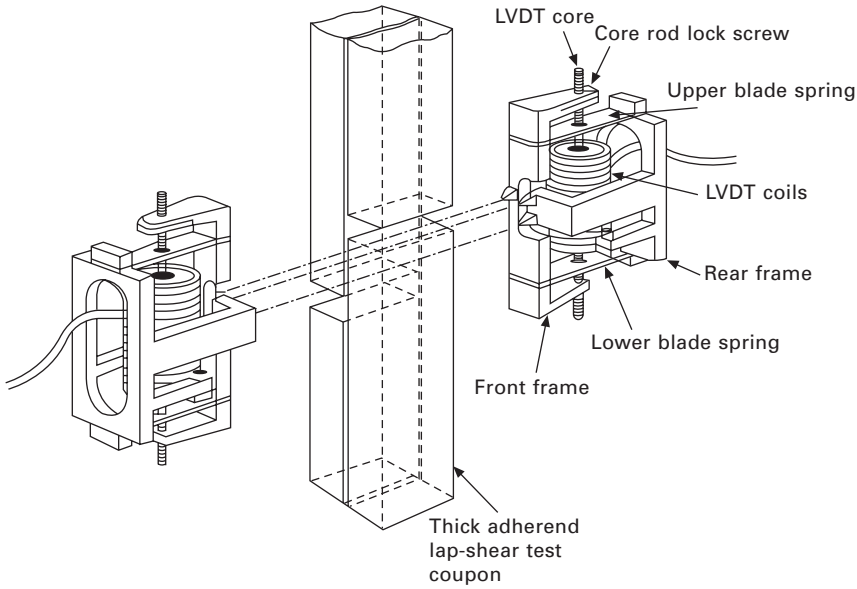

*14.5* Thick adherend shear test specimen (a) made with pre-shaped adherends (b) cut from bonded plates (c) top view showing loading pin locations.

centre of each adherend, since small misalignments can result in unwanted rotation and uneven loading of the joint, thus compromising the test data.

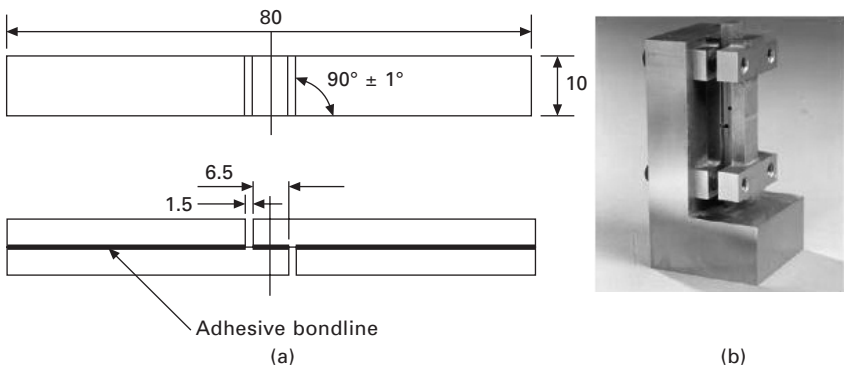
The relative displacement of the adherends is best measured using a pair of purpose-built transducers as described in ASTM D 5656, such as those developed by Althoff and Brockmann (1976) and Krieger (1975), making contact at three location points straddling the bondline on each edge of the specimen, see Fig. 14.6. Knife-edged extensometers straddling the bond or non-contact strain measurement techniques (e.g. video extensometry) can also be used. For the highest accuracy, the results should be corrected for the effects of adherend displacement, for example by using FE analysis. The use of a dummy, shaped metal test piece to generate corrections should be avoided because, since the stress distributions are very different, the results lead to errors. Corrections will be small owing to the high stiffness of the adherends.

A modified version of the thick adherend shear test using a smaller joint specimen loaded in compression offers the combination of good quality results with high throughput. The specimen and test fixture are shown in Fig. 14.7. Although pre-shaped adherends can be used, for ease of manufacturing it is usual for specimens to be machined from bonded sheets. Although the thickness of the plates is not fixed, a practical minimum is around 2.5 mm.

© Woodhead Publishing Limited, 2010




*14.6* Thick-adherend shear test specimen using contact extensometers.



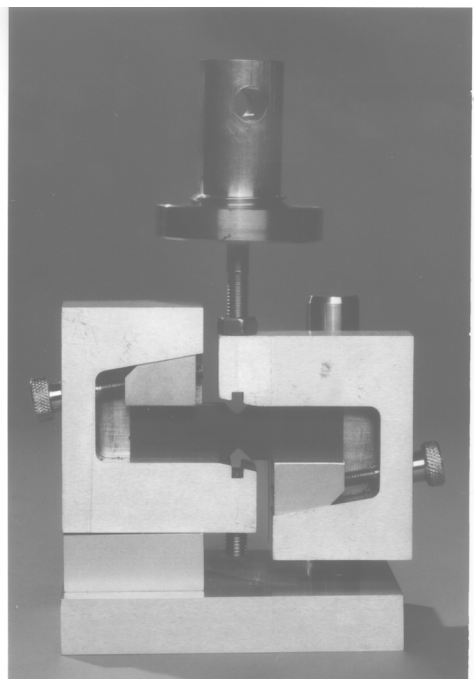

*14.7* Miniature TAST specimen tested in compression: (a) specimen geometry, (b) loading fixture which prevents buckling.

The test fixture crosspieces restrain buckling. The fixture is placed between the parallel platens of a test machine and compressed. The test provides shear strength data that are comparable with the results obtained from the full size TAST. Displacement transducers that straddle the platens can monitor platen movement and these measurements, corrected for adherend strain, can be used to determine shear strain in the adhesive layer.

© Woodhead Publishing Limited, 2010

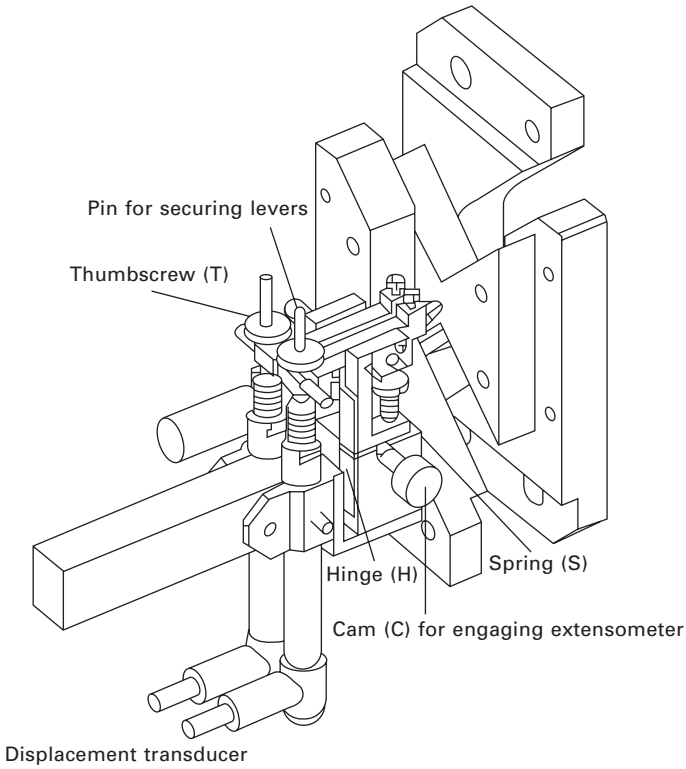
*Alternative shear tests*

Tests designed for bulk materials, illustrated in Figs. 14.8 and 14.9, such as the notched beam (Iosipescu, 1967, ASTM D 5379) and notched plate (Arcan *et al.*, 1978; Weissberg and Arcan, 1988) can be adapted for adhesive testing by using shaped adherends. The adherends are bonded so that the bondline forms the centre of the sample and deforms in shear when loads are introduced to the adherends via test fixtures. Tests will provide modulus, yield curve and strength data. Shear stress is calculated from the applied force divided by bonded areas. The peak stresses at the end of the bondline can be reduced by machining blunt radiuses at both the adherend ends and the adhesive fillet. Shear strain can be determined by measuring the relative displacements of reference points on either side of the bond (e.g. by using a contacting extensometer such as shown in Fig. 14.9) and dividing the difference by the bond thickness. Ideally the reference points should be as close to the bondline as possible to minimise the contribution of the adherend deformation relative to the adhesive deformation. Some contribution is inevitable and corrections can be made using either simple elastic analyses or through FE calculations. Out-of-plane bending or twisting, which can lead



*14.8* V-notched beam (from Iosipescu, 1967) shear test specimen and test fixture.

© Woodhead Publishing Limited, 2010

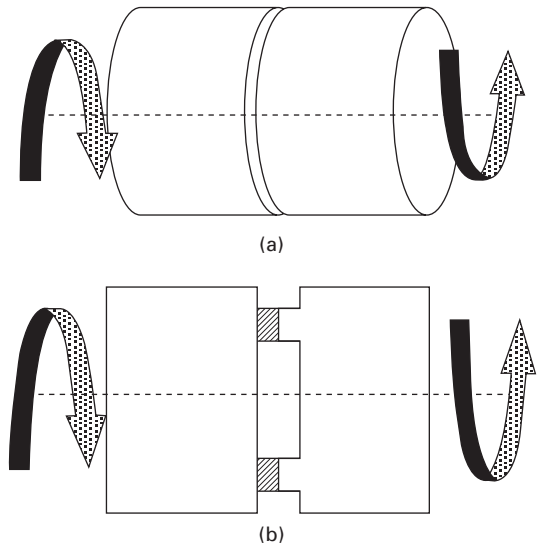



*14.9* Arcan specimen, test fixture and extensometer.

to premature failure, should be minimised through the use of thick adherends and appropriate test machine fixtures.

The torsion of a cylindrical rod or napkin ring (ISO 11003-1), Fig. 14.10, is an alternative method of measuring shear properties (modulus and yield curves). Tests are performed with one end of the specimen fixed and a rotational load applied to the opposite end (using either a rotary motor or via a lever). Napkin ring samples are preferred as the stress state in the adhesive is relatively uniform and straightforward to analyse. The torsion method has an advantage over other shear tests as it produces very low peel stresses within the adhesive with the result that premature failure arising from peel stress is much less likely. Large shear strains to failure can be achieved and tests have shown that even relatively brittle adhesives (such as early generation epoxies) can be tested to beyond their yield points. However, torsion tests are rarely performed as test equipment is rare in laboratories in comparison to tensile test equipment.

© Woodhead Publishing Limited, 2010




*14.10* Torsion tests: (a) cylindrical rod, (b) napkin ring.

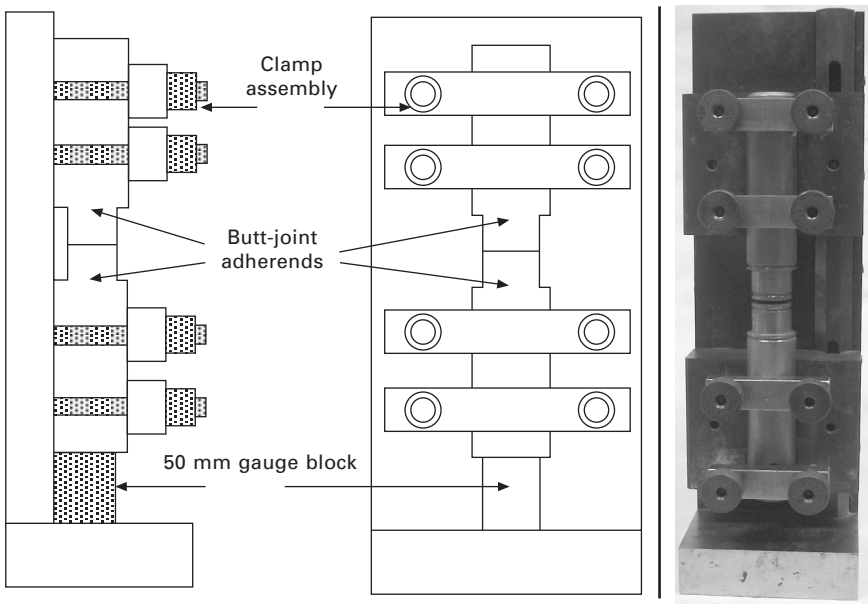
## 14.2.2 Tension and peel tests

*Butt tension*

Butt tension tests were originally used to assess the tensile strength of bonds but following improvements in analysis methods (e.g. Adams *et al.*, 1978; Oschner *et al.*, 2007) have been used to evaluate the elastic and plastic yield properties of adhesives to provide modulus, yield curve and strength data. Although conceptually simple, the butt joint test (ISO 6922, ASTM D 2095) is difficult to perform repeatably and accurately. As the adhesive layer is very thin in relation to the length of the adherends, the axial direction of the loading path is critical. Careful alignment of the sample during manufacture and testing is vital to avoid cleavage loads that cause premature fracture.

Sample alignment can be controlled during sample preparation by using precisely machined V-blocks, see Figure 14.11. The bond layer thickness is set by using gauge blocks to position the adherends precisely with respect to each other before they are clamped. The adherends are pressed together with the end being a gauge block of the desired thickness placed between the lower adherend and the end stop. The top adherend is then clamped. The lower adherend and gauge block are removed and adhesive applied to the adherend. This is replaced in the mould and positioned against the end stop, leaving a gap equal to the thickness of the gauge block which sets the bondline. The alignment of the test machine can be checked using dummy specimens (strain gauged metal rods). Any misalignments can be corrected using adjustable mounting plates, which can be obtained

© Woodhead Publishing Limited, 2010



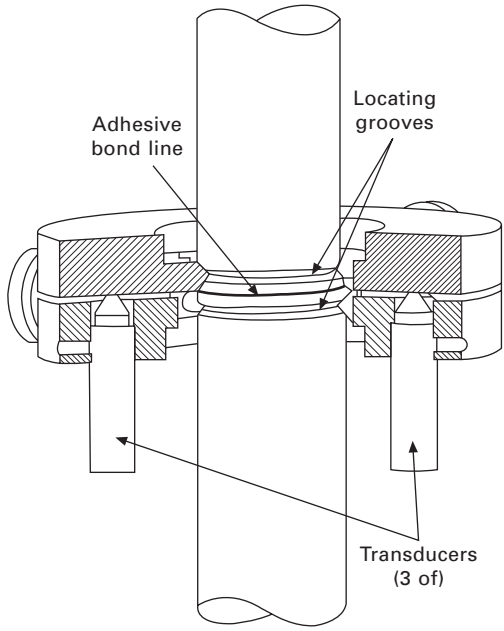

*14.11* Bonding fixture to control alignment of butt-joint specimens made by bonding rods.

commercially from test equipment suppliers, until all the gauges on different locations on the circumference of the specimen read a uniform level of strain when loaded.

Purpose-built extensometers provide the best means of measuring extensions and monitoring bending. The extensometer shown in Fig. 14.12 uses three displacement transducers, which are spaced equally at 120° intervals around the circumference of the sample. The extensometer is clamped to both adherends. The transducers measure the changes in separation of the adherends and the readings are averaged to determine the extension of the bond. These displacement transducers detect the onset of cleavage in the sample through divergence of the measured extensions. Circumferential grooves, carefully machined very close to the ends of the adherends, act as locaters for the extensometers. By positioning the extensometer close to the bondline, the correction for extension of the adherends included in the measurement is minimised.

The stress state in the butt joint test is relatively uniform in the centre of the specimen, a combination of normal stress, from the applied tensile extension, and radial stresses, generated by the rigid adherends constraining the Poisson's contraction. Shear stresses are extremely low. Peaks in stress appear at the rim of the adhesive layer. The specimen can be modified to reduce these stress concentrations, for example by profiling the edges by

© Woodhead Publishing Limited, 2010




*14.12* Extensometer system for accurate measurement of bondline extension in a butt-joint test.

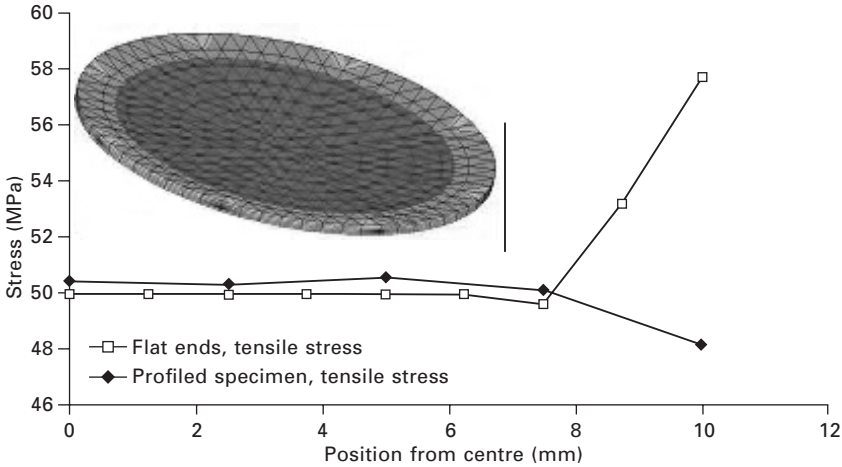
rounding the rim edge. Altering the shape of the adherend bonding surface can also improve the uniformity of the stress distribution to simplify the interpretation of the results. FE analyses (Fig. 14.13) suggest that when the butted adherend ends were profiled as interlocking concave and convex hemispheres with 50 mm radii of curvature, producing a bowl-shaped adhesive layer with a constant adhesive bond thickness, the region of highest stress extends from the centre of the specimen over the majority of the adhesive layer. The stress values near the rim are lower. The highest stress predicted in the FE analysis is only a few percent greater than the average stress (calculated from the force divided by the bonded area).

Oschner *et al*. (2007) have developed techniques for interpreting butt joint test results which provide full elastic constants. The technique requires simultaneous measurement of tensile extension and transverse contractions of the adhesive layer during tests, as is common for bulk specimen tests. Numeric analysis is carried out on the results to determine the Young's modulus and Poisson's ratio.

### *Scarf joint*

Scarf joints are overlap joints where the angle ($\theta$) between the axis of the adhesive layer and the axis of the adherends (of equal width and thickness) is

© Woodhead Publishing Limited, 2010




*14.13* Effect of profiling the adherends on the tensile stress distribution within the adhesive layer.

greater than 0° (butt joint) and less than 90°, see Fig. 14.14. This test method requires the use of relatively thick adherends, 10 mm being the practical minimum. Through varying the scarf angle the ratio of normal stresses to shear stresses within the bondline can be controlled. This control over stress ratios provides an extremely useful tool for exploring yield and failure criteria in adhesives and can be used to validate constitutive models.

A mechanical analysis approach presented by Clarke (1996) can be used to determine shear stress $\tau$ and normal stress $\sigma_T$ in a simple scarf joint. The analysis predicts a shear stress in the adhesive layer given by:

$$\tau = P \sin\theta \cos\theta / t$$

and a normal stress in the adhesive given by:

$$\sigma_T = P \cos^2\theta / t$$

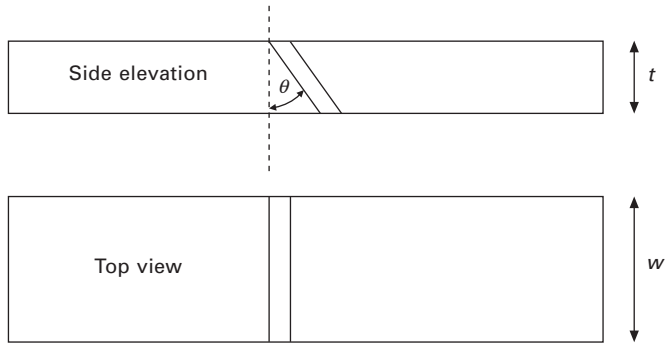
where $P$ is the applied (end) load per unit width, $t$ is the adherend thickness and $\theta$ is the taper angle. The ratio of shear stress to normal stress is given by:

$$\tau/\sigma_T = \tan\theta$$

Ideally, for the strongest joints the scarf angle should be as large as possible.

FE analyses have shown that scarf joints produce relatively uniform stress distributions in the interior of the joint. If the sharp corners of the adherends are profiled (rounded) appropriately it is possible to reduce the peaks in stresses associated with the edges of the bondline significantly.

© Woodhead Publishing Limited, 2010




*14.14* Scarf joint.

Samples are manufactured from pretapered adherends, for example bars that have been cut or spark eroded at the desired angle. These are positioned and aligned using slotted jigs. Bondline thickness can be set using a process similar to that described for butt joints. Samples are tested in tension with loads introduced either via wedge action grips or pins. The bond extension is measured using clip on extensometers that straddle the bondline.

### *Peel tests*

Peel tests are used to assess bond quality since the predominant stress, as the name suggests, is peel or tension. Thus, they are extremely useful in assessing the effects of process (e.g. surface treatment) or service (environmental exposure) on the strength of the adhesive adherend interface. Peel testing requires at least one flexible adherend. The term 'flexible' refers to the ability of the adherend to bend through 90° without breaking or cracking. The result quoted for peel tests is the constant load per unit width required to continue peeling the joint after initiation, determined from the flat portion of the force–extension curve. The maximum load, corresponding to the initiation of failure, is sometimes used, as it can be sensitive to environmental degradation.

The main differences between the methods are the angles of peel and whether the peel angle remains constant during the test. Research, such as that performed by Crocombe and Adams (1981b, 1982) and Sargeant (1998), has shown that much of the energy is dissipated in the adherends rather than the adhesive and therefore accurate data for the elastic–plastic mechanical properties of both the adhesive and the adherends are important in the analysis of the test data. Peel tests, while providing useful comparative data, are unlikely to provide quantitative measures of interface strength. There is no guarantee that the fracture path will be along the interface. Stress distributions depend significantly on local geometrical features such as crack

© Woodhead Publishing Limited, 2010

sharpness and peel angle. The conversion between peel load per unit area to stress requires assumptions about the extent of the peel zone that are likely to be inaccurate.

The T-peel test has been adopted by most standards bodies (e.g. ISO 11339, ASTM D 1876) and is widely used to evaluate surface treatments and the environmental durability of adhesively bonded systems. Specimens (Fig. 14.15(a)) are typically 25 mm wide, have a minimum bonded length of 150 mm and 50 mm long arms. The recommended thickness is 0.5 mm for steel and 0.7 mm for aluminium, although to test the strongest adhesives it may be necessary to use thicker adherends to minimise bending and avoid failure of the specimen arms. The external radius of the sample and the length of the adhesive fillet affect the result, particularly the load at which failure initiates. The fillet size can be controlled using a special tool shaped to fit within the bonded joint. Adhesive layer thickness is not specified in standards but should be controlled to ensure repeatability. A miniature T-peel specimen with a short bonded length takes up less space in an environmental conditioning system and is often used to assess environmental performance in screening programmes, see Fig. 14.15(b).

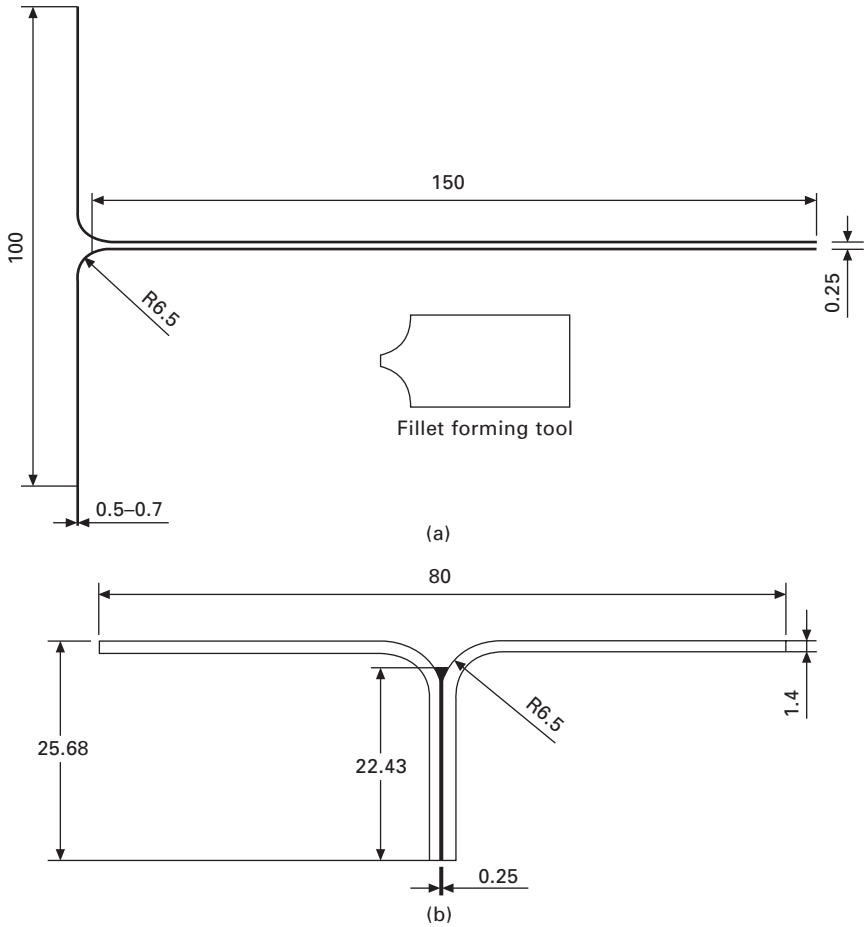
There are several peel tests for assessing the bonding of a flexible adherend to a rigid adherend. The 180° peel test (ISO 8510-2, ASTM D 903) requires one flexible adherend to be sufficiently flexible to be bent back through 180° before being stripped from a more rigid adherend at a constant peel rate. This test is favoured for non-structural adhesives, for example pressure sensitive adhesives and tapes. The floating roller test method (ISO 14676, ISO 4578, ASTM D 3167) enables a constant angle of peel to be maintained throughout the test and can be adjusted to vary the peel angle. The climbing drum peel test (ASTM D 1781), used in the aerospace industry to determine the bonding of flexible skins to rigid sandwich structures, also ensures that the flexible skin is peeled from the rigid structure at a constant peel angle.

### *Cleavage and fracture*

Fracture mechanics tests provide information on the growth of a fracture within a material and have been extensively applied to polymers and adhesives (e.g. Kinloch and Young, 1983; Moore *et al.*, 2001; Williams *et al.*, 2003). The quantities determined through fracture mechanics tests are the critical stress intensity factor ($K_c$) and the critical strain energy release rate ($G_c$). The stress intensity factor is related to the geometry of the test specimen and crack tip. $G_c$ is a material property.

The common fracture test methods for adhesives are based on the double-cantilevered beam (mode I) and end notch flexure (mode II) tests. Mode I (crack opening) tests impose severe cleavage stresses on bonded joints; some common test specimens are illustrated in Fig. 14.16. Fracture tests require

© Woodhead Publishing Limited, 2010

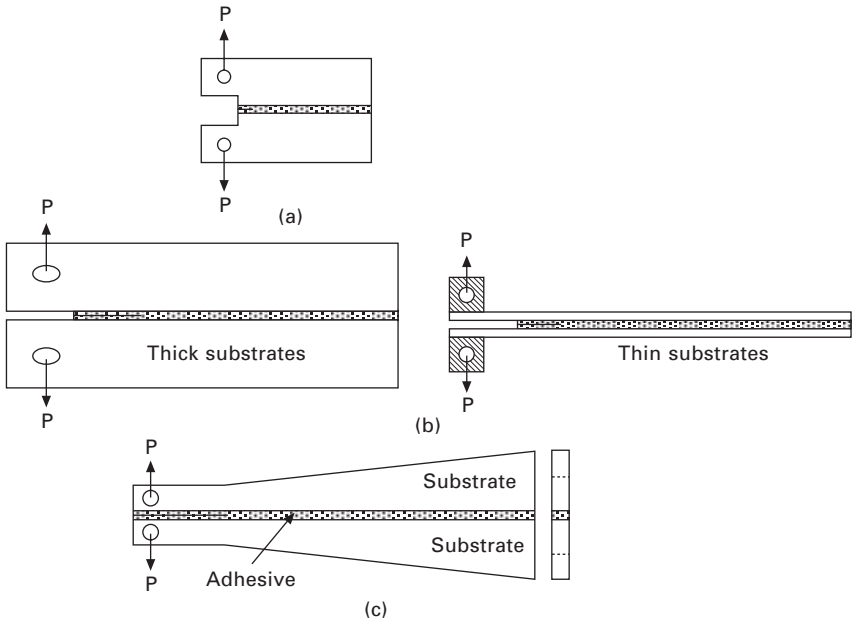



*14.15* (a) Standard T-peel specimen and tool to control fillet form, (b) miniature T-peel used in creep rupture testing.

an initial notch or pre-crack and the precise geometry of this notch will influence the results and is a source of uncertainty (variability) in the tests. Results from the initial part of the test are normally excluded from analyses with $G$ determined from the regions of steady state crack growth. Fracture toughness is recognised as an important adhesive property, contributing to mechanical and impact performance.

The wedge cleavage test (ISO 10354, ASTM D 3762), commonly referred to as the Boeing wedge test, uses the introduction of a wedge between two flat surfaces to force the adherends apart and impose cleavage stresses in the region of the crack tip, which are driven by the elastic stored energy in the adherends. Crack length is monitored with time, often using ruled scales attached to the adherends. The stressed specimen can be exposed to hostile

© Woodhead Publishing Limited, 2010




*14.16* Cleavage and fracture tests; (a) compact tension, (b) double cantilevered beam, (c) tapered double cantilevered beam.

environments and the presence of chemicals at the crack tip can be expected to accelerate degradation. Commonly a crack growth limit is reached within several days making this test attractive as a simple and reliable method for rapidly assessing durability.

Fracture energies, $G$, can be determined from the crack length, $a$, wedge displacement, $w$, adherend modulus, $E$, and adherend thickness, $h$:

$$G = \frac{Ew^2h^3}{16}\left[\frac{3(a+0.6h)^2+h^2}{(a+0.6h)^3+ah^2}\right]$$

This test is not considered particularly accurate for fracture toughness measurements as the driving force depends on the wedge insertion distance and the stiffness of the adherends. The accuracy of the fracture energy can be compromised by plastic deformation of the adherends (reducing cleavage forces) and of the adhesive. Although specimens can be manufactured with the initial crack at the interface there is no certainty that the crack will continue to run along the interface. FEA suggests that the regions of maximum strain and stress in the specimen, prior to crack propagation, are close to the interface.

Compact tension test samples (ASTM D 1062) are manufactured by bonding shaped adherends with the same geometry as the solid compact

© Woodhead Publishing Limited, 2010

tension specimen, Fig. 14.16(a). Specimens are 25 mm wide, with a 25 mm long bondline. The depth of adherend is typically 12 mm at either side of the bondline. The specimen is loaded at one end of the bond producing a cleavage force. The test is run at a constant loading rate or crosshead speed until the joint has completely failed. The maximum load is recorded.

The double-cantilevered beam (DCB) test described in ASTM D 3433, Fig. 14.16(b), is used to measure the initiation and propagation energy of a mode I crack. The critical strain energy release rate ($G_{IC}$) depends on crack length and is calculated using:

$$G_{IC} = \frac{4P^2(3a^2 + h^2)}{Eb^2h^3}$$

where $P$ is the applied load, $E$ is the Young's modulus of the adherend, $b$ is the specimen width, $a$ is the crack length and $h$ is the adherend thickness. Specimen preparation is straightforward. Thick adherend parts can be bonded and tested directly. Where the beams are formed from thin sheet material, end tabs need to be attached to allow the beams to be gripped. The dependence of specimen compliance and strain energy release on crack length adds to the complexity of carrying out and analysing this test.

The specimen compliance in the tapered double-cantilevered beam (TDCB) test described in ASTM D3433, Fig. 14.16(c), is independent of crack length. Compliance, $C$, is directly related to load, $P$, width, $b$, adherend modulus, $E$, and bending moment, $m$. $G_{IC}$, proportional to the rate of change of compliance with cracklength, $a$, is given by:

$$G_{IC} = \frac{4P^2}{Eb^2} m$$

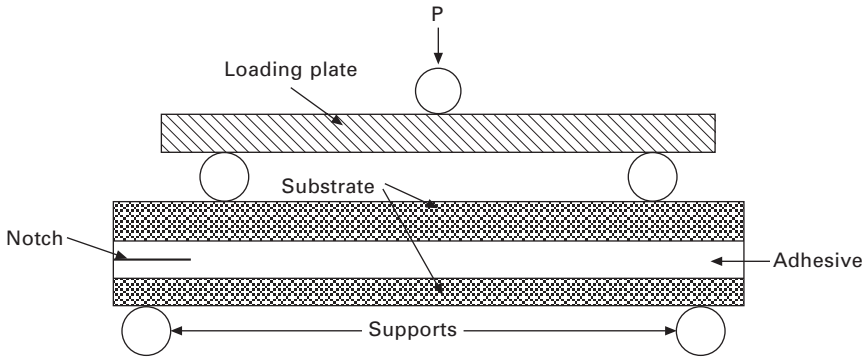
The taper height is chosen such that $m$ is constant with crack length $a$ from the relationship:

$$m = \frac{3a^2}{h^3} + \frac{1}{h}$$

Mode II tests for adhesives are limited. Tests based on a bonded version of the end notch flexure specimen, a composites test method (ASTM D 6671), have been used with limited effect to determine in-plane (shear) fracture toughness. The specimen is essentially the double-cantilevered beam specimen loaded in three- or four-point flexure, see Fig. 14.17. For small displacements (and negligible transverse shear deformation), strain energy release is calculated using:

$$G_{IIC} = \frac{9P^2a^2}{16Eb^2h^3}$$

© Woodhead Publishing Limited, 2010




*14.17* Schematic of the four-point end notch flexure test for mode II fracture toughness.

### 14.2.3 Compression tests

Compressive stresses are usually seen as desirable within structural joints since designs normally seek to reduce the risk of failure initiating from tensile stresses within the adhesive. However, adhesive joints may experience stress states with considerable components of compressive stress. No standard tests exist to measure the compressive properties of adhesives and design calculations cannot be easily verified. A normal assumption is that the compressive modulus is equal in magnitude to the tensile modulus and that behaviour can be modelled using the tensile modulus and Poisson's ratio is normally a reasonable assumption within the elastic limit. However, little is known about behaviour beyond the (unknown) elastic limit. Uniaxial compression properties can be measured using bulk specimen tests, for example ISO 604. However, the stress state lacks the constraints occurring within joints and there is a risk that buckling of the sample could be interpreted as yield.

In theory, test specimens such as butt or scarf could be tested in compression with the free lengths of the adherends reduced so that "stub" specimens can be tested between parallel platens without buckling. Comparison of results with FE predictions would help establish which material models are most appropriate for such stress states.

## 14.3 Specimen manufacture issues

Ultimately, the relevance and reliability of the test data provided through joint testing can be affected by many factors such as the type of test employed, care and attention to detail paid whilst fabricating specimens, the suitability of the testing equipment employed and the means employed to analyse the results. A number of factors, often not included in written standards, can

© Woodhead Publishing Limited, 2010

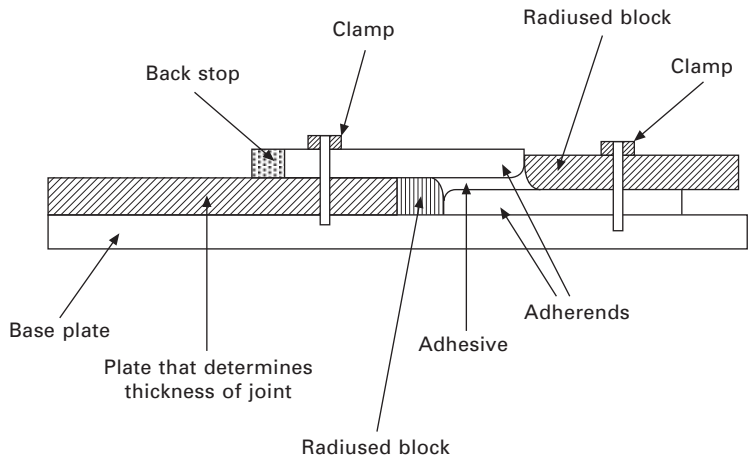
significantly affect the reliability (i.e. repeatability and reproducibility) of data obtained from testing adhesive joints:

- specimen manufacture and alignment
- surface treatments
- sample curing and residual stress
- specimen dimensions (including adherend size, bond thickness and bond areas)
- end effects (edge shape/profile and end fillets).

### 14.3.1 Alignment and jigging during fabrication

To ensure reproducibility of results when conducting tests, the alignment and positioning of the adherends need to be controlled when manufacturing joints. It is normally best to use a bonding fixture to ensure correct bond length (in the case of lap joints), accurate alignment and uniform bondline thickness. To reduce stress and increase the 'apparent' shear strength of single lap joint compared with square-ended bondlines, a fillet or spew can be formed at the overlap ends. Further increases in strength may be achieved by rounding the ends of the adherends. A fixture for making such samples is shown in Fig. 14.18.

An alternative approach is to bond large test panels and cut specimens from these plates, for example a plate 180 mm wide will be capable of providing 6 single lap joint specimens. However, mechanical damage caused by machining or clamping (i.e. adherend bending) is a potential problem. Also, it is more difficult to ensure that the adhesive fully fills the overlap than when making single specimens.




*14.18* Preparation fixture for controlling fillet during specimen manufacture, profiled adherends with rounded edges are shown.

© Woodhead Publishing Limited, 2010

The clamping force applied by the fixture to the specimen should be checked during the curing process to ensure that clamping force remains constant and has not relaxed through adhesive flow. Mould release agent or thin polytetrafluorene (PTFE) film may need to be used to guarantee easy release of bonded components from the clamping fixture. There should be no transfer of release agent into the adhesive layer or onto the bonded surfaces.

The mixing and dispensing of the adhesive onto the bonding surfaces can also affect the results. If a multi-part adhesive requires mixing, this needs to be done consistently when preparing samples. Sufficient adhesive should be dispensed to fill the joint fully and form consistent fillets, but excess adhesive should be avoided as this makes joints difficult to close and creates the problem of cleaning the excess. Application should be done carefully to prevent the inclusion of voids within the bond layer.

### 14.3.2 Surface preparation

Surface preparation is a critical step in the adhesive bonding. Correct surface preparation is essential for good joint strength and maintaining long-term structural integrity of bonded joints. Unsatisfactory surface preparation will result in the bond failing adhesively and unpredictably at the adhesive/adherend interface (adhesive failure). Surface preparation is covered comprehensively in many text books and therefore is not covered in detail in this chapter. Adherend surfaces, unless specified otherwise, should be prepared according to standards, such as ISO 17212 and ISO 2818. Checks should always be made to ensure that there is no mechanical damage caused by machining or handling before bonding.

The preparation and the stability of the treatment needs to be considered when devising test plans, as samples may be manufactured over a period of time and it is important that the adherends do not undergo physical or chemical changes whilst being stored or handled. For example, moisture can alter the chemistry of both the surface and substrate of the adherend, thus compromising the performance of bonded joints. Before and after machining, adherends sensitive to environmental attack or hygroscopic in nature should be stored in sealed containers to prevent moisture ingress and contamination. This is particularly important for moisture absorbing materials such as composites, since release of absorbed moisture during hot curing can significantly degrade the strength of the joint.

### 14.3.3 Curing

The curing temperature is important as the thermal history of the adhesive affects its properties. Curing conditions should be controlled so that the

© Woodhead Publishing Limited, 2010

adhesive in each specimen under test experiences the same thermal history, which is consistent with the conditions experienced in the actual component. Adjustments to cure cycles may be needed to control temperatures in systems that have different masses or thermal conductivity. For example, in a typical cure process using a preheated oven, joints that have a large mass will heat up more slowly than low mass joints and as a consequence the highest temperature reached by the adhesive in the large joint may be far lower than the adhesive in the smaller joint. Exothermic cure reactions may have a significant impact on the thermal history. Generally, a large mass of adhesive and/or a joint with poor thermal conductivity will experience a greater rise in temperature than one with a small adhesive mass and/or high thermal conductivity. In extreme cases the temperature can rise sufficiently to lead to thermal degradation of the adhesive or adherend. When defining cure samples it is often useful to embed thermocouples in the bonds to determine the actual temperatures experienced by the adhesive.

Many adhesives cure under ambient conditions, often taking a considerable period of time to reach full cure and their optimum properties. This can be inconvenient for testing, particularly when monitoring production. For many of these adhesives, increasing the cure temperature can accelerate the rate of cure but often this can lead to different final properties. Post-cure at elevated temperatures following a period of cure under ambient conditions can also be used to accelerate the completion of cure. The differences that these practices make on the final properties need to be fully understood (through comparison tests) before such short cuts can be taken with confidence. Differential scanning calorimetry (DSC), ISO 11357 and dynamic mechanical thermal analysis (DMTA), ISO 6721, measurements can be used to assess the state of cure.

Adhesive joint tests assume that all stress in the adhesive layer is generated by the application of load through the adherends. However, residual stress in the adhesive layer may already be present following manufacture of the specimens, generated by:

- physical shrinkage of the adhesive during cure
- differences in the residual thermal expansion of the adhesive and adherends generating strain when the joint is cooled from the cure (or post-cure) temperature.

The extent of shrinkage may be determined through dilatometry or internal strain measurements (e.g. using embedded fibre Bragg strain sensors) of the adhesive during cure and cooling. These measurements will provide data on both the cure shrinkage and the coefficient of thermal expansion (CTE). Shrinkage whilst the adhesive is still a viscous liquid/paste will have little effect on internal stress generation and, therefore, the technique for monitoring cure shrinkage only needs to be capable of measuring the

© Woodhead Publishing Limited, 2010

behaviour following the gel point of the adhesive, where it changes state from viscous liquid to viscoelastic solid.

### 14.3.4 Bondline thickness

Bondline thickness in test specimens needs to be consistent and accurately controlled (i.e. a uniform adhesive layer thickness across the entire bonded area) in order to obtain consistent and reliable results. Non-uniformly thick bondlines will introduce greater end peel stresses and reduce measured bond strengths. With thick bondlines there is higher the risk of incorporating voids and stresses at the corners of the joint tend to be larger as it is difficult to maintain axial loading with a very thick bondline. Thick adhesive layers can change the cure properties producing internal stresses, thereby reducing short and long-term performance. Conversely very thin bondlines can result in adhesive starvation and debonding. Optimum bond thickness will depend on the type of adhesive used. The method used to control bondline thickness must not introduce voids in the adhesive or the joint performance will be compromised.

Control of bondline thickness can be achieved by:

- mechanical means (i.e. separation of adherends physically controlled by the bonding fixture)
- thin wire spacers (e.g. stainless steel) inserted between the adherends; It is essential that wire spacers used to control bondline thickness are located well within the bonded area away from the specimen edges and regions of high stress concentrations (i.e. ends of joints).
- ballotini glass balls, which can be mixed with single- and two-part adhesive pastes (typically 1% by mass); the distribution of glass beads in the adhesive must be uniform and therefore glass beads should be thoroughly mixed into the adhesive before application to the adherend surfaces.
- film adhesives available with carriers (e.g. nylon mat or mesh), which control bondline thickness.

The final thickness of the bondline should be measured, particularly if design data are required from the tests (as the bond thickness is the effective gauge length of the specimen). Bondline thickness can be determined by various methods, such as:

- Measuring the total thickness of the joint at the bonded region using callipers or micrometers and subtracting the thickness of the adherends (measured before bonding) – this may lead to large uncertainties and is not possible to do with all types of joint.
- Directly measuring the thickness using a travelling microscope – requires an easily visible interface between the adherend and adhesive.

© Woodhead Publishing Limited, 2010

- Through thickness scanning techniques (such as X-ray tomography or ultrasound) may be options but these techniques will need to be calibrated for the specific adherend/adhesive system and validated using conventional measurements.

Bondline thickness should be measured at different positions over the bond to evaluate uniformity. Most practically, this will be done at different positions along both the visible sides of the joint. Accuracy is important as the small thickness of the bondline increases the significance of any measurement uncertainty, for example an accuracy of 0.1 mm in the measurement is equivalent to a relatively high uncertainty of 10% for a relatively thick 1 mm bond but would be almost insignificant in the uncertainty of bulk specimen measurements made using a 50 mm gauge length.

### 14.3.5 End effects

Variations in fillets (size and shape) and adherend edges (shape) at the ends of the bond will affect the test results as the stress at the peaks at the ends of the bond depend on local factors, including geometry, for example see Adams and Harris (1987), Lang and Mallick (1998), Crocombe and Adams (1981a). In FE models, perfectly square adherend edges lead to mathematical singularities and the prediction of large stress concentrations in the adhesive at the ends of the overlap. However, in real joints the adherend edges will vary in shape and perfect squareness is extremely unlikely (particularly if an abrasive surface treatment is employed). These random shapes cannot easily be modelled. To simplify the analysis of such joints, it is often preferable to profile the adherend edges (e.g. by rounding to a defined radius) to provide consistency between specimens and reduce the stress concentration at the edge. In some joint types (e.g. strap joints) the adherends can be tapered to reduce stress concentrations at the edges of the bond layer. Similar arguments favour the control of fillet size and shape through the use of shaped spacers as shown in Fig. 14.18.

## 14.4 Test variables

### 14.4.1 Test machine and specimen alignment

It is important when loading test specimens that no lateral or angular offset is introduced to the specimen. Eccentric acting or off-axis forces should be avoided as small lateral (1 to 2 mm) or angular (1 to 2 degrees) offsets in the loading train can lead to additional shear and bending stresses, resulting in premature joint failure. Specimens should be attached to the test frame so that the major axis of the test specimen coincides with the direction of force through the centreline of the gripping assembly and loading axis of

© Woodhead Publishing Limited, 2010

the test machine. The test machine should have high lateral rigidity and accurate alignment between the upper and lower gripping faces. The load train should be as short and as stiff as possible. If the grips are articulated, as in the case of universal joints, the specimen may be subjected to large bending and twisting loads, resulting in reduced joint strength.

The alignment of the test machine and the test specimen should be checked at the centre of the gauge length using a strain gauged alignment specimen to monitor bending strains. Rectangular or circular bars provide the best checks and these specimens need to be accurately machined to ensure errors in parallelism are < 0.2 mm $m^{-1}$ and in concentricity (lateral offset) of 0.03 mm (Kandil, 1998). Bending strains should be less than 3–5% of the average axial strain. Alignment fixtures that adjust lateral movement, tilt and rotation of the machine grip or loading rod can also be included in the loading train to minimize angular and lateral offset between the upper and lower machine grips or loading rods.

Rotating the grips when tightening should be avoided as this can cause large bending and twisting loads. If the grips are articulated they should be tightened first to avoid stressing the specimen. Grips should be slowly tightened with any induced loads removed by progressively adjusting the crosshead position to prevent axial stress on the specimen whilst the grips are being tightened. Gripping pressure should be sufficient to prevent specimen slippage throughout the duration of the test, but not excessive as this will initiate failure of the specimen at the grips. Loading via pins through the adherends is an alternative approach which is less likely to overstress the sample. The holes should be accurately drilled to avoid misalignments.

### 14.4.2 Strain and displacement measurement techniques

Determination of strain within the adhesive layer is vital for the acquisition of materials properties data for design. Contact and non-contact techniques suitable for measuring strain and displacement include contact extensometers, video extensometers, strain mapping, strain gauges and crosshead movement. Direct measurement of strain within the adhesive is becoming possible through new technologies, such as digital image correlation (DIC) or electronic speckle pattern interferometry (ESPI), but is far from routine. The most common method of determining strain is to measure the deflection of the bond (often determined from change in separation of points on opposite adherends) and divide by the bondline thickness. The strain will be an average strain in the bondline. Determination of strain from the relative movements of the adherends will include some deflection of the adherends. The inclusion of adherend deflection in the measurement should be minimised and, therefore, the measurement points (e.g. contact points or gauge marks) should be as close to the bond layer as possible.

© Woodhead Publishing Limited, 2010

It is possible to correct the strain causing deformation of the adherends by calculating the adherend extensions, for example by simple mechanical analysis (if joint geometry is simple) or by FE analysis, and subtract these from the measurement. Where the stiffness of the adherends is very much greater than that of the adhesive layer, corrections may be minimal. However, if the measurement system is not optimised, the correction of the deflection measurement could be very large. For example in deflections of a lap shear joint measured via the crosshead, extension of the adherends can easily be over ten times the bond layer deflection.

Tests can be optimised to reduce the contribution from extension of the adherends by:

- minimising the distance between the measurement points and the bondline to reduce the amount of adherend deformation included in the measurement.
- using adherends with modulus values very much greater than the adhesive.

The first of these approaches suggests the use of either non-contacting extensometers with gauge marks close to the interface or purpose built extensometers that contact the adherends close to the interface. However, where this is not possible it is preferable to use general purpose extensometers rather than rely on crosshead movement.

In many joint tests, the loading path may cause bending of the specimen. In order to cope with specimen bending, extensometers measuring opposite faces of the specimen should be used to determine displacement (Dean and Duncan, 1998). Although the average of the measured extensions is used to calculate test results, individual transducer measurements should be recorded so that the quality of the test data can be checked. Any bending of the specimen will be apparent from diverging displacement measurements. Errors caused by minor bending are minimised by taking the average measurement of the two displacement transducers.

In selecting extensometry methods both the required level of accuracy and the measurement range need to be considered. As the bondline thickness defines the gauge length, the resolution of the measuring device needs to be sufficient to provide accurate measurements. Any extensometer used should be capable of measuring the change in gauge length with a resolution of at least 1% of the relevant applied displacement or better (i.e. equivalent to ± 0.05 μm for 1% strain over a typical bond thickness of 0.5 mm). High precision extensometers may have limited travel and have insufficient range to measure the full load–extension curve to failure. It may be necessary to use one type of extensometer for accurate measurements at low strains and another to capture the behaviour to failure.

© Woodhead Publishing Limited, 2010

*Contact extensometers*

Contact extensometers are the preferred method for measuring displacement and hence strain in the adhesive or the stiffness of bonded joints. Positioning of the contact points is critical for the successful use of contact extensometers. Extensometers can be general purpose (e.g. knife-edged materials testing extensometers) or specially constructed for the joint. Extensometers should be used as pairs to accommodate bending.

General purpose knife-edged tensile extensometers, with displacement sensors based on either linear variable differential transformers (LVDTs) where movement is sensed through changes in the inductance or strain gauged flexure elements, can be used to measure joints. Knife-edged extensometers are often used in pairs, straddling the bondline, to accommodate bending. Some adaptation may be needed to ensure that contact is correctly made between the knife edge and the adherend (e.g. using different length knife edges to cope with the 'step' in a lap joint). General purpose extensometers have sufficient resolution to sense the small displacements in the bondline and costs are relatively modest.

Theoretically, special purpose built extensometers should provide more accurate measurements than general purpose extensometers. An example of the use of purpose built extensometers is illustrated in Fig. 14.6, which shows two extensometers attached to a TAST specimen for measuring shear deformation. The three-point contact minimises rotation of the extensometers. The contact points are close to the bond, reducing the adherend deflection contained in the measurements. Purpose-built extensometers are relatively expensive and generally limited in use to a specific joint type.

Where samples have low stiffness, it is advisable to support the weight of the extensometer because allowing the extensometer to hang unsupported from the specimen may cause bending and introduce contact stresses. Contact forces need to be sufficient to prevent slippage between the extensometer and the specimen, but not so large that the specimen surface is cut or nicked as this may cause the specimen to fail prematurely. Failure can be a violent event, releasing considerable energy that can damage the extensometer; therefore it may be necessary to remove extensometers prior to failure. Extensometers need to be able to operate satisfactorily within the test environment (i.e. temperature and humidity) and be resistant to chemical attack when used in hostile environments.

*Non-contact extensometers and strain mapping*

Non-contact or optical extensometers (e.g. video extensometers) avoid the problems of contact damage and use up to failure. There are no temperature or environmental restrictions, as video extensometers can be located outside

© Woodhead Publishing Limited, 2010

the test chamber (provided that the specimen can be imaged clearly). Standard systems measure the separation of marks in one direction, mimicking general purpose contact extensometers but some systems provide capabilities for dot location measurements, which allow two-dimensional measurements and a limited strain mapping capability. Dot location provides versatility and, potentially, enables measurement of many different types of joint using a single system.

Remote cameras and image analysis software are used to monitor the separation of high contrast marks or lines inscribed on the test specimen. The initial separation of the marks defines the gauge length and the change in separation of the marks is recorded throughout the test. Gauge marks should not be made on the specimen in any way that may cause damage to the specimen.

Early generations of video extensometers were not particularly suitable for measuring small strains (e.g. movements of a few micrometres), which limited their applicability to structural adhesive joints. However, developments in resolution, sensitivity and speed of digital imaging and data processing are leading to improved capabilities. One limitation of the technology is that, unless a dual camera system is used, measurement is normally only possible at one side of the joint and bending cannot be evaluated.

Developments in image analysis and pattern recognition technology have produced non-contacting methods for the determination of strain. Full field strain mapping techniques, such as DIC or ESPI, provide information on relative displacements in the adherends and the adhesive layer. These techniques can measure strains in complex geometries; this data can be used to verify model predictions and to derive material properties.

ESPI is a non-contact technique, based on the measurement of laser interference fringes, and is capable of measuring and monitoring non-uniform strain fields at high resolution. The system can measure the deformation and thus the strain under mechanical and/or thermal loads along the three specimen axes (i.e. three-dimensional (3D) strain measurement). ESPI systems are capable of measuring local deformation with a resolution of approximately 0.1 μm, equivalent to 0.02% strain for a 0.5 mm thick bond. The technique needs minimal specimen preparation and is capable of inspecting large and small areas, but capital outlay for equipment is generally prohibitive for most test facilities.

DIC techniques use computer image analysis to track the movement of points of applied speckle patterns on the surface of the specimen. Speckle patterns are usually applied by spraying with contrasting coloured paints. Displacements can be resolved with sub pixel accuracy to give an effective resolution of typically 0.01% strain. Calculation of 3D strains is possible if two or more imaging cameras are used. Calibration of the camera by using a calibration plate is straightforward.

© Woodhead Publishing Limited, 2010

*Strain sensors*

Strain gauges can be attached to adherends and used to monitor strain in the adherends of bonded structures. The usefulness of such measurements in interpreting the behaviour of the bond layer is limited except in cases where changes in joint performance are manifested in measurable changes in the adherend strain. One such application is back-face strain gauging of thin lap shear joints where crack growth in the adhesive layer can be monitored through strains measured by gauges bonded to the external surface of the adherends at the overlap.

Structural monitoring, using strain sensing devices embedded in materials, is the subject of much research and may yield developments that can be applied to adhesive joints. Devices that can be embedded within the adhesive layer, such as strain sensing optical fibres with Bragg gratings, or particles with strain sensitive properties that can be probed, using measurement techniques such as Raman spectroscopy or X-ray diffraction, offer the prospect of directly measuring the strain within the bond layer. However, there are many practical obstacles to be overcome before these techniques are adopted for routine adhesive joint testing or used outside research laboratories.

*Crosshead movement*

An approximate measurement of joint deflection and hence strain can be obtained from measuring the crosshead displacement of the test frame. Any slippage or compliance within the loading train will produce errors in the strain measurement in addition to those resulting from the deflection of the adherends.

If crosshead movement is the only available measurement, the displacement measurements need to be corrected to take into account the stiffness of the loading train. The stiffness of the machine can be estimated by testing a specimen, such as a metal rod or bar with similar dimensions to the joint specimen, that has a large and known stiffness. The difference between the measured deflection and the expected deflection of the specimen can be used to determine machine stiffness. However, even with an estimate for the machine stiffness, the accuracy of strains determined using crosshead displacements must be considered suspect. The adhesive layer deflections, even those that occur at large strains, are likely to be small compared with the machine compliance corrections. This leads to large errors and uncertainties in the corrected values, which are obtained by, effectively, subtracting one large calculated extension from a large measured extension. It is not unknown for corrected bond deflections to be negative. Therefore, the strain results will have extremely high uncertainties associated with them and are really suitable only for qualitative purposes.

© Woodhead Publishing Limited, 2010

### 14.4.3 Test conditions

Polymeric adhesives are viscoelastic materials. Their mechanical properties will be sensitive to applied strain rate and temperature, particularly under conditions close to the glass transition temperature of the adhesive. These test parameters need to be controlled to reduce variability in test results and to ensure that data generated using different joint types can be compared. The influence of the specimen bondline thickness on the applied strain rate should be considered when deciding test speeds. As a general rule of thumb, the ratio of test speed to bondline thickness should be approximately the same for each joint.

## 14.5 Detection of failure

An important output of adhesive joint tests is the identification of the point where failure initiates. In many cases, joint failure initiates through the formation of cracks within the adhesive layer or fillet before the ultimate extension or load of the joint is reached. Designing for a long-term service life requires that joints never be loaded to the extent that these failures can initiate (whether through cohesive rupture or adhesion failure). Therefore, identification of the failure initiation point is a critical part of a joint test. By knowing this point, analyses can be performed to calculate stress and strain distributions immediately prior to the initiation of the crack, because if a fracture is present in the bond, the analyses will be inaccurate.

### 14.5.1 Shape of the force–extension curve

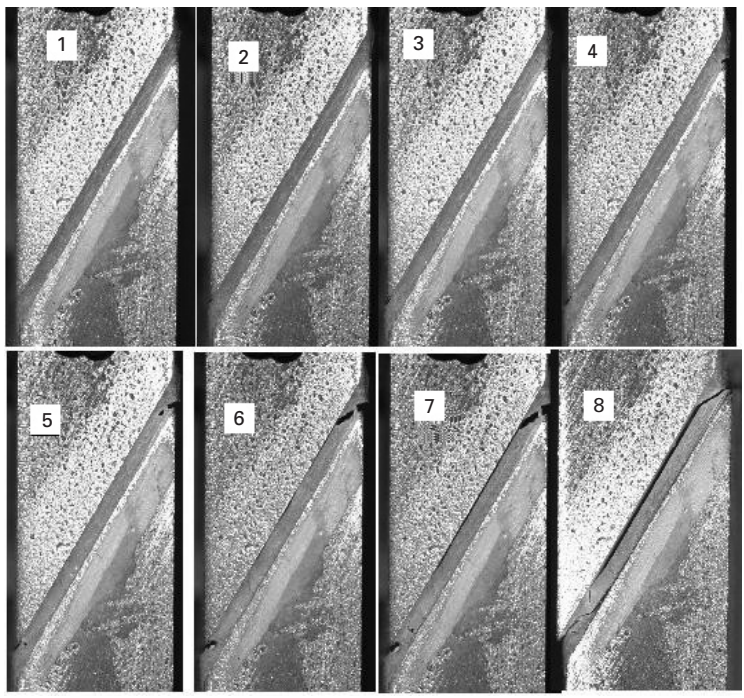
The formation of a crack will result in a redistribution of load and, in principle, failure could be detected from a change in the shape of the measured force–extension or stress–strain curve at the point of crack initiation, see Fig. 14.2. The slope of the loading curve should fall as a crack forms because the load-bearing area of the bond is reduced. In many tests the initiation of fracture is readily apparent. However, in other tests the joint stiffness can reduce as load is applied, for example as a toughened adhesive yields plastically. In these situations, particularly if crack growth is slow, it may be very difficult to distinguish the effects caused by crack formation from those owing to yield. FE predictions may be used to establish the load at which the measured force–extension response of a joint deviates from the predicted behaviour. However, for these analyses to have any reliability, the models of the material properties and boundary conditions need to be extremely accurate.

© Woodhead Publishing Limited, 2010

### 14.5.2 Visual inspection

It is possible to detect a crack forming and growing on the edges of the adhesive by viewing the bond. Obviously cracks forming in the interior of the bondline will not be visible until the crack has grown to the edge of the joint. High magnification of the region of the joint where failure is expected is needed to view the beginning of a crack and photography or video recordings can record the formation and growth of the crack, see Fig. 14.19. By referencing these images, by synchronising the time index of the test data and the photographs to the force–extension or stress–strain curves, further information can be gathered on the conditions that generate the fracture.

Visual detection of cracks can be difficult, particularly where heterogeneity and surface structures at the joint edge mask the presence of a crack until it has grown. The edges of the adhesive bond could be polished to reduce these effects and penetrant dyes used to improve the contrast between the crack and the surface. The tests need to be performed at slow strain rates in order to capture the crack growth meaningfully, unless high-speed photography facilities are available. A fast propagating crack is likely to be




*14.19* Initiation and propagation of a crack in a scarf joint.

© Woodhead Publishing Limited, 2010

associated with sudden, catastrophic failure of the joint, the situation where the maximum load is most likely to correspond to the load that will initiate failure.

### 14.5.3 Acoustic emission of fracture energy

The fracture of an elastic material or bond is accompanied by a release of energy and a portion of this energy will be acoustic. Thus, fracture can be heard, a loud crack occurs as a brittle adhesive bond fails. Sensitive acoustic transducers placed near the bondline should be able to detect acoustic emission from a crack forming. Analysis of the acoustic signal, particularly if multiple transducers are used, may yield additional information about the crack location and growth rate. Acoustic emission (AE) is a technique being applied to many systems (e.g. composites, coatings) as a research and structural monitoring tool. The technique relies on the operator having sufficient experience to be able to identify particular defect types from the AE data. The sound intensity emitted by the initiation of a slow propagating crack in a tough adhesive is low and may be difficult to detect above any background noise. Although the technique is essentially a laboratory tool, however, AE is used for proof and qualification tests of pressure vessels prior to installation and routine in-service inspection.

### 14.5.4 Strain mapping techniques

Mapping strain, either in the adhesive layer or in the adherends in the vicinity of the bond, can reveal the presence of a fracture. The initiation of a crack will alter the distribution of strain in its immediate vicinity. Local surface strain measurements ought to give an indication of the initiation of a fracture, even if the fracture originates within the bulk of the adhesive. Strain mapping can be carried out using a variety of techniques, including ESPI and DIC described in the section on strain measurement. The absolute accuracy of strain maps in small regions of critical stress may be questionable but the initiation of a crack should have sufficient effect on the strain map to be readily apparent.

Internal strains can be characterised by Raman microscopy provided that the materials are transparent at the wavelengths used. The adhesive may need to be doped with particles that have molecular bonds with suitable strain sensitive characteristic vibration properties. With a suitable calibration curve, Raman spectroscopy can be used to determine strains in local regions (de Lange *et al.*, 2001). X-ray diffraction can characterise strain in metal adherends close to the adhesive interface. These strains can be used to calculate stress in the adherend close the interface and, by inference, provide information on the stress near the interface (Predecki *et al.*, 1986). Photoelasticity measurements

© Woodhead Publishing Limited, 2010

can also be applied where one of the adherends is transparent (Mullville and Vaishnav, 1986).

Strain gauges can be attached to monitor strain in rigid adherends. This technique is known as 'back face strain gauging' and can be a cost-effective monitoring method. Strain gauges will also enable the identification of the point of plastic yield of the adherends, which is another precursor to failure of the joint.

### 14.5.5 Non-destructive fracture detection

The presence of fractures can be determined using non-destructive testing (NDT) techniques. Measurements providing real time data can be integrated into the test system to provide a direct link between mechanical data and fracture behaviour.

Thermography can yield information about the flow of heat through the joint, which could indicate internal defects or cracks generated under load. Thermal imaging cameras are used to produce heat maps of the sample. Conventional thermal images of joints under test (particularly under continuous cyclic loading) can reveal 'hot spots' where high stresses and strains dissipate mechanical energy as heat. Flash thermography is a technique where the heat loss from the sample is assessed following a brief intense pulse of heat.

Some NDT methods may be impractical or unsafe to carry out in real time as samples are tested. However, this limitation can be overcome by testing specimens at defined proof loads and inspecting afterwards.

## 14.6 Case study in the use of joint tests: cryogenic liquid containment system

Prototype testing of full-scale components is desirable to validate designs but often may not possible owing to the size of the structures. In such situations, representative joint tests are used in combination with FE modelling to validate the design. For example, bonded insulating membrane systems for transporting liquefied natural gas that are constructed in the hold of sea tankers can contain thousands of cubic metres of liquefied gas. The insulation system has to be able to contain the cargo while sustaining the displacements and stresses arising from large temperature changes (on filling and emptying the tank) and wave motion transmitted from the hull (via mastic pads).

The manufacture of cryogenic tanks for transporting liquefied gases presents many challenges in design and fabrication. The process of materials selection, design validation and quality assurance testing demonstrates the need for different types of joint testing to meet different requirements. FE modelling

© Woodhead Publishing Limited, 2010

is employed in both the structural design process and the interpretation of test results.

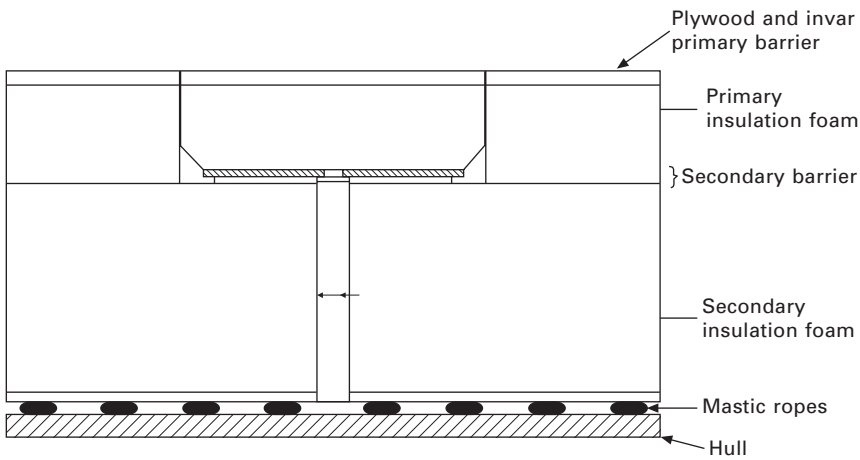
### 14.6.1 Design

One of these membrane insulation systems consists of two layers of insulated foam (rigid PUF) separated by a rigid composite secondary barrier film (RSB) bonded to the bottom layer of foam and subsequently, in most of the membrane, also to the top foam layer (Fig. 14.20). At regular intervals there are expansion gaps between the panels to allow for movement; these gaps are bridged by a top-bridging pad, to which a flexible composite barrier film (FSB) is bonded. The bonds between the flexible layer covering the top bridging pad and the rigid layer covering the lower layer of foam are critical to the structural performance. The secondary barrier film provides a back up to the primary invar barrier film and needs to contain the liquid gas in the event of primary barrier failure.

The rigid barrier, the flexible barrier and the epoxy adhesive used to bond the rigid and flexible barrier layers were qualified for use in the application through a series of tests that screened the adhesive for compatibility with the adherends, chemical resistance and low temperature performance. A double lap shear specimen was used for many of these acceptance tests.

### 14.6.2 Validation

Owing to the size of the structure it is very difficult to carry out meaningful full-scale tests. FE modelling predicts the system performance but representative

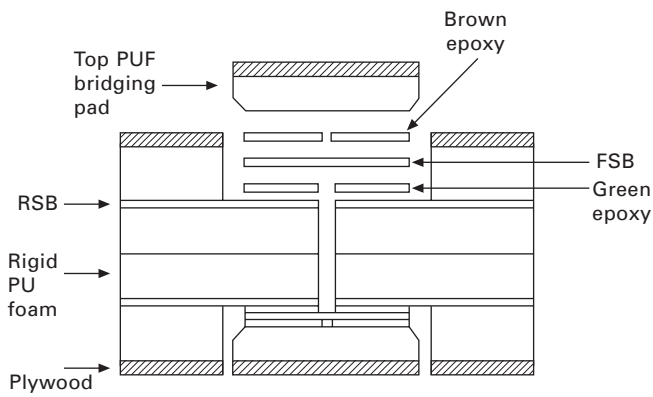



*14.20* Schematic of insulation membrane system (courtesy of GazTransport and Technigaz).

© Woodhead Publishing Limited, 2010

joint tests are needed to provide validation. Global FE models of the ship and insulation system are analysed to provide predictions of temperature distributions and local forces/deflections acting on the bonds. These predictions form the boundary conditions for more detailed analyses of the bonds that provide calculations of stress in the adhesives and barrier films. Stress in the adhesive layer results from differential thermal contractions of the different materials used in the insulation system and from deformations resulting from the deflections (hogging and sagging) of the hull. Owing to limitations in the availability of full, multi-axial materials properties data and failure criteria for the materials (particularly for the adhesives and barrier films), full non-linear analyses could not be performed. Therefore, the absolute quantitative values obtained for stress contain unknown uncertainties. As a consequence, FE modelling could not be used as the sole means of predicting failure and, therefore, could not directly calculate safety factors in the design.

The primary validation test employed was the sandwich specimen shown in Fig. 14.21. Although being of a slightly different geometry (owing to the need for a symmetrical specimen), the sandwich specimen replicates the key features of the insulation system (foam layers, bridging pads and barrier films). It is prepared under identical conditions to the system in tanks. This specimen is tested in a tensile test machine under temperature control. The sample is clamped and cooled to the normal operation temperature of the bond (–100°C), with a resulting increase in load caused by thermal contraction, before extensions are applied. The global system FE analyses predict that the membrane must sustain a minimum of 0.6 mm extension per metre length of the system, which is equivalent to an extension of 0.4 mm (or 8 kN load) applied to the sandwich panel. Failure extensions of 4



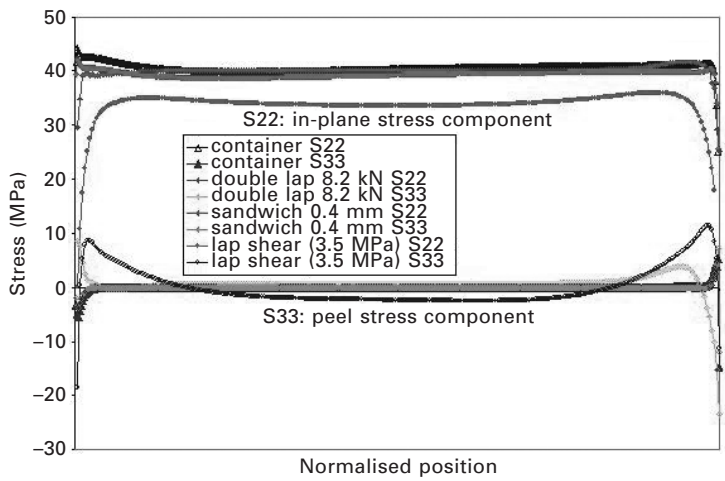

*14.21* Sandwich panel specimen (courtesy of GazTransport and Technigaz).

© Woodhead Publishing Limited, 2010

mm (20 kN load) were obtained by tests, providing an empirical proof of the design.

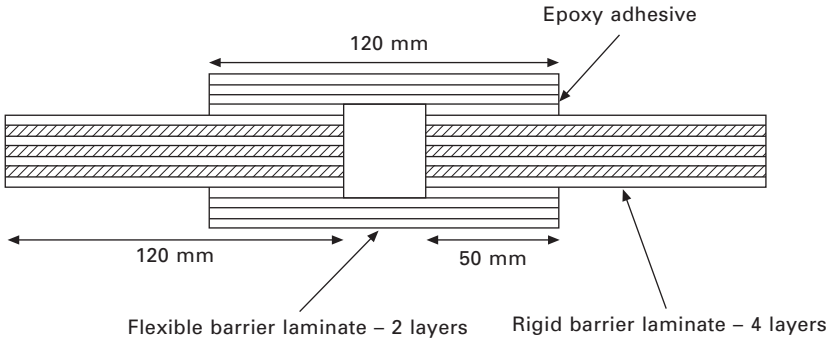
However, to ratify the design it was necessary to provide evidence that the stresses within the adhesive layer in the test specimen are comparable to those experienced in the full structure. There was a possibility that differences in specimen geometry, boundary conditions and temperature distributions could reduce the relevance of the sandwich test. The FE models of the sandwich specimen contain the same inherent assumptions as the models of the complete insulation system. Therefore, whilst there was still relatively low confidence in the absolute stress values there was high confidence in any comparisons between the models, as the same assumptions were made for materials properties in each model. This comparison, shown in Fig. 14.22, reveals that under design service conditions, the sandwich specimen is under a similar state of stress as the full insulation system. Stress values close to the failure load of the sandwich specimen are significantly greater than the design requirements.

A double lap joint, using adherends made from laminates of the barrier films (Fig. 14.23) was also used to validate the design. FE predictions showed that the state of stress in the adhesive layer in samples cooled to –100°C and loaded to approximately 8 kN would be comparable to the in-service stress in the membrane. Tests on the double lap sample showed that the sample comfortably exceeded this level and the failure load was greater than 24 kN. The stresses in the adhesive near failure are significantly higher than the design requirements.




*14.22* FE analyses comparing stress in different joints under proof loads.

© Woodhead Publishing Limited, 2010




*14.23* Double lap joint specimen.

### 14.6.3 Quality assurance

The sandwich panel and double lap joint specimens are difficult to prepare in the production environment, which limits their use for quality control or screening purposes. Therefore, quality control testing during the construction of the insulation system is mainly carried out using a single lap shear test. Dummy samples (50 mm by 50 mm) of the rigid barrier film are bonded to the flexible barrier film. These are cured *in situ* before being bonded to shaped aluminium adherends to form lap joints, which are 50 mm wide and 10 mm thick at the overlap. The joints are tested at low temperatures and acceptable construction is demonstrated through cohesive failure (rather than adhesive failure from either of the barrier films) above a minimum failure load (8.75 MPa), which is less than one-third of the failure load achieved with well-bonded samples.

FE modelling shows, as partly illustrated in Fig. 14.3, that this sample replicates the levels of peel and shear stress in the membrane system but does not produce the same in-plane stresses (which originate mainly from differential thermal contraction). The stress state sustained in the sample, particularly the critical peel stress, is sufficiently close to the stress state in the structure to provide a reasonable assessment of the quality of the bond. However, the overall state of stress, including the thermal shrinkage induced in-plane stress, is different from the structure and this test, while providing additional information about the capability of the adhesive and interface, is insufficient by itself to validate the design.

## 14.7 Case study in the use of joint tests: using T joints to validate materials models

A joint test study to validate a FE design illustrates many of the measurement challenges of joint tests. Dean *et al*. (2004) developed a cavitation model

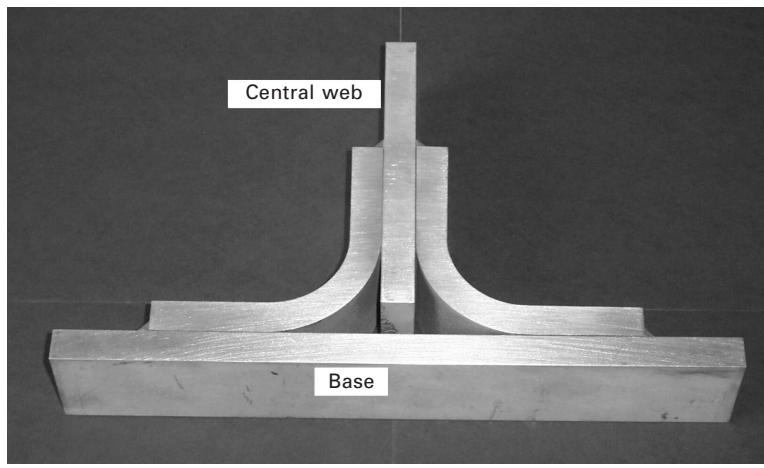
© Woodhead Publishing Limited, 2010

to describe the non-linear yield behaviour of toughened epoxy adhesives. The materials data for use in the model were derived from sets of bulk specimen tests in tension, shear and compression. Scarf and butt joint tests were used to determine the parameters describing the multi-axial yield stresses. Several candidate failure criteria were proposed from the results of these tests. The resulting model was coded into a FE package. A validation exercise was performed to assess the accuracy of the model, in comparison with elastic and elastic–plastic material models, and to assess the reliability of the proposed failure criteria.

A T-joint specimen, as shown in Fig. 14.24, was designed for this study to evaluate the accuracy of the FE model in predicting the strength and stiffness. The specimen was constructed from both aluminium and composite adherends. Two types of loading were employed in testing and analysis, tension (central web loaded perpendicular to the crosspiece) and transverse (central web loaded parallel to the crosspiece). Full details were reported by Broughton *et al.* (2004).

### 14.7.1 Manufacture

The manufacture, testing and analysis of these T-joint specimens illustrates many of the challenges in joint testing. Carefully positioning the adherends and fixing their positions using clamps accomplishes alignment of samples during manufacture. The bondline thickness was controlled by mixing approximately 1% by weight of ballotini (glass balls), with a nominal diameter of 0.25 mm, into the single part epoxy adhesive before application. Checks after curing using a travelling microscope showed that the bondline thickness of the four bonded regions was consistently around 0.25 mm.




*14.24* T-joint specimen made of epoxy bonded aluminium.

© Woodhead Publishing Limited, 2010

The biggest challenge during manufacture was control of the thermal history of the adhesive during cure. The optimum adhesive cure cycle is to place samples in an oven preheated to 180°C for 30 minutes. However, the large mass of the adherends in the T-joint sample provide a degree of thermal lag in the temperature seen by the adhesive. A series of measurements using thermocouples embedded in the bond was used to determine a new cure cycle, with the cure time extended but the temperature of the oven reduced (thermocouple measurements on bulk and smaller joint samples found that the adhesive never reached the oven temperature during the cycle).

### 14.7.2 Testing

Three modes of testing were chosen so that the samples could be tested within a tensile test machine. Before tests could be carried out, jigs were made to fix the sample crosspieces to the test machine base and fittings made to attach the stem to the moving crosshead. The fixing jigs were designed to attach the crosspiece firmly to the machine and be sufficiently stiff and strong to sustain the loads applied. The fixing jigs were also designed so that they can be readily modelled as constraints within the FE analyses. Movement of the central web in the direction of loading was measured by using an LVDT transducer attached near the point of load application.

The strain in the structure was also monitored by full field strain mapping (DIC) and by strain gauging the joint. The strain mapping methods were able to provide information on strain in the adherends and locations of strain concentrations in the adherends and the adhesive layer. However, the magnification used to image the full joint provided limited resolution of the adhesive bonds and results were not sufficient to quantify strains in the adhesive layer. The onset of local damage, that is cracks in either the adherends or adhesive layer, was detected using strain mapping techniques. Strain gauges could provide local values of strain in the adherends but did not provide information about the adhesive layer. Strain gauges, if positioned close to the expected locus of failure, provided a means of detecting the onset of failure.

### 14.7.3 Results

FE analysis showed that load–displacement response, initial stiffness and failure load for both aluminium and GRP T-joints could be predicted in direct tension and transverse loading with reasonable accuracy using a combination of cavitation model and a hydrostatic stress failure criterion. Cohesive failure occurred as predicted in the internal adhesive fillets between the flanges and centre web. Failure was sudden and catastrophic.

© Woodhead Publishing Limited, 2010

## 14.8 Future trends

Increasingly, engineers will seek to perform virtual tests on joints and structures using computerised tools such as FE analysis with the aim of predicting long-term performance and design safety factors. To enable this, joint tests will need to provide the accurate materials property data required for non-linear, multi-axial material models used for predictive modelling of the performance of the adhesive layer. Development of test configurations, test fixtures, data analyses techniques and extensometry to generate accurate materials property data will continue.

Testing programmes will need to be developed that generate data for predicting structural lifetime performance in real situations with varying loading and environmental conditions. This will require tests that provide good quality data that can be performed relatively cheaply. Use of miniaturised versions of tests that provide design data, such as TAST or butt joints, is likely to increase. As data requirements for lifetime performance modelling are potentially huge, the use of statistical 'design of experiments' will increase to produce the most efficient testing programmes. Structural health monitoring, using embedded sensors or non-destructive examination, will provide additional understanding of lifetime performance and are likely to be implemented for management of real bonded structures.

Modelling techniques are being developed continuously and tests will need to evolve as well. New approaches, such as adaptive meshing and cohesive zone damage which combine continuum mechanics and fracture energy, aim to provide predictions of the initiation and growth of defects that will enable designers to predict strengths of structures. Tests are needed to provide accurate failure criteria. These would need to generate local measurements of stress and strain in critical regions of the overlap where fractures originate and grow, probably using strain mapping techniques combined with measurement of the size and shape of the fracture notch from image analysis. The level of precision required suggests that tests will need to be carried out with samples within the field of view of optical or even scanning electron microscopes.

The growing field of micro- and nano-technology will create a need to understand adhesion and adhesive joints at much smaller scales than are currently covered by standard tests. There is limited understanding about whether continuum properties derived from bulk material or standard joints are relevant at extremely small length scales where the influence of surfaces will dominate, for example through locally altering the cure reaction. Research using scanning probe techniques, such as depth sensing indentation (Ashcroft, 2004), to map the spatial variations of the properties of adhesives (e.g. viscoelastic and viscoplastic) within bondlines seeks to understand better near surface properties. Research into the use of scanning probe techniques to

© Woodhead Publishing Limited, 2010

measure adhesive properties in high-throughput (combinatorial) experiments is also likely to produce new approaches to performing adhesive screening studies.

## 14.9 Acknowledgements

The author is grateful for the assistance of many colleagues at NPL, in particular Bill Broughton, Greg Dean, Louise Crocker, Maria Lodeiro and Richard Mera. The support of UK National Measurement Systems through funding for research on the measurement of adhesives through the Performance of Adhesive Joints and similar programmes is acknowledged. The author is thankful for the advice and backing over many years from the Adhesives Industrial Advisory Group. GazTransport & Technigaz are thanked for their permission to publish material in Section 14.6.

© Crown copyright 2009 Reproduced with the permission of the Controller of HMSO and Queen's Printer for Scotland

## 14.10 Sources of further information and advice

All of the many reports and good practice guides produced by the UK initiative on the measurement of the performance of adhesives and adhesive joints are available from the National Physical Laboratory (www.npl.co.uk).

The Adhesives Design Toolkit (www.adhesivestoolkit.com) that was produced by collaboration between NPL, TWI, MERL and ESR Technology, has a large resource of information and advice on the use of adhesives.

International Organisation for Standardization (ISO) can be accessed at www.iso.ch

ISO 527-4, *Plastics – Determination of Tensile Properties. Test Conditions for Isotropic and Orthotopic Fibre-reinforced Plastic Composites*.
ISO 604, *Plastics – Determination of Compressive Properties*.
ISO 2818: *Plastics – Preparation of Test Specimens by Machining*.
ISO 4578, *Adhesives – Determination of Peel Resistance of High-Strength Adhesive Bonds: Floating Roller Method*.
ISO 4587, *Adhesives – Determination of Tensile Lap-Shear Strength of Rigid-to Rigid Bonded Assemblies*.
ISO 6721, *Plastics – Determination of Dynamic Mechanical Properties*.
ISO 6922, *Adhesives – Determination of Tensile Strength of Butt Joints*.
ISO 8510-2, *Adhesives – Peel test for a Flexible-Bonded-to-Rigid Test Specimen Assembly. Part 2: 180 Degree Peel*.
ISO 9142, *Adhesives – Guide to the Selection of Standard Laboratory Ageing Conditions for Testing Bonded Joints*.
ISO 9653, *Adhesives – Test Method for Shear Impact Strength of Adhesive Bonds*.

© Woodhead Publishing Limited, 2010

ISO 10354, *Adhesives – Characterization of Durability of Structural Adhesive Bonded Assemblies – Wedge Rupture Test*.
ISO 10365, *Adhesives – Designation of Main Failure Patterns*.
ISO 11003-1, *Adhesives – Determination of Shear Behaviour of Structural Bonds. Part 1: Torsion Test Method Using Butt-Bonded Hollow Cylinders*.
ISO 11003-2, *Adhesives – Determination of the Shear Behaviour of Structural Bonds. Part 2: Thick-Adherend Shear Test Method*.
ISO 11339, *Adhesives – 180° Peel Test for Flexible-to-Flexible Bonded Assemblies (T-Peel Test)*.
ISO 11343, *Adhesives – Determination of Dynamic Resistance to Cleavage of High-Strength Adhesive Bonds Under Impact Conditions – Wedge Impact Method*.
ISO 11357, *Plastics – Differential Scanning Calorimetry*.
ISO 14615, *Adhesives – Durability of Structural Adhesive Joints – Exposure to Humidity and Temperature Under Load*.
ISO 14676, *Adhesives – Evaluation of the Effectiveness of Surface Treatment Techniques for Aluminium – Wet-Peel Test by Floating-Roller Method*.
ISO 15107, *Adhesives – Determination of Cleavage Strength of Bonded Joints*.
ISO 15166-1, *Adhesives – Methods of Preparing Bulk Specimens. Part 1: Two Part Systems*.
ISO 15166-2, *Adhesives – Methods of Preparing Bulk Specimens. Part 2: Elevated-Temperature-Curing, One-Part Systems*.
ISO 17212: *Structural adhesives – Guidelines for the Surface Preparation of Metals and Plastics Prior to Adhesive Bonding*.
ISO 19212, *Adhesives – Determination of Temperature Dependence of Shear Strength*.

*ASTM International*

www.astm.org

ASTM D 695, *Standard Test Method for Compressive Properties of Rigid Plastics*.
ASTM D 897, *Standard Test Method for Tensile Properties of Adhesive Bonds*.
ASTM D 903, *Standard Test Method for Peel or Stripping Strength of Adhesive Bonds*.
ASTM D 950, *Standard Test Method for Impact Strength of Adhesive Bonds*.
ASTM D 1002, *Standard Test Method for Apparent Shear Strength of Single-Lap Joint Adhesively Bonded Metal Specimens by Tension Loading (Metal-to-Metal)*.

© Woodhead Publishing Limited, 2010

ASTM D 1062, *Standard Test Method for Cleavage Strength of Metal-to-Metal Adhesive Bonds*.

ASTM D 1781, *Standard Test Method for Climbing Drum Peel of Adhesives*.

ASTM D 1876, *Standard Test Method for peel resistance of adhesives (T-peel test)*.

ASTM D 2093, *Standard Guide for Preparation of Surfaces for Plastics Prior to Adhesive Bonding*.

ASTM D 2095, *Standard Test Method for Tensile Strength of Adhesive by Means of Bar and Rod Specimens*.

ASTM D 2651, *Standard Guide for Preparation of Metal Surfaces for Adhesive Bonding*.

ASTM D 3167, *Standard Test Method for Floating Roller Peel Resistance of Adhesives*.

ASTM D 3433, *Standard Test Method for Cleavage of Adhesives in Bonded Metal Joints*.

ASTM D 3528, *Standard Test Method for Strength Properties of Double-Lap Shear Adhesive Joints by Tension Loading*.

ASTM D 3762, *Standard Test Method for Adhesively-Bonded Surface Durability of Aluminium (Wedge Test)*.

ASTM D 3933, *Standard Guide for Preparation of Aluminum Surfaces for Structural Adhesives Bonding (Phosphoric Acid Anodizing)*.

ASTM D 5379, *Standard Test Method for Shear Properties of Composite Materials by the V-Notched Beam Method*.

ASTM D 5656, *Standard Test Method for Thick-Adherend Metal Lap-Shear Joints for Determination of Stress-Strain Behaviour of Adhesives in Shear by Tension Loading*.

ASTM D 6671, *Standard Test Method for Mixed Mode I-Mode II Interlaminar Fracture Toughness of Unidirectional Fiber Reinforced Polymer Matrix Composites*.

## 14.11 References

Adams, R.D. and Harris, J.A. (1987). 'The influence of local geography on the strength of adhesive joints', *Int. J. Adhesion and Adhesives*, **7**, 69–80.

Adams, R.D., Coppendale, J. and Peppiatt, N.A. (1978). 'Stress analysis of axisymmetric butt joints loaded in torsion and tension', *J. Strain Anal.*, **13**, 1–10.

Adams, R.D., Comyn, A. and Wake, W.C. (1997). *Structural Adhesive Joints in Engineering*, second edition, Chapman and Hall, UK.

Althof, W. and Brockmann, W. (1976). 'New test methods for the prediction of the environmental resistance of adhesive bonded joints', *Proceedings Bicentennial of Materials Progress 21*, Society for the Advancement of Material and Process Engineering, USA, 581–691.

Arcan, M., Hashin, Z. and Voloshin, A. (1978). 'A method to produce uniform plane-

© Woodhead Publishing Limited, 2010

stress states with applications to fiber-reinforced materials', *Experimental Mechanics*, **18**, 141–6.

Ashcroft, I.A. (2004). 'Depth sensing indentation of epoxy adhesives', *Proceedings of the 27th Annual Meeting of the Adhesion Society*, Wilmington, NC, Chaudhury M.K (ed.).

Bikerman, J.J. (1968). *Science of Adhesive Joints*, 2nd edition, Academic Press.

Blackman, B.R.K, Kinloch, A.J. and Paraschi, M. (2001). 'The failure of adhesive joints under modes I and II loading', *Proceedings of Structural Adhesives in Engineering VI*, Bristol, IoM.

Broughton, W.R., Crocker, L.E., Gower, M.R.L. and Shaw, R.M. (2004). *Assessment of Predictive Analysis for Bonded and Bolted T-Joints*, NPL Report DEPC-MPR 002, National Physical Laboratory.

Clarke, J.L. (1996). 'Structural design of polymer composites', *EUROCOMP Design Code and Handbook*, Chapman and Hall, UK.

Construction Industry Research and Information Association, (1997). *Joining of Fibre-Reinforced Polymer Composite Materials*, Project Report 46, Construction Industry Research and Information Association.

Crocombe, A.D. and Adams, R.D. (1981a). 'Influence of the spew fillet and other parameters on the stress distribution in the single lap joint', *J Adhesion*, **13**, 141–55.

Crocombe, A.D. and Adams, R.D. (1981b). 'Peel analysis using the finite element method', *J Adhesion*, **12**, 127–42.

Crocombe, A.D. and Adams, R.D. (1982). 'An elasto-plastic investigation of the peel test', *J Adhesion*, **13**, 241–67.

Dean, G. and Duncan, B. (1998). *Preparation and Testing of Bulk Specimens of Adhesives*, NPL Measurement Good Practice Guide No 17, National Physical Laboratory, 1998.

Dean, G., Crocker, L., Read, B. and Wright, L. (2004). 'Prediction of deformation and failure of rubber-toughened adhesive joints', *Int. J. Adhesives and Adhesion*, **24**, 295–306.

European Space Agency, (1990). *Adhesive Bonding Handbook for Advanced Structural Materials*, European Space Research and Technology Centre, European Space Agency, Noordwjik, The Netherlands.

Institution of Structural Engineers, (1999). *Guide to The Structural Use of Adhesives*, The Institution of Structural Engineers.

Iosipescu, N. (1967). 'New accurate procedure for single shear testing of metals', *J. Materials*, **2**, 537–66.

Kandil, F.A. (1998). *Measurement of Bending in Uniaxial Low Cycle fatigue Testing*, NPL Measurement Good Practice Guide No 1, National Physical Laboratory.

Kinloch, A.J. (1987). *Adhesion and Adhesives – Science and Technology*, Chapman and Hall, UK.

Kinloch, A.J. and Young, R.J. (1983). *Fracture Behaviour of Polymers*, Applied Science Publishers, UK.

Krieger, R.B. (1975). *Stiffness Characteristics of Structural Adhesives for Stress Analysis in Hostile Environment*, American Cyanamid, Havre de Grace, MD.

Lang, T.P. and Mallick, P.K. (1998). 'Effect of spew geometry on stresses in single lap adhesive joints', *Int. J. of Adhesion and Adhesives*, **18**, 167–77.

de Lange, P.J., Mader, E., Mai, K., Young, R.J. and Ahmad, I. (2001). 'Characterisation and micromechanical testing of aramid-reinforced epoxy composites', *Composites A*, **32**, 331–42.

© Woodhead Publishing Limited, 2010

Moore, D.R., Williams, J.G. and Pavan, A. (2001). *Fracture Mechanics Testing Methods for Polymers, Adhesives and Composites*, European Structural Integrity Society, Elsevier Science, 1st edition.

Mullville, D.R. and Vaishnav, R.N. (1986). 'Interfacial crack propagation', *J. Adhesion*, **7**, 215–33.

Ochsner, A., Stasiek, M., Mishuris, G. and Gracio, J. (2007). 'A new evaluation procedure for the butt-joint test of adhesive technology: determination of the complete set of linear elastic constants', *Int. J. Adhesion and Adhesives*, **27**, 703–11.

Predecki, P., Barret, C.S., Lankford, A.B. and Gutierrez-Lemini, D. (1986). 'Stresses in an adhesive bond at an adhesive/adherend interface under load', *J. Adhesion*, **19**, 207–18.

Sargeant, J.P. (1998). 'Microextensometry, the peel test and the influence of adherend thickness on the measurement of adhesive fracture energy', *Int. J. of Adhesion and Adhesives*, **18**, 215–24.

Weissberg, V. and Arcan, M. (1988). 'A uniform pure shear testing specimen for adhesive characterisation', *Adhesively Bonded Joints: Testing, Analysis and Design, ASTM STP 981*, Johnson W.S. (ed.), American Society for Testing and Materials, Philadelphia, 28–38.

Weitzenböck, J. R. and McGeorge, D. (2005). *BONDSHIP Project Guidelines*.

Williams, J.G., Pavan, A., Blackman, B. (2003). *Fracture of Polymers, Composites and Adhesives II: 3rd ESIS TC4 Conference*, European Structural Integrity Society, Elsevier Science, 1st edition.

© Woodhead Publishing Limited, 2010

# 15
# Advances in testing adhesively bonded composites

J.-Y. COGNARD, ENSIETA, France;
P. DAVIES, IFREMER, France; and
L. SOHIER, Université de Bretagne Occidentale (UBO), France

**Abstract**: This chapter will briefly present the current state of the art with respect to tests for composite assemblies, before describing an improved testing approach. The lap shear test is first examined in detail, through a series of results from tests on glass/epoxy and carbon/epoxy specimens. Numerical modelling is used to show the difficulties in analysing results for this specimen configuration. An original approach is then presented, based on modification of the Arcan test method. This allows the determination of adhesive failure envelopes from tests on metal substrates. The approach is then extended to composite assemblies and test results are given. The chapter concludes with a discussion of future testing requirements.

**Key words**: Arcan, failure envelope, lap shear, numerical model.

## 15.1 Introduction

The use of adhesive bonding has developed considerably in recent years and the pressing requirement for lighter weight in all areas of transportation to reduce energy consumption will inevitably result in more applications. Composite materials are a key element in weight reduction strategies, so assembly of composite modules and connections between composite and metallic structures are of great importance. Several recent books provide up-to-date overviews of this area.[1, 2] However, in spite of an awareness of their significance, tests to characterize assemblies have developed very little since the simple lap shear specimen on bonded metal substrates was standardized in the 1980s.[3] In addition, few of the standard adhesive tests are suitable to characterize composite assemblies as will be shown below. As a result, the lack of appropriate tests may be considered to be one of the factors currently limiting adhesive bonding.

This chapter will present the current state of the art with respect to composite bonding and briefly describe the tests used today. Then in Section 15.3 the lap shear test approach will be examined, through a series of results from tests on glass/epoxy and carbon/epoxy specimens. Numerical modelling will be used to show the difficulties in analysing results for this specimen



© Woodhead Publishing Limited, 2010

configuration. In Section 15.4 a new approach will be presented, based on modification of the Arcan test method. This allows the determination of adhesive failure envelopes from tests on metal substrates. In Section 15.5, extension of the approach to composite assemblies is presented and test results are given. The chapter concludes with a discussion of future testing requirements.

## 15.2 State of the art

### 15.2.1 Adhesively bonded composite design

The use of adhesively bonded composite assemblies is not new; extensive test programmes in the 1970s and 1980s in the aerospace industry recognized the potential of adhesive bonding in metallic structures and provided large material databases such as those of the Primary Adhesively Bonded Structure Technology (PABST) programme.[4] The latter was started in February 1975 for the purpose of validating the concept of adhesive bonding primary fuselage structural members instead of using rivets. Several references treat the subject of composite assembly design; Hart-Smith provides a good overview.[5]

### 15.2.2 Testing bonded composite assemblies

The designer who wishes to assemble composite structures with adhesives needs certain properties. In order to assess the integrity of the adhesive, he or she requires a failure envelope for the adhesive. In addition, provided the composite/adhesive interface remains intact, the designer will need a through-thickness failure envelope to evaluate the delamination resistance of the composite plies close to the adhesive. The standard test methods for adhesive properties, described in Chapter 14, will provide a shear strength from the Thick Adherend Shear test (TAST),[6] but little else. While adhesives are generally designed to work in shear, geometrical features frequently result in a normal stress component and the designer must estimate how this will affect the pure shear strength in order to check the integrity of the assembly. One approach is to use the lap shear test for this. Testing this specimen generates both shear and normal stress components but, as will be shown below, the peel stresses are very localized and analysis of this test to produce a failure envelope is a hazardous exercise. There is a real need for a more reliable approach to identification of the mechanical properties needed for design. The work described below, based on a development of the Arcan test method first proposed in the 1970s[7] and subsequently applied to composites by Jurf and Pipes,[8] is a contribution to this effort. Identification of parameters to characterize through-thickness damage development and failure in composites is an area which has been addressed

© Woodhead Publishing Limited, 2010

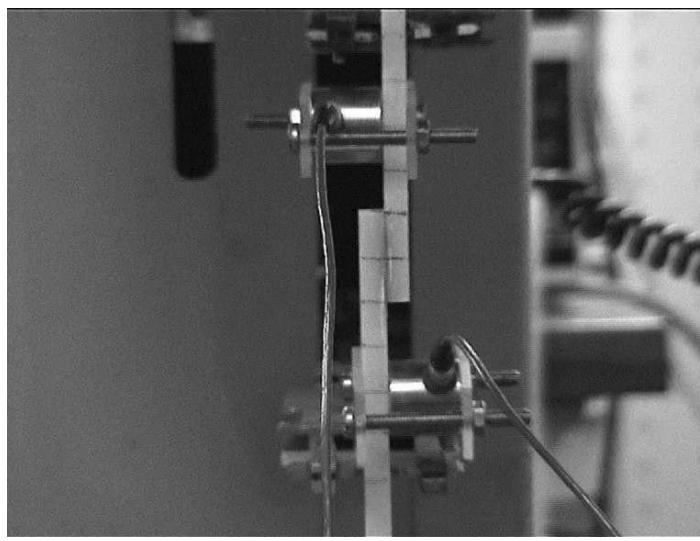
by various authors in recent years[9–11] but has resulted in few standard test methods.

## 15.3 Examples of results from traditional tests of adhesively bonded composites

Given that the lap shear test remains by far the most popular test for providing information on joint performance, it is interesting first to examine what this test measures when composite substrate assemblies are tested. Within a European Network (DOGMA) a series of unidirectional (UD) glass/epoxy samples was tested at IFREMER,[12] in order to provide data to compare to models. Some of the results from the tests are shown below. A second series was performed more recently on UD carbon/epoxy specimens and these results are also provided. These results are then interpreted in terms of stress distributions and the limits of the tests are discussed.

### 15.3.1 Bonded glass/epoxy lap shear tests

Testing a single lap shear specimen is the most frequently used way of evaluating adhesively bonded composite joints today. A series of tests was performed on bonded glass/epoxy specimens (Fig. 15.1) as described in Table 15.1 below.



15.1 Glass/epoxy SLS specimen, 3 mm thick, 20 mm overlap, showing two acoustic emission transducers, above and below the bonded section.

© Woodhead Publishing Limited, 2010

*Table 15.1* Details of glass/epoxy lap shear specimens

| Substrates | Adhesive | Overlap (mm) | SLS width (mm) |
|---|---|---|---|
| 8 layers 300 g $m^{-2}$ quasi-UD E glass, 3 mm thick. Epoxy SR1500/2505, 6h 90°C cure | Redux 420 0.2 mm thick, 4h 50°C cure | 10, 20, 30 | 20 |
| 16 layers same fibres, and resin, 6 mm thick<br>$E_1$ = 25.6 GPa,<br>$T_c$ = 375 MPa<br>$R_c$ = 16 MPa, $S_c$ = 52 MPa | Redux 420 0.2 mm thick, 4h 50°C cure | 20 | 20 |

Figure 15.2 shows the influence of overlap length on failure load. In this range the apparent shear strength (maximum load divided by bonded area) is roughly constant, in the range 20–25 MPa for all specimens.

In order to understand what is happening in these tests, it is important to examine the sequence of events leading to failure. Inspection of fracture surfaces, using optical or scanning electron microscopy (SEM) is ambiguous. These show many features including adhesive deformation, traces of fibres and areas where cracks appear to have run along the adhesive/adherend interface.

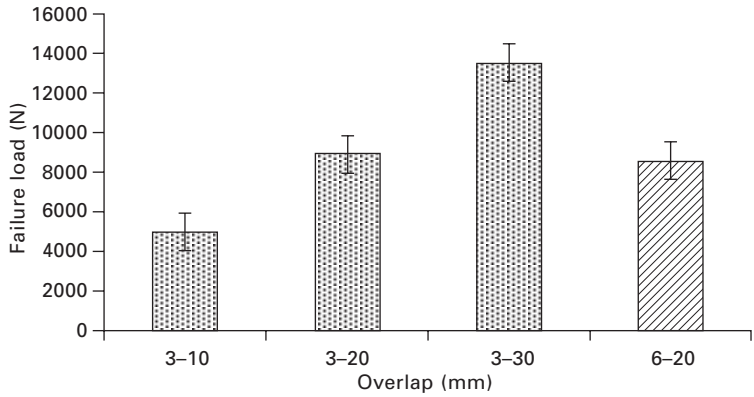
A second series of tests was therefore run on the 6 mm thick 20 mm overlap single lap shear (SLS) specimens under different loads as a percentage of the mean break load $F_r$, stopping the tests after the acoustic emission was recorded but before final failure, to try to determine the nature of the damage. Table 15.2 shows the results.

All the damage detected was within the adhesive bondline, see Fig. 15.3.

This shows that damage is certainly present in the adhesive layer before final failure, in the form of shear cracks which initiate at defects, particularly voids. However, it does not exclude the possibility that damage is also present in the composite. Once the specimen is unloaded, matrix cracks or delaminations will close and it is unlikely that they will be detected by SEM observations. Dye penetrants were used to try to detect such damage but none was found.

These observations highlight the difficulties in analysing what happens in a multi-material specimen with a complex stress state even during quasi-static tests. However, from a practical viewpoint, the plasticity and damage tolerance of tough structural adhesives such as this one result in a more uniform stress state along the joint.

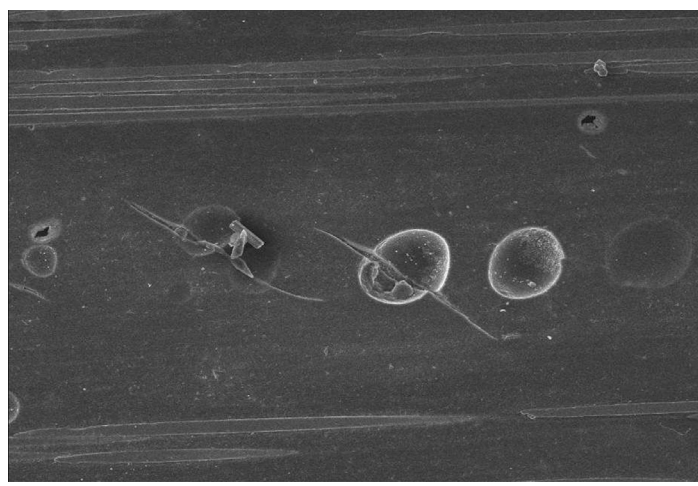
© Woodhead Publishing Limited, 2010




*15.2* Glass/epoxy joints: influence of overlap length for 3 and 6 mm thick substrates described in Table 15.1.

*Table 15.2* SLS tests with acoustic emission recording (AE), shown in Fig. 15.1, stopped at different loads and examined in the SEM (scanning electron microscope)

| Force (kN) | $F_r$ (%) | Non-linearity, force–strain plot (kN) | AE max. (dB) | Surface damage (SEM) | Centre damage (SEM) |
|---|---|---|---|---|---|
| 6 | 68 | Linear | 60 | 1 small | 1 small |
| 7 | 79 | Linear | 75 | None | 1 small |
| 8 | 90 | 7 | 70 | 2 cracks (on voids) | 1 on void |
| 8.5 | 96 | 7.5 | 70 | None | 2 from voids |
| 9.5 | 107 | 7.5 | >90 | Several cracks, both ends of joint | Fillet and interior |



*15.3* Damage within specimen before final failure.

© Woodhead Publishing Limited, 2010

### 15.3.2 Bonded carbon/epoxy lap shear tests

A series of tests was then performed on bonded carbon/epoxy specimens. One example is described in Table 15.3 below.

The mean tensile failure load obtained from tests on four carbon/epoxy specimens was 9.57 kN (standard deviation 0.39 kN). This value is slightly higher than the values obtained on the thicker glass/epoxy specimens with the same overlap (8.93 and 8.55 kN for 3 mm and 6 mm thick substrates, respectively). Failure was again mixed and difficult to interpret: some areas of damaged adhesive were visible, while other regions exhibited debonded fibres, suggesting composite damage. There have been some recent studies addressing the damage development in carbon fibre composite lap shear specimens; Potter and co-workers examined crack propagation during fatigue tests and proposed crack deflection mechanisms to improve joint performance.[13, 14]

### 15.3.3 Numerical analyses of stress distributions

In this section we present the influence of different parameters on the stress distributions through the adhesive thickness and the composite substrate using two-dimensional (2D) finite element simulations. CAST3M FE software was used here and for all the simulations presented throughout this chapter.[15] For simplicity, computations are made assuming linear elastic behaviour of the components and small displacements. The aim is only to analyse the influence of edge effects on the behaviour of SLS specimens at the beginning of loading, before non-linear material and geometrical effects become significant. However, even with these simplifying assumptions, numerical models are needed in order to model perfect interfaces in these multi-material structures. Various previous studies have highlighted the difficulties in obtaining reliable results. References 16–22 are a non-exhaustive selection of studies performed since 2000 which have presented models of this type. With the standard finite element method, based on the variational principle of minimum potential energy whose single variable is the displacement field, the continuity of the displacement field is satisfied but the continuity of the

*Table 15.3* Details of carbon/epoxy lap shear specimens

| Substrates | Adhesive | Overlap (mm) | SLS width (mm) |
|---|---|---|---|
| 4 layers 300 g $m^{-2}$ UD T700, 1.3 mm thick<br>$E_1$ = 110 GPa<br>$T_c$ = 1600 MPa<br>$R_c$ = 16 MPa, $S_c$ = 52 MPa | Redux 420, 0.4 mm thick, 4h 50°C cure | 20 | 20 |

© Woodhead Publishing Limited, 2010

stress vector is not exactly verified. Therefore, refined meshes are also needed near the interface, in order to obtain good numerical results, especially for assemblies with large material heterogeneities.[23] Various simulations have shown that good numerical results are obtained using meshes with 20 linear rectangular elements for a 0.1 mm adhesive thickness. Computations were made in two dimensions (plane stress) on half of the specimen by applying suitable boundary conditions. Results are presented for glass/epoxy and carbon/epoxy substrates assuming orthotropic behaviour; the material parameters for the adhesive joint, whose behaviour is assumed here to be isotropic, are $E_j = 2.0$ GPa and $\nu_j = 0.3$.

The elastic limit equivalent stress $\sigma$ for the adhesive used has been identified experimentally under 2D tension–shear loadings (this will be presented in Section 15.4 below) such that:

$$\sigma_{yy}^2/R_j^2 + \sigma_{xy}^2/S_j^2 = 1 \qquad [15.1]$$

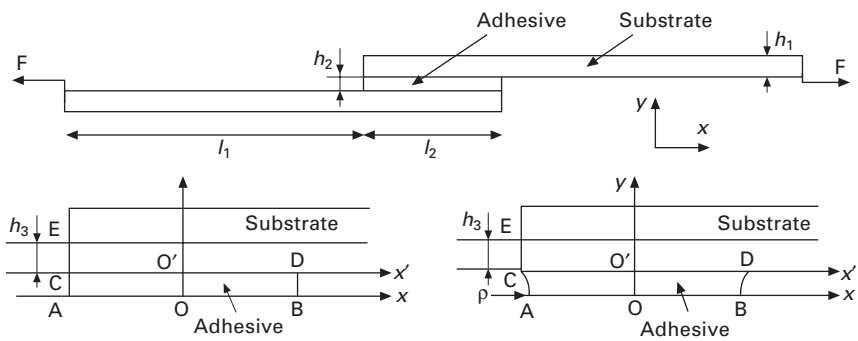
with $R_j = 40$ MPa and $S_j = 25$ MPa.

For the composite substrate the following classical elastic limit equivalent stress is used:

$$\sigma_{yy}^2/R_c^2 + \sigma_{xy}^2/S_c^2 + \sigma_{xx}^2/T_c^2 = 1 \qquad [15.2]$$

Values taken for composite strengths $R_c$ (interlaminar tensile), $S_c$ (interlaminar shear) and $T_c$ (in-plane tensile) are given in Tables 15.1 and 15.3.

Two geometries of the free edges of the adhesive joints are used in order to emphasise the influence of this geometrical parameter (straight edges and cleaned edges, see Fig. 15.4). Other geometries can be used to limit the edge effects,[24, 25] but the two geometries examined here are associated with constant thickness of the adhesive joint (a modification of the adhesive thickness can change the mechanical behaviour of the joint). Another important parameter



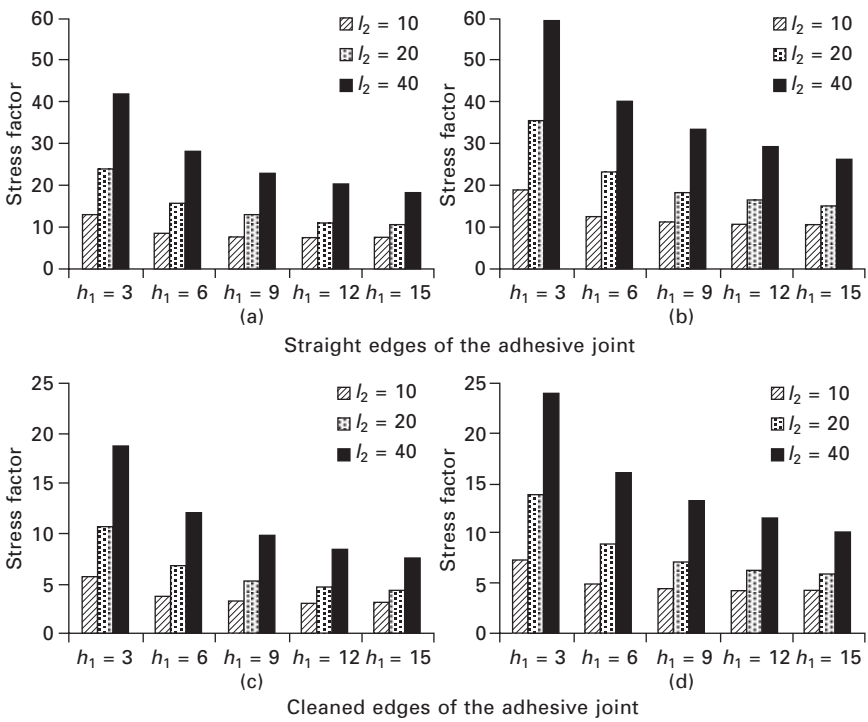

*15.4* Geometry of the single lap shear specimen.

© Woodhead Publishing Limited, 2010

is the overlap length, which influences the stress distribution in the adhesive joint. With the assumptions proposed above, the problem to be solved is linear; thus the stress state in the SLS can be normalized in order to obtain a constant average shear stress.

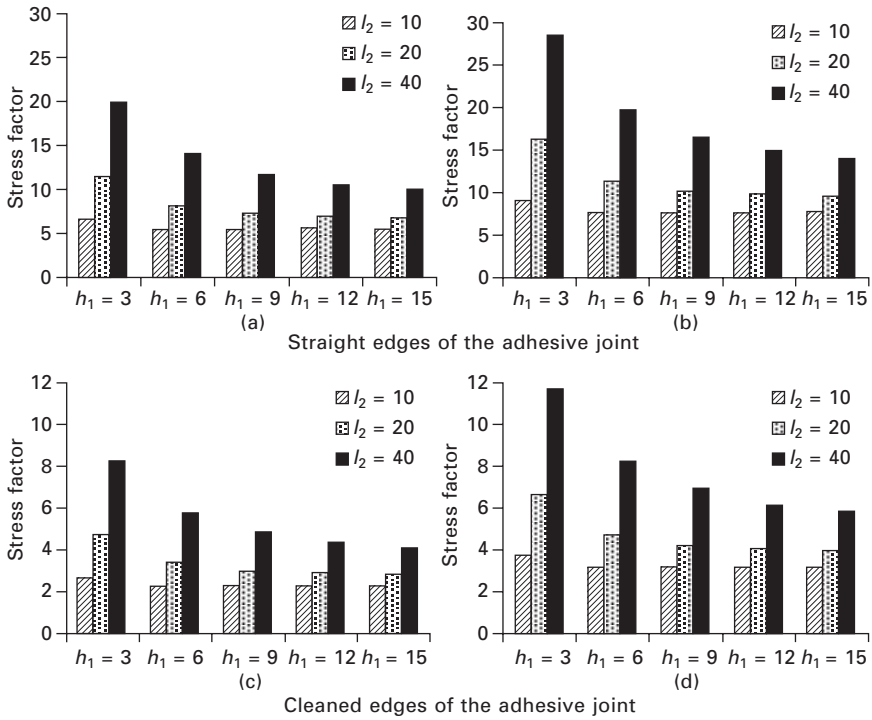
Results are presented for an adhesive joint thickness of $h_2 = 0.4$ mm, $h_1 = 80$ mm, different thicknesses of the substrates ($h_1 = 3, 9, 12, 15$ mm), different overlap lengths ($l_2 = 10, 20, 40$ mm) and for the two materials used as substrates. For the different 2D simulations, the cleaned edges are defined by the following relationship for the radius of curvature $\rho$: $\rho = 0.75 \times h_2$ (Fig. 15.4).

Figures 15.5 and 15.6 present the so-called stress factor, which is the maximum value of the equivalent stress in the component considered (adhesive or substrates) normalized with respect to the mean value. A stress factor lower than 1 indicates that the most highly stressed regions of the joint are not close to the free edges (i.e. that the edge effects are low). Note that an increase in the overlap length or a decrease in the thickness of the substrates lead to an increase in stress factor. Moreover, edge effects are lower for carbon than for glass with the same thickness, which can be explained by




*15.5* Influence of different geometric parameters in glass/epoxy substrates. (a) (c), adhesive joint, (b) (d) composite substrate.

© Woodhead Publishing Limited, 2010

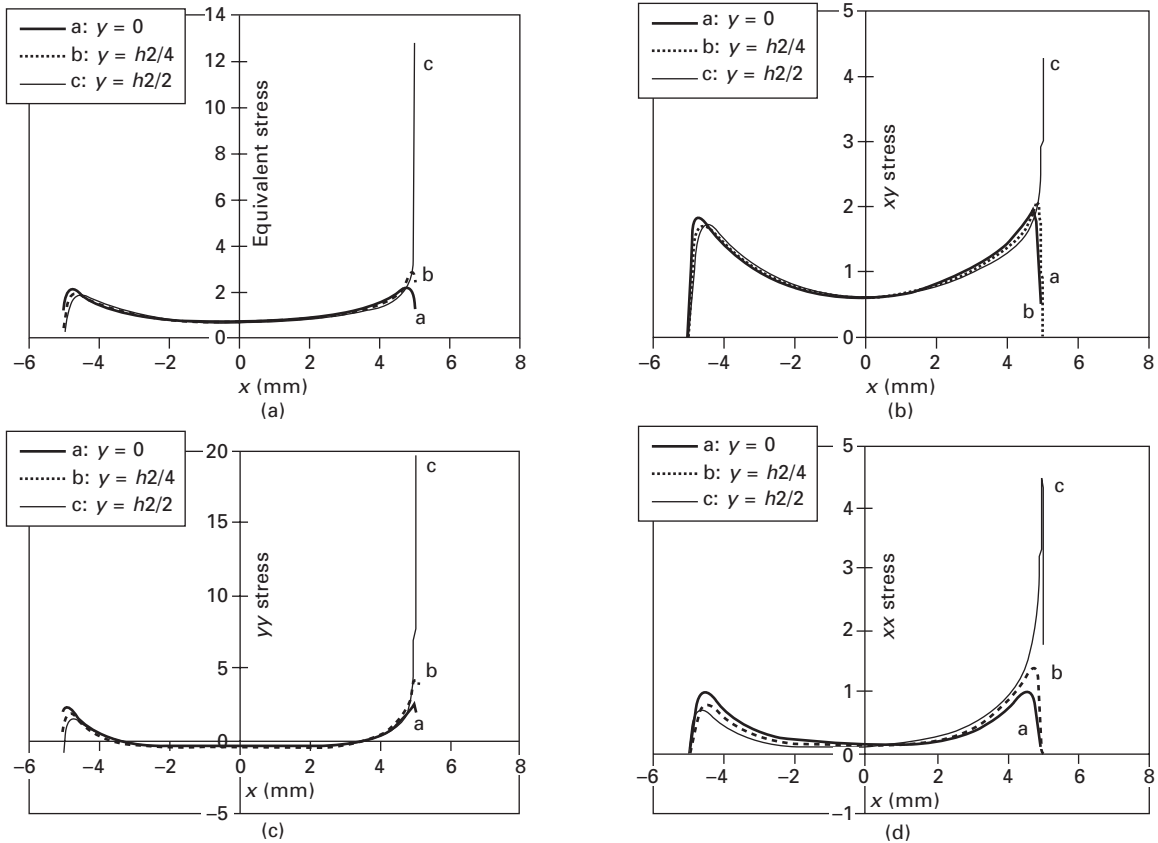



*15.6* Influence of different geometric parameters for carbon/epoxy substrates. (a) (c), adhesive joint; (b) (d), composite substrate.

the influence of the material on the stiffness of the substrates. The results from tests (Fig. 15.2) indicate that doubling the overlap area does not result in doubling the failure load, which only increased in those tests by a factor of 1.8

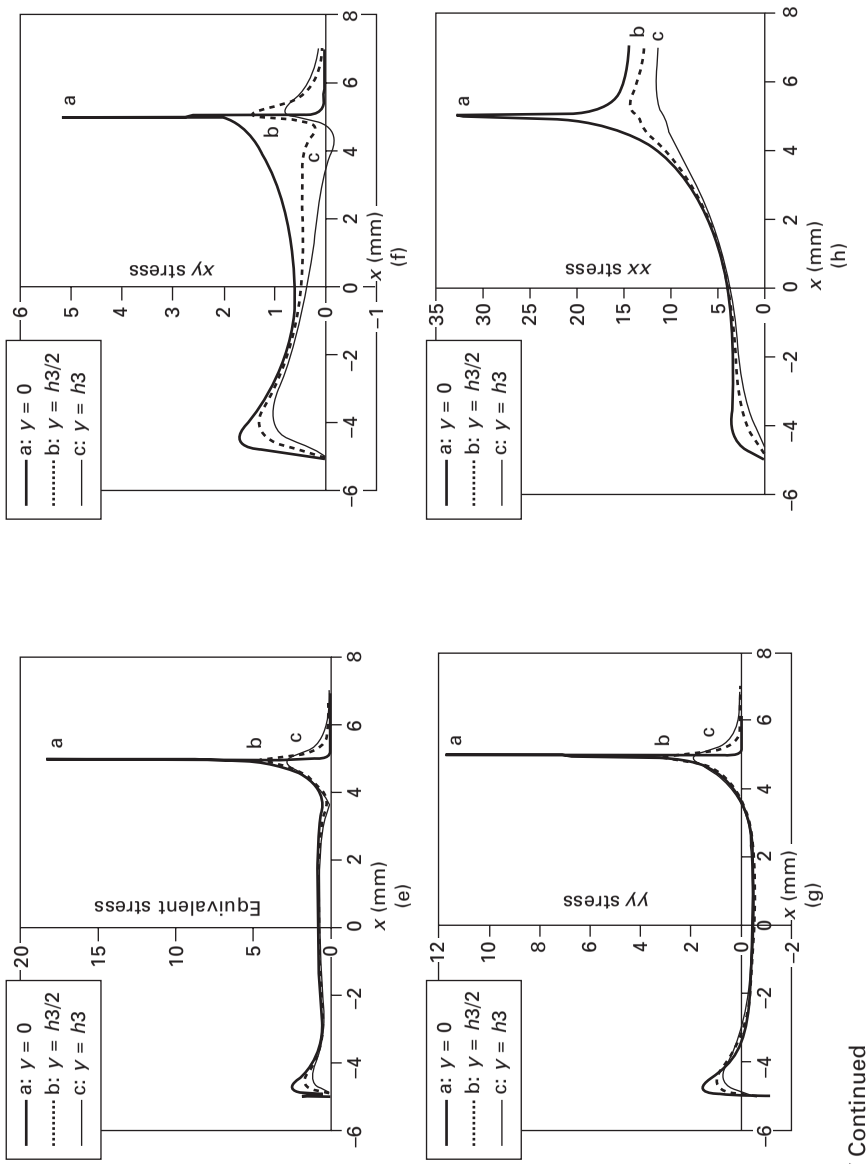
Figure 15.7 presents the stress distribution in the adhesive joint (a)–(d) and in the composite substrate (e)–(h). The parameter $h_3$ in Fig. 15.4 is taken as $h_2$ here and varied in order to examine the stress gradient close to the interface in the substrate. Results are presented for different lines with respect to the position $y$ in the adhesive joint ($y = 0$ is the mid-plane of the adhesive and $y = h_2/2$ corresponds to a line close to the adhesive–substrate interface) extrapolated to the node point next to the interface. For the composite substrate, results are only presented for a thickness of $h_1 = 3$ mm and an overlap of $l_2 = 10$ mm. It is important to note that, for the adhesive, the edge effects are mainly associated with a strong evolution of the normal stress, close to the free edge of the adhesive near the adhesive–substrate interface; this result can be explained by the boundary conditions. For the substrate, there are also large edge effects close to the substrate–adhesive interface; moreover for the substrate, the stress component $s_{xx}$ is not equal to zero close

© Woodhead Publishing Limited, 2010




*15.7* Normalized stress distribution on the adhesive joint (a)–(d) and the composite substrate (e)–(h) (glass substrate; $h_1$ = 3 mm; $l_2$ = 10 mm; straight edges)

© Woodhead Publishing Limited, 2010

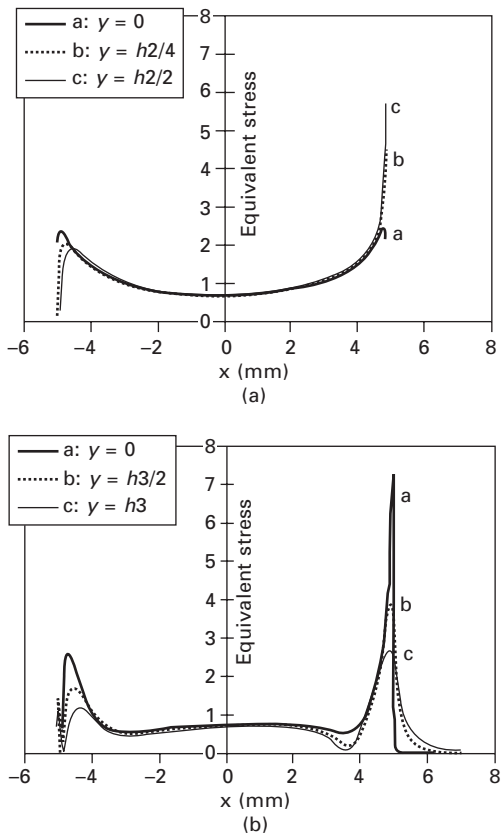



*15.7* Continued

© Woodhead Publishing Limited, 2010

to point D (Fig. 15.4) associated with the loading of the specimen, but this stress component has only a small influence on the equivalent stress as it acts in the fibre direction.

Figure 15.8 presents the evolution of the equivalent stress for the case of cleaned edges in the adhesive joint. As presented in Fig. 15.6, this geometry leads to strong reductions in edge effects with respect to straight edges and the levels of the equivalent stress are similar for the adhesive and for the composite substrate. These results underline that the geometry of the free edges of the adhesive has a strong influence on the edge effects; but it would be difficult to cancel out the edge effects by simply modifying the geometry of the adhesive free edges for SLS specimens. In practice, manufacturing SLS adhesive joints often leads to geometries with a blend radius close to the free edges of the adhesive joint. Thus, the maximum values of the equivalent stress




*15.8* Stress distribution of the adhesive joint (a) and the composite substrate (b) (glass substrate; $h_1$ = 3 mm; $l_2$ = 10 mm; cleaned edges).

© Woodhead Publishing Limited, 2010

are likely to be similar for the adhesive joint and the substrates. Therefore degradation starts close to the most stressed point (point D, Fig. 15.4) and can propagate either in the adhesive or in the composite.

Numerically, it is quite difficult to analyse such problems because it is necessary to use non-linear models with a reliable failure criterion and reliable interlaminar strength data. Moreover, it is difficult to modify the geometry of the substrates close to point D in order to limit the edge effect. An alternative strategy is to propose an experimental fixture which intrinsically promotes low edge effects for testing adhesively bonded assemblies, in order to prevent crack initiation close to the free edges of the adhesive. In the following, such a fixture is proposed.

## 15.4 Modified Arcan test

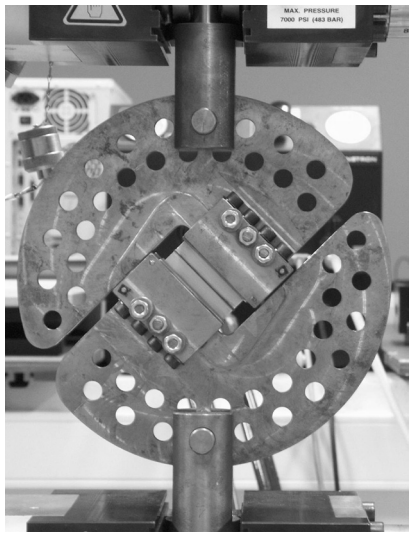
As shown in the previous section, edge effects can be very large for adhesively bonded assemblies and thus a key point in analysing the behaviour of such assemblies is to propose experimental fixtures which limit the stress singularities, in order to determine the influence of the material behaviour, rather than the response of the structure. This section presents the main properties of a methodology developed in order to obtain a 'reliable' characterization of the behaviour of adhesives in an assembly. Some experimental results are then shown for one structural adhesive.

### 15.4.1 Test development

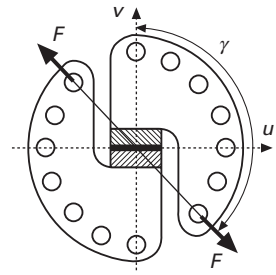
In order to be able to study the behaviour of the adhesive as a function of the normal stress component, a modified Arcan fixture has been developed, which enables compression or tension to be combined with shear loads (Fig. 15.9). Numerical simulations in linear elasticity, for bi-material structures show that the use of a special geometry for the substrate (a beak close to the adhesive joint) makes it possible to limit the contribution of the singularities caused by edge effects.[26] Moreover the system fixing the substrates to the supporting fixture has been optimized in order to prevent preloading of the adhesive joint.[27]

To preserve the simplicity associated with the Arcan fixture,[7] and the use of a standard tensile testing machine, a specimen with rectangular section ($10 \times 66$ mm$^2$) was selected. This experimental fixture that is associated with a non-contact extensometry system based on image correlation allows us to analyse, for radial loadings, the non-linear behaviour of an adhesive joint. The results for the epoxy adhesive Huntsman™ Araldite® 420 A/B[28] will be shown here as an example.

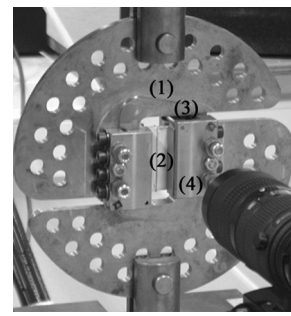
© Woodhead Publishing Limited, 2010



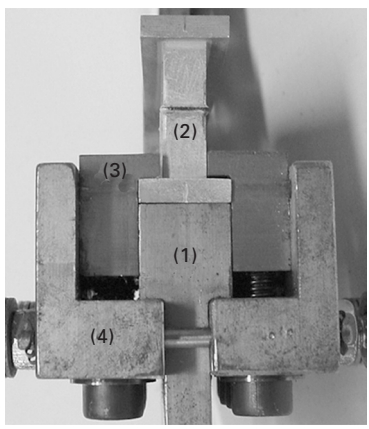

(a)



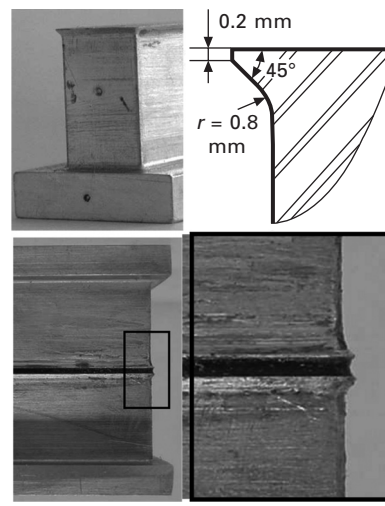

(b)




(c)




(d)




(e)

*15.9* Arcan fixture and geometry of the substrates with beak. (a) Modified Arcan fixture; (b) principle; (c) shear loading; (d) specimen mounting: 1, Arcan fixture support; 2, bonded specimen; 3, clamping system; 4 clamping system support; (e) geometry of substrates.

© Woodhead Publishing Limited, 2010

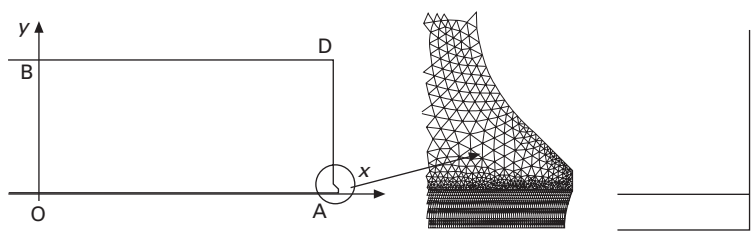
## 15.4.2 Numerical validation

Determination of the stress distributions through the thickness of the adhesive joint allows us to analyse the stress singularities. Computations were made in 2D (plane stresses) on half of the specimen by applying adequate boundary conditions. Results are presented for both aluminium substrates (Young's modulus: $E_a$ = 80 GPa, Poisson's ratio: $\nu_a$ = 0.3) and steel substrates ($E_s$ = 220 GPa, $\nu_s$ = 0.3); the material parameters for the adhesive joint are: $E_j$ = 2.2 GPa, $\nu_j$ = 0.3.

The geometry of the specimens designed for the modified Arcan fixture is presented in Fig. 15.10 (OA = 32.5 mm, OB = 15 mm). The boundary conditions of the computation are anti-symmetric on the segment [OA], in order to model only half of the structure, and prescribed displacements on the upper bound of the substrate [CD] (in the *y*-direction for tensile loading and in the *x*-direction for shear loading).

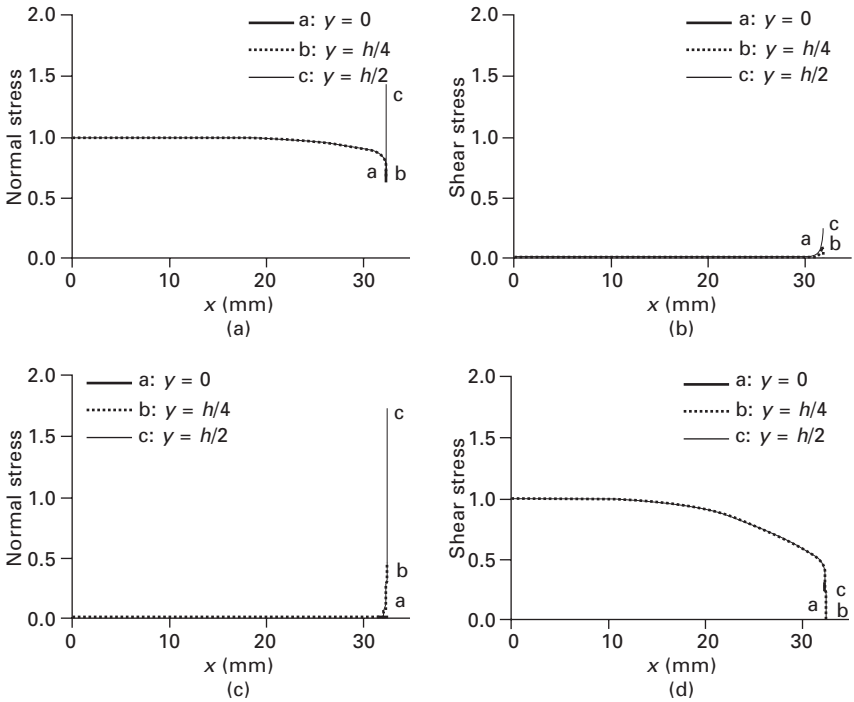
It has been shown that, in the case of elastic behaviour, the relative elastic properties of the materials, the geometry of the substrate close to the edge of the joint and the local geometry of the joint near the free edge are important parameters needed to limit the stress singularities of adhesively bonded joints. Results are presented for two geometries. On one hand the geometry which has been designed for the modified Arcan fixture with a beak on the substrate and cleaning of the free end of the adhesive joint before curing (geometry 'a', Fig. 15.10) and, on the other hand, without a beak on the substrate and a straight edge of the adhesive (geometry 'b', Fig. 15.10). The latter geometry is the one used for the TAST specimen.

Results presented in Figs. 15.11 and 15.12, for a thickness of the adhesive joint of $h$ = 0.4 mm, show that the use of a beak can limit the stress singularities near the free edge of the adhesive. Figure 15.11 presents the stress distribution in the adhesive joint for tensile and shear loadings. Results are presented on different lines with respect to the position $y$ in the adhesive joint ($y$ = 0 is the middle plane of the adhesive and $y = h/2$ corresponds to a line close to the adhesive–substrate interface). It is important to note that the edge effects are mainly associated with a strong evolution of the normal




*15.10* Model and different geometries near the edge of the joint.

© Woodhead Publishing Limited, 2010




*15.11* Stress distribution for geometry 'b': (a), (b) tensile loading; (c), (d) shear loading.

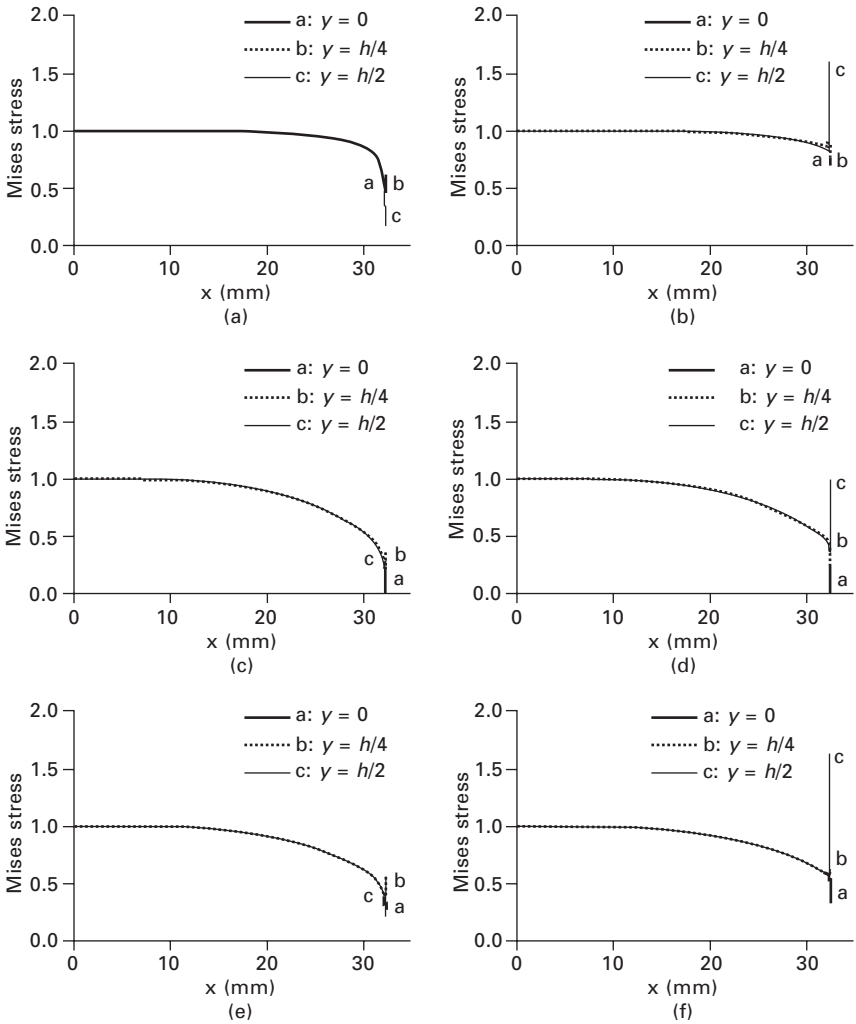
stress, close to the free edge of the adhesive; this result can be explained by the stress boundary conditions.

Figure 15.12 presents the evolution of the von Mises equivalent stress for different loadings: tensile ($\gamma = 0°$, Fig. 15.9b), shear ($\gamma = 90°$) and tensile-shear ($\gamma = 45°$). In order to make the comparisons of stress states easier, the equivalent von Mises stress has been normalized to one at the centre of the adhesive joint.

These results underline the strong influence of the local geometry of the joint near the edge on the stress singularities. The geometry proposed for the modified Arcan test, with a beak and cleaning of the adhesive before curing, limits the edge effects significantly. A comparison of the experimental results in shear from the standardized TAST fixture[6] and those obtained with the modified Arcan fixture for shear loadings underlines the influence of the edge effects on the analysis of the adhesive behaviour.[23] Moreover analysis of some aspects of the non-linear behaviour of the adhesive has been performed on the stress distribution in the adhesive joint.[23]

For geometry '*b*', the zones close to the interfaces are the most highly stressed regions of the joint. These results can explain why cracks appear in that area, as can be observed, for instance, in the case of TAST specimens.

© Woodhead Publishing Limited, 2010




*15.12* Influence of geometry and loading: (a), (b) tensile loading; (c), (d) shear loading; (e), (f) tensile–shear loading; (a), (c), (e) geometry 'a'; (b), (d), (f) geometry 'b'.

It has been shown that for adhesives with plastic behaviour, large stress singularities, computed under elastic behaviour, lead to localization of plastic zones close to the adhesive–substrate interface near the free edge of the adhesive which may also result in crack initiation.[23] It is important to note that the adhesive–substrate interface is often the weakest part of the assembly, either due to defects on the surface or to local variations in chemistry[29] and that it is difficult to analyse the non-linear behaviour of the adhesive starting from experiments with crack propagations.

© Woodhead Publishing Limited, 2010

For the modified Arcan test, steel substrates generate higher edge effects than aluminium ones and an increase of the joint thickness also leads to an increase of the edge effects. More detailed results can be found in Cognard.[30]

Figure 15.12 also underlines the influence of the loading on the stress distribution in the middle plane of the adhesive joint, for computations performed using linear behaviour of the constituents. Under the assumptions of the calculation, the maximum values of the components of the stress are obtained from the finite element results and from the average stress obtained based on the loads measured during the experimental test and the section of the adhesive plane ($S_c$):

$$\sigma_{n\ maxi} = 1.12\ \sigma_{n\ average} \quad \text{with} \quad \sigma_{n\ average} = F_N/S_c \qquad [15.3]$$

$$\sigma_{t\ maxi} = 1.29\ \sigma_{t\ average} \quad \text{with} \quad \sigma_{t\ average} = F_T/S_c$$

where $F_N$ and $F_T$ are the components of the applied load respectively in the normal and tangential directions in the mean plane of the adhesive joint.

Moreover, as a non-uniform evolution of the stress state in the adhesive joint is observed, it is necessary to use inverse techniques in order to identify the parameters of the material behaviour model for the Arcan test.[6]

### 15.4.3 Example of failure envelope for an epoxy adhesive

The experimental results which are presented in the following were obtained with aluminium alloy (2017) substrates and with the epoxy resin Huntsman™ Araldite® 420 A/B, using simple preparation of surfaces (abrasion with 120 grade paper) and cure at a low temperature (techniques used in boatyard environments). The adhesive is left for 12 hours at 20°C after assembly on aluminium substrates then cured at 50°C for 4 hours; the thickness of the adhesive joint was 0.4 mm, obtained using a special calibrated fixture, and an imposed displacement rate of 0.5 mm $min^{-1}$ (crosshead of the tensile testing machine) was used. The relative displacements of both ends of the adhesive joint in the normal and tangential directions are denoted by $D_N$ and $D_T$ respectively in the mean plane of the adhesive joint.

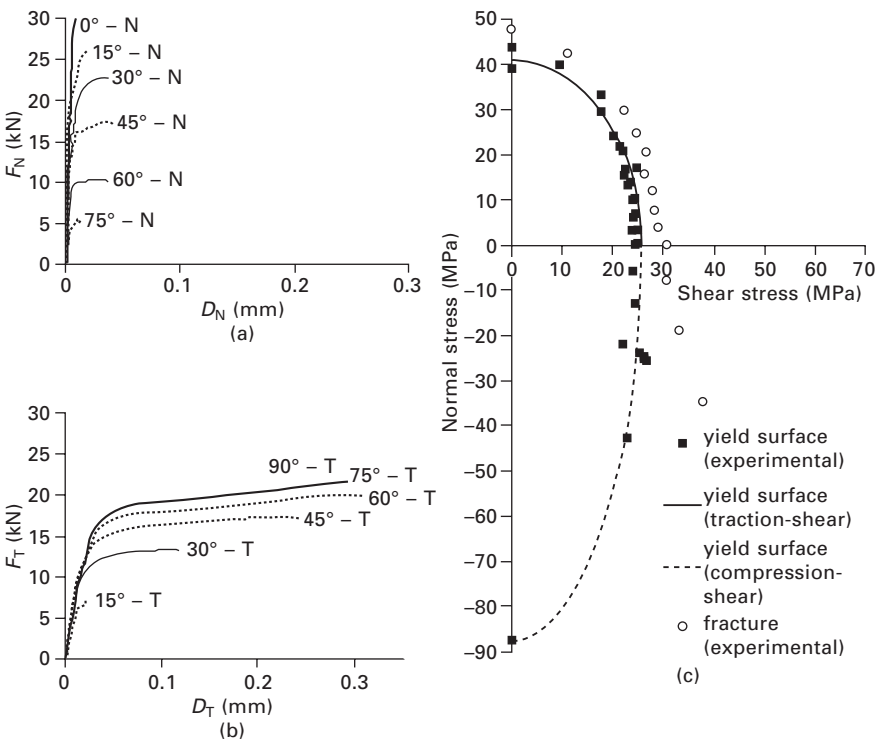
Elastoplastic behaviour can be seen under monotonic loading. Under cyclic loading with increasing load and under more complex loadings, viscoplastic behaviour of the adhesive joint can be detected. Results can be found in Cognard *et al.*[31] It is also important to note that the normal component ($D_N$) of the displacement of the adhesive is much lower than the tangential component ($D_T$) (of the order of 1:20 in compression-shear (135°) and 1:10 in tension-shear (45°)). For monotonic loadings, elastoplastic behaviour with isotropic hardening allowed the experimental results to be represented accurately.[31]

© Woodhead Publishing Limited, 2010

Figures 15.13(a) and 15.13(b) present, with respect to the angle of the loading (Fig. 15.9) to the normal of the main plane of the adhesive, the behaviour of the adhesive in the load–displacement diagram for tension–shear monotonic loading (curves are marked by the angle).

The strength envelopes, presented in Fig. 15.13(c) have been obtained from monotonic loading tests. For each angle, between 5 and 10 tests have been performed. An inverse identification procedure allows us to determine the fracture envelope and the so-called yield surface associated with the experimental parameters.

The behaviour observed for the fracture envelope is interesting, the strength (based on maximum stress) under normal tension is higher than that under shear loading. Compression increases the shear stress of the adhesive joint at failure significantly, which is very important for underwater applications. Examination of fracture surfaces shows an adhesive (at the adhesive–substrate interface) and cohesive (within the adhesive) type failure when the normal




*15.13* Experimental results for tension–shear tests for monotonic loadings; $v$ = 0.5 mm min$^{-1}$ and tension/compression–shear fracture and 'elastic' envelopes, Huntsman™ Redux 420. Behaviour in (a) the normal direction; (b) the tangential direction; (c) elastic yield and fracture envelope.

© Woodhead Publishing Limited, 2010

stress is dominant and a mixed-cohesive type failure (failure at interfaces linked by cracks through the adhesive perpendicular to the mean plane) when the shear stress is dominant. For practical use of the strength envelope in terms of stresses it may be more useful to determine the 'elastic' domain (yield surface) in the case of monotonic loading; this is plotted with the maximum stress values computed under elastic assumptions (Equation 15.1).

## 15.5 Characterization of composite assemblies with the modified Arcan test

Having shown that the modified Arcan fixture can provide a failure envelope for the adhesive, the next step is to apply this test to a composite assembly. This will be described in three sections. First the test set-up will be described briefly, then numerical analysis will be presented and finally some test results will be discussed.

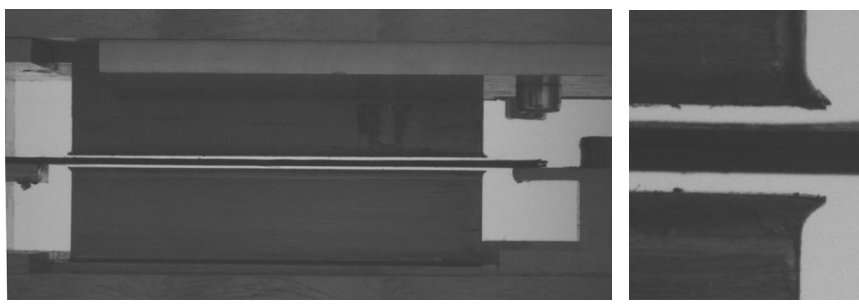
### 15.5.1 Experimental fixture

To analyse the behaviour of mixed assemblies, that is a metal–adhesive–composite–adhesive–metal assembly, the experimental procedure was adapted.[32] To ensure correct positioning of the substrates and composite plate, an assembly fixture was developed (Fig. 15.14). The Arcan fixture can then be used directly (Fig. 15.15).

Figure 15.16 presents the geometry proposed for testing of these mixed bonded assemblies. Substrates with beaks are used to limit the edge effects.

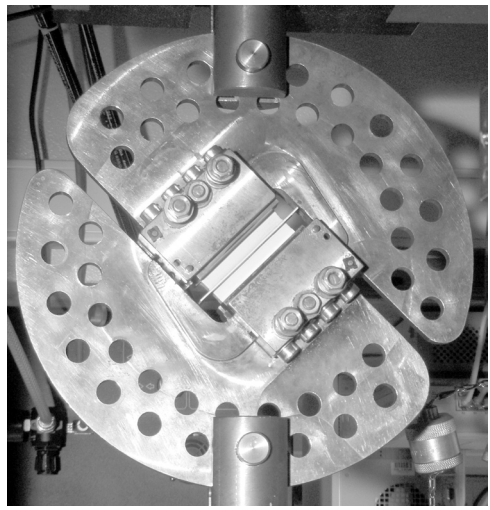
### 15.5.2 Numerical analysis of stress distribution

In order to analyse the possibilities of the proposed experimental test some numerical simulations have been performed using a linear elastic assumption for the different components, taking into account the previously used

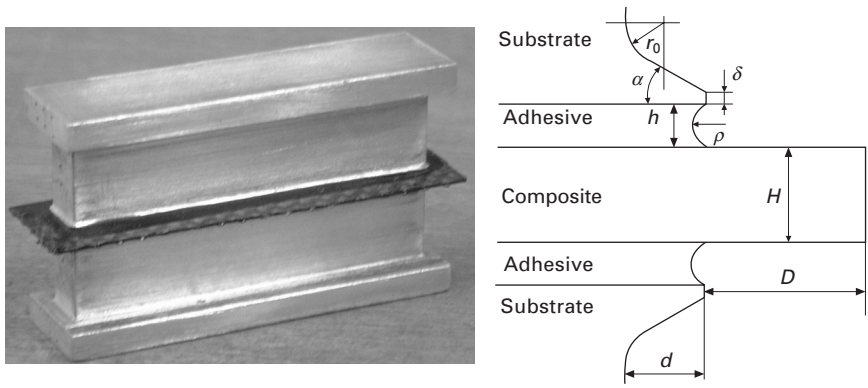


*15.14* Bonding fixture for mixed assemblies with composites.

© Woodhead Publishing Limited, 2010



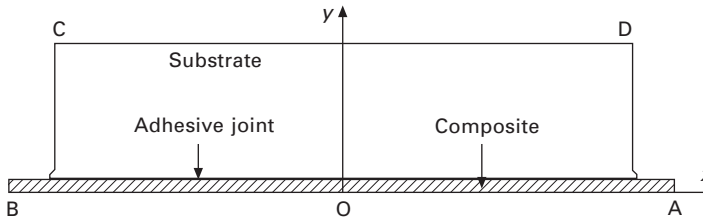
*15.15* Experimental fixture with mixed bonded assembly (tensile–shear loading).




*15.16* Geometry of the mixed bonded assembly.

equivalent limit stress of the adhesive and the unidirectional carbon/epoxy composite (Table 15.3). As presented in the previous section computations are made in 2D (plane stresses) on half of the bonded specimen (i.e. one substrate, one adhesive joint and half of the composite plate), using adequate boundary conditions on segment [AB], Fig. 15.17. The loading is prescribed on segment [CD]. In order to obtain precise numerical results, meshes with 20 linear rectangular elements for each 0.1 mm thickness, of both adhesive and composite, are used, so there is a very large number of elements through the thickness direction.

© Woodhead Publishing Limited, 2010




*15.17* Model used for numerical simulations.

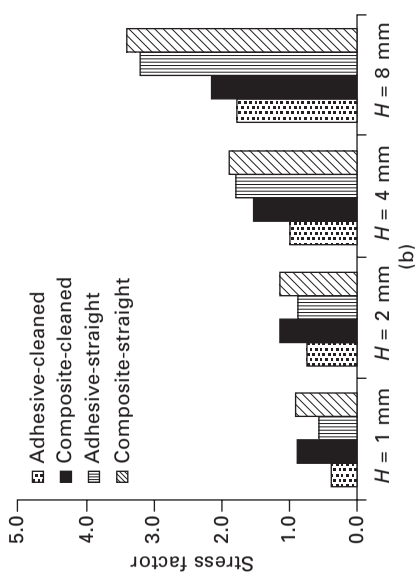
Figure 15.18 presents results for two different free edges of the adhesive (straight edges, $\rho = 0.75 * h$ and cleaned edges, $\rho = \infty$; Fig. 15.16), and for three different loadings (tensile, $\gamma = 0°$; shear, $\gamma = 90°$ and tensile-shear, $\gamma = 45°$). The other geometric parameters are: $\alpha = 30°$, $r_0 = 0.8$ mm and $d = 0.5$ mm (Fig. 15.16).

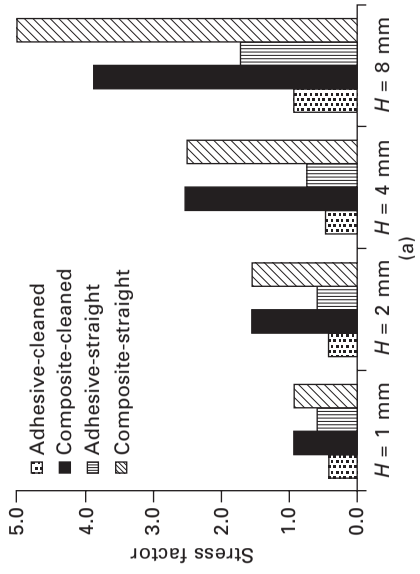
As the problem to be solved is linear, results can be normalized in order to obtain the equivalent stress at the centre of the adhesive equal to one; Table 15.4 presents the associated value of the equivalent stress at the centre of the composite for the three loadings. Thus, without taking into account the influence of the edge effects, one can note that with this pair of materials (adhesive and composite), the non-linear behaviour (and perhaps failure) will start first in the adhesive for shear loadings and in the composite with tensile–shear and tensile loadings (the non-linear behaviour starts when the equivalent stress reaches one with our notation). Therefore, for this pair of materials, the proposed test cannot be used to analyse the behaviour of the composite under shear loading.

The second step is to analyse the influence of edge effects on the equivalent stress for the adhesive and for the composite. Figure 15.18 presents the stress factor for different composite thicknesses and for the two geometries of the free edges of the adhesive. It may be noted that to limit the edge effects in both the adhesive joint and the composite plate it is necessary to use a thin adhesive joint ($2h = 0.2$ mm) and a thin composite plate ($2H = 1$ mm).

Figure 15.19 presents the evolution of the equivalent stress in the thickness of the adhesive and the composite for a tensile loading. Since the solution is symmetric with respect to the $y$ axis for such loadings, results are only shown for $x > 0$ (Fig. 15.17). Moreover, as the evolution of the equivalent stress through the thickness of the adhesive and the composite is quite small far from stress singularity points, only the maximum and the minimum values of the equivalent stress are drawn for a given abscissa $x$. It may be noted that the edge effects are quite low for a composite plate of 1 mm thickness while for a composite plate of 8 mm thickness the edge effects are more important in the adhesive joint than in the composite.

© Woodhead Publishing Limited, 2010







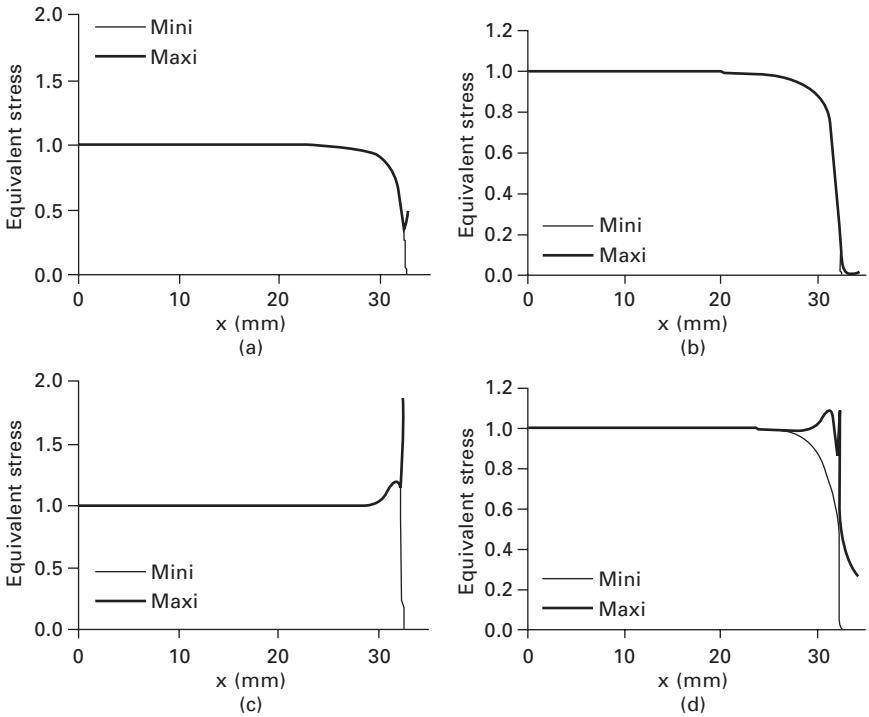



*15.18* Edge effect for mixed bonded assemblies. (a) Shear loading, $h = 0.2$ mm; (b) tensile shear, $h = 0.2$ mm; (c) tensile loading, $h = 0.2$ mm; (d) tensile loading, $h = 0.4$ mm.

© Woodhead Publishing Limited, 2010

*Table 15.4* Maximum value of the equivalent stress at the centre of the specimen

| | Shear | Tensile–shear | Tensile |
|---|---|---|---|
| Adhesive | 1 | 1 | 1 |
| Composite | 0.49 | 1.39 | 2.50 |

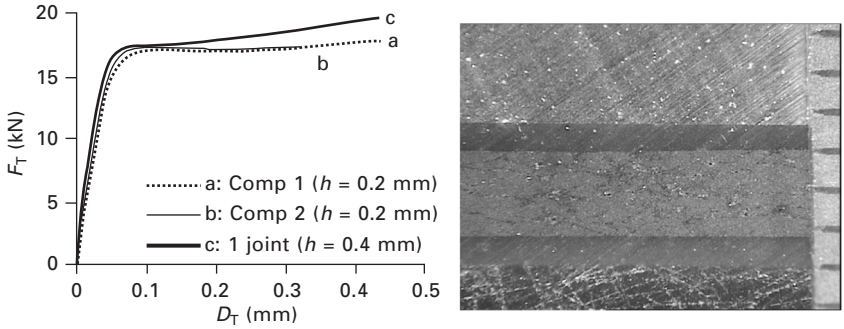



*15.19* Tensile loading for straight edges ($h$ = 0.2 mm). (a), (c) adhesive; (b), (d) composite; (a) (b) $H$ = 1 mm; (c), (d) $H$ = 8 mm.

## 15.5.3 Experimental results for UD carbon/epoxy composite

The UD carbon/epoxy composites, which were presented in Section 15.3, have been used to validate the proposed test. Adhesive joints with a thickness of 0.2 mm have been used to limit the edge effect. Figure 15.20 presents experimental results for shear loading tests (two results are presented: Comp 1 and Comp 2). For these tests we obtain a failure of the adhesive close to the adhesive–substrate interface as predicted by the numerical analyses. Figure 15.20 also presents the experimental result for a test without the composite but with a joint thickness of 0.4 mm (one joint). Note that the global behaviour of the two different tests are quite similar, in fact the most loaded part of the

© Woodhead Publishing Limited, 2010




*15.20* Experimental results for shear loadings. The photo shows a section through the specimen, with failure at the adhesive/aluminium interface (bottom of photo), scale graduations 0.5 mm

assembly is the adhesive. But there are four interfaces with the composite layer present and only two without the composite plate.

Figure 15.21 shows results for tensile tests which are associated with fracture in the composite plate.

Figure 15.22 presents results for tensile-shear loading tests which are also associated with fracture in the composite. Similar results to those from the tensile tests are observed. Tests in which the composite plate was replaced by an aluminium plate (of nearly the same thickness) make it possible to estimate the deformation of the composite plate. More work is needed in order to analyse the evolution of the deformation and damage development in the composite.

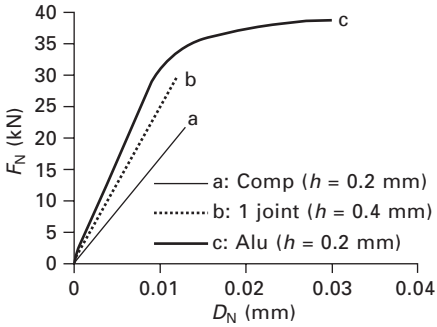
Moreover, Figs. 15.20 and 15.22 underline that the scatter in the experimental results is quite low for tests on mixed bonded assemblies with composites when experimental conditions are carefully controlled. The scatter in results tends to be lower than that found in those from conventional joint tests, such as those shown in Fig. 15.2.

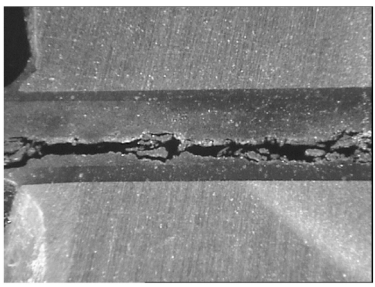
## 15.5.4 Industrial applications

Following the development of the modified Arcan test on unidirectional composites the test has been applied to a number of more realistic sequences used in industrial applications. One example will be briefly described, concerning the design of racing yachts; for this application, adhesive bonding of the mainsail rail to the composite mast would limit the use of mechanical fastening, which requires drilling a large number of holes in the structure, Fig. 15.23 (typically every 50 mm). This would result in both a weight gain and elimination of potentially damaging stress concentrations.

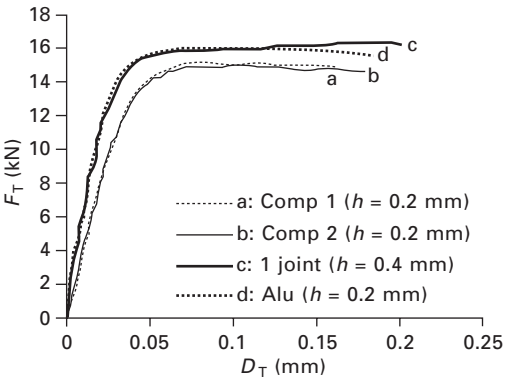
This is a complex problem; masts may be over 30 m long so bondline thickness variation, surface treatments and a range of loading conditions

© Woodhead Publishing Limited, 2010



*15.21* Experimental results for tensile loadings. The photo shows a section through a specimen, failure within the composite.




*15.22* Experimental results for tensile–shear loadings.





*15.23* Mainsail rail and detail of mechanical fasteners.

must be considered. The interface between the composite and the aluminium is particularly important.

In order to increase the loads transmitted by such hybrid bonded assemblies, an optimization of the design of the composite based on resistance to delamination under out-of-plane loadings has to be performed. In one recent

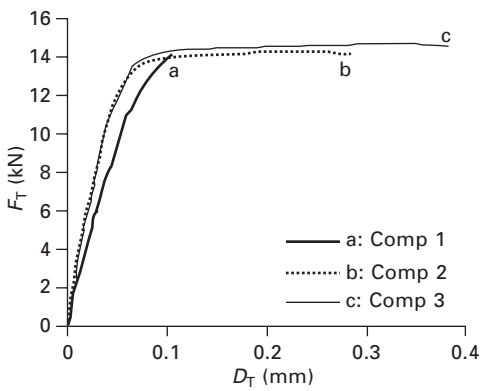
© Woodhead Publishing Limited, 2010

study, a range of materials and interfaces have been examined. One example of the results is shown below, three multidirectional composite plates, manufactured by a boatyard with different peel plies, have been tested with the modified Arcan fixture under tensile–shear loadings. These results (Fig. 15.24) underline that the proposed test is able to analyse the behaviour of thin composite plates under out-of-plane loadings. More work is underway to clarify the role of composite failure mechanisms in mixed joints.

## 15.6 Conclusion and future trends

Although adhesives and bonding technology have developed considerably in recent years there are few appropriate test methods available to characterize their non-linear response. The widely used lap shear geometry can only be used to provide qualitative information on surface treatments or to compare adhesives. In order to address this problem and to obtain the data needed to design adhesively bonded assemblies, a modified Arcan test has been developed. This was first applied successfully to simple metallic assemblies; here a new version is presented which enables composite/metal assemblies to be characterized, which is of direct interest in industrial applications. Numerical analysis and test results are presented which suggest that this approach may also lead to a better understanding of out-of-plane composite strengths. However, further studies, both numerical and experimental, are needed if reliable interlaminar damage development and strength data are to be obtained. The results to date have mainly focussed on unidirectional composites, tests have been performed on multidirectional materials but the analysis needs to be extended to these.

New material developments such as through-thickness reinforcements offer great potential for improving joint efficiency. However, unless more




*15.24* Experimental results for different multidirectional composites under tension–shear loadings, (h = 0.4 mm).

© Woodhead Publishing Limited, 2010

effort is directed towards the characterization of these new systems they will remain underexploited. The work described here is part of this effort. Studies in progress are directed towards understanding and quantifying durability,[33] another critical issue in adhesively bonded joint optimisation.

## 15.7 References


1. Adams RD. *Adhesive bonding: Science, Technology and Applications*, Woodhead Publishing, Cambridge, UK, 2005.
2. Tong L and Steven GP. *Analysis and Design of Structural Bonded Joints*, Kluwer Academic, Boston, 1999.
3. *ASTM Standard Test Method for Apparent Shear Strength of Single Lap Joint Adhesively Bonded Metal Specimens by Tension Loading (metal-to-metal)*, D1002, 1994.
4. Potter DL, *Primary Adhesively Bonded Structure Technology (PABST). Design Handbook for Adhesive Bonding*, 1979.
5. Hart-Smith LJ, 'Design of adhesively bonded joints', *Joining Reinforced Plastics*, Matthews FL (ed.), Elsevier, Barking, UK, Chapter 7, 1987.
6. *ASTM D5656-95. Standard Test Method for Thick-Adherend Metal Lap-Shear Joints for Determination of the Stress–Strain Behavior of Adhesives in Shear by Tension Loading*, ASTM 1995.
7. Arcan M, Hashin Z and Voloshin A, 'A method to produce uniform plane stress states with applications to fiber reinforced materials', *Exp Mechanics*, 1978, **18**, 141–6.
8. Jurf RA and Pipes RB. 'Interlaminar fracture of composite materials', *J Composite Mater*, 1982, **16**(5), 386–94.
9. Mespoulet S, Hodgkinson JM and Matthews FL, 'Design, development and implementation of test methods for determination of through thickness properties of laminated composites', *Plast Rubber Composites*, 2000, **29**(9), 496–502.
10. Lodeiro MJ, Broughton WR and Sims GD, 'Understanding the limitations of through thickness test methods', *Proceedings 4th European Conference on Composites Testing and Standardization*, London, 1998, 80–90.
11. Weaver H.J., Yang J., Evans A.G. and Zok F.W. 'A modified test for measuring the interlaminar tensile strength of fiber-reinforced ceramic composites', *Composites Sci Technol*, 2008, **68**, 10–16.
12. Davies P, Loaec H, Reynaud S, Ferreira A, Hentinen M, Hildebrand M, Mustakangas M, Gaarder R, Carli F, van Straalen IJ, Sargent J, Adams RD, Broughton J and Beevers AJ, 'Failure of bonded glass/epoxy composite joints: A benchmark study and correlation with test results', *Proceedings SAEVI*, Bristol, July 2001, 233–8.
13. Potter KD, Guild FJ, Harvey HJ, Wisnom MR and Adams RD, 'Understanding and control of adhesive crack propagation in bonded joints between carbon fibre composite adherends I. Experimental', *Int J Adhesion Adhesives*, 2001, **21**, 435–43.
14. Guild FJ, Potter KD, Heinrich J, Adams RD and Wisnom MR, 'Understanding and control of adhesive crack propagation in bonded joints between carbon fibre composite adherends II. Finite element analysis, *Int J Adhesion Adhesives*, 2001, **21**, 445–53.
15. Cognard JY, Thomas F and Verpeaux P. 'An integrated approach to solving mechanical problems on parallel computers', *Adv Eng Software*, 2000, **31**, 885–99.


© Woodhead Publishing Limited, 2010

16. Cheikh M, Coorevits P and Loredo M. 'Modelling the stress vector continuity at the interface of bonded joints', *Int J Adhesion Adhesives*, **22**, 2001, 249–57.
17. Pandley PC and Narasimhan S, 'Three-dimensional nonlinear analysis of adhesively bonded lap joints considering viscoplasticity in adhesives', *Computers & Structures*, **79**, 2001, 769–83.
18. Qian ZQ. 'On the evaluation of wedge stress intensity factor of bi-material joints with surface tractions', *Computers & Structures*', 2001, **79**, 53–64.
19. Leguillon J, Laurencin and Dupeux M, 'Failure initiation in an epoxy joint between two steel plates', *Eur J Mech A/Solids*, 2003, **22**, 509–24.
20. Zgoul M and Crocombe AD. 'Numerical modeling of lap joints bonded with rate-dependent adhesive', *Int J Adhesion Adhesives*, 2004, **24**, 355–66.
21. Wu Z. 'Design free of stress singularities for bi-material components', *Composite Structures*, 2004, **65**, 339–45.
22. Magalhães AG, De Moura MFSF and Goncalves JPM, 'Evaluation of stress concentration effects in single-lap bonded joints of laminate composite material', *Int J Adhesion Adhesives*, 2005, **25**, 313–9.
23. Cognard JY, Créac'hcadec R, Sohier L and Davies P, 'Analysis of the non-linear behavior of adhesives in bonded assemblies, Comparison of TAST and ARCAN tests', *Int J Adhesion Adhesives*, 2008, **28**(8), 393–404.
24. Da Silva LFM and Adams RD, 'Techniques to reduce the peel stresses in adhesive joints with composites', *Int J Adhesion Adhesives*, 2007, **27**, 227–35.
25. Adams RD, Comyn J and Wake WC, *Structural Adhesives Joints in Engineering*, Chapman & Hall, London, 2nd edition, 1997.
26. Cognard JY, Davies P, Gineste B and Sohier L, 'Development of an improved adhesive test method for composite assembly design', *Composite Sci Technol*, 2005, **65**, 359–68.
27. Cognard JY, Créac'hcadec R, Davies P and Sohier L, 'Numerical modelling of the non-linear behavior of adhesively-bonded assemblies', in *Innovation In Engineering Computational Structures Technology*, Saxe-Coburg Publications, Stirling, Scotland, Chapter 11, 225–47.
28. *Huntsman™ Structural Adhesives – Araldite® 420 A/B*, Publication No A 161, UK, 2004.
29. Roche AA, Bouchet J and Bentadjine S, 'Formation of epoxy-diamine/metal interphases', *Int J Adhesion Adhesive*, 2002, **22**, 431–44.
30. Cognard JY, 'Numerical analysis of edge effects in adhesively-bonded assemblies. Application to the determination of the adhesive behaviour', *Computers & Structures*, 2008, **86**, 1704–17.
31. Cognard JY, Davies P, Sohier L and Créac'hcadec R, 'A study of the non-linear behavior of adhesively-bonded composite assemblies', *Composite Structures*, 2006, **76**, 34–46.
32. Cognard J-Y, Créac'hcadec R, Davies P and Sohier L, 'Experimental study and modelling of the behavior of hybrid bonded assemblies in marine applications', *Proceedings 16th International Conference on Composite Materials (ICCM-16)*, Kyoto, Japan.
33. Bordes M, Davies P, Cognard JY, Sohier L, Sauvant-Moynot V and Galy J, 'Prediction of long term strength of adhesively bonded joints in sea water', *Int J Adhesion Adhesives*, 2009, **29**(6), 595–608.

© Woodhead Publishing Limited, 2010

# 16

# Designing adhesive joints for fatigue and creep load conditions

I. ASHCROFT, Loughborough University, UK; and
P. BRISKHAM, Coventry University, UK

**Abstract**: Fatigue and creep, along with environmental effects, are the primary concerns in the long-term performance of structural adhesives in-service. This chapter discusses the effects of creep and fatigue loading on adhesively bonded joints and describes the main methods that have been used to model both phenomena. The final section in the chapter discusses how creep and fatigue can be accounted for in industrial design, with particular emphasis on applications in the aerospace and automotive sectors.

**Key words**: fatigue, creep, damage mechanics, fracture mechanics, viscoelasticity, viscoplasticity.

## 16.1 Introduction

Fatigue of an engineering structure relates to cyclic or repetitive loads. The significance of fatigue loading is that failure can occur when the maximum fatigue load is significantly lower than that required to cause instantaneous, or quasi-static, failure of the structure in its original, i.e. non-fatigue-damaged, state. Failure may occur after many millions of cycles, with loads significantly below those required to cause plastic deformation; this is termed high cycle fatigue (HCF). The failure may be progressive, in which case damage can be monitored and parts replaced before a critical crack length is reached, or may occur very rapidly after a long period in which there is little outward sign of damage, known as 'sudden death' failure. If the applied stresses are high enough to cause plastic deformation, the fatigue life is considerably shorter and this is termed low cycle fatigue (LCF). In some cases the fatigue life is determined principally by the number of cycles whereas in others, such as when corrosion or creep contribute to failure, it may have a complex dependence on both the number of cycles and the elapsed time. In some materials a limit is seen, below which fatigue failure does not occur, or fatigue damage progresses at a low enough rate to be considered negligible. This is known as the endurance limit or fatigue threshold.

Creep is the time dependent deformation of a material under load. Creep in polymeric adhesives is a characteristic of their time dependent material behaviour. This means that there is no unique relationship between stress and



© Woodhead Publishing Limited, 2010

strain and hence constitutive models will instead represent the relationship between stress and strain rate. Structural adhesives tend to be highly cross-linked and have glass transition temperatures significantly higher than normal ambient conditions and hence may be adequately represented by a time-independent material model for much of their in-service life. However, even with these materials, a combination of elevated temperature and absorbed moisture can result in creep that can contribute to failure. Most structures are subjected to complex load spectra in which elements of both fatigue and potential creep loading are present. The environmental conditions are also likely to be fluctuating and this will affect the response of the structure to the imposed loads. Adhesively bonded joints are likely to be designed so that quasi-static failure under normal service loads will not occur. The designer must then be concerned with in-service failure from the effects of fatigue or creep loading, environmental effects, or a combination of these.

A number of approaches are available to the designer contemplating fatigue and/or creep of a bonded structure, ranging from the purely experimental to the purely theoretical. In practice, elements of both experimentation and calculation are usually employed, the particular mix being dependent on many factors, including:

- knowledge of service conditions,
- cost and complexity of structure,
- severity of loading,
- criticality of failure,
- availability of reliable design codes and analysis methods,
- certification requirements.

The main job of the designer is to ensure that appropriate materials and geometry are used for the predicted service conditions, maximising performance whilst minimising cost. In order to do this, some knowledge of the service loads and conditions, candidate material properties and manufacturing constraints are required. This basic information must come from testing and measurement. The design process will then entail stages of initial design, design modification and prototyping, which for any load bearing structure is likely to involve both physical testing and some form of analysis. As physical testing is expensive, the concept of virtual testing is gaining popularity in industry. This is a branch of computer-aided engineering in which computer-generated models are used to predict performance, often using the finite element method. These tools can be used with confidence when predicting whether a metal structure can safely withstand the maximum applied load seen in service. Indeed, it is very rare that a structure designed with these tools will show quasi-static failure under normal loads.

© Woodhead Publishing Limited, 2010

Failure is generally because of an abnormal load, fatigue, environmental effects or a combination of these. In the case of materials with time-and environment-dependent behaviour, such as adhesives, subjected to complex loading spectra and fluctuating environments, accurate predictions are more difficult, resulting in the use of high safety factors and rigorous mechanical testing programmes. This is not ideal, as any over-design can add cost and weight to the structure and testing of structures is expensive.

The development of accurate, validated predictive methods for the long-term performance of bonded joints under service conditions would, therefore, be of great benefit to the designer. If the analysis method is mechanistically accurate then the predicted stages of progression of damage leading to failure can be used to design effective in-service monitoring schemes, ensuring parts are replaced before failure occurs. There are a number of methodologies open to the designer, including:

- total life design,
- safe life design,
- fail safe design,
- design with in-service life monitoring.

This chapter reviews the main methods currently available for characterising and predicting the fatigue and creep behaviour of bonded joints. Section 16.2 discusses fatigue in bonded joints. Some of the major issues concerning fatigue in bonded joints are discussed, as well as the various mechanical tests that are used to characterise fatigue behaviour. The main methods of characterising and predicting fatigue in bonded joints are then reviewed.

In Section 16.3, creep in bonded joints is discussed. Methods of modelling the time-dependent behaviour of adhesives are reviewed, followed by a discussion of the characterisation of crack growth in a creeping material. Section 16.4 discusses creep–fatigue interactions in bonded joints and extends the concepts of time-dependent fracture mechanics introduced in section 16.3.4 to adhesives tested under cyclic loading.

Section 16.5 summarises the current situation regarding analysis of creep and fatigue in bonded joints in industry, focussing on the aerospace and automotive sectors. Current design methods are reviewed and possible directions in which improved analysis and design methods may be developed are suggested.

Throughout the chapter, the emphasis is on high performance structural adhesives, as these are the adhesives in which fatigue and creep failure are of most concern and also for which most published data are available. However, many of the methods discussed can easily be applied, perhaps with some modification, to other classes of adhesive.

© Woodhead Publishing Limited, 2010

## 16.2 Fatigue in adhesive joints

### 16.2.1 Introduction

The analysis of fatigue in bonded joints is largely based on techniques developed for other materials, mainly metals. Although, polymeric adhesives share many of the characteristics of fatigue failure with metals, there are also a number of important differences. The mechanisms of fatigue failure in polymers differ from those in metals, as will susceptibility to environmental factors such as moisture and temperature. Also, the time-dependent material behaviour of many adhesives at relatively modest temperatures may affect their response to cyclic loads. The study of fatigue in bonded joints is further complicated by the fact that the joint comprises different materials that will react to fatigue loading in different ways. Adhesively bonded joints are affected by many factors, including: service environment, test frequency and load history, and hence any comprehensive predictive methodology must be able to take all these factors into account. However, adhesive joints are generally considered to have good fatigue resistance compared with alternative joining techniques, such as spot welding or bolting. This can be attributed to a reduction in the stress concentrations associated with both mechanical fasteners and welds. Also, the adherend material is less affected by the joining process compared with the hole drilling required for mechanical fastening and the thermal effects of welding.

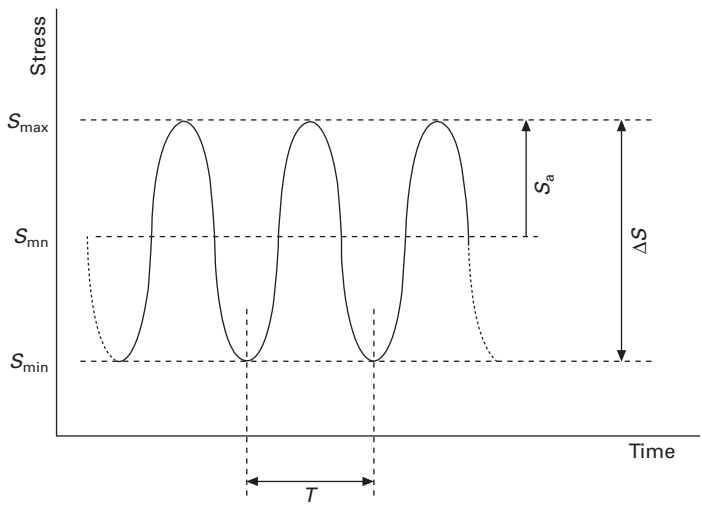
It is common practice to separate the fatigue life of a structure into initiation and propagation phases. In adhesively bonded joints, the differentiation between these two phases is difficult as fatigue initiation in adhesives is complex and can vary with material, geometry and environment. Adhesives tend to be multi-component systems, with fillers, carrier mats and toughening phases often added to the basic matrix material. Fatigue failure of an adhesive may involve many mechanisms, including matrix micro-cracking (initiation, growth and coalescence), filler particle debonding or fracture, cavitation of rubber toughening particles and debonding of carrier mat fibres. Fatigue failure in a bonded joint may also involve failure, or damage, in the adherends or in the interfacial region between adherend and adhesive and hence these possible modes of failure should also be considered in any predictive model. An additional difficulty in characterising fatigue initiation in bonded joints is that the initial damage tends to be internal and hence detection is difficult. However, for the designer, differentiation between initiation and propagation may be necessary in order to select appropriate methods for life prediction and in-service monitoring. A pragmatic approach then is to define the initiation phase as the period until a sufficient crack has formed that further growth can be predicted using fracture mechanics or until the damage can be detected using in-service monitoring techniques.

© Woodhead Publishing Limited, 2010

Various methods of modelling the fatigue behaviour of bonded joints have been proposed, varying in complexity, applicability and degree of empiricism. The aims of the models are either to (1) predict a fatigue limit or threshold, below which failure will not occur within a specified time, (2) predict the number of load cycles (or time) until a certain event occurs (such as macro-crack initiation or complete failure) or (3) predict the rate of change of crack length (or some other measure of damage) as a function of cycles. The following sections discuss the nature of fatigue loading and mechanical testing before reviewing the various methods that can be used to characterise and predict the fatigue response of bonded joints.

## 16.2.2 Fatigue spectra

The main feature of fatigue is that the load varies with time and it is useful to characterise the load spectrum in terms of peaks and troughs in this varying load, with a cycle being defined as the time between adjacent peaks (or troughs) and the frequency being the number of cycles in a unit time. It is common in laboratory experiments to represent fatigue as a constant amplitude, sinusoidal waveform, as shown in Fig. 16.1. In real applications, however, it is more likely that frequency, amplitude, mean and waveform will all vary with time. The designer, therefore, needs to think first about how to characterise the fatigue spectra seen in-service and second how to use this information in the design process. There has been a great deal of work on this subject and a full treatment is beyond the scope of this chapter. However, it would be useful to briefly discuss some of the approaches available.




*16.1* Constant stress amplitude showing sinusoidal fatigue load.

© Woodhead Publishing Limited, 2010

It is possible to characterise the in-service load spectra through simulation, however, it is more commonly done through measurement. In some cases a typical spectrum may be repeated throughout the structure's life, but for many applications, cars for example, the spectra will vary widely for each individual part. In this case, a 'worst case scenario' approach may have to be taken. Once the load spectrum has been generated it can be used in simulations and/or testing. In order to accelerate the testing it is generally preferable to reduce the spectrum. In metals, where the materials are generally rate insensitive, an easy method of accelerating tests is to compress the spectrum and test at high frequency, although any time-dependent effects, such as corrosion, will not be represented accurately in such a test. When devising accelerated service simulation tests for adhesive joints, care must be taken when introducing acceleration techniques that any influential time-dependent or load sequencing effects are retained in the spectrum. Another way of reducing the spectrum is to remove cycles from the spectrum that do not contribute to the fatigue damage. When producing a reduced spectrum for accelerated testing, care must still be taken to retain any important load sequencing effects.

### 16.2.3 Mechanical testing

Mechanical testing can range from inexpensive coupon tests through testing of structural elements to testing of full prototypes, which may be extremely expensive. In all cases, fatigue testing will be considerably lengthier and more costly than quasi-static testing. The coupon tests can fulfil a number of roles. Single material tests may be used to generate material property data whilst joint tests can be used to compare material systems or joint geometries, evaluate performance over a range of loading and environmental conditions, generate design data or provide validation data for predictive models.

Typical joint samples are similar to those used in quasi-static testing. Simple lap joints are generally used to generate *S–N* curves, as described in Section 16.2.4, and standard fracture mechanics tests, such as the double cantilever beam, are used to generate fatigue crack growth curves. Fatigue testing of these joints will generally be carried out with uniaxial, constant amplitude, sinusoidal waveforms. In most cases the waveform will have a positive maximum, such that the sample remains in tension throughout, avoiding buckling of the sample. As these tests are relatively inexpensive they are often used to explore the effects of contributing factors to the fatigue life of bonded joints, such as test environment, preconditioning, frequency and *R*-ratio (the ratio of minimum to maximum fatigue load). This information can then be used to select the most damaging cases for use in structural element or prototype testing. The structural element tests are designed to represent

© Woodhead Publishing Limited, 2010

accurately a particular joint (or joints) in a structure. Samples will be more complex than the simple coupon tests and loading may now be multiaxial. The increased cost of these tests means that fewer will be carried out. The final testing is of a prototype in which the bonded joints will only be one part of what is being tested. Testing will be under simulations of severe in-service use. Failure at this point can have significant financial repercussions.

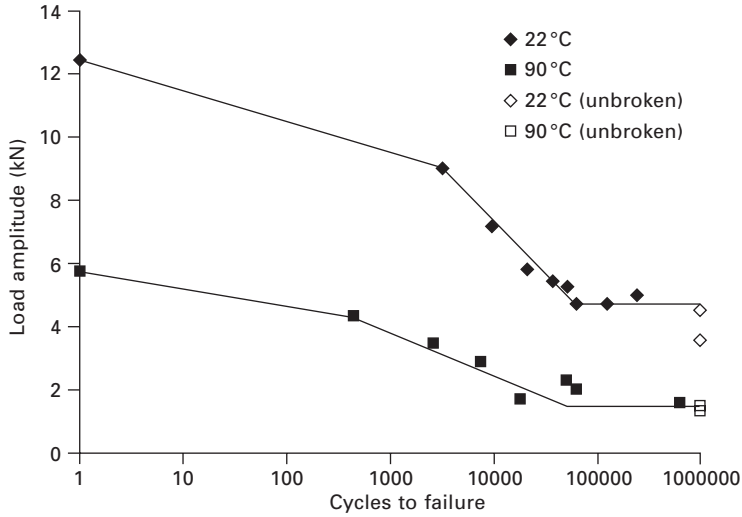
Fatigue testing adhesive lap joints is covered by the standards BS EN ISO 9664:1995 and ASTM D3166-99. The former recommends that at least four samples should be tested at three different stress amplitude values for a given stress mean, such that failure occurs between $10^4$ and $10^6$ cycles. This standard also provides advice about statistical analysis of the data. In general, fatigue data exhibit greater scatter than quasi-static data and this needs to be taken into account when using safety factors with fatigue data. Further advice on the application of statistics to fatigue data is found in BS 3518-5:1966.

### 16.2.4 Total life approach

In the total life approach, the number of cycles to failure ($N_f$) is plotted as a function of a variable such as stress or strain amplitude. Where the loading is low enough for the deformation to be predominantly elastic, a stress variable ($S$) is usually chosen and the resultant plot is termed an *S–N* curve, or Wöhler plot, and this is known as the stress–life approach. Under these conditions a long fatigue life would be expected and hence this is sometimes termed high cycle fatigue (HCF). The *S–N* data is either plotted as a log-linear or a log-log plot and a characteristic equation can be obtained by empirical curve fitting. The constants in the curve fitted equations are dependent on many factors, including: material, geometry, surface condition, environment and mean stress. Hence, caution should be used when trying to apply *S–N* data beyond the samples used to generate the data. The standard stress–life method gives no indication of the progression of damage, although in some cases the onset of cracking is indicated on the plot in addition to the complete failure, allowing the initiation and propagation phases to be differentiated. The above factors mean that the *S–N* curve is of rather limited use in predicting fatigue behaviour, however, it is still useful as a validation tool in fatigue modelling.

A further limit in the application of *S–N* curves to fatigue prediction in bonded joints is that there is no unique relation between the easily determined average shear stress in the adhesive layer and the maximum stress. For this reason, load rather than stress is often used in total life plots for bonded joints and these are known as *L–N* curves. A typical *L–N* curve for epoxy bonded double lap joints can be seen in Fig. 16.2. The *L–N* curve can be divided into a LCF region below approximately 1000 cycles, a HCF region

© Woodhead Publishing Limited, 2010




*16.2* Load–life (*L–N*) curve for bonded lap joints (data from Ashcroft *et al.*, 2001).

between approximately 1000 and 100,000 cycles and an endurance limit region above approximately 100,000 cycles.

Fatigue life not only depends on the stress amplitude but also on the mean stress, as either increasing the mean or increasing the amplitude tends to result in a reduction of the fatigue life. The relationship between amplitude and mean on the fatigue life plot can be illustrated in constant life diagrams in which a given fatigue life is plotted against both mean and amplitude.

In some cases efforts have been made to differentiate between the initiation and propagation phases in the *S–N* behaviour of bonded joints (Harris and Fay. 1992; Zhang and Shang, 1995; Crocombe *et al*., 2002, 2005; Graner-Solana *et al*., 2007; Shenoy *et al*., 2009a; Dessureault and Spelt, 1997; Quaresimin and Ricotta, 2006). Shenoy *et al*. (2009a) used a combination of back-face strain measurements and sectioning of partially fatigued joints to measure damage and crack growth as a function of number of fatigue cycles. It was seen from the sectioned joints that there could be extensive internal damage in the joint without external signs of cracking. Therefore, determination of an initiation phase from external observations alone is likely to lead to an overestimation.

Shenoy *et al*. (2009a) identified three regions in the fatigue life of an aluminium/epoxy single lap joint. An initiation period (CI) in which damage starts to accumulate, but a macro-crack has not yet formed, a stable crack growth (SCG) region in which a macro-crack has formed and is growing slowly and a fast crack growth region (FCG), which leads to rapid failure of the joint. They found that the percentage of life spent in each region varies

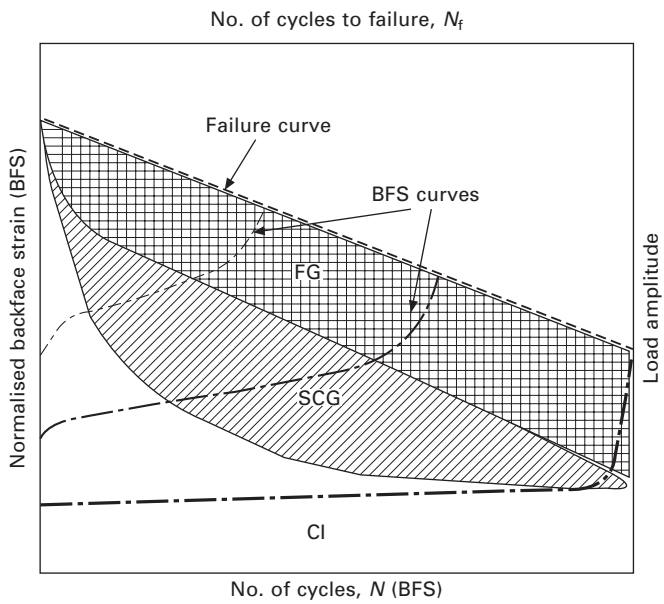
© Woodhead Publishing Limited, 2010

with the fatigue load. At low loads the fatigue life is dominated by crack initiation, whereas crack growth dominates at high loads. This is illustrated schematically in the extended *L–N* curve of Fig. 16.3. It can also be seen in Fig. 16.3 that the back-face strain signal associated with each phase of fatigue damage can be used to monitor damage.

The *S–N* curve is only directly applicable to constant amplitude fatigue whereas in most practical applications for structural joints a variable amplitude fatigue spectrum is more likely. A simple method of using *S–N* data to predict variable amplitude fatigue is that proposed by Palmgren (1924) and further developed by Miner (1945). The so called Palmgren–Miner (P–M) rule can be represented by:

$$\Sigma \frac{n_i}{N_{\mathrm{fi}}} = 1 \qquad [16.1]$$

where $n_i$ is the number of cycles in a constant amplitude block. $N_{\mathrm{fi}}$ is the number of cycles to failure at the stress amplitude for that particular block and can be obtained from the *S–N* curve. It can be seen that using Equation 16.1, the fatigue life of a sample in variable amplitude fatigue can be predicted from an *S–N* curve obtained from constant amplitude fatigue testing of similar samples. However, there are a number of serious limitations to this method, primarily, the assumptions that damage accumulation is linear and that there are no load history effects.




*16.3* Extended *L–N* diagram (from Shenoy *et al.*, 2009a).

© Woodhead Publishing Limited, 2010

Modifications to the P–M rule have been suggested to address some of the deficiencies, for example Marco and Starkey (1954), Henry (1955), Leve (1969), Owen and Howe (1972) and Bond (1999). However, any improvements are at the expense of increased complexity and/or increased testing requirements and the basic flaw in the method, that it bears no relation to the actual progression of damage in the sample, is still not addressed.

Erpolat *et al*. (2004a) used the P–M law and the extended P–M law, in which cycles below the endurance limit also contribute to damage accumulation, to predict failure in an epoxy-CFRP (carbon fibre reinforced polymer) double lap joint subjected to a variable amplitude (VA) fatigue spectrum. The resulting Miner's sum was significantly less than one, varying between 0.04 and 0.3, and decreased with increasing load. This indicates that load sequencing is causing damage acceleration, that is that the P–M rule is non-conservative.

Wöhler (1867) noted a stress below which a nominally infinite life is seen, which is termed the fatigue or endurance limit. If a fatigue limit is seen, it may be possible to use the data from one sample to predict the fatigue limit for a different geometry or loading condition. The approach is similar to that for predicting failure under quasi-static loading and similar multiaxial failure criteria, for example von Mises or maximum principal stress, should be used. Abdel Wahab *et al*. (2001a) compared the predicted fatigue limit (or fatigue threshold) in bonded lap-strap joints using a variety of stress- and strain-based failure criteria.

Under high stress amplitudes, plastic deformation occurs and the fatigue life is considerably shortened. This is known as low cycle fatigue (LCF). Under constant stress amplitude fatigue with strain hardening, the strain amplitude decreases after the first cycle and the subsequent hysteresis loop is repeated a number of times before micro-cracking occurs. In LCF the high loads involved mean that cracks are usually still small when failure occurs. This behaviour leads to a horizontal asymptote to the quasi-static strength in the LCF region, as seen in Fig. 16.2. In constant strain amplitude testing, if there is a positive strain mean, the mean tends to decrease as the sample is fatigued, a phenomenon known as plastic shakedown. This can be compared with the effect of creep in constant stress amplitude testing, which leads to an increase in the mean strain with cycling. The strain–life approach is more difficult to implement than the stress–life method, particularly for complex systems such as bonded joints. Structural bonded joints tend to be used in HCF applications so the strain–life method has seen little application to adhesively bonded joints.

© Woodhead Publishing Limited, 2010

### 16.2.5 Strength and stiffness wearout

An alternative phenomenological approach to the total life methods described above is to characterise fatigue damage as a function of the reduction in the strength or stiffness of the joint during its fatigue life. Stiffness wearout has the advantage of being non-destructive. However, it is not directly linked to a failure criterion and may not be very sensitive to the early stages of damage. The strength wearout method provides a useful characterisation of the degradation of residual strength but requires extensive destructive testing.

In the strength wearout method the joint's strength is initially equal to the static strength, $S_u$, but decreases to $S_R(n)$ as damage accumulates through the application of $n$ fatigue cycles. This degradation can be represented by:

$$S_R(n) = S_u - f(S_u, S_{max}, R)n^{\kappa} \quad [16.2]$$

where $\kappa$ is a strength degradation parameter, $S_{max}$ is the maximum stress and $R$ is the ratio of minimum to maximum stress (i.e. $R = S_{min}/S_{max}$). Failure occurs when the residual strength equals the maximum stress of the spectrum, that is when $S_R(N_f) = S_{max}$. Shenoy *et al.* (2009b) proposed a modified version of this equation that they termed the normalised non-linear strength wearout model (NNLSWM), which is given by:

$$L_n = 1 - \frac{(L_u - L_{max})}{L_u}(N_n)^{\eta} \quad [16.3]$$

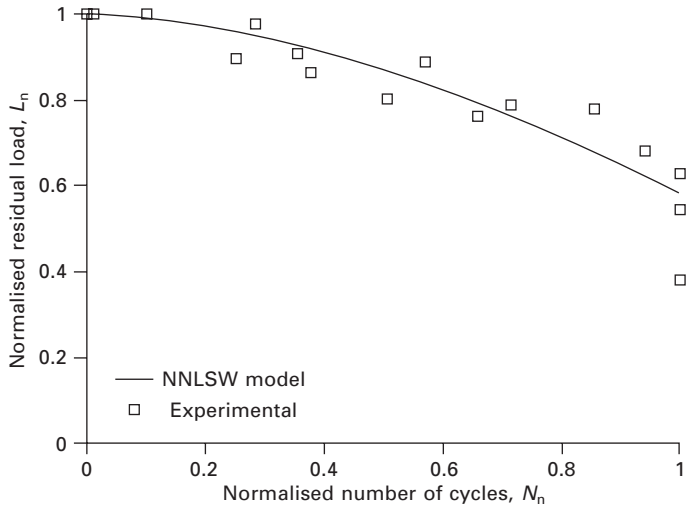
the normalised residual failure load, $L_n$, and normalised cycles to failure, $N_n$, are defined as:

$$L_n = L_R(n)/L_u$$
$$N_n = n/N_f$$

where $L_R(n)$ is the quasi-static failure load after $n$ fatigue cycles, $L_u$ is the quasi-static failure load prior to fatigue loading and $N_f$ is the number of cycles to failure. Figure 16.4 shows an experimental plot of $L_n$ against $N_n$ for various fatigue loads, together with the best fit of Equation 16.3. It can be seen that the proposed phenomenological model agrees well with the experimental results. A single curve can be reasonably drawn for the entire range of fatigue loads wherein, the experimental parameter $\eta$ is independent of the applied fatigue load.

Schaff and Davidson (1997a, b) extended Equation 16.2 to enable the residual strength degradation of a sample subjected to a variable amplitude loading spectrum to be predicted. However, they noted a crack acceleration effect in the transition from one constant amplitude (CA) block to another, a phenomenon they termed the cycle mix effect, and proposed a cycle mix factor (CM) to account for this. Erpolat *et al.* (2004a) proposed a modified form of Shaff and Davidson's cycle mix equation to model the degradation

© Woodhead Publishing Limited, 2010




*16.4* Normalised non-linear strength wearout model (from Shenoy *et al.*, 2009b).

of CFRP-epoxy double lap joints subjected to a variable amplitude fatigue spectrum. They showed that this model represented the fatigue life of bonded joints under variable amplitude fatigue more accurately than Palmgren–Miner's law. Shenoy *et al*. (2009c) proposed further modifications to this approach based upon a non-linear strength wearout model with a damage-dependent cycle mix parameter.

As with strength degradation, stiffness degradation can be considered as a power function of the number of load cycles, using a similar equation to Equation 16.2 (Dibenedetto and Salee, 1979; Yang *et al.*, 1990; Whitworth, 1990). A failure criterion for a stiffness-based wearout model is not as straightforward as that for the strength-based wearout models. One approach is to relate degraded stiffness, $E(N_f)$, to stress, for example:

$$\frac{E(N_f)}{E(0)} = \frac{S_{max}}{S_u} \qquad [16.4]$$

where $E(0)$ is the initial stiffness.

## 16.2.6 Fracture mechanics (or fatigue crack growth) approach

The fracture mechanics approach deals predominantly with the crack propagation phase. Hence, it must be assumed that crack initiation occurs during the early stages of the fatigue cycling or that there is a pre-existing crack. The rate of fatigue crack growth, d$a$/d$N$, is then correlated with an

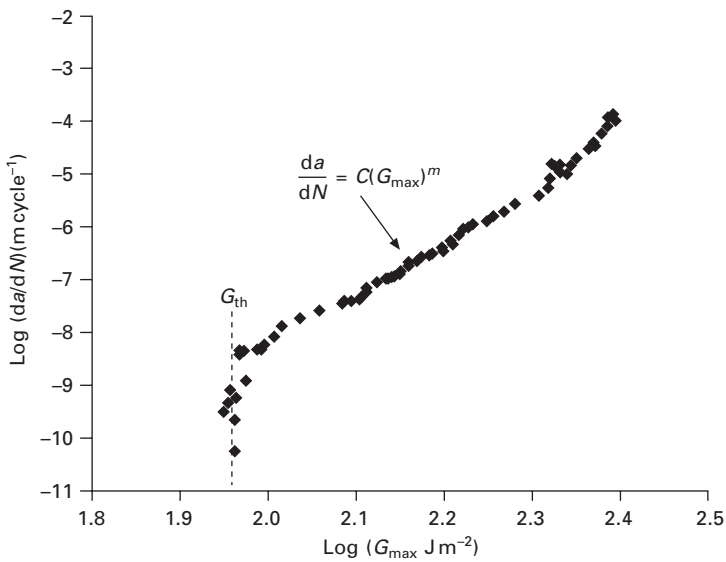
© Woodhead Publishing Limited, 2010

appropriate fracture mechanics parameter, such as Griffith's (1921) strain energy release rate, $G$, or Irwin's (1958) stress intensity factor, $K$. Paris *et al*. (1961) proposed that d$a$/d$N$ was a power function of the stress intensity factor range, $\Delta K$ (= $K_{max} - K_{min}$):

$$\frac{da}{dN} = C\,\Delta K^m \qquad [16.5]$$

where $C$ and $m$ are empirical constants, dependent on factors such as the material, the fatigue frequency, the $R$-ratio and the environment. Although $K$ is the most widely used fracture mechanics parameter for the analysis of metals, it is more difficult to apply to bonded joints, where the constraint effects of the substrates on the adhesive layer complicates characterisation of the stress distribution around the crack tip. Therefore, $G$, is often used as the governing fracture parameter for adhesives if linear elastic fracture mechanics (LEFM) is applicable (i.e. localised plasticity).

If an elastoplastic fracture mechanics (EPFM) parameter is required, owing to more widespread plasticity, then Rice's (1968) $J$-integral ($J$) is generally used. A plot of the experimentally measured crack growth rate against the calculated $G_{max}$ or $\Delta G$ often exhibits three regions, as illustrated in Fig. 16.5. Region I is defined by the threshold strain energy release rate, $G_{th}$, in which crack growth is slow enough to be deemed negligible. Region II is described by a power law equation analogous to Equation 16.5 and is hence




*16.5* Fatigue crack growth (FCG) curve generated from fatigue testing epoxy film bonded CFRP DCBs (from Ashcroft and Shaw, 2002).

© Woodhead Publishing Limited, 2010

sometimes referred to as the Paris region. In region III there is unstable fast crack growth as $G_{max}$ approaches the critical strain energy release rate, $G_c$.

In a general form, the relationship between the fatigue crack propagation rate and a relevant fracture parameter, $\Gamma$, can be represented by:

$$\frac{da}{dN} = f(\Gamma) \quad [16.6]$$

The number of cycles to failure can be determined from:

$$N_f = \int_{a_0}^{a_f} \frac{da}{f(\Gamma)} \quad [16.7]$$

where $a_0$ is the initial crack length and $a_f$ is the final crack length. Equation 16.7 is often solved using numerical crack growth integration (NCGI). Abdel Wahab *et al*. (2003, 2004) proposed a general method of predicting crack growth and failure in bonded lap joints incorporating NCGI and finite element analysis (FEA). The crack growth law was determined from tests using a double cantilever beam (DCB) sample and this was used to predict the fatigue crack growth in single and double lap joints.

The numerical integration technique can easily be adapted to the prediction of fatigue crack growth in variable amplitude (VA) fatigue. Erpolat *et al*. (2004b) applied the NCGI technique to the prediction of crack growth in CFRP/epoxy DCB joints subjected to periodic overloads. This tended to underestimate the experimentally measured crack growth, indicating crack growth acceleration caused by the spectrum loading, and an unstable rapid crack growth period was also seen when high initial values of $G_{max}$ were applied. This behaviour was attributed to the generation of increased damage in the process zone ahead of the crack tip when the overloads were applied. Ashcroft (2004) presented evidence of these damaged regions through X-radiography and microscopy and proposed a simple extension to the NCGI method to enable these load history affects to be predicted.

Adhesives and polymer composites tend to exhibit fast fracture and hence it may be preferable to design for a service life with no crack growth, using $G_{th}$ as the design criteria. Abdel Wahab *et al*. (2001a) investigated this approach for bonded lap-strap joints. Elastic ($G$) and elastoplastic ($J$) fracture parameters, crack placement and initial crack size were investigated. The approach of Abdel Wahab *et al*. (2001a) has also been extended to samples subjected to environmental ageing by incorporating the method into a coupled transient hygro-mechanical finite element analysis (Ashcroft *et al*., 2003).

The fatigue crack growth approach outlined above is directly applicable if the fatigue life is dominated by the fatigue propagation phase. However, if the initiation phase is significant, this approach will underestimate the fatigue life and a method of predicting the number of cycles before the macro-crack

© Woodhead Publishing Limited, 2010

forms is required. This can be done empirically in a similar fashion to the stress–life approach, with the number of cycles to fatigue initiation, $N_i$, being plotted as a function of a suitable stress (or other) parameter rather than cycles to total failure, $N_f$ (Shenoy *et al.*, 2009a). An alternative approach, suggested by Lefebvre and Dillard (1999), is to use a stress singularity parameter as the fatigue initiation criterion.

### 16.2.7 Damage mechanics

The damage mechanics approach has the advantage of representing both initiation and propagation phases. In continuum damage mechanics (CDM) a damage variable, $D$, is defined (Lemaitre, 1984, 1985; Kachanov, 1986) which is equal to zero for undamaged material and one at complete failure. The damage variable is related to a damage equivalent effective stress, $\sigma^*_{\text{eff}}$, which can be calculated for a sample under load to determine the location and severity of damage. Lemaitre (1984, 1985) derived an equation relating the change in the damage variable per cycle in fatigue, $\mathrm{d}D/\mathrm{d}N$, to $\sigma^*_{\text{eff}}$. This was extended by Abdel Wahab *et al.* (2001b) to predict fatigue thresholds in bonded lap-strap and double lap joints. They found that the predictions using CDM compared favourably with those using fracture mechanics. This method has also been used to predict fatigue damage in bulk adhesive samples (Hilmy *et al.*, 2006) and aluminium/epoxy single lap joints (Hilmy *et al.*, 2007).

### 16.2.8 Summary

A number of different approaches have been successfully used to characterise or predict the response of adhesively bonded joints to fatigue loading. The most appropriate approach for a given application depends on numerous factors, as discussed in the introduction to this chapter. A significant current development is the unification of the various approaches into a general set of related analysis tools. This approach starts with a progressive damage modelling tool, of which the various fracture mechanics-based methods may be seen as a sub-set. Ideally, the progressive damage modelling should be able to represent accurately both the initiation and propagation phases. This model can then be used to generate *S–N* curves, strength wearout plots, fatigue thresholds, and so on, for different sample geometries. The model can also be used to investigate measurable signs of fatigue damage, such as back-face strain, which can be used to develop effective in-service monitoring methods. A further challenge in creating effective fatigue design tools for bonded joints is to ensure that the tools are based on accurate physical models of the fatigue response of the joints and that the models

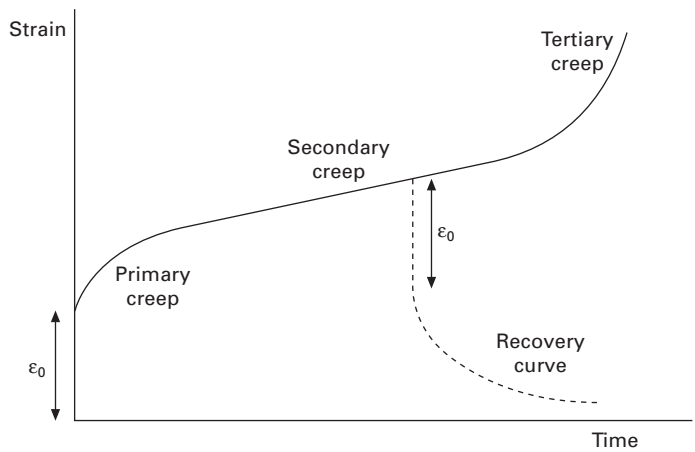
© Woodhead Publishing Limited, 2010

can accurately represent the complex response of bonded joints to realistic in-service loading and environmental conditions.

## 16.3 Creep in adhesive joints

### 16.3.1 Introduction

Creep is defined in ASTM (D2293) as 'the dimensional change with time of a material under load, following the initial instantaneous elastic or rapid deformation'. Various coupon tests and standards have been developed to evaluate the creep resistance of adhesives, either by monitoring the time-dependent displacement of an adhesive specimen under load or by recording the time to failure. Established test standards include ASTM D2294-96, ASTM D1780–99, ISO 15109 and EN 1943. In static load creep experiments, a dead load is applied to the adhesive joint. The initial displacement and the change in displacement, or strain, over time are recorded. It is important that environmental conditions are kept constant throughout the test. Figure 16.6 shows a typical creep curve under conditions of constant (and uniform) stress, temperature and humidity. At $t = 0$ the curve shows an instantaneous strain, $\varepsilon_0$, in response to the applied load, which, depending on the magnitude of the stress, could be elastic, where $\varepsilon_0 = \varepsilon_e$, or elastic–plastic, where $\varepsilon_0 = \varepsilon_e + \varepsilon_p$. After this initial response, the creep curve can be separated into three regions, classified as: primary (or transient), secondary (or steady state) and tertiary creep. Failure occurs at the end of the tertiary creep regime and is known as creep rupture. The total strain prior to the tertiary phase is the sum of the instantaneous strain, $\varepsilon_0$, the transient strain, $\varepsilon_t$, and the steady




*16.6* Schematic constant stress and temperature creep curve for a viscoelastic polymer.

© Woodhead Publishing Limited, 2010

state strain, $\varepsilon_s$. The creep strains are dependent on stress, $\sigma$, as well as time, $t$, and this can be represented by the following equation:

$$\varepsilon = \varepsilon_0 + B\sigma^m t + D\sigma^\alpha (1 - e^{-\beta t}) \quad [16.8]$$

where the second term in Equation 16.8 represents the steady state creep strain and the third term the transient creep strain. $B$, $m$, $D$, $\alpha$ and $\beta$ are empirical constants determined by curve fitting to experimental creep data. In some cases the transient creep region can be ignored, in which case differentiation of Equation 16.8 gives:

$$\dot{\varepsilon} = B\sigma^m \quad [16.9]$$

The constants in Equation 16.9 can be determined by plotting the log of the steady state strain rate, $\dot{\varepsilon}$, against the log of stress. However, there are numerous other ways in which the creep behaviour in adhesively bonded joints can be modelled and these are discussed further in Section 16.3.2.

The time-dependent behaviour of adhesives can be illustrated in a number of different ways. If the creep curve in Fig. 16.6 is repeated for different stresses then tables of stress and strain values at a given time can be generated from the curves. Plots of stress against creep strain for a given time are called isochronous stress–strain curves and a family of such curves can be plotted for different times. The gradient of an isochronous stress–strain plot is called the creep compliance. In the case of linear viscoelasticity, the isochronous stress–strain plots are linear, so that the creep compliance for a given time is constant. Another way of representing creep data is to plot the log of time to rupture from a creep test against stress. This gives a plot similar to the *S–N* curve generated from fatigue testing.

If the load is removed before creep rupture in a dead load creep test and strain continues to be monitored, an instantaneous decrease in strain equal to the elastic strain when the load was applied will be followed by a time-dependent decrease in strain in a process called recovery, as shown in Fig. 16.6. The degree of recovery is dependent on the material and the creep mechanisms. A high degree of cross-linking in a polymer will tend to increase the proportion of recovered strain.

An alternative method of experimentally investigating creep behaviour is the relaxation test. In this test a constant strain is applied to the specimen and creep of the material results in a decrease in stress over time. This is termed relaxation and should not be confused with recovery. Another popular method of illustrating the time-dependent nature of an adhesive is to plot stress against strain at different constant strain rates.

Viscoelasticity may also be characterised using dynamic mechanical analysis, in which a small oscillatory strain is applied to a sample and the

© Woodhead Publishing Limited, 2010

resultant stress measured. In an elastic material the stress is in phase with the strain, whereas in a viscous material there is a 90° phase lag. In a viscoelastic material there will be a phase lag, $\delta$, of less than 90°. Hence stress and strain can be represented by:

$$\varepsilon = \varepsilon_0 \sin(\omega t) \quad [16.10]$$

$$\sigma = \sigma_0 \sin(\omega t + \delta) = \sigma_0 \cos\delta \sin\omega t + \sigma_0 \sin\delta \cos\omega t \quad [16.11]$$

where $\omega$ is the angular frequency. Equation 16.11 shows that the stress consists of a component of magnitude ($\sigma_0 \cos\delta$) in phase with strain and a component of magnitude ($\sigma_0 \sin\delta$) 90° out of phase with strain. Similarly, the stress–strain relationship can be defined by a modulus component, $E'$, in phase with strain, called the storage modulus, and a component, $E''$, 90° out of phase with strain, called the loss modulus:

$$\sigma = \varepsilon_0 E'' \sin\omega t + \varepsilon_0 E'' \cos\omega t \quad [16.12]$$

where:

$$E' = \frac{\sigma_0}{\varepsilon_0}\cos\delta \quad \text{and} \quad E'' = \frac{\sigma_0}{\varepsilon_0}\sin\delta$$

Other useful parameters defined from dynamic mechanical testing are the complex modulus, $E^* = E' + iE''$, and the loss factor, $\tan\delta = E''/E'$. Dynamic testing is commonly carried out over a range of frequencies. At low frequencies polymers are 'rubbery' and have a low modulus that is relatively independent of frequency. At very high frequencies, 'glassy' behaviour is seen in which modulus is high and again relatively frequency independent. In the intermediate region, in which viscoelastic behaviour is observed, peaks in the loss modulus and tan $\delta$ are seen.

The tests described above are generally carried out by testing tensile test samples. However, in the case of adhesives, the stress state can have a significant effect on the time-dependent behaviour. This can be investigated by testing under other modes of loading; bending, shear and compression testing being the most popular.

Creep failure can generally be classified as being either widespread or localised. The former occurs when stresses are fairly uniform; hence the whole part creeps and fails by creep rupture. In cases where stresses are localised, a localised crack forms and failure is characterised by propagation of this crack in the creeping material. In these cases standard linear elastic or elastic–plastic fracture mechanics methods may not be sufficient to characterise the crack growth and time-dependent fracture mechanics may need to be implemented. This is discussed further in Section 16.3.4.

© Woodhead Publishing Limited, 2010

### 16.3.2 Time-dependent material models

If strain rates are reasonably uniform within a specimen, or timescales are short in relation to creep rates, then the effects of loading an adhesive may be adequately modelled using an appropriate time-independent model, with material constants taken from tests carried out at rates similar to those seen in the application sample. If the creep of the adhesive is significant over the timescale under consideration and the strain rates are non-uniform, then an appropriate time-dependent material model must be incorporated into the stress analysis. Ideally, the time-dependent model should be capable of representing all the time-dependent features observed in the adhesive, which may include linear or non-linear viscoelasticity, viscoplasticity, hydrostatic stress sensitivity and large degrees of non-linear recovery. Finding a model that can successfully represent all the observed time-dependent characteristics for different stress states may be difficult and determining the parameters for such a model both time consuming and costly. In many cases only certain stress states and types of loading need to be considered, in which case a simpler, though not generally applicable, model may be sufficient. There are many ways of modelling time-dependent behaviour and only a brief introduction to the main approaches that have been applied to structural adhesive materials is presented here. One of the numerous texts, such as Ferry (1970), Nielsen and Landel (1994), Shames and Cozzarelli (1997), Christensen (2003) or Ward and Sweeney (2004), should be consulted for a more complete treatment of the subject.

Mechanical behaviour can be modelled as a combination of simple mechanical elements, called rheological models. The simplest elements are the linear or Hookean spring, in which strain, $\varepsilon$, is proportional to stress, $\sigma$, and the linear or Newtonian viscous dashpot, in which strain rate, $\dot{\varepsilon}$, is proportional to stress. Combinations of these two elements comprise the family of linear viscoelastic rheological models. The simplest rheological models comprise two linear elements. A dashpot in parallel with a spring, shown in Fig. 16.7 (a), is called a Kelvin or Voigt model. When loaded, the stress is divided between the two elements.

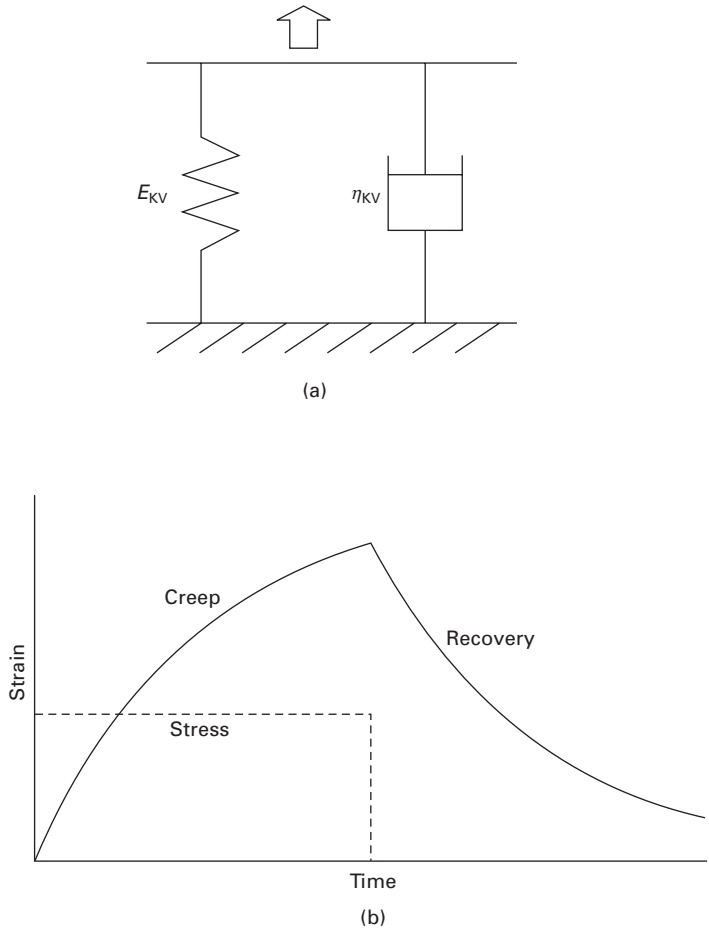
$$\sigma = E_{\mathrm{KV}}\varepsilon + \eta_{\mathrm{KV}}\dot{\varepsilon} \qquad [16.13]$$

where $E_{\mathrm{KV}}$ is the modulus of the spring, $\eta_{\mathrm{KV}}$ is the viscosity of the dashpot and $\dot{\varepsilon}$ is the strain rate. The strain is the same in both elements and is given by:

$$\varepsilon(t) = \frac{\sigma}{E_{\mathrm{KV}}}[1 - \exp(-t/\tau')] \qquad [16.14]$$

where $t$ is time and $\tau'(= \eta_{\mathrm{KV}}/E_{\mathrm{KV}})$ is the retardation time, which is a measure of the rate at which deformation occurs. Equation 16.14 provides a reasonable

© Woodhead Publishing Limited, 2010

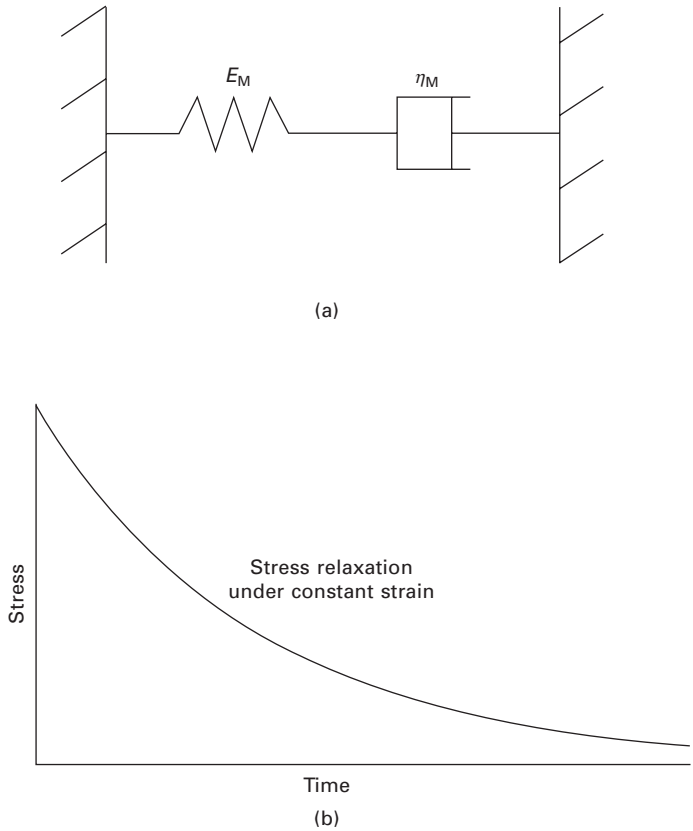



*16.7* (a) Kelvin–Voigt model, (b) creep and recovery curves.

approximation of transient creep, shown in Fig. 16.7(b), however, representation of recovery is poor as the instantaneous and unrecovered components are not accounted for. It can be seen from Equation 16.14 that strain increases with time under constant stress in creep. This indicates a creep compliance, $J(t) = \varepsilon(t)/\sigma$, which also increases exponentially with time. From Equation 16.13, it can be seen that when the strain rate is zero, only an elastic response is seen, hence the Kelvin–Voigt model is unable to represent relaxation.

A linear spring and dashpot in series, shown in Fig. 16.8(a), is called a Maxwell model. In this case the stress is the same for the dashpot and the spring and the total strain, $\varepsilon$, is the sum of the strain in the spring, $\varepsilon_s$ and the dashpot, $\varepsilon_d$. The total strain rate is, hence, given by:

© Woodhead Publishing Limited, 2010




*16.8* (a) Maxwell model, (b) stress relaxation curve.

$$\dot{\varepsilon} = \dot{\varepsilon_s} + \dot{\varepsilon_d} = \frac{\dot{\sigma}}{E_M} + \frac{\sigma}{\eta_M} \qquad [16.15]$$

Equation 16.15 shows that under creep conditions, at $\dot{\sigma} = 0$, there is a constant rate of strain, that is, Newtonian flow, which is generally a poor representation of creep in polymers. In the case of stress relaxation, where $\dot{\varepsilon} = 0$, integrating Equation 16.15 gives:

$$\sigma(t) = \sigma_0 \exp\left(\frac{-t}{\tau}\right) \qquad [16.16]$$

where $\sigma_0$ is the initial stress and $\tau (= \eta_M/E_M)$ is the relaxation time. This provides a reasonable approximation of relaxation, shown in Fig. 16.8(b). It can be seen from Equation 16.16 that in relaxation, stress decreases with time under constant strain. This points to a relaxation modulus, $E_r = \sigma(t)/\varepsilon$, which also decreases exponentially with time.

© Woodhead Publishing Limited, 2010

The two element models described above indicate a single relaxation time for creep and a single retardation time for stress relaxation. In a real polymer there will be a range of relaxation and retardation times and these can be represented by using multi-element models with varying spring and dashpot constants. An array of Kelvin–Voigt units in series can be used for creep simulation and an array of Maxwell units in parallel can be used to model stress relaxation. For example, from Equation 16.16, it can be seen that stress relaxation for an array of Maxwell units at the same strain can be represented by:

$$\sigma(t) = \varepsilon \sum_n E_n \exp\left(\frac{-t}{\tau_n}\right) \qquad [16.17]$$

where there are $n$ Maxwell units and $E_\mathrm{n}$ and $\tau_\mathrm{n}$ are the modulus and retardation time of the $n$th Maxwell unit, respectively. Equation 16.17 is in the form of a Prony series and one of the many methods suggested for solving this class of problem can be used to determine an appropriate Prony series to fit experimental stress relaxation or creep data (e.g. Ferry, 1970; Soussou *et al*., 1970; Chen, 2000).

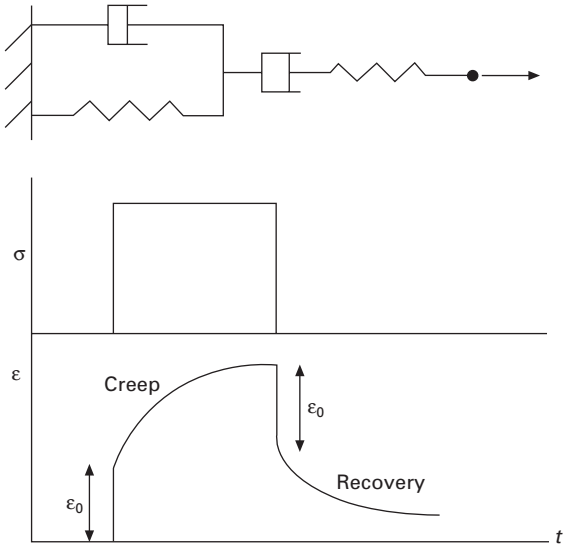
More generally applicable models of viscoelasticity can be obtained by increasing the number of elements and a number of three and four element models have been proposed. Hojjati *et al*. (2004) proposed a three element model to characterise stress relaxation in the epoxy-based adhesive FM73, from Cytec Engineered Materials. In this model a Maxwell unit is put in parallel with a spring, which enables relaxation to a non-zero stress under constant strain, which is more characteristic of a cross-linked polymer such as an epoxy adhesive than the relaxation to zero stress seen in the Maxwell model. They also proposed that a simpler method than using a Prony series to represent a more complex relaxation behaviour than accounted for in the Maxwell model is to use a 'stretched' exponential, in which the exponent term is raised to a power. The modified equation for relaxation modulus can be represented by:

$$E_\mathrm{r} = E_\mathrm{s} + E_0 \exp\left[-\left(\frac{-t}{\tau}\right)^b\right] \qquad [16.18]$$

where $E_\mathrm{s}$ is the modulus of the spring in series with the Maxwell unit, $E_0$ is the initial modulus of the Maxwell unit and $b$ is an experimentally determined material constant. A four element model can be obtained by putting the Maxwell and Kelvin models in series that exhibits transient and steady state creep as well as partial recovery. This is called a Burger's fluid and is illustrated in Fig. 16.9.

Plasticity is represented in the rheological models by a frictional slider, also known as a Saint-Venant element, which represents rigid, perfectly plastic

© Woodhead Publishing Limited, 2010




*16.9* Four element linear viscoelastic model (Burgers fluid).

behaviour, or in series with a spring, elastic-perfectly plastic behaviour. A slider in parallel with a dashpot is a linear viscoplastic or Bingham element. Once the yield stress is exceeded, this element exhibits rate-dependent strain hardening. Combinations of viscoelastic and viscoplastic elements may be useful when a number of different stress-dependent creep mechanisms are present.

In many real cases, non-linear viscoelasticity or viscoplasticity is observed. This behaviour can be represented by substituting the linear elements in the linear visoelastic and viscoplastic models with non-linear elements, such as non-linear elastic springs (Hencky elements) or non-linear dashpots (e.g. Stokes fluid). However, such models are complex, difficult to implement and have many parameters requiring data.

An easier method of representing non-linear viscoelastic behaviour is to adopt a purely phenomenological approach, such as the power law creep equation given in Equation 16.8. The drawback to such an approach is that the phenomenological models have limited application beyond the loading conditions to which the empirical equation has been fitted. Another empirical approach is to use a classical elastic–plastic model, but with strain rate dependent parameters. The most suitable elastic–plastic models are those which include hydrostatic stress sensitivity, such as Mohr–Coulomb and Drucker–Prager models. Yu *et al.* (2001) used this approach to model creep and strain rate-dependent stress–strain curves for an epoxy adhesive and showed that this was more successful than the application of a power law creep model.

© Woodhead Publishing Limited, 2010

A final class of models that have been proposed to represent the mechanical behaviour of adhesives are the unified theory models, which attempt to represent observed behaviour, such as non-linear viscoelasticity and plasticity, in a single theory. Cernocky (1982), Kitagawa *et al*. (1989) and Chiu and Jones (1995) can be referred to for examples of unified theory models. Overstress models are a type of unified theory model based on the concept that there is an equilibrium or back stress–strain response at very slow strain rates. Loading at higher strain rates results in an applied stress that is greater than the back stress and the difference between the two is called the overstress. Strain rate in the material increases as the overstress increases. Crocombe *et al*. (2001) proposed an overstress model with the following basic formulation:

$$\dot{\varepsilon} = A(\sigma - s)\exp(k|(\sigma - s)|) \qquad [16.19]$$

where $\sigma$ is the applied stress, $s$ is the back stress and $A$ and $k$ are material constants. Crocombe *et al*. (2001) showed that this model could be used to model the creep, recovery and constant strain rate stress–strain behaviour of a structural adhesive.

The above discussion demonstrates that there are a number of potential methods of modelling the time-dependent behaviour of adhesives, varying in their complexity and ability to characterise different aspects of the observed time-dependent behaviour. It would seem that an essential starting point in the adoption of a suitable model is to characterise the behaviour of the material over the range of loading and environmental conditions likely to be experienced in-service. This may include creep, recovery, relaxation, constant strain rate and cyclic testing for different stress states and temperatures. This testing will indicate the requirements of a suitable material model as well as providing data for the model parameters and model validation.

### 16.3.3 Effect of temperature and absorbed moisture

The preceding sections have addressed the time dependency of the mechanical behaviour of polymeric adhesives. However, the mechanical behaviour is also highly dependent on temperature and absorbed moisture. Moreover, the effects of time, temperature and moisture are analogous, with longer times having a similar effect to higher temperatures and greater concentrations of absorbed moisture. The effect of temperature on the viscoelastic properties of polymers has been dealt with in depth in numerous texts (e.g. Ferry, 1970), therefore, this section will only attempt to summarise some of the main points that may be of interest in relation to polymeric adhesives.

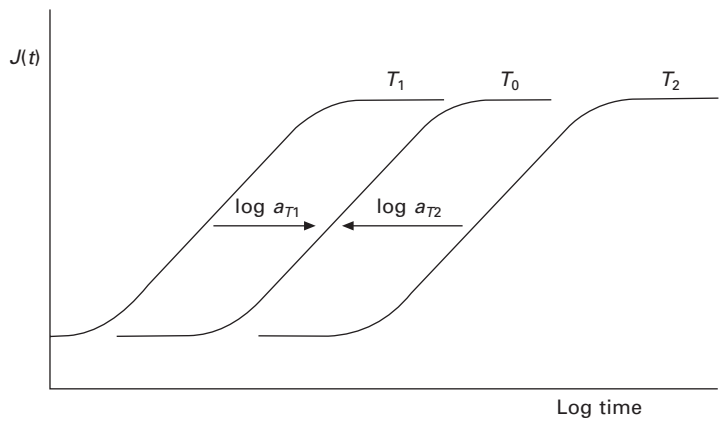
As temperature or timescale increase, polymers change from a glassy to a rubbery state. In the glassy state the polymer is brittle and deformation

© Woodhead Publishing Limited, 2010

relates to the small displacement of molecules about an equilibrium position. In the rubbery state, segmental molecular rotations and translations occur on loading, giving the polymer much greater flexibility than in the glassy state. The transition between the glassy and rubbery states is characterised by a large change in modulus and is often defined by a glass transition temperature, $T_g$. The polymer is sometimes defined as 'leathery' in the transition region. Moisture has the effect of lowering the $T_g$. Jurf and Vinson (1985) noted that epoxy adhesives were relatively insensitive to moisture in the glassy and rubbery regions but that moisture reduced modulus in the transition region. They concluded that the effect of moisture was equivalent to raising temperature in epoxy adhesives but warned against moisture-induced effects such as micro-cracking and chemical decomposition which would invalidate this relationship.

It has already been noted that the effects of time and temperature are analogous and this leads to the time–temperature superposition principle which posits that creep or stress relaxation curves can be superimposed by horizontal shifts along a logarithmic time axis. This is achieved by applying a shift factor, $a_T$, with respect to a reference temperature, $T_0$, to create a single 'master' curve. The process is illustrated in Fig. 16.10. The shift factor is temperature dependent and this relationship can be described by an Arrhenius relationship in the glassy region and the WLF (Williams, Landel and Ferry) equation (Ferry, 1970) in the rubbery region, given by Equations 16.20 and 16.21, respectively.

$$\log(a_T) = \frac{\Delta H}{2.303R}\left(\frac{1}{T} - \frac{1}{T_0}\right) \qquad [16.20]$$




*16.10* Schematic illustration of time–temperature superposition of creep compliance.

© Woodhead Publishing Limited, 2010

$$\log(a_T) = \frac{-C_1(T - T_0)}{C_2 + T - T_0} \quad [16.21]$$

where $\Delta H$ is the activation energy and $R$ is the universal gas constant. $C_1$ and $C_2$ are material constants. A small vertical shift has also been proposed when performing a time–temperature superposition (Williams *et al.*, 1955; McCrum and Morris, 1964).

Examples of the application of the time–temperature superposition principle to adhesives can be found in Jurf and Vinson (1985) and Hojjati *et al.* (2004). Jurf and Vinson also looked at the effect of moisture on the viscoelastic properties of epoxy adhesives and proposed a horizontal shift factor caused by moisture, $a_M$, that was analogous to $a_T$. This idea of the equivalence of time–temperature superposition and time–moisture superposition was expanded upon by Yao and Ziegmann (2006), who went on to define empirical relationships between $a_m$ and $a_T$ for an epoxy resin/glass fibre composite. The advantage of such superposition methods is that it allows long-term effects to be simulated in short times by increasing temperature or moisture concentration.

### 16.3.4 Creep crack growth and time-dependent fracture mechanics

In structures in which stresses and temperature are fairly uniform, any creep damage will also be fairly uniform and failure will be by creep rupture. In bonded joints this situation will only generally occur when the adhesive layer is very flexible compared to the adherends. In most cases, stress concentrations are seen in bonded joints and hence creep damage will tend to be more localised. Hence, failure is more likely to be by the formation of a crack in the region of high stress and its subsequent propagation through the structure. In this case, creep rupture data may be useful in predicting the initiation of localised failure but will not be able to represent accurately the failure of the whole structure.

Although there is considerable literature on the characterisation and modelling of the time-and rate-dependent behaviour of adhesives, there is relatively little on the effect that this has on crack growth. In practically all the published literature on the application of fracture mechanics to predicting crack growth in structural adhesives, either a linear elastic fracture mechanics (LEFM) parameter, such as strain energy release rate, or elastic–plastic fracture mechanics parameter (EPFM), such as the $J$-integral, is used. In many cases this is perfectly acceptable as the rate of crack growth far exceeds the rate of creep in the process zone ahead of the crack tip. However, where this is not the case, LEFM and EPFM cannot uniquely define the crack tip conditions as they will vary as a function of time. In this case a time-dependent fracture

© Woodhead Publishing Limited, 2010

mechanics (TDFM) approach is required in which creep deformation is included in the formulation of the fracture parameter.

Landes and Begley (1976) and Nikbin *et al*. (1976) independently proposed a TDFM parameter that is analogous to Rice's *J*-integral. Landes and Begley called this new integral *C** and defined it as follows:

$$C^* = \int_\Gamma W^* \mathrm{d}y - T_\mathrm{i} \left\{ \frac{\partial \dot{u}_\mathrm{i}}{\partial x} \right\} \mathrm{d}s \qquad [16.22]$$

where

$$W^* = \int_0^{\dot{\varepsilon}_{ij}} \sigma_{ij} \mathrm{d}\dot{\varepsilon}_{ij} \qquad [16.23]$$

Γ is a line contour taken counter clockwise from the lower crack surface to the upper crack surface, $W^*$ is the strain energy rate density associated with the stress $\sigma_{ij}$ and strain rate $\dot{\varepsilon}_{ij}$, $T_i$ is the traction vector defined by the outward normal, $n$ along Γ, $\dot{u}_i$ is the displacement rate vector and $s$ is the arc length along the contour. $C^*$ is valid only for extensive steady-state creep condition and alternative parameters have been proposed for when this is not the case. Saxena (1986) proposed a parameter $C_t$ that was suitable for characterising creep crack growth from small scale to extensive creep conditions. This was defined as:

$$C_t = -\frac{1}{B} \frac{\partial U_t^*(a, t, \dot{V}_\mathrm{c})}{\partial a} \qquad [16.24]$$

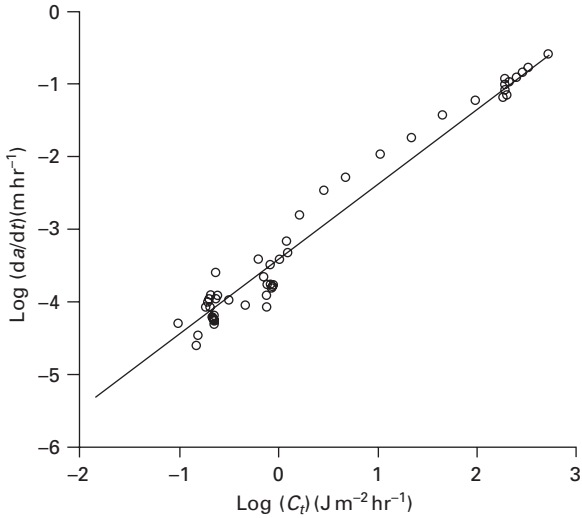
where $B$ is sample width, $a$ is crack length, $t$ is time, $U_t^*$ is an instantaneous stress-power parameter and $\dot{V}_\mathrm{c}$ is the load line deflection rate.

Although there has been very little application of TDFM to adhesively bonded joints, Al-Ghamdi (2004) investigated the suitability of $C^*$ and $C_t$ for characterising creep crack growth in epoxy–steel double cantilever beam samples. He showed that $C_t$ was the more suitable parameter and a plot of creep crack growth rate ($\mathrm{d}a/\mathrm{d}t$) as a function of $C_t$ for samples tested at 120°C can be seen in Fig. 16.11. A straight line can be drawn through the data points that represents the following equation:

$$\frac{\mathrm{d}a}{\mathrm{d}t} = DC_t^n \qquad [16.25]$$

where $D$ and $n$ are experimentally determined material parameters. It can be seen that Equation 16.25 is similar in form to Equation 16.5 which describes the relationship between fatigue crack growth and a LEFM parameter.

© Woodhead Publishing Limited, 2010




*16.11* Creep crack propagation rate as a function of creep parameter, $C_t$, for epoxy/steel DCB joints tested at 120°C.

## 16.3.5 Summary

This section shows that structural adhesives can exhibit time-dependent behaviour, such as creep, recovery and stress relaxation, when under load. It also shows that the mechanical behaviour of polymeric adhesives is highly dependent on temperature and moisture concentration and that the effects of time, temperature and moisture are analogous. This has lead to the time–temperature and time–moisture superposition principles, which allow long-term effects to be simulated over shorter times by increasing temperature or moisture content. Designers intending to use adhesively bonded joints need to be aware of the time-, temperature- and moisture-dependent behaviour of adhesives and account for this behaviour in their analysis procedures. However, adhesive material behaviour can be complex and serious consideration must be given to which material model is most appropriate for the material in question under the prevailing operating conditions.

If creep is accumulative and widespread then undesirable permanent deformations may be observed in bonded structures, eventually leading to failure through creep rupture. This can be eliminated or reduced by using appropriate materials for the loading and environmental conditions or by building structural redundancy into the joints so that accumulative creep is avoided. If stresses are more localised, creep rupture will also be more localised and the problem becomes one of crack propagation through a creeping medium. If the rate of crack growth is fast in relation to the rate of creep in the adhesive, the LEFM and EPFM parameters generally used

© Woodhead Publishing Limited, 2010

to characterise crack growth in bonded joints may be adequate. However, if the rate of crack growth is slow in relation to the rate of creep, such as at elevated temperatures, then a TDFM parameter must be used. This is an area that has received little consideration to date.

## 16.4 Creep–fatigue interactions in adhesive joints

Evidence of creep in fatigue testing bonded lap joints has been observed by a number of authors (e.g. Hart-Smith, 1981a; Harris and Fay, 1992). Ashcroft and Shaw (2002) used the fracture mechanics approach discussed in Section 16.2.6 to predict the fatigue thresholds in lap strap and double lap joints at different temperatures, using $G_T$ determined from testing double cantilever beam samples as the failure criterion. The predictions were reasonably good, apart from those for double lap joints tested at 90°C, which failed at far lower loads than predicted. This was attributed to accumulative creep in the double lap joint, which was observed in the plots of displacement against cycles at constant load amplitude in the fatigue tests for these joints. It was noted that accumulative creep was prevented in the lap-strap joint as the CFRP strap adherend spanned the loading points.

As many adhesives exhibit some degree of viscoelastic or viscoplastic behaviour over a part of their operating range, it is not surprising that the combined effects of creep and fatigue are seen when bonded joints are tested in fatigue with a non-zero mean load. The effects of this superimposed creep and fatigue behaviour include a strong frequency, mean load and temperature dependency for fatigue crack growth. Fatigue crack growth in such circumstances may still be adequately represented by LEFM or EPFM parameters. However, different fatigue crack growth curves will be required for different frequencies and temperatures, as seen in Al-Ghamdi *et al*. (2003). However, if creep is significant, fatigue crack growth may be better represented by a TDFM parameter, such as $C_t$. In cyclic loading $C_t$ will vary with the applied load and an average value of $C_t$, $C_{t(\text{ave})}$, may be used to characterise the fatigue–creep crack growth.

Al-Ghamdi *et al*. (2004) proposed three methods of predicting creep–fatigue crack growth in bonded joints. The first method is the empirical crack growth law approach. In this approach an appropriate fracture mechanics parameter is selected and plotted against the fatigue crack growth rate (FCGR = d$a$/d$N$) or the creep crack growth rate (CCGR = d$a$/d$t$). A suitable crack growth law is fitted to the experimental data and crack growth law constants are determined at different temperatures and frequencies. Empirical interpolation can then be used to determine crack growth law constants at unknown temperatures and frequencies. This method can also be used to predict crack growth under conditions of varying frequency, load and temperature.

© Woodhead Publishing Limited, 2010

The second method is the dominant damage approach. This assumes that fatigue and creep are competing mechanisms and that crack growth is determined by whichever is dominant. In this case, crack growth should be predominantly either cycle or time dependent. For example, if creep is the dominant damage mechanism, plots of d$a$/d$t$ against a suitable TDFM should be independent of frequency.

The third method is the crack growth partitioning approach. This assumes that crack growth can be partitioned into cycle-dependent (fatigue) and time-dependent (creep) components and that the total crack growth can be determined by summing these components. This method can be represented by the following equation:

$$\frac{\mathrm{d}a}{\mathrm{d}N} = \left(\frac{\mathrm{d}a}{\mathrm{d}N}\right)_{\text{fatigue}} + \frac{1}{f}\left(\frac{\mathrm{d}a}{\mathrm{d}t}\right)_{\text{creep}} \qquad [16.26]$$

Al-Ghamdi *et al*. (2004) proposed the following form of Equation 16.26:

$$\frac{\mathrm{d}a}{\mathrm{d}N} = D(G_{\max})^n + \frac{mC_{t(\text{ave})}^q}{f} \qquad [16.27]$$

The fatigue crack growth constants $D$ and $n$ were determined from high frequency tests where it was assumed that creep effects were negligible and the creep crack growth constants $m$ and $q$ were determined from constant load crack growth tests. In many cases this method produced an excellent prediction of crack growth. However, under some conditions crack growth was underestimated. To solve this problem, Ashcroft *et al*. (2005) proposed the addition of a creep–fatigue interaction term:

$$\frac{\mathrm{d}a}{\mathrm{d}N} = D(G_{\max})^n + \frac{mC_{t(\text{ave})}^q}{f} + CF_{\text{int}} \qquad [16.28]$$

where $CF_{\text{int}} = R_{\text{f}}^p R_{\text{c}}^y C_{\text{fc}}$. $R_{\text{f}}$ and $R_{\text{c}}$ are scaling factors for the cyclic- and time-dependent components, respectively, and

$$R_{\text{f}} = \frac{(\mathrm{d}a/\mathrm{d}N)}{(\mathrm{d}a/\mathrm{d}N) + (\mathrm{d}a/\mathrm{d}t)/f}$$

and

$$R_{\text{c}} = \frac{(\mathrm{d}a/\mathrm{d}t)/f}{(\mathrm{d}a/\mathrm{d}N) + (\mathrm{d}a/\mathrm{d}t)/f}$$

and $p$, $y$ and $C_{\text{fc}}$ are empirical constants.

© Woodhead Publishing Limited, 2010

## 16.5 Applications of fatigue and creep analysis of adhesively bonded joints

### 16.5.1 Introduction

Transport structures such as aerospace airframes and automotive body structures are exposed to a wide range of fatigue loading conditions and provide an excellent example of real life applications where fatigue and creep analysis are playing an increasingly significant role in the design process. Aerospace joints represent one of the most advanced and safety critical applications of bonded joints. Automotive joints highlight the tremendous benefits that can be gained by combining adhesives with complimentary point joining methods such as spot welds or self piercing rivets. In this section, analysis methods in current use by designers and analysts in the automotive and aerospace industries are discussed and suggestions are made for future developments in this area.

### 16.5.2 Aerospace

The benefits of adhesives are utilised to manufacture stiff and lightweight structures for flight control components, such as elevators. These parts often comprise metal skins with honeycomb cores. Heat curing adhesives, which become very fluid for a short time before cross-linking occurs, are employed on these parts to ensure large fillets are produced between the sheet and core material. Adhesive bonding is also widely employed to attach stringers to wing and fuselage skin panels to increase the structural stiffness of airframes. The growing need to minimise fuel consumption in new aircraft is encouraging the increased use of reinforced polymer composites and there is a clear advantage to bonding these materials adhesively.

#### *Designing for fatigue and creep in aerospace*

The most widely adopted approach to joint design in aerospace applications is to incorporate redundant load paths in the airframe. The main function of these redundant design features is to significantly reduce the risk of a serious failure occurring in service in the event that a portion of a bond line on a prime load path becomes damaged or weakened. Incorporating multiple load paths gives the airframe sufficient structural integrity to continue flying after the failure of a structural element, preventing a crash and allowing time for the failure to be detected by a safety inspection and repaired. This topic is discussed in more detail in publications by Tomblin *et al*. (2005), Molent and Barter (2007), Higgins (2000) and Hart-Smith (1981b).

The structural arrangement is a deciding factor in the loading of redundant

© Woodhead Publishing Limited, 2010

load paths after the structure is damaged. Hence the load paths and the expected load levels over time are key criteria in the design of fail safe features. This 'fail-safe' approach is also used to combat creep and production flaws in bonds by employing large joint overlaps that provide sufficient residual strength to accommodate an appropriate level of creep and bondline flaws. The highest service temperature must be considered when choosing the overlap length. If the $T_g$ is below the maximum service temperature, it is good practice to employ sufficient lightly loaded adhesive away from the edges to prevent accumulative creep. A sensible design approach is to make the bond area large enough to give the joint a greater load-carrying capacity than the parts being joined. Tomblin *et al.* (2005) reported that this approach is effective for aluminium joints subjected to shear loading conditions up to a sheet thickness of around 3.5 mm. The overlap length required is influenced by the requirements of structural stiffness and shape, as well as stress and strain levels.

Except for cases where the margins of safety are shown to be large, certification of bonded joints is usually accomplished by mechanical testing. The main objective of the testing being to cover all aspects of the usage of the joints to ensure that there are no unexpected surprises in service. An important part of airframe design and certification is full-scale airframe fatigue testing under variable amplitude loads representative of those predicted to occur over the service lifetime.

### *Combining adhesives with rivets or bolts*

Combining bonding and fasteners has many advantages. The adhesive increases stiffness, improves the load transfer and reduces the stress concentrations at the fastener holes. Aerospace designers often refer to fasteners added to bonded joints to prevent peel as 'chicken rivets'. The fasteners act as peel stoppers, preventing the bond line unzipping in areas of criticality. The main drawbacks of mechanical fasteners are the added weight and cost, and being the most common source of structural cracking. Interference-fit fasteners are usually used on aircraft joints to prevent fretting movement and improve structural fatigue performance.

The complex stress states occurring around a mechanical joint make it difficult to predict the joint lifetime reliably and extensive testing is usually conducted to evaluate the performance and lifetime of mechanical joint configurations. The development of entirely bonded primary aircraft structures has the potential to save significant weight and cost compared to conventional bonded-bolted designs and was the main focus of work in the Navy ManTech Program (2005).

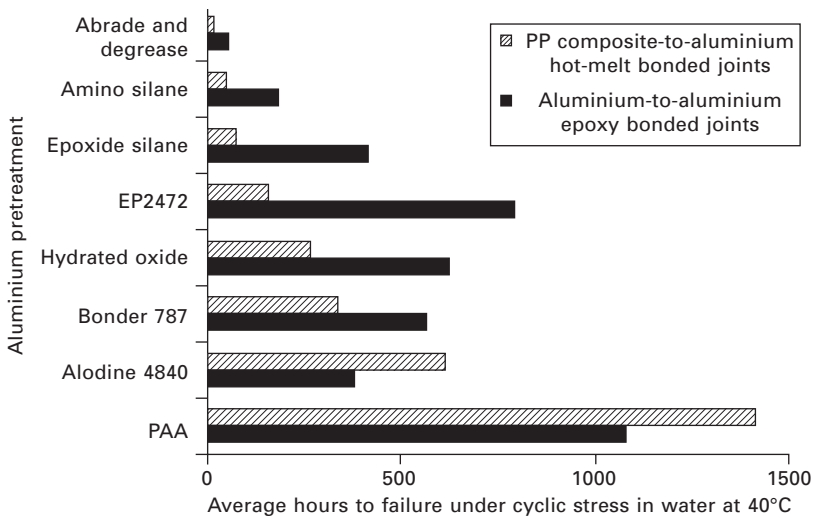
© Woodhead Publishing Limited, 2010

*Environmental degradation*

The most important lifetime prediction topic remains the degradation of bond performance following exposure to harsh environmental conditions. Long-term environmental durability should be substantiated for all structural bonding systems. Adhesive bonds can become weakened by exposure to harsh environmental conditions and the effect of this on fatigue and creep performance can be significant. Significant emphasis must be given to the importance of assessing long-term durability of bonded structures particularly when considering new adhesives or changes to existing suppliers or manufacturing processes.

It is well established that extremely durable adhesive bonds can be made to aluminium provided an appropriate anodising surface pretreatment has been employed; the two most established pretreatments for aerospace components are phosphoric acid and chromic acid anodising. Cyclic stress testing of bonded aluminium joints immersed in hot-wet conditions by Briskham (1999) demonstrated the significant fatigue lifetime benefits of using aerospace standard anodising pretreatments compared to more basic automotive surface treatments, as shown in Fig. 16.12.

The pressing environmental need to remove toxic hexavalent chromium from pretreatment tanks created an urgent need for the development of a viable chromate-free anodising system. Critchlow *et al*. (2006, 2007) have made significant advances in the development of chromate-free anodising pretreatments, with combined corrosion and bond durability performance to rival the effective chromate systems.




*16.12* Average fatigue life in hours of lap shear joints exposed to cyclic stress while immersed in water at 40°C (from Briskham, 1999).

© Woodhead Publishing Limited, 2010

*Modelling and analysis of bonded joints*

The basic properties of bonded joints can be defined by mechanical testing and a joint property database can be populated by testing each bonding system and joint configuration, to enable a range of standard design tools to be employed by the designer. In a recent survey of industry practices for bonded joints by Tomblin *et al*. (2005), 40% of designers reported having had some success in applying analysis methods for fatigue and damage tolerance assessments of bonded structures.

A typical design approach is to calculate the load capacity of a joint using elastic–plastic analysis and then compare this against the structural loading requirements to determine the overlap length required to carry the loads by elastic behaviour. As a precaution against creep, this overlap length is usually extended to provide a lightly loaded region in the joint that can help to prevent the accumulation of irreversible creep strain. Experimental data of the effect of maximum and minimum service temperatures is then used to ensure that the joint will provide the required load capacity in the full range of service conditions. In most cases the design analysis also takes residual stresses in the bonded joint into account.

A local strain-based approach is widely used for fatigue crack initiation analysis, with consideration being given to the plastic deformation that may occur in localized regions where fatigue cracks begin. The stresses and strains in these localised regions are analysed and used as a basis for crack initiation life predictions. Coupon tests are conducted for each location and loading spectrum to obtain mean test lives, crack initiation and failure times. The damage for each full or half-cycle is calculated using a strain–life curve and the total fatigue damage is summed. The equivalent flight hour time is measured in terms of number of cycles. A strain-based approach is especially appropriate for ductile airframe materials, such as aluminium or titanium, as these materials experience local yielding associated with occasional severe loading events.

Molent and Barter (2007) conducted an extensive review of crack growth in metals on a range of airframes in service and concluded that the relatively simple crack growth model shown in the following equation adequately represents typical crack growth:

$$Ln(a) = \psi t_F + Ln(a_0) \qquad [16.29]$$

where $t_F$ is the flight hours, $\psi$ is a parameter dependent on geometry, material and load spectrum, $a$ is the crack depth at $t_F$ and $a_o$ is the initial crack size.

*Fatigue tracking of aircraft in service*

Fatigue life tracking primarily involves monitoring the fatigue stresses

© Woodhead Publishing Limited, 2010

experienced by each individual airframe in order to prevent the airframe being used after it has exceeded agreed fatigue life limits and maximise the service life of the airframe. Tracking an individual aircraft's usage is paramount since the loads experienced may vary significantly.

Molent and Barter (2007) concluded from their review of crack growth in airframes that despite the best efforts of designers, fatigue cracking is likely to develop in all airframes in service, making fatigue tracking essential during the lifetime of airframes. Early fatigue tracking systems used crack initiation as a retirement criterion for airframes. However, the extensive development of total life and risk assessment approaches for aircraft have led to significant improvements in this field and the development of advanced systems for fatigue tracking and crack growth analysis. Onboard recorders monitor a broad spectrum of loading events such as bending and torsion. The fatigue tracking system employed for each aircraft model is validated by comparing the calculated damage with test results and service experience. The design requirements of the airframe are influenced by the method of fatigue tracking; see Sarkar *et al*. (2007) for more in depth information on this topic.

The structural lives of aircraft are generally defined by using one of three approaches: safe-life, fail-safe and damage-tolerant. The safe-life approach, aims to retire a component from service before the formation of a fatigue crack by using safety factors calculated from crack initiation data. This approach has the advantage of low inspection requirements and is employed in service applications where detailed inspection is difficult, such as aircraft carriers.

The fail-safe approach requires multiple load paths to be included at the design stage so that even after the failure of a structural element, the structural integrity of the aircraft is not impaired, allowing sufficient time for scheduled inspections to find and repair the damage.

The damage-tolerant approach aims to detect cracks before they reach catastrophic or critical sizes by imposing inspection schedules appropriate to the crack growth characteristics of each component. The application of a damage tolerance approach depends on the component's inspectability. If a component is non-inspectable, then service life must be demonstrated through crack growth analysis.

### 16.5.3 Automotive

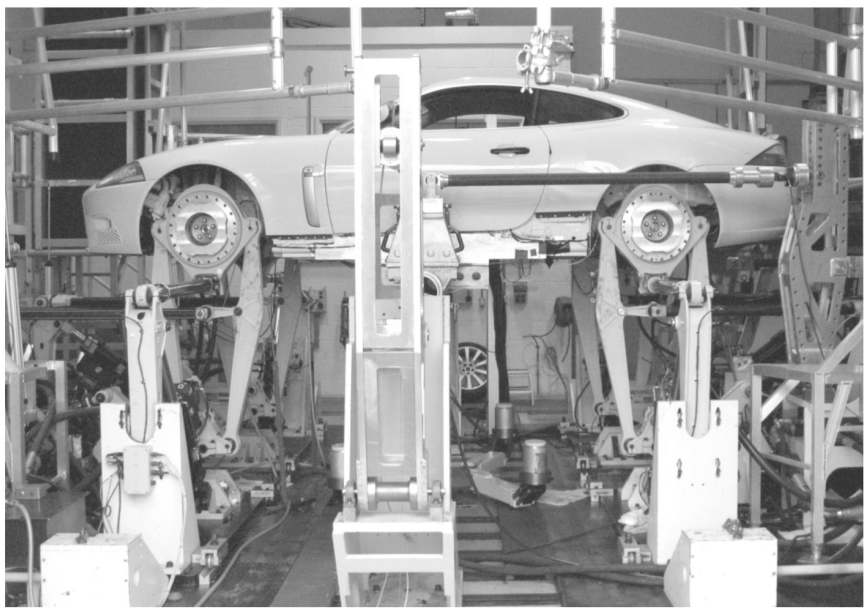
The analysis of structural adhesives for fatigue life prediction is a relatively new requirement in the automotive industry and is being investigated in several research projects. It is currently difficult for car designers to predict the fatigue durability of bonded and hybrid joints. Therefore most designers take a conservative approach and over-engineer the body structure to ensure

© Woodhead Publishing Limited, 2010

the joints will not fail under normal service conditions. This adds extra weight and cost to the vehicle and has a knock on effect on other related areas such as such as acceleration, braking and fuel consumption. Figure 16.13 shows the durability testing of a full car body structure. This testing is accompanied by road testing on a track surface designed to accelerate the effects of loading. This testing is expensive and any problems identified at this late design stage will result in potentially expensive 'fixes'. Car designers responsible for durability analysis have highlighted the need for a software tool to analyse and predict the durability of bonded or hybrid car body joints to enable the design of optimised structures whilst minimising the risk of in-service failure. Researchers at Coventry University are currently working with fatigue software suppliers to develop a tool for this purpose.

*Adhesive and hybrid joints*

A typical car body has between 4000 and 6000 point joints; most car bodies are made from pressed steel panels and the point joints on these cars are almost entirely produced using resistance spot welding. Some luxury and sports car bodies are made from pressed aluminium panels; the point joints on aluminium cars can be made using either self pierce riveting or resistance spot welding. Recent advances in the electrode life of aluminium spot welding by



*16.13* Photograph showing durability testing of a full car body structure (courtesy of Jaguar Cars Ltd).

© Woodhead Publishing Limited, 2010

Briskham *et al*. (2006) means that the same point joining method so widely and effectively employed on steel cars can now be applied in a similar fashion to aluminium cars. Both of these point joining methods apply a sufficiently high clamping force via a two sided gun to squeeze a viscous wet adhesive out of the localised area between the tips of the gun before the point joint is made. Combining point joining with adhesive bonding to produce hybrid joints in this way is commonly known as weld-bonding and riv-bonding.

Hybrid joining is so effective that it has become common practice in both steel and aluminium car body structures. Several studies, such as by Booth *et al*. (2000), have reported significant improvements in structural connectivity gained through the use of hybrid joints and the resulting enhancements in stiffness, NVH (noise, vibration and harshness), and fatigue and crash performance. Low volume sports cars with aluminium body structures and hybrid joints combining mechanical point joints with adhesives have proved the performance and durability benefits of this approach. Point joints remain the primary joining method in high volume cars, but many manufacturers now enhance these joints by adding adhesive in high stress or high fatigue locations, such as in the A or B post joints forming the passenger safety cell.

Figure 16.14 shows the significant fatigue life improvement available by adding adhesives to riveted aluminium joints. The riveted joint failed after 1.5 million cycles at 3 kN, $R = 0.1$, whereas bonded and riv-bonded joints both showed no visible sign of damage after 6 million cycles under the same test conditions.

Larger amounts of adhesive can usually be found in the joints of executive car bodies where ride quality is of paramount importance. Most hybrid joining applications in high volume car plants employ single part heat curing adhesives, avoiding the need for clamping by using the point joints to hold the wet bonded parts together and utilising the e-coat baking process to cure the adhesive.

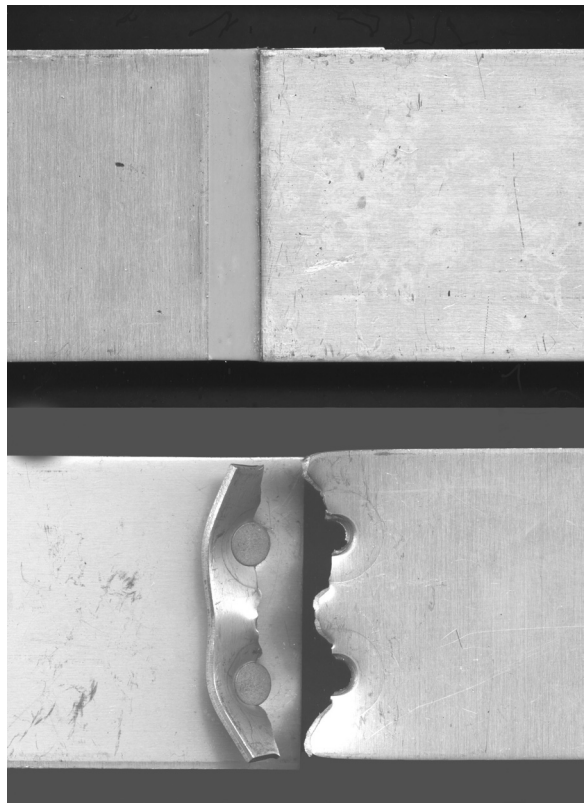
### *Design and analysis approaches*

A conservative approach is normally used in which the acceptable limits are based on data from axial tests. The automotive industry is currently using a number of different design approaches to predict joint durability under fatigue loading conditions, these include:

- controlling the stresses in the adhesives within acceptable limits
- controlling forces in the adhesives within acceptable limits
- calculating the strain energy release rate and ensuring that this is below the threshold value for the adhesive.

A typical approach could be described as follows. Small joints representing

© Woodhead Publishing Limited, 2010



*16.14* Aluminium lap shear joints produced by bonding and self-pierce riveting, showing the earlier failure of the riveted joint.

each joint on the vehicle are mechanically tested to determine a range of properties, including maximum strength, energy absorption and fatigue life, under a range of loading and environmental conditions. These results are used to generate a database of joint property data and fatigue life curves. The test samples are then modelled to determine the values of selected design criteria, which can then be applied to adhesive or hybrid joints in a vehicle.

### *Constant and variable amplitude loading*

The majority of bond durability studies conducted to date have focussed on constant amplitude loading, but joints in service on cars are mainly exposed to variable loading with occasional peak loading events. It is important to test joints using variable amplitude loads in order to simulate real life conditions more closely. Occasional spikes in a variable amplitude loading profile have been shown to initiate joint failures more quickly than constant amplitude

© Woodhead Publishing Limited, 2010

loads. A recent study by Erpolat *et al*. (2004b) found occasional overload cycles accelerated the damage caused by repetitions of smaller cycles. Predicting fatigue crack growth in bonded metals under random loadings is a difficult task, in particular because of load history effects, which stem from load sensitivity of the process, or a damage zone in the adhesive ahead of the crack tip.

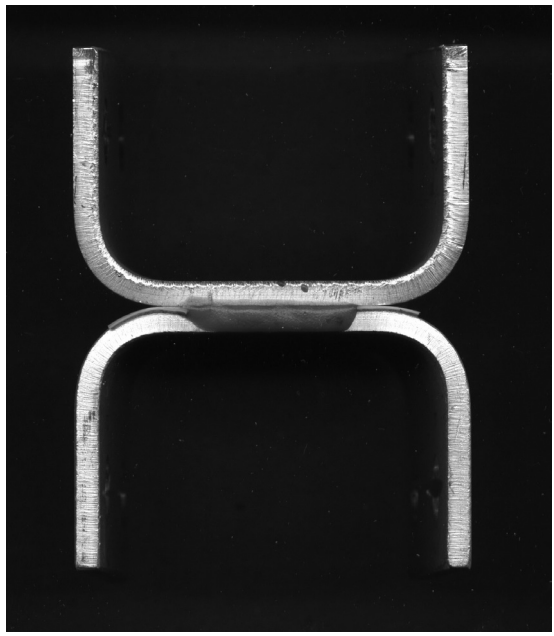
### *Cyclic stress testing to generate joint property data*

Cyclic stress durability modelling of adhesives requires the initiation and growth behaviour of cracks to be evaluated and the threshold value, where no further crack growth occurs, to be investigated. For example, at low cyclic loads the fatigue life of a bonded joint can be dominated by crack initiation, but at high cyclic loads the fatigue life can be dominated by crack growth. An effective analysis system needs to account for the cumulative damage caused by exposure to different types of loading. The favoured approach for assessing the fatigue resistance of adhesive systems and conducting fatigue life predictions is based on fracture mechanics. The basis of the approach is for bonded joints to be designed to remain below the fatigue growth threshold $G_{th}$ value to avoid crack growth in service. This approach is generally favoured over stress–life based methods. More information on this topic can be found in studies by Ashcroft (2004), Harris and Martin (1998) and Nolting *et al*. (2008).

In order to generate results that are useful for conducting fatigue–life predictions on a specific joint configuration, it is good practice to employ a material thickness, bond area and corner radii that closely represent the real life joints. Joint types commonly employed by automotive engineers in fatigue testing include lap shear, t-peel, cantilever beam, U shape, box section and top hat. U-shape joints are one of the joint geometries available for investigating hybrid joints, and were recommended by the American Welding Society (1966) for testing spot welded joints. The geometry employed by Briskham and Maddison (2008) in a recent study of hybrid aluminium joints is shown in Fig. 16.15.

Quasi-static and fatigue strength are both influenced by the adhesive fillet size. Therefore, the amount of adhesive in the fillet region is one of the most important factors to consider when making fatigue test specimens. It is common practice to have a manual wiping operation on low volume sports car bodies to remove excess adhesive flowing from squeezed joints and it is beneficial to create an angled bond fillet to improve stress distribution and maximise the bond performance. In high volume vehicle production the flow of excess adhesive from joints is usually seen as undesirable, and in order to avoid operator skin contact and minimise waste, a zero or minimal

© Woodhead Publishing Limited, 2010



*16.15* Bonded aluminium U shape testpiece.

fillet size is usually preferred. This explains why test pieces manufactured to investigate the fatigue properties of high volume car joints are usually manufactured with a minimal or zero fillet size.

Testing one joint at a time on single station testing frames requires long testing periods to generate the volume of data required to populate a joint properties database. A fully instrumented multi-station approach enables these tests to be conducted in days rather than weeks. A multi-station system constructed to test up to 12 lap shear or U shape joints under load control is shown in Fig. 16.16.

### *Testing for degradation of bonds in hostile environments*

It is well established that exposure to water, extreme temperature changes, or chemicals can significantly accelerate crack growth in bonded joints under fatigue loading conditions and that the temperature of the water has a significant effect on the joint life. Exposure to wet conditions can cause the crack propagation path to change from running through the adhesive, which is the usual propagation path in dry conditions, to the adhesive–metal interface. Briskham (Briskham 1998; Briskham and Smith, 2000) showed cyclic stress testing of joints under water caused extremely rapid joint failures to occur in some bonding systems and highlighted the significant

© Woodhead Publishing Limited, 2010



*16.16* Multi-station fatigue testing apparatus for testing twelve lap shear, T-peel or U-shape joints, either in air, inside a humidity chamber or immersed in water.

extra durability gained by employing aerospace anodising pretreatments for aluminium joints.

Many of the adhesive joints in a car body structure are protected from exposure to water or do not become wet for long enough to suffer from significant levels of accelerated fatigue failure caused by water ingress. This, plus the use of point joints as the primary joining method and adhesives as the secondary method, enables car manufacturers to employ less expensive surface pretreatments than the anodising systems employed for aerospace parts. However, it is important to evaluate the fatigue life under hot–wet conditions for every bonding system and multi-station testing provides an effective way to run comparative tests against systems which have proved their long-term durability in service applications.

### *Joint quality monitoring in production*

Many car manufacturers protect themselves against potential legal claims by employing data logging systems that provide a traceability record, demonstrating how each joint was made, in the event of this being required

© Woodhead Publishing Limited, 2010

to investigate a fatigue or crash failure in service. Some luxury car makers have recently introduced automated photography systems to record the size of the adhesive fillet on key joints and provide a traceability record that adhesive was present in the joint.

### 16.5.4 Summary

Adhesive bonding is ideal for transport applications, providing many advantages such as weight efficiency, fatigue resistance and the ability to produce aerodynamically smooth surfaces. There is significant scope for the further development of more powerful analytical tools to aid the design of bonded joints in transport applications and to reduce the requirement for mechanical testing of coupons, assemblies and complete structures. Useful design tools can take the form of generic design guidelines, such as process window charts, as well as powerful software programs for predicting failures and enabling further optimisation of designs. Increasing fuel consumption and environmental considerations mean the demand for optimised lightweight structures and extended service lifetimes will continue to increase. Efficient production of highly durable joints in a range of different materials and at the same time development of cost effective methods for repair or end of life separation is one of the main challenges facing engineers in this field.

## 16.6 Overall summary and future trends

Both fatigue and creep can have a significant bearing on the performance and failure of structural adhesive joints and must be considered if efficient and safe bonded structures are to be designed. A number of tools for predicting both creep and fatigue behaviour of bonded joints are already available to the designer. However, each of these has limitations and selection of appropriate analytical methods which the designer can fully trust is still a problem. In the future two separate developments are needed.

First, models that more accurately represent the physical behaviour of bonded joints under complex loading and environmental conditions must continue to be developed. This will be aided by continuing developments in computational mechanics and experimental damage characterisation techniques. Second, there must be a concerted effort to translate the increased ability to model complex adhesive joint behaviour accurately to trustworthy and easy to use tools for the designer. There are currently many design tools available to the designer but these tend to be fragmented, poorly supported and offer limited functionality. Some of the larger automotive and aerospace companies have developed their own methodologies and software for analysing and predicting joint durability, but creating, updating and validating in-house software is a costly exercise and there is a strong argument for working in

© Woodhead Publishing Limited, 2010

collaborative partnerships to bring specialist resources and skills together to develop and update commercially available software tools. One of the biggest decisions a designer has to make is how conservative to be in ensuring a product will not fail in service. The continued development of tools to enable more reliable predictions of fatigue and creep failures will enable further optimisation of designs to reduce key factors such as cost and fuel consumption, without endangering lives or reputation.

## 16.7 References

Abdel Wahab MM, Ashcroft IA, Crocombe AD, Hughes DJ and Shaw SJ (2001a). 'The effect of environment on the fatigue of bonded composite joints. Part 2: fatigue threshold prediction'. *Composites Part A*, **32**, 59–69.

Abdel Wahab MM, Ashcroft IA, Crocombe AD, Hughes DJ and Shaw SJ (2001b). 'Prediction of fatigue threshold in adhesively bonded joints using damage mechanics and fracture mechanics'. *J Adhesion Sci Technol*, **15**, 763–82.

Abdel Wahab MM, Ashcroft IA, Crocombe AD and Smith PA (2003). 'Fatigue crack propagation in adhesively bonded joints'. *Key Eng Mater*, **251**, 229–34.

Abdel Wahab MM, Ashcroft IA, Crocombe AD and Smith PA (2004). 'Finite element prediction of fatigue crack propagation lifetime in composite bonded joints'. *Composites Part A*, **35**, 213–22.

Al-Ghamdi (2004). *Fatigue and Creep of Adhesive Bonded Joints*, PhD Thesis, Loughborough University.

Al-Ghamdi AH, Ashcroft IA, Crocombe AD and Abdel Wahab MM (2003). 'Crack growth in adhesively bonded joints subjected to variable frequency fatigue loading'. *J Adhesion*, **79**, 1161–82.

Al-Ghamdi AH, Ashcroft IA, Crocombe AD and Abdel Wahab MM (2004). 'Creep and fatigue crack growth in DCB joints'. In: *Proceedings 7th International Conference on Structural Adhesives in Engineering*, IOM Communications, London, 22–5.

American Welding Society (1966). *Recommended Practices for Resistance Welding*, American Welding Society, AWS C1.1–66.

Ashcroft IA (2004). 'A simple model to predict crack growth in bonded joints and laminates under variable amplitude fatigue'. *J Strain Anal*, **39**, 707–16.

Ashcroft IA and Shaw SJ (2002). 'Mode I fracture of epoxy bonded composite joints, Part 2: fatigue loading'. *Int J Adhesion and Adhesives*, **22**, 151–67.

Ashcroft IA, Abdel Wahab MM, Crocombe AD, Hughes DJ and Shaw SJ (2001). 'Effect of temperature on the quasi-static strength and fatigue resistance of bonded composite double lap joints'. *J Adhesion*, **75**, 61–88.

Ashcroft IA, Abdel Wahab MM and Crocombe AD (2003). 'Predicting degradation in bonded composite joints using a semi-coupled FEA method'. *Mech Adv Mater Struct*, **10**, 227–48.

Ashcroft IA, Al-Ghamdi AH, Crocombe AD and Wahab MA (2005). 'Creep-fatigue interactions and the effect of frequency on crack growth in adhesively bonded joints'. In: *Proceedings 9th International Conference on the Science and Technology of Adhesives*, Oxford, IOM Communications, London, 110–13.

Bond IP (1999). 'Fatigue life prediction for GRP subjected to variable amplitude loading'. *Composites Part A*, **30**, 961–70.

Booth GS, Olivier CA, Westgate SA, Liebrecht F and Braunling S (2000). 'Self-piercing

© Woodhead Publishing Limited, 2010

riveted joints and resistance spot-welded joints in steel and aluminium'. *Proceedings of the International Body Engineering Conference*, Detroit, MI, 2000, SAE International, SAE Paper No. 2000-01-2 681.

Briskham P (1998). 'Cyclic stressing of lap shear joints in a hostile environment', *Fifth International Conference on Adhesion and Surface Analysis*, Loughborough University, 31st March–2nd April 1998.

Briskham P (1999). *Strong and Durable Fusion Bonding of Glass Reinforced Polypropylene to Pre-treated Aluminium*, PhD Thesis, University of Warwick.

Briskham P and Smith G (2000). 'Cyclic stress durability testing of lap shear joints exposed to hot-wet conditions'. *Int J Adhesion Adhesives*, **20**, 33–8.

Briskham P and Maddison A (2008). 'Long term performance and prediction of bonded joint behaviour'. *International Rapra Conference Automotive Adhesives Sealants and Coatings*, 10–11 June, Stuttgart, Germany.

Briskham P, Boomer D, Blundell N, Han L, Hewitt R and Young K (2006). 'Comparison of self-pierce riveting, resistance spot welding and spot friction joining for aluminium automotive sheet'. *Proceedings of SAE 2006 World Congress & Exhibition*, April 2006, Detroit, MI, USA, Session: Welding and Joining and Fastening. SAE International, SAE Paper No. 2006-01-0774.

Cernocky EP (1982). 'Comparison of the unloading and revesred loading behaviour of three viscoplastic constitutive theories'. *Int J Non-Linear Mech*. **17**, 255–66.

Chen T (2000). *Determining a Prony Series for a Viscoelastic Material from Time Varying Strain Data*. NASA TM-2000-210123, ARL-TR-2206.

Chiu WK and Jones R (1995). 'Unified constitutive model for thermoset adhesive FM73'. *Int J Adhesion Adhesives*, **15**, 131–6.

Christensen RM (2003). *Theory of Viscoelasticity*, Dover Publications, New York, USA.

Critchlow GW, Yendall KA, Bahrani D, Quinn A and Andrews F (2006). 'Strategies for the replacement of chromic acid anodising for the structural bonding of aluminium alloys'. *Int J Adhesion Adhesives*, **26**, 419–53.

Critchlow G, Ashcroft I, Cartwright T and Bahrani D (2007). *Anodising Aluminium Alloys*, UK Patent no. GB 3421959A.

Crocombe AD, Yu X and Richardson G (2001). 'A unified visco-plastic model for the stress analysis of adhesively bonded structures', *J. Adhesion Sci Technol*, **15**(3), 279–302.

Crocombe AD, Ong AD, Chan CY, Abdel Wahab MM and Ashcroft IA (2002). 'Investigating fatigue damage evolution in adhesively bonded structures using backface strain measurement'. *J Adhesion*, **78**, 745–78.

Crocombe AD, Wahab MA and Ashcroft IA (2005). 'Characterising adhesive joint fatigue damage evolution using multiple backface strain gauges'. In: *Proceedings 28th Annual Meeting of the Adhesion Society*, Vorvolakos K (ed.), The Adhesion Society, 211–13.

Dessureault M and Spelt JK (1997). 'Observations of fatigue crack initiation and propagation in an epoxy adhesive'. *Int J Adhesion Adhesives*, **17**, 183–95.

Dibenedetto AT and Salee G (1979). 'Fatigue crack propagation in graphite fibre reinforced nylon 66'. *Polym Eng Sci*, **19**, 512–18.

Erpolat S, Ashcroft IA, Crocombe AD and Abdel Wahab MM (2004a). 'A study of adhesively bonded joints subjected to constant and variable amplitude fatigue'. *Int J Fatigue*, **26**, 1189–96.

Erpolat S, Ashcroft IA, Crocombe AD and Abdel Wahab MM (2004b). 'Fatigue crack

© Woodhead Publishing Limited, 2010

growth acceleration due to intermittent overstressing in adhesively bonded CFRP joints'. *Composites A*, **35**, 1175–83.
Ferry JD (1970). *Visoelastic Properties of Polymers*, John Wiley & Sons Ltd, New York, USA.
Graner-Solana A, Crocombe AD, Wahab MA and Ashcroft IA (2007). 'Fatigue initiation in adhesively bonded single lap joints'. *J Adhesion Sci Technol*, **21**, 1343–57.
Griffith AA (1921). 'The phenomenon of rupture and flow in solids'. *Phil Trans R Soc A*, **221**, 163–97.
Harris JA and Fay PA (1992). 'Fatigue life evaluation of structural adhesives for automotive applications'. *Int J Adhesion Adhesives*, **12**, 9–18.
Harris JA and Martin RH (1998). *Development of a Life Assessment Method for Bonded and Weld-Bonded Automotive Structures*, MERL Ltd. 1998, SAE 980692.
Hart-Smith LJ (1981a). *Developments in Adhesives 2*, Applied Science Publ, London, 1–44.
Hart-Smith L J (1981b). *Further Developments in the Design and Analysis of Adhesive-Bonded Structural Joints*. ASTM special technical publication, ISSN 0066-0558, CODEN ASTTA8, no 749, 3–31.
Henry DL (1955). 'A theory of fatigue damage accumulation in steel'. *Trans Am Soc Mech Eng*, **77**, 913–8.
Higgins A (2000). 'Adhesive bonding of aircraft structures, *Int J Adhesion Adhesives*, **20**, 367–76.
Hilmy I, Abdel Wahab MM, Ashcroft IA and Crocombe AD (2006). 'Measuring of damage parameters in adhesive bonding'. *Key Eng Mater*, **324**, 275–8.
Hilmy I, Abdel Wahab MM, Crocombe AD, Ashcroft IA and Solano AG (2007). 'Effect of triaxiality on damage parameters in adhesive'. *Key Eng Mater*, **348**, 37–40.
Hojjati M, Johnston A, Hoa SV and Denault J (2004). 'Viscoelastic behaviour of Cytec FM73 adhesive during cure'. *J Appl Polym Sci*, **91**, 2548–57.
Irwin GR (1958). 'Fracture'. *Handbuch der Physic VI*, Flugge S (ed.), Springer, Berlin, 551–90.
Jurf RA and Vinson JR (1985). 'Effect of moisture on the static and viscoelastic shear properties of epoxy adhesives'. *J Mater Sci*, **20**, 2979–89.
Kachanov LM (1986). *Introduction to Continuum Damage Mechanics*, Martinus Nijhoff, Dordrecht.
Kitagawa M, Mori T and Matsutani T (1989). 'Rate dependent nonlinear constitutive equation of polypropylene'. *J Polym Sci Polym Phys*, **27**, 85–95.
Landes JD and Begley JA (1976). *A Fracture Mechanics Approach to Creep Crack Growth*. ASTM STP 590, 128–48.
Lefebvre DR and Dillard DA (1999) A stress singularity approach for the prediction of fatigue crack initiation. Part1: theory. *J Adhesion*, **70**, 119–38.
Lemaitre J (1984). 'How to use damage mechanics'. *Nuclear Eng Design*, **80**, 233–45.
Lemaitre J (1985). 'A continuous damage mechanics model for ductile fracture'. *J Eng Mater Technol*, **107**, 83–9.
Leve HL (1969). 'Cumulative damage theories. In: *Metal Fatigue: Theory and Design*, John Wiley & Sons, NY, USA, 170–203.
Marco SM and Starkey WL (1954). 'A concept of fatigue damage'. *Trans Am Soc Mech Eng*, **76**, 626–62.
McCrum NG and Morris EL (1964). 'On the measurement of the activation energies for creep and stress relaxation'. *Proc Roy Soc A*, **281**, 258–73.
Miner MA (1945). 'Cumulative damage in fatigue'. *J Appl Mech*, **12**, 159–64.

© Woodhead Publishing Limited, 2010

Molent L and Barter SA (2007). 'A comparison of crack growth behaviour in several full-scale airframe fatigue tests'. *Int J Fatigue*, **29**, 1090–9.

Navy ManTech Program (2005). *Aircraft Primary Structure Adhesive Bonding Development*, Navy ManTech Program, Rev A, September, Office of Naval Research, USA.

Nielsen LE and Landel RF (1994). *Mechanical Properties of Polymers and Composites*, Marcel Dekker, New York, USA.

Nikbin KM, Webster GA and Turner CE (1976). *Relevance of Nonlinear Fracture Mechanics to Creep Cracking*. ASTM STP 601, 47–62.

Nolting AE, Underhill PR and DuQuesnay DL (2008). 'Variable amplitude fatigue of bonded aluminum joints', *Int J Fatigue*, **30**, 178–87.

Owen MJ and Howe RJ (1972). 'The accumulation of damage in a glass-reinforced plastic under tensile and fatigue loading'. *J Phys D: Appl Phys*, **5**, 1637–49.

Palmgren A (1924). 'Die Lebensdauer von Kugellargen', *Zeitschrift des Vereins Deutscher Ingenieure*, **68**, 339–41.

Paris PC, Gomez MP and Anderson WE (1961). 'A rational analytic theory of fatigue life'. *Trend in Engineering*, **13**, 9–14.

Quaresimin M and Ricotta M (2006). 'Fatigue behaviour and damage evolution of single lap bonded joints in composite material'. *Comp Sci Technol*, **66**, 176–87.

Rice JR (1968). 'A path independent integral and the approximate analysis of strain concentration by notches and cracks'. *J Appl Mech*, **35**, 379–86.

Sarkar S, Iyyer N, Merrill R and Phan N (2007). 'Aircraft life management using crack initiation and crackgrowth models – P-3C aircraft experience'. *Int J Fatigue*, **29**, 1584–607.

Saxena A (1986). *Creep Crack Growth under Nonsteady-State Conditions*, ASTM STP 905, 185–201.

Schaff JR and Davidson BD (1997a). 'Life prediction methodology for composite structures, Part I: Constant amplitude and two-stress level fatigue'. *J Comp Mater*, **31**, 128–57.

Schaff JR and Davidson BD (1997b). 'Life prediction methodology for composite structures, Part II: Spectrum fatigue'. *J Comp Mater*, **31**, 158–81.

Shames IH and Cozzarelli FA (1997). *Elastic and Inelastic Stress Analysis*. Taylor and Francis, Philadelphia PA.

Shenoy V, Ashcroft IA, Critchlow GW, Crocombe AD and Abdel Wahab MM (2009a). 'An investigation into the crack initiation and propagation behaviour of bonded single lap joints using backface strain'. *Int J Adhesion Adhesives*, **29**, 361–71.

Shenoy V, Ashcroft IA, Critchlow GW, Crocombe AD and Abdel Wahab MM (2009b). 'Strength wearout of adhesively bonded joints under constant amplitude fatigue'. *Int J Fatigue*, **31**, 820–30.

Shenoy V, Ashcroft IA, Critchlow GW, Crocombe AD and Abdel Wahab MM (2009c). 'An evaluation of strength wearout models for the lifetime prediction of adhesive joints subjected to variable amplitude fatigue'. *Int J Adhesion Adhesives*, **29**, 639–49.

Soussou JE, Moavenzadeh F and Gradowczyk MH (1970). 'Application of Prony series to viscoelasticity', *J Rheol*, **14**, 573–84.

Tomblin J, Strole K, Dodosh G and Ilcewicz L (2005). *Assessment of Industry Practices for Aircraft Bonded Joints and Structures*, DOT/FAA/AR-05/13, Office of Aviation Research, Washington, DC 20591, July 2005, Final Report.

Ward IM and Sweeney J (2004). *An Introduction to the Mechanical Properties of Solid Polymers*. John Wiley & Sons, Chichester, England.

Whitworth HA (1990). 'Cumulative damage in composites'. *J Eng Mater Technol*, **112**, 358–61.

© Woodhead Publishing Limited, 2010

Williams ML, Landel RF and Ferry JD (1955). 'The temperature dependence of relaxation mechanisms in amorphous polymers and other glass-forming liquids'. *J Am Chem Soc*, **77**, 3701–07.

Wöhler A (1867). 'Versuche über die Festigkeit der Eisenbahnwagenachsen'. *Zeitschrift für Bauwesen*, **10**, 'English summary', *Engineering*, **4**, 160–1.

Yang JN, Jones DL, Yang SH and Meskini A (1990). 'A stiffness degradation model for graphite/epoxy laminates'. *J Comp Mater*, **24**, 753–69.

Yao J and Ziegmann G (2006). 'Equivalence of moisture and temperature in accelerated test method and its application in prediction of long-term properties of glass-fiber reinforced epoxy pipe specimen'. *Polym Testing*, **25**, 149–57.

Yu XX, Crocombe AD and Richardson G (2001). 'Material modelling for rate-dependent adhesives', *Int J Adhesion Adhesives*, **21**, 197–210.

Zhang Z and Shang JK (1995). 'A backface strain technique for detecting fatigue crack initiation in adhesive joints'. *J Adhesion*, **49**, 23–36.

© Woodhead Publishing Limited, 2010

# 17

# Improving bonding at high and low temperatures

L. F. M. DA SILVA, University of Porto, Portugal

**Abstract**: A full study of the effects of temperature on joints must cover shrinkage of the adhesive, differential coefficients of thermal expansion and variation of adhesive mechanical properties with temperature such as the stress–strain curve and the toughness. These three aspects are treated in the present chapter in detail, supported by the most up-to-date data. Methods of modelling and experimental results are presented and it is shown that variation of the adhesive mechanical properties with temperature is generally the most critical factor. As the glass transition temperature of the adhesive is approached, a dramatic change in properties occurs. Techniques to improve the joint behaviour are proposed, especially the mixed adhesive joint concept where a low temperature adhesive and a high temperature adhesive are used together in a joint. Geometrical solutions are also proposed. Functionally graded adhesive joints are discussed as future trends.

**Key words**: high temperature adhesives, thermal analysis, finite element analysis, glass transition temperature, mechanical properties of adhesives, joint design.

## 17.1 Introduction: key problems caused by high and low temperature conditions

One of the main advantages of using adhesive bonding is the possibility of bonding dissimilar materials, such as carbon fibre reinforced plastics (CFRP) to aluminium in many aeronautical applications. However, dissimilar adherends may have very different coefficients of thermal expansion (CTE). Thus, temperature changes may introduce thermal stresses in addition to the externally applied loads. Adhesive curing and the resulting thermal shrinkage may also introduce internal stresses. Deformations or even cracks can appear. A full study of the effects of temperature on joints must cover the three following aspects:

1. shrinkage of the adhesive
2. differential thermal expansion
3. variation of adhesive mechanical properties with temperature.

It is important to consider thermal effects because these generally lead to a joint strength reduction (Apalak *et al.*, 2003a; Srivastava, 2003; Al-Samhan and Darwish, 2005), even though in some cases the opposite happens (da



© Woodhead Publishing Limited, 2010

Silva *et al*., 2004). Several authors have found that the stresses caused by adhesive shrinkage have much less effect on the lap joint strength than those generated by the adherend thermal mismatch (Adams *et al*., 1992; Adams and Mallick, 1993; Coppendale, 1977; Yu, 1999). Thermal loads are especially important when bonding adherends with different CTEs (Hart-Smith, 1973; Rastogi *et al*., 1998; Apalak and Gunes, 2002; Kaye and Heller, 2005). However, the change in adhesive properties with temperature is the main challenge for low and high temperature applications. While most metals used in structural applications are relatively insensitive to temperature variations from –50 to 150ºC, most adhesives show a dramatic change in their mechanical properties.

This chapter starts with a description of the three aspects mentioned above (shrinkage of the adhesive, differential thermal expansion and variation of adhesive mechanical properties with temperature). Methods of modelling thermal loads are then discussed for uniform and non-uniform temperature distribution cases. Experimental joint strength results are presented to illustrate the importance of temperature. Techniques to improve the joint behaviour at low and high temperatures are proposed. Finally future trends are discussed.

## 17.2 Shrinkage of the adhesive

Yu (1999) developed a device to measure the cure shrinkage of adhesives. A volume shrinkage of 5% for several adhesives was obtained, about a third of which takes place after gelation. This is an important point since volume reduction occuring after the start of gel in the adhesive will introduce internal stresses. Yu (1999) also showed experimentally with a metallic strip coated with an adhesive that the residual stresses caused by the shrinkage of the adhesive during cure are much lower than those caused by differences in CTEs. The same conclusion was obtained by Yu *et al*. (2006).

Lu and Wong (2000) measured the adhesive shrinkage of three conductive epoxy adhesives with a thermomechanical analyser (TMA) and the resin dimensional change during cure ranged between 2.98 and 4.33%. Hudson *et al*. (2002) developed an optical method to measure shrinkage accurately during the cure of adhesives treated with UV light. An average value for the volume shrinkage of 8.7% was obtained with a fairly small scatter of ±0.2%. Zhang *et al*. (2005) developed an experimental technique to measure the cure force and consequently the volume shrinkage during the curing process. A droplet of liquid adhesive is applied between two glass rods with low CTE. The adhesive is then cured by infrared heating. A micro-tester is used to measure the force required to keep the glass rods at a constant distance during the curing process. The volume cure shrinkage of a non-conductive adhesive was 4.29%.

© Woodhead Publishing Limited, 2010

Coppendale (1977) studied the effect of adhesive cure shrinkage in lap joints using a two dimensional finite element (FE) analysis. In the overlap region, the predominant stress is longitudinal tensile. It is uniform in the central region and decreases towards each end. Around the adherend corner with a fillet, the maximum tensile stress caused by shrinkage is at an angle of approximately 45° to the maximum tensile stress caused by an external applied load. For relatively high applied mechanical loads, Coppendale (1977) concluded that for 0.5% shrinkage, shrinkage stresses are not important (for 10 kN the effect is less than 10%).

Mallick (1989) studied CFRP/aluminium single lap joints (SLJs) typically used in aircraft structures. He studied the thermal stresses caused by adhesive contraction, the thermal stresses caused by different thermal expansion of the two adherends and a temperature reduction of 150ºC and the stresses caused by a 5 kN applied load. After superimposing all the stresses, he found that the adhesive shrinkage stresses have much less effect than adherend mismatch.

## 17.3 Effect of differential thermal expansion

Coefficients of thermal expansion for different substrates and adhesives are presented in Table 17.1. The CTEs can be determined by dilatometry, by strain gauges (da Silva and Adams, 2008) or by a bi-material curved beam method (Yu *et al.*, 2003; Loh *et al.*, 2005).

Let us look at the residual stresses in a joint with aluminium and a CFRP for example. With a negative thermal load, that is with a decrease in temperature from the stress-free temperature ($T_{SF}$), and a compliant adhesive, the aluminium and the composite adherends can contract freely (see Fig. 17.1a). Note that, in fact, the length of the composite adherend does not

*Table 17.1* Typical coefficients of thermal expansion (CTE) of various adherends and adhesives (da Silva *et al.*, 2007)

| Material | CTE ($\times 10^{-6}$ °C$^{-1}$) | |
|---|---|---|
| Aluminium | 24 | |
| Steel | 12 | |
| Titanium | 9 | |
| Glass fibre | 6 | |
| Carbon fibre (axial) | –0.5 | |
| Carbon fibre (radial) | 10 | |
| Carbon fibre reinforced epoxy (longitudinal) | –0.1 | |
| Carbon fibre reinforced epoxy (transverse) | 30 | |
| | Below $T_g$ | Above $T_g$ |
| Epoxy | 60 | 180 |
| Bismaleimide | 35 | 114 |
| Polymethyl methacrylate | 26 | 53 |

© Woodhead Publishing Limited, 2010

change because its longitudinal CTE is close to zero. However, for a stiff adhesive in its glassy region, the adherends cannot contract freely so that the composite is subjected to a compressive axial load and the aluminium adherend is under tension (see Fig. 17.1b). However, the axial load causes bending of the joint as indicated in Fig. 17.1(c). The resultant stress will then be the sum of the uniform component caused by the axial load plus the linearly varying (through the thickness) contribution caused by bending. Whether the bending component is higher than the uniform direct component depends on the geometry and the material properties.

However, more important than the thermal stresses in the adherends are the stresses in the adhesive. For metal/composite joints for example, the metal tends to shrink as the temperature is decreased from the cure value (generally a high temperature) and this is partially resisted by the composite (lower CTE), thereby inducing residual bond stresses especially at the ends of the joint. One end has positive residual shear stresses and the other end has negative residual shear stresses (see Fig. 17.2).

The thermal stresses are beneficial at one end of the joint but have the reverse effect on the other side of the joint. The thermal load $\Delta T$ is given by Equation 17.1:

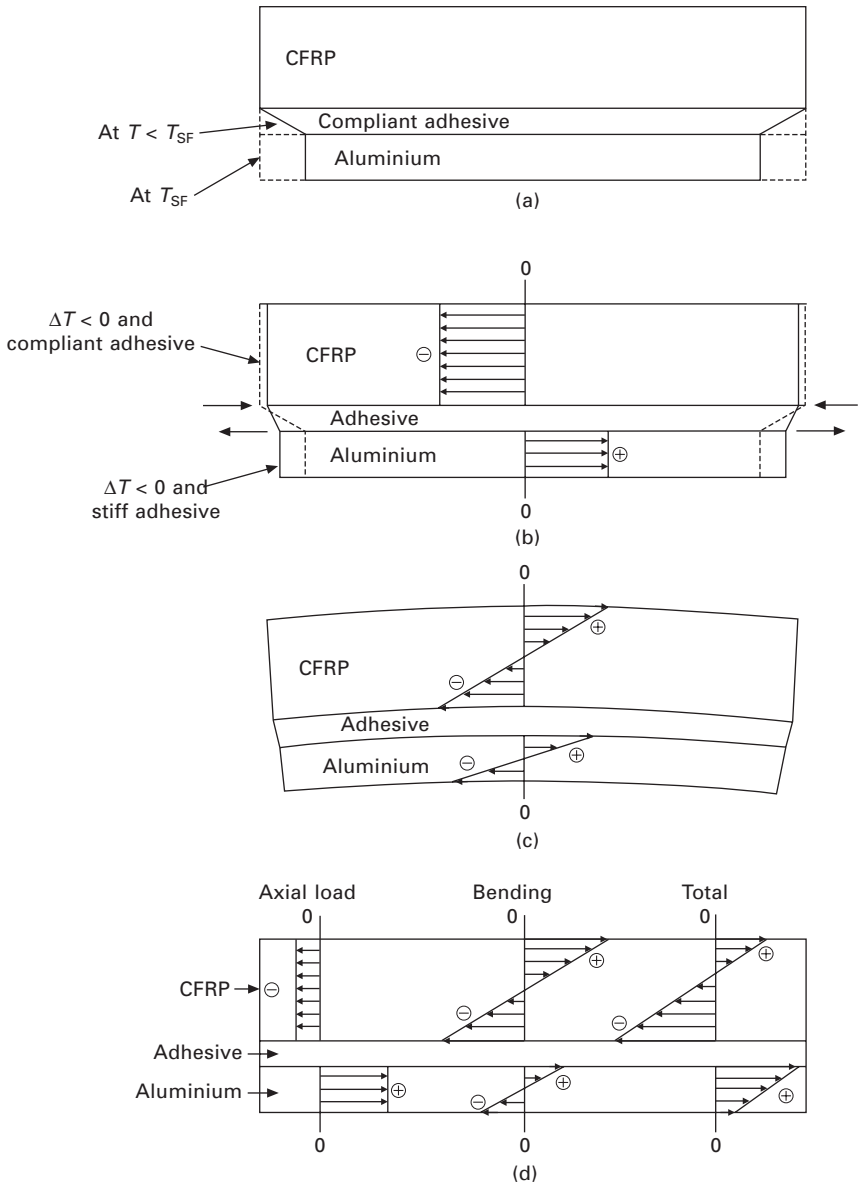
$$\Delta T = T_O - T_{SF} \quad [17.1]$$

where $T_O$ is the operating temperature and $T_{SF}$ is the stress-free temperature. According to Hart-Smith (1973), the stress-free temperature is the cure initiation temperature of the adhesive, which is usually slightly lower than its normal cure temperature. It is reasonable to consider the stress-free temperature as the normal cure temperature of the adhesive. However, this is valid only if the adhesive always operates below its glass transition temperature ($T_g$). When the adhesive is heated above its $T_g$, thermal stresses are relaxed because the adhesive is very compliant (Yu, 1999; Comyn, 1990).

Upon subsequent cooling, once the adhesive becomes hard again, below its $T_g$, thermal stresses start to build up, so that the stress-free temperature is no longer its cure temperature but its $T_g$. This was proved experimentally in da Silva and Adams (2006) by the measurement of the thermal strains, and hence stresses, of aluminium-adhesive-CFRP sandwich specimens with strain gauges, as shown in Fig. 17.3.

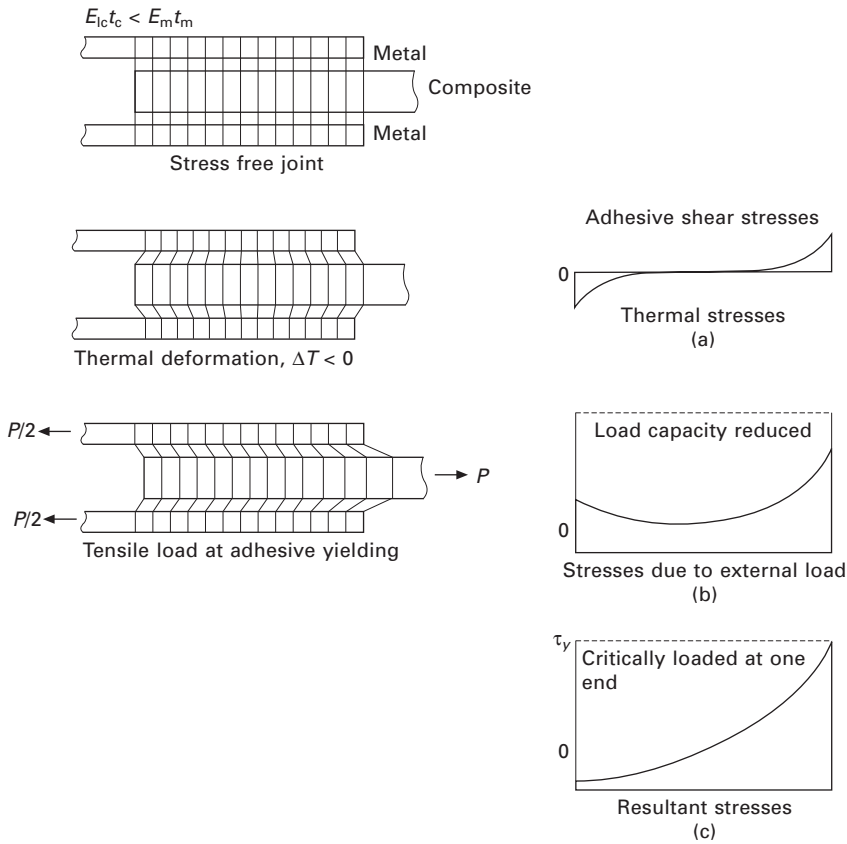
The strain gauges were bonded at room temperature after curing the joint, giving a zero value of strain at that temperature, which obviously does not correspond to reality. In a bonded joint above the $T_g$, there is no stress on the adherends as the adhesive is very compliant and the adherends can expand as if they were free. Note that this might not be true in every case. If sufficiently thin, even relatively soft adhesives can induce significant stresses in adherends if the bond plane is sufficiently large. The strain gauge data were adjusted so that the strain above the $T_g$ coincided with the strain of the

© Woodhead Publishing Limited, 2010

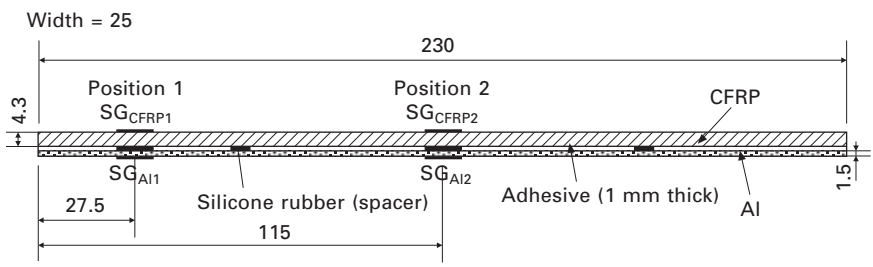



*17.1* Stresses in adherends: (a) for a negative thermal load ($\Delta T < 0$) and a compliant adhesive; (b) for $\Delta T < 0$ and a stiff adhesive, axial component; (c) for $\Delta T < 0$ and a stiff adhesive, bending component; (d) for $\Delta T < 0$ and a stiff adhesive, axial plus bending components (da Silva and Adams, 2006).

© Woodhead Publishing Limited, 2010




*17.2* Adhesive shear stresses in a metal/composite double lap joint for the case where the composite has a lower longitudinal stiffness than the metal ($E_{lc}\ t_c < E_m\ t_m$) under a tensile load and a thermal load, at adhesive yielding ($\tau_y$).




*17.3* Sandwich specimens for determination of the stress-free temperature (dimensions in mm). SG is the strain gauge (da Silva and Adams, 2006).

© Woodhead Publishing Limited, 2010

respective adherend when it was free but thermally expanded. This shifting enables us to know the real value of strain after the cure of the sandwich. Then, the subtraction of the free expansion values of the adherends from the values measured in the sandwich beam gives the elastic strains caused by thermal effects. The procedure is shown in Fig. 17.4.

Note that the strain gauges used are compensated for steel (whose CTE is $12 \times 10^{-6}$ °C$^{-1}$) so that when bonded to a free piece of CFRP, the strain gauge will be under compression when heated (CTE of CFRP is effectively close to zero). As the joint is heated from room temperature to a temperature above its $T_g$, the strains decrease and go to zero at the cure temperature, then increase in the opposite sign and eventually decrease again to zero as the $T_g$ is attained. The strain decreases as the $T_g$ is approached because the adhesive becomes too soft to cause any strain on the substrates. In the explanation of the data treatment shown in Fig. 17.4, this effect is clearly seen in the graph corresponding to Step 3. On cooling from a temperature above the adhesive $T_g$, strains start to build up from $T_g$ and increase until room temperature.

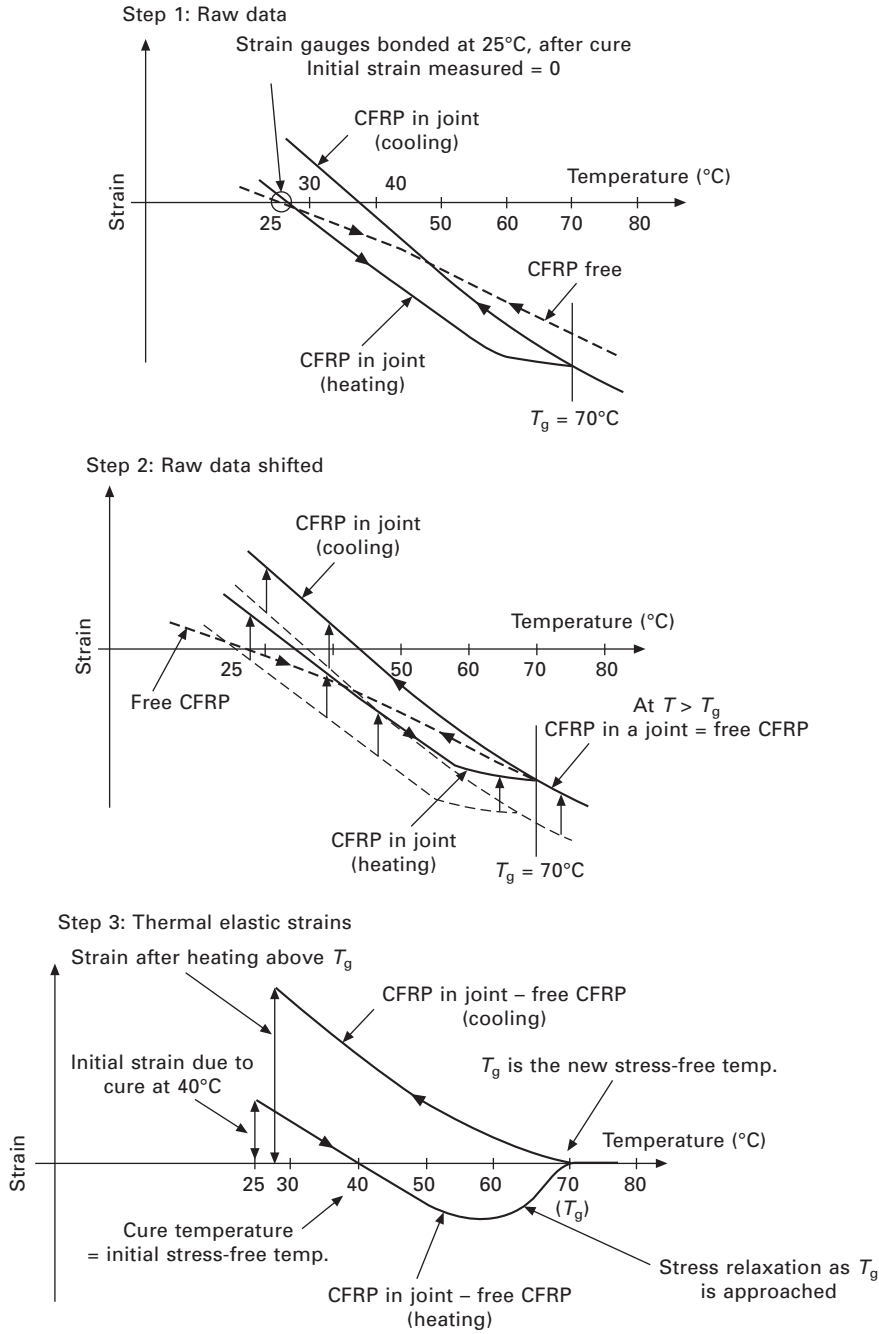
## 17.4 Effect of temperature on adhesive properties

The temperature stresses may be important and they must be taken into account, especially those due to different CTEs. However, owing to the polymeric nature of adhesives, variation in the mechanical properties of the adhesives (stress–strain curve and toughness) with temperature may be the most important factor to consider. For high temperature applications (above 200ºC), the adhesives used are often either bismaleimides or polyimides and are generally supplied as films. Film adhesives can be supported, with a carrier, or be unsupported, without a carrier. In general, carriers can be nylon, polyester or glass (usually preferable at high temperatures) fibres and their structure can be nonwoven, woven or knitted.

Although polyimides have good high temperature properties, bismaleimides offer advantages such as the fact that they do not generate volatiles during cure, resulting in less porosity. When temperatures higher than 300ºC are desired, ceramic adhesives may be used (Bhowmik *et al.*, 2006). These are based on inorganic binding compounds such as alkali silicates and metal phosphates.

Carbon, silica, magnesia or zirconia powder are commonly used as fillers. The adhesives are usually available in two part systems, in which one of the components is the binder and the other is the filler. Joining these two components results in a slurry that must be quickly applied to the substrate. The assembly must then be cured, which requires temperatures between 260 and 1000ºC. The different combinations of binder and filler can be optimised

© Woodhead Publishing Limited, 2010




*17.4* Data treatment procedure to obtain the thermal elastic strain from strain measurements (strain gauge 2 on the CFRP adherend) (da Silva and Adams, 2006).

© Woodhead Publishing Limited, 2010

to match more closely the CTE of the substrate and reduce the stresses during heating and cooling phases.

Currently used ceramic adhesives do not offer a hermetic connection or a high degree of reliability. Their reliability and strength is below that offered by high performance ceramics and this can result in cracking under thermal stresses. The use of these adhesives is therefore a very complex proposition and requires careful design.

For aerospace applications, not only do extremely high temperatures have to be considered but sometimes extremely low temperatures as well. When in orbit, the outside temperature is of the order of –80ºC. Adhesives for cryogenic engines should maintain their mechanical performance to temperatures as low as –200ºC. High temperature adhesives can be used at low temperatures. However, they are very sensitive to defects because of their brittle nature. It is more appropriate to use rubber-like adhesives such as polyurethanes or silicones. Most conventional sealants, such as polysulphides, flexible epoxies, silicones, polyurethanes and toughened acrylics are flexible enough for use at intermediate low temperatures to –30°C. Aerospace applications for these materials include their use as sealants for fuel tanks (Giannis *et al.*, 2008) or to bond the ceramic tiles of the space shuttle.

The mechanical properties of an adhesive depend on the operational temperature in relation to the glass transition point. As the temperature decreases below the glass transition temperature ($T_g$), the modulus and strength increase while the ductility decreases. At $T_g$ there is a rapid reduction in the modulus and strength as the temperature increases and the adhesive can no longer carry a substantial load. Knowledge of $T_g$ is therefore very important. Table 17.2 presents typical $T_g$ values for different types of adhesives.

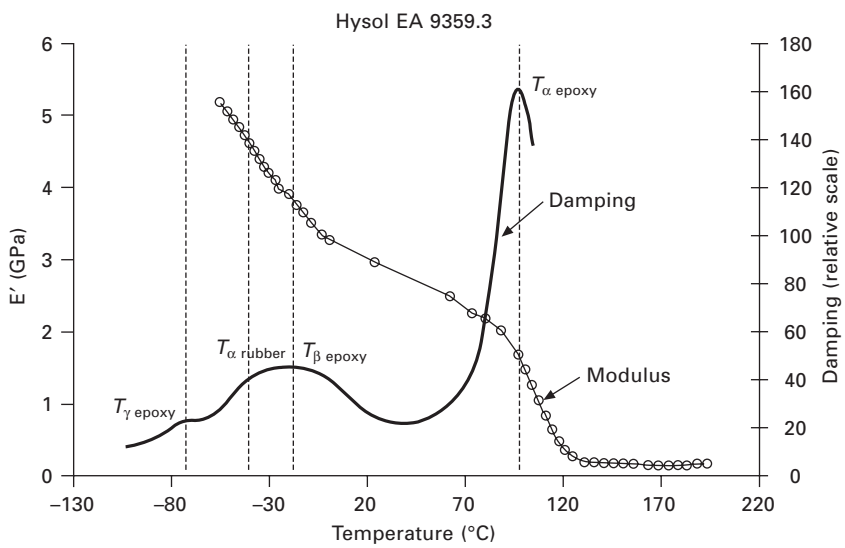
*Table 17.2* Glass transition temperature ($T_g$) of various adhesives (approximate values) (da Silva *et al.*, 2007)

| Adhesive | $T_g$ (°C) |
|---|---|
| *Epoxies* | |
| Toughened epoxy | 50–150 |
| Epoxy phenolic | 200 |
| Epoxy nylon | 50 |
| Epoxy polysulfide | 50 |
| *Phenolics* | |
| Nitrile phenolic | 120 |
| Vinyl phenolic | 70 |
| Neoprene phenolic | 70 |
| *High temperature adhesives* | |
| Bismaleimide | 210–280 |
| Polyimide | 340–430 |
| *Polyurethanes* | 20–50 |
| *Anaerobics* | 120 |
| *Cyanoacrylates* | 80 |
| *Modified acrylics* | 60–120 |

© Woodhead Publishing Limited, 2010

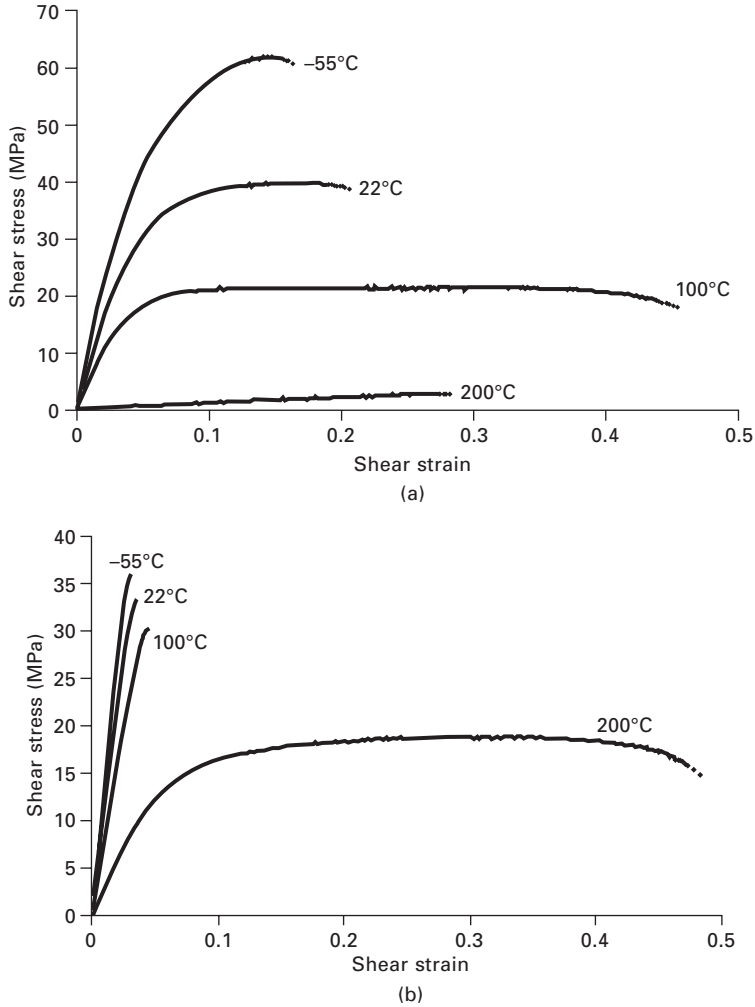
$T_g$ can be determined by various methods such as dynamic mechanical thermal analysis (DMTA), thermomechanical analysis (TMA) or differential scanning calorimetry (DSC) (Rieger, 2001). Figure 17.5 presents the results obtained by da Silva and Adams (2005) from a DMTA-type apparatus where the modulus and the damping as a function of temperature are given for an epoxy adhesive (Hysol 9359.3, Loctite Aerospace). The high damping and modulus drop is clearly seen in the vicinity of $T_g$.

The effect of temperature from –55 to 200ºC on the shear stress–shear strain properties of an epoxy adhesive (Supreme 10HT, Master Bond) and a bismaleimide adhesive (Redux 326, Hexcel Composites) is shown in Fig. 17.6 (da Silva and Adams, 2007a). The bismaleimide adhesive has a maximum service temperature, according to the manufacturer, of 230°C for long periods and 270°C for short periods. The epoxy has a $T_g$ close to 100°C. Figure 17.6 clearly shows a dramatic decrease in strength of the epoxy adhesive at 200ºC. The bismaleimide adhesive strength decreases with temperature but its ductility increases, which can be an advantage when used in a joint. Jensen *et al*. (1995) tested the tensile properties of a polyimide adhesive in the film form (without carrier) at 25, 150 and 177ºC. The tensile strength and tensile modulus decreased with temperature (48% and 39%, respectively) whereas the elongation increased by 31%. Stress–strain curves for other types of adhesives have also been presented by Adams and Mallick (1993) and Chiu *et al*. (1994) with similar conclusions.




*17.5* Dynamic flexural modulus (*E*′) of composite specimens and damping using a DMTA-type apparatus for adhesive Hysol 9359.3 (da Silva and Adams, 2005).

© Woodhead Publishing Limited, 2010




*17.6* Adhesive shear curves obtained with the thick adherend shear test (TAST): (a) Supreme 10HT, (b) Redux 326 paste (da Silva and Adams, 2007a).

Dixon *et al*. (1998) tested an epoxy in lap shear and peel at high temperatures and a bismaleimide in lap shear and peel from –55 to 130ºC. Both contained a carrier. They found that the bismaleimide adhesive has a more consistent strength over the temperature range tested than does the epoxy. Dixon *et al*. (1998) found that failures begin with small cracks at the specimen ends and that catastrophic failure is often seen to occur through the support cloth. Moreover, the bismaleimide adhesive failed in such a way that at 20°C and –55ºC, the support cloth was cleanly debonded, whereas at 130ºC the adhesive remained attached to the cloth fibres after fracture, probably due

© Woodhead Publishing Limited, 2010

to an increase in adhesive ductility. More recent results on the influence of temperature on adhesive properties are presented by Deb *et al*. (2008) using double lap shear tests.

Besides the stress–strain variation, the toughness of the adhesive is also an important factor to consider as this material property is increasingly being used for adhesive joints design (Curley *et al*., 2000; Wang *et al*., 2003; de Moura, 2008). Information on the critical strain energy release rate at low or high temperatures is more difficult to find in the literature than the stress–strain curves of the adhesives and this is certainly an area that needs to be investigated. The area under the stress–strain curve is an estimate of the toughness. As the temperature increases, the strength decreases but the ductility increases giving an additional plastic deformation at the crack tip and hence an increase in toughness. Fracture tests in mode I at cryogenic, room and high temperatures have indicated this (Kim *et al*., 2005; Melcher and Johnson, 2007). However, a rapid decrease in toughness is expected as the $T_g$ of the adhesive is approached.

The instantaneous response of a polymer material above its $T_g$ is a small fraction of its total response to the load, with an important time-dependent component. The models used to represent this behaviour are based on arrangements of Hookean springs or Newtonian dashpots. If the time during which the stress is applied is small compared to the time of relaxation, the response is determined more by the spring than the dashpots. For a polymer at a temperature below its $T_g$, the time to relaxation is almost infinitely long and therefore the response is almost elastic. As the temperature increases and approaches $T_g$, the modulus starts to decline and the viscous component becomes increasingly important. Generally, structural adhesives are used at temperatures below the vitreous state of the adhesive.

Richardson *et al*. (2003) proposed and evaluated a multiaxial, temperature, and time-dependent failure criterion for an epoxy adhesive. The failure criterion has been shown to be applicable at temperatures ranging from –29ºC to 46ºC. An important aspect of viscoelasticity occurs when the polymers are cyclically deformed. Even at temperatures below $T_g$ there is always a viscous component that leads to a loss of energy during the cyclic deformation. One advantage of this phenomenon is that it can induce a vibration damping. However, energy converted to heat increases the temperature. In theory, the rise in temperature may affect the modulus and strength but, in practice, a large interfacial area provides excellent conditions for the release of heat. In the case of joints between metal materials, the increase in temperature under dynamic deformation is negligible. This cannot be assumed in the case of other substrates, such as composites with carbon or glass fibres.

As seen above, thermal loads are a particular challenging condition for adhesives. The modifications in mechanical properties can be permanent or temporary. The ageing mechanism can be divided into physical and chemical.

© Woodhead Publishing Limited, 2010

Physical ageing, which consists in a progressive loss of the free volume, can be recovered by heating the adhesive above the $T_g$ and quenching (Parvatareddy *et al.*, 1998). However, when the chemistry of the adhesive is altered after a stage at high temperatures, the damage is permanent. This aspect is particularly important and the service temperature of the structure should never go beyond the chemical degradation temperature of the adhesive. There are cases, however, where the chemical changes are used as an advantage. Wang *et al.* (2006) have shown that the residue derived from the carbonisation of organic synthetic resin possesses excellent thermal–physical properties.

## 17.5 Modelling high and low temperature conditions

Most studies consider that all joint members have a uniform temperature distribution (Lee and Lee, 1995; Reedy and Guess, 1996; Ioka *et al.*, 1996; Anifantis *et al.*, 1997; Kim *et al.*, 1997; Kim and Lee, 1998; Rastogi *et al.*, 1998; Abedian and Szyszkowski, 1999; Nagakawa *et al.*, 1999, Nabulsi and Mall, 1997; Nakagawa and Sawa, 2001; da Silva and Adams, 2007a). The residual thermal stresses can be easily calculated if the CTE of the adherends and the stress-free temperature are known (see Section 17.3). Some analytical models include the thermal stresses such as those of Hart-Smith (1973), Sinha and Reddy (1976), Adams and Mallick (1992), Suhir (2000), Rossetos (2003), Zhong *et al.* (2005) and Wang *et al.* (2007). For example, in the closed-form model of Hart-Smith (1973) for double lap joints, the thermal load due to differential CTE between the adherends is simply taken into account in the adherend stress–strain relation by adding the term CTE ($\alpha$) times $\Delta T$:

$$\frac{\mathrm{d}u_o}{\mathrm{d}x} = \frac{P_o}{E_o t_o} + \alpha_o \Delta T, \quad \frac{\mathrm{d}u_i}{\mathrm{d}x} = \frac{P_i}{E_i t_i} + \alpha_i \Delta T \qquad [17.2]$$

where $u$ is the axial displacement of the adherend, $P$ is the applied load per unit width, $E$ is the Young's modulus, $t$ is the thickness and the subscripts o and $i$ represent the external and internal adherends of the double lap joint. The adhesive elastic stress ($\tau$)–strain ($\gamma$) relation is given by:

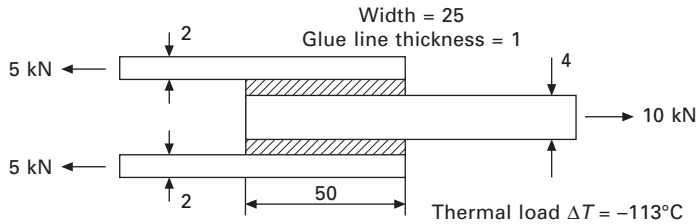
$$\tau = G_a \gamma = \frac{G_a}{t_a}(u_i - u_o) \qquad [17.3]$$

where $G$ is the shear modulus and the subscript a is for the adhesive. Equation 17.3 shows that the residual thermal stresses in the adhesive increase as the difference in thermal expansion between the adherends increases.

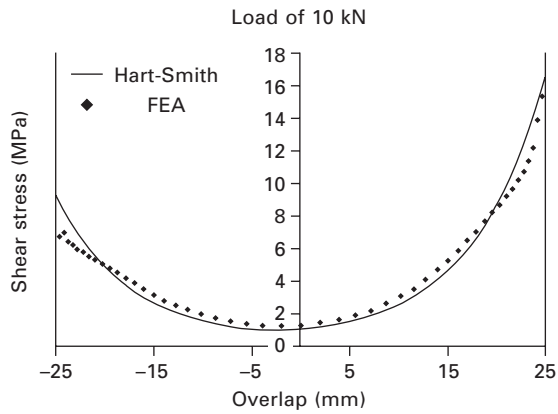
However, most studies are done using the finite element method. A

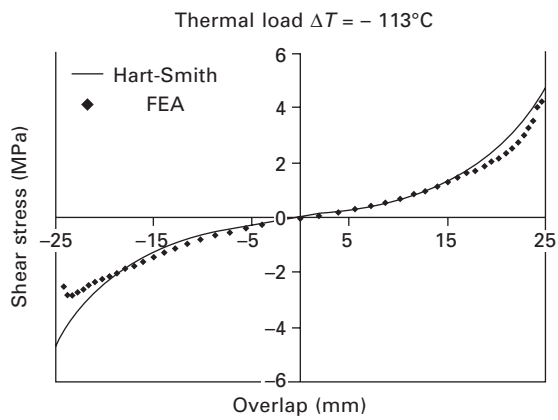
© Woodhead Publishing Limited, 2010

comparison between the FE method and the closed-form analysis of Hart-Smith (1973) is shown in Fig. 17.7 for a double lap joint between titanium and a fibre-reinforced composite (da Silva and Adams, 2007a). The thermal




Adhesive: Supreme 10HT at 22°C
Inner adherend: bismaleimide composite
Outer adherend: titanium




*17.7* Comparison between Hart-Smith's closed-form analysis and the finite element analysis. All dimensions in mm (da Silva and Adams, 2007a).

© Woodhead Publishing Limited, 2010

stress in the adhesive given by the model of Hart-Smith (1973) and the FE analysis are very similar.

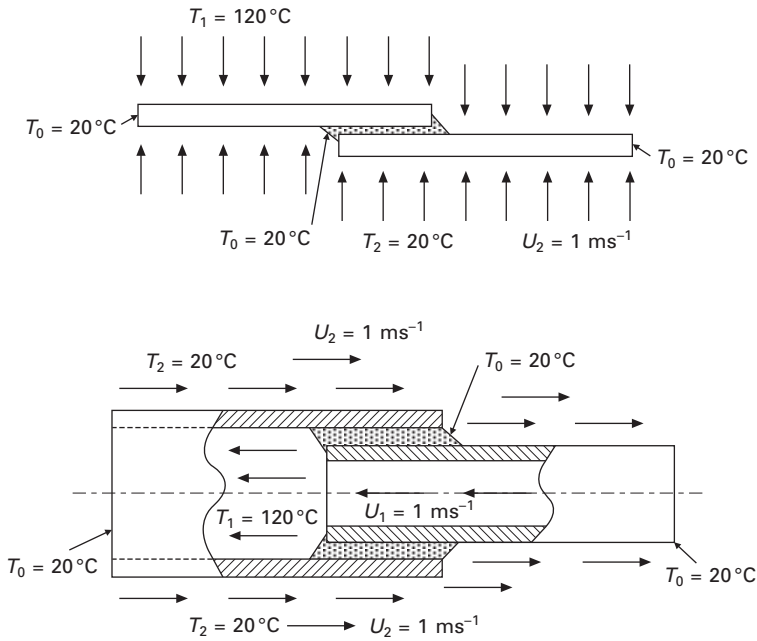
For more complex thermal analyses such as localised thermal loads, analytical models are more difficult to implement. An exception is the work of Katsuo *et al*. (1999) who carried out transient thermal stress analysis of an adhesive butt joint. They assumed the upper and lower end surfaces of the joint are at different temperatures at a certain instant and analysed the effects of CTE and Young's modulus ratios of the adhesive and adherends on the transient thermal stress distribution.

The previous analyses prescribe the final temperature distributions along the boundary of the adhesive joints and in the adhesive joints and then compute the thermal strains using the temperature differences relative to the initial uniform joint temperature. However, the materials in an adhesively bonded joint have different heat conduction/convection properties. Therefore, heat transfer through the adhesive joint members should be analysed in detail in order to understand the different heat transfer mechanisms.

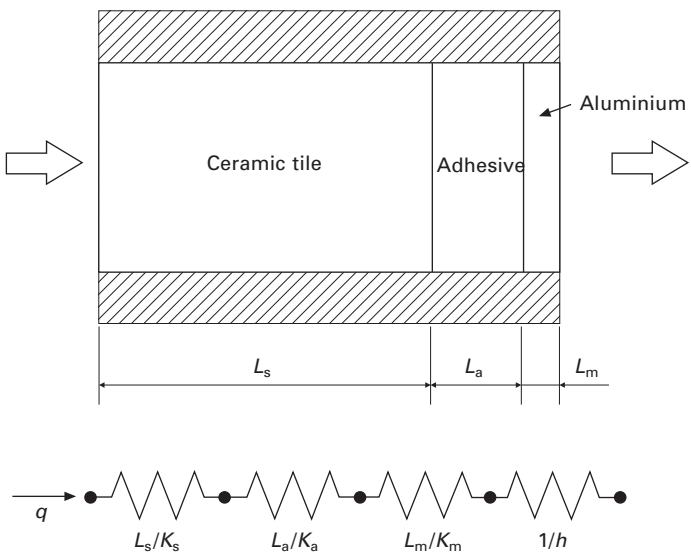
Apalak and co-workers (Apalak and Gunes, 2002; Apalak *et al*., 2003(a)–(d), Apalak *et al*., 2004) performed thermal analyses in the case where the outer surfaces of the adhesive joint are subjected to fluid flows at different temperature and velocity, and where the adherends have different edge conditions (see Fig. 17.8). The fuselage of an aircraft is a typical practical example of the thermal boundary condition of the single lap joint (outside temperature can reach –55ºC) whereas the tubular joint is a good simulation of pipes for transporting hot substances. The heat transfer throughout the adhesive joint takes place by conduction, whereas it occurs by convection from the joint surfaces to the fluids, or the fluids to the joint surfaces. These thermal boundary conditions make the heat transfer problem of the adhesive joint complex but are very important to study in order to have a real insight into the practical thermal conditions found in adhesively bonded joints.

Another possibility for investigating temperature distributions through adhesive joints is to use purely thermal simulations. For example, Marques (2008) studied the temperature distribution along a ceramic–adhesive–aluminium sandwich specimen when an incident power corresponding to 1000ºC was applied on the ceramic side, simulating the connection of the ceramic tiles to the fuselage of the space shuttle (see Fig. 17.9). A diagram of equivalent resistances was built and the temperature distribution with time was calculated using the software Engineering Equation Solver (F-Chart Software, Madison, WI) with a finite difference method. A parametric study showed that for the most common aerospace configuration, the maximum temperature that the adhesive layer encounters is approximately 300ºC.

© Woodhead Publishing Limited, 2010




*17.8* Thermal boundary conditions studied by Apalak and co-workers for a single lap joint (top) and a tubular joint (bottom) ($U$ is the fluid velocity).




*17.9* Thermal model (top) and thermal resistance diagram (bottom) studied by Marques (2008). The resistance is expressed by the $K$ parameter in W m$^{-1}$ K$^{-1}$.

© Woodhead Publishing Limited, 2010

## 17.6 Experimental joint strength results in high and low temperature conditions

Althof (1971) tested titanium and composite joints from ambient temperature to 175ºC. In the case of titanium the strength was approximately constant while for the CFRP joints the strength fell to about half that at room temperature. Two reasons were given: the interlaminar strength of the CFRP decreases with increasing temperature and the adhesion between the adhesive and the CFRP is reduced with increasing temperature. Stone (1981) tested metal/carbon fibre-reinforced composites joints and found a great reduction in strength at –55ºC. This joint strength reduction was attributed to the differential adherend contraction on cooling from the cure temperature and the effect of adhesive properties. Al-Hamdan (1989) analysed thermal stresses in bonded joints. Mild steel lap joints were tested over a temperature range from –60 to 200ºC. It emerged that the joints were strongest in the region 0–70ºC. At low temperatures, the brittleness of the adhesive causes a loss in strength. At high temperatures, the adhesive is soft and leads to failure by total plastic yielding in the joint.

Matsui (1990) studied the effects of curing and test temperatures on the strength of adhesive joints. Experimental data were presented along with empirical formulae. The test temperatures ranged from 5–100ºC. The adherends were of aluminium or steel. At the lower temperature, interface failure (adhesive failure) occurred. At high temperatures cohesive failure took place and the joint strength decreased markedly with increasing temperature. Contrary to the results obtained by Al-Hamdan (1989), the joint strength decreases with temperature because the loss in adhesive strength is more important than the gain in ductility.

Adams and Mallick (1993) studied a series of aluminium/CFRP SLJs, with three different adhesives, at 20ºC and –55ºC. Joints were tested at various overlap lengths and the three adhesives were cured at 60ºC. Predictions were based on a continuum mechanics approach and were compared with experimental measurements. The authors found that the model was capable of accurate joint strength predictions for elastoplastic adhesives but, when the adhesive was brittle, the predictions were less accurate. They suspected that this may be due to scatter in the mechanical property data: the percentage deviation of the fracture quantities at 20ºC was far less than at –55ºC. For the three adhesives, there was a severe reduction of joint strength with the lowering of temperature.

Cho *et al*. (1998) studied the effect of curing temperature on the adhesion strength of polyamideimide/copper joints and showed that the adhesion strength decreased as the thermal stress increased with the increase in both curing temperature and time. Kim and Lee (2001) investigated the effects of environmental temperature and filler on the tensile modulus and failure

© Woodhead Publishing Limited, 2010

strength of an epoxy adhesive. From the tensile tests on tubular single lap adhesive joints, it was found that the average tensile strength of the tubular single lap adhesive joint did not decrease much compared to the adhesive properties because the tensile residual thermal stress in the joint decreased as the environmental temperature increased.

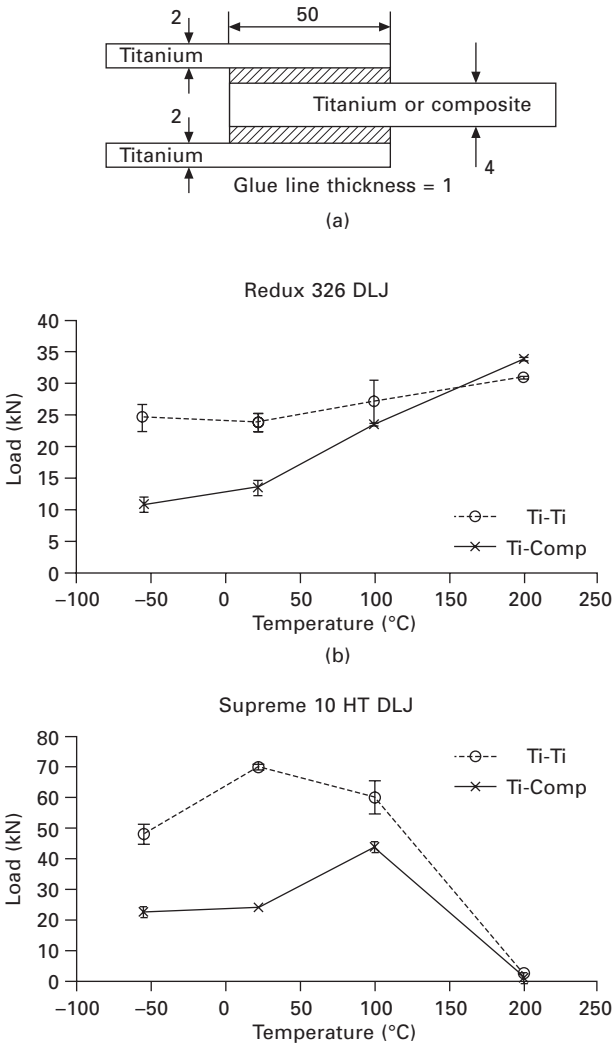
Double lap joints (DLJ) with similar (titanium–titanium, Ti–Ti) and dissimilar adherends (titanium–composite, Ti–Comp), were tested from low to high temperatures by da Silva and Adams (2007b). The composite was a carbon fabric 0/90º laminate impregnated with a bismaleimide resin. Two kinds of adhesives were tested, a stiff and brittle high temperature adhesive Redux 326 (bismaleimide) with a cure of 175ºC and a post-cure of 230ºC ($T_g$ = 260ºC), and a ductile and less stiff low temperature adhesive Supreme 10HT (epoxy) with a cure at 120ºC and a $T_g$ of 135ºC. Redux 326 Ti–Ti joints (Fig. 17.10a) have a higher strength at high temperatures than at low temperatures because Redux 326 is ductile at high temperatures.

The failure load at –55, 22 and 100ºC is approximately constant which suggests that the thermal stresses do not play a major role in similar adherends. Compared with the Ti–Ti joints, the failure load of the Ti–Comp joints is much reduced, especially at –55 and 22ºC. The Redux 326 Ti–Comp joints have a much lower strength at low temperatures because the thermal loads involved are very high owing to the high stress-free temperature of Redux 326 (230ºC).

Supreme 10HT Ti–Ti joints (Fig. 17.10b) are much stronger than Redux 326 at low temperatures but have very little strength at high temperatures. The thermal loads are also important for the Supreme 10HT Ti–Comp joints but to a lesser extent since the stress-free temperature is much lower (120ºC). The main reason for the huge decrease at –55 and 22ºC is the composite transverse failure which does not allow Supreme 10HT to give its full potential. It is known that an internal taper in the adherend and an adhesive fillet transfers the failure from the composite to the adhesive (Adams *et al.*, 1986). However, the joint strength at low temperatures of a joint with an internal taper and adhesive fillet is not much higher than the regular geometry with no taper and fillet owing to the high thermal load generated in the fillet (da Silva and Adams, 2007c).

Joints subjected to high and low temperatures have to retain their strength for many cycles. Humfeld and Dillard (1998) studied the effect of thermal cycling on the state of residual stress in thermoviscoelastic polymeric materials. Their major finding is that in cyclic temperature conditions, at high temperatures, compressive residual stresses in the adhesive can relax significantly whereas at low temperatures, residual stresses give rise to increasingly larger tensile stresses more difficult to accommodate because of the reduced molecular mobility. This asymmetrical behaviour leads

© Woodhead Publishing Limited, 2010




*17.10* Experimental failure load of (a) Redux 326 DLJs and (b) Supreme 10HT double lap joints.

eventually to a situation in which relatively large tensile stresses can result at cold temperatures.

## 17.7 Techniques for optimising adhesive bonds in high and low temperature conditions

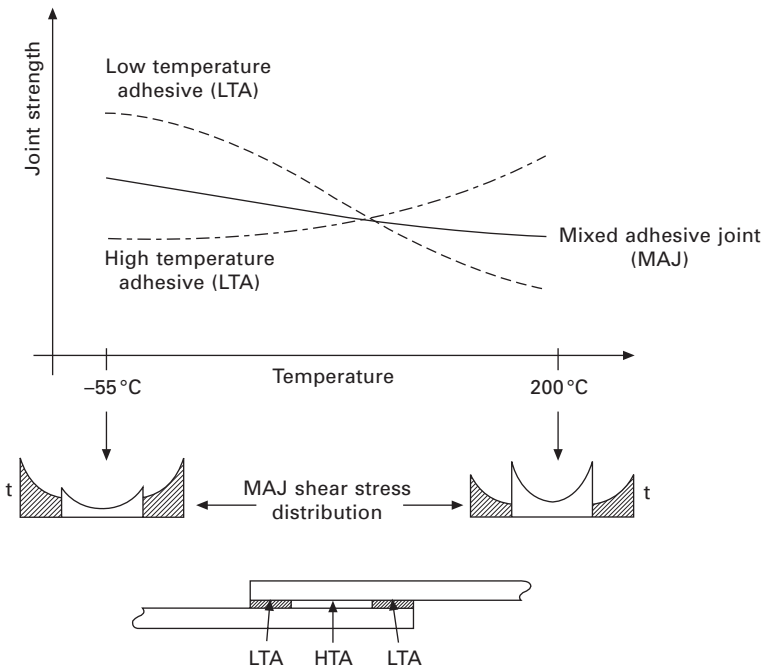
Adhesives suitable for high temperatures are generally too brittle for use at low temperatures. Owing to their brittleness and high stiffness, the strength

© Woodhead Publishing Limited, 2010

in such a joint is often poor at low temperatures (da Silva and Adams, 2005). On the other hand, adhesives suitable for low temperatures are usually too weak or degrade at high temperatures. It may eventually be possible for chemists to develop an adhesive which will exhibit a good joint strength from –55 to 200°C, but this is unlikely in the near future. One solution therefore is to make a joint with a combination of two adhesives, consisting of a low temperature adhesive (LTA) which is tough at low temperatures and has a high modulus, but which does not degrade at the highest required operating temperature, and a high temperature adhesive (HTA) which has high strength at high temperatures but may be very brittle at low temperatures (see Fig. 17.11).

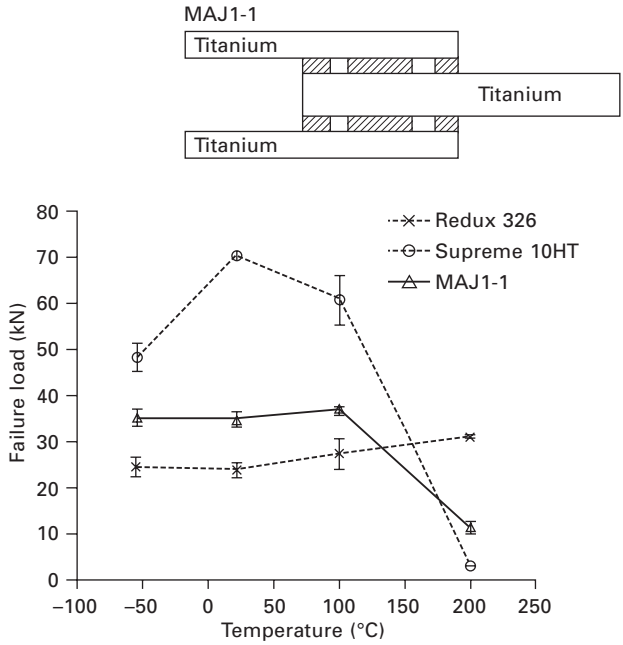
Adhesive double lap joints with dual adhesives to be used over a wide temperature range (–55 to 200°C) were studied theoretically (da Silva and Adams, 2007a) and experimentally (da Silva and Adams, 2007b). The joint strength predictions have shown that for identical adherends (e.g. titanium), the mixed adhesive approach is of little benefit (see Fig. 17.12). However, for titanium/composite double lap joints, there is a real improvement (see Fig. 17.13), especially if the difference in the CTE is high.

As shown in Fig. 17.2, the shear stress distribution caused by an external tensile load is non-symmetric in dissimilar adherends. The shear stress peaks

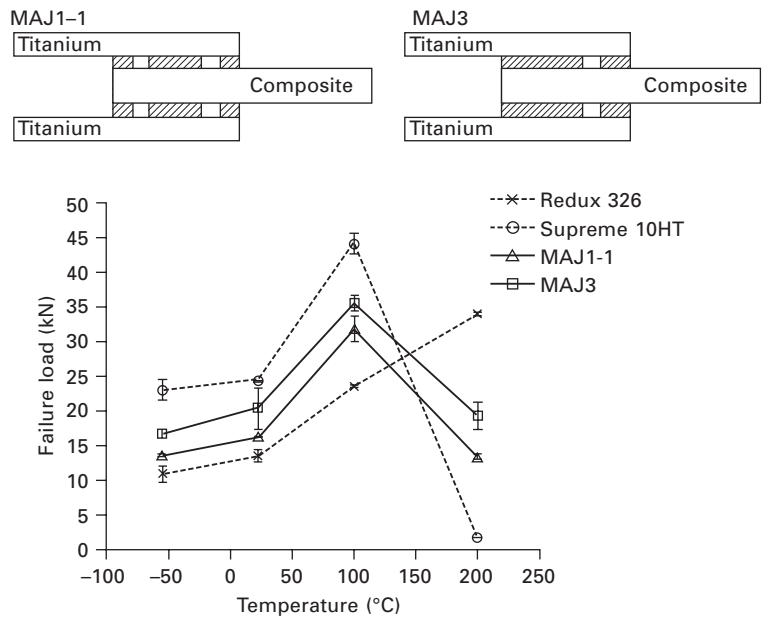



*17.11* Mixed adhesive joint concept.

© Woodhead Publishing Limited, 2010




*17.12* Experimental failure load for titanium/titanium DLJs. The error bars correspond to the maximum and minimum values (da Silva and Adams, 2007b).




*17.13* Experimental failure load for titanium/composite DLJs. The error bars correspond to the maximum and minimum values (da Silva and Adams, 2007b).

© Woodhead Publishing Limited, 2010

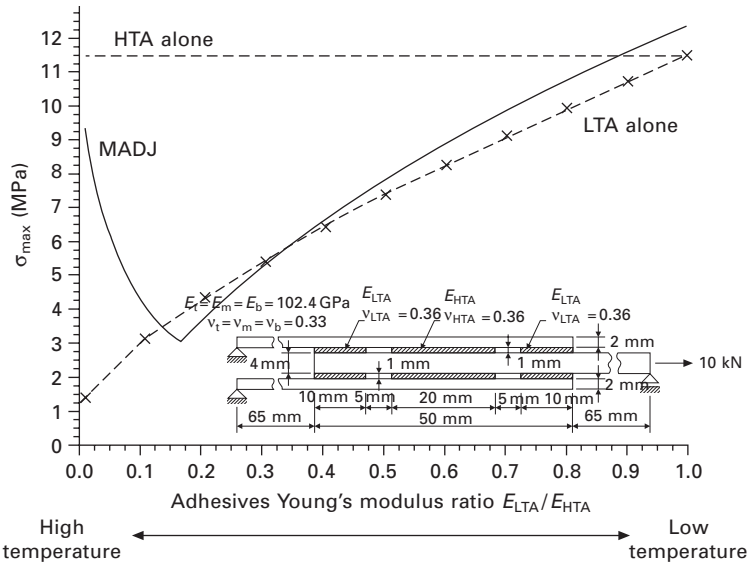
at the overlap end where the inner composite adherend has a lower stiffness. The thermal residual stresses are beneficial at the end from which the stiff adherend extends, but detrimental at the other end, creating a case where the resultant stress is biased to one end. This will result in a decrease of the load capacity of the joint. Depending on the combination of the adherends and their relative moduli, the thermal loads can create a joint critically loaded at one end. For these, the classic mixed adhesive joint design (see Fig. 17.11) can be modified so that the ductile adhesive is located only on the critical side (design MAJ3 in Fig. 17.13).

Recently, an analytical analysis based on Frostig's model (Frostig *et al*., 1999), was developed by da Neves *et al*. (2009a) to study a SLJ and a DLJ with one or more adhesives along the overlap. It was observed that the adhesive stress distributions of the model developed and that of a FE analysis are in very close agreement over almost the entire overlap length. The analytical models developed for mixed adhesive single lap joints (MASJ) and mixed adhesive double lap joints (MADJ) were used to make a parametric study (da Neves *et al*., 2009b). The effect of the ratio LTA Young's modulus / HTA Young's modulus ($E_{LTA}/E_{HTA}$) (which is equivalent to studying the temperature variation) on the maximum adhesive shear and peel stresses in a MASJ and in a MADJ were investigated. The overlap of the low and high temperature adhesives and the effect of the high temperature adhesive modulus were also studied. The main conclusion is that MASJs and MADJs show similar behaviour with temperature. However, at high temperatures, the reduction in the adhesive peel stress over a joint with a HTA alone is much higher in the case of a MASJ (see Fig. 17.14 and Fig. 17.15) and makes the use of mixed adhesive joints more efficient for SLJs than for DLJs.

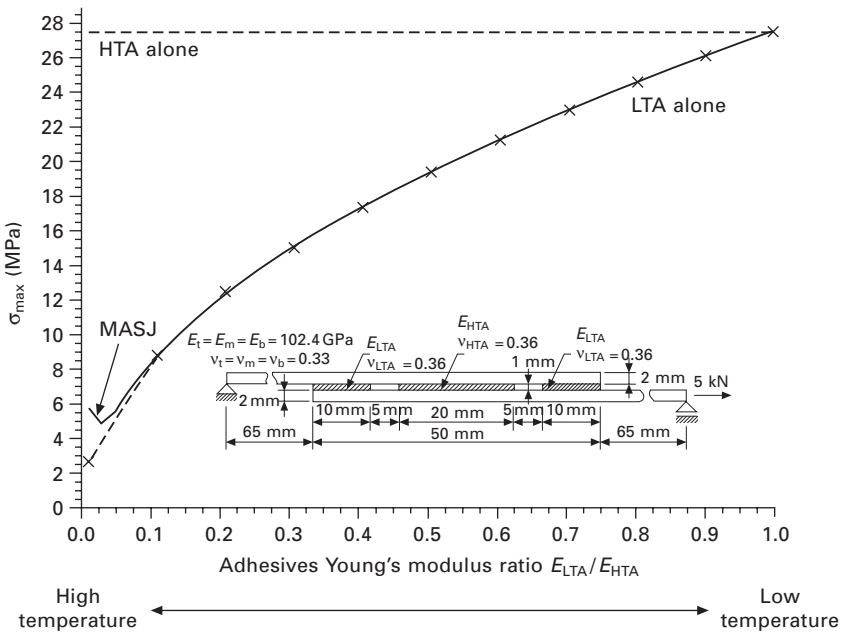
At high temperatures, the maximum stresses occur in the HTA until a certain value of $E_{LTA}/E_{HTA}$ ratio at which they start to occur in the LTA. This transition $E_{LTA}/E_{HTA}$ ratio, and consequently this transition temperature, correspond to a minimum of the adhesive stresses in a MAJ. At the transition, the maximum adhesive stresses in the LTA and in the HTA of the MAJ are equal (see Fig. 17.16), making the stress distribution along the overlap length smoother.

At high temperatures, the high temperature adhesive (HTA) in the middle of the joint retains the strength and transfers the entire load while the low temperature adhesive (LTA) is the load bearing component at low temperatures, making the high temperature adhesive relatively lightly stressed. At low temperatures, the load must essentially be supported by the LTA. If its modulus is of the same order as the modulus of the HTA, most of the load will be carried by the LTA. However, if its modulus is much lower than the modulus of the HTA, the HTA might still be critically loaded. One possibility is to stiffen the ends of the overlap where the LTA is as shown in Fig. 17.17.

© Woodhead Publishing Limited, 2010

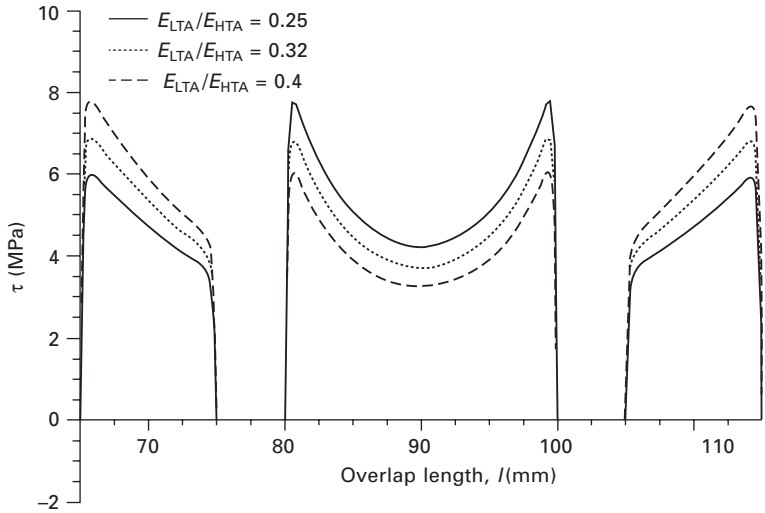



*17.14* Effect of the adhesives Young's modulus ratio on the maximum adhesive peel stress in a MADJ (da Neves *et al.*, 2009b).

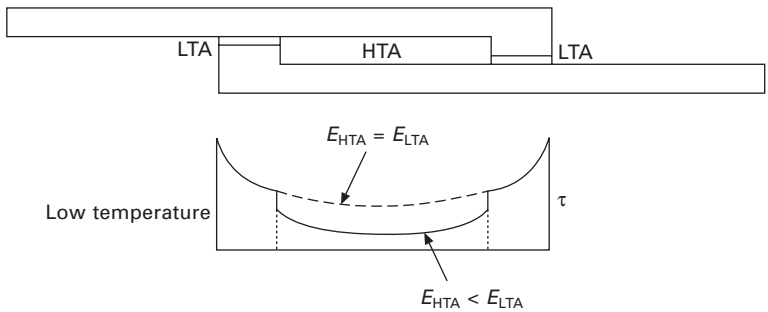



*17.15* Effect of the adhesives Young's modulus ratio on the maximum adhesive peel stress in a MASJ (da Neves *et al.*, 2009b).

© Woodhead Publishing Limited, 2010



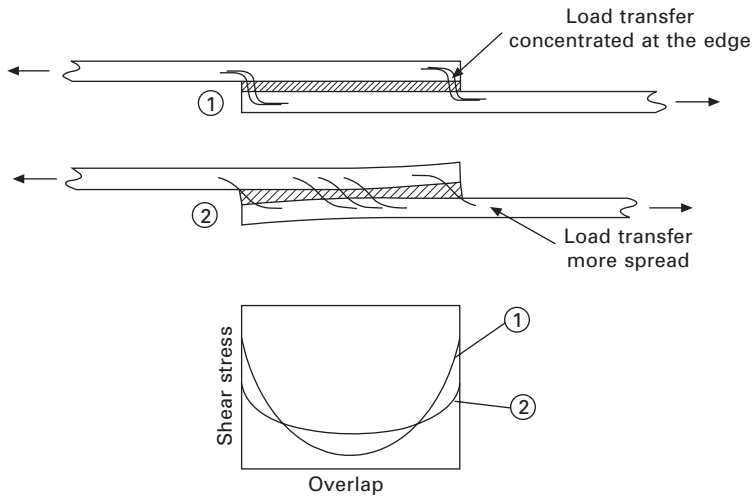

*17.16* Transition of the maximum overall adhesive shear stress from the HTA to the LTA in a MADJ (da Neves *et al.*, 2009b).




*17.17* Stiffening of the ends of the overlap in a mixed adhesive joint.

The problem with using a brittle adhesive in a lap joint at low temperatures is the high stress concentration at the ends of the overlap. This problem can be reduced by adherends which are slightly bent along the overlap. The bent adherends give rise to a gradual change in adhesive thickness that can give a smother stress distribution along the overlap (see Fig. 17.18). Other techniques to decrease the adhesive stress concentration at the ends of the overlap such as 'wavy' lap joints (Ávila and Bueno, 2004; Fessel *et al.*, 2007) should also be effective in improving the joint performance at low temperatures.

© Woodhead Publishing Limited, 2010




*17.18* Load transfer and shear stress distribution in single lap joints with bent adherends.

## 17.8 Summary and future trends

This chapter identifies and discusses the key problems caused by high and low temperature conditions. These are shrinkage of the adhesive, differential thermal expansion and differing adhesive mechanical properties with temperature. It is shown that the variation of adhesive properties with temperature is often the most critical factor. Analytical and numerical methods of modelling high and low temperature conditions are presented. For complex boundary conditions, a numerical approach is more appropriate. Experimental results for adhesive joints as a function of temperature generally show a decrease in strength at low and high temperatures. At low temperatures, the cause is the high thermal stresses whereas at high temperatures, it is the low adhesive strength. To increase the temperature range of application of adhesive joints, a joint with two adhesives along the overlap is proposed. A HTA in the middle of the overlap is the load bearing adhesive at high temperatures whereas a LTA at the ends of the overlap protects the HTA at low temperatures. This idea is supported by analytical, numerical and experimental results.

The work previously presented on mixed adhesive joints could be extended to space applications such as in the bonding of ceramic tiles in the space shuttle. A ceramic adhesive with a higher strength than the silicone adhesive currently used could provide better strength at high temperatures (+1200ºC) during the re-entry of space vehicles into the atmosphere and the silicone adhesive would be the load-carrying adhesive when the space shuttle is in orbit (–80ºC). This is currently under investigation by the author.

© Woodhead Publishing Limited, 2010

The use of functionally graded adhesives or adherends is a promising technique for optimising adhesive bonds in high and low temperature conditions. With the objective of reducing the peak stress and non-uniform stress distribution in the adhesive of a single-lap joint, a new concept of adherend modulus grading was implemented with ceramic-metal graded adherends (Apalak and Gunes, 2006, 2007) and fibre grading (Ganesh and Choo, 2002). Adhesive grading along the overlap has never been studied before but is certainly the natural extension of the mixed adhesive concept presented above. The gradual modification of adhesive properties along the overlap could be obtained by several techniques such as a differentiated cure, adhesive toughening by micro or nano particles or differentiated adhesive formulation.

## 17.9 Sources of further information and advice

The papers of Comyn (1990) and Adams *et al*. (1992) give an excellent overview of thermal effects in adhesive joints. A recent book chapter by Apalak (2008) describes the complex modelling of adhesive joints under non-uniform thermal loads. For heat transfer mechanisms, the book of Holman (1992) is an excellent reference. Adhesives for high temperatures such as aromatic adhesives are well described in the book of Petrie (2000). Ceramic adhesives are less common and information about them is scarce. The Welding Institute (TWI) site (http://www.twi.co.uk/j32k/index.xtp) gives some information on ceramic adhesives and the Cotronics company (Brooklyn, NY, USA) (http://cotronics.com/vo/cotr/) commercialises various types of adhesive indicating the main physical and mechanical properties.

Thermal loads are an important aspect of adhesive joints and numerous articles can be found in journals dedicated to adhesion, polymers and composites. A search by the author for the preparation of the present chapter in the Web of Science database indicated that there are 290 articles related to the terms ‘temperature’ AND ‘adhesive’ AND ‘joints’ from 2000 to 2008. Useful information on thermal testing and data analysis can be found in international standards such as ASTM D1151, D1183 and D2557.

## 17.10 Acknowledgements

The author thanks the Portuguese Foundation for Science and Technology for supporting part of the work presented here, through the research projects POCTI/43525/EME/2000 and PTDC/EME-PME/67022/2006.

The author also wishes to thank Prof. R D Adams for his advice and comments on the work presented in this chapter.

© Woodhead Publishing Limited, 2010

## 17.11 References

Abedian A and Szyszkowski W (1999), 'Effects of surface geometry of composites on thermal stress distribution—a numerical study', *Compos Sci Technol*, **59** (1), 41–54.

Adams RD and Mallick V (1992), 'A method for the stress analysis of lap joints', *J Adhesion*, **38**, 199–217.

Adams RD and Mallick V (1993), 'The effect of temperature on the strength of adhesively-bonded composite-aluminium joints', *J Adhesion*, **43**, 17–33.

Adams RD, Atkins RW, Harris JA and Kinloch AJ (1986), 'Stress analysis and failure properties of carbon-fibre-reinforced-plastic/steel double-lap joints', *J Adhesion*, **20**, 29–53.

Adams RD, Coppendale J, Mallick V and Al-Hamdam H (1992), 'The effect of temperature on the strength of adhesive joints', *Int J Adhesives Adhesion*, **12**, 185–90.

Al-Hamdan HS (1989), *Thermal Stresses in Bonded Joints*, Master Thesis, Department of Mechanical Engineering, University of Bristol, UK.

Al-Samhan A and Darwish SM (2005), 'Factors influencing thermo-mechanical stresses developed in bonded tools', *Int J Adhesives Adhesion*, **25**, 379–88.

Althof W (1971), *Strength Properties of Bonded Joints of Carbon Fibre Reinforced Composites*, RAE Library Trans. No. 1616.

Anifantis NK, Kakavas PA and Papanicolaou GC (1997), 'Thermal stress concentration due to imperfect adhesion in fiber reinforced composite', *Compos Sci Technol*, **57** (6), 687–96.

Apalak MK (2008), 'Non-linear thermal stresses in adhesive joints', in *Modeling of Adhesively Bonded Joints*, da Silva LFM and Öchsner A (eds), Heidelberg, Springer.

Apalak MK and Gunes R (2002), 'On non-linear thermal stresses in an adhesively bonded single lap joint', *Computers and Structures*, **80**, 85–98.

Apalak MK and Gunes R (2006), 'Thermal residual stresses in an adhesively-bonded functionally graded single-lap joint', *J Adhesion Sci Technol*, **20** (12), 1295–320.

Apalak MK and Gunes R (2007), 'Elastic flexural behaviour of an adhesively bonded single lap joint with functionally graded adherends', *Mater Design*, **28**, 1597–617.

Apalak MK, Apalak ZG, Gunes R and Karakas ES (2003a), 'Steady-state thermal and geometrical non-linear stress analysis of an adhesively bonded tee joint with double support', *Int J Adhesives Adhesion*, **23** (2), 115–30.

Apalak MK, Apalak ZG and Gunes R (2003b), 'Thermal non-linear elastic stress analysis of an adhesively bonded T-joint', *J Adhesion Sci Technol*, **17** (7), 995–1016.

Apalak MK, Gunes R and Fidanci L (2003c), 'Geometrically non-linear thermal stress analysis of an adhesively bonded tubular single lap joint', *Finite Elem Anal Design*, **39**, 155–74.

Apalak MK, Gunes R, Turaman MO and Cerit AA (2003d), 'Thermal and geometrically non-linear stress analyses of an adhesively bonded composite tee joint', *Composites A*, **34**, 135–50.

Apalak MK, Apalak ZG and Gunes R (2004), 'Thermal and geometrically non-linear stress analyses of an adhesively bonded composite tee joint with double support', *J Thermoplastic Compos Mater*, **17**, 103–36.

Ávila AF and Bueno PO (2004), 'Stress analysis on a wavy-lap bonded joint for composites', *Int J Adhesives Adhesion*, **24**, 407–14.

Bhowmik S, Bonin HW, Bui VT and Weir RD (2006), 'Durability of adhesive bonding

© Woodhead Publishing Limited, 2010

of titanium in radiation and aerospace environments', *Int J Adhesives Adhesion*, **26**, 400–05.

Chiu WK, Chalkley PD and Jones R (1994), 'Effects of temperature on the shear stress-strain behaviour of structural adhesives (FM73)', *Computers and Structures*, **53**, 483–9.

Cho JH, Kong DI, Park CE and Jin MY (1998), 'Effect of curing temperature on the adhesion strength of polyamideimide/copper joints', *J Adhesion Sci Technol*, **12** (5), 507–21.

Comyn J (1990), 'Thermal effects on adhesive joints', in Brinson HF and Dostal CA, *Engineered Materials Handbook, Vol 3: Adhesives and Sealants*, ASM International, Metals Park, Ohio, 616–21.

Coppendale J (1977), *The Stress and Failure Analysis of Structural Adhesive Joints*, PhD Thesis, Department of Mechanical Engineering, University of Bristol, UK.

Curley AJ, Hadavinia H, Kinloch AJ and Taylor AC (2000), 'Predicting the service-life of adhesively-bonded joints', *Int J Fracture*, **103**, 41–69.

da Neves PJC, da Silva LFM and Adams RD (2009a), 'Analysis of mixed adhesive bonded joints – Part I: Theoretical formulation', *J Adhesion Sci Technol*, **23**, 1–34.

da Neves PJC, da Silva LFM and Adams RD (2009b), 'Analysis of mixed adhesive bonded joints – Part II: Parametric study', *J Adhesion Sci Technol*, **23**, 35–61.

da Silva LFM and Adams RD (2005), 'Measurement of the mechanical properties of structural adhesives in tension and shear over a wide range of temperatures', *J Adhesion Sci Technol*, **19** (2), 109–42.

da Silva LFM and Adams RD (2006), 'Stress-free temperature in a mixed adhesive joint', *J Adhesion Sci Technol*, **20** (15), 1705–26.

da Silva LFM and Adams RD (2007a), 'Joint strength predictions for adhesive joints to be used over a wide temperature range', *Int J Adhesives Adhesion*, **27**, 362–79.

da Silva LFM and Adams RD (2007b), 'Adhesive joints at high and low temperatures using similar and dissimilar adherends and dual adhesives', *Int J Adhesives Adhesion*, **27**, 216–26.

da Silva LFM and Adams RD (2007c), 'Techniques to reduce the peel stresses in adhesive joints with composites', *Int J Adhesives Adhesion*, **27**, 227–35.

da Silva LFM and Adams RD (2008), 'Effect of temperature on the mechanical and bonding properties of a carbon reinforced bismaleimide', *J Mater: Design Applications – Part L*, **222**, 45–52.

da Silva LFM, Adams RD and Gibbs M (2004), 'Manufacture of adhesive joints and bulk specimens with high temperature adhesives', *Int J Adhesives Adhesion*, **24**, 69–83.

da Silva LFM, de Magalhães AG and de Moura MFSF (2007), *Juntas Adesivas Estruturais* (in Portuguese), Porto, Publindústria.

Deb A, Malvade I, Biswas P and Schroeder J (2008), 'An experimental and analytical study of the mechanical behaviour of adhesively bonded joints for variable extension rates and temperatures', *Int J Adhesives Adhesion*, **28**, 1–15.

de Moura MFSF (2008), 'Progressive damage modeling', in *Modeling of Adhesively Bonded Joints*, da Silva LFM and Öchsner A (eds), Heidelberg, Springer.

Dixon DG, Harris SJ, Dempster M and Nicholls P (1998), 'The effect of PEEK fibres and powder on joints made with a high temperature adhesive', *J Adhesion*, **65**, 131–62.

Fessel G, Broughton JG, Fellows NA, Durodola JF and Hutchinson AR (2007), 'Evaluation of different lap-shear joint geometries for automotive applications', *Int J Adhesives Adhesion*, **27**, 574–83.

© Woodhead Publishing Limited, 2010

Frostig Y, Thomsen OT and Mortensen F (1999), 'Analysis of adhesive-bonded joints, square-end, and spew-fillet – high order theory approach', *J Eng Mech*, **125**, 1298–307.

Ganesh VK and Choo TS (2002), 'Modulus graded composite adherends for single-lap bonded joints', *J Compos Mater*, **36** (14), 1757–67.

Giannis S, Adams RD, Clark LJ and Taylor MA (2008), 'The use of a modified peel specimen to assess the peel resistance of aircraft fuel tank sealants', *Int J Adhesives Adhesion*, **28**, 158–75.

Hart-Smith LJ (1973), *Adhesive-Bonded Double-Lap Joints*, NASA CR-112235.

Holman JP (1992), *Heat Transfer*, McGraw-Hill, New York.

Hudson AJ, Martin SC, Hubert M and Spelt JK (2002), 'Optical measurements of shrinkage in UV-cured adhesives', *J Electronic Packaging, Trans ASME*, **124** (4), 352–4.

Humfeld GR and Dillard DA (1998), 'Residual stress development in adhesive joints subjected to thermal cycling', *J Adhesion*, **65** (1–4), 277–306.

Ioka S, Kubo S, Ohji K and Kishimoto J (1996), 'Thermal residual stresses in bonded dissimilar materials and their singularities', *Japan Soc Mech Eng Int J Ser A: Solid Mech Mater Engng*, **39**(2), 197–203.

Jensen BJ, Hou TH and Wilkinson SP (1995), 'Adhesive and composite properties of LARCTM-8515 polyimide', *High Perform Polym*, **7**, 11–21.

Katsuo M, Nakano Y and Sawa T (1999), '2-Dimensional transient thermal stress analysis of adhesive butt joints', *J Adhesion*, **70** (1–2), 75–93.

Kaye R and Heller M (2005), 'Through-thickness shape optimisation of typical double lap-joints including effects of differential thermal contraction during curing', *Int J Adhesives Adhesion*, **25**, 227–38.

Kim YG and Lee DG (1998), 'Influence of fabrication residual thermal stresses on rubber-toughened adhesive tubular single lap steel–steel joints under tensile load', *J Adhesion*, **65** (1–4), 163–85.

Kim JK and Lee DG (2001), 'Thermal characteristics of tubular single lap adhesive joints under axial loads', *J Adhesion Sci Technol*, **15** (12), 1511–28.

Kim YG, Lee SJ, Lee DG and Jeong KS (1997), 'Strength analysis of adhesively bonded tubular single lap steel–steel joints under axial loads considering residual thermal stresses', *J Adhesion*, **60** (1–4), 125–40.

Kim K-Y, Ye L and Yan C (2005), 'Fracture behavior of polyetherimide (PEI) and interlaminar fracture of CF/PEI laminates at elevated temperatures', *Polym Compos*, **26**, 20–8.

Lee SJ and Lee DG (1995), 'Optimal-design of the adhesively bonded tubular single lap joint', *J Adhesion*, **50** (2–3), 165–80.

Loh WK, Crocombe AD, Abdel Wahab MM and Ashcroft IA (2005), 'Modelling anomalous moisture uptake, swelling and thermal characteristics of a rubber toughened epoxy adhesive', *Int J Adhesives Adhesion*, **25**, 1–12.

Lu D and Wong CP (2000), 'Effects of shrinkage on conductivity of isotropic conductive adhesives', *Int J Adhesives Adhesion*, **20**, 189–93.

Mallick V (1989), *Stress Analysis of Metal/CFRP Adhesive Joints Subjected to the Effects of Thermal Stresses*, PhD Thesis, Department of Mechanical Engineering, University of Bristol, UK.

Marques EAS (2008), *Analysis of Adhesive Joints for Aerospace Applications*, Master Thesis, Department of Mechanical Engineering and Industrial Management, Faculty of Engineering, University of Porto, Portugal.

Matsui K (1990), 'Effects of curing conditions and test temperatures on the strength of adhesive-bonded joints', *Int J Adhesives Adhesion*, **10**, 277–84.

© Woodhead Publishing Limited, 2010

Melcher RJ and Johnson WS (2007), 'Mode I fracture toughness of an adhesively bonded composite–composite joint in a cryogenic environment', *Compos Sci Technol*, **67**, 501–6.

Naboulsi S and Mall S (1997), 'Thermal effects on adhesively bonded composite repair of cracked aluminium panels', *Theor Appl Fracture Mech*, **26**, 1–12.

Nakagawa F and Sawa T (2001), 'Photoelastic thermal stress measurements in scarf adhesive joints under uniform temperature changes', *J Adhesion Sci Technol*, **15** (1), 119–35.

Nakagawa F, Sawa T, Nakano Y and Katsuo M (1999), 'A 2-dimensional finite element thermal stress analysis of adhesive butt joints containing some hole defects', *J Adhesion Sci Technol*, **13** (3), 309–23.

Parvatareddy H, Dillard JG, MacGrath JE and Dillard DA (1998), 'Environmental aging of the Ti-6Al-4V/FM-5 polyimide adhesive bonded system: Implications of physical and chemical aging on durability', *J Adhesion Sci Technol*, **12** (6), 615–37.

Petrie E M (2000), *Handbook of Adhesives and Sealants*, New York, McGraw-Hill.

Rastogi N, Soni SR and Nagar A (1998), 'Thermal stresses in aluminium-to-composite double-lap bonded joints', *Adv Engi Software*, **29** (3–6), 273–81.

Reedy ED and Guess TR (1996), 'Butt joint strength and effect of residual-stress and stress-relaxation', *J Adhesion Sci Technol*, **10** (1), 33–45.

Richardson DE, McLennan ML, Anderson GL, Macon DJ and Batista-Rodriguez A (2003), 'Multiaxial, temperature, and time-dependent (MATT) failure model', *J Adhesion*, **79**, 157–74.

Rieger J (2001), 'The glass transition temperature $T_g$ of polymers–Comparison of the values from differential thermal analysis (DTA, DSC) and dynamic mechanical measurements (torsion pendulum)', *Polym Testing*, **20**, 199–204.

Rossetos JN (2003), 'Thermal peel, warpage and interfacial shear stresses in adhesive joints', *J Adhesion Sci Technol*, **17** (1), 115–28.

Sinha PK and Reddy MN (1976), 'Thermal analysis of composite bonded joints', *Fibre Sci Technol*, **9**, 153–9.

Srivastava VK (2003), 'Characterization of adhesive bonded lap joints of C/C–SiC composite and Ti–6Al–4V alloy under varying conditions', *Int J Adhesives Adhesion*, **23**, 59–67.

Stone MH (1981), 'The effect of adhesive properties on the low temperature strength of joints between metals and carbon fibre reinforced plastics', *Int J Adhesives Adhesion*, **1**, 203–7.

Suhir E (2000), 'Adhesively bonded assemblies with identical nondeformable adherends and "piecewise continuous" adhesive layer: predicted thermal stresses in the adhesive', *Int J Solids Struct*, **37**, 2229–52.

Wang RX, Sinclair AN and Spelt JK (2003), 'Strength of adhesive joints with adherend yielding: II. Peel experiments and failure criteria', *J Adhesion*, **79** (1), 49–66.

Wang JG, Jiang N and Jiang HY (2006), 'The high-temperatures bonding of graphite/ceramics by organ resin matrix adhesive', *Int J Adhesives Adhesion*, **26**, 532–6.

Wang X, Geng H, He S, Pokhyl YO and Koval KV (2007), 'Effect of thermal expansion coefficient on the stress distribution in solar panel', *Int J Adhesives Adhesion*, **27**, 288–97.

Yu H (1999), *Experimental Determination of Shrinkage, Modulus and Residual Stresses in Adhesives During the Cure Process*, PhD Thesis, Department of Mechanical Engineering, University of Bristol, UK.

Yu J-H, Guo S and Dillard DA (2003), 'Bimaterial curvature measurements for the CTE of adhesives: optimization, modeling, and stability', *J Adhesion Sci Technol*, **17** (2), 149–64.

© Woodhead Publishing Limited, 2010

Yu Y, Ashcroft IA and Swallowe G (2006), 'An experimental investigation of residual stresses in an epoxy–steel laminate', *Int J Adhesives Adhesion*, **26**, 511–19.

Zhang X, Wong EH, Rajoo R, Iyer MK, Caers JFJM and Zhao XJ (2005), 'Development of process modeling methodology for flip chip on flex interconnections with non-conductive adhesives', *Microelectronics Reliability*, **45**, 1215–21.

Zhong WH, Zhamu A, Aglan H, Stone J and Gan YX (2005), 'Effect of residual stresses on fatigue crack growth behaviour of aluminum substrate repaired with a bonded composite patch', *J Adhesion Sci Technol*, **19** (12), 1113–28.

© Woodhead Publishing Limited, 2010

# 18

# Assessing and improving bonding in wet conditions

K. TAN, C. WHITE and D. HUNSTON,
National Institute of Standards and Technology, USA;
B. VOGT, Arizona State University, USA;
A. HAAG, Haag Chemistry LLC, USA

**Abstract**: Moisture is a key culprit in degrading adhesive bonds. This chapter reviews recent developments in test methods and techniques that have been used to assess and understand the role moisture plays in bond degradation, placing emphasis on accelerated destructive aging and testing, as well as non-destructive evaluation. Current understanding of interfacial water accumulation and advances in techniques for quantifying interfacial water distribution and diffusion are discussed. Finally, progress in surface pretreatment techniques, modification of bulk properties, engineering of novel biological adhesives and joint design considerations for improving adhesive bonds in wet conditions are presented.

**Key words**: durability, moisture, degradation, aging, biological adhesives, accelerated testing, interfacial water distribution.

## 18.1 Introduction

Water is ubiquitous in any uncontrolled setting and affects worldwide commerce by initiating device and structural failures like corrosion, electrical shorting or adhesive failure. In adhesive failure, environmental attack of water leads to significant deterioration in joint strength and subsequently to premature failure of the adhesive bond. Water, in either the liquid or vapor phases, penetrates the adhesive and causes great problems in both durability and reliability of adhesive joints. Since water molecules exhibit a strong dipole, they interact with charged or polar surfaces such as high surface energy substrates, and can permeate polymers. This susceptibility to moisture has led to significant efforts to evaluate the effects of moisture on adhesion and to the development of better understanding of the mechanisms of water attack.

It is well documented that the presence of moisture in joints not only weakens the physical and chemical properties of a bulk adhesive itself via plasticization, swelling, degradation, cracking and crazing, and so on (Weitsman, 1977; Sargent and Ashbee, 1981; Bowditch, 1996; Gazit, 1978; Su *et al.*, 1992; Xiao and Shanahan, 1997; Wylde and Spelt, 1998; Loh *et al.*, 2002), but also attacks the interface between the adhesive and the substrate.



© Woodhead Publishing Limited, 2010

Hydrolysis of secondary interfacial bonds, hydration of substrate oxide layer and cathodic delamination are examples of degradation mechanisms caused by moisture at the interface (Watts and Castle, 1984; Venables, 1984; Watts, 1989; Brewis *et al.*, 1990; Kalashnikova *et al.*, 1996; Kinloch *et al.*, 2006, 2007; Nguyen *et al.*, 2005). Additionally, in some cases, moisture degradation may also lead to gross corrosion or dimensional changes in the substrates, for example if a hydrolytically unstable substrate, such as mild steel, is utilized. With such potentially deleterious effects of water, many adhesive joints are unlikely to achieve their anticipated service life. Research undertaken during the past two to three decades, however, has provided significant progress in understanding the effects of wet conditions on bonding and has helped develop measures to improve the bonding in wet conditions. The present chapter is devoted to consideration of the wet adhesion properties of structural adhesive joints.

## 18.2 Testing and modeling adhesive bonds in wet conditions

Understanding the kinetics and mechanisms of moisture attack is central to the development of more durable adhesive bonding. To acquire this fundamental knowledge, in turn, requires the development and application of test methods and models to assess the durability of adhesive bonds in wet conditions. In any such testing, it is critical that the failure mode matches that which occurs in the actual application of interest. The failure mode may depend on the presence or absence of load, the type of load, and/or the load level. Measurements made under inappropriate conditions may produce misleading or even incorrect predictions of behavior. Relevant, useful approaches and analysis techniques that have enhanced understanding of the role of moisture in bond degradation briefly will be reviewed.

### 18.2.1 Accelerated aging and testing

The durability of adhesive joints may be assessed using long-term field exposure and this is likely to decrease the risk of introducing poorly performing joints into the marketplace. However, the cost of developing new adhesive materials and systems is directly related to the time-to-market, which strongly correlates with research and development time. Added time in the pipeline results in a decreased return on investment and lost product market competition battles. Also, the durability data accumulated from long-term field tests over years may be of little relevance if the materials fail to meet expectations or there is any change in the formulation. Therefore, accelerated tests must be employed to assess the durability, within reasonable time scales, particularly in an era where there is an increasing demand for shorter research and development

© Woodhead Publishing Limited, 2010

cycles. A number of approaches have been used to accelerate such tests; the two most common are increasing the temperature and applying increased mechanical loading. With any such approach, however, there are two important questions: 'Does the acceleration alter the failure mechanism?' and 'How much is the aging accelerated?' For qualitative and ranking experiments, the second question may not be important, but if any behavioral predictions are desired, the amount of acceleration needs to be determined. The usual ways of addressing these questions are to characterize the failure mode and to test at intermediate values of the accelerating parameters to see if the process follows the same kinetics at all times.

A popular form of accelerated aging for load-bearing structural joints involves the use of static or dynamic stress, particularly at or near adhesive/substrate interfaces, and simultaneous exposure to hostile environments, such as high humidity, elevated temperature or corrosive conditions. The ready ingress of water molecules into bonds near the propagating crack tip, coupled with the high stress concentration which is present at the crack tip, leads to an easily observable acceleration factor. Thus, this test method circumvents a problem associated with accelerating environmental attack through the use of unrealistically high temperatures. Some well-known methods are the Boeing wedge test, constant displacement rate test, peel test, cyclic fatigue test, pull-off test, blister test, and so on whose strengths and limitations have been discussed elsewhere (Kinloch, 1987; Adams *et al.*, 1997; Lacombe, 2006).

In the Boeing wedge test (ASTM D-3762), bonded joints are loaded by driving a wedge between the substrates to produce a constant displacement. This test, developed by Boeing during the 1960s, remains one of the most popular accelerated assessments providing rapid screening of durability performance, particularly when analyzed in terms of fracture energy. The wedge test has been shown to be sensitive to test environments, surface pretreatments, and so on. Further, its qualitative correlation to long-term in-service performance has been demonstrated (Marceau and Thrall, 1985) for some material systems. However, the wedge test can be misused because ASTM D-3762 is not fully prescriptive. For the wedge test to have the potential for reliable quantitative evaluation, several critical experimental considerations must be taken into account or avoided altogether. These include gross plastic deformation of substrates, crack blunting effects around the crack tip and stress relaxation caused by creep of adhesives (Arnott and Kindermann, 1995a; Yang *et al.*, 1999; Sargent, 2005). Furthermore, the wedge test is not suitable for service life prediction because it provides data for a very limited set of conditions.

In recent years, the constant displacement rate test method has been used extensively (Arnott and Kindermann, 1995a, 1995b; Kook and Dauskardt, 2002; Korenburg *et al.*, 2004; Kinloch *et al.*, 2007). Since the displacement

© Woodhead Publishing Limited, 2010

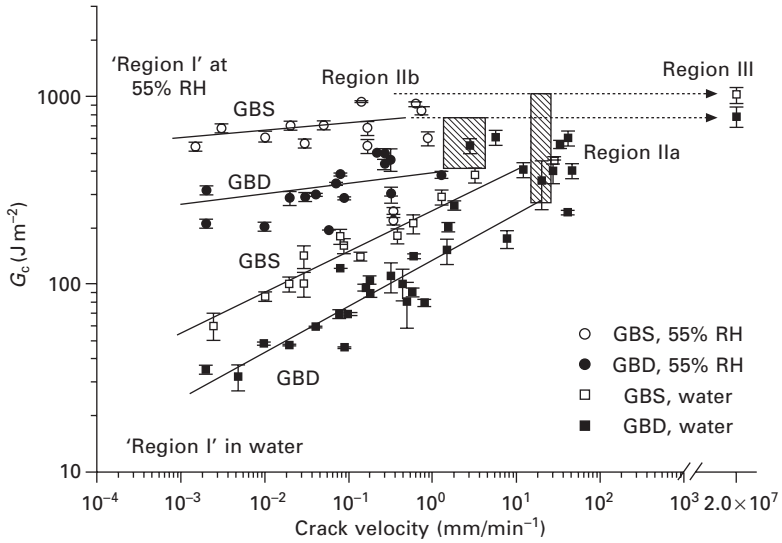
rate strongly influences crack growth rate, the displacement rate can be selected to drive the crack at a velocity that is either faster or slower than the degradation rate of bonds ahead of the crack tip. This relationship is illustrated in Fig. 18.1, which shows that the dependence of adhesive fracture energy on the crack velocity exhibits distinct regions that have been well-documented in the literature (Wiederhorn, 1967; Kook and Dauskardt, 2002; Korenburg *et al*., 2004; Kinloch *et al*., 2007).

Of particular interest in the study of durability is the lowest crack velocity region, which is associated with water molecule diffusion to the propagating crack tip at a rate faster than the crack velocity, thus allowing water molecules to reach and weaken the crack tip. Therefore, the durability of adhesive joints is readily discernable in this low crack velocity region (Arnott and Kindermann, 1995a, 1995b; Kinloch *et al*., 2007). On the other hand, when joints are loaded at a fast displacement rate, crack extension may occur at a rate faster than the diffusion rate of water molecules, suppressing any potential effect of water attack. Indeed, Kinloch *et al*. (2007) found that adhesive fracture energy recorded at 21°C ± 1°C for 55% relative humidity (RH) was greater than that recorded for 21°C ± 1°C liquid water tests, but the values of adhesive fracture energy were of statistically the same magnitude for both the environments if relatively fast rates were employed. Thus, the durability ranking obtained from high displacement rate tests can be misleading.

Data collection to establish the dependence of adhesive fracture energy upon the crack velocity as illustrated in Fig. 18.1 is usually time consuming, as each data point is obtained from a single displacement rate for each specimen. To accelerate the rate of experimentation, Kindermann *et al*. (1997) proposed that multiple different displacement rates may be applied to a single specimen. Using an adhesive system similar to that used in a prior study (Arnott and Kindermann, 1995a), eight decreasing displacement rates were applied to a specimen with each rate sustained for the time needed for a displacement of 1 mm. The researchers constructed a plot of adhesive fracture energy versus crack velocity within eight days. This plot was found to be statistically identical to those obtained previously on other specimens using a single displacement rate for each specimen which took three months to complete (Arnott and Kindermann, 1995a). This method, of course, can reduce experimental time, but it also can enable a reduction in variations introduced by using different specimens. However, it should be noted that a relatively simple fracture-mechanics relation was used.

The adhesive fracture energy mechanical relation depends only on load and displacement and is independent of crack length. Thus, the adhesive fracture energy may be calculated readily from the load–displacement data. It is important when conducting these tests to ensure that each successive step has a fracture energy that is equal to or higher than that for the previous step. The growing crack will have a crack-tip deformation zone whose size

© Woodhead Publishing Limited, 2010




*18.1* Relationship between the adhesive fracture energy, $G_C$, and the crack velocity for aluminum-alloy/epoxy joints recorded at 55% RH and in liquid water at 21°C ± 1°C. GBD denotes substrates that were grit blasted and degreased; GBS denotes substrates that were grit blasted, degreased and had substrates that were also silane-pretreated prior to bonding (Kinloch *et al.*, 2007).

depends on fracture energy. If the next step normally would have lower fracture energy, the measurement may be influenced by the larger deformation zone generated in the previous step. This is particularly important for tough materials in which the zone size may not be small compared to 1 mm. It remains to be demonstrated whether such an approach provides a sound basis for an accelerated test if more complex fracture-mechanics relations, such as those whose equations explicitly include crack length, are required. In such cases, the lack of data points for determining adhesive fracture energy at each displacement rate may well compromise both the accuracy and reliability of results.

The fluctuating loads used in cyclic fatigue tests always lead to much lower resistance to crack growth than those seen under monotonic loads. Thus, the combination of a hostile environment and cyclic fatigue loading constitute a very severe test environment. Cyclic fatigue loading represents an accelerated test method extensively used to increase the rate of water attack on the joints without the detrimental effects associated with the common practice of raising the test temperature or crack blunting caused by water plasticization occurring in specimens subjected to monotonic loading (Kinloch, 1987; Ashcroft *et al.*, 2001). However, most cyclic-fatigue tests commonly are undertaken using expensive servo-hydraulic test machines. The disadvantage

© Woodhead Publishing Limited, 2010

of these machines is that usually only one specimen can be tested at a time, leading to both extended testing and extensive financial outlay. One approach that has been adopted to accelerate the rate of experimentation is the use of multi-specimen machines that are capable of independently testing many specimens simultaneously (Tan, 2005).

The ingress of water into full adhesive joints usually takes a relatively long time, in the region of years, to reach saturated conditions (Chang *et al.*, 1997; Tan, 2005). Modifications to test geometries have been proposed to accelerate water uptake. One of these accelerating routes is via the use of an open-faced configuration (Chang *et al.*, 1997; Wylde and Spelt, 1998). Specimens are made by coating a thin layer of adhesive over the substrates, which are then placed in environments with different levels of relative humidity and temperature. Owing to a larger exposed surface area for water ingress and shorter diffusion path, equilibrium is achieved very quickly, usually within days. Adhesion loss is then measured using the notched coating test (Chang *et al.*, 1997; Dillard *et al.*, 1999), shaft-loaded blister test (O'Brien *et al.*, 2005; Tan *et al.*, 2008a, 2008b) or scrape test (Knox and Cowling, 2000) as examples.

Similarly, Wylde and Spelt (1998) have used an open-faced joint, but proposed to bond a second substrate to the adhesive layer using a second adhesive to form a double cantilever beam joint. Chang *et al.* (1997) demonstrated that the open-faced configuration provided a sound basis for an accelerated test by showing that the results agreed well with those from double cantilever beam joints which have been conditioned for one year. Of course, the specimens need to be checked so that the failure path is known. For adhesive systems which are prone to corrosion, however, the build-up of corrosion products at buried interfaces without the constraint imposed by two substrates may introduce a different failure mechanism compared to the full adhesive joint configuration (Vine *et al.*, 2001).

### 18.2.2 Non-destructive test methods

The development of reliable non-destructive test (NDT) methods for adhesive joints has long been sought, since a lack of such methods can limit the use of bonding in critical load-bearing applications. Such techniques are also potentially useful for both in-process and on-site evaluation and monitoring. The challenge is that adhesives can fail in many different ways so that the variety of features that need to be obtained to anticipate a failure cover a very wide range. No single technique or group of techniques can measure all of these features. Some features, such as changes in chemistry, are not easily measured. In other cases, techniques may be available, but lack sensitivity either because the changes are too small or they occur in a very small volume, such as the region near the interface. Finally, there are

© Woodhead Publishing Limited, 2010

characteristics that are observable only at high strains. For example, the basic mechanical properties of a simple epoxy and a toughened epoxy are nearly identical at small strains and yet the fracture energies may differ by more than an order of magnitude.

In the case of moisture attack, the situation is complicated, as the changes involved occur at the sub-micrometer scale, whereas the thickness of the adhesive layer and substrate are on the micrometer scale. Nonetheless, it has been shown that empirical correlations between NDT parameters and failure characteristics are very helpful in interpreting the failure mechanism. For example, Fernandes *et al.* (2002) employed electrochemical impedance spectroscopy (EIS) to correlate pitting corrosion of a plasma-coated aluminum alloy. Simpson *et al.* (1992) reported a correlation between low-frequency impedance measurements and the loss in tensile strength for polymer/steel joints. Boinard *et al.* (2001) used dielectric spectroscopy to establish correlations between dielectric signals with the degradation of adhesive properties of the joints during aging caused by water absorption. In the case of a normal-incidence ultrasonic technique, a correlation may be found between adhesive toughness during environment attack and ultrasonic scans (Vine *et al.*, 2001).

Correlations between non-destructive measurements and mechanical or electrochemical properties may allow non-destructive monitoring of adhesive joints to provide early warning if moisture attack in joints has reached a critical stage. For example, Davis *et al.* (2000, 2002) used correlations between low-frequency impedance and loss in mechanical properties of adhesive joints to develop such sensors to detect early stages of degradation. The key is that the sample failure mode(s) must be known and the techniques must be sensitive to an appropriate feature. Moreover, NDT results are often only qualitative, so it is not possible to evaluate quantitatively the hygroscopic stability of adhesive/substrate interfaces. Thus, quantitative NDT for quality inspection and durability evaluation is currently still lacking.

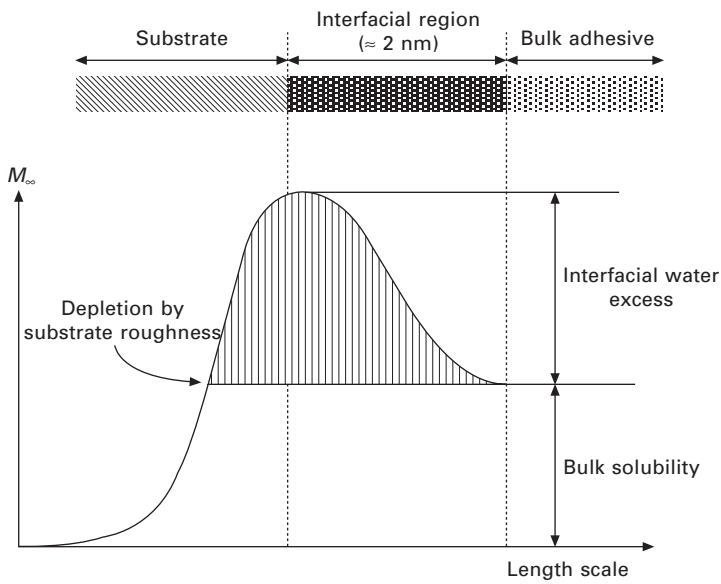
### 18.2.3 Interfacial water distribution and diffusion

When water attacks an adhesive joint, the failure occurs usually at or near the adhesive/substrate interface. As a result, it is important to know not only how much water the adhesive absorbs, but also how the water is distributed throughout the bonded joint. Water uptake in bulk adhesives has received significant attention and is typically measured gravimetrically, but solid state nuclear magnetic resonance (NMR) spectroscopy (Hodge *et al.*, 1996) has also been utilized. More recently, metrologies for measuring water ingression into thin adhesive coatings have been explored, including EIS (Bellucci and Nicodemo, 1993), quartz crystal microbalance (Moylan *et al.*, 1991), specular X-ray reflectivity (Vogt *et al.*, 2005b), dielectric properties (Pethrick *et al.*,

© Woodhead Publishing Limited, 2010

1996) and attenuated total reflection Fourier transform infrared spectroscopy (ATR-FTIR) (Fieldson and Barbari, 1993; Sammon *et al*., 1998; Cotugno *et al*., 2001). Quantifying the moisture distribution near an interface, however, has remained virtually impossible until recently. Early attempts to measure interfacial water content utilized a perforated joint configuration that only yielded qualitative information about interfacial diffusion. Given the fundamental importance of this question, a growing number of studies have attempted to determine water concentration at or near the adhesive/substrate interface.

It has been shown that water-rich layers exist at the interface of several types of adhesive/substrate interface, after exposure to air saturated with water at room temperature, (see Fig. 18.2). Using neutron reflectivity, Wu *et al*. (1995) mapped the concentration of deuterated water in polyimide film as a function of the distance from the buried polyimide/silicon oxide interface and found that the water concentration at this interface exceeded that of the bulk film by more than 500%. Nguyen *et al*. (1995) used FTIR-multiple total internal reflection spectroscopy (MTIR) to measure the water absorption in a series of epoxy, asphalt and pigmented polyester films on silicon oxide. In all cases, water concentration at the interface was greater than that of the bulk adhesive. Kent *et al*. (1996) employed neutron reflectivity to show




*18.2* Schematic of water concentration profile near a polymer/substrate interface. The higher concentration of water at the interface is due to the stronger affinity of water for the substrate than the bulk polymer. The lower concentration very near the substrate oxide interface is attributed to intrinsic roughness of the oxide layer.

© Woodhead Publishing Limited, 2010

that a large concentration of water (> 80 vol.%) existed at a polyurethane/molybdenum interface.

This accumulation of water multilayers at the interface is not surprising since high surface energy surfaces are highly hydrophilic, creating a thermodynamic driving force for water accumulation. Indeed, there is substantial evidence confirming the formation of multilayers of water on high surface energy free surfaces at relative humidities below 100% (Bowden and Throssell, 1951). In addition, the presence of hygroscopic contaminants at the interface would contribute to the multilayer adsorption at the interface (Bascom, 1970; Nguyen *et al*., 1995). These contaminants include hydrophilic unreacted and partially reacted resins and curing agents, additives and impurities, either accrued during specimen preparation or leached out from the adhesive during exposure to water (Nguyen *et al*., 1995). Ions produced during the corrosion process also may increase the affinity of the interface for water (Leidheiser and Funke, 1987).

While many adhesive joints do contain multilayers of water at the adhesive/substrate interface, the interfacial moisture content is strongly dependent on the surface chemistry of the substrates (Kent *et al*., 1999a, 1999b; Vogt *et al*., 2005a; O'Brien *et al*., 2006). Wu *et al*. (1995) employed neutron reflectivity to investigate deuterated water adsorption at the interface between a polyimide and silicon oxide pretreated with a silane coupling agent. They found that the water in the interfacial region reached a maximum concentration of 12% by volume when the silane finish was present, but 17% by volume was accumulated at an untreated silicon oxide surface. Similarly, using FTIR-MTIR, Nguyen *et al*. (2007) measured the thickness of the interfacial water layer for both untreated and silane-treated epoxy/silicon oxide systems. They found little water accumulation at the epoxy/silicon-treated oxide interface, but about 3 nm of water layer accumulated at the epoxy/untreated silicon substrate following 100 h of exposure at 24°C. Also, Vogt *et al*. (2005a) demonstrated that water accumulation near the buried interface of poly(4-tert-butoxycarboxystyrene) film and $Al_2O_3$ can be reduced substantially by treating the substrate surface with phenylphosphonic acid (a hydrophobic agent). The reduction in the interfacial water concentration increased the adhesive fracture energy of the joints by a factor of five (O'Brien *et al*., 2006).

The influence of bulk polymer chemistry on the interfacial water concentration has been reported for limited number of systems. For example, Vogt *et al*. (2004) exposed poly(4-hydroxystryene) (PHOSt) and poly(tert-butoxycarboxystyrene) (PBOCSt) films on silicon wafers to saturated water vapor, and measured water accumulation at the buried interface by neutron reflectivity. The water absorption in bulk PBOCSt was found to be 1% by volume, which was considerably lower than that of bulk PHOSt (10% by volume). However, closer to the silicon substrate, the water concentration

© Woodhead Publishing Limited, 2010

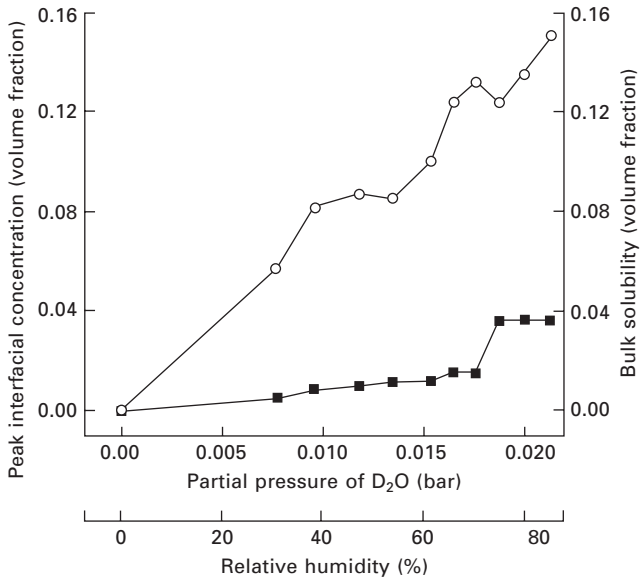
attained at the buried interfaces of both systems is independent of the polymers. The lack of polymer chemistry influence on the interfacial excess water distribution was ascribed to the weak dependence of the forces controlling the adsorption of these polymers at the interface (i.e. the van der Waals interactions) on the maximum water uptake. However, it is unclear if the lack of influence of polymer on the interfacial moisture content is universal for all polymers. In fact, previous studies (Vogt *et al*., 2005b) have suggested that the extent of swelling at a polymer/substrate interface may be related to the mechanical properties of polymers. Additionally, indirect evidence from recent work by Tan *et al*. (2008a, 2008b) showed that hydroscopic swelling stresses in a bulk polymer may have an influence on the interfacial water uptake.

Many studies of water near buried interfaces have focused on exposure either to saturated vapor or liquid (Kent *et al*., 1999a, 1999b; Vogt *et al*., 2005a, 2005b, 2005c; O'Brien *et al*., 2006). Tan *et al*. (2008a, 2008b) has recently investigated samples exposed to different levels of relative humidity. These studies were motivated by observations (Brewis *et al*., 1990; Lefebvre *et al*., 1991) that some adhesive joints show a dramatic drop in strength when exposed to humidity levels above a certain critical value. Tan *et al*. (2008a, 2008b) studied poly(methyl methacrylate) films supported on silicon oxide, and showed that loss of adhesion strength is initiated at a critical relative humidity.

Figure 18.3 shows moisture concentrations in the polymer both at the interface and at a distance away from the interface. The latter curve provides an indication of bulk sorption properties of the adhesive and increases linearly with relative humidity up to a value of 60% RH. Between 60% RH and 68% RH there is a large increase in concentration which corresponds to the humidity range where there is rapid loss in adhesion strength (Lefebvre *et al*., 1991; Tan *et al*., 2008a, 2008b). In contrast, the curve in Fig. 18.3 for water concentration at the interface shows no discontinuity, but rather a steady increase with relative humidity. When the actual distribution profile for the high water concentration near the interface was examined, however, Tan *et al*. (2008b) found that a significant broadening of the high water concentration region near the interface occurred at the same relative humidity as the critical relative humidity for loss of adhesion strength. Consequently, although the maximum water concentration increases linearly with relative humidity, the total quantity of water near the interface shows a dramatic increase at the critical relative humidity.

There are conflicting theories indicating that water resides at the interface in either heterogeneous condensed droplets or in a homogeneously distributed layer (Kinloch, 1987; Leidheiser and Funke, 1987). *In situ* atomic force microscopy (AFM) images of ultrathin polymer films supported on silicon wafers exposed to water strongly suggest separation of liquid water and vapor

© Woodhead Publishing Limited, 2010

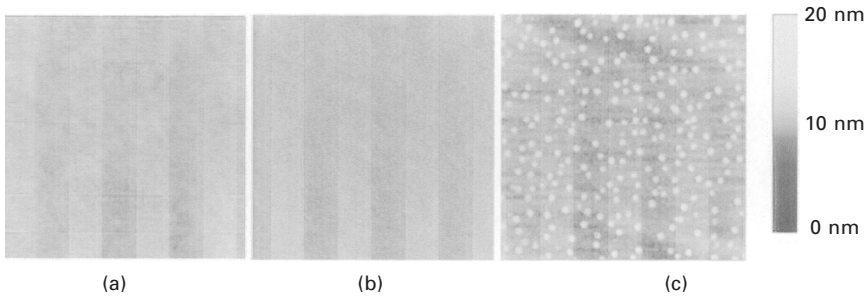



*18.3* Comparison of interfacial and bulk water concentrations determined using neutron reflectivity. A significant excess is observed at the interface (○) which increases approximately linearly with humidity. The bulk solubility of water in PMMA (■) shows a discontinuity near the critical relative humidity (Tan *et al.,* 2008b).

at the interface (Tan *et al*., 2008b). Figure 18.4(a) shows a representative AFM image of the dry film which is relatively featureless, as expected. Two different surfaces, a native silicon oxide and a methylated surface, were examined. The former surface is extremely hydrophilic and known to exhibit poor adhesion in wet environments. The latter surface is somewhat hydrophobic and exhibits minimal adhesion loss when exposed to moisture. The *in situ* AFM images of these two polymer films with nearly identical thickness, but extremely different surface chemistries are shown in Figs 18.4(b) and 4(c). The polymer film on the hydrophobic surface remains relatively featureless, but the film on the hydrophilic surface exhibits a blistered surface. The presence of small isolated water-filled blisters can be attributed to the formation of heterogeneous condensed droplets at the interface (Leidheiser and Funke, 1987; Vogt *et al*., 2005c; Tan *et al*., 2008b).

Note that the strength of silicon oxide–water interaction does not generally favor multiple occupancy of sites until the next layer is sorbed (Thiel and Madey, 1987). However, structural heterogeneities or local differences in film thickness may allow water molecules to arrive at the interface at locally different rates, causing such phase separation to occur (Leidheiser and Funke, 1987). Additionally, the water concentration at the interface is in excess of

© Woodhead Publishing Limited, 2010




*18.4* AFM images (5 μm × 5 μm) of (a) a dry polymer film surface, and polymer films supported on (b) a hydrophobic and (c) a hydrophilic surface exposed to water. The dry film and the water-exposed film supported on the hydrophobic surface are relatively featureless, while the water-exposed film supported on the hydrophilic surface exhibits a blistered surface. The height scale is shown on the right of the images (adapted from Tan *et al.*, 2008b).

the bulk solubility within the polymer, so multiple phases might be expected from a simple thermodynamic (equilibrium) argument.

The moisture absorption rates into polymers and interfaces can be different owing to the properties of bulk polymers and interfacial regions (Dillingham and Boerio, 1987; Roche *et al.*, 2002). For example, in a recent study on water diffusion along an epoxy/iron interface using ATR-FTIR, Wapner *et al.* (2006) found that the interfacial diffusion of water is about two orders of magnitude faster than the transport through the polymer itself. An indirect measurement of interfacial water diffusion rate into full adhesive joints has been reported by Zanni-Deffarges and Shanahan (1995). Based on a common observation that progressive diffusion of water degrades bulk mechanical properties, these workers attempted to correlate changes in the overall elastic behavior of a modified epoxy adhesive to estimate mass water uptake. A 'composite' model was developed in which the elastic moduli are assumed to be a combination of rigidities from the relative fractions of 'wet' and 'dry' adhesive under load. A comparison was made with the results obtained using classic gravimetric analysis. As shown in Table 18.1, the 'composite' model gave values of the coefficient of diffusion, $D$, for the bulk adhesive in satisfactory agreement with those obtained by gravimetric analysis. Applying the same reasoning, these workers attempted to estimate water ingress into cylindrical torsional full adhesive joints. The coefficient of diffusion was deduced using measured torque of the joints as a function of immersion time. They found that the value of $D$ for torsional joints is considerably greater, thus indicating the important role of interfacial water diffusion in adhesive bond durability.

© Woodhead Publishing Limited, 2010

*Table 18.1* Calculated values of the coefficient of diffusion, *D*, obtained from gravimetric analysis and the 'composite' model (Zanni-Deffarges and Shanahan, 1995)

| | $D$ ($10^{-12}$ $m^2s^{-1}$) | |
|---|---|---|
| | From gravimetric analysis | From 'composite' model |
| Tensile specimen | 1.4 ± 0.1 | 0.8 ± 0.01 |
| Compressive specimen | 1.4 ± 0.1 | 0.5 ± 0.005 |
| Bonded joint | – | 5.3 ± 0.1 |

## 18.3 Techniques for optimizing adhesive bonds in wet conditions

The procceeding discussion has clearly highlighted the importance of both the hydrolytic stability of adhesive/substrate interfacial regions and the bulk properties of adhesives. Therefore, to optimize adhesion in wet conditions, attention should be given to the enhancement of the interaction between the adhesive and the substrate surface, in addition to the bulk properties of adhesive. Through these considerations, a variety of techniques have been developed to improve the durability of adhesive joints exposed to wet environments.

### 18.3.1 Surface pretreatment routes

One of the most common approaches to enhance adhesive/substrate interfacial hydrolytic stability is to use surface pretreatments for substrates prior to bonding. Surface pretreatments are important not only to clean the surface, remove weak boundary layers and engineer surface topography and morphology, but also to provide specific chemical properties. There are many examples of this in the literature. In the case of metallic substrates, conventional chemical pretreatment processes, including chromium acid etching, chromium acid anodizing, or phosphoric acid anodizing are still commonly used to create durable bonded interfaces (Venables, 1984; Kinloch, 1987). However, these pretreatments involve aggressive and toxic chemicals, such as hexavalent chromium (Cr-VI) compounds, volatile organic compounds, strong acids or alkalis, and so on. Owing to ever-increasing environmental regulations regarding such etching and anodizing processes, there has been a growth in interest in alternative processes that are environmentally benign. The use of coupling agents provides greener alternatives. Organofunctional silanes are the most commonly used to increase the environmental resistance of joints prepared from steel (Hong and Boerio, 1994; Korenburg *et al.*, 2004; Kinloch *et al.*, 2007), aluminum alloy (Abel *et al.*, 2000; Johnsen *et al.*, 2002; Korenburg *et al.*, 2004; Kinloch *et al.*, 2007), glass (Hunston *et al.*, 1996; Ritter *et al.*, 2002; Kinloch *et al.*, 2006) and molybdenum oxide

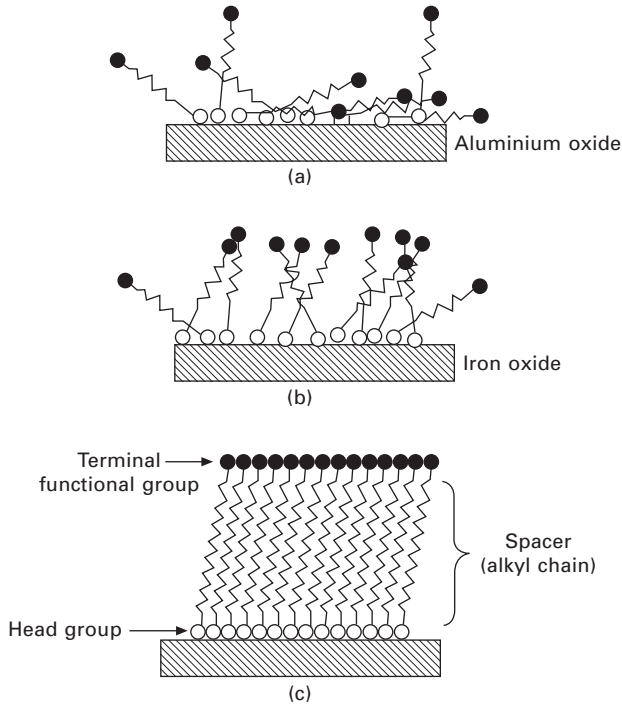
© Woodhead Publishing Limited, 2010

(Kent *et al*., 1996). Direct evidence from surface analysis indicated that the adhesion promotion is a condensation reaction between silanols of the hydrolyzed silane and hydroxyl groups present on the substrate surface forming covalent bonds (Gettings and Kinloch, 1977; Abel *et al*., 2000). Such strong bonds between the substrate and adhesive lead to better water barrier properties and more robust interfaces (Kent *et al*., 1996; Nguyen *et al*., 2007). Studies on glass substrates (Hunston *et al*., 1996) have suggested that although the covalent bonds between the adhesive and the coupling agent are important for the strength of the interface, the bonds between the glass and the coupling agent play an important role in durability. It was suggested that these covalent bonds tie up the OH groups on the glass surface and thus inhibit moisture attachment at the interface.

Despite all that is known about coupling agents, the selection of appropriate silane formulations and application procedures is accomplished empirically. The optimization of silane application is difficult, because adsorption of silanes is a complex phenomenon depending on numerous variables. These include substrate surface chemistry, solution pH, silane concentration, solvent, hydrolysis time, drying temperature and time lag between silane application and bonding. While conventional, serial experimental methods are feasible, a combinatorial and high throughput approach would be more fruitful in establishing the optimum processing variables.

Commercial short chain silanes typically adsorb as disordered multilayers. For example, $\gamma$-glycidoxypropyltrimethoxysilane (GPS) usually forms a disordered polysiloxane layer which is between 5 and 25 molecular layers in thickness (Kinloch, 1997) and has 50% of silanol groups pointing up and 50 % pointing down (van Ooij *et al*., 1996). The formation of such disordered multilayers is expected owing to the complicated hydrolysis, competing interactions, adsorption and reactivity of head-end groups of silane with polar species on the substrate surface (Fendler, 2001; Love *et al*., 2005). Although these disordered multilayer primers may form strong covalent bonds across the adhesive/substrate interface, the presence of a thick and weak polysiloxane layer can lead to a cohesive failure within this layer, which enables water to permeate through the polysiloxane reaching the silane/substrate interface, where it may disrupt even primary interfacial bonding. In addition, molecular orientation of silane molecules has a significant effect on the ability of silane to promote adhesion (Sennett *et al*., 1995; Ulman, 1996). For example, using molecular dynamics simulations, Sennett *et al*. (1995) found significant differences in molecular alignment of silane molecules on aluminum oxide and iron oxide. They showed that both ends of silane molecules tend to align flat on aluminum oxide, making the organofunctional groups unavailable for reaction with the adhesives (Fig. 18.5a). In the case of iron oxide, silane molecules align normal to the substrate surface (Fig. 18.5b).

© Woodhead Publishing Limited, 2010




*18.5* (a) Both ends of short alkyl chain silane molecules tend to align flat on an aluminum oxide surface, making terminal functional groups unavailable to react with adhesives. (b) In the case of iron oxide, silane molecules align normal to the substrate surface. (c) The long alkyl chain silane with a critical chain length enables alkyl chains to pack densely with the head groups of the silane molecules chemisorbed at the substrate surface and terminal functional groups oriented away.

This molecular alignment may explain why silanes enhance joint performance more effectively for steel than for aluminum alloy. Thus, silane performance might be improved significantly if ordered, densely packed self-assembled monolayers (SAMs) can be deposited. Several reviews have discussed this subject (Ulman, 1996; Onclin *et al.*, 2005). In SAMs, alkyl chains are densely packed with silanols of silane molecules chemisorbed at the surface of the substrate and organofunctional groups that are compatible with the adhesive of interest are oriented away from the substrate. Consequently, this would result in the formation of a highly ordered covalently bonded 'bridge' between the substrate and adhesive, but now without the presence of a thick layer of polysiloxane. Also, in a silane with long alkyl chains, the intermediate alkyl chains are highly hydrophobic, so the ordered monolayer film would impede water diffusion to the silane/substrate interface. All these features should contribute to improved joint water resistance.

© Woodhead Publishing Limited, 2010

It has been shown that the deposition of a monolayer of silane with such a controlled architecture requires a critical minimum alkyl chain length of 18 and a particular substrate/head group combination (Cave and Kinloch, 1992; Hobbs and Kinloch, 1998). Kinloch *et al.* (2006) used X-ray photoelectron spectroscopy (XPS) to show that a vinyl-terminated long alkyl chain silane with a 20 alkyl chain length indeed adsorbed as a monolayer at approximately 60° to the plane of the substrate surface with vinyl terminal groups oriented away from the substrate surface. A simplified schematic representation of the adsorbed silane is shown in Fig. 18.5(c). This observation was supported by a fracture-mechanics test in that the adhesive fracture energy for the vinyl-terminated long alkyl chain silane pretreated joints was relatively low compared with ultrasonically cleaned joints and the GPS pretreated joints. This is an expected result, which arises from the relatively poor wetting and intrinsic adhesion between the epoxy and vinyl terminal groups (which are unreactive with respect to the epoxy).

An advantage of the vinyl terminal groups is that it may be possible to activate these functional groups *in situ* so that they may chemically react with an adhesive to form covalent bonds between the adhesive and substrate. Such chemical activation processes are challenging because not all functional groups can be introduced conveniently in the SAMs owing to the inherent reactivity of the silanes (Onclin *et al.*, 2005). Also, functional groups might interact with the polar substrate surfaces, thus disrupting the ordered monolayers (Ulman, 1996). However, extensive research now has led to precise chemical controls of SAMs that are chemisorbed on substrate with varied surface chemistry (Netzer and Sagiv, 1983; Brzoska *et al.*, 1994; Onclin *et al.*, 2005).

A cautionary note is offered by Holmes *et al.* (2003), who studied SAMs made with a mixture of two silanes. They were identical except that one had a group which could bond with the adhesive, while the other did not. The results showed that the bond strength improved as the fraction of bonding silane was increased, but soon reached a maximum beyond which little improvement in strength was achieved. The authors postulated that in the closely packed SAM layer, steric hindrance limited the number of bonding groups that could react with the adhesive. Thus, a number of factors must be considered in developing an optimum coating.

### 18.3.2 Modification of bulk adhesive properties

Two important factors in improving adhesion are minimization of cure shrinkage and residual adhesive stresses. Cure shrinkage can arise from two sources. First, for most reaction chemistries utilized in adhesives, the products have a lower volume than the starting materials, particularly when water or volatiles are generated that leave the adhesive during cure. The

© Woodhead Publishing Limited, 2010

second factor, which is important for systems cured at elevated temperatures, is that differences in thermal expansion may exist between the adhesive and substrate. These two factors can produce shrinkage in the adhesive during the fabrication process and this shrinkage can result in the formation of gaps or flaws, which facilitate water ingress and collection. In addition, the thermal history and any internal stresses that develop due to shrinkage will affect the free volume in the adhesive which can influence water diffusion rates and concentration levels in a polymer.

One way to minimize these problems is to develop adhesive systems that do not undergo changes in volume during cure (Endo *et al.*, 1982; Ishida and Allen, 1996). Generally, the monomers involved are cyclic molecules which open during cure. The ring opening produces expansion that compensates for any shrinkage generated by the subsequent reactions. Although this approach is very effective, the systems are often specialty resins that do not meet the criteria for most applications. A far more common solution is the addition of fillers. This reduces the amount of resin and therefore the overall cure shrinkage. Moreover, the fillers often have a thermal expansion coefficient that is more similar to the substrate, which reduces thermal shrinkage.

The second important factor for improving adhesion is minimization of residual stresses (Plepys and Farris, 1990). Obviously, cure shrinkage can be a factor in generating residual stresses, so the approaches described above are relevant here. In addition, moisture-induced swelling in the adhesive can be an important factor. The stress mismatch between the constrained adhesive and the substrate would weaken the interface, eventually leading to interfacial failure.

Kinloch *et al.* (1991) found that residual stresses induced at the adhesive/substrate interface from post-curing the adhesive (thermal stress) promote interfacial failure. Tan *et al.* (2008a, 2008b) suggested that moisture-induced swelling stress plays a role in the sudden drop in adhesion strength that occurs when certain adhesives are exposed to humidities above a critical value for a significant time. These stresses will contribute to the crack tip stress field and reduce the external load that needs to be applied to cause failure. Further, such stresses may render interfacial bonds more susceptible to water attack (Sharpe, 1966; Kinloch, 1987). As mentioned earlier, the rate of diffusion and the solubility of water in adhesive bonds may be increased if mechanical stresses are present. There are many approaches to decreasing residual stresses in bulk adhesives, including incorporating plasticizers or additives, forming an elastic finish coat on adhesive/substrate interface, introducing interpenetrating networks, using more flexible or thicker adhesives, and so on (Nakamura *et al.*, 1986; Kinloch, 1987; Veselovsky and Kestelman, 2002).

As previously discussed, the multi-stage silane surface pretreatments are able to improve the durability of adhesive joints. However, they increase the manufacturing complexity of the joint significantly. One way to avoid

© Woodhead Publishing Limited, 2010

such complex surface pretreatments is to add silanes directly into adhesive formulations. This also provides a cost-effective method of employing silanes in adhesive bonding, which has been used for many years (Walker, 1980). Its efficacy in improving the durability of adhesive bonds has been reported (Brockmann, 1983; Nakamura *et al.*, 2007). The exact mode of action, however, is poorly understood and the concentration of silanes is chosen on an *ad hoc* basis. Abel and Watts (2008) have employed XPS and time-of-flight secondary ion mass spectroscopic analyses on specimens prepared by ultramicrotomy at locations ranging from the adhesive/substrate interface to the bulk of adhesive. They found that $\gamma$-aminopropyltriethoxysilane (APS) migrated from the bulk adhesive to the interfacial region and condensed at the aluminum surface to form covalent bonds. There also is evidence indicating that cross-linking of the silane may occur. Thus, the mode of action is similar to that of an adhesion promoter when used as a primer and the silane diffuses towards the interface where it hydrolyzes and forms a covalent bond. However, silane primers that promote adhesion do not necessarily perform well when used as additives (Nakamura *et al.*, 2007). Indeed, effective coupling between adhesives and the silane depend on the compatibility between the solubility parameters and reactivities of adhesives and silane and the stability of the silane in storage (Witucki, 1993; Nakamura *et al.*, 2007).

### 18.3.3 Engineering novel biological adhesives

Biological adhesives are remarkable in their ability to form strong bonds in the presence of water and maintain a high moisture resistance, both of which are valuable features for industrial adhesives. Since their large scale production is generally not economical at this time, much effort currently is being devoted to understanding the basic concepts involved in their bonding for use in synthetic adhesive design.

Much progress in the understanding of biological adhesives has been achieved via the study of mussels and barnacles, although a number of adhesives from other organisms have also been investigated (Smith and Callow, 2006). In these organisms, the adhesive is essential to their existence, providing access to resources necessary for life, protection from predators and improvement in reproduction. Requisite adhesive features are displacement of water from the surface to which it will bond, spreading, cleaning of biofilm, adhesion to surfaces with diverse compositions, curing (strength development) and resistance to water and aggressive solutes including enzymes/microbes throughout their lifetime.

The adhesive materials in mussels, barnacles and bacteria are chemically and morphologically different. Mussel adhesive is composed of protein with high levels of a unique amino acid, 3,4-dihydroxyphenylalanine (DOPA),

© Woodhead Publishing Limited, 2010

which has been attributed to having strong and non-specific surface adhesion properties as well as the ability to cross-link and develop high cohesive strengths in the presence of water (Sagert *et al.*, 2006). Barnacle adhesive is similarly composed of proteins but, in an interesting contrast, contains only common amino acid subunits and does not become cross-linked (Kamino, 2008). Its *modus operandi* involves a set of at least six proteins with specialized interfacial adhesive and bulk cohesive properties, including water resistance. The proteins self-assemble as the adhesive is formed and 'applied' in sea water as a result of hydrophobic molecular interactions that occur upon conformational change. Elucidation of the composition and properties of these proteins and the mechanism of self-assembly during the bonding process is a key step in the application of these concepts in material science, especially for practical water-resistant adhesives.

Progress continues in the understanding of another adhesive material produced by the *Caulobacter crescentus* bacterium (Tsang *et al.*, 2006). Studies are still in the early stages, but this adhesive is one of the strongest found in nature. The critical strength-producing component appears to contain oligosaccharide-units based on N-acetylglucosamine (the repeat unit found in chitin, a key component in structural biological materials such as crustacean exoskeletons).

These basic studies of natural adhesives have led to the design and synthesis of fascinating biomimetic adhesives, especially materials based on the DOPA-concept from mussel adhesives. Strong interfacial adhesion properties have been achieved by incorporation of the 3,4-dihydroxyphenyl, or catechol, moiety into synthetic polymers. This unit notably provides strong bonding to surfaces ranging from metals and oxides to a variety of polymers, including polytetrafluorethylene.

Where stronger bulk properties, that is higher cohesive strength, are desired, the catechol moiety can be cross-linked in the presence of oxidants and multifunctional nucleophiles. For example, adherent, multifunctional coatings have been formed on a variety of surfaces using a very simple process by dip-coating in an aqueous solution of dopamine (3,4-dihydroxyphenylethylamine) at pH 8.5. Air alone initiates polymerization and cross-linking forming a thin coating which then can be further modified with other compounds to form ad-layers with diverse properties (Lee *et al.*, 2007a). Thus, the polymerized dopamine, owing to its adhesion to diverse surfaces, becomes a 'universal primer'. Modification of an adhesive surface to improve both its wet and dry adhesion also has been accomplished via the catechol moiety (Lee *et al.*, 2007b). In a unique system modeled after the gecko lizard's adhesive feet, a nanofabricated surface was coated with a thin film of catechol-functionalized polyacrylate. The resulting material exhibited high adhesion to a variety of surfaces in AFM studies. Both wet and dry adhesion were improved markedly and were also reversible, maintaining adhesive performance after a thousand

© Woodhead Publishing Limited, 2010

contact cycles. At this early stage of development, mechanical property testing on these coatings and adhesives has been performed mostly on the microscopic scale, such as with AFM. In one instance involving larger scale testing, derivatization of polystyrene with catechol was shown to improve greatly its shear strength in binding aluminum substrates in the presence of oxidative cross-linking (Westwood *et al*., 2007).

The catechol moiety has been used successfully as a component in wood adhesives to produce strong and water-resistant bonds (Liu and Li, 2006; Li and Geng, 2007). The driving force for this research has been replacement of adhesives based on formaldehyde, a suspected carcinogen and also derived from depleting petroleum resources. For this technology to be truly useful on a commercial scale, as for any of the biological adhesives, economics is an issue. Thus, condensed tannins, demethylated kraft lignin and even decayed wood have been identified as economical catechol-substituted raw materials, which have exhibited excellent shear strengths with high water resistance comparable with commercial wood adhesives.

In summary, recent discoveries in the science of biological adhesives have pointed to the powerful and versatile catechol moiety as found in the DOPA-containing mussel protein adhesives. It offers strong binding to surfaces with widely varying compositions. Upon oxidative cross-linking, it yields high water-resistant cohesive strengths. These functional properties are making the catechol-derivatized materials extremely attractive. A key task now is to advance these concepts into wide practice by identifying inexpensive analogs of the catechol functionality or cheaper production processes for catechol-bearing raw materials. In addition, lessons being learned from barnacle adhesion will help us design materials with suitable structures that will self-assemble, when triggered, to form strong water-resistant adhesives.

### 18.3.4 Bonded joint design considerations

Improved bonded joint durability can be promoted by proper design and optimization. The design of bonded joints must take into consideration stress distributions and potential moisture intrusion into the joints. Joint performance can be optimized via minimization of joint stresses and uniform distribution of stresses across of the entire bonded area, that is the absence of high stress concentration. The stress distribution in adhesive bonds may be modified by altering adhesive thickness, joint length and geometry, in addition to using adhesives with different mechanical properties (Minford, 1993; Adams *et al*, 1997). Design concepts and approaches that reduce direct exposure of bonded joints to moisture or that increase the diffusion path for moisture should also be employed. To accomplish this, sealants may be used around bond edges, which not only create a primary and secondary barrier to moisture penetration, but also provide enhancement of visual appearance.

© Woodhead Publishing Limited, 2010

## 18.4 Future trends

Surface pretreatments of substrates remain one of the most important steps in adhesive bonding in order to ensure good bond strength and durability. Physical, topographical, morphological and chemical changes introduced by surface pretreatments are known to be critical to the subsequent durability performance of adhesive bonds. However, the present approach used in industries to promote good adhesion is through conventional surface pretreatment methods which are time-consuming, expensive, labor intensive and high in technical manpower requirements. Thus, the search for cheaper and simpler alternative techniques that are capable of attaining the best current standards of adhesive bond performance should be given priority. Additionally, low-cost, precise molecular engineering of interfacial regions is highly desirable considering that conventional pretreatments usually result in incomplete coverage of substrates that produce heterogeneous surface properties (Kinloch, 1987). In these pretreatments, weak sites may occur that are mechanically weak and enable water ingress to the interface. Molecular self-assembly techniques offer considerable promise in overcoming this problem, but the use of such precise molecular engineering of surface has yet to be realized in structural adhesive bonding.

Conventional durability screening tests such as wedge tests or constant displacement rate tests are time consuming and labor intensive. They often lack predictive capability and may provide only qualitative information under a very specific set of conditions. The ever-increasing demand for shorter product research and development cycles has led to an obvious need for faster, cost-effective, reliable and predictive durability tests. One potential approach to accelerate the rate of experimentation is to use combinatorial and high-throughput methodology. This methodology has been used widely in the pharmaceutical, agrochemical and biotechnology industries (Chisholm and Webster, 2007). Unlike conventional serial experimental methods, this methodology explores a relatively large number of chemically and physically distinct properties, such as surface chemistry, roughness, and substrate type, and so on in a single experiment. It must be remembered, however, that simply generating more data cannot compensate for a poor test methodology, so it is just as important to have a sound scientific basis for combinatorial testing as it is for conventional methods. Finally, there is a continuing need in the adhesives community for better experimentation designs for aging procedures, joint geometries and test methodologies, to provide sound test techniques for assessing durability. An ideal test methodology should be capable of producing accurate, reproducible quantitative durability ranking of adhesive joints while not requiring expensive equipment and well-trained personnel. Furthermore, models are needed to make reliable service life predictions of real bonded components.

© Woodhead Publishing Limited, 2010

## 18.5 References

Abel, M.L. and Watts, J.F. (2008), 'Effect of incorporation of silanes within epoxy adhesives on interface chemistry: a surface analysis study', in *Proceedings 31th Annual Meeting of the Adhesion Society*, Anderson, G. (ed.), 51–3.

Abel, M.L., Digby, R.P., Fletcher, I.W. and Watts, J.F. (2000), 'Evidence of specific interaction between $\gamma$-glycidoxypropyltrimethoxysilane and oxidized aluminum using high-mass resolution ToF-SIMS', *Surface Interface Anal.*, **29**, 115–25.

Adams, R.D., Comyn J. and Wake, W.C. (1997), *Structural Adhesive Joints in Engineering*, Chapman & Hall, NY.

Arnott, D.R. and Kindermann, M.R. (1995a), 'Constant displacement-rate method for testing epoxy adhesive bonds', *J. Adhesion*, **48**, 85–100.

Arnott, D.R. and Kindermann, M.R. (1995b), 'Durability testing of epoxy adhesive bonds', *J. Adhesion*, **48**, 101–19.

Ashcroft, I.A., Wahab, M.M.A., Crocombe, A.D., Hughes, D.T. and Shaw, S.J. (2001), 'The effect of environment on the fatigue of bonded composite joints. Part 1: testing and fractography', *Compos. Part A – Appl. Sci. Manufacturing*, **32**, 45–58.

Bascom, W.D. (1970), 'Water at the interface', *J. Adhesion*, **2**, 161–83.

Bellucci, F. and Nicodemo, L. (1993), 'Water transport in organic coatings', *Corrosion*, **49**, 235–47.

Boinard, P., Pethrick, R.A., Banks, W.M. and Crane, R.L. (2001), 'Novel non-destructive technique to assess the degradation of adhesively bonded composite structures', *Insight*, **43**, 159–62.

Bowden, F.P. and Throssell, W.R. (1951), 'Adsorption of water vapor on solid surfaces', *Nature*, **167**, 601–2.

Bowditch, M.R. (1996), 'The durability of adhesive joints in the presence of water', *Int. J. Adhesion Adhesives*, **16**, 73–9.

Brewis, D.M., Comyn, J., Raval, A.K. and Kinloch, A.J. (1990), 'The effect of humidity on the durability of aluminum-epoxide joints', *Int. J. Adhesion Adhesives*, **10**, 247–53.

Brockmann, W. (1983), 'Steel adherends', in *The Durability of Structural Adhesives*, Kinloch, A.J. (ed.), Applied Science, London, 281.

Brzoska, J.B., Ben Azouz, I. and Rondelez, F. (1994), 'Silanization of solid substrates: a step toward reproducibility', *Langmuir*, **10**, 4367–73.

Cave, N.G. and Kinloch, A.J. (1992), 'Self-assembling monolayer silane films as adhesion promoters', *Polymer*, **33**, 1162–70.

Chang, T., Sproat, E.A., Lai, Y.H., Shephard, N.E. and Dillard, D.A. (1997), 'A test method for accelerated humidity conditioning and estimation of adhesive bond durability', *J. Adhesion*, **60**, 153–62.

Chisholm, B.J. and Webster, D.C. (2007), 'The development of coatings using combinatorial/high throughput methods: a review of the current status', *J. Coat. Technol. Res.*, **4**, 1–12.

Cotugno, S., Larobina, D., Mensitieri, G., Musto, P. and Ragosta, G. (2001), 'A novel spectroscopic approach to investigate transport processes in polymers: the case of water-epoxy system', *Polymer*, **42**, 6431–8.

Davis, G.D., Krebs, L.A., Drzal, L.T., Rich, M.J. and Askeland, P. (2000), 'Electrochemical sensors for non-destructive evaluation of adhesive bonds', *J. Adhesion*, **72**, 335–58.

Davis, G.D., Thayer, K., Rich M.J. and Drzal L.T. (2002), 'Inspection of composite and

© Woodhead Publishing Limited, 2010

metal adhesive bonds with an electrochemical sensor', *J. Adhesion Sci. Tech.*, **16**, 1307–26.

Dillard, D.A., Chen, B., Chang, T. and Lai, Y-H. (1999), 'Analysis of the notched coating adhesion test', *J. Adhesion*, **69**, 99–120.

Dillingham, R.G. and Boerio, F.J. (1987), 'Interphase composition in aluminum/epoxy adhesive joints', *J. Adhesion*, **24**, 315–35.

Endo, T., Okawara, M. and Bailey, W.J. (1982), 'New materials which cure without shrinkage – preparation and polymerization of diurethanes containing bicyclic ortho ester structure', *Polymer J.*, **14**, 927–30.

Fendler, J.H. (2001), 'Chemical self-assembly for electronic applications', *Chem. Mater.*, **13**, 3196–210.

Fernandes, J.C.S., Ferreira, M.G.S., Haddow, D.B., Goruppa, A., Short, R. and Dixon, D.G. (2002), 'Plasma-polymerized coatings used as pretreatment for aluminum alloys', *Surface Coat. Technol.*, **154**, 8–13.

Fieldson, G.T. and Barbari, T.A. (1993), 'The use of FTIR-ATR spectroscopy to characterize penetrant diffusion in polymers', *Polymer*, **34**, 1146–53.

Gazit, S. (1978), 'Dimensional changes in glass filled epoxy resins as a result of absorption of atmospheric moisture', *J. Appl. Polym. Sci.*, **22**, 3547–58.

Gettings, M. and Kinloch, A.J. (1977), 'Surface analysis of polysiloxane-metal oxide interfaces', *J. Mater. Sci.*, **12**, 2511–18.

Hobbs, P.M. and Kinloch, A.J. (1998), 'The computational molecular modeling of organosilane primers', *J. Adhesion*, **66**, 203–28.

Hodge, R.M., Bastow, T.J., Edward, G.H., Simon, G.P. and Hill, A.J. (1996), 'Free volume and the mechanism of plasticization in water-swollen poly(vinyl alcohol)', *Macromolecules*, **29**, 8137–43.

Holmes, G.A., Feresenbet, E. and Raghavan, D. (2003), 'Using self-assembled monolayer technology to probe the mechanical response of the fiber interphase–matrix interphase interface', *Compos. Interfaces*, **10**, 515–46.

Hong, S.G. and Boerio, F.J. (1994), 'Effect of silane on the interfacial compositions of epoxy metal adhesive bonds – XPS and RAIR analyses', *Surface Interface Anal.*, **21**, 650–8.

Hunston, D.L., Macturk, K.S., Schultheisz, C.R., Holmes, G., McDonlugh, W.G. and Schutte, C.L. (1996), 'The role of silane surface treatments in strength and durability of fiber-matrix bonding in composites', Vol. 2, in *Proceedings EurAd'96, European Adhesion Conference*, The Institute of Materials, London, 427–32.

Ishida, H. and Allen, D.J. (1996), 'Physical and mechanical characterization of near-zero shrinkage polybenzoxazines', *J. Polym. Sci. Part B – Polym. Phys.*, **34**, 1019–30.

Johnsen, B.B., Olafsen, K., Stori, A. and Vinje, K. (2002), 'Silanisation of adhesively bonded aluminum alloy AA6060 with gamma-gylcidoxypropyltrimethoxysilane. 1. durability investigation', *J. Adhesion Sci. Technol.*, **16**, 1931–48.

Kalashnikova, I.V., Matveev, V.V. and Arslanov, V.V. (1996), 'Spontaneous recovery of the strength of polymer-aluminum adhesive systems in aqueous medium: II. structure-morphological and chemical transformations in the transition region', *Colloid J.*, **58**, 722–9.

Kamino, K. (2008), 'Underwater adhesive of marine organisms as the vital link between biological science and material science', *Marine Biotechnol.*, **10**, 111–21.

Kent, M.S., Smith, G.S., Baker, S.M., Nyitray, A., Browning, J., Moore, G. and Hua, D.W. (1996), 'The effect of a silane coupling agent on water adsorption at a metal/polymer interface studied by neutron reflectivity and angle-resolved X-ray photoelectron spectroscopy', *J. Mater. Sci.*, **31**, 927–37.

© Woodhead Publishing Limited, 2010

Kent, M.S., McNamara, W.F., Fein, D.B., Domeier, L.A. and Wong, A.P.Y. (1999a), 'Water adsorption in interfacial silane layers by neutron reflection: 1. silane finish on silicon wafers', *J. Adhesion*, **69**, 121–38.

Kent, M.S., McNamara, W.F., Baca, P. M., Wright, W., Domeier, L.A., Wong, A.P.Y. and Wu, W.L. (1999b), 'Water adsorption in interfacial silane layers by neutron reflection: 2. epoxy plus silane finish on silicon wafers', *J. Adhesion*, **69**, 139–63.

Kinderman, M.R., Wilson and Arnott, D.R. (1997), 'A multiple constant displacement-rate tensile testing machine', *Measurement Sci. Technol.*, **8**, 390–7.

Kinloch, A.J. (1987), *Adhesion and Adhesives: Science and Technology*, Chapman & Hall, London.

Kinloch, A.J. (1997), 'Adhesives in engineering', *Proc. Inst. Mech. Eng. Part G*, **211**, 307–35.

Kinloch, A.J., Thrusabanjong, E. and Williams, J.G. (1991), 'Fracture at bimaterial interfaces – the role of residual stresses', *J. Mater. Sci.*, **26**, 6260–70.

Kinloch, A.J., Tan, K.T. and Watts, J.F. (2006), 'Novel self-assembling silane for abhesive and adhesive applications', *J. Adhesion*, **82**, 1117–32.

Kinloch, A.J., Korenburg, C., Tan, K.T. and Watts, J.F. (2007), 'Crack growth in structural adhesive joints in aqueous environments', *J. Mater. Sci.*, **42**, 6353–70.

Knox, E.M. and Cowling, M.J. (2000), 'A rapid durability test method for adhesive', *Int. J. Adhesion Adhesives*, **20**, 201–8.

Kook, S-Y. and Dauskardt, R.H. (2002), 'Moisture-assisted debonding of a polymer/metal interface', *J. Appl. Phys.*, **91**, 1293–303.

Korenburg, C.F., Kinloch, A.J. and Watts, J.F. (2004), 'Crack growth of structural adhesive joints in humid environments', *J. Adhesion*, **80**, 169–201.

Lacombe, R. (2006), *Adhesion Measurement Methods Theory and Practice*, Taylor & Francis, Florida.

Lee, H., Dellatore, S.M., Miller, W.M. and Messersmith, P.B. (2007a), 'Mussel-inspired surface chemistry for multifunctional coatings', *Science*, **318**, 426–30.

Lee, H., Lee, B.P. and Messersmith, P.B. (2007b), 'A reversible wet/dry adhesive inspired by mussels and geckos', *Nature*, **448**, 338–41.

Lefebvre, D.R., Takahashi, K.M., Muller, A.J. and Raju, V.R. (1991), 'Degradation of epoxy coatings in humid environments: the critical relative humidity for adhesion loss', *J. Adhesion Sci. Technol.*, **5**, 201.

Leidheiser, H., Jr. and Funke, W. (1987), 'Water disbondment and wet adhesion of organic coatings on metals: a review and interpretation', *J. Oil Color Chem. Assoc.*, **70**, 121–32.

Li, K. and Geng, X. (2007), *Adhesive compositions and methods of using and making the same*, United States Patent 7,265,169.

Liu, Y. and Li, K. (2006), 'Preparation and characterization of demethylated lignin-polyethylenimine adhesives', *J. Adhesion*, **82**, 593–605.

Loh, W.K., Crocombe, A.D., Abdel Wahab, M.M., Watts, J.F. and Ashcroft, I.A. (2002), 'The effect of moisture on the failure locus and fracture energy of an epoxy: steel interface', *J. Adhesion Sci. Technol.*, **16**, 1407–29.

Love, J.C., Estroff, L.A., Kriebel, J.K., Nuzzo, R.G. and Whitesides, G.M. (2005), 'Self-assembled monolayers of thiolates on metals as a form of nanotechnology', *Chem. Rev.*, **105**, 1103–69.

Marceau, J.A. and Thrall, E.W. (1985), 'Environmental-durability testing', in *Adhesive Bonding of Aluminum Alloys*, Thrall, E.W. and Shannon, R.W. (eds), Marcel Dekker, NY, 177.

© Woodhead Publishing Limited, 2010

Minford, J.D. (1993), '*Handbook of Aluminum Bonding Technology and Data*', Marcel Dekker, NY.

Moylan, C.R., Best, M.E. and Ree, M. (1991), 'Solubility of water in polyimides – quartz crystal microbalance measurements', *J. Polym. Sci. Part B – Polym. Phys.*, **29**, 87–92.

Nakamura, Y., Tabata, H., Suzuki, H., Iko, K., Okubo, M. and Matsumoto, T. (1986), 'Internal stress of epoxy-resin modified with acrylic core-shell particles prepared by seeded emulsion polymerization', *J. Appl. Polym. Sc.*, **32**, 4865–71.

Nakamura, S., Pavlovic, E. and Kramer, E.J. (2007), 'Fracture energy of epoxy interfaces with layers of different silane coupling agents', *J. Adhesion*, **83**, 351–65.

Netzer, L. and Sagiv, J. (1983), 'A new approach to construction of artificial monolayer assemblies', *J. Am. Chem. Soc.*, **105**, 674–6.

Nguyen, T., Byrd, E. and Bentz, D. (1995), 'Quantifying water at the organic film/hydroxylated substrated interface', *J. Adhesion*, **48**, 167–94.

Nguyen, T., Byrd, E.W., Bentz, D. and Martin, J. (2005), '*In situ* spectroscopic study of water at the asphalt/siliceous substrate interface and its implication in stripping', *J. Adhesion*, **81**, 1–28.

Nguyen, T., Byrd, W.E., Ashed, D., Chin, J., Clerici, C. and Martin, J. (2007), 'Relationship between interfacial water layer adhesion loss of silicon/glass fiber-epoxy systems: a quantitative study', *J. Adhesion*, **83**, 587–610.

O'Brien, E.P., Case, S.L. and Ward, T.C. (2005), 'Critical and subcritical adhesion measurements of a model epoxy coating exposed to moisture using the shaft-loaded blister test', *J. Adhesion*, **81**, 41–58.

O'Brien, E.P., White, C.C. and Vogt, B.D. (2006), 'Correlating interfacial moisture content and adhesive fracture energy of polymer coatings on different surfaces', *Adv. Eng. Mater.*, **8**, 114–118.

Onclin, S., Ravoo, B.J. and Reinhoudt, D.N. (2005), 'Engineering silicon oxide surfaces using self-assembled monolayers', *Angew. Chem. Int. Ed.*, **44**, 6282–304.

Pethrick, R.A., Hollins, E.A., McEwan, I., MacKinnon, A.J., Hayward, D., Cannon, L.A., Jenkins, S.D. and McGrail, P.T. (1996), 'Dielectric, mechanical and structural, and water absorption properties of a thermoplastic-modified epoxy resin: poly(ether sulfone)-amine cured epoxy resin', *Macromolecules*, **29**, 5208–14.

Plepys, A.R. and Farris, R.J. (1990), 'Evolution of residual-stresses in 3-dimensionally constrained epoxy-resins', *Polymer*, **31**, 1932–6.

Ritter, J.E., Jacome, G.S., Pelch, J.R., Russell, T.P. and Lardner, T.J. (2002), 'Controlling subcritical crack growth at epoxy/glass interface', *T. ASME*, **124**, 328–33.

Roche, A.A., Bouchet, J. and Bentadjine, S. (2002), 'Formation of epoxy-diamine/metal interphases', *Int. J. Adhesion Adhesives*, **22**, 431–41.

Sagert, J., Sun, C. and Waite, J.H. (2006), 'Chemical subtleties of mussel and polychaete holdfasts', in *Biological Adhesives*, Smith, A.M. and Callow, J.A. (eds), Springer, NY, 125–45.

Sammon, C., Mura, C., Yarwood, J., Everall, N., Swart, R. and Hodge, D. (1998), 'FTIR-ATR studies of the structure and dynamics of water molecules in polymeric matrixes. a comparison of PET and PVC', *J. Phys. Chem. B*, **102**, 3402–11.

Sargent, J.P. (2005), 'Durability studies for aerospace applications using peel and wedge tests', *Int. J. Adhesion Adhesives*, **25**, 247–56.

Sargent, J.P. and Ashbee, K.H.G. (1981), 'On the occurrence of osmosis during water uptake by adhesively bonded titanium joints', *J. Phys. D: Appl. Phys.*, **14**, 1933–8.

Sennett, M.S., Wentworth, S.E. and Kinloch, A.J. (1995), 'Investigation of the interaction

© Woodhead Publishing Limited, 2010

of silane-based adhesive primers with metal oxide surfaces using molecular dynamics simulations', *J. Adhesion,* **54**, 23–31.

Sharpe, L.H. (1966), 'Some aspects of the permanence of adhesive joints', *Appl. Polym. Symp.*, **3**, 353–9.

Simpson, C.T., Hampel, H., Davis, G.D., Arah, C.O., Fritz, T.L., Moran, P.J., Shaw, B.A. and Zankel, K.L. (1992), 'Evaluation of the effects of acidic deposition on coated steel substrates', *Prog. Org. Coat.*, **20**, 199–216.

Smith A.M. and Callow J.A. (eds) (2006), *Biological Adhesives*, Springer, NY.

Su, N., Mackie, R. and Harvey, W. (1992), 'The effects of aging and environment on the fatigue life of adhesive joints', *Int. J. Adhesion Adhesives*, **12**, 85–93.

Tan, K.T. (2005), *The Mechanics and Mechanisms of Environmental Attack on Structural Adhesive Joints*, PhD Thesis, Imperial College, London, UK.

Tan, K.T., White, C.C., Hunston, D.L., Clerici, C., Steffens, K.L., Goldman, J. and Vogt, B.D. (2008a), 'Fundamentals of adhesion failure for a model adhesive (PMMA/Glass) joint in humid environments', *J. Adhesion*, **84**, 339–67.

Tan, K.T., Vogt, B.D., White, C.C., Steffens, K.L., Goldman, J., Satija, S., Clerici, C. and Hunston, D.L. (2008b), 'On the origins of sudden adhesion loss at a critical relative humidity: examination of bulk and interfacial contributions', *Langmuir*, **24**, 9189–93.

Thiel, P.A. and Madey, T.E. (1987), 'The interaction of water with solid-surfaces: fundamental aspects', *Surface Sci. Rep.*, **7**, 211–385.

Tsang, P.H., Li, G., Brun, Y.V., Freund, L.B. and Tang, J.X. (2006), 'Adhesion of single bacterial cells in the micronewton range', *Proc. Natl Acad. Sci.*, **103**, 5764–8.

Ulman, A. (1996), 'Formation and structure of self-assembled monolayers', *Chem. Rev.*, **96**, 1533–54.

Van Ooij, W.J., Zhang, B.C., Conners, K.D. and Hornstrom, S-E. (1996), 'On the use, characterization and performance of silane coupling agents between organic coatings and metallic or ceramic substrates', *AIP Conference Proceedings*, **354**, 305–23.

Venables, J.D. (1984), 'Adhesion and durability of metal–polymer bond', *J. Mater. Sci.*, **19**, 2431–53.

Veselovsky, R.A. and Kestelman, V.N. (2002), *Adhesion of Polymers*, McGraw-Hill, NY.

Vine, K., Cawley, P. and Kinloch, A.J. (2001), 'The correlation of non-destructive measurements and toughness changes in adhesive joints during environmental attack', *J. Adhesion*, **77**, 125–61.

Vogt, B.D., Soles, C.L., Jones, R.L., Wang, C.Y., Lin, E.K., Wu, W.L., Satija, S.K., Goldfarb, D.L. and Angelopoulos, M. (2004), 'Interfacial effects on moisture absorption in thin polymer films', *Langmuir*, **20**, 5285–90.

Vogt, B.D., Prabhu, V.M., Soles, C.L., Satija, S.K., Lin, E.K. and Wu, W.L. (2005a), 'Control of moisture at buried polymer/alumina interfaces through substrate surface modification', *Langmuir*, **21**, 2460–4.

Vogt, B.D., Soles, C.L., Lee, H.J., Lin, E.K. and Wu, W. (2005b), 'Moisture absorption into ultrathin hydrophilic polymer films on different substrate surfaces', *Polymer*, **46**, 1635–42.

Vogt, B.D., Soles, C.L., Wang, C-Y., Prabhu, W.M., McGuiggan, P.M., Douglas, J.F., Lin, E.K., Wu, W-I; Satija, S.K., Goldfarb, D.L. and Angelopoulos, M. (2005c), 'Water immersion of model photoresists: interfacial influences on water concentration and surface morphology', *J. Microlith. Microfab. Microsyst.*, **4**, 013003.

© Woodhead Publishing Limited, 2010

Walker, P. (1980), 'Organosilanes as adhesion promoters for organic coatings', *J. Coat. Technol.*, **52**, 49–61.

Wapner, K., Stratmann, M. and Grundmeier, G. (2006), '*In situ* infrared spectroscopic and scanning kelvin probe measurements of water and ion transport at polymer/metal interfaces', *Electrochim. Acta*, **51**, 3303–15.

Watts, J.F. (1989), 'Mechanistic aspects of the cathodic delamination of organic coatings', *J. Adhesion*, **31**, 73–85.

Watts, J.F. and Castle, J.E. (1984), 'The application of X-ray photoelectron spectroscopy to the study of polymer-to-metal adhesion', *J. Mater. Sci.*, **19**, 2259–72.

Weitsman, Y. (1977), 'Stresses in adhesive joints due to moisture and temperature', *J. Comps. Mater.*, **11**, 378–94.

Westwood, G., Horton, T.N. and Wilker, J.J. (2007), 'Simplified polymer mimics of cross-linking adhesive proteins', *Macromolecules*, **40**, 3960–4.

Wiederhorn, S.M. (1967), 'Influence of water vapor on crack propagation in soda-lime glass', *J. Amer. Ceram. Soc.*, **50**, 407–14.

Witucki, G.L. (1993), 'A silane primer: chemistry and applications of alkoxy silanes', *J. Coat. Technol.*, **65**, 57–60.

Wu, W.-L., Orts, W.J., Majkrzak, C.J. and Hunston, D.L. (1995), 'Water adsorption at a polyimide/silicon wafer interface', *Polym. Eng. Sci.*, **35**, 1000–4.

Wylde, J.W. and Spelt, J.K. (1998), 'Measurement of adhesive joint fracture properties as a function of environmental degradation', *Int. J. Adhesion Adhesives*, **18**, 237–46.

Xiao, G.Z. and Shanahan, M.E.R. (1997), 'Water absorption and desorption in an epoxy resin with degradation', *J. Polym. Sci. – Part B: Polym. Phys.*, **35**, 2659–70.

Yang, Q.D., Thouless, M.D. and Ward, S.M. (1999), 'Numerical simulations of adhesively-bonded beams failing with extensive plastic deformation', *J. Mech. Phys. Solids*, **47**, 1337–53.

Zanni-Deffarges, M.P. and Shanahan, M.E.R. (1995), 'Diffusion of water into an epoxy adhesive: comparison between bulk behaviour and adhesive joints', *Int. J. Adhesion Adhesives*, **15**, 137–42.

© Woodhead Publishing Limited, 2010

# 19

# Improving bonding in hostile chemical environments

W. BROUGHTON, National Physical Laboratory, UK

**Abstract**: This chapter is primarily concerned with the effects and resistance of structural adhesives to various chemical agents, other than water (moisture and humidity) or salt solutions, which may modify or degrade the characteristics and properties of adhesives and consequently the performance of adhesive joints. It covers chemicals, such as organic solvents, acids and alkalis, and aviation fluids (jet fuel, hydraulic oil and de-icing fluids). Environmental factors, such as thermal ageing, weathering and photo-oxidation, high-energy radiation and biological degradation are also covered along with environmental stress cracking (ESC). The chapter identifies factors that need to be considered when designing and manufacturing bonded structures for use in chemical environments, including adhesive selection and surface treatments. The use of sealants and design of adhesive joints are also discussed. Test methods and standards for assessing chemical degradation of adhesives and adhesive joints are also included.

**Key words**: accelerated, adhesives, bonded, chemical, degradation, durability, environmental, joints, resistance, stress cracking, test methods.

## 19.1 Introduction

Chemical resistance considerations are of prime importance in the design of bonded structures for operation in hostile environments and, hence, the importance of long-term durability of an adhesive joint in the service environment in which the structure may be exposed for a prolonged period of time. The resistance of adhesive joints to degradation agents often becomes apparent within a short period. In some circumstances, only a few hours of exposure may lead to failure or seriously compromise joint performance. Irreversible property changes in adhesive joints can be induced by any number of chemical agents (or factors) acting alone or collectively. In many applications, bonded structures will be exposed to a combination of two or more factors, often resulting in complex synergistic degradation of the material. Exposure to elevated temperatures or the application of applied stresses can accelerate the degradation effects of chemical agents. Degradation caused by one agent can also alter the resistance to other agents, similar to biological systems. In addition to inducing chemical reactions, absorbed chemicals induce important physical effects within the adhesive (i.e. dimensional changes, resin plasticization and leaching of adhesive constituents) and degradation



© Woodhead Publishing Limited, 2010

of the substrate–adhesive interface. In the absence of environmental stress cracking (ESC), the amount and type of chemical absorbed by a polymer in a given time can be a useful guide to the probable extent of physical changes or damage induced.

This chapter is primarily concerned with the effects on structural adhesives and their resistance to various chemical agents, other than water (moisture and humidity) or salt solutions, which may modify or degrade the characteristics and properties of adhesives and consequently the performance of adhesive joints. It covers chemicals, such as solvents, acids and alkalis, and aviation fluids (jet fuel, hydraulic oil and de-icing fluids). Environmental factors, such as thermal ageing, weathering and photo-oxidation, high-energy radiation and biological degradation are also covered along with environmental stress cracking, synergistic effects of mechanical stress in combination with chemical agents. The chapter identifies factors to be considered when designing and manufacturing bonded structures for use in chemical environments, including adhesive selection and surface treatments. The use of sealants and design of adhesive joints are also discussed. Test methods and standards to assess chemical degradation of adhesives and adhesive joints are also included.

## 19.2 Chemical agents and degradation mechanisms

### 19.2.1 Introduction

Irreversible changes in properties can be induced by any number of degradation agents (factors) acting alone or collectively (excluding water, humidity and salt solutions):

- thermal (heat ageing or sub-zero exposure)
- acid and alkali solutions
- solvents (including paint strippers and cleaning agents)
- diesel and engine fuels, oils and greases
- high-energy radiation
- mechanical stress (static and fatigue)
- electrical (including galvanic reactions)
- microbial (e.g. fungal and bacteria).

In order to determine the chemical resistance of adhesive systems, it is advisable to expose the adhesive and/or adhesive joint to various environmental and loading conditions that simulate actual service conditions (ASM International Handbook on Adhesives and Sealants, 1990; Cognard, 2005; Petrie, 2007). Short-term tests conducted under standard laboratory conditions (23°C/50% relative humidity (RH)) are inadequate, failing to provide the necessary information required to assess service life. The environmental consequences can be so severe that it is advisable to conduct laboratory and field trials on

© Woodhead Publishing Limited, 2010

representative bonded components under conditions that closely represent the actual service conditions that will be experienced by the adhesive joint.

Although the list of environmental factors is too numerous to elaborate, the common denominator is the possible detrimental effect on the adhesive properties, particularly, creep. Hence creep or stress rupture tests should be conducted on adhesive joints to determine the maximum load the adhesive joint will withstand for extended periods of time without failing. Factors that will most probably affect the durability of the adhesive joint are listed below (Petrie, 2007):

- maximum stress and average constant stress levels
- environmental conditions (e.g. chemical and temperature)
- cyclic effects of stress and environment (including rate and period)
- exposure time.

It is therefore of paramount importance to select an adhesive appropriate for the service application. This applies equally to the selection of adherends. Many structural adhesives are far more resistant to strong acids, salt solutions and oxidative agents than stainless steel or aluminium alloys. It is not unusual in environmental trials for the adhesive to outlast the adherend, with the adhesive remaining unaffected whilst the adherend has degraded. Certain combinations of adhesive and adherends may pose chemical incompatibility problems with constituents in either the adhesive or adherend migrating to the interface and chemically reacting with the other material, or the service conditions can trigger chemical reactions at the interface.

Consideration needs to be given to the surface treatment applied to the adherends. Good design can be easily undermined by poor surface preparation. Most failures in adhesive joints are initiated by interfacial degradation. Moisture and other chemicals can diffuse rapidly along the adhesive–adherend interface through capillary action and trigger chemical reactions with the adherend surface that result in debonding. In the case of poorly prepared metal surfaces, hydrated oxides will form on the surface displacing the chemical bonds between the adhesive and adherend and the adhesive bond will be compromised (failing prematurely). Chemicals may also permeate through the adherend (e.g. fibre-reinforced plastics) entering the interface region from beneath and adversely affecting the interfacial bond strength.

This section examines the degrading effects of various chemical environments on adhesive joint performance and considers the synergistic effects of chemical agents, temperature and mechanical stress on degradation. Weathering and photo-oxidation, high-energy radiation and biological (microbial) effects are also considered. A full list of recognized chemical agents and test methods to assess the effects of chemical exposure are given in ISO 175. A list of standards relating to chemical resistance testing is presented at the end of this chapter.

© Woodhead Publishing Limited, 2010

### 19.2.2 Chemical agents and degradation

Adhesive joints can come into contact with a number of chemicals and organic solvents during service life, sometimes inadvertently through maintenance (e.g. cleaning fluids and paint strippers) and accidents. Absorption of any fluid (liquids and gases) plasticizes the adhesive, lowering the glass-transition temperature $T_g$ and reducing the stiffness and strength of the adhesive. Other physical changes that can occur include swelling and leaching of soluble constituents (additives) of the adhesive, thus compromising its chemical resistance. Exposure to chemicals and organic solvents will often result in degradation of the substrate–adhesive interface. The higher the concentration of absorbed fluid, the greater the level of degradation in the process which is accelerated at elevated temperatures and in the presence of applied stress. The influence of diffusion and absorption of fluids on the rate of chemical degradation and the interaction between factors such as concentration, temperature and stress is key to predicting long-term performance of bonded structures under different service conditions.

Joints bonded by structural adhesives have two attributes in their favour when exposed to chemical or solvent environments: a high degree of polymer cross-linking and low exposure area (Petrie, 2007), both of which impart considerable protection against chemical attack. Most structural adhesives, such as epoxies, phenolics, polyurethanes and modified acrylics are highly resistant to chemicals and organic solvents at temperatures below the $T_g$ of the adhesive. The adhesive bondline is usually sufficiently thin and well protected from the surrounding environment, especially where the adherends are non-porous and impermeable to the chemicals or solvents present in the surrounding environment.

Chemical resistance can be further enhanced through the application of a protective coating and/or sealant around the edges of the adhesive joint. Polyurethanes and silicones are two sealant materials particularly suited to harsh environments at sub-zero and elevated temperatures. The operating temperature range of these sealants is typically –250ºC to 250ºC and –160ºC to 250ºC, respectively. Fluorosilicones are able to offer improved chemical resistance compared with silicones and resistance to aviation fluids (including oils, fuels and greases), oxidation, ozone and weathering is excellent. In a functional temperature range of –60ºC to 200ºC these materials seem well suited for applications involving harsh environments, but the high costs and special nature of these materials has restricted their use to specific applications, such as seal materials in jet fuel components.

Each adhesive has specific attributes that provide protection against a range of chemicals. The problem for designers and engineers is selecting an adhesive that will guarantee the required design life performance when exposed to the chemicals and solvents that the bonded product is expected

© Woodhead Publishing Limited, 2010

to experience during its service life. This includes secondary environments, such as maintenance activities involving chemical cleaners and paint strippers. There is no single adhesive that offers a universal solution and protection from all environments. Being impervious to one environment is no guarantee of resistance to other environments. An adhesive with maximum resistance to acids generally has poor resistance to bases, and vice-versa. Adhesives with dense cross-linked molecular structures generally have good resistance to chemicals and organic solvents and to high temperatures. Most thermosetting adhesives tend to be hydrolytically stable in the presence of most organic solvents and moderate acids and bases (Kinloch, 1987), although at elevated temperatures (above 70°C), these types of adhesive are susceptible to hydrolysis, showing considerable loss in mechanical performance. Thermoplastic adhesives can be appreciably degraded when exposed to a range of organic solvents, acids or bases.

As previously mentioned, structural adhesives offer good chemical resistance over a wide range of temperatures. The chemical resistance of various types of adhesives are summarized in Table 19.1; exceptions do exist and a proper assessment would be required on a case-by-case basis.

Epoxy adhesives generally tend to exhibit higher resistance to a variety of chemicals and solvents (see www.engineeringtoolbox.com) compared with other adhesive systems, although the resistance to specific chemical agents is strongly dependent on the type of epoxy curing agent used. Aromatic amine curing agents are generally recommended in preference to other curing agents in epoxy systems for long-term chemical resistance applications (see Petrie, 2007). There are exceptions, such as exposure to oxidizing acids (e.g. concentrated perchloric acid, chromic acid, nitric acid and the glass cleaning mixture of chromium trioxide). Epoxies are capable operating over the temperature range –250°C to 175°C, although in practice the maximum operating temperature is reduced to 120°C and 50°C for heat-cured and room-temperature cured systems, respectively. Special formulations are available at higher operating temperatures (~215°C), although for only short time periods (~3000 h).

*Table 19.1* Chemical resistance of adhesive families

| Adhesive | Chemical environment | | | | | |
|---|---|---|---|---|---|---|
| | Aliphatic solvents | Aromatic solvents | Esters and ketones | Strong oxidants | Strong acids | Strong bases |
| Acrylics | H | L | L | L | L | M-H |
| Bismaleimides | H | H | L-M | M | M | M |
| Epoxies | M-H | M-H | M-H | L | M | M |
| Phenolics | H | H | M-H | L-M | H | M |
| Polyimides | H | H | M-H | M | M | M |
| Polyurethanes | M-H | L-M | M | M-H | M-H | L-M |

L = low resistance M = moderate resistance H = strong resistance

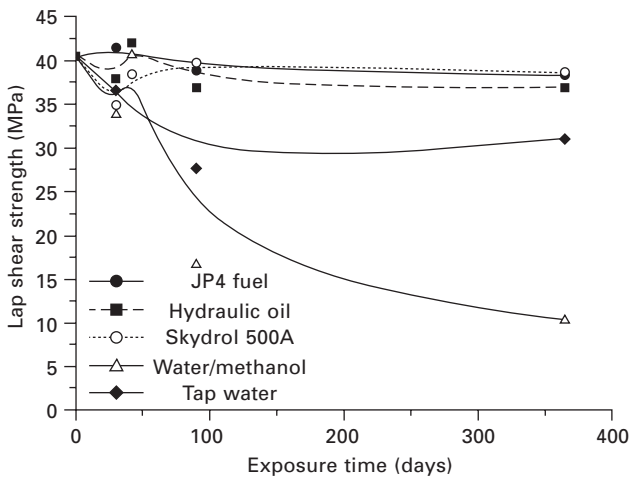
© Woodhead Publishing Limited, 2010

Figure 19.1 compares the long-term effect of various chemical environments at 22°C on the lap-shear strength (Bishopp, 2005) of an epoxy film adhesive (Hexcel Redux 319). The lap joints, constructed using Alclad 2024-T3 aluminium alloy metal sections, were vapour degreased, pickled in chromic–sulphuric acid prior to adhesive application and then cured for 60 min at 175°C. Water/methanol is particularly aggressive and tap water to a lesser degree. JP4 jet fuel, hydraulic oil and Skydrol 500A have far less effect. As the temperature increases, the fluid absorbed by the adhesive joint generally increases and the degradation rate accelerates. Chemicals, such as hydraulic oil and Skydrol 500A which are relatively benign at room temperature may become highly aggressive at elevated temperatures.

Phenolics are particularly durable at both elevated temperatures and under harsh environments (good solvent resistance) and would see much greater use in engineering industries if they were easier to use and less susceptible to shock. Phenolic adhesives tend to be more durable than epoxies. The basic resins can be modified with rubbery polymers to increase toughness (e.g. vinyl acetal and nitrile phenolics). Epoxy phenolics have a wide operating temperature range from –250ºC to 260ºC, although these adhesives have low impact resistance.

Modified thermosetting acrylics are considered to be excellent candidates for structural bonding applications at temperatures as low as –70ºC for operation in hostile environments, as they possess good impact and peel properties. Acrylics are highly sensitive to paint strippers, such as methylene chloride, a common ingredient in many paint strippers used on aircraft.

Polyurethanes show good resistance to a wide range of chemicals, solvents, oils and greases, providing strong, resilient joints that are impact




*19.1* Effect of various chemical environments at 22°C on Redux 319 epoxy film adhesive (Bishopp, 2005).

© Woodhead Publishing Limited, 2010

resistant and have good low-temperature strength compared with many other adhesives. Some grades of polyurethane offer excellent cryogenic performance. Polyurethanes are not recommended for use with strong acid and alkali solutions.

Polyimides and bismaleimides: Few adhesives are suitable for prolonged use at temperatures between 200°C and 350°C, however polyimides and bismaleimides are superior to most other adhesive types with regard to long-term strength retention at elevated temperatures. Like most polymers, these adhesives are vulnerable to chemical attack by chlorinated solvents and ketones. Thermoplastic polyimides are susceptible to environmental stress cracking when exposed to organic solvents, such as acetone, methyl-ethyl-ketone (MEK), toluene and ethylene glycol (deicing fluid), and aircraft fuels (Parvatareddy *et al.*, 1999). The combination of stress and solvent can lead to rapid cracking of the adhesive. Chemical resistance to strong acids and alkalis is moderate. Bismaleimides are purported to have very high resistance to solvents even at elevated temperatures, although like other adhesive systems, chemical resistance decreases at elevated temperatures.

Product data sheets supplied by a number of adhesive manufacturers contain tensile (lap) shear strength values for a range of chemical environments in addition to standard laboratory conditions, distilled and deionised water (ambient and boiling), water vapour and saltwater spray. Chemical environments include acetic acid, ethyl acetate, acetone, MEK, methanol, isopropanol, xylene, antifreeze (anti-icing fluid), gasoline (petrol), JP4 fuel and hydraulic oil. Often other constituents, such as fillers, fire retardants and curing agents are more reactive than the resin. Formulators and users, although usually aware of the potential durability problems associated with these additives, often overlook constituents like catalysts, hardeners and pigments. A number of chemical agents and situations most relevant to adhesive joints are briefly discussed below.

Organic solvents: High-performance structural adhesives used in the aircraft industry (Parvatareddy *et al.*, 1999), like epoxy and thermoplastic polyimide adhesives, are highly sensitive to organic solvents (e.g. acetone, MEK, ethyl acetate and toluene) even at room temperature. Solvent uptake is rapid and the effects on adhesive strength and $T_g$ are generally irreversible. Solvents tend to have a plasticization (softening) effect on the adhesive and in combination with mechanical stress can result in crazing or cracking of the adhesive (i.e. ESC). Exposure to acetone for short periods (1–3 months) can result in 10% (or higher) tensile strength reduction of structural adhesives, with higher levels of strength loss recorded after exposure to MEK and toluene (≥25%).

Aircraft structures may be repainted between 10 and 15 times during a service life of 30 to 40 years, which requires old paint to be removed before recoating. Paint strippers, such as methylene chloride, phenol, benzyl alcohol and benzene alcohol blends will soften and dissolve adhesives. Methylene

© Woodhead Publishing Limited, 2010

chloride is highly aggressive towards acrylic and epoxy resin systems. In the view of solvent sensitivity of structural adhesives, it is important to prevent solvents coming into contact with the adhesive and/or joint during service life. Chemical paint strippers are banned from use with composite aircraft components.

Acids and bases: Many acids and alkaline agents are known to degrade structural adhesives, although the degree of degradation by specific chemical agents is dependent on the chemical composition of the adhesive, chemical concentration levels, exposure time and temperature. Acetic acid is considered to provide a severe environment along with chromic, hydrochloric, hydrofluoric, nitric and sulphuric acids. Dilute mineral acids are frequently encountered, not only in the chemical plant industry, but are also present in industrial and household effluent and sewage.

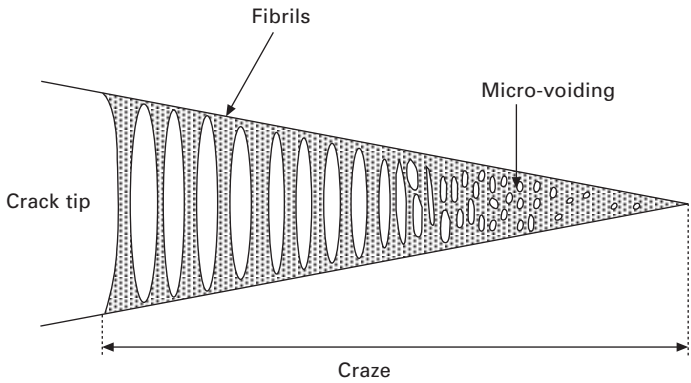
Aviation fluids: Gasoline (petrol), JP4 fuel and hydraulic fluid are known to plasticize some structural adhesives and consequently lower joint strength, although the level of degradation induced generally tends to be far less than most other chemicals or solvents (Doyle and Pethrick, 2009). Whilst deicing fluid ethylene glycol has been found to have a minimal effect on the mechanical properties of structural adhesives, exposure to diethylene glycol monoethyl ether (DGME) can cause severe deterioration of these materials (Rider and Yeo, 2005).

Oxidation: This is the primary degradation process at elevated temperatures with the rate of degradation increasing with the amount of oxygen present. Oxygen diffusion through the adhesive resin and along the adherend–adhesive interface can be rapid at elevated temperatures. Oxidation can result in strength reduction and discolouration of the adhesive. Differential scanning calorimetry (DSC) can be used to ascertain the extent and rate of material oxidation. A majority of polymers (thermosetting and thermoplastic) are susceptible to oxidation by any one of numerous chemical agents including hydrogen peroxide, certain bleaches (e.g. sodium hypochlorite) and oxidizing acids, such as chromic and nitric acid.

### 19.2.3 Environmental stress cracking (ESC)

Exposure to moderate levels of applied stress for extended periods of time can induce crazing and cracking in polymers and is the underlying cause of long-term transition to brittle behaviour in ductile polymers. This mechanism, known as creep (or stress) rupture is a common cause of polymer failure (Arnold, 1996; Greenwood, 1997; Wright, 1996). Crazes are voids that are held together by highly drawn fibrils (Fig. 19.2), which bridge the void allowing the craze to transmit stress and preventing the craze from propagating and coalescing (joining together). Craze initiation is considered to evolve from microdeformation processes in localized regions about 30 nm in diameter. As

© Woodhead Publishing Limited, 2010




*19.2* Schematic of craze formation (Maxwell and Pilkington, 2008).

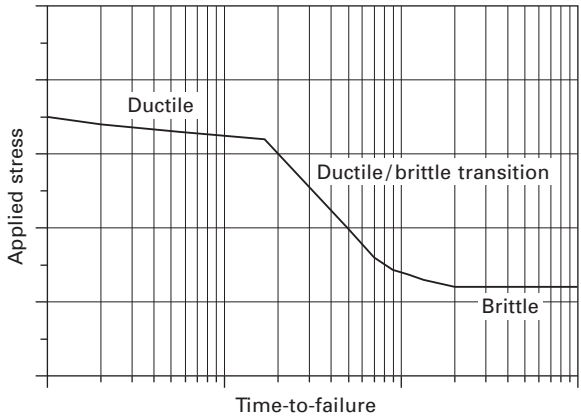
the deformation region develops, further localized deformation is induced. The growth and coalescence of such deformed nuclei create a narrow plastic zone. In the presence of dilatational stress, voids develop. The voided structure is considered to be the precursor of the fibrillated craze structure which ultimately leads to unstable crack growth and failure. Ingress of stress-cracking agents causes the fibrils to soften, allowing the cracks to grow. Pressure exerted by the swollen polymer drives the crack tip; eventually the swollen region grows rapidly, resulting in brittle fracture.

High stress promotes ductile failure, whereas low stress promotes delayed brittle failure, as shown in Fig. 19.3. There is an 'apparent' threshold strain below which crazing is not expected to occur for a very long time. A number of factors are known to accelerate this embrittlement process, including stress (or strain) concentration, exposure to elevated temperatures, dynamic (cyclic) fatigue loading and contact with specific chemical environments.

ESC is essentially the physical interaction of highly localized plasticization through stress enhanced fluid absorption in the presence of stress concentrating defects, which does not involve chemical change or molecular degradation of the polymer (Wright, 1996). Defects (e.g. voids) are invariably present in adhesive joints and in the presence of stress concentrations they are prime sites for localized yielding. Absorption of any fluid will plasticize the polymer, and reduce its yield strength. Once the fluid has penetrated the polymer it becomes locally dissolved promoting cracking and crazing in the polymer. Cracking is normally preceded by the formation of crazes initiated at sites of stress concentration or in regions of local microstructure inhomogeneity. The higher the concentration of the absorbed fluid, the lower the yield strength.

ESC remains one of the most common causes of polymer failure (Arnold, 1996; Comyn, 1994; Wright, 1996). It can inadvertently be initiated through exposure to cleaning fluids and paint strippers, rather than caused by exposure

© Woodhead Publishing Limited, 2010




*19.3* Typical time-dependent creep rupture curve of an amorphous polymer (http://www.rapra.net/consultancy/environmental-testing-environmental-stress-cracking.asp).

to the primary service environment. ESC is a complex phenomenon, with aspects such as chemical compatibility, liquid diffusion, craze formation and crack development all making a contribution (Comyn, 1994; Wright, 1996). While semi-crystalline and amorphous polymers (e.g. thermosetting adhesives) are both susceptible to ESC, amorphous thermoplastics are considerably more susceptible. These materials are most susceptible at temperatures approaching the $T_g$ of the polymer. Fluids with high molar volume, high viscosity and high boiling points are less likely to be severe stress cracking agents compared with fluids containing low hydrogen bonding (e.g. ethers, ketones and esters). Non-hydrogen bonded fluids (e.g. aliphatic hydrocarbons) and highly hydrogen-bonded fluids (e.g. water and alcohol) tend to be less severe in comparison with low hydrogen bonded fluids. Stress cracking fluids are most aggressive near their boiling point.

It is difficult to source ESC data for a given chemical/adhesive combination owing to the large number of chemicals and adhesives available and therefore it is necessary to conduct ESC tests to ascertain if an adhesive is safe to use in contact with particular chemicals. Tests should be carried out on adhesive joints as the chemical agent may attack the adherend/adhesive interface.

### 19.2.4 Weathering and photooxidation

Weathering or more specifically photooxidation of polymers refers to the chemical and physical changes that occur when ultraviolet (UV) radiation is absorbed by a polymer. The UV radiation spectrum comprises wavelengths of between 290 and 400 nm, which corresponds to energies of between 415 and 300 kJ $mol^{-1}$. These energies are in the same range as the bond energies of many organic compounds. Chemical reactions are induced when

© Woodhead Publishing Limited, 2010

specific functional groups absorb UV radiation. Free radicals liberated in the process will trigger further reactions. The deleterious effect will be dependent on the chemical nature of the material, environmental factors, such as temperature and humidity, and exposure time. Material changes include discoloration (yellowing and bleaching), embrittlement and loss of mechanical and physical properties. Photooxidative sensitivity may also increase with prolonged exposure to pollutants (Brown and Greenwood, 2002; Maxwell *et al.*, 2005).

UV radiation can be divided into three groups of wavelengths described below:

- UVA (315–400 nm) – least harmful to polymers, forming 6% of the total solar radiation reaching earth
- UVB (280–315 nm) – more damaging to polymers, forming 0.1% of the total solar radiation reaching earth
- UVC (<280 nm) – most harmful to polymers, but filtered out by the earth's atmosphere.

UV radiation below 350 nm is absorbed by window glass, thus eliminating UVB radiation indoors.

When a polymer is exposed to solar radiation, the energy absorbed by the polymer results in the formation of free radicals within the polymer by the dissociation of the C–H bonds in the polymer chains. The extent of this chemical reaction depends on the radiation exposure, that is the quantity of ultraviolet light (<350 nm) to which it is exposed. Once free radicals have been produced, reaction with oxygen generates hydroperoxides (Wypych, 2008), which can dissociate further, producing a series of decomposition products including aldehydes and ketones. The presence of these carbonyl groups in a degraded polymer can be used as a chemical index for degradation. Once formed these free radicals can continue to react via propagation reactions long after the initial UV exposure has ended.

The formation and propagation of free radicals in itself does not seriously affect the mechanical properties of the polymer, as free radicals do not significantly alter the long-chain nature of the polymer molecules. Degradation of the mechanical properties occurs because the free radicals produced are highly unstable and readily undergo chain scission reactions. This results in the formation of two smaller polymer chains, one of which is a free radical and capable of further reactions (Wypch, 2008).

The intensity of the UV radiation decreases with increasing depth in the material, so that the reaction tends to be a near surface process. Shorter wavelengths have a far more deleterious effect on material properties than longer wavelengths. Longer wavelengths will penetrate deeper into the material, but are not easily absorbed, whereas the total energy of shorter wavelengths tends to be absorbed within a few micrometres of the surface.

© Woodhead Publishing Limited, 2010

Since oxygen is involved in the reaction process, there is an important balance between UV radiation and oxygen diffusion and, of course, temperature since that will also determine the kinetics of reaction and the transport of reactive species. Under natural exposure conditions there will be wetting and drying cycles and dark periods. The significance of the latter is that some recovery of the oxygen concentration in the material can occur, which otherwise is confined to the very near surface owing to consumption by reaction with the polymer radicals. Since the concentration of these radicals diminishes by a termination reaction during the dark period, oxygen ingress can extend to a greater depth.

Geographical location, seasonal variations and time of day play a significant role in the length, intensity and wavelengths experienced. Equatorial latitudes are particularly hostile in terms of UV exposure where, because of the high solar angle, the levels of UV radiation and temperature are higher and the range of wavelengths transmitted by the earth's atmosphere extends even lower (i.e. shorter wavelengths). At higher altitudes, a thinner atmosphere absorbs less UV radiation. The presence of water increases UV degradation, because the dissolved oxygen in water is more active in promoting photooxidation than oxygen in the air.

UV resistance can be improved by including additives, such as antioxidants, thermal and UV stabilizers and pigments in the adhesive formulation. Antioxidants slow down the process of oxidative degradation, prolonging the life of the product. Thermal stabilizers are added to protect the adhesive system from chemical breakdown caused by heat and UV radiation, whilst UV stabilizers protect against UV degradation and exposure to fluorescent light and filtered daylight. Pigments alter the absorption characteristics of the material acting as a screen against UV radiation when compounded with the adhesive. Carbon black, titanium dioxide, zinc oxide and barium sulphate are examples of commonly used pigments. The costs of additives can often be prohibitive and also may adversely alter mechanical performance. Carbon black is particularly effective in protecting against UV radiation and is inexpensive. It absorbs UV radiation and protects the polymer chains. Certain types of pigment can cause the polymer to be photosensitive and thus accelerate UV degradation.

### 19.2.5 High-energy radiation

High-energy radiation covers a wide range of different forms of high-energy particulate and electromagnetic radiation including X-rays, gamma rays, neutrons, alpha particles and beta particles. When a polymer is irradiated, the ionizing radiation induces degradation by the formation of free radicals or ions in the polymer. These reactive intermediates are capable of initiating chemical reactions which occur by free radical or ionic mechanisms and

© Woodhead Publishing Limited, 2010

which result in scission as well as in cross-linking reactions. Free radicals with a long lifetime can be present in the bulk of the material after irradiation and still cause changes in properties even a long time after exposure. The intensity of ionizing radiation on the earth's surface is not normally high enough to affect most structural adhesives significantly, as these materials tend to be highly cross-linked and exhibit high temperature resistance. Nitrile–phenolic adhesives are more resistant to radiation than epoxy-based adhesives. Radiation resistance of epoxy adhesives is improved by using aromatic curing agents. Radiation exposure tests are required for products used in the nuclear industry and applications where radiation is used (e.g. medical X-rays and sterilization). ASTM D 1879 specifies methods of evaluating resistance to radiation.

### 19.2.6 Biological degradation

Biological degradation is not a common form of degradation as most polymers are resistant to microbiological attack by fungi or bacteria. It is the chemical additives and pigments that are usually susceptible to microbial attack (Campo, 2007), which tends to occur on exposed surfaces owing to oxidation of the additives. Polyurethanes in particular are sensitive to microbial attack, although polyether polyurethanes are more resistant to biological degradation than polyester polyurethanes (Brown and Greenwood, 2002; Chanda and Roy, 2009). Polymers that have good water and weather resistance generally have greater resistance to microbial attack. Geographical location and seasonal effects are important because microorganism growth is more rapid in warm, humid climates than cold, dry climates.

Resistance to mould, fungi and bacteria can be improved by including antimicrobial additives (also known as fungicides or biocides), uniformly distributed throughout the polymer (or adhesive), during the compounding process or alternatively by applying a suitable protective coating and/or sealant around the exposed edges of the adhesive joint. Antimicrobials can provide protection against mould, mildew, fungi and bacterial growth, which can cause discoloration, embrittlement and sometimes product failure. These additives are known to be highly toxic and care needs to be taken in handling and storing these materials. The effectiveness of antimicrobials depends on their ability to migrate to the edges of the bonded structure where microbial attack initially occurs. Antimicrobials are usually carried in plasticizers, which are mobile. It is important for the adhesive system to be able replenish any surface loss caused through leaching or erosion, but only sufficient to maintain protection. High mobility can cause significant leaching of the antimicrobial via weathering which compromises its ability to protect the adhesive joint from the surrounding environment. As silicone rubbers have good resistance to microbial attack, they are used as sealants.

© Woodhead Publishing Limited, 2010

Microbial testing generally consists of exposing materials to an outdoor environment in geographical locations where weather conditions are favourable to microbial growth (see ASTM G 21 and ISO 846). The angle of exposure to sunlight and weather conditions will influence the extent and duration of microbial attack. An alternative approach (known as soil burial) is to bury specimens for set periods of time and then to exhume and examine the specimens for the effects of microbial attack. The conditions involved in soil burial tests have been optimized to ensure maximum degradation (Brown and Greenwood, 2002).

## 19.3 Chemical resistance testing

### 19.3.1 Introduction

In order to determine the effectiveness of different adhesive systems, processing variables and surface treatments, it may be necessary to expose adhesive joints to various environmental and loading conditions that simulate actual service conditions. The resistance of the bonded structure to degradation agents often becomes apparent within a short period. In some circumstances only a few hours of exposure may lead to catastrophic failure or seriously compromise the structural integrity of the joint.

It is impractical in most cases to carry out testing for prolonged periods of time in order to assess long-term performance (or durability) of bonded systems. In these situations, accelerated ageing is required to assist the process of determining long-term performance from short-term tests. A number of techniques have been employed to accelerate testing of adhesives joints. These tests tend to be laboratory based and the environments involved are harsher than actual in-service conditions. The usual approach in accelerated chemical resistance testing has been to increase the temperature, chemical concentration or pressure. However, there is a temperature limit to which most adhesives can be raised without effecting a change in the degradation mechanisms. Above this critical temperature, there is a strong possibility of altering the degradation mechanism. It is important that the ageing conditions selected recreate the same failure mechanisms that would be experienced in service.

The use of smaller specimens for longer times under moderate conditions can potentially be employed, provided the data generated can be scaled up to predict the long-term performance of more realistic size structures. Perforating the bondline of coupon specimens (e.g. single-lap joints) with small diameter holes can also accelerate fluid uptake by reducing diffusion path lengths (Arrowsmith and Madison, 1987). The ability to correlate laboratory test data with service performance is key to the success of accelerated testing. Although accelerated ageing is widely used (Packham, 2005), it is seldom

© Woodhead Publishing Limited, 2010

possible to establish a one-to-one correlation between the rate of degradation in the accelerated test and actual service conditions. A full understanding of chemical degradation effects is not yet available and there is no consensus about a satisfactory accelerated test.

### 19.3.2 Diffusion kinetics and solubility

The degree of degradation that occurs in adhesive systems when in service can often be linked directly with the amount of fluid absorbed. The fluid absorption kinetics of adhesive systems will differ widely and also change with physical ageing. An understanding of permeation of chemical species is essential to develop testing methodologies and accelerated ageing protocols for polymeric materials (Duncan *et al.*, 2005; Duncan and Broughton, 2007). The process of permeation of chemicals through polymers is a combination of two interrelated processes, dissolution in the polymer and diffusion through the polymer. Dissolution is the process of absorption of the chemical in the polymer and depends on the affinity (interaction energy) of the polymer for the absorbing molecules, the volume available for absorption and the concentration of absorbing chemical. There is a limit, the solubility, to the amount of the chemical that can be absorbed under any particular set of conditions. Permeability is the product of solubility and diffusion. Where solubility obeys Henry's law, permeability, $P$, can be related to diffusion coefficient, $D$, and solubility, $S$, by the following relation (Chanda and Roy, 2009):

$$P = DS \qquad [19.1]$$

Diffusion in adhesive joints occurs when molecules of the diffusing species pass through voids and other gaps between the polymer molecules of the adhesive, or by capillary action along the interface. The diffusion rate is dependent on the size of the diffusing species and the size of the gaps within the adhesive and at the interface, and tends to be higher along the latter. Absorption is dependent on the level of porosity, with the rate of fluid absorbed and fluid concentration at saturation increasing with the level of porosity. For diffusing species with similar solubility parameters, the smaller molecules will diffuse faster in a polymer than larger molecules.

Amorphous polymers are particularly susceptible to solvation because solvent molecules can diffuse readily through the 'free volume' of the polymer. Solvent molecules facilitate segmental motion in the polymer and as a result $T_g$ and first order phase transitions tend to be shifted to lower temperatures. The rate of diffusion in amorphous polymers will depend on the state of the polymer (glassy < $T_g$ < rubbery). In the rubbery state, there is substantial 'free volume' in the polymer mass and considerable molecular segment mobility, which enables easier passage of the diffusing species through the polymer.

© Woodhead Publishing Limited, 2010

In the glassy state, the 'free volume' is far less and molecular segments are immobile, and as a result the diffusion rate is lower. Diffusion rates tend to be higher in amorphous adhesives compared with thermoplastic adhesives. In semi-crystalline polymers, the crystalline regions are almost impermeable owing to the ordered arrangement of molecules and high degree of molecular packing in these regions, with diffusion restricted to the amorphous regions. Reducing the 'free volume' of the polymer will increase the diffusion barrier characteristics, thereby increasing resistance to solvent attack. This can be achieved by increasing crystalline content, crystallite size, molecular weight, degree of cross-linking and packing density, or adding inert fillers.

As the concentration of liquid solvent in the polymer increases, the polymer begins to swell owing to a reduction in the intermolecular forces between polymer chains. The swelling process is considered to be reversible if the polymer returns to its original dimensions and weight on removal of the solvent (i.e. no chemical reaction). The process is considered to be irreversible if a chemical reaction occurs, resulting in the leaching of polymer components, such as plasticizers. The presence of solvents in polymers can be detected using DSC by measuring the effect on $T_g$ of the polymer.

Diffusion of a chemical species within a polymeric material, such as an adhesive, is a time- and temperature-dependent process and can often be expressed by Fick's second law:

$$\frac{dC}{dt} = D\,\frac{d^2C}{dx^2} \qquad [19.2]$$

where $C$ is the chemical concentration of the diffusing species, $D$ is the diffusion coefficient ($m^2\ s^{-1}$) and $x$ is the direction of diffusion (usually taken as the thickness direction for an infinitely long and wide section).

The 'apparent' diffusion coefficient $D_A$ for a polymer resin specimen can be determined from the initial linear region of the Fickian diffusion curve (Fig. 19.4) using the following relationship:

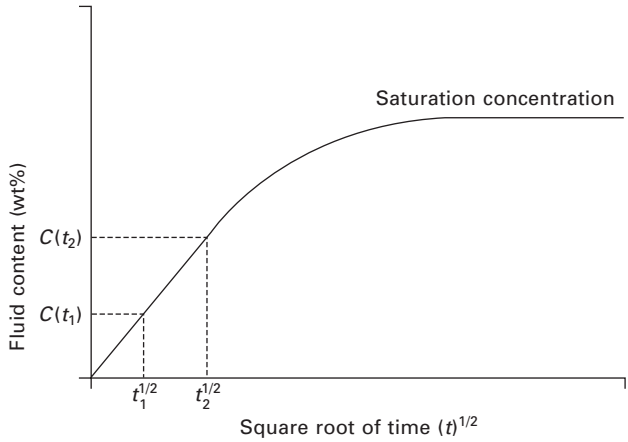
$$D_A = \frac{\pi}{16}\left(\frac{h(C(t_2) - C(t_1))}{C_S(\sqrt{t_2} - \sqrt{t_1})}\right)^2 \qquad [19.3]$$

where $C_S$ is the chemical saturation or equilibrium concentration (weight percentage), $C(t_1)$ is the fluid uptake after time $t_1$, $C(t_2)$ is the fluid uptake after time $t_2$ and $h$ is the specimen thickness.

The absorbed fluid concentration $C(t)$, which is often expressed as a percentage of the specimen dry mass, is calculated from the mass $M(t)$, initial mass $M_0$ and the reconditioned mass $M_c$ after drying the specimen (if there is no loss of fluid-soluble matter then $M_c = M_0$):

$$C(t) = \frac{M(t) - M_c}{M_0} \qquad [19.4]$$

© Woodhead Publishing Limited, 2010




*19.4* Fickian diffusion curve.

The analysis used to derive $D$ assumes that the specimen is an infinite rectangular plate with no diffusion from the specimen edges. In fact, diffusion occurs from all six surfaces of a rectangular section. A correction factor to account for edge effects has been derived, which enables the true one-dimensional diffusion coefficient $D$ to be determined as follows (Shen and Springer, 1976):

$$D = D_A\left(1 + \frac{h}{l} + \frac{h}{b}\right)^{-2} \qquad [19.5]$$

where $l$, $b$ and $h$ are the length, width and thickness of the rectangular specimen, respectively.

By considering the one dimensional diffusion case, analytical solutions for the temporal and spatial distribution of fluid concentration $C(t)$ at a distance $x$ inside the material in the direction of diffusion can be determined by the relationship:

$$\frac{C(t) - C_0}{C_M - C_0} = 1 - \frac{4}{\pi}\sum_{j=0}^{\infty}\frac{1}{(2j+1)}\sin\left[\frac{(2j+1)\,\pi x}{h}\right]\exp\left[-\frac{(2j+1)^2\pi^2 D \cdot t}{h^2}\right] \qquad [19.6]$$

where $C_0$ is the initial concentration of the diffusing species within the material of thickness $h$ for $t \leq 0$ and $C_M$ is fluid concentration at the specimen surface for $t > 0$. It is assumed that concentration of the diffusing species at the specimen surface remains constant and the concentration of the diffusing species in the fully saturated material is in equilibrium with the surrounding environment.

© Woodhead Publishing Limited, 2010

The mass gain of fluid in the material as a function of time can be obtained by integrating Equation [19.6] over the section thickness (Jost, 1960):

$$\frac{M(t) - M_0}{M_M - M_0} = 1 - \frac{8}{\pi^2} \sum_{j=0}^{\infty} \frac{1}{(2j+1)^2} \exp\left[ - \frac{(2j+1)^2 \pi^2 D \cdot t}{h^2} \right] \quad [19.7]$$

where $M_0$ is the initial weight of the fluid in the material (i.e. the weight prior to environmental exposure) and $M_M$ is the weight of the fluid in the material when the material is fully saturated.

For a closed rectangular adhesive sandwich (i.e. adhesive layer between two metal sections) with a width $2w$ and length $2l$, the equation expressing fluid concentration at any point $(x, y)$ in the adhesive sandwich as a function of time, $t$, can be determined using the following relation (see Wylde and Spelt, 1998):

$$\frac{C(x, y, t)}{C_M} = 1 - \frac{16}{\pi^2} \sum_{j=0}^{\infty} \sum_{k=0}^{\infty} \frac{(-1)^j (-1)^k}{(2j+1)(2k+1)} \times [(\cos\sqrt{\lambda}x)(\cos\sqrt{\mu}y)\exp(-D(\lambda + \mu)t)] \quad [19.8]$$

where:

$$\lambda = \left( \frac{(2j+1)\,\pi}{2l} \right); \mu = \left( \frac{(2k+1)\,\pi}{2w} \right) \quad [19.9]$$

Diffusion coefficients increase with temperature and for ideal systems the relationship between $D$ and temperature, $T$(K), can be expressed by an Arrhenius relationship:

$$D = D_0 \exp\left( - \frac{E_D}{kT} \right) \quad [19.10]$$

where $E_D$ is the energy barrier to diffusion and $k$ is Boltzmann's constant. Material parameters $D_0$ and $E_D$ can be determined by plotting log $D$ against $1/T$ graph, which is often linear.

International standard ISO 62 describes a procedure for determining liquid absorption properties and/or diffusion coefficients in the 'through-the-thickness' direction of flat and curved solid plastics. ISO 62 is suitable for use with adhesives specimens and is applicable to both vapour exposure and liquid immersion.

Solubility measurements of an adhesive in different solvents are important in assessing the chemical resistance and potential applications for the material. It is also essential to assess the solubility of the different additives, such as plasticizers, anti-oxidants and pigments in the adhesive, which can have an impact on chemical resistance. Although the solubility relations in polymer systems are complex, empirical solubility rules have been derived that enable

© Woodhead Publishing Limited, 2010

solubility predictions for a number of polymer-chemical species combinations. The solubility parameter, δ, is defined in terms of the cohesive energy density in the liquid state ($\Delta E_V/V$), in which $\Delta E_V$ is the molar energy of vaporization and $V$ is the volume of the liquid (Chanda and Roy, 2009):

$$\delta = \left(\frac{\Delta E_V}{V}\right)^{1/2} \quad [19.11]$$

Cohesive energy density provides a measure of the intermolecular attraction forces in the material, which approximately equals the heat of vaporization for liquids or sublimation for solids per mole. The total cohesive energy $\Delta E_t$, which holds a liquid together, can be divided into contributions from dispersion forces $\Delta E_d$, polar forces $\Delta E_p$ and hydrogen bonding forces $\Delta E_h$ (Hansen, 2000):

$$\Delta E_t = \Delta E_d + \Delta E_p + \Delta E_h \quad [19.12]$$

The total solubility parameter can be expressed in terms of solubility parameters $\delta_d$, $\delta_p$ and $\delta_h$ due to dispersion forces, dipole forces and hydrogen bonding, respectively.

$$\delta_t^2 = \delta_d^2 + \delta_p^2 + \delta_h^2 \quad [19.13]$$

The three parameters, known as Hansen solubility parameters (HSPs), have been derived empirically from experiments conducted on a large number of solvents. For each polymer, a three-dimensional spherical volume of solubility in $\delta_d$, $\delta_p$ and $\delta_h$ space can be defined by an interaction radius, $R_O$. The distance of the coordinates of any solvent i from the centre point of the spherical volume of polymer j is:

$$d^2 = \left\lfloor 4(\delta_d^i - \delta_d^j)^2 + (\delta_p^i - \delta_p^j)^2 + (\delta_h^i - \delta_h^j)^2 \right\rfloor \quad [19.14]$$

The scale on the dispersion axis is usually doubled, as indicated in the above equation, to improve the spherical nature of the volume. This distance can be compared with the radius $R$ of the solubility sphere of the polymer. If $d < R$, the probability of solvent i dissolving polymer j is high. This approach has proved effective in predicting chemical degradation of structural adhesives (Storm *et al.*, 2005).

### 19.3.3 Accelerated conditioning and testing

Conditioning can be carried out using either full immersion (where solution chemistry needs to be considered) or in a gas atmosphere (where vapour pressure should be controlled). The test specimens can be either unstressed or subjected to constant stress or strain whilst being conditioned. A note of caution, some adhesives may remain unaffected by the surrounding chemical media, but fail rapidly when exposed to the same chemical environment

© Woodhead Publishing Limited, 2010

whist in a stressed state. Absorption and diffusion rates are also temperature dependent. Equilibrium fluid concentrations normally increase with increasing vapour pressure.

The natural process of fluid absorption in engineering components/structures is normally very slow and this makes it very difficult to reach an adequate degree of degradation in a structural test element in practical timescales. It has been found necessary, therefore, to speed up the fluid diffusion process by employing an accelerated conditioning technique that can ensure a representative level of degradation in a significantly reduced time.

There are two basic methods of fluid conditioning:

- fixed-time conditioning, where a test specimen is exposed to a conditioning environment for a specified period of time; and
- equilibrium conditioning, where a specimen is exposed until the material reaches equilibrium with the conditioning environment.

The first technique is routinely employed for screening adhesives (including surface treatments). This approach results in non-uniform fluid distribution through the bondline thickness of the test specimen. Test data obtained from specimens conditioned in this manner are only considered suitable for comparing different batches of the same material or for quality control tests. Ideally, comparative studies of chemical or solvent absorption effects on adhesive properties should be carried out only using specimens where the fluid content has reached saturation and where the specimens have been exposed to identical conditions. Equilibrium fluid concentration is most likely to indicate 'worst-case' material properties. The larger the specimen the longer the time required to reach equilibrium, requiring the use of relatively small specimens to determine fluid diffusion coefficients.

It is recommended that when comparing the effects of adhesive systems, surface treatments and processing variables on the chemical resistance of adhesive joints, all specimens have identical geometry and dimensions and are prepared and conditioned together to account for any variability in the conditioning environment. Also, control specimens are recommended to check changes in the system's performance.

Pressurized fluid testing: The rate of fluid (liquid or vapour) uptake of specimens immersed in a fluid under pressure, such as deep-sea environments, may be expected to increase with an increase in pressure. Porous materials (i.e. high porosity) or poorly bonded systems tend to absorb fluid more rapidly under pressurized conditions than would occur under atmospheric conditions. Tests simulating high-pressure conditions can be carried out in specially designed pressure autoclaves, which can be heated internally using heating elements or externally using a heating blanket. The autoclave material needs to be inert to the chemicals within the autoclave.

© Woodhead Publishing Limited, 2010

### 19.3.4 Creep-rupture testing

Creep-rupture (also known as stress-rupture or static fatigue) tests are performed to assess the extension of materials or structures (e.g. adhesive joints) under load, to predict long-term behaviour or to assess the long-term strength of the system under load. Strain levels in excess of those normally experienced during service are applied to the test component. The first requirement needs high precision extensometers to monitor extension and the tests must be performed under stable environmental conditions (temperature and humidity) to avoid artefacts in the measurement.

Two approaches have been adopted to assess the degree of degradation under combined static load and environment:

- Rate of strength loss with time (i.e. residual strength): This approach determines the time taken for the strength of the materials system to decline to a design stress limit, below which the joint is no longer considered safe. Specimens are removed at regular intervals to assess strength reduction.
- Time-to-failure: This approach attempts to determine the probable average life expectancy of a materials system at a prescribed stress level or to determine the percentage of failures that can be expected to occur within a given exposure period.

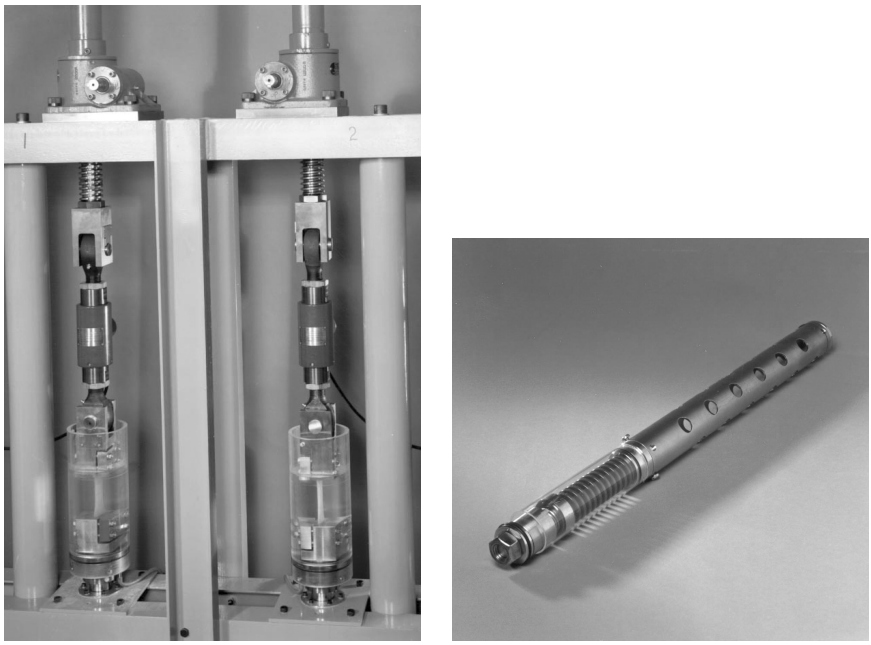
Creep-rupture tests could, in theory, be performed using any of the loading options outlined below, but for the greatest accuracy the first two options are preferred:

- mechanical (servo-hydraulic or motor driven) test machines;
- dead-weight and lever creep testing machines;
- a screw jack in series with a load cell (Fig. 19.5);
- self-stressing fixture where specimens are placed in either a tube equipped with a pre-calibrated spring system (Fig. 19.5) for loading specimens or a circular ring.

The use of a mechanical test machine is not an economic option in most cases. A bank of small creep machines can be assembled at a considerably lower cost compared with the capital outlay involved in purchasing and operating such machines. Self-stressing fixtures (Fig. 19.5), which are light and economic to produce and maintain, are particularly suitable for field trials and for large batch testing.

Self-stressing tubes have been successfully used to test many different types of specimen, for example small single-lap and T-peel adhesive joints. Testing consists of placing specimens (1–6) in a tube equipped with a precalibrated spring system for loading the specimens. The spring system can be compressed and locked in place in order to apply the required load

© Woodhead Publishing Limited, 2010



(a) (b)

*19.5* Tensile creep fixtures. (a) Screw-jack test machines; (b) self-stressing tubes.

with the spring stiffness determining the load range. The amount of load is determined by measurement of the spring compression. The specimens are bolted together with either stainless steel or polyamide bolts.

The stress tubes need to be inspected at frequent intervals to check the condition of the test specimens (i.e. failed or intact). Failed joints are replaced by spacers and the remaining specimens are restressed. The failure times are measured at which the first three specimens fail. When the third specimen fails, the remaining specimens are removed from the loading tube and tested to failure to determine residual strength. The average lifetime of the failed specimens and the residual strength of the remaining specimens should be recorded. The large uncertainty associated with time-to-failure measurements, especially at the high stress levels will require either electromechanical or optical devices to monitor load or deformation in order to determine time-to-failure accurately.

Specimens loaded by springs can often be in an unstressed state for a considerable period of time (overnight or weekends) before the failed joint is replaced (by a 'dummy' specimen) and the loading train is retensioned. There is a tendency for surviving specimens to be damaged in the restressing process with the probability of this occurring increasing at high stresses. Creep/relaxation histories of specimens may be different owing to the replacement

© Woodhead Publishing Limited, 2010

of failed specimens and subsequent reloading. This contributes further to the uncertainty of creep rupture data. For long-term tests over months or years, this effect will probably be minimal. For short duration tests (i.e. static loads close to the maximum load at failure) load relaxation occurs and it is therefore necessary continuously to adjust the manual screw jack on the creep frame or the loading spring on the self-stressing tube in order to maintain a constant load. The use of controlled mechanical test frames avoids this problem. Manually operated systems are best suited to long-term testing where loads are relatively low and load relaxation is minimal.

Design limits for load and stress levels need to be established for any particular system tested. Typically these are between 10 and 50% of the short-term strength of the polymeric system. It is generally recommended that the sustained stress in an adhesive bonded joint under service conditions should be kept below 25% of the short-term strength of the joint. Some design guides suggest a knockdown factor of 10 (i.e. stress level of 10%). The onset of failure tends to be catastrophic. In general, damage and stiffness loss prior to failure is minimal. Methods of accelerating the testing process based on mechanical load tend to use stress levels that are significantly higher than stress levels used in design, thus the limiting design strains are reached in shorter times than in actual service.

The large uncertainty associated with creep test results implies that the current approach of conducting three tests per stress level is inadequate and that considerably more data points are required to generate reliable creep rupture curves for engineering design purposes. Five (preferably 10) specimens per stress level with five stress levels per condition should provide a reasonable number of data points. For characterization purposes it is recommended that specimens are mechanically loaded at each of five stress levels (i.e. 80%, 70%, 55%, 40% and 25% of the short-term tensile strength of the material).

### 19.3.5 Environmental stress cracking (ESC)

The evaluation of ESC resistance is covered by a number of national and international standards (Turnbull and Maxwell, 1999). These test methods can be divided roughly into two groups: those that are based on an applied deformation and those based on applied load. The main international standards for testing ESC resistance are:

- Constant deformation tests
  - Bent strip (ISO 22088-3)
  - Bent strip test for flexible materials (ASTM D 1693)
  - Ball and pin impression (ISO 22088-4)
  - Constant tensile deformation (ISO 22088-5)

© Woodhead Publishing Limited, 2010

  - Slow strain rate testing (ISO 22088-6).
- Constant load tests
  - Constant tensile stress (ISO 22088-2 and ISO 16770).
  - C-ring tests (ASTM F 1248) – essentially for pipes and tubes.

Bent strip test: This test involves clamping the test specimen to a semi-circular former and applying a known strain to the specimen. The radius of curvature of the former can be varied to induce different levels of stress in the specimen. The resultant strain ε may be calculated using the following equation:

$$\varepsilon(\%) = \frac{d}{2r + d} \times 100 \qquad [19.15]$$

where $d$ is the thickness of the specimen and $r$ is the radius of the former.

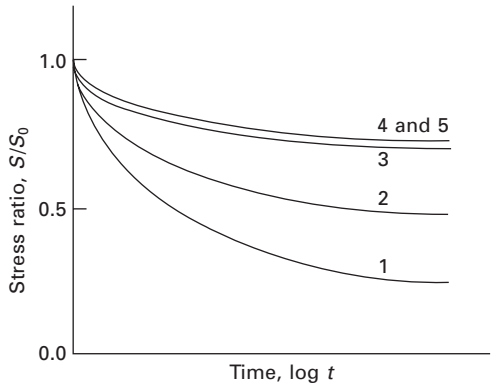
Once the specimen has been strained it is brought quickly into contact with the chemical environment. After a set time the specimen is removed from the apparatus and either visually inspected for crazing or mechanically tested to assess residual strength. The test is most commonly used to assess the ESC susceptibility of amorphous polymers. It is unsuitable for semi-crystalline polymers, which are susceptible to rapid stress relaxation; applied stress to the specimen will decrease during the test.

Bent strip for flexible materials: This technique is suitable for flexible polymers but only for quality control purposes. The specimens used in this test are notched rectangular strips that are clamped in a jig so that the sample folds over on itself at an angle of 180° producing stress within the specimen. Once loaded into the jig, the specimens are immediately exposed to the chemical environment under the required test conditions. The specimens are then inspected either visually or using an automatic inspection technique at set time intervals and the time required for 50% of the specimens to fail is noted.

Ball and pin impression: This test is used primarily for complex finished components. The method involves drilling a series of holes of a specific diameter into the polymer. A series of oversized balls or pins are inserted into the holes to induce a range of different stresses. One hour after the pins have been inserted, the specimens are immersed in the environment for 20 hours. The specimens are then dried and visually examined for crazes. The smallest ball to cause visible crazing is used to determine the ESC resistance of the polymer.

Constant tensile deformation: The test method involves applying a constant deformation to the specimen and monitoring the stress relaxation that occurs while it is immersed in the chemical environment. The test is repeated using progressively smaller levels ($1 > 5$) of deformation until the stress relaxation curves of consecutive tests superimpose on one another (Fig. 19.6). $S_0$ is the initial stress and $S$ is the stress at time $t$. The applied stress required to

© Woodhead Publishing Limited, 2010



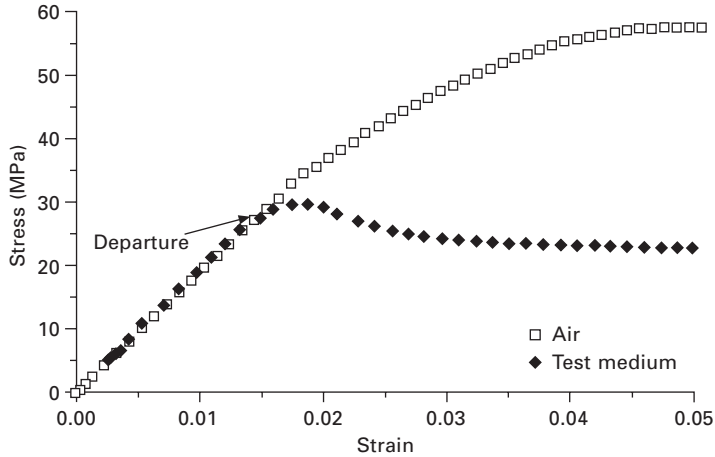

*19.6* Stress relaxation curves for progressively smaller levels of deformation (1 > 5) until consecutive curves superimpose on one another (4 and 5).

produce this level of deformation is defined as the critical stress. The ESC resistance of the material is determined by comparing the critical stress obtained in the environment to that obtained in air.

Slow strain rate testing: The test involves subjecting a specimen to a gradually increasing strain at a constant displacement rate whilst it is exposed to the chemical environment. The tests are conducted under uniaxial tension at low strain rates to enhance the influence of the environment on the specimen. Load and displacement are monitored continuously to enable stress–strain curves to be produced. The development of crazes within the specimen causes the strain to be taken up locally at the crazes, such that the stress required to deform the specimen is reduced compared to that in an inert environment. The onset of craze initiation can therefore be detected by the departure of the stress–strain curve in the chemical environment from that in air (see Fig. 19.7). The main advantages of the slow stain rate test are that it is relatively rapid, requires few specimens and can be automated.

Constant tensile stress test: The distinctive feature of this test is that a constant load is applied to the specimens, thereby avoiding the problem of stress relaxation that is found in the constant strain test methods. The technique involves subjecting the specimen under investigation to a constant tensile stress at a stress below the tensile yield stress of the polymer (see Fig. 19.8). This can be achieved in a number of ways including using a dead weight that is suspended from one end of the specimen, while the specimen is immersed in a cell containing the stress-cracking agent. The specimen is inspected at regular intervals to establish the onset of crazing. The time required for crazes/cracks to appear after the specimen has been exposed, or the threshold stress below which no crazes appear in a specific time period (typically 1000 h) can be used as a measure of the ESC resistance.

© Woodhead Publishing Limited, 2010




*19.7* Typical stress–strain plots for a polymer in air and in a test medium.



*19.8* Typical environmental cell used for the constant load test.

## 19.3.6 Artificial weathering

As the ultimate aim of accelerated ageing is to improve lifetime prediction under service conditions, the most appropriate conditions are those that match the service environment exactly. These are most easily obtained by naturally exposing specimens at outdoor exposure sites. The problem with

© Woodhead Publishing Limited, 2010

this approach is that the exposure period required would have to be at least as long as the life expectancy of the product, necessitating accelerated (artificial) weathering procedures that simulate the effects of natural weathering in realistic timescales.

The predominant factors in climatic exposure are humidity, temperature and solar (UV) radiation. The severity of these factors will depend on the geographical location and need to be taken into account when designing bonded structures. For marine applications, seawater and salt spray exposure also form part of the service environment. Accelerated weathering procedures (Broughton and Maxwell, 2007; Mitchell, 2004) generally involve cyclic exposure to a combination of salt spray, elevated and/or sub-zero temperatures and ultraviolet (UV) radiation. At present, there is no universally agreed performance-based specification for accelerated weathering. Performance-based specifications are being developed by a number of recognized standards bodies including BSI, ISO, NACE and customer end-users (e.g. Norsok). It is important to note that there is no 'foolproof' test that will provide an accurate prediction of service performance and life expectancy or that will accommodate the wide range of climatic conditions experienced geographically.

Artificial weathering involves exposing test specimens to an artificial UV light source in a cabinet in which the temperature, humidity and water spray are controlled. The problem with this approach is determining synergistic effects (interactions) between the different parameters in the weathering process. The key parameter in all accelerated weathering apparatus is the UV light source, which should ideally simulate solar radiation (see ASTM G 53). The main types of artificial light sources used are carbon-arc, xenon-arc and fluorescent tube (see ASTM D 1499, ASTM D 2565, ASTM D 4329 and ISO 4892).

Accelerated weathering standards tend to exclude the effect of the sub-zero temperatures that are often experienced in practice or in external exposure testing. When selecting a procedure for accelerated weathering, consideration should be given to including a sub-zero temperature excursion. A freeze cycle (–20°C for 24 h) has been included in ISO 20340 in an attempt to produce more realistic results. The inclusion of the freeze cycle has been shown to produce results much more typical of those seen in practice or in external exposure testing (Mitchell, 2004).

Weathering chambers: The conditioning chamber and support equipment (i.e. racking) is constructed from corrosion-resistant material (e.g. stainless steel). Specimens are supported within the test chamber using an open holding frame, which can be adjusted to allow double-sided or single-sided exposure. In order to simulate actual topside service conditions, only one surface is exposed to salt spray and UV radiation. A solid backing can be inserted into the holding frame for single-sided exposure. In addition to

© Woodhead Publishing Limited, 2010

controlling irradiance, the test chamber should have controlled temperature and, if required, controlled humidity. The chamber should also include facilities for the provision of salt spray or the formation of condensation on the specimen surfaces or for immersion of the specimens in water. Irradiance at any position in the area used for the specimen exposure should be at least 80% of the maximum irradiance. For some materials with high reflectivity, periodic repositioning of specimens is recommended to ensure uniformity of exposure (see ISO 4892).

### 19.3.7 Designing and planning an accelerated test programme

In order to conduct an effective accelerated test programme, it is essential to spend time designing and planning the test programme (Brown and Greenwood, 2002). The more consideration given to this process the more likely that the outcome of the exercise will meet expectations. The process is iterative and will need to be repeated several times in order to establish a programme that will meet budget and technical requirements. The test programme needs to be suitably flexible in case unexpected results or technical problems occur. It may be necessary in some cases for test parameters to be changed during the test programme. Short-term tests at high stress levels and high temperatures are generally set-up first to check the procedure and to identify technical issues that may not have been apparent prior to testing. It is often possible to establish the timescale of the longer term tests on the basis of these short-term results. This is important where measurements need to be completed within a set period of time, as specified in a number of standards.

Steps that need to be considered when designing, planning and managing an accelerated test programme (see Brown and Greenwood, 2002; ISO 11403) are:

- Define clearly the purpose and objectives of the test programme.
- Specify the service life that needs to be predicted and the level of uncertainty in life expectancy that is acceptable.
- Identify critical degradation agents and levels (e.g. temperature, humidity and pressure), which are often dependent on resources and time available.
- Consider environmental and safety issues in relation to handling, storage and disposal of chemicals.
- Consider specimens and products to be exposed.
- Define synergistic effects (e.g. humidity and temperature): establish requirements and whether or not conditions can be achieved.
- Monitor loading requirements and test parameters (e.g. temperature, salt concentration, humidity, pH level, displacement, load, etc.).

© Woodhead Publishing Limited, 2010

- Give detailed test conditions and specimen numbers to be tested per condition.
- Consider environmental and monitoring equipment requirements and include a contingency plan to allow for possible equipment failure.
- Undertake performance tests (destructive and non-destructive) on the conditioned material.
- Devise methods for analysing data and predictive model(s) for extrapolating short-term data to service conditions.
- Consider timing and sequencing of exposures.
- Ensure equipment, labour costs and time agree with budget and available timescale.
- Identify specimen/product machining and preparation requirements.

## 19.4 Modelling and predictive analyis

This section provides a brief overview of different modelling approaches including analytical modelling, stress analysis and fracture mechanics to predicting joint behaviour in hostile chemical environments. The use of finite element analysis (FEA) with different modelling approaches is also covered. For more details on the different models see Brown and Greenwood, 2002; Maxwell *et al.*, 2005.

### 19.4.1 Analytical models

Although a number of analytical models have been proposed for polymers, relating the rate of property change to the level of degrading agent, they tend to be used for comparative purposes and not for design, as there is no conclusive evidence of their universal validity. The Arrhenius equation is one of the best-known models for assessing the lifetime of polymers and is often used to predict the combined effects of temperature and time:

$$K(T) = A \exp\left(-\frac{E}{RT}\right) \qquad [19.16]$$

where, $K(T)$ is the reaction rate for the process (change of parameter with time), $E$ is reaction energy, $R$ is the gas constant, $T$ is absolute temperature and $A$ is an empirically derived constant. A plot of $K(T)$ against $1/T$ will often yield a straight line with a slope $E/R$, which can be extrapolated with caution. Various forms of this relationship have been used to relate the rate of strength degradation with the rate of fluid uptake (i.e. diffusivity) for adhesives and adhesive joints.

Correlation factors: An empirical approach uses simple algebraic expressions to relate loss of joint strength to the level of absorbed fluid (or degradation

© Woodhead Publishing Limited, 2010

agent) in the adhesive layer. This approach is usually only applicable to a narrow range of materials (i.e. material specific) and conditions. It is assumed that a simple relationship exists between the mechanical properties of the conditioned adhesive (or adhesive joint) and the mechanical properties of the unconditioned adhesive (or adhesive joint) as a function of time and temperature.

Extrapolation of accelerated test data: Mechanical, thermal and chemical properties of adhesives change during the service life of a bonded structure. Considerable timescales (months or years) are often involved, which for material qualification and design purposes is impractical. Hence the need for accelerated testing methods and prediction techniques that simulate long-term service conditions. The approach generally employed is to extrapolate the accelerated test data to service conditions, which is less demanding, using an acceleration factor (Kinloch, 1995). Mathematical functions that relate degradation, acceleration and time are often limited in their application. The effect of degradation differs between materials and different material properties. Degradation mechanisms are sensitive to small changes in the controlling parameters, such as temperature, stress and level of degradation agent. In addition, the interaction of degradation agents (i.e. synergistic effects) is generally not known with sufficient accuracy or certainty.

### 19.4.2 Stress analysis

In this approach, finite element modelling is carried out on the adhesive joint to determine the stress, strain and fluid distributions throughout the bonded structure as a function of time (coupled mechanical-diffusion analyses). An appropriate failure criterion is then applied to determine what is allowed in the design. A continuum-based FE model of the adhesive joint is appropriate when the adhesive has a finite thickness. The elastic and strength properties and stress–strain response of the adhesive and substrate materials can be measured experimentally and used directly for modelling purposes. Where the bondline is extremely thin, the macroscopic properties of the adhesive are not relevant directly and the analyst needs to resort to a fracture mechanics approach, which employs cohesive elements to model interfacial rupture (i.e. crack initiation and propagation), see Section 19.4.3.

The stress analysis approach seems to produce reasonable stiffness predictions (within 5% of measured values) and strength predictions, providing that failure is essentially the cohesive failure of the adhesive or adherend. Failure is dependent on a number of factors, including the adherend–adhesive system, surface treatment, and stress, fluid and temperature distributions within the structure. Interfacial or near interfacial failure makes this approach difficult to apply and usually results in a poor correlation between theoretical and experimental results.

© Woodhead Publishing Limited, 2010

### 19.4.3 Fracture mechanics

Adhesive joint failure can be considered to involve the initiation and propagation of naturally occurring (intrinsic) flaws or defects. These mechanisms can be described by fracture mechanics, thus providing a basis for estimating the fracture, fatigue and service life of joints. Fracture mechanics may be considered to be complimentary to stress-based approaches, which are useful in initial design. Generally, fracture mechanics might be applied once an initial joint geometry has been determined in order to provide a more detailed design assessment. It may also be used for damage tolerance calculations, which are required by certain design codes particularly for military applications. Two parameters are used to quantify crack growth behaviour: the stress intensity factor, $K$, which considers crack tip stresses and the strain energy release rate, $G$, which considers the energy required to create new crack surfaces.

The general approach is to relate the rate of crack growth, d$a$/d$t$, through the joint to the applied strain-energy release rate, $G$, or the stress intensity factor, $K$. This approach assumes a pre-existent crack of length, $a$, and uses FEA to determine the stress state in the vicinity of the crack tip. Although $K$ and $G$ can be related, the stress intensity method is less useful for adhesives, as $K$ values are more difficult to calculate, and is limited to linear–elastic behaviour. With the strain energy release rate method, the nonlinear effects of viscoelasticity and plasticity can be more readily accounted for in the analysis. In design analysis, $G$ can be used to assess the onset of fracture under extreme loads, the time for the onset of crack growth under static loads (creep failure) and the rate of crack growth under cyclic loads (fatigue failure). It is most commonly employed for the latter. Fracture toughness test data are experimentally obtained for mode I and mode II fracture under environmental conditions relevant to the bonded structure.

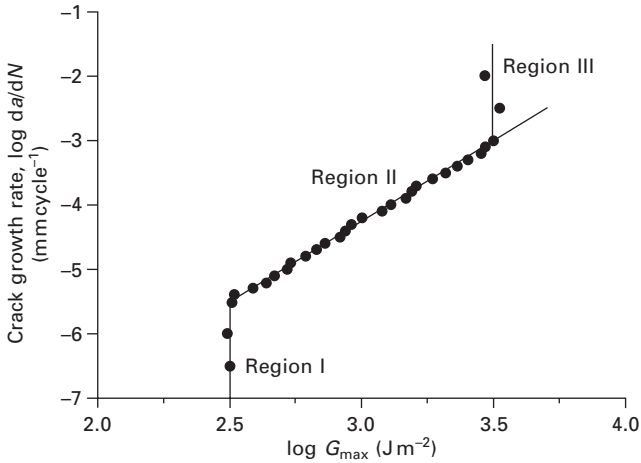
A form of the Paris equation (Broek, 1978) can be used to relate crack growth rate per loading cycle, d$a$/d$N$, to the maximum value of the applied strain energy release rate $G_{MAX}$ (Kinloch and Osiyemi, 1993):

$$\frac{da}{dN} = C(G_{MAX})^n \qquad [19.17]$$

where $C$ and $n$ are empirically determined constants dependent on the material system and environmental conditions. The above relationship applies only to the linear portion of the log–log plot of $G_{MAX}$ versus d$a$/D$N$ (Fig. 19.9). Two extreme levels of strain energy release rate are identified: high catastrophic or critical level $G_c$, at which rapid fracture occurs, and a low threshold level $G_{TH}$, below which low crack growth occurs.

The relationship between d$a$/d$N$ and $G_{MAX}$ can be described as follows (Ashcroft *et al.*, 1996: Fernlund *et al.*, 1994):

© Woodhead Publishing Limited, 2010




*19.9* Typical log–log crack growth rate versus $G_{MAX}$ plot. Region I – Threshold region ($G_{TH}$) is associated with low crack growth rate and $G_{MAX}$ values ($G_{TH} \approx 0.1\ G_C$). Region II – Linear region is defined by the Paris Law. Region III – Value of $G_{MAX}$ approaches the adhesive fracture toughness $G_C$ measured under monotonic loading conditions.

$$\frac{da}{dN} = C(G_{MAX})^n \left[ \frac{1 - \left( \frac{G_{TH}}{G_{MAX}} \right)^{n_1}}{1 - \left( \frac{G_{MAX}}{G_c} \right)^{n_2}} \right] \qquad [19.18]$$

where $G_{TH}$ is the minimum (or threshold) value of the adhesive fracture energy, $G_c$, and $C$, $n$, $n_1$ and $n_2$ are material constants. $G_c$ is determined from constant rate of displacement tests (i.e. monotonic fracture energy).

The main advantage of the fracture mechanics approach in design analysis is that geometry-independent results are generated from the laboratory tests. The strain energy release rate $G$ is measured from the test specimens during cyclic fatigue testing, together with the associated crack growth rates d$a$/d$N$. Crack growth testing is performed over a range of $G$ values including the threshold value, the $G$ value below which negligible crack growth would ever be expected (see http://www.adhesivestoolkit.com/Introduction.xtp). The threshold value can itself be used during joint design as a limiting criterion, whereby the designer limits the maximum $G$ value within the joint to or below the measured threshold value. This would be classed as a damage-intolerant design. If a damage-tolerant system is acceptable, the designer can predict the expected life of the component by applying the measured crack growth model.

Fracture mechanics can be implemented in FEA through the use of cohesive elements and traction-separation based modelling. This general

© Woodhead Publishing Limited, 2010

framework allows the combination of several damage mechanisms to act simultaneously on the same material. Each failure mechanism consists of a damage initiation criterion, a damage evolution law and a choice of element removal upon reaching the completely damaged state. Damage initiation refers to the commencement of degradation of the response of a material point. The process of degradation begins when the stresses and/or strains satisfy certain specified damage initiation criteria. This will be dependent on fluid concentration at the material point; material properties will be dependent the fluid concentration. Damage initiation criteria can be used to evaluate the propensity of the material to undergo damage. The damage evolution law describes the rate at which material stiffness is degraded once the corresponding initiation criterion is reached (including the effects of mechanical, thermal and chemical degradation mechanisms). A scalar damage variable, $D$, which has an initial value of zero and evolves towards one, is used to represent the overall damage.

At any given time during analysis the stress tensor in the material is given by the scalar damage equation:

$$\sigma = (1 - D\overline{\sigma}) \qquad [19.19]$$

where $D$ is the overall damage variable and $\overline{\sigma}$ is the effective (or undamaged) stress tensor (i.e. stresses that would exist in the absence of damage). The overall damage variable captures the combined effect of all active mechanisms and is computed in terms of individual damage variables, in accordance with damage evolution laws associated with each damage mechanism. The cohesive element is removed from the mesh when $D = 1$ for all material points within the element (i.e. lost its load-carrying capacity). Once removed, cohesive elements offer no resistance to subsequent penetration of the surrounding components. Cracks are restricted to propagating along the layer of cohesive elements in a self-similar manner.

## 19.5 Optimizing chemical resistance of adhesive joints

It is important to define accurately the environmental conditions which the adhesive joint must withstand and to select an adhesive capable of operating under these conditions with no adverse effects. Factors to be considered include the chemical species present in the service environment, the operating temperature and pressure, mechanical loading conditions and expected duration (i.e. service life) of exposure in the chemical environment. This should include any chemicals used in maintenance activities. The resistance of adhesive joints to chemicals and organic solvents can be improved by chemically modifying the adhesive to reduce fluid permeation. Including inert fillers and additives, or increasing the crystalline phase (thermoplastic

© Woodhead Publishing Limited, 2010

adhesives) will lower the volume of adhesive that can be influenced by chemical or solvent ingress. Adhesives containing protective additives, such as corrosion inhibitors, antioxidants, UV stabilizers and antimicrobials are available and users are advised to discuss their industrial requirements with adhesive manufacturers/suppliers.

The next step is to select a surface treatment that will ensure the long-term durability of the adhesive joint under the service conditions. Surface preparation is recognized as a critical step in the adhesive bonding process and no matter how well a joint is designed if the surface preparation is inadequate the joint will not survive, particularly in hostile conditions. Correct surface preparation is essential for good joint strength and to maintain the long-term structural integrity of bonded joints. Unsatisfactory surface preparation will result in the bond failing adhesively and unpredictably at the interface. The adherend should also be protected with a suitable primer or chemically treated to improve adhesion and protect the interface from the permeation of chemical species. Surface treatments should be applied just before bonding to ensure maximum effectiveness. It is generally assumed that by maximizing moisture resistance, the resistance to attack from other chemical agents is also maximized.

For a given adhesive type and surface treatment, the durability of adhesive bonds depends on the permeability of the adhesive to the chemical agents present in the surrounding environment. Steps need to be taken to ensure that permeation is minimized. Increasing the fluid content in a bonded structure results in a reduction in mechanical performance (i.e. stiffness, strength, and static and cyclic fatigue resistance) whose effect is accelerated at elevated temperatures or in the presence of applied stress.

The basic rules of good design of adhesive joints apply to most loading and environmental conditions. For example, thickening the adhesive at the ends of the bondline using large adhesive fillets or internal tapering can reduce peel and shear stresses in these regions, thus improving creep and fatigue performance. It also provides added protection against environmental attack. Increasing the bondline spreads strain over a larger volume, resulting in lower strain in the adhesive and therefore a lower stress concentration. The presence of residual stresses induced by resin shrinkage and thermal mismatch between adherends and the adhesive pose a problem since complete removal is practically impossible. The presence of residual stresses will lower the adhesives resistance to ESC. Residual stresses can be minimized through good design and by optimizing the processing conditions.

An important way of improving the chemical resistance of an adhesive joint is to increase the bond area. A large bond area will guarantee a longer period of time before the chemical species can fully diffuse through the adhesive joint. Minimizing the exposed surface area of the adhesive to the surrounding environment will also contribute to improved chemical resistance.

© Woodhead Publishing Limited, 2010

The presence of flaws or porosity in the adhesive or at the interface will promote chemical ingress.

Note that there will still be a need to test entire substructures under end-use service conditions for safety conformance purposes, although the amount of data required from coupon testing should decrease with improvements in predictive modelling.

## 19.6 Future trends

Fracture mechanics is proving a useful tool for predicting the structural performance of adhesively bonded joints, particularly with the development of adaptive meshing and cohesive zone damage modelling approaches, which combine continuum mechanics and fracture energy. Future developments can be expected to include the effects of chemical degradation of the adhesive and interfacial properties in modelling static and dynamic performance of bonded structures. The use of fracture mechanics should eliminate the need for the large databases that are required when using stress-based FEA.

Molecular modelling should lead to improved predictive analysis of material behaviour, thus enabling designers and engineers to predict material performance prior to mechanical assessment. It may be possible to synthesize polymer molecules and their interactions with different chemicals and solvents using this approach, thereby eliminating a considerable amount of testing involved in evaluating the efficacy of the adhesive and different additives (antioxidants, thermal stabilizers, UV stabilizers, etc.) in test environments.

Hansen solubility parameters potentially provide a means of rapid chemical resistance evaluation of adhesive systems or at least useful information regarding the behaviour of adhesive systems (including additives) in a chemical reagent environment. This approach could be used in conjunction with combinatorial analysis and statistical 'design of experiments (DOE)' to evaluate the effects of concentration levels and temperature on chemical resistance. Combinatorial analysis and DOE can also be used to assess surface treatments and joint design.

Novel measurement techniques, such as nanoindentation, nanoscratch, atomic force microscopy (AFM) and scanning electrochemical microscopy are being assessed as methods of characterising interfacial properties. These methods potentially offer rapid and/or low cost alternatives to mechanical testing for quality assurance (production) and environmental degradation assessment. It should be possible to miniaturize tests to enable rapid material selection and development and to accelerate tests reducing the need for large and time-consuming test programmes. No single ideal or universally applicable interfacial measurement method exists that can provide quantitative data for engineering or design purposes. Future developments are expected to include

© Woodhead Publishing Limited, 2010

embedded sensors, such as fibre Bragg gratings, to monitor the chemical and structural integrity of bonded structures from 'cradle-to-grave'. Real-time chemical sensors for monitoring *in situ* moisture, pH, and ionic or organic (e.g. processing) species in engineering structures should be possible.

## 19.7 Sources of further information and advice

Further information and advice on various aspects of adhesive technology including chemical resistance can be obtained by accessing the following websites.

http://www.adhesivestoolkit.com/Toolkits/AdhesiveSelector/Introduction.xtp
http://www.ascouncil.org/
http://www.astm.org/
http://www.basaonline.org/
http://www.bpf.co.uk
http://www.bsigroup.com/en/Standards-and-Publications/
http://www.engineeringtoolbox.com
http://www.materialssolutions.info/
http://iom3.org
http://www.iom3.org/content/society-adhesion-adhesives
http://www.iso.org/iso/iso_catalogue.htm

## 19.8 Acknowledgements

The background information included in this chapter owes considerable debt to a series of research programmes funded by the United Kingdom Department of Business, Innovation, and Skills (National Measurement System Policy Unit). This chapter has also benefited from the technical support and advice provided by my colleagues Dr Louise Crocker, Dr Greg Dean, Mr Bruce Duncan and Dr Tony Maxwell at the National Physical Laboratory and Mr John Bishopp (Star Adhesion Limited). The author gratefully acknowledges their contributions.

## 19.9 References

Arnold, J.C. (1996). 'Environmental stress crack initiation in glassy polymers', *Trends in Polymer Science*, **4**, 403–8.

Arrowsmith, D.J. and Madison, A. (1987). 'The use of perforated lap shear specimens to test the durability of adhesive-bonded aluminium', *International Journal of Adhesion and Adhesives*, **23**, 15–24.

Ashcroft, I.A., Gilmore, R.B. and Shaw, S.J. (1996). 'Cyclic fatigue and environmental effects with adhesively bonded joints', *AGARD 83rd SMP Meeting*, Florence, Italy.

© Woodhead Publishing Limited, 2010

ASM International (1990). 'Adhesives and sealants', *Engineered Materials Handbook*, Volume 3, ASM International, Ohio, USA.

Bishopp, J.A. (2005). 'Surface pretreatment for structural bonding, *HandBook of Adhesives and Sealants*, Volume 1, Cognard, P. (ed.), Elsevier, Amsterdam, 163–214.

Broek, D. (1978). *Elementary Engineering Fracture Mechanics*, Sijthoff and Noordhoff, The Netherlands.

Broughton, W.R. and Maxwell, A.S. (2007). 'Accelerated environmental ageing of polymeric materials', *NPL Measurement Good Practice Guide*, No. 103, National Physical Laboratory, Teddington, United Kingdom.

Brown, R.P. and Greenwood, J.H. (2002). *Practical Guide to the Assessment of Useful Life of Plastics*, RAPRA Technology Limited, Shropshire, UK.

Campo, A. (2007). *Selection of Polymeric Materials: How to Select Design Properties from Different Standards*, PDL Handbook Series, William Andrew, New York.

Chanda, M. and Roy, S.K. (2009). *Plastics Fundamentals, Properties and Testing,* Plastics Engineering Series, CRC Press, Taylor & Francis Group, Abingdon, UK.

Cognard, P. (2005). 'Technical characteristics and testing methods for adhesives and sealants', *Handbook of Adhesives and Sealants*, Volume 1, Chapter 2, Cognard, P. (ed.), Elsevier, Amsterdam.

Comyn, J. (ed.), (1994). *Polymer Permeability*, Chapman and Hall, London, UK.

Doyle, G. and Pethrick, R.A. (2009). 'Environmental effects on the ageing of epoxy adhesive joints', *International Journal of Adhesion and Adhesives*, **29**(1), 77–90.

Duncan, B.C. and Broughton, W.R. (2007). *Absorption and Diffusion of Moisture in Polymeric Materials*, NPL Measurement Good Practice Guide No. 102, National Physical Laboratory, Teddington, United Kingdom.

Duncan, B., Urquhart, J. and Roberts, S. (2005). *Review of Measurement and Modelling of Permeation and Diffusion in Polymers*, NPL Report DEPC MPR 012, National Physical Laboratory, Teddington, United Kingdom.

Fernlund, G., Papini, M., McCammond, D. and Spelt, J.K. (1994). 'Fracture load predictions for adhesive joints', *Composites Science and Technology*, **51**, 587–600.

Greenwood, J.H. (1997). *Life Prediction in Polymers*, ERA Technology Report No. 97-0782R.

Hansen, C.M. (2000). *Hansen Solubility Parameters: A User's Handbook*, CRC Press LLC, Boca Raton, FL.

Jost, W. (1960). *Diffusion in Solids, Liquids and Gases*, Academic Press, New York.

Kinloch, A.J. (1987). *Adhesion and Adhesives – Science and Technology*, Chapman and Hall, London.

Kinloch, A.J. (1995). *Predicting the Lifetime of Adhesive Joints in Hostile Environments*, MTS Adhesive Programme, Project 3: Environmental Durability of Adhesive Bonds, Report No. 5, ESR Technology (formerly AEA Technology), Harwell, United Kingdom.

Kinloch, A.J. and Osiyemi, S.O. (1993). 'Predicting Fatigue Life of Adhesively-Bonded Joints', *Journal of Adhesion*, **43**, 79–90.

Maxwell, A.S. and Pilkington, G. (2008). 'Prediction of environmental stress cracking resistance in polyethylenes', *Polymer Engineering and Science*, **48**, 360–4.

Maxwell, A.S., Broughton, W.R., Dean, G.D. and Sims, G.D. (2005). *Review of Accelerated Ageing Methods and Lifetime Prediction Techniques for Polymeric Materials*, NPL Report DEPC MPR 016, National Physical Laboratory, Teddington, United Kingdom.

Mitchell, M.J. (2004). 'Testing of offshore systems – is there a realistic testing scenario

© Woodhead Publishing Limited, 2010

or is there still work to be done', *Proceedings of NACE 2004 Corrosion Conference, Progress in Offshore Coatings*, New Orleans, USA.
Packham, D.E. (2005). *Handbook of Adhesion*, 2nd edition, John Wiley and Sons, Chichester, West Sussex, UK.
Parvatareddy, H., Dillard, J.G., McGrath, J.E. and Dillard, D.A. (1999). 'Solvent effects on high temperature polyimides and their bonded joints', *Journal of Adhesion*, **69**, 83–98.
Petrie, E.M. (2007). *Handbook of Adhesives and Sealants*, 2nd edition, McGraw-Hill Handbooks, New York.
Rider, A. and Yeo, E. (2005). *The Chemical Resistance of Epoxy Adhesive Joints Exposed to Aviation Fuel and its Additives*, Report No. DSTO-TR-1650, Defence Science and Technology Organisation Platforms Sciences Laboratory, Fishermans Bend, Victoria, Australia.
Shen, C.H. and Springer, G.S. (1976). 'Moisture absorption and desorption of composite materials', *Journal of Composite Materials*, **10**, 2–20.
Storm, B.K., Gwisdalski, M., Lindvang, D. and Rann, M. (2005). 'Investigation of degradation of structural adhesives under influence of chemicals', *Macromolecular Symposia*, **225**(1), 205–19.
Turnbull, A. and Maxwell, A.S. (1999). 'Test methods for environment stress cracking of polymeric materials', *National Physical Laboratory Technical Review*, **3**, 1999.
Wright, D.C. (1996). *Environmental Stress Cracking of Plastics*, RAPRA Technology, Shropshire, UK.
Wylde, J.W. and Spelt, J.K. (1998). 'Measurement of adhesive joint fracture properties as a function of environmental degradation', *International Journal of Adhesion and Adhesives*, **18**, 237–46.
Wypych, G. (2008). *Handbook of Materials Weathering*, 4th edition, ChemTec Publishing, Ontario, Canada.

## 19.10 Appendix: Standards

### 19.10.1 ISO Standards

*Thermal degradation*

| | |
|---|---|
| ISO 176 | *Determination of Loss of Plasticisers – Activated Carbon Method* |
| ISO 177 | *Plastics – Determination of Migration of Plasticiser* |
| ISO 291 | *Plastics – Standard Atmospheres for Conditioning and Testing* |
| ISO 305 | *Determination of Thermal Stability of Polyvinyl Chloride Related Chlorine Containing Polymers, and their Compounds – Discoloration Method* |
| ISO 554 | *Standard Atmospheres for Conditioning and/or Testing – Specification* |
| ISO 1137 | *Plastics: Determination of Behaviour in a Ventilated Tubular Oven* |
| ISO 1599 | *Cellulose Acetate – Determination of Viscosity* |

© Woodhead Publishing Limited, 2010

| | |
|---|---|
| ISO 2578 | *Plastics: Determination of Time/Temperature Limits after Exposure to Prolonged Action of Heat* |
| ISO 3205 | *Preferred Test Temperatures* |
| ISO 3671 | *Determination of Volatile Matter of Amino-plastics Moulding Materials* |

*Environmental stress cracking (ESC)*

| | |
|---|---|
| ISO 4599 | *Plastics – Determination of Resistance to Environmental Stress Cracking (ESC) – Bent Strip Method* |
| ISO 4600 | *Plastics – Determination of Environmental Stress Cracking (ESC) – Ball and Pin* |
| ISO 6252 | *Plastics – Determination of Resistance to Environmental Stress Cracking (ESC) – Constant Tensile Stress Method* |
| ISO 16770 | *Plastics – Determination of Environmental Stress Cracking (ESC) of Polyethylene – Full-Notch Creep Test (FNCT)* |
| ISO 22088 | *Plastics – Determination of Resistance to Environmental Stress Cracking (ESC)* |

*Effect of liquids*

| | |
|---|---|
| ISO 62 | *Plastics – Determination of Water Absorption* |
| ISO 175 | *Plastics – Determining the Effect of Liquid Chemical Including Water* |
| ISO 483 | *Plastics – Small Enclosures for Conditioning and Testing Using Aqueous Solutions to Maintain Relative Humidity at Constant Value* |
| ISO 4611 | *Plastics – Determination of the Effect of Exposure to Damp Heat, Water Spray and Salt* |

*Weathering*

| | |
|---|---|
| ISO 877 | *Plastics – Determination of Resistance to Change upon Exposure under Glass to Daylight* |
| ISO 2579 | *Plastics – Instrumental Evaluation of Colour Differences* |
| ISO 3557 | *Plastics – Recommended Practice for Spectrophotometry and Calculation of Colour in CIE Systems* |
| ISO 3558 | *Plastics – Assessment of the Colour of Near-White or Near-Colourless Materials* |
| ISO 4582 | *Plastics – Determination of Changes in Colour and Variations in Properties after Exposure to Daylight under Glass, Natural Weathering or Laboratory Light Sources* |
| ISO 4607 | *Plastics – Methods of Exposure to Natural Weathering* |

© Woodhead Publishing Limited, 2010

| | |
|---|---|
| ISO 4892 | *Plastics – Methods of Exposure to Laboratory Light Sources* |
| ISO 9370 | *Guide for the Instrumental Determination of Radiant Exposure in Weathering Tests* |
| ISO TR 9673 | *Solar Radiation and its Measurements for Determining Outdoor Weather Exposure Levels* |
| ISO 11403-3 | *Environmental Influences on Properties* |
| ISO 20340 | *Paints and Varnishes – Performance Requirements for Protective Paint Systems for Offshore and Related Structures* |

*Biological attack*

| | |
|---|---|
| ISO 846 | *Plastics – Evaluation of the Action of Micro-organisms* |

*Mechanical (creep)*

| | |
|---|---|
| ISO 899 | *Plastics – Determination of Creep Behaviour* |

### 19.10.2 ASTM Standards

*Thermal degradation*

| | |
|---|---|
| D 1151 | *Standard Practice for Effect of Moisture and Temperature on Adhesive Bonds* |
| D 1203 | *Standard Test Methods for Volatile Loss From Plastics Using Activated Carbon Methods* |
| D 3045 | *Standard Practice for Heat Aging of Plastics Without Load* |

*Environmental stress cracking (ESC)*

| | |
|---|---|
| D 1693 | *Environmental Stress Cracking of Ethylene Plastics* |
| D 3929 | *Standard Test Method for Evaluating Stress Cracking of Plastics by Adhesives Using the Bent Beam Method* |
| F 1248 | *Determination of Environmental Stress Crack Resistance (ESCR) of Polyethylene Pipe* |

*Ageing*

| | |
|---|---|
| D 1183 | *Standard Practices for Resistance of Adhesives to Cyclic Laboratory Aging Conditions* |
| D 2295 | *Standard Test Method for Strength Properties of Adhesives in Shear by Tension Loading at Elevated Temperatures (Metal-to-Metal)* |

© Woodhead Publishing Limited, 2010

| | |
|---|---|
| D 2918 | *Standard Test Method for Durability Assessment of Adhesive Joints Stressed in Peel* |
| D 2919 | *Standard Test Method for Determining Durability of Adhesive Joints Stressed in Shear by Tension Loading* |
| D 3632 | *Standard Test Method for Accelerated Aging of Adhesive Joints by the Oxygen-Pressure Method* |
| D 3762 | *Standard Test Method for Adhesive-Bonded Surface Durability of Aluminium (Wedge Test)* |
| D 4498 | *Standard Test Method for Heat-Fail Temperature in Shear of Hot Melt Adhesives* |

*Effect of fluids*

| | |
|---|---|
| D 543 | *Standard Practices for Evaluating the Resistance of Plastics to Chemical Reagents* |
| D 986 | *Standard Practice for Resistance of Adhesive Bonds to Chemical Reagents* |
| D 570 | *Standard Test Method for Water Absorption of Plastics* |
| D 1653 | *Standard Test Method for Water Vapour Transmission of Organic Coating Films* |
| D 1712 | *Standard Practice for Resistance of Plastics to Sulfide Staining* |
| E 96 | *Standard Test Methods for Water Vapour Transmission Rate of Materials* |

*Weathering*

| | |
|---|---|
| D 1435 | *Standard Practice for Outdoor Weathering of Plastics* |
| D 1499 | *Standard Practice Filtered Open-Flame Carbon-Arc Type Exposures of Plastics* |
| D 2565 | *Standard Practice for Xenon Arc Exposure of Plastics Intended for Outdoor Applications* |
| D 4329 | *Standard Practice for Fluorescent UV Exposure of Plastics* |
| D 4364 | *Standard Practice for Performing Outdoor Accelerated Weathering Tests of Plastics Using Concentrated Sunlight* |
| G 24 | *Standard Practice for Conducting Exposures to Daylight Filtered Through Glass* |
| G 53 | *Standard Practice for Operating Light-and Water-Exposure Apparatus (Fluorescent UV-Condensation Type) for Exposure of Nonmetallic Materials* |
| G 156 | *Standard Practice for Selecting and Characterizing Weathering Reference Materials Used to Monitor Consistency of Conditions in an Exposure Test* |

© Woodhead Publishing Limited, 2010

| | |
|---|---|
| G 178 | *Standard Practice for Determining the Activation Spectrum of a Material (Wavelength Sensitivity to an Exposure Source) Using the Sharp Cut-On Filter or Spectrographic Technique* |

*Biological and high energy radiation*

| | |
|---|---|
| D 1879 | *Standard Practice for Exposure of Adhesive Specimens to High Energy Radiation* |
| G 21 | *Standard Practice for Determining Resistance of Synthetic Polymeric Materials to Fungi* |

*Mechanical (creep)*

| | |
|---|---|
| D 1780 | *Standard Practice for Conducting Creep Tests of Metal-to-Metal Adhesives* |
| D 2290 | *Standard Test Methods for Tensile, Compressive, and Flexural Creep and Creep-Rupture of Plastics* |
| D 2293 | *Standard Test Method for Creep Properties of Adhesives in Shear by Compression Loading (Metal-to-Metal)* |
| D 2294 | *Standard Test Method for Creep Properties of Adhesives in Shear by Tension Loading (Metal-to-Metal)* |

© Woodhead Publishing Limited, 2010

# Index


AA 2024 T3, 212
  vs GLARE fatigue crack growth, 216
AA 7075-T6, 212
ABAQUS, 376
AC-130, 205
AC TECH, 205
accelerated conditioning, 592–3
accelerated testing, 548–52
accelerators, 115
acetic acid, 581
acetyl phenylhydrazine, 99, 105
acids, 581
acoustic emission, 423
acrylic, 579
  anaerobic, 7
  reactive, 6, 10
  toughened, 6–7, 12
acrylic adhesives
  advances, 132–50
    advanced technologies, 135–6
    cure systems, 133–4
    first and second generation, 135
    future trends, 149–50
    historical evolution, 133
    manufactures, 149
  advantages/disadvantages and unique characteristics, 140–4
    cure profile comparison, 142
    formulation variables, 140–2
    potential formulating variables, 141
  applications, 145–8
    boat stringer bonding, 146–7
    bonding low energy surfaces, 148
    heavy truck assembly, 147
    marine and wind blade thick gap bonding, 148
    school bus assembly, 147–8
    thermoplastic bumpers, 145–6
  classification, 137–40
    elastomer modified methyl methacrylate-based, 137–8
    non-methyl methacrylate, 138–40
    polymer blends as modifiers, 140
  structural methacrylates
    advantages, 142–4
    disadvantages, 144
adaptive meshing, 431
addition cure chemistry, 72–3
  formulation ingredients and their functions, 75
adherend flexibility, 372–3
adherend thickness, 274–5
adhesion, 237
  performance, 237
  promoters, 78, 115–16
Adhesive and Sealant Council, 18
adhesive bonding, 265, 295
  assessment and improvement in wet conditions, 547–67
    future trends, 567
  chemical agents and degradation mechanisms, 575–87
    adhesive families chemical resistance, 578
    biological degradation, 586–7
    chemical environments effect on Redux 319, 579
    craze formation, 582
    environmental stress cracking, 581–3
    high-energy radiation, 585–6
    typical time-dependent creep rupture curve, 583




© Woodhead Publishing Limited, 2010

weathering and photooxidation, 583–5
chemical resistance testing, 587–602
accelerated conditioning and testing, 592–3
accelerated test programme design and planning, 601–2
artificial weathering, 599–601
constant load test environmental cell, 599
creep-rupture testing, 594–6
deformation stress relaxation curves, 598
diffusion kinetics and solubility, 588–92
environmental stress cracking, 596–8
Fickian diffusion curve, 590
stress-strain plots for polymer, 599
tensile creep fixtures, 595
effect of adhesives Young's modulus ratio
mixed adhesive double lap joints, 538
mixed adhesive single lap joints, 538
experimental failure load
Redux 326 DLJs and Supreme 10HT double lap joints, 534
titanium/composite double lap joints, 536
titanium/titanium double lap joints, 536
high and low temperature applications, 516–41
adhesive shear curves, 526
adhesive shrinkage, 517–18
composite specimens dynamic flexural modulus, 525
differential thermal expansion effect, 518–22
experimental failure load, 534
experimental joint strength results, 532–4
future trends, 540–1
glass transition temperature, 524
Hart-Smith's close form analysis vs finite element analysis, 529
key problems, 516–17
load transfer and shear stress distribution, 540
maximum overall adhesive shear stress transition, 539
mixed adhesive joint concept, 535
modelling temperature conditions, 528–30
overlap ends stiffening in mixed adhesive joint, 539
sandwich specimens for stress-free temperature determination, 521
shear stresses in metal/composite double lap joint, 521
stresses in adherends, 520
temperature effect on adhesive properties, 522–8
thermal boundary conditions, 531
thermal elastic strain data treatment procedure, 523
thermal model and thermal resistance diagram, 531
typical coefficients of thermal expansion, 518
improvement in hostile chemical environments, 574–609
future trends, 608–9
optimising adhesive joints chemical resistance, 606–8
modelling and predictive analysis, 602–6
analytical models, 602–3
fracture mechanics, 604–6
log-log crack growth rate vs SERR maximum value, 605
stress analysis, 603
optimising adhesive bonds techniques, 534–9, 559–66
bonded joint design considerations, 566
bulk adhesive properties modification, 562
engineering novel biological adhesives, 564–6
silane molecules, 561
surface pre-treatment routes, 559–62
testing and modelling in wet conditions, 548–58
accelerated ageing and testing, 548–52

© Woodhead Publishing Limited, 2010

adhesive fracture energy and crack velocity, 551
coefficient of diffusion calculated values, 559
dry polymer film surface AFM images, 558
interfacial vs bulk water concentrations, 557
interfacial water distribution and diffusion, 553–8
non-destructive test methods, 552–3
water concentration profile schematic, 554
adhesive joints
aerospace, 499–503
aircraft fatigue tracking, 502–3
combining adhesives with rivets and bolts, 500
designing for fatigue and creep, 499–500
environmental degradation, 501–2
lap shear joints average fatigue life, 501
automotive, 503–9
adhesive and hybrid joints, 504–5
bonded aluminium U shape test piece, 506
bonds degradation testing, 508–9
constant and variable amplitude loading, 506–7
cyclic stress testing, 507–8
design and analysis approaches, 505–6
full car body structure durability testing, 504
joint quality monitoring in production, 509
multi-station fatigue testing apparatus, 509
riv-bonded aluminium U shape testpiece, 508
case study in use of joint tests, 424–30
cryogenic liquid containment system, 424–8
using T joints to validate materials models, 428–30
creep, 484–97
crack growth and time-dependent fracture mechanics, 494–5
crack propagation rate, 496
creep compliance time-temperature superposition, 493
four element linear viscoelastic model, 491
Kelvin-Voigt model, creep and recovery curves, 488
Maxwell model, 489
schematic constant stress and temperature creep curve, 484
temperature and absorbed moisture effect, 492–4
time-dependent material models, 487
current and emerging types of testing, 392–410
compression tests, 410
shear tests, 393–400
tension and peel tests, 401–9
designing for fatigue and creep load conditions, 469–511
creep-fatigue interactions, 497–8
future trends, 510–11
developments in testing, 389–432
failure detection, 421–4
fracture energy acoustic emission, 423
non-destructive fracture detection, 424
shape of force–extension curve, 421
strain mapping techniques, 423–4
visual inspection, 422–3
fatigue, 472–84
bonded lap joints load-life curve, 476
constant stress amplitude, 473
crack growth curve, 481
creep analysis applications, 499–510
damage mechanics, 483
extended L-N diagram, 477
fracture mechanics approach, 480–3
mechanical testing, 474–5
normalised non-linear strength wearout model, 480
spectra, 473–4
strength and stiffness wearout, 479
total life approach, 475–8
future trends, 431–2
preparation fixture for controlling fillet during manufacture, 411

© Woodhead Publishing Limited, 2010

role of testing, 389–92
design and verification, 391–2
process and material screening, 390
quality assurance, 390
specimen manufacture issues, 410–15
alignment and jigging during fabrication, 411–12
bondline thickness, 414–15
curing, 412–14
end effects, 415
surface preparation, 412
test variables, 415–21
strain and displacement measurement techniques, 416–20
test conditions, 421
test machine and specimen alignment, 415–16
adhesive primers, 206
adhesive sandwich, 591
adhesive sealants *see* silicone
adhesively bonded composites
advances in testing, 437–64
future trends, 463–4
composite assemblies characterisation, 456–63
bonding fixture, 456
different multidirectional composites analysis, 463
edge effect, 459
equivalent stress maximum value, 460
experimental fixture, 456
geometry, 457
industrial applications, 461–3
mainsail rail and mechanical fasteners, 462
mixed bonded assembly experimental fixture, 457
numerical simulations model, 458
shear loadings experimental results, 461
stress distribution numerical analysis, 456–8
tensile loading for straight edges, 460
tensile loadings experimental results, 462
tensile-shear loadings experimental results, 462
UD carbon/epoxy composite experimental results, 460–1
geometric parameters
influence in carbon/epoxy substrates, 445
influence in glass/epoxy substrates, 444
modified Arcan test, 449–56
Arcan fixture and geometry of substrates with beak, 450
epoxy adhesive failure envelope, 454–6
influence of geometry and loading, 453
model and different geometries near joint edge, 451
numerical validation, 451–4
shear distribution for geometry, 452
tension–shear tests results for monotonic loadings, 455
test development, 449
results from traditional tests, 439–49
bonded carbon/epoxy lap shear tests, 442
bonded glass/epoxy lap shear tests, 439–40
carbon/epoxy lap shear specimen details, 442
damage within specimen before final failure, 441
glass/epoxy lap shear specimen details, 440
glass/epoxy single lap shear specimen, 439
overlap length influence on failure load, 441
single lap shear specimen geometry, 443
single lap shear tests with emission recording, 441
stress distribution on adhesive joint and composite substrate, 446–7, 448
stress distributions numerical analyses, 442–9
state of the art, 438–9
composite design, 438
testing bonded composite assemblies, 438–9

© Woodhead Publishing Limited, 2010

adhesives
chemistry, 4–10
anaerobic acrylic, 7
cyanoacrylate, 7–8
epoxy, 5–6
other systems, 8–9
polyurethane, 6
reactive acrylic, 6
silicone, 8
solvent cements, 9–10
toughened acrylic, 6–7
key issues in selection, 3–19
aesthetics, 16
cure mechanism, 11–12
end of life requirements, 16
form and structure, 10–11
future trends, 18–19
Internet provision, 17–18
joint design, 14
joint function and operating environment, 13–14
manufacturing demands, 14
quality control, 14–15
substrate compatibility, 12–13
surface pre-treatment, 13
testing and evaluation, 15
selector software, 16–17
stand-alone systems, 16–17
Adhesives Design Toolkit, 18
adsorption theory, 240–3
primary bond formation, 241
secondary bond formation, 241–2
AFM *see* atomic force microscopy
ageing, 548–52
Air Products and Chemicals, 77
Airbus A380, 29, 215, 220
Ajicure PN-23, 108
Alclad 2024-T3, 579
alkyl 2-cyanoacrylate, 111
alkyl 2-cyanopentadienoate, 121
alkyl trithiadiazapentalenes, 107
allyltriphenylphosphonium bromide, 107
Alteco, 124
aluminium, bonding improvements, 185–229
aluminium alloys
surface treatment, 196–200
anodising processes, 199–200
CAA oxide electron micrograph, 199
chromium-free anodising treatments, 200
conversion coatings, 200
etching processes, 197–8
methods overview, 197
American Cyanamid, 28
American Sealants Company, 97
AMRL Melbourne, 205
anaerobic adhesives, 7
advances, 96–110, 126–7
breakaway and breakloose testing configuration, 98
metals standard electrode potential, 101
monomer and resin suppliers, 99
chemistry, 98–103
proposed redox initiation system, 100
urethane block copolymers preparation, 102
future trends
products with improved physical properties, 127
sustainable products, 127
recent developments in technology, 103–10
accelerated cure speed, 108, 110
anhydride coreactants with phenylhydrazine, 106
APH vs SPH breakaway strength, 106
breakaway and breakloose strength comparison, 105
dental applications, 110
new curatives, 103–7
semi-solid anaerobic adhesives and controls formulations, 104
semi-solid form, 103
surface insensitive, 107
thermal resistance, 108
tensile shear strength comparison
magnesium lapshear specimens with and without ATPB, 108
magnets bonded to epoxy steel with Chartwell B545, 110
steel lapshear specimens with Ajicure PN-23, 109
steel lapshear specimens with and without DABPA, 109
Anaerobic Permafil, 96, 97

© Woodhead Publishing Limited, 2010

anhydrides, 123
anodising process, 199–200, 204
  brush, 205
Ansys 11.0 finite element environment, 334
Ansys environment, 340
APH *see* acetyl phenylhydrazine
apparent diffusion, 589
Appendix of Standards, 611–15
Arall, 29
Aramid Reinforced Aluminium Laminates, 213
Arcan fixture, 449
aromatic isocyanates, 49
Arrhenius equation, 602
Arrhenius relationship, 591
artificial weathering, 599–601
ASTM, 389
ASTM 647-00, 338
ASTM B117, 203
ASTM D 903, 406
ASTM D 1002, 394
ASTM D 1062, 408–9
ASTM D 1499, 600
ASTM D 1693, 596
ASTM D 1781, 406
ASTM D 1876, 406
ASTM D 1879, 586
ASTM D 2095, 401
ASTM D 2293, 484
ASTM D 2565, 600
ASTM D 3167, 406
ASTM D 3433, 409
ASTM D 3528, 395
ASTM D 3762, 407, 549
ASTM D 4329, 600
ASTM D 5379, 399
ASTM D 5649, 97, 105
ASTM D 5656, 396, 397
ASTM D 6671, 409
ASTM D 1002-05, 98, 119
ASTM D 1780-99, 484
ASTM D 2294-96, 484
ASTM D 3166-99, 475
ASTM D 3433-99, 2001, 359
ASTM D 4501-01, 98, 119
ASTM F 1248, 597
ASTM G 21, 587
ASTM G 53, 600
Aston Martin Vanquish, 272
atmospheric plasma, 273
  pre-treatment, 301
atomic force microscopy, 556
ATPB *see* allyltriphenylphosphonium bromide
ATR-FTIR, 558
Australian Air Force, 29
Automotive Composites Consortium, 276, 278
aviation fluids, 581

ball and pin impression, 597
barnacle adhesive, 565
bases, 581
bent strip test, 597
  flexible materials, 597
benzosulfimide *see* saccharin
Berlaymont building, 88
BETAMATE LESA Adhesive, 258
Big Dig 2006, 28
biological adhesives, 564
biological degradation, 586–7
biomimetic adhesives, 565
bismaleimide, 269, 580
bitumen, 185
blockshear testing, 98
blooming, 119
Boeing, 204, 205
Boeing, 787, 281
Boeing wedge test, 407, 549
Boltzmann's constant, 591
bonded joints
  corner locations and definition technical crack, 327
  crack initiation
    corner geometry, 330
    overlap strength, 331
  crack propagation phase, 338–43
    actual vs average nominal crack length, 339
    crack length averaging, 338
    crack length evolution, 339
    crack propagation scatter band for all joints tested, 342
    cracked joint deformed shape and FE model details at interface crack, 341
    influence of corner geometry, 331
    influence of overlap strength, 332
    Paris curve data calculated for

© Woodhead Publishing Limited, 2010

different survival probabilities, 343
square edge vs spew fillet joint, 330
trends in SERR components and influence of adherend stacking sequence, 342
experimental fatigue data
spew fillet joints, 320
square edge joints, 320
statistical analysis results, 321
fatigue damage mechanics overview and analysis, 322–31
fraction of fatigue life to crack initiation, 332
generalised SIF approach and life to crack initiation assessment, 333–7
FE models adopted reference local frame, 335
properties of adherends and adhesive used as input data, 334
strength of singularity and normalised values for generalised SIF, 336
stress distribution at adhesive–adherend interface, 335
life prediction
composite material, 316–48
model, 331–3
procedure and application, 343–5
procedure flow chart, 344
single lap bonded joints fatigue behaviour, 318–22
bondpreg, 229
breakaway test, 97
breakloose test, 97
Bridgestone, 124
brush anodising process, 205
BS EN ISO 9664:1995, 475
Bueche-Cashin-Debye equation, 244–5
Burger's fluid, 490, 491
butt joints, 296–7

CalcuRep, 219
calender, 160
calixarenes, 116
carbon black, 151, 153, 157, 165, 585
carbon/epoxy cracked lap shear joints, 317
carbon fibre, 269, 270, 283
carbon nanofibres, 154, 155–6
scanning electron micrograph in epoxy matrix, 156
carbon nanotubes, 154
multi-walled, 155
single-walled, 155
transmission electron micrograph in epoxy matrix, 155
carbon reinforced plastic (CRP), 304
carbon steel
surface treatment, 201–2
CAST3M FE, 442
catalysts
addition-cure, 77
condensation-cure, 77
T-series, 77
cathecol moiety, 565, 566
*Caulobacter crescentus,* 565
CentrAl, 228–9
centric force transmission, 297
ceramic whiskers, 154, 156
Chartwell B-545.1, 108, 110
Chemence, 124
chemical resistance testing, 587–602
chemical vapour deposition, 155
Chevrolet Corvette, 272
Chevron-Philips, 27
chromate conversion coatings, 200
chromic acid anodising process, 199, 200
chromium and sulphuric acid, 197–8
Chrysler LLC, 276
cleavage load, 297–8, 299
climbing drum peel test, 406
clinching, 301
Closure Medical, 126
co-bonding process, 276
coefficient of thermal expansion, 413, 518, 528
cohesive energy density, 592
cohesive zone damage, 431
cohesive zone model, 357, 378–9
traction plotted against separation distance, 379
complex modulus, 486
Composite Construction Laboratory, 28
compression tests, 410
computer aided engineering modelling, 281
condensation cure chemistry, 70–2
formulation ingredients and their functions, 75

© Woodhead Publishing Limited, 2010

constant displacement test, 549–50
constant tensile deformation, 597–8
constant tensile stress test, 598
contact angle techniques, 357
continuum damage mechanics, 483
Convair B-58, 28
conversion treatment, 204
corona discharge, 255
corrosion resistant steels *see* stainless steel
crack growth
  behaviour, 604
  creep crack growth rate, 497
  partitioning approach, 498
  rates, 338, 347
  stable, 476
  testing, 605
crack nucleation phase, 316
crack propagation life, 343
crack velocity region, 550
CRAS, 219
creep, 469–70, 484
  compliance, 485
  failure, 486
  load conditions, 469–511
creep rupture, 484, 581
  testing, 594–6
critical debonding, 360–1
critical fracture, 354
critical peel stress, 428
critical strain energy release rate, 406, 409
critical stress intensity factor, 406
cross-linkers, 76–7
  RTV condensation-cure, 76
  RTV/LTV addition cure, 76–7
crown ether, 116
CRP *see* carbon reinforced plastic
cryogenic liquid containment system
  case study in use of joint tests, 424–8
    design, 425
    quality assurance, 428
    validation, 425–7
  double lap joint specimen, 428
  insulation membrane system, 425
  sandwich panel specimen, 426
  stress FE analyses in different joints under proof loads, 427
CSA *see* chromium and sulphuric acid
cumene hydroperoxide, 99
cure inhibitor, 73
cure profile, 142–3
cure retarder, 73
cure shrinkages, 562–3
curing, 412–14
cyanate esters, 8–9
cyanoacrylate, 7–8, 12
cyanoacrylate adhesives
  2001-2006 patenting activity, 124
  advances, 96, 110–27
    advantages and disadvantages, 112
    anionic charge delocalisation by tautomeric structures, 113
    chemical structures of different esters, 113
    chemistry, 111–14
    history, 110–11
    poly(alkyl cyanoacrylates), 114
    zwitterionic polymerisation, 113
  durability, 119
  formulations and types, 114–19
  future trends
    products with improved physical properties, 127
    sustainable products, 127
  glass transition temperatures of poly(alkyl cyanoacrylates), 114
  moisture resistance, 123–4
  polymer property modifiers, 115–16
    adhesion promoters, 115–16
    hydrophobic additives, 117
    miscellaneous, 117
    plasticizers, 116–17
    thermal stabilisers, 117
    toughenes, 117
  polymerisation process modifiers, 114–15
    accelerators, 115
    stabilisers, 114–15
  technology advances, 124–6
    adding acids on shock resistance, 125
    industrial adhesive bonding, 124–6
    tissue bonding, 126
  thermal resistance, 119–23
    steel lapshear specimens tensile shear strength comparison, 122
  types, 118–19
    flexible, 118
    low bloom, 119
    low surface energy substrates, 119
    standard ethyl, 118

© Woodhead Publishing Limited, 2010

surface insensitive ethyl, 118
thermally resistant ethyl, 118
toughened ethyl, 118
typical tensile shear bond strengths, 120
UV curable ethyl, 118
cycle mix effect, 479
cycle mix factor, 479
cyclic fatigue debonding, 361–3
cyclic fatigue loading, 551
cyclic stress testing, 507–8
Cytec-Fiberite, 29
Cytech Engineered Materials, 490
CZM *see* cohesive zone model

d-spacing, 161
DABPA *see* diallyl ether of bisphenol A
damage initiation, 606
damage mechanics approach, 483
damage-tolerant approach, 503
DAPCOtreat, 204
degradation, 548
D.E.R. 332-Versamide, 239
Dexter Corporation, 149
di-*p*-toluylsulfonimide, 107
diallyl ether of bisphenol A, 108
structure, 109
diaryliodonium salt, 74
differential scanning calorimetry, 581, 589
diffusion kinetics, 588–92
diffusion theory, 243–6
digital image correlation, 228
digital image correlation techniques, 416, 419
DIN 53283, 38
DIN 54451, 39, 40
disbond arrestment, 269
dispersion, 158–9
dissolution, 588
DMTA *see* dynamic mechanical thermo analysis
Dodge Viper, 272, 283
bonded-only joint, 268
carbon fibre SMC fender support, 283
glass/carbon hybrid SMC door inner panel, 283
headlamp, 267
DOGMA, 439
dominant damage approach, 498
double cantilever beam, 359, 379, 409
double lap joint, 427
Douglas Aircraft Company, 28
Dow BETAMATE 1484, 277
dry ice blasting, 301
duPont, 134
dynamic mechanical analyser, 374
dynamic mechanical thermo analysis, 46, 413

e-beam curing, 285
ε-Caprolactones, 125
e-coat *see* electrocoat
EA9628/EA9202, 28
Eastman Kodak, 111
Ecole Polytechnique Federale de Lausanee, 28
elastoplastic fracture mechanics, 481, 494
electrocoat, 275
electronic speckle pattern interferometry, 416, 419
electronic theory, 246
empirical crack growth law approach, 497
EN 1943, 484
EN 22553, 310
energy release rate, 355, 356
Engineering Adhesive Selector, 17
Engineering Equation Solver, 530
environmental exposure debonding, 365–7
environmental stress cracking, 581–3, 596–8
epoxide *see* epoxy
epoxy, 5–6, 143, 144, 145, 270, 304
epoxy adhesives, 188–92, 578
advances, 20–30
fast cure epoxy compositions US patent activity, 21
main applications and limitations, 21–2
applications, 27–30
aerospace, 28–30
aluminium-glass-fibre/epoxy laminate diagram, 29
construction, 27–8
assembly bonding, 190–2
automotive bonding, 189–90
modified adhesives, 188–9
out of autoclave curing methods, 189
recent developments, 22–30

© Woodhead Publishing Limited, 2010

aryl cyanate ester-epoxy reactions, 23
bisphenol-C diglycidyl ether structure, 24
chronoaniline-acetaldehyde condensate, 26
nano-silica filler on epoxy fracture energy, 25
renewable materials, 26–7
toughening, 24–6
vegetable oil based epoxy resins addition, 27
websites of interest, 30
epoxy-phenolic adhesives, 187
epoxy resin, 185
etch primers, 255
etching treatment, 204
European Economic Community Medical Device Directive, 68
extensometry methods, 417

F-111 bomber, 220
F-Chart Software, 530
fail-safe approach, 500, 503
failure load prediction, 223–4
fast crack growth region, 476
fatigue
crack growth, 480–3, 497, 498, 506
GLARE vs AA 2024 T3, 216
propagation rate, 482
designing adhesive joints, 469–511
high-cycle, 469, 475
low-cycle, 469, 478
variable amplitude, 482
fatigue life, 469, 476
fatigue life tracking, 502–3
Federal Aviation Regulation, 269
Fibre Bragg gratings, 227
fibre metal laminates, 29, 213–15
fibre-reinforced polymer, 27, 304–5
Fickian diffusion, 366
Fick's second law, 589
fillers, 78–9, 563
electrically conductive, 80
non-reinforcing, 79
reinforcing, 79
semi-reinforcing, 79
thermally conductive, 80–1
flame retardants, 79–80
flame treatment, 249
flash thermography, 424
flexible, 405
flexible composite barrier film, 425
floating roller test method, 406
fluid concentration, 589, 590
fluid conditioning, 593
fluorosilicones, 577
FM/73, 29, 490
FM/300, 29
FM73/BR127, 28
FM55/XA3950, 28
Fokker, 204, 213
Fokker 100, 190
Fokker F28, 190
Ford Motor Company, 273, 276
Forest Products Laboratory, 198
FPL etch, 198
fracture
toughness, 165–9
fracture energy, 358, 360, 408
fracture mechanics, 604–6, 608
adhesive joint design improvement, 350–81
approach, 224–5
design implications of other singularities, 375–6
design insights, 372–5
adherend flexibility, 372–3
adhesive thickness effects, 373
plot of fracture energies measured in falling wedge test, 375
rate and temperature effects, 374–5
designing to resist fracture, 360–7
resist critical debonding, 360–1
resist subcritical debonding, 361–7
future trends, 379–80
insensitivity of continuum-based strength criteria to dominant flaw size, 352
issues related to mixed mode fracture, 367–72
locus of failure, 372
mode mixity effects, 371–2
measuring adhesion fracture energies, 357–60
characterising fracture energies, 359–60
corrected beam theory application, 360
measured fracture energies, 357–9

© Woodhead Publishing Limited, 2010

thermodynamic, intrinsic and practical adhesion, 359
numerical analysis, 376–9
CZM, 378–9
*J*-integral method, 377–8
virtual crack closure method, 376–7
overview, 354–7
general loading for a cracked bilayer, 356
three fractured modes, 355
FRANC2D, 376
FRANC3D, 376
FRP *see* fibre-reinforced polymer
FTIR-MTIR, 554, 555

General Motors, 276
generalised SIF, 333, 343
GENOA, 376
GLARE, 29, 30, 213–14, 215, 216, 225
stress-strain curve, 216
vs AA 2024 T3 fatigue crack growth, 216
Glare 2, 215
Glare 3, 214, 215
glass/carbon hybrid SMC door, 283
glass/epoxy single lap joints, 317
glass fibre, 270
glass fibre reinforced aluminium laminate *see* GLARE
glass/polypropylene single lap joints, 317
glass transition temperature, 87, 193–5, 519, 524, 525
Gluedo, 17
grit-blast/silane process, 205
grit blasting, 271–2

Halpin Tsai model, 162
Hansen solubility parameters, 592, 608
heat stabilisers, 79
hem flange joints, 303
hemming, 304
Henkel, 124
Henkel AG & Co KGaA, 149
Henkel Terobaka 5087-02P, 277
Henry's law, 588
Hexcel Composites, 525
Hexcel Redux 319, 579
high temperature adhesive, 535
high-temperature vulcanising, 70
Hookean spring, 487
hot strength, 119–20
Huntsman Araldite 420 A/B, 449
hybrid joining, 301, 505
hybrid process, 302
hydroxyethyl methacrylate, 138, 139
hydroxypropyl methacrylate, 138, 139
Hypalon, 134
Hysol, 28

incremental polynomial method, 338
inductive curing, 285, 312
inductive heating, 302
injection bonding, 308
set up, 309
instant adhesives *see* cyanoacrylate adhesives
integral C*, 495
inter-adherend-fibres, 305
interference-fit fasteners, 500
intrinsic adhesion, 358
IPS, 149
ISO 62, 591
ISO 175, 576
ISO 604, 410
ISO 846, 587
ISO 2818, 412
ISO 4578, 406
ISO 4587, 394
ISO 4892, 600
ISO 6721, 413
ISO 6922, 401
ISO 10354, 407
ISO 11339, 406
ISO 14676, 406
ISO 15109, 484
ISO 15166, 391
ISO 16770, 597
ISO 17212, 412
ISO 20340, 600
ISO 527-4, 391
ISO 8510-2, 406
ISO 11003-1, 400
ISO 11003-2, 396
ISO 22088-2, 597
ISO 22088-3, 596
ISO 22088-4, 596
ISO 22088-5, 596
ISO 22088-6, 597
isochronous stress-strain curves, 485

© Woodhead Publishing Limited, 2010

isopropyl alcohol, 272

*J*-integral, 357, 377–8, 481
  mesh discretisation, 378
Jeffamine, 257
JKR method, 357
joints
  *see also* specific joints
  adhesive, developments in testing, 389–432
    case study in use of joint tests, 424–30
    current and emerging types of testing, 392–410
    failure detection, 421–4
    future trends, 431–2
    role of testing, 389–92
    specimen manufacture issues, 410–15
    test variables, 415–21
  automobile bonnet anti flutter bonding, 304
  basics, 296–9
    design optimisation, 298
    possible geometries, 297
    stiffness of joints and joint geometry, 300
  bonded, life prediction in composite material, 316–48
    crack propagation phase, 338–43
    fatigue damage mechanics overview and analysis, 322–31
    generalised SIF approach and life to crack initiation assessment, 333–7
    life prediction model, 331–3
    life prediction procedure and application, 343–5
    single lap bonded joints fatigue behaviour, 318–22
  configuration for an optimised pipe joint, 308
  design and fabrication techniques selection, 295–312
  design improvement using fracture mechanics, 350–81
    design implications of other singularities, 375–6
    design insights from fracture mechanics, 372–5
    designing to resist fracture, 360–7
    fracture mechanics overview, 354–7
    future trends, 379–80
    issues related to mixed mode fracture, 367–72
    measuring adhesion fracture energies, 357–60
    numerical analysis, 376–9
  design selection, 299, 301
  experimental values for strength degradation, 306
  fabrication techniques, 301–2
  for different materials, 302–10
    closed profiles bonding, 307–8
    concrete structures reinforcement, 310
    FRP bonding, 304–5
    sandwich structures bonding, 304–5
    sheet metals bonding, 306–7
  graphic representation in engineering drawings, 310–11, 312
    graphic symbol and secondary technical factors, 312
    symbols for different joint geometries, 311
  injection bonding set up, 309
  inter-adherend-fibre joint illustration, 306
  quality monitoring in production, 509
  repair joint in CRP sample, 305
  schematic model of two phases in joint fatigue life, 333
  suitable for sandwich panels, 307
  typical flanges for joining sheet metals, 303

Kaneka, 158
Kelvin-Voigt model, 487, 488
kissing bond, 266, 274
knife-edged extensometers, 397, 418
Knoevenagel condensation, 111

L–N curve, 475
lap shear strength, 38–9
lap shear test, 98, 390, 438, 439
laser pre-treatment, 301
life prediction model, 318, 331–3
linear elastic fracture mechanics, 357, 481, 494

© Woodhead Publishing Limited, 2010

linear variable differential transformers, 418, 430
lithium tri-sec-butyl borohydride, 257
local stress field, 327
locking compounds *see* anaerobic adhesives
Loctite Corporation, 97, 111, 149
Lord Corporation, 149
L'Oreal, 124
loss factor, 486
loss modulus, 486
low temperature adhesive, 535
low temperature vulcanising, 70, 72, 73, 75, 76–7
Lycurgus cup, 151

M1133/6740, 28
3M Corporation, 28, 79
Macrolite Ceramic Spheres, 79
manual multi-step sanding, 271
Master Bond, 525
maximum nominal stress, 319
Maxwell model, 488, 489, 490
mean shear stress, 393
mechanical interlocking theory, 238–9, 245–6
metal alkyl borohydrides, 257
metal bonding
  adhesive bonded joints effectiveness modelling and testing, 220–8
    analytical solutions, 221–2
    bonded lap joint shear and peel stresses, 221
    calculated stresses and strains, 224
    failure load prediction, 223–4
    fibre optic sensors bondline strains, 227
    fracture mechanics approach, 224–5
    improved analytical methods for fatigue crack growth, 225
    numerical tools, 222–3
    optical digital videomicroscopy development, 227–8
    test methods overview, 226
    testing adhesive bonded joints, 226
  developments in the range of metal adhesives, 186–96
    adhesive temperature resistance improvements, 193–6
    decrease in adhesive modulus with temperature, 195
    epoxy adhesives, 188–92
    epoxy film and 2-C epoxy paste adhesive shear-strain curves, 191
    epoxy vs MS polymer adhesive overlap joints, 194
    Fokker 100 extent of adhesive bonding, 187
    high flexibility adhesives, 193
    lap joints S-N curves, 190
    methyl methacrylate adhesives, 192–3
    modified phenolic adhesives, 187–8
    polyurethane adhesives, 192
    strength of various adhesive types, 196
    structural adhesives glass transition temperature range, 195
  improvements in bonding metals, 185–229
    adhesive bonded joints effectiveness modelling and testing, 220–8
    CentrAl concept, 229
    future trends, 228–9
    key problems, 185–6
  joint design developments, 206–20
    AA 7075-T6 vs AA 2024-T3 residual strength, 213
    adherends elastic deformations, 207
    adhesive bonded laminates, 211–13
    adhesive bonded stepped lamination, 211
    bonded repairs, 218–20
    bonded vs solid aluminium alloy laminate fracture surface, 214
    bonded window frames, 220
    effect of joint geometry, material and type of adhesive for lap joints, 208
    fatigue crack growth life improvement, 212
    fatigue cracks bridging, 215
    fibre metal laminates, 213–15
    Fokker F28 outer wing skin, 214
    GLARE stress-strain curve, 216
    GLARE vs AA 2024-T3 fatigue crack growth, 216
    joint optimisation, 209–10
    large fuselage panel, 217

© Woodhead Publishing Limited, 2010

load transfer in various types of joints, 206
overlap joints eccentricity, 208–9
peel stresses, 210
sandwich structures, 217–18
scarf joint, 210
shear stress distribution of bonded overlap joints, 207
vertical tail plane leading edge, 217
weight and cost reduction, 216–17
metal surface treatment techniques developments, 196–206
aluminium alloys, 196–200
aluminium alloys surface treatment methods, 197
bonding primers developments, 206
PSA oxide electron micrograph, 201
sol-gel surface treatment for aluminium, steel, titanium, 203–5
stainless steel wedge test specimens crack extensions, 203
steel and stainless steel, 200–3
surface configurations after etch process, 198
titanium, 203–4
shear stress distribution
effect of overlap length, 208
unequal axial stiffness adherends effect, 209
methacrylates, 132–50
advantages, 142–4
bondline properties, 143–4
cure profile, 142–3
potential formulating variables, 141
methoxybenzoyl toluylsulfonamide, 107
methyl methacrylate, 133, 144
adhesives, 192–3
methylbenzoyl toluylsulfonamide, 107
microwave curing, 285
mixed adhesive double lap joints, 537
effect of adhesives Young's modulus ratio, 538
mixed adhesive single lap joints, 537
effect of adhesives Young's modulus ratio, 538
mixed mode fracture, 367–72
correlation between measured fracture energy and tan value, 370
effect of specimen type and fracture mode on locus of failure, 371
locus of failure, 372
mode mixity effects, 371–2
moisture, 547
moisture curing adhesives
reactivity, 51–4
bubbling, 53–4
low initial strength, 52–3
slow curing speed, 51–2
slow strength build-up, 52
strength build up and curing speed of different PUR technologies, 53
Mori-Tanaka model, 162
MTS 858 servo-hydraulic testing device, 318
multi-walled nanotubes, 155, 160
multifunctional adhesives and composites, 286
mussel adhesive, 564

*N*-methyl-*N*-phenylglycine, 106
nano ferrites, 302
nano-fillers, 24
nanoclays, 153, 157
-modified polymers microstructures, 157
nanoparticle reinforcement, 152–3
advances in structural adhesives, 151–74
assembly of nanoparticles using diblock polymers, 173
future trends, 172–4
incorporation methods, 158–61
alignment, 161
cyanate ester polymer with 10 wt% titania nanoparticles, 158
dispersion, 158–9
mixing, 159–60
sonication, 160–1
nanoparticles types and key attributes, 153–7
definition, 153
equi-axed, 154
nanoclay-modified polymers microstructures, 157
nanotubes and nanofibres, 154–6
other nanoparticles, 157
plate-like, 156–7
opportunities and limitations, 151–3

© Woodhead Publishing Limited, 2010

nanotechnology, 152
silica nanoparticles in epoxy, 154
typical property variations, 161–72
conductivity vs filler content, 166
electrical properties, 164–5
epoxy and nanoclay-modified epoxy films oxygen permeability data, 163
epoxy insulation breakdown time, 166
epoxy vs silicate fracture toughness, 168
fatigue performance, 169–71
fracture energy vs silica nanoparticles content, 169
fracture toughness, 165, 167–9
functional properties, 163–4
hybrid epoxy lap-shear and roller peel strength, 172
logarithmic crack growth rate per cycle vs logarithmic range of applied SIF, 170
mechanical properties, 161–2
nanoclay-modified epoxy polymer relative modulus, 162
peel and lap shear performance, 171–2
silica particle-dispersed composite normalised total light transmittance, 165
nanoparticles
definition, 153–4
equi-axed, 154
plate-like, 156–7
types and key attributes, 153–7
Nanopox, 158
Nanoresins, 158
Nanostrength E20, 24
nanotechnology, 151–2
Narmco, 28
National Institutes of Standards and Technology, 163
National Starch and Chemical, 149
near surface mounting technique, 28
neutral line method, 219
Newtonian flow, 489
nitric acid anodising process, 202–3
nitrile-phenolic adhesives, 187
*N,N*-dialkyl arylamine, 99
Nomex, 218
nominal cracks, 327–8
non-destructive evaluation, 267, 361
non-destructive test, 424, 552
normalised non-linear strength wearout model, 479
numerical crack growth integration, 482
nylon, 270, 271–2

Oak Ridge National Lab, 277
operating temperature, 519
organic solvents, 580
organosilane, 78
out-of-autoclave bonding, 285
overlap joints, 296
overstress model, 492
Owens and Corning, 29
oxidation, 581

palladium, 77
Palmgren–Miner rule, 362, 477, 478
Paris equation, 604
Paris-Erdogan law, 170
Paris law, 362, 364
Paris region, 482
Park Avenue Tower, 85
Pasa-Jell, 29
Pasa-Jell 107, 204
peel load, 297–8, 299
peel plies, 271–2
peel stoppers, 277
Permabond Adhesive Selector, 17
PET *see* polyethylene terephthalate
phenolic adhesives, 579
phenolics, 9
phenylene diamines, 107
phenylhydrazine, 105
phosphonium salt, 107
phosphoric acid anodising, 199, 200
containment system, 205
phosphoric-sulphuric acid anodising, 200
photoelasticity, 423–4
photooxidation, 583–5
phthalic anhydride, 117
PLANE82, 334
plasma treatment, 251–5
plastic bonding
adhesion mechanisms, 238–46
adsorption theory, 240–1
butt tensile strengths improvements, 239

© Woodhead Publishing Limited, 2010

chemical treatments effect on bond strength, 242
diffusion theory, 243–6
electronic theory, 240
mechanical interlocking theory, 238–9
polyamide bonded samples peeling strength, 245
surface geometry effect on butt tensile strength, 240
thermal treatment effect on joint strength, 242
advances, 237–62
future trends, 261–2
liquid droplet on solid surface, 247
organoboron chemistry uses, 256–8
surface characteristics, 246–7
limitations, 258–61
advancing and receding contact angle measurements for PE and PP, 259
durability, 258–61
lap shear test values, 261
polyethylene advancing and receding contact angle measurements, 258
shear testing results, 260
stud pull off testing results, 260
versatility, 261
surface treatments, 247–56
BETAMATE LESA adhesive lap shear strength, 258
changing the distance between inner tip and polypropylene surface, 250
chemical treatments, 255–6
corona discharge, 255
flame treatment, 249–51
ionising environments, 251
PET AFM images before and after plasma treatment, 253
plasma treatments, 251–5
polymers adhesion and surface properties, 252
polyurethane-painted polypropylene tensile strength, 250
primer type effect on metallocene polyolefin T-peel strength, 256
PVDF AFM images before and after plasma treatment, 254
solvent treatment, 248–9
surface energies of common adherends, 248
plasticizers, 116–17
platinum, 77, 80
Plexus, 149
podands, 116
Poisson's contraction, 402
Poisson's ratio, 391, 403, 410
poly(alkyl cyanoacrylates), 114
polyalkylene oxides, 116
polyamide thickener, 103
polybismalaeimides, 8
polyester, 270
polyetheretherketone, 269
polyethylene terephthalate, 251
polyimide adhesive, 366
polyimides, 8, 580
polymer matrix composites
bonding, 265–87
common bonding requirements, 266–9
bonded-only joint in the Dodge Viper, 268
glass fibre-polypropylene composite spare wheel well, 267
future trends in aerospace and automotive composites, 281–7
automotive front end module, 284
composite and metal usage in Boeing 787 primary structure, 282
concept for reinforcing metal with bonded polymer composite stiffener, 282
joint design considerations, 274–7
aerospace applications developments, 275–6
automotive applications developments, 276–7
schematic of weld-bond joint concept, 277
Z-pin stubble in composite substrate, 276
joints modelling and testing, 277–81
adhesively bonded composite joints, 278–80
testing adhesively bonded composite joints, 280–1
pre-treatment and surface characterisation, 271–4

© Woodhead Publishing Limited, 2010

aerospace applications, 272–4
automotive applications, 274
unique bonding requirements
aerospace applications, 269–70
automotive applications, 270
polymeric anchor, 307
polymers, 74–5
silanol-terminated PDMS, 74
vinyldimethysiloxy-terminated PDMS, 75
polyolefins, 148, 301
polyphenylene sulphide, 269
polypropylene, 270, 283
common application, 284
polytetrafluorene, 412
polyurethane, 6, 143, 145, 147, 577, 579–80, 586
adhesives, 192–3
advances in structural adhesives, 35–65
education, 35
surface treatment strategy, 57
applications, 57–64
automotive, 58–60, 60
bonded wooden panels for laminated beams, 63
bonding insulating glass into a window frame, 64
bonding panels finger joint design, 64
bus floor and side panels bonding, 59
bus roof and air conditioning bonding, 58
buses, 58
laminated beams, 62
leisure boat, 61
marine, 60
rail, 58
rail applications bonding, 59
roof structure laminated beams, 63
rotor blades for wind turbines, 61
rotor blades principle design for wind turbines, 62
sandwich panels, 60–1
sandwich panels bonding, 61
windows, 62–4
building blocks schematic, 48
characterisation, 38–48
2-C PUR Wöhler curve, 45
adhesion and ageing, 47–8
bonded lap shear specimen, 39
2C PUR DMTA measurement, 46
1C PUR Wöhler curve, 44
2C structural adhesives stress-elongation, 43
crash resident adhesive stress-strain diagram, 42
durability, 43–6
glass transition temperature and temperature dependence, 46–7
high modulus 1C PUR DMTA, 47
lap shear specimen, 38
lap shear strength, 38–9
PUR adhesives stress-strain diagram, 42
shear modulus G, 39
stress-strain diagram, 40–3
sun roof lid stiffness, 40
thick adherent test specimen, 41
Wöhler curves for different adhesive types, 44
chemistry, 48–54
building blocks, 48–50
2C adhesives reactivity, 50–5
moisture curing adhesives reactivity, 51–4
nanophases formation during curing, 50
peel force measurements, 51
design principles, 54–6
bonding area, 54
bondline thickness, 54
strength dependence from bondline thickness, 55
stress distribution schematic view, 55
stress through thermal elongation, 56
thermal elongation difference, 56
landscape of adhesives, 37
positioning, 37–8
polyvinyl chloride, 9
power law creep equation, 491
PP *see* polypropylene
pressure sensitive adhesives, 10
pressurised fluid testing, 593
Primary Adhesively Bonded Structure Technology, 28, 438
Prony series, 490

© Woodhead Publishing Limited, 2010

propagation modes, 355
PSA *see* phosphoric-sulphuric acid anodising
PUR *see* polyurethane
pure mode, 355
  fracture energy, 369
Pyrosil, 301

Quickstep technology, 189

R-glass fibre, 29
R-ratio, 474
radiation, 585–6
Raman microscopy, 423
Raman spectroscopy, 420, 423
reactive acrylic adhesives, 192
reactive plasticizers, 76
redox initiation system, 99
Redux 326, 525, 533
Redux 775, 186, 187
residual stress, 563
resin transfer moulding, 189
rigid composite secondary barrier film, 425
robot dispensing process, 301
room temperature vulcanising, 69–70
Rose model, 219
Royal Australian Air Force, 218
RTV *see* room temperature vulcanising

S2-glass, 29
S-N curve, 475, 477
SAAB 2000, 220
SAAB aircraft, 213
saccharin, 99, 106–7
safe-life approach, 503
Saint Gobain, 29
Saint-Venant element, 490
sandwich panels, 60
  bonding, 61
scalar damage equation, 606
scanning probe techniques, 431–2
scarf joint, 298–9, 403–5
  crack initiation and propagation, 422
  illustration, 405
scatter bands, 336, 347
scrim layer, 368
scuff sanding, 268, 272
Seal Texipreg CC206, 318
sealer bead, 303–4
self-assembled monolayers, 561, 562
self-catalytic cure systems, 70
SERR *see* strain energy release rate
sewing, 305
shear lag theory, 220, 222
shear modulus, 37
shear strain, 399
shear stress, 369–70, 399
shear tests, 393–400
  alternative tests, 399–400
    Arcan specimen, test fixture and extensometer, 400
    torsion tests, 401
    V-notched beam shear test specimen and test fixture, 399
  double lap, 395
    strap joint with tapered adherends, 396
  lap strap, 395–6
  single lap shear, 393–5
  stress-strain curve, 394
  thick adherend shear, 396–8
    miniature specimen tested in compression, 398
    test specimen made with pre-shaped adherends and cut from bonded plates, 397
    test specimen using contact extensometers, 398
  thin-lap shear specimen with dimensions specified by standards, 395
  typical lap joint configurations, 393
sheet moulding compound, 272, 283
SIF *see* stress intensity factor
Sika, 28
silane, 78, 559–60
silicone, 8, 272, 577
  adhesive formulations, 74–81
    adhesion promoters, 78
    catalysts, 77
    cross-linkers, 77
    fillers, 78–9
    formulation ingredients and their functions, 75
    plasticizer, 76
    polymers, 74–5
  advances, 66–90
    future trends, 90
    properties, 67–9

© Woodhead Publishing Limited, 2010

product forms and cure chemistry, 69–74
addition cure chemistry, 72–3
condensation cure chemistry, 70–2
electron-beam and photo-cure induced addition chemistry, 73–4
special additives, 79–81
electrically conductive fillers, 80
flame retardants, 79–80
heat stabilisers, 79
thermally conductive fillers, 80–1
structural adhesive applications, 81–9
automotive, 82–4
aviation and aerospace, 84–5
construction, 85–8
domestic appliances, 88
electronics, 88–9
lamp bonding application, 82
solar/photovoltaic renewable energy industry, 89
silicone fluid *see* trimethylsiloxy-terminated PDMS polymer
silicone reactive hot melt adhesives, 83–4
siloxane polymers, 70
single lap bonded joints
fatigue behaviour, 318–22
geometry, 319
single lap shear test, 389–90, 428
single-walled nanotubes, 155, 160
Skydrol 500A, 579
slow strain rate testing, 598
SMC *see* sheet moulding compound
*S–N* plots, 362
snap cure, 20
solubility, 588–92
parameter, 592
solvent, 248
solvent-based primers, 255
sonication, 160–1
Specialchem - Adhesives and Sealants, 18
spew fillet joints, 336
crack length evolution, 325
crack patterns from corner, 324
experimental 10-90% scatter band
fatigue data at failure (overlap 20 mm), 346
fatigue data at failure (overlap 40 mm), 346
life to crack initiation, 345
life to crack propagation, 345
experimental fatigue data, 320
fillet crack initiation, 323
fracture surface morphology over entire overlap length, 325
scatter bands for fatigue to crack initiations, 337
side views of cracks nucleated at the fillet toe and upper corner, 326
stress distribution at adhesive–adherend interface, 335
SPH *see* succinic phenylhydrazine
spot curing, 304
spot weld, 302
square edge joints, 336
crack growth rates vs normalised crack length, 340
crack initiation and intralaminar/interlaminar crack path, 326
crack length evolution, 339
crack propagation vs normalised fatigue life, 329
experimental fatigue data, 320
fracture surface morphology, 329
interface crack initiation and propagation path, 326
scatter bands for fatigue to crack initiations, 337
SSG *see* structural sealant glazing
stabilisers, 114–15
stainless steel, 202–3
static fatigue, 364
static overdetermination, 297, 307
steel, bonding improvements, 185–229
stitching, 305
storage modulus, 486
strain, measurement techniques, 416–20
contact extensometers, 418
crosshead movement, 420
non-contact extensometers and strain mapping, 418–19
strain sensors, 420
strain energy density, 378
strain energy release rate, 317, 332, 339, 354
strain gauges, 430
strain mapping techniques, 423–4
stress factor, 444
stress intensity factor, 332, 354, 355, 356
stress-life approach, 475

© Woodhead Publishing Limited, 2010

stress rupture *see* creep rupture
stress-strain curve, 40
structural adhesive bonding
  definition, 35–6
  necessary skills, 36
structural modelling, 278
structural sealant, 67
  *see also* silicone
  glazing, 85, 86
subcritical debonding, 361–7
  crack length and fracture energy values, 367
  cyclic fatigue debonding, 361–3
  debond rate data collected at different applied energy release rate, 364
  environmental exposure debonding, 365–7
  rate dependence of epoxy adhesive, 365
  rubber toughening component on model epoxy fatigue resistance, 362
  time-dependent debonding, 364–5
succinic phenylhydrazine, 106
sulfonation, 274
sulphuric acid anodising process, 199–200
superglue *see* cyanoacrylate adhesives
Supreme 10HT, 525, 533
surface energy, 246
surface treatment
  aluminium alloys, 196–200
  metal bonding, 186
  plastic bonding, 247–56
  steel and stainless steel, 200–3
  titanium, 203

t-butylbenzoyl toluylsulfonamide, 107
T joints, 297
  materials models validation, 428–30
    manufacture, 429–30
    results, 430
    testing, 430
  specimen made of epoxy bonded aluminium, 429
T-series catalysts, 77
Taoka, 124
tapered double-cantilevered beam, 409
technical crack nucleation, 327
Teflon, 272
tension and peel tests, 401–9
  butt tension, 401–3
    adherends profiling on tensile stress distribution, 404
    extensometer system, 403
    precisely machined V-blocks, 402
  cleavage and fracture, 406–9
    common test specimens, 408
    four-point end notch flexure test, 410
  peel tests, 405–6
    standard specimen and tool to control fillet form, 407
  scarf joint, 403–5
    illustration, 405
tetrahydrofurfuryl methacrylate, 138
thermal load, 519
thermal stabilisers, 117
thermally conductive adhesives, 80, 89
thermography, 424
thick-adherend shear test, 396, 398, 418
thin lap shear test, 393–4
Three Bond, 124
three-roll mill, 160
time–moisture superposition principle, 366
time–temperature superposition principle, 358, 365, 374
tin catalysts, 71
tissue bonding, 126
titanates, 71
titanium
  surface treatment, 203–4
    anodising treatments, 204
    etching and conversion treatments, 204
TnBB-MOPA complex, 257
Toagosei, 125
total vision system, 85
toughening, 117
  polymeric, 140
traction separation laws, 379
trimethylsiloxy-terminated PDMS polymer, 76
Turco 5578, 204
Tyzor, 77

UD carbon/epoxy composite, 460–1
UHU, 124
ultrasonic bath, 160, 161
unified theory models, 492

© Woodhead Publishing Limited, 2010

urethane block copolymers, 101
preparation, 102
UV curing, 73, 285, 312
system, 74
UV radiation, 584–5

vacuum assisted resin transfer moulding, 189
Van der Waals forces, 196, 241
vehicle-level modelling, 278
vinyl esters, 270
virtual crack closure technique, 339, 376–7
nodal forces and displacements used, 377
viscoelasticity, 527
visual inspection, 422–3
von Mises stress, 299

water break test, 271
weathering, 583–5
artificial, 599–601
chambers, 600–1
wedge cleavage test, 407
Weibull statistics, 353
weld-bond doubler, 277
welding, 302
wide-angle X-ray scattering, 156–7
Wöhler plot, 475

X-ray diffraction, 420, 423
X-ray photoelectron spectroscopy, 562

Young's modulus, 296, 304, 391, 403, 409, 528

Z Light Spheres, 79
Z-pins, 275–6
stubble in composite substrate, 276
Zecosphere, 79
zwitterion, 113
polymerisation, 112–13

© Woodhead Publishing Limited, 2010